Oceanologia

Official Journal of the Polish Academy of Sciences: Institute of Oceanology and Committee on Maritime Research

This journal is supported by the Ministry of Science and Higher Education, Warsaw, Poland

Indexed in: ISI Journal Master List, Science Citation Index Expanded, Scopus, Current Contents, Zoological Record, Thomson Scientific SSCI, Aquatic Sciences and Fisheries Abstracts, DOAJ

IMPACT FACTOR ANNOUNCED FOR 2016 IN THE 'JOURNAL CITATION REPORTS' IS 1.500; 5-year IF is 1.341

Publisher
Elsevier Sp. z o.o.
22, Jana Pawła II Avenue
00-133 Warsaw, Poland

Associate Publisher
Justyna Kasprzycka
j.kasprzycka@elsevier.com
+31 20 485 3846

ISSN 0078-3234

Oceanologia (2017) 59, 397—412

Available online at www.sciencedirect.com

ScienceDirect

journal homepage: www.journals.elsevier.com/oceanologia/

ORIGINAL RESEARCH ARTICLE

Kongsfjorden and Hornsund hydrography — comparative study based on a multiyear survey in fjords of west Spitsbergen

Agnieszka Promińska *, **Małgorzata Cisek**, **Waldemar Walczowski**

Institute of Oceanology, Polish Academy of Sciences, Sopot, Poland

Received 14 July 2016; accepted 7 July 2017
Available online 25 July 2017

KEYWORDS
Hornsund;
Kongsfjorden;
Summer hydrography;
Atlantic Water;
Transports

Summary A recent study has shown increased warming in the fjords of west Spitsbergen. Their location is critical, as they are situated along the main northward pathway of Atlantic Water (AW) which is a great source of heat to the Arctic Ocean and the fjords. In the light of ongoing warming, we aim to discuss differences between the fjords under northward transformation of oceanic waters. We compared summer hydrographic conditions in two fjords located in two opposite ends of west Spistbergen: Hornsund in the south and Kongsfjorden in the north. The study is based on high resolution CTD measurements collected during Arctic cruises between 2001 and 2015. The emphasis was put not only on differences in water temperature, salinity and water masses but also the freshwater content (*FWC*), AW transport and heat delivery to the fjords. In general, the water in Kongsfjorden is on average 1°C warmer and its salinity is higher by 0.5 compared to Hornsund. It is also characterized by two times greater transport of AW and heat delivery to the fjord. On the other hand, Hornsund reveals two times higher *FWC*. Both fjords undergo a gradual warming due to an increased presence of Atlantic origin waters. The ongoing warming is accompanied by an increase in variability of temperature and salinity dependent on the domination of the Sørkapp Current (SC) or the West Spitsbergen Current (WSC) on the West Spitsbergen Shelf (WSS). Nonetheless, Hornsund remains more Arctic-type fjord compared to Kongsfjorden, due to stronger blocking by SC.

* Corresponding author at: Institute of Oceanology, Polish Academy of Sciences, Powstańców Warszawy 55, 81-712 Sopot, Poland.
E-mail address: promyk@iopan.gda.pl (A. Promińska).
Peer review under the responsibility of Institute of Oceanology of the Polish Academy of Sciences.

Production and hosting by Elsevier

http://dx.doi.org/10.1016/j.oceano.2017.07.003

1. Introduction

Fjords of the west coast of Spitsbergen are located in a critical area – along the main pathway of the Atlantic Water (AW) toward the Arctic Ocean. AW, carried by the West Spitsbergen Current (WSC) with its core following the continental slope, brings a huge amount of heat to the Arctic Ocean through the deep Fram Strait (Schauer et al., 2004). WSC is separated from the fjords by the Sørkapp Current (SC) which transports cold and fresher Arctic Water (ArW) from the Barents Sea along the West Spitsbergen Shelf (WSS) toward the north. Both currents meet and mix along the Polar front (Swerpel, 1985; Walczowski, 2013) which is also called the Arctic Front (Saloranta and Svendsen, 2001). On its way to the north, WSC undergoes significant transformation, cooling and freshening (Nilsen et al., 2006; Saloranta and Haugan, 2004). This is mostly due to heat loss to the atmosphere or ice melting and heat transfer to coastal waters (Saloranta and Haugan, 2004; Tverberg et al., 2014), which is why WSC plays a significant role as a source of heat to the fjords as well. The terrestrial boundary of the Arctic fjords is characterized by numerous tidewater glaciers which constitute the main source of freshwater in the fjords (Weslawski et al., 1995), thus leading to strong stratification in summer (Cottier et al., 2010).

A long-term analysis show the warming of the west Spitsbergen fjords, which is manifested by an increase in water temperature (Pavlov et al., 2013), acceleration of tidewater glaciers (Blaszczyk et al., 2013) as well as changes in the sea ice cover in the fjords (Muckenhuber et al., 2016). The increase in maximum water temperature in autumn of approximately 2°C over the last century is mainly explained by the changes observed in WSC and the wind pattern in the Arctic and the Fram Strait (Pavlov et al., 2013). Blaszczyk et al. (2013) show significant acceleration of tidewater glaciers in Hornsund in the last decade due to changes in air temperature and increased water temperature in the fjord. Observations from the last 14 years clearly show that the area of sea ice cover that usually formed in winter in the Svalbard fjords (Hornsund and Isfjorden) reduced in response to increased winter air temperature and AW inflows (Muckenhuber et al., 2016). In all the cases AW is mentioned as an important factor leading to the observed changes.

AW enters the fjords in an annual cycle during the shift from winter to summer conditions (Cottier et al., 2010; Nilsen et al., 2008). However, AW inflow is also observed during winter time (Cottier et al., 2007; Promińska et al., unpublished data), which is linked with a growing number of winter cyclones passing through the Fram Strait (Nilsen et al., 2016).

In this study, we aim to compare the summer hydrography of two Arctic fjords, Hornsund and Kongsfjorden, as the southernmost and the northernmost component of the west Spitsbergen fjords' network. So far, a comparison of hydrographic conditions was done in Isfjorden and Grønfjorden (a small fjord being a part of the Isfjorden system), and it was based on long time series (Pavlov et al., 2013). The major part of the comparative study regarding Kongsfjorden and Hornsund has been dedicated to biology and usually been based on a short time period (Gluchowska et al., 2016; Węsławski et al., 1995, 2006). Here, we provide two comparable hydrographic data sets collected by the Institute of Oceanology PAN during Arctic cruises that took place in the years 2001–2015. The purpose of the paper is to answer the question: what is the difference between the west Spitsbergen fjords in the light of the warming that they experience? More, what is the difference between the fjords located in the south and those up north, taking into consideration the northward transformation of oceanic waters? Many important aspects of the study are related to the content of Promińska et al. (unpublished data) devoted to interannual changes in temperature, salinity and water masses in Hornsund. In this paper we extend the analysis to discuss the differences between Kongsfjorden and Hornsund not only in water temperature, salinity and water masses distribution but also water column stability, freshwater content and transport of AW toward the fjords. Moreover, we test the hypothesis that the ongoing warming is accompanied by an increase in water temperature and salinity in the studied fjords.

2. Fjords description

Two glaciated fjords, Hornsund and Kongsfjorden, are the southernmost and one of the northernmost fjords on the west coast of Spitsbergen, the largest island of Svalbard Archipelago (Fig. 1). Hornsund is about 35 km long with a width ranging between 2 and 12 km. The hypsometric curve and volume calculated for both fjords are presented in Fig. 2a and b. Bathymetry is based on electronic charts developed by Primar and distributed by NavSim Polska sp. z o.o. The data from NavSim are interpolated on a regular grid matrix of 1000 × 1000 elements. A grid cell resolution is 32.1 m and 22.6 m in latitudinal and longitudinal direction for Hornsund and 26.6 m and 23 m for Kongsfjorden. The surface area and corresponding volume is 284.48 km^2 and 22.63 km^3 for Hornsund (Fig. 2a) and 267.81 km^2 and 27.98 km^3 for Kongsfjorden (Fig. 2b).

There is a significant difference in bathymetry between the studied fjords. Fig. 3 shows cross-fjord (a) and along-fjord (b) sections bathymetry in Hornsund (solid line) and Kongsfjorden (dash-dotted line), which location is shown in Fig. 1. Both fjords have no pronounced entrance sill, which facilitates the inflow of waters from the outside. However, the entrance to Hornsund is rather flat and shallow with maximum depth slightly exceeding 150 m (Fig. 3a, solid line). In Kongsfjorden the maximum depth along the cross section is almost 400 m on the southern side (Fig. 3a, dash-dotted line). The along-fjord sections reveal clear division into Main part (green) and Inner part (blue) in both fjords. Here the area of Brepollen (the Inner part of Hornsund) is larger and locally deeper than the Inner part of Kongsfjorden. Additional geometrical aspect, which makes the fjords different, is that Hornsund has more complex coastline including several bays (e.g. Burgerbukta, Samarinvågen), which cannot be found in Kongsfjorden.

The ubiquitous tidewater glaciers in Svalbard shape the landscape of the fjords and are the main source of freshwater (Weslawski et al., 1995 and references herein). The annual freshwater discharge into Hornsund has been estimated to 1.8 km^3 (Weslawski et al., 1995 and references herein), while in Kongsfjorden it is 1.4 km^3 (Svendsen et al., 2002). Calculations based on momentary hydrographic measurements gave also higher values of 0.7 km^3 (for July 1987) for Hornsund

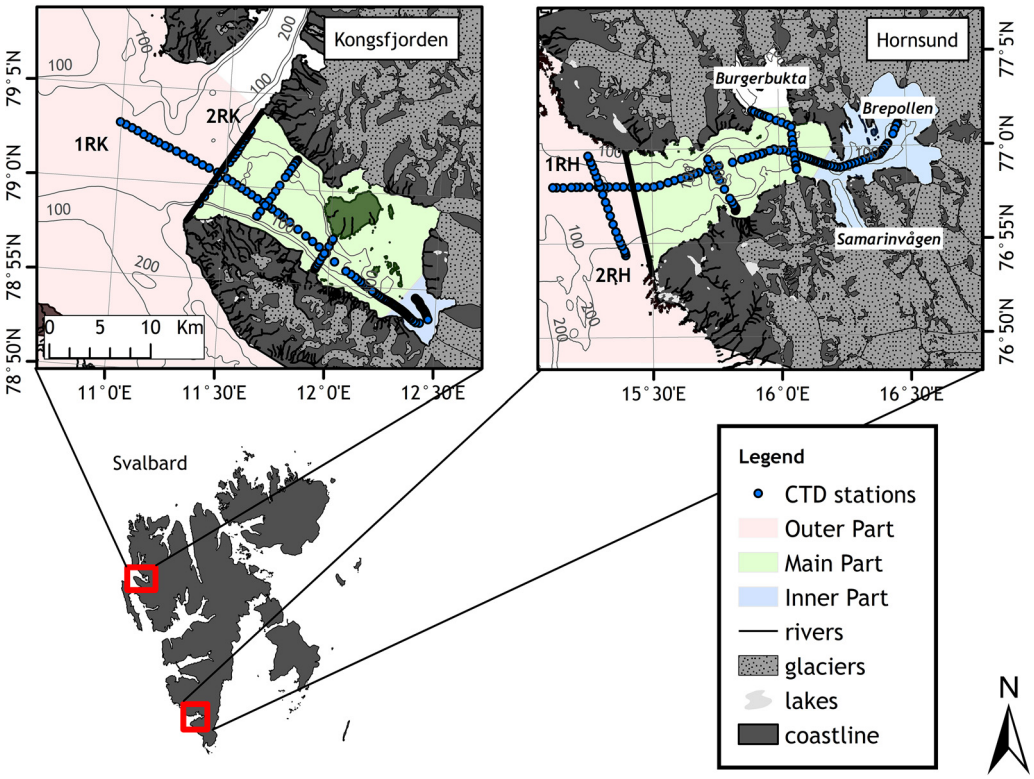

Figure 1 Study area. Location of CTD stations in Kongsfjorden and Hornsund. Black lines indicate geographical boundaries of the fjords. Different colors represent different parts of the fjords: Outer part (light coral), Main part (light green), Inner part (light blue). (For interpretation of the references to color in this figure legend, the reader is referred to the web version of the article.)

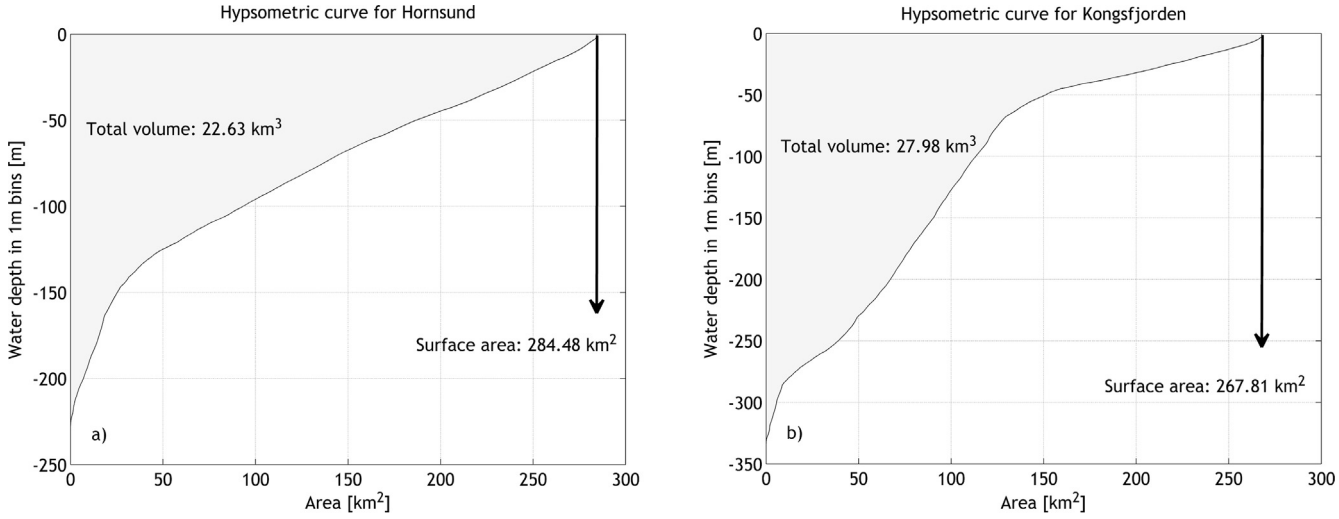

Figure 2 Hypsometric curve for Hornsund (a) and Kongsfjorden (b) based on area calculations for every 1 m depth interval. Bathymetric data based on electronic charts developed by Primar and distributed by NavSim Polska sp. z o.o.

compared to 0.3 km^3 (for July 1988) for Kongsfjorden (Węsławski et al., 1991).

3. Material and methods

3.1. Hydrographic measurements

The study is based on high resolution CTD measurements along monitoring sections, which locations are shown in Fig. 1. Measurements along longitudinal sections are carried out almost every year and only the number of cross sections differs in some years. The towed CTD system were used, which means that the measurements are taken continuously from the surface to the bottom, while the ship is moving with more or less constant speed of 3—3.5 knots. Data on water temperature and salinity were collected during summer cruises onboard r/v *Oceania*, under the long-term monitoring program AREX between 2001 and 2015. The average time

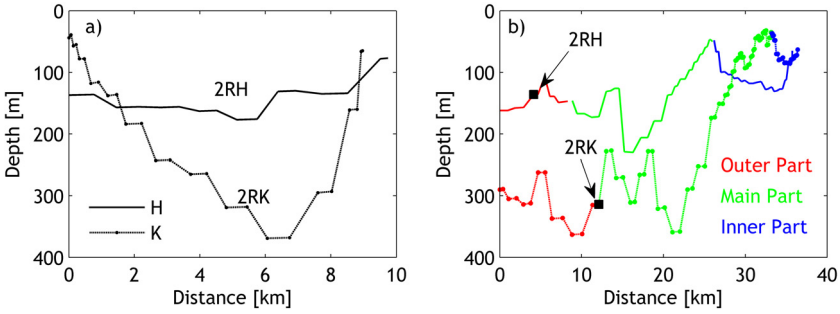

Figure 3 Bathymetry of cross sections 2RH and 2RK (a) and along-fjord sections 1RH and 1RK (b) in Hornsund (solid line) and Kongsfjorden (dash-dotted line). Different colors represent different parts of the fjords: Outer part (red), Main part (green), Inner part (blue). Black squares indicate intersection with section 2RH and 2RK. (For interpretation of the references to color in this figure legend, the reader is referred to the web version of the article.)

difference between the measurements in both fjords was about 7 days. All the data were filtered and vertically averaged every 1db. Further the data were interpolated into a regular grid of 1 m in vertical and 0.5 km bins in horizontal using kriging method.

Mean values of potential temperature (hereafter temperature) and practical salinity (hereafter salinity) were calculated using weighted average, where the weight was a cube with a dimensions 0.5 km × 1 m × 1 m (defined as a unit volume). Each value in each profile was multiplied by the unit volume and then the sum of it was divided by the volume of the section (the volume of a 1 m wide section along the Main part of section 1RK and 1RH). Mean values of temperature and salinity presented in the paper are calculated for the Main part (light green in Fig. 1) of the longitudinal sections, defined by the black lines (boundaries of the fjords in Fig. 1) and longitude 16.14 E for Hornsund and 12.35 E for Kongsfjorden (location of a shallow sill). Detailed device specification and characteristics of hydrographic measurements can be found in Table S1 of supplementary material.

3.2. Freshwater calculation

Freshwater calculations were based on the methodology described in Beszczynska-Möller et al. (1997 and references herein) as well as recent study of freshwater in Hornsund (Dølven, 2015). Freshwater content (*FWC*) was calculated by the integration of measured salinity relative to a reference salinity over water column:

$$FWC = \int_{z}^{0} \frac{S_{ref} - S}{S_{ref}} dz,$$

where *FWC* is the height of the freshwater portion of the water column [m], S_{ref} is the reference salinity, S is the measured salinity, z is the depth [m].

For the salinity data with vertical resolution of 1 m the expression above is discretized to:

$$FWC = \sum_{z=z_0}^{n} \frac{S_{ref} - S}{S_{ref}}.$$

Each value of measured salinity in each CTD profile was subtracted from the reference salinity and then divided by reference value and the sum of it gave the *FWC* – the height of the freshwater portion in each CTD profile. To avoid negative values of *FWC*, all the data where measured salinity is higher than the reference salinity were excluded from the calculation. The total volume of freshwater (FWC_{total}) was calculated by multiplying the average of all calculated *FWC* values in the fjord by its surface area. The percentage of the total volume of a given fjord is presented as well. *FWC* calculations in this study were based on the data covering the Main parts of the fjords (light green in Fig. 1).

Reference salinity of 34.2 was taken from Dølven (2015) based on measurements taken in Hornsund in April 2012 and May 2011 and 2013 and the assumption that all the freshwater was flushed out before winter (Dølven, 2015).

3.3. Stability of water column

Stability of water column is represented by the square of the Brunt–Väisälä frequency (a measure of stratification):

$$N^2 = -\frac{g}{\rho}\frac{d\rho}{dz},$$

where g is the acceleration of gravity, ρ is the potential density.

For stability calculations data are averaged every 5 db to eliminate noise.

3.4. Transports

For sections located at the mouth of the fjords (sections 2RK and 2RH in Fig. 1) transport of volume and heat was calculated. Geostrophic currents were calculated with use of dynamic height method, with reference to the no-motion layer (*NML*). Here, the bottom was adopted as the *NML*. Transports of properties were calculated using gridded velocity and property fields.

4. Results

4.1. Water mass distribution

The general overview of water masses is contained in supplementary material. Ranges of temperature and salinity are defined in Table S2. Fig. 4 shows distribution of water masses along the longitudinal sections in Hornsund and Kongsfjorden for summers 2001–2015 according to ranges of temperature

and salinity defined in Table S2 of the supplementary material. The black lines separate the Outer part, Main part and the Inner part of the fjords (starting from the left side of each figure). The Surface Water (SW, light orange) was found along Kongsfjorden in all years. In most years a layer of SW was very thin (~10 m) but in some years it extended to ~50 m (2003, 2004, 2010, 2011, 2015). Below SW there is an Intermediate Water (IW, green). Only in 2004 it was covered by the Local Water (LW, blue), which typically was observed in deeper parts. The thickness of IW was typically ~50 m but in 2002,

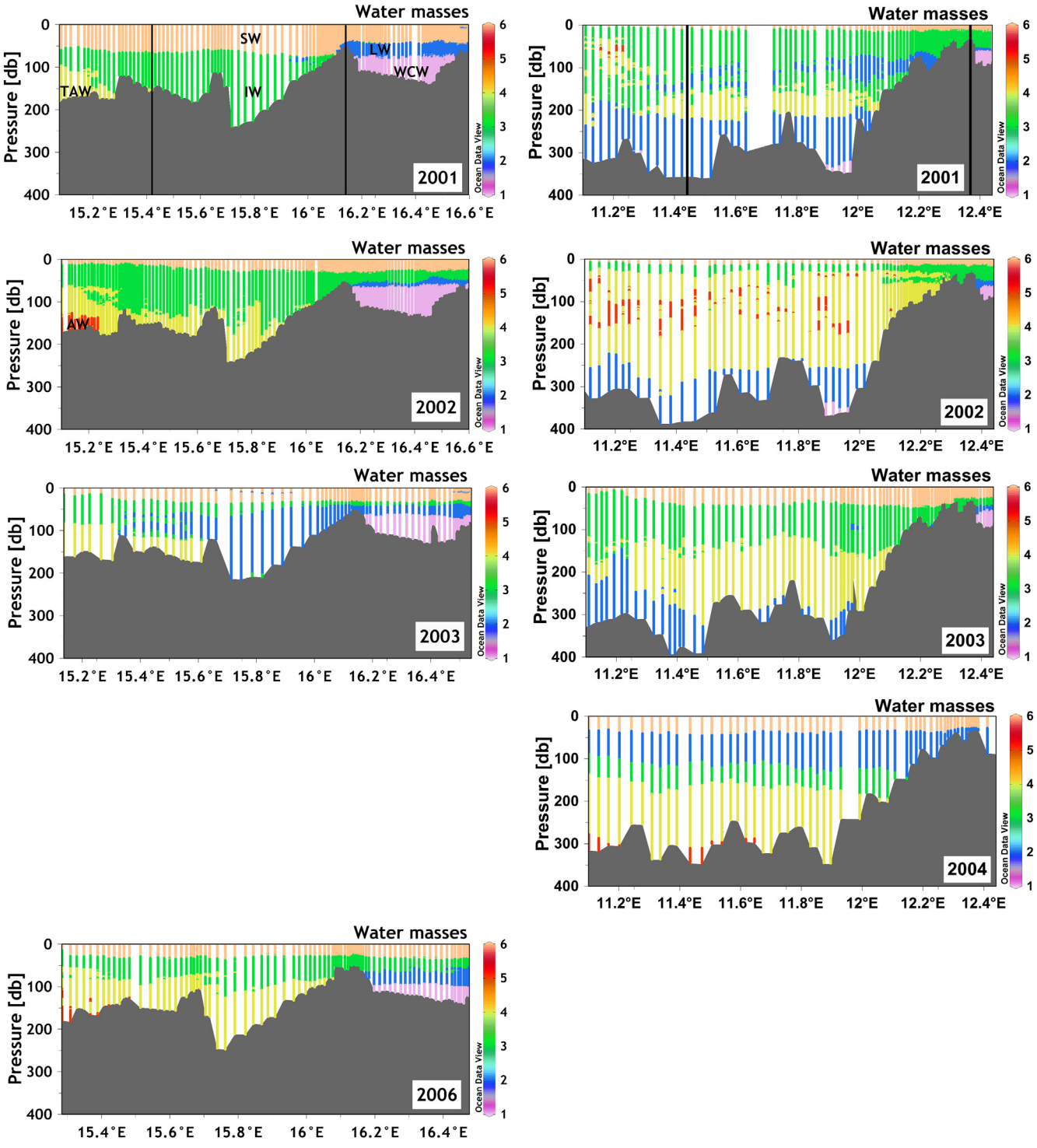

Figure 4 Distribution of particular water masses along fjord axis in Hornsund Fjord (left column) and Kongsfjorden (right column) for years 2001–2015. The left side of figures is the seaward site and on the right side are the innermost fjords parts. The following numbers are assigned to particular water masses (see Table S2 in supplementary material): 1 – Winter Cooled Water (WCW, pink); 2 – Local Water (LW, blue); 3 – Intermediate Water (IW, green); 4 – Transformed Atlantic Water (TAW, yellow); 5 – Atlantic Water (AW, red); 6 – Surface Water (SW, orange). (For interpretation of the references to color in this figure legend, the reader is referred to the web version of the article.)

2010 and especially in 2014 there was almost no IW at all. Transformed Atlantic Water (TAW, yellow) is a typical water of Atlantic origin found in Kongsfjorden. It usually spreads below IW and extends to the bottom. The exceptional years are 2001, 2002, 2003 when TAW was observed at the intermediate depths with LW below. In 2004 and 2010 LW was much lighter than TAW and filled the upper 50–100 m below the SW. Pure Atlantic Water (AW, red) defined by $\theta > 3^{\circ}$C and $S > 34.9$ was found in the Main Basin at the bottom (2004) or as patches at intermediate depths in 2002, 2007, 2013 and 2015. In 2014 AW filled the fjord from 20 m up to 250 m. It also reached the Inner part for the first time in study period.

The extent of Atlantic origin waters differs significantly in both fjords. In Hornsund AW typically occurred at the entrance to the fjord and TAW was the only water of Atlantic origin that reached the Main Basin. In Kongsfjorden TAW filled

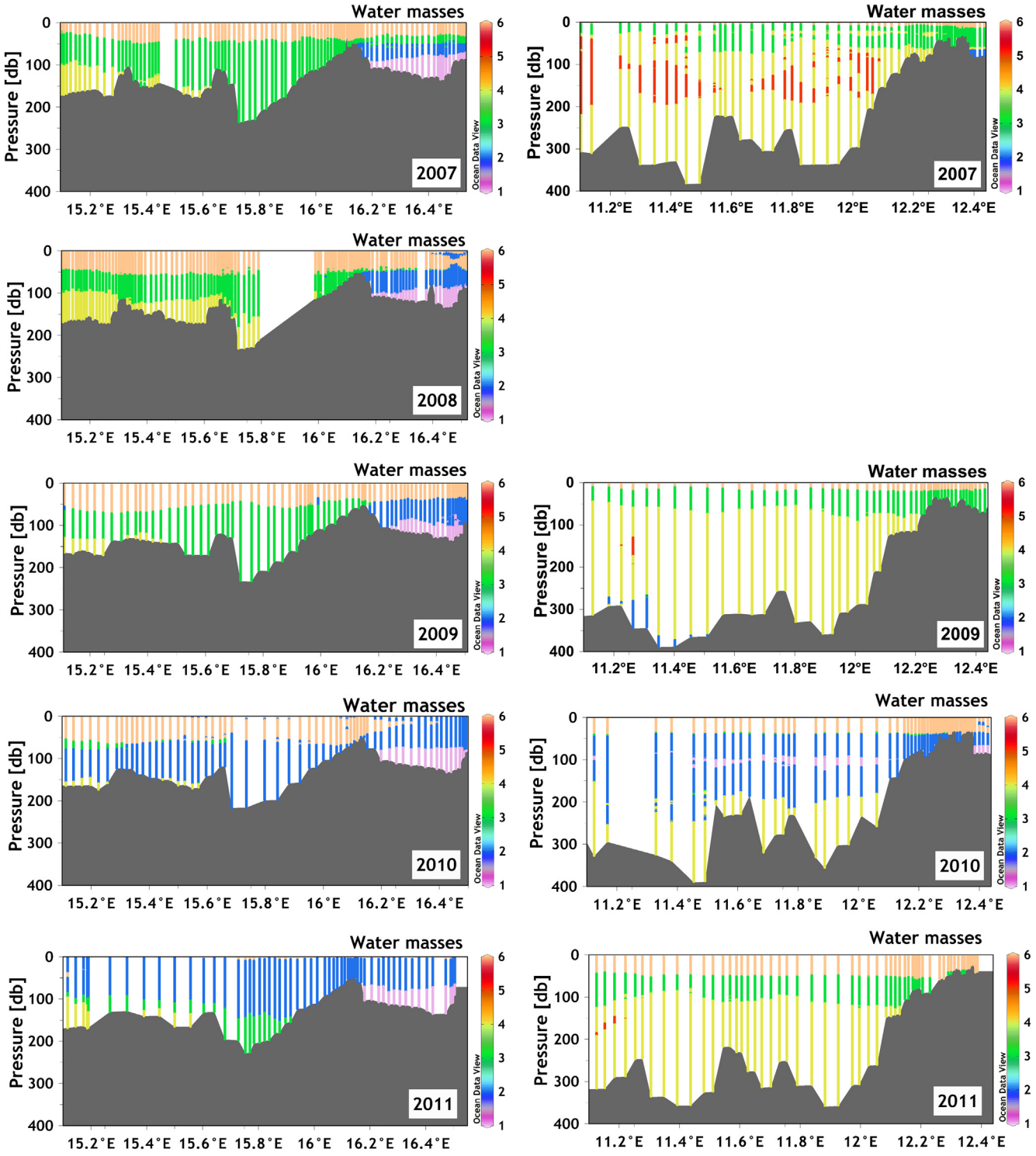

Figure 4 (*Continued*)

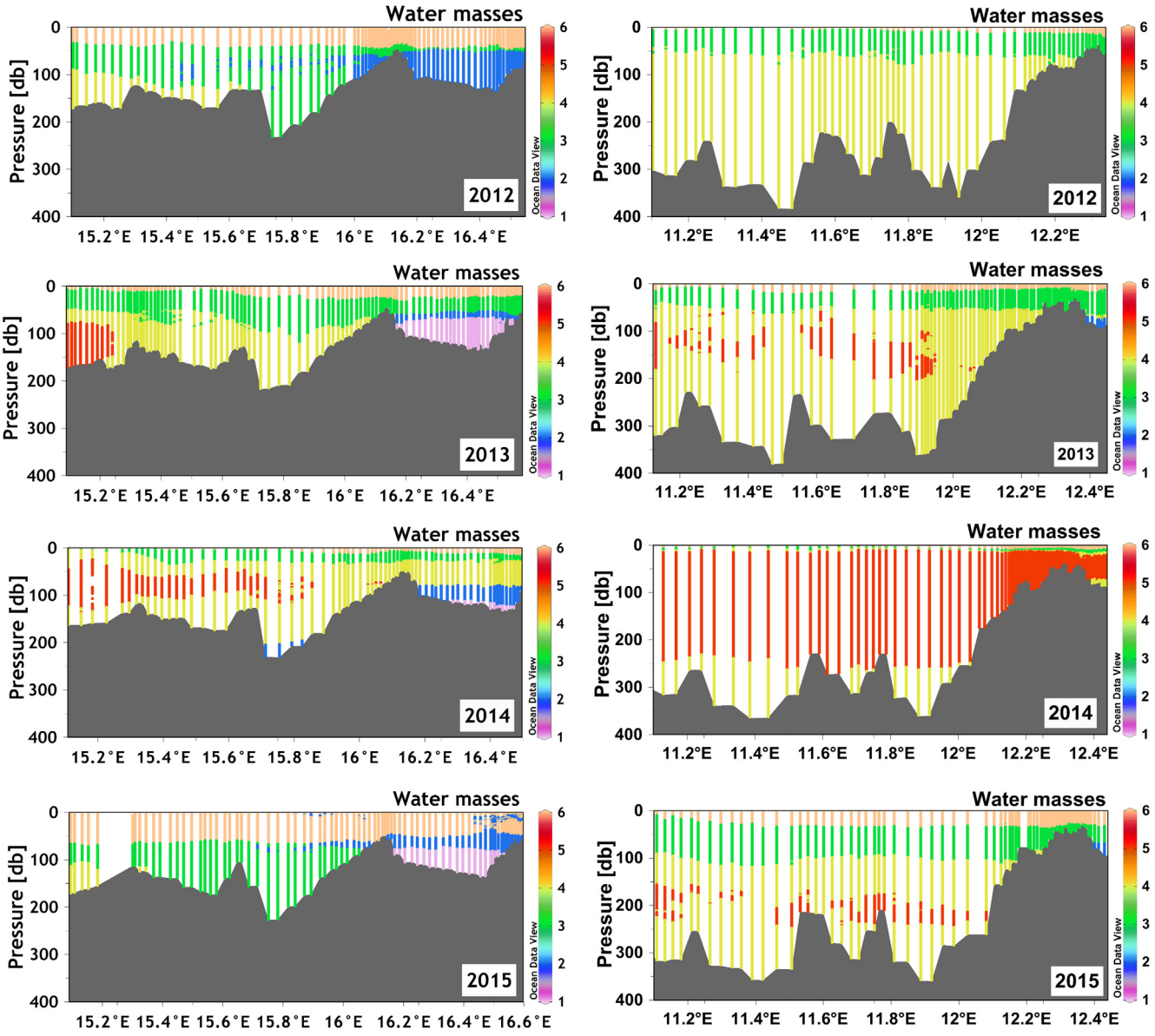

Figure 4 (*Continued*).

the large part of the fjord almost in all years and AW was observed also in the fjord's Main Basin. However, summer 2014 was extreme for both fjords. AW covered the largest extent in the fjords and TAW reached their Inner parts.

4.2. Interannual variability in hydrography

Table 1 shows mean values of temperature and salinity calculated for along-fjord sections 1RH and 1RK, only for the Main part of the sections. Differences in both variables between Hornsund and Kongsfjorden are shown as well. Graphical representation can be found in Fig. 5. Mean water temperature in Hornsund ranges between 0.45°C (2011) and 3.63°C (2014) and is on average 0.92°C lower than in Kongsfjorden, where it ranges between 1.06°C (2010) and 4.54°C (2014). Mean water salinity in Hornsund ranges between 33.33 (2011) and 34.67 (2014) and is on average 0.46 lower than in Kongsfjorden, where it reaches values between 34.00 (2004) and 35.00 (2014). Fig. 5 shows that changes in temperature and salinity correspond very well in Hornsund ($r = 0.88$). In Kongsfjorden the situation is more complex, resulting in lower correlation of temperature and salinity ($r = 0.67$).

The long-term (2001—2015) summer mean temperature and salinity is equal to 2.17°C and 34.06 for Hornsund and 2.90°C and 34.46 for Kongsfjorden. Temperature and salinity anomalies clearly show periods of warming and salinification, as well as periods of cooling and freshening of waters in both fjords (Fig. 6). The strongest negative anomalies were observed in 2010 (in Kongsfjorden) and 2011 (in Hornsund). Generally, after 2011, positive temperature and salinity anomalies were observed with the strongest in 2014 for both fjords, when water temperature was ca. 1.5°C higher than the long-term mean values.

Changes in water temperature and salinity can be seen in the entire water column, which is evident in Figs. 7 and 8. Fig. 7a and b shows longitudinal changes in water

Table 1 Mean water temperature, salinity, temperature and salinity difference for Hornsund and Kongsfjorden for summers 2001–2015.

Year	Mean T		Mean S		ΔT	ΔS
	Hornsund	Kongsfjorden	Hornsund	Kongsfjorden		
2001	1.92	1.80	33.79	34.43	0.13	0.64
2002	2.78	3.20	34.29	34.65	0.42	0.35
2003	1.46	2.86	34.13	34.23	1.40	0.10
2004	–	1.63	–	34.00	–	–
2005	–	–	–	–	–	–
2006	2.85	–	34.25	–	–	–
2007	2.71	2.89	34.14	34.71	0.18	0.57
2008	2.09	–	34.02	–	–	–
2009	1.80	3.11	33.87	34.56	1.32	0.70
2010	1.07	1.06	33.90	34.11	0.01	0.21
2011	0.45	3.30	33.33	34.21	2.85	0.87
2012	1.98	3.09	34.10	34.63	1.11	0.53
2013	3.20	3.31	34.34	34.62	0.12	0.28
2014	3.63	4.54	34.67	35.00	0.91	0.33
2015	2.27	3.96	33.90	34.35	1.69	0.45
Mean	2.17	2.90	34.06	34.46	0.92	0.46

temperature and salinity at the depth of 25 m in Hornsund between 2001 and 2015. Black lines divide the section into Outer part (west of the black line in Fig. 1), Main part and Brepollen, the innermost part of Hornsund. The years 2001–2009 are characterized by a small variability in both temperature and salinity. Temperature ranges between 2.5°C in colder years (2001, 2003, 2008 and 2009) and 3.5–4°C in warm years (2002, 2006 and 2007). Salinity ranges between 33.1 and 33.5 (2001, 2008, 2009 and 2010) and 33.9 and 34.1 (years 2002–2003 and 2006–2007). Typically salinity at 25 m did not exceed 34, except for 2002 in the Outer part of Hornsund. Years 2010–2015 are characterized by much larger variability in both temperature and salinity. Minimum temperature (~0°C) was noted in the coldest year (2011) in all parts of Hornsund with a corresponding minimum salinity of 31.9. The strongest warming and even the most pronounced increase in salinity was observed in 2014 in all parts of Hornsund. That year the temperature exceeded 4.5°C, also in Brepollen, and salinity reached values above 34.5 in the Main part and Brepollen and 34.7 in the Outer part.

Fig. 7c and d presents longitudinal changes in water temperature and salinity at 25 m depth in Kongsfjorden between 2001 and 2015. The black line divides the section into Outer part (west of the black line in Fig. 1) and Main part.

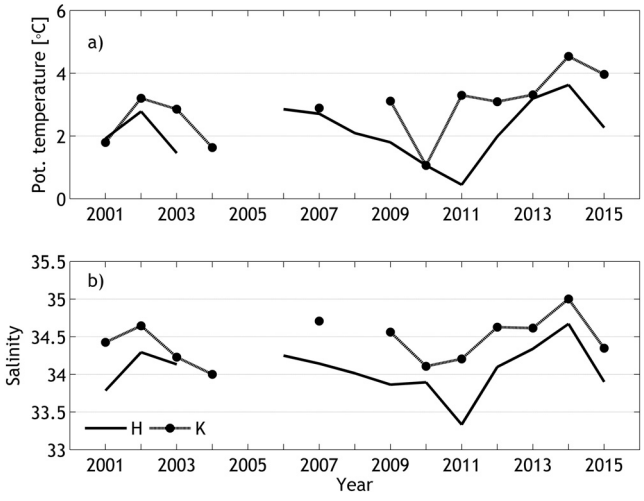

Figure 5 Time series of water temperature and salinity for Hornsund (solid line) and Kongsfjorden (dashed-dotted) in summers 2001–2015.

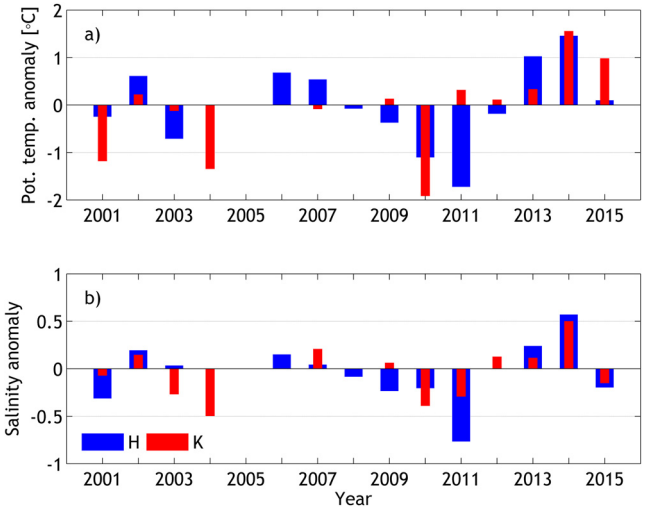

Figure 6 Time series of temperature (a) and salinity (b) anomalies in Hornsund (blue bars) and Kongsfjorden (red bars). (For interpretation of the references to color in this figure legend, the reader is referred to the web version of the article.)

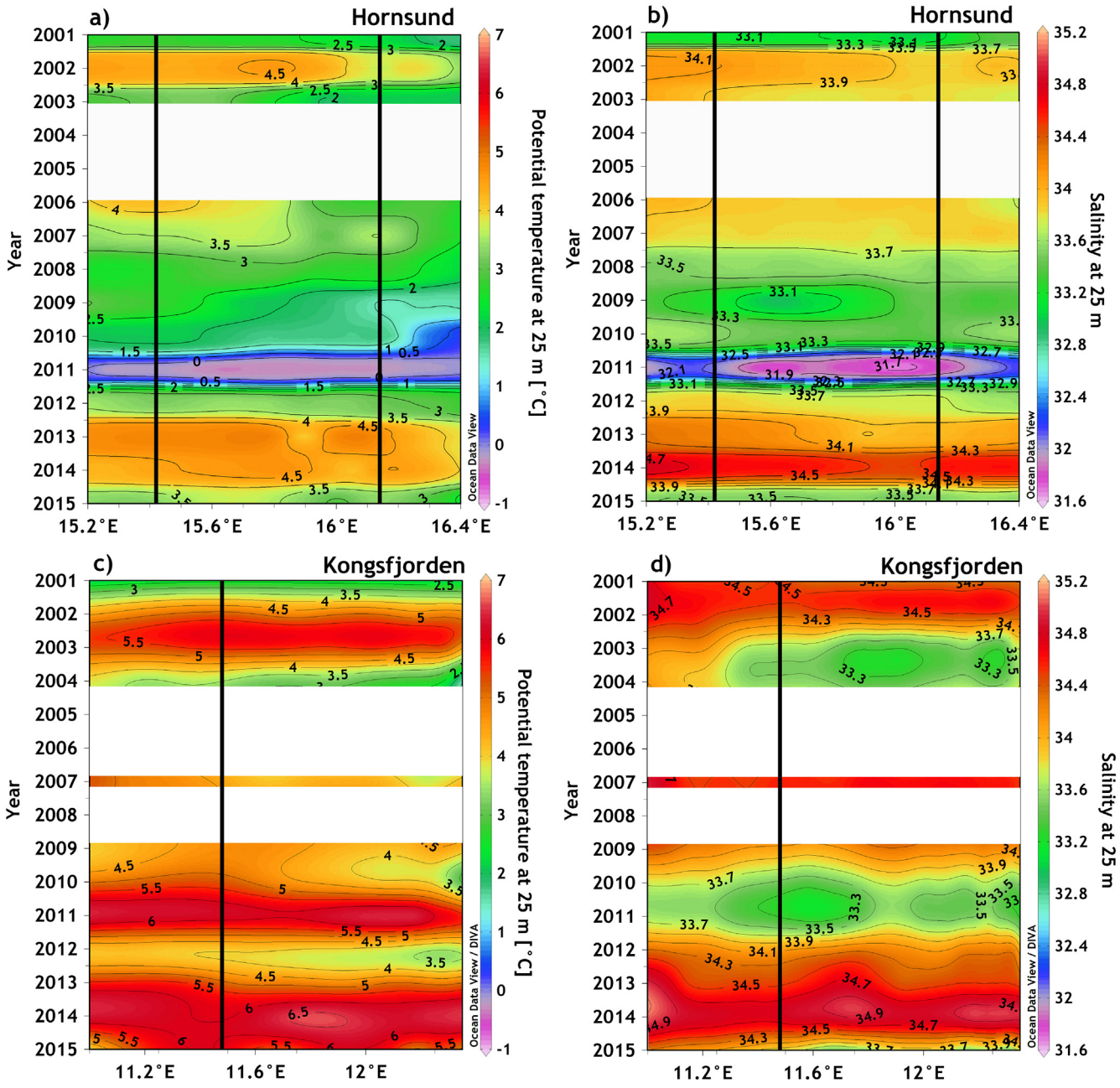

Figure 7 Longitudinal water temperature and salinity distribution at 25 m in Hornsund (a and b) and Kongsfjorden (c and d). Black lines indicate boundaries between Outer part, Main basin and Inner part of the fjords.

There are not sufficient data to show the Inner part of the fjord. Temperature ranges from 3.5°C to 4.5°C in years 2001, 2007, 2009 and 2012 to more than 5°C in the years 2002, 2010—2011 and 2013—2015. Salinity ranges from 33.1 to 33.7 in the years 2003—2004, 2010—2011. In the other years studied, salinity typically exceeded 34 with a significant increase between 2002 and 2003, and the highest value was recorded in 2014 (above 34.9).

Fig. 8a and b presents longitudinal changes in water temperature and salinity at 100 m depth in Hornsund. There is a clear difference between Brepollen and the remaining part of the section. One can clearly see significantly low values of water temperature (∼−1.5°C) in Brepollen between 2001 and 2003, while after that period the recorded values were remarkably higher, with the highest temperatures observed in 2012 and 2014 (below −0.5°C). In the period 2001—2009, the strongest warm signal was observed in the Outer part of Hornsund in the years 2001—2003, 2006—2008 and 2012—2015. In 2006 and 2007 that warm signal was observed partly in the Main Basin and in 2014 it was observed all over the Main part almost throughout its entire depth. 2014 was also a year with the highest salinity on record in the study period in all parts of the section. The lowest salinity (less than 34.4) was observed in Brepollen in 2012. Relatively low values were also recorded in Brepollen in 2009 and almost in the entire section in 2010.

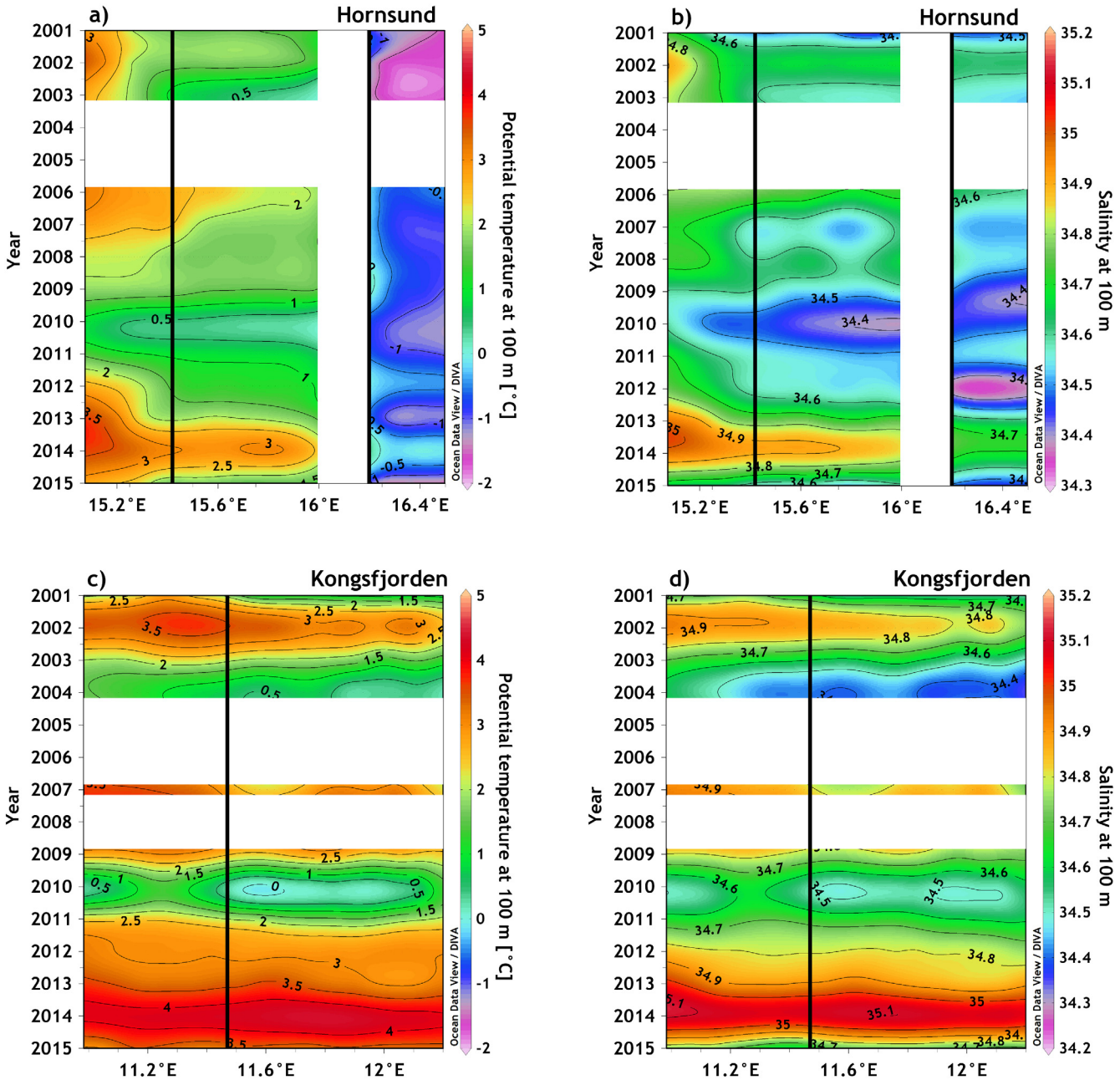

Figure 8 Longitudinal water temperature and salinity distribution at 100 m in Hornsund (a and b) and Kongsfjorden (c and d). Black lines indicate boundaries between Outer part, Main basin and Inner part of the fjords.

In Kongsfjorden, strong warming at the depth of 100 m was observed in the years 2002, 2007 and 2012–2015, when temperature exceeded 3°C (Fig. 8c). The corresponding high salinity was observed in the years 2002 and 2013–2014 (Fig. 8d). In the other years of the study (2007, 2012 and 2015), despite the warming shown in Fig. 8c, salinity was relatively low (Fig. 8d). 2014 is the year when the highest temperature (above 4°C) and salinity (above 35) was recorded in the study period in Kongsfjorden. A significant cooling and freshening was observed in 2003–2004 and 2010.

To look closer to the differences between the fjords, we chose years 2010, 2011 and 2014 in a case study of different hydrographic conditions. In summer 2010 both fjords experienced cooling and freshening (Fig. 9). In Hornsund, below the 70 m fresh surface layer, cold water filled the fjord almost down to the bottom in the Outer and Main part. In Brepollen the entire water column was cold, its temperature centered around 0°C in the upper 50 m and it was colder below the sill. Water mass distribution shows LW (blue) in large part of the fjord. In the Outer part, at the bottom, there are some patches of TAW (yellow). In Kongsfjorden, very cold water temperature was observed from 50 m down to 150–200 m and water mass distribution shows LW (with patches of WCW characteristics, pink) in this area. Below 200 m water had properties typical for TAW ($\theta > 1$°C, S > 34.7).

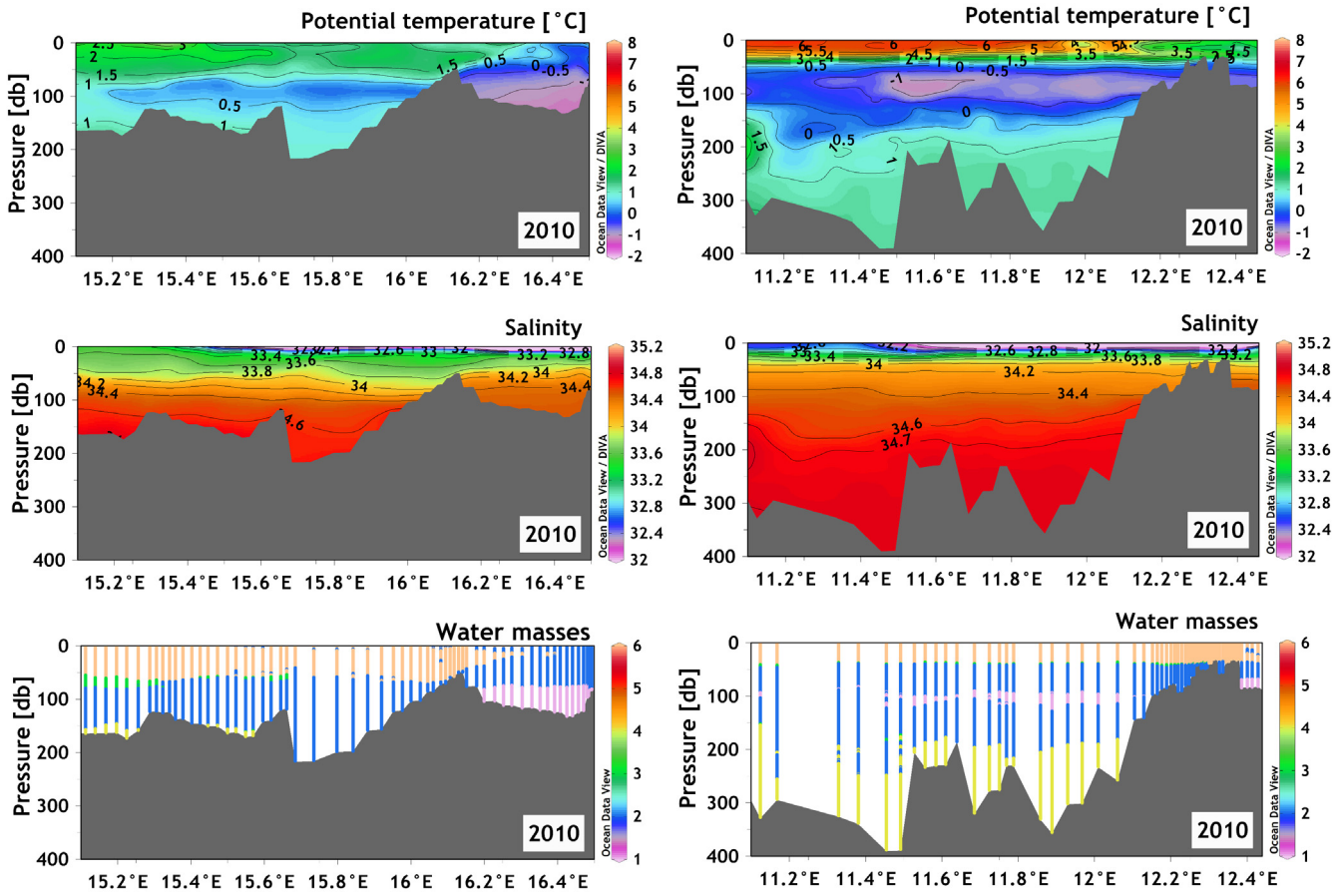

Figure 9 Longitudinal distribution of temperature, salinity and water masses in summer 2010 in Hornsund (left column) and Kongsfjorden (right column). The left side of each figure is the seaward site and on the right side are the innermost fjords parts. The following numbers are assigned to particular water masses (see Table S2 in supplementary material): 1 — Winter Cooled Water (WCW, pink); 2 — Local Water (LW, blue); 3 — Intermediate Water (IW, green); 4 — Transformed Atlantic Water (TAW, yellow); 5 — Atlantic Water (AW, red); 6 — Surface Water (SW, orange). (For interpretation of the references to color in this figure legend, the reader is referred to the web version of the article.)

In 2011 hydrographic conditions differed between the fjords (Fig. 10). In Hornsund the upper 75 m was filled with cold and very fresh water all over the fjord, resulting in the lack of layer that could be classified as the SW (light orange). In the Outer and Main part patches of TAW (yellow) and IW (green) could be observed. In Kongsfjorden there was a completely different distribution. There was no cold and fresh signal at all, unlike the situation observed in Hornsund. The upper 50 m was very warm and relatively fresh, representing SW. Below that level, a ~50 m thick layer of IW could be observed, and from 100 m down to the bottom the fjord was filled with warm and saline TAW. In the Outer part patches of pure AW (red) occurred.

In summer 2014 the highest values of temperature and salinity in the fjords during the study period (Fig. 11) were recorded. For the first time the isohaline of 34.9 (a threshold salinity value for the pure AW) occurred in the Main part of Hornsund, resulting in the greatest extent of AW in the fjord. In Brepollen TAW was observed for the first time. The thickness of AW in Hornsund ranged between ~100 m in the Outer part and ~50 m in the Main part. In Kongsfjorden that warming was even greater. The fjord was filled in large extent with AW (25—250 m), reaching far into the fjord. Deeper parts of the fjord were filled with TAW. In both fjords there was hardly any SW. LW was observed only in Hornsund, in the deepest area of the Main part and in Brepollen. WCW (pink) reached the lowest thickness in Hornsund compared to 2010 and 2011, and it disappeared completely in the Inner part of Kongsfjorden.

4.3. Stability of water column

Different hydrographic conditions described above also indicate a different stability of water column. Fig. 12 shows vertical profiles of temperature, salinity and corresponding stratification (Brunt — Väisälä frequency squared). For all the presented years Hornsund (blue) is characterized by higher values of stratification than Kongsfjorden (red). In 2010 the range of temperature (Fig. 12a) and salinity (Fig. 12b) was similar in both fjords. Only upper 50 m was significantly warmer in Kongsfjorden. The highest values of water column stability were observed at 5 m in Hornsund and decreased down to 150 m where the value centered around 0 (Fig. 12c). In Kongsfjorden the maximum of water column stability was observed at 23 m and below 150 m it was close to 0.

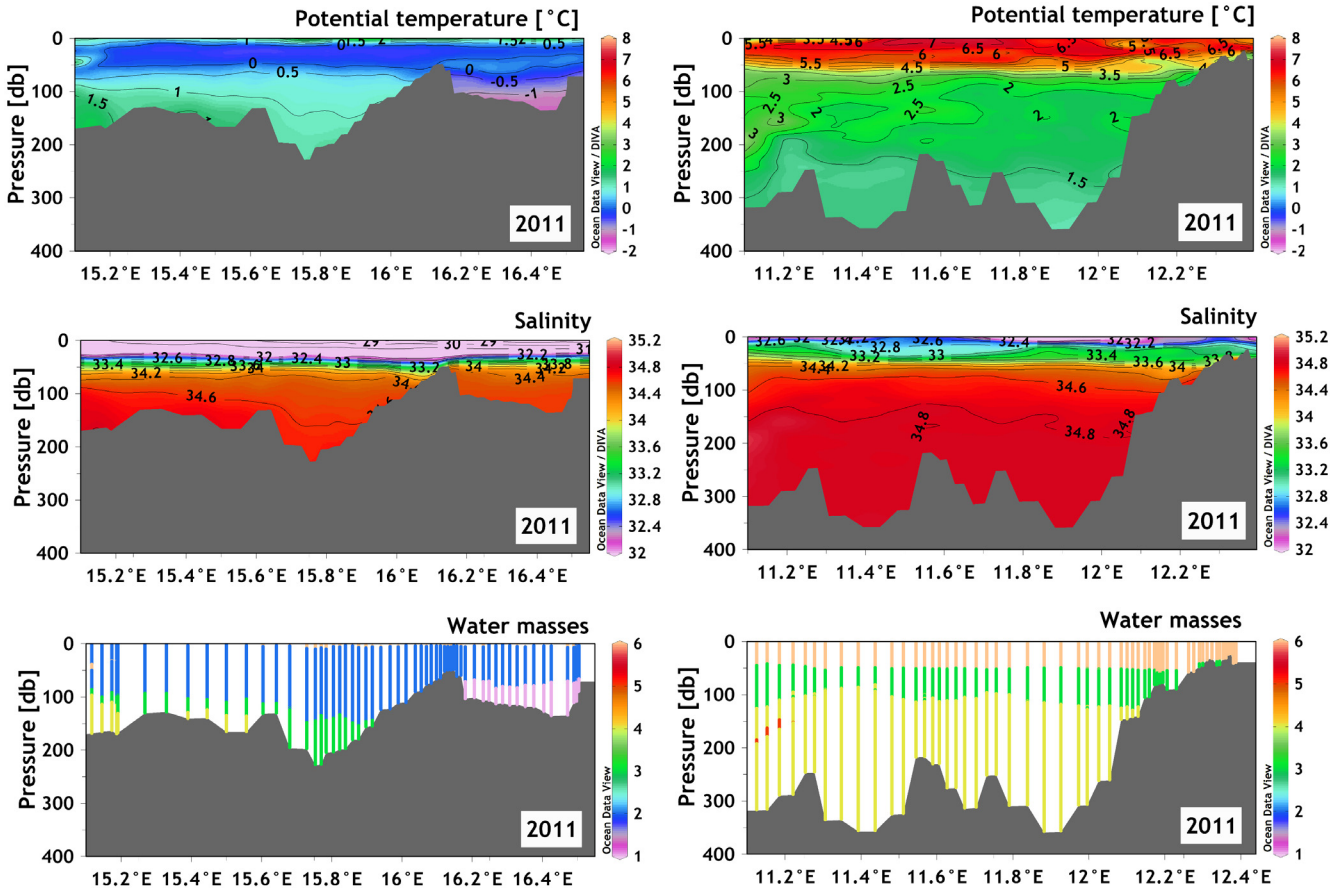

Figure 10 Longitudinal distribution of temperature, salinity and water masses in summer 2011 in Hornsund (left column) and Kongsfjorden (right column). The left side of each figure is the seaward site and on the right side are the innermost fjords parts. The following numbers are assigned to particular water masses (see Table S2 in supplementary material): 1 — Winter Cooled Water (WCW, pink); 2 — Local Water (LW, blue); 3 — Intermediate Water (IW, green); 4 — Transformed Atlantic Water (TAW, yellow); 5 — Atlantic Water (AW, red); 6 — Surface Water (SW, orange). (For interpretation of the references to color in this figure legend, the reader is referred to the web version of the article.)

Very different conditions were observed in 2011 (Fig. 12d—f). A great difference was noted in the upper 50 m, where the fjords are in the opposite phase. In Hornsund (blue) temperature decreased from ~4°C in the surface layer to ~0°C at 15 m with a relatively low salinity. In Kongsfjorden (red) very warm water occurred, of temperature reaching almost 7°C and salinity was remarkably higher than in Hornsund. However, there was a similar pattern in water column stability. In the upper 100 m of both fjords, high values occurred with two-fold maxima, at 5 m and 40 m in both fjords.

In 2014 very warm and saline water occurred in both fjords (Fig. 12g—i), yet in the case of Hornsund it was less saline and shifted toward colder waters (a shift of about 2°C). Water column stability was highest at 4—5 m in both fjords. Moreover, in Kongsfjorden high values could be observed at 70 m and 260 m.

4.4. Freshwater content

Calculations of the total *FWC* in Hornsund provide values ranging from 0.06 km^3 to 0.81 km^3 (Fig. 13a, blue bars), which represents 0.27—3.58% of the fjord volume (Fig. 13b, blue bars). The minimum of total *FWC* occurred in 2014. Summer 2011 was the most outstanding year with the highest total *FWC*. The years 2001, 2009 and 2015 are characterized by significantly lower values of total *FWC* (less than 2% of Hornsund volume) relative to summer 2011. However, compared to the other years, the summers of 2001, 2009 and 2015 can be considered as years with high total *FWC*.

Total *FWC* in Kongsfjorden ranges between 0.03 km^3 and 0.42 km^3 (Fig. 13a, red bars), which represents 0.12—1.5% of the fjord's volume (Fig. 13b, red bars). Similar to Hornsund, summer of 2014 was the year with the lowest total *FWC*. Similar values are showed for the years 2004 and 2011.

4.5. Transports

To compare both fjords, the baroclinic currents were calculated for the years 2001—2003 and 2010—2015, when sections across the Hornsund (2RH) and Kongsfjorden (2RK) mouths were performed. Mean baroclinic inflow to Hornsund equals approximately 20 mSv (10^3 m^3 s^{-1}) with 238 MW of heat delivered to the fjord (Table 2). On average 1.4 mSv of AW delivers 24.7 MW of heat to Hornsund. Mean baroclinic inflow to Kongsfjorden is about 40 mSv (10^3 m^3 s^{-1}) with 525 MW of

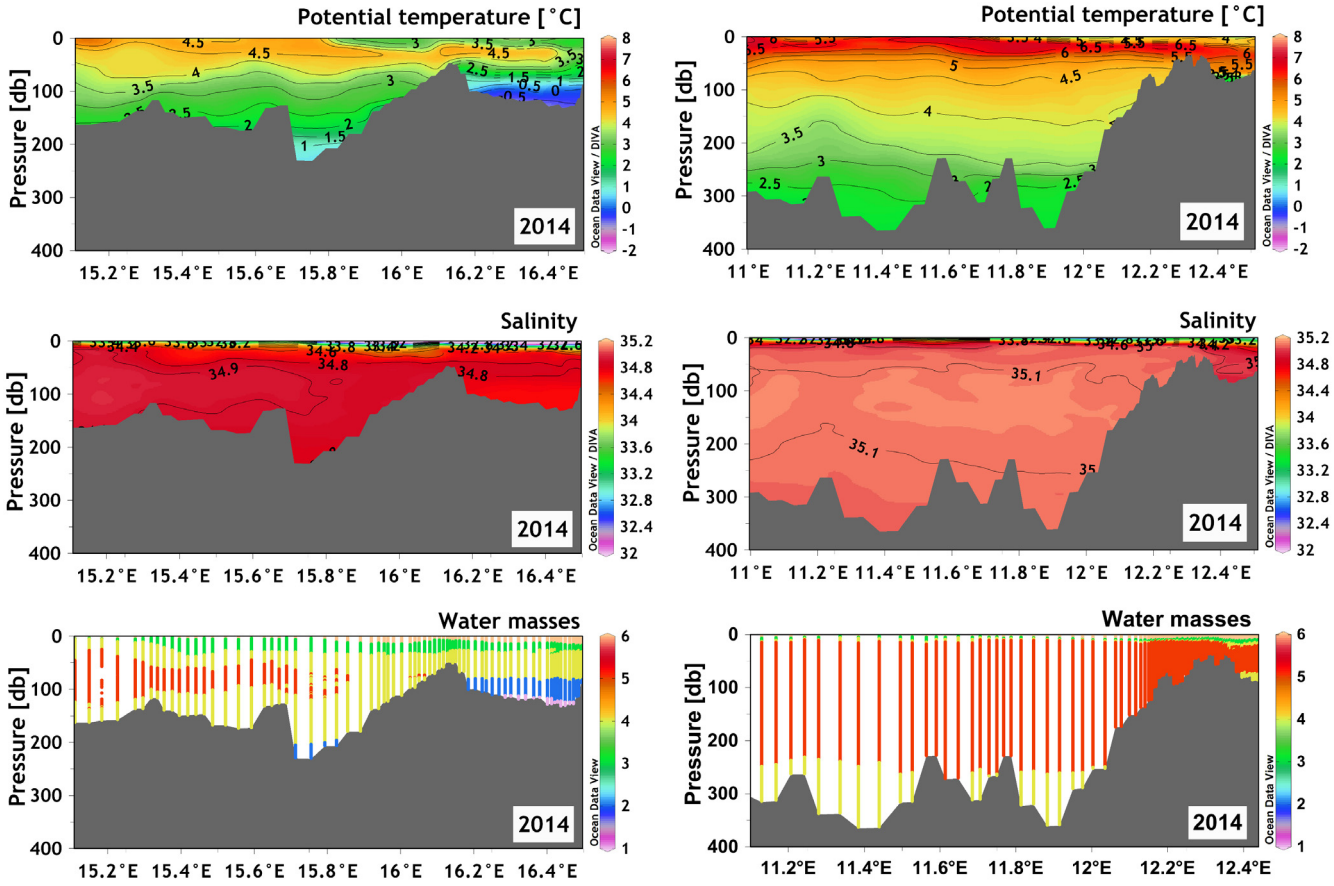

Figure 11 Longitudinal distribution of temperature, salinity and water masses in summer 2014 in Hornsund (left column) and Kongsfjorden (right column). The left side of each figure is the seaward site and on the right side are the innermost fjords parts. The following numbers are assigned to particular water masses (see Table S2 in supplementary material): 1 — Winter Cooled Water (WCW, pink); 2 — Local Water (LW, blue); 3 — Intermediate Water (IW, green); 4 — Transformed Atlantic Water (TAW, yellow); 5 — Atlantic Water (AW, red); 6 — Surface Water (SW, orange). (For interpretation of the references to color in this figure legend, the reader is referred to the web version of the article.)

Table 2 Mean characteristics of water temperature and salinity, transport of volume and heat through the cross sections in Hornsund (2RH) and Kongsfjorden (2RK).

	Vol [mSv]	Vol+ [mSv]	Vol− [mSv]	Temp [°C]	Sal	Heat [MW]	Heat+ [MW]	Heat− [MW]	AW_Vol [mSv]	AW heat [MW]
2RH mean	−2.7	20.9	−23.6	2.55	34.27	−43.9	238	−282	1.4	24.7
2RK mean	3.1	36.3	−33.1	2.86	34.61	37	525	−488	3.4	46

heat delivered to the fjord. On average 3.4 mSv of AW delivers 46 mW of heat to Kongsfjorden.

5. Discussion

Our comparable hydrographic data set shows that under the continuing warming in Svalbard fjords, both Hornsund and Kongsfjorden significantly differ in water temperature, salinity, freshwater content and AW presence. Our main finding is that Hornsund is approximately 1°C colder and its salinity is on average lower by 0.5 compared to Kongsfjorden. More waters of the Atlantic origin are found in Kongsfjorden. The fjord is characterized by approximately 2 times higher inflow of AW and the corresponding heat delivery, but 2 times lower total *FWC* in comparison to Hornsund. As the fjords are located on the main pathway of AW into the Arctic Ocean, one can assume that the fjords experience more (less) inflow of AW within a similar time period. Even so, the present study shows that in some years the fjords may demonstrate very different conditions. Moreover, we observed increased variability of water temperature and salinity during summer in Hornsund and Kongsfjorden with the exceptional and unprecedented warming and increase in salinity in the summer of 2014 in the period 2001—2015 for both fjords.

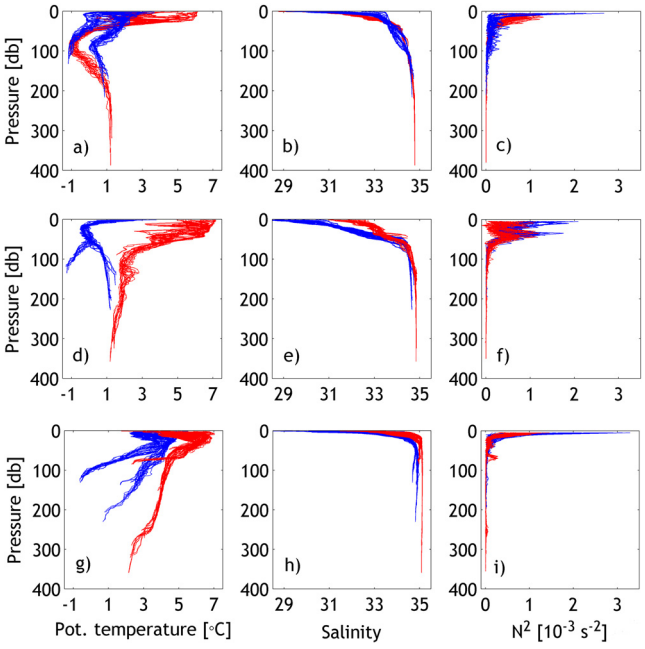

Figure 12 Potential temperature, salinity and stratification profiles for data collected along fjords' axis for Kongsfjorden (red) and Hornsund (blue) in 2010 (a–c), 2011 (d–f) and 2014 (g–i). (For interpretation of the references to color in this figure legend, the reader is referred to the web version of the article.)

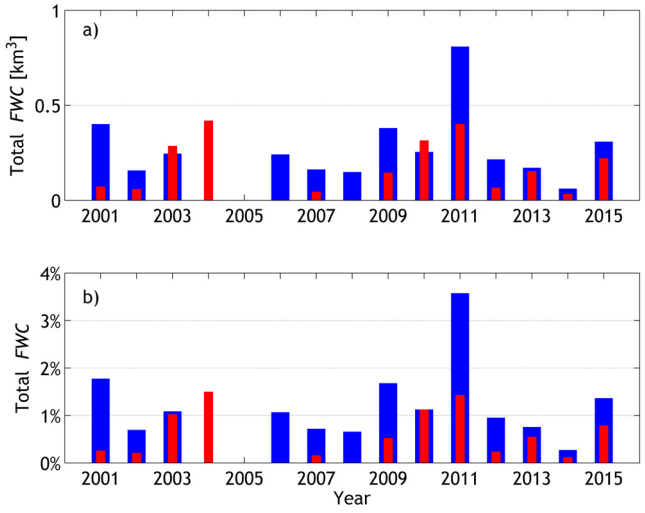

Figure 13 Total freshwater volume (a) and percentage of the fjord volume (b) in Hornsund (blue) and Kongsfjorden (red) in summers 2001–2015. (For interpretation of the references to color in this figure legend, the reader is referred to the web version of the article.)

In most years both fjords experienced warming or cooling at the same time (Fig. 6). Since the fjords on the west coast of Spitsbergen have no entrance sill there is a direct influence of waters from the outside. The Inner parts of the fjords are of more Arctic character due to remnants of water from the previous winter. However, Fig. 4 shows clearly that the fjords undergo a transition toward more Atlantic type. It is particularly evident after 2006, when deeper parts of the fjords have been replaced by TAW instead of LW or IW, and in summer 2014 when large areas of the fjords were filled with pure Atlantic Water. That was an exceptional year of the analyzed period. Moreover, in Inner parts, where typically WCW was found, there were years with no WCW at all (Fig. 4). The warming may be a result of an increased inflow of AW into the fjords due to changes in the atmosphere (Cottier et al., 2005, 2007; Nilsen et al., 2016).

A previous study of Hornsund hydrography showed a weak occupation by the AW explained with stronger blocking by SC compared to other fjords west of Spitsbergen (Promińska et al., unpublished data). They presented yearly mean Sea Ice Concentration (SIC) as a proxy for SC and showed high correlation with water temperature and salinity in Hornsund. The extremely low temperature and salinity in summer 2011 in Hornsund was explained by the sea ice inflow brought by the SC from the Barents Sea, which was also documented by Kruszewski (2012). The sea ice events in July occurred several times between 2001 and 2015, with the highest sea ice concentration in July 2004 and 2011 but they were also present in July 2001, 2005 and 2008 (Promińska et al., unpublished data). Fig. 4 shows that the cold signal is not observed in Kongsfjorden (summer 2011), since the sea ice can melt completely on its way north due to heat gain from the atmosphere and mixing of cold water with surrounding warm water from WSC (Saloranta and Haugan, 2004; Tverberg et al., 2014). On the other hand, the presence of LW in the upper layer (Fig. 4) and negative temperature and salinity anomalies in summer 2004 (Fig. 6) may be linked to a sea ice event in July 2004. This shows that despite a great number of papers concentrated on the variability of WSC and processes governing the inflow of AW into the fjords, variability in SC and relation with WSC is still poorly documented and understood.

Kongsfjorden is characterized by on average 1°C higher water temperature and 0.5 higher salinity compare to Hornsund. That difference results from a combination of geographical and environmental settings. First of all, Węsławski et al. (unpublished data) showed essential difference between frontal zone demarcating the WSC from the SC, which is much more pronounced at Hornsund foreground. Despite the northward cooling of the WSC (Saloranta and Haugan, 2004) AW is more available for Kongsfjorden than for Hornsund. Another limiting factor are deep troughs across the WSS, playing an important role in supplying water from the outside (Nilsen et al., 2016). The trough leading to Hornsund is very narrow and shallower than in case of Kongsfjorden. The geometry of Hornsund (numerous inner bays), as well as higher freshwater content (Fig. 13), leads to higher water mass transformation in the fjord toward more Arctic characteristics, resulting in lower temperature and salinity.

Approximately twice higher total *FWC* in Hornsund compared to Kongsfjorden may result from landscape diversity as one source of freshwater comprising glacial water (ablation and melting of a glacier, melting of icebergs), river runoff, precipitation. At first sight, there are more tidewater glaciers distributed along the fjord coastline in Hornsund (97% of glacierized area, Blaszczyk et al., 2013). In Kongsfjorden, there are only 5 tidewater glaciers with the ice front positions distributed mainly along the coastline of the Inner

fjord basin (Fig. 1). On the other hand, the southern coast of Kongsfjorden is rich in branched river network. However, assuming that rivers are a minor source of freshwater in the fjords (Węsławski et al., 1991 and references herein) and considering the fact that among all tidewater glaciers on Svalbard those in Hornsund retreat fastest (Blaszczyk et al., 2013), the landscape contrast of both fjords could serve as a sufficient explanation of higher total *FWC* in Hornsund. Our result shows that the seaward boundary is an additional factor influencing the total *FWC* in the fjord. The strongest manifestation of the seaward influence in Kongsfjorden and Hornsund is summer 2004 and 2011, respectively (Fig. 4), where the evident contributor to the total *FWC* was SC.

It is worth recalling that our calculations of the total *FWC* are based on momentary observations representing hydrographic conditions at the specific time. Another limitation of the method is that it gives overall *FWC* without specifying contribution of particular freshwater source. Moreover, the choice of the reference salinity may also influence the results. A previous study of freshwater in Hornsund and Kongsfjorden was based on the reference salinity taken for the summer measurements outside the fjords (S_{ref} = 35.23 for Hornsund and S_{ref} = 34.56 for Kongsfjorden, Węsławski et al., 1991), which, besides the fact that those values do not represent the fjords' waters, can significantly overestimate the FWC calculations.

Our results show that despite the continuing warming, both Kongsfjorden and Hornsund experience increased variability in temperature and salinity (Fig. 6) dependent on the domination of SC (Figs. 9 and 10) or WSC (Fig. 11). This increase is likely to be more pronounced in the future as a result of growing number of extreme weather events. Increased inflow of AW into the fjords is possible due to increased frequency of winter cyclones passing through the Fram Strait, which drives the mostly barotropic Spitsbergen Trough Current — transformed Atlantic Water circulating along the WSS troughs (Nilsen et al., 2016). More unmodified AW during winter may influence the local climate (Walczowski and Piechura, 2011) and sea ice cover (Muckenhuber et al., 2016). Warmer winters and lack of sea ice cover lead to an increased occurrence of years with no Winter Cooled Water (Promińska et al., unpublished data), which in turn is one of the factors controlling the AW inflow (Nilsen et al., 2008).

The baroclinic calculations usually underestimate total flow, but on the other hand it allows to assess the average flows and fluxes. Calculations give reasonable results, in case of both fjords maximal currents velocities are up to 30 cm s^{-1}. The inflow is usually situated at the deeper layer along the southern coast of the fjord and the outflow along the northern coast of the fjord. However, there is also the inflow of warm water into the fjord observed in the middle or close to the northern coast of the fjord. Results show that during the summer the intensity of exchange processes in Kongsfjorden is almost two times higher than in the case of Hornsund (Table 2). Greater inflow and higher water temperature result in much higher heat transport into Kongsfjorden than into Hornsund (525 MW vs 238 MW). The Atlantic Water plays important role in this transport. The water exchange in the Outer parts of the fjords is more intensive and residence time in this region is even shorter. The Inner parts of the fjords exchange water much slower. It is visible especially in the case of Hornsund, where WCW in Brepollen is observed in most summer observations. Nevertheless, even in Brepollen the upper layer of the water column has exchanged.

To conclude, both fjords located at two opposite ends of west Spitsbergen experience the ongoing warming accompanied by an increased variability in water temperature and salinity. Nonetheless, weaker occupation by AW, less heat transport to Hornsund as well as higher freshwater content in the fjord lead to lower values of water temperature and salinity in Hornsund compared to Kongsfjorden resulting in a more Arctic character of Hornsund.

Acknowledgements

The paper is a result of collaboration in GAME project (Growing of the Arctic Marine Ecosystems) financed from the Polish National Science Center funds under the no. DEC-2012/04/A/NZ8/00661. A major part of the study is also supported by the statutory research (subject I.4) carried out at the Institute of Oceanology PAN. Here, the authors would like to thank the crew of r/v *Oceania* for fieldwork assistance and all the people who actively participated in the data collection during Arctic cruises in the period 2001—2015. The analysis of archival data from Hornsund was also performed as part of the Polish-Norwegian project AWAKE-2 (Arctic climate system of ocean, sea ice and glacier interactions in Svalbard; PolNor/198675/17/2013). The analysis and interpretation of hydrographic data was performed under a doctoral project that is conducted at the Centre for Polar Studies KNOW (Leading National Science Centre). We also thank Joanna Pardus for providing basemap shapefiles for map preparation and Dr. Anna Przyborska from the Physical Oceanography Department IO PAN for providing hypsometric data for Hornsund and Kongsfjorden. Finally, we would like to sincerely thank two anonymous reviewers for their suggestions to improve the manuscript.

Appendix A. Supplementary data

Supplementary data associated with this article can be found, in the online version, at https://doi.org/10.1016/j.oceano.2017.07.003.

References

Beszczynska-Möller, A., Weslawski, J.M., Walczowski, W., Zajaczkowski, M., 1997. Estimation of glacial meltwater discharge into Svalbard coastal waters. Oceanologia 39 (3), 289—298.

Blaszczyk, M., Jania, J.A., Kolondra, L., 2013. Fluctuations of tidewater glaciers in Hornsund Fjord (Southern Svalbard) since the beginning of the 20th century. Pol. Polar Res. 34 (4), 327—352, http://dx.doi.org/10.2478/popore-2013-0024.

Cottier, F., Nilsen, F., Inall, M., Gerland, S., Tverberg, V., Svendsen, H., 2007. Wintertime warming of an Arctic shelf in response to large-scale atmospheric circulation. Geophys. Res. Lett. 34 (10), L10607, http://dx.doi.org/10.1029/2007GL029948.

Cottier, F., Tverberg, V., Inall, M.E., Svendsen, H., Nilsen, F., Griffiths, C., 2005. Water mass modification in an Arctic fjord through cross-shelf exchange: the seasonal hydrography of Kongsfjorden, Svalbard. J. Geophys. Res. 110 (C12), C12005, http://dx.doi.org/10.1029/2004JC002757.

Cottier, F., Nilsen, F., Skogseth, R., Tverberg, V., Skarðhamar, J., Svendsen, H., 2010. Arctic fjords: a review of the oceanographic environment and dominant physical processes. In: Howe, J.A., Austin, W.E.N., Forwick, M., Paetzel, M. (Eds.), Fjord Systems and Archives. Geol. Soc. Spec. Publ., 344, 35—50, http://dx.doi.org/10.1144/SP344.4.

Dølven, K.O., 2015. Interannual variations of freshwater content in Hornsund. (Master's thesis). University of Bergen and University Centre in Svalbard.

Gluchowska, M., Kwasniewski, S., Prominska, A., Olszewska, A., Goszczko, I., Falk-Petersen, S., Hop, H., Weslawski, J.M., 2016. Zooplankton in Svalbard fjords on the Atlantic-Arctic boundary. Polar Biol. 39 (10), 1785—1802, http://dx.doi.org/10.1007/s00300-016-1991-1.

Kruszewski, G., 2012. Zlodzenie Hornsundu i wód przyległych (Spitsbergen) w sezonie zimowym 2010—2011.(Ice conditions in Hornsund and adjacent waters (Spitsbergen) during winter season 2010—2011). Probl. Klimatol. Polar. 22, 69—82.

Muckenhuber, S., Nilsen, F., Korosov, A., Sandven, S., 2016. Sea ice cover in Isfjorden and Hornsund, Svalbard (2000—2014) from remote sensing data. Cryosphere 10 (1), 149—158, http://dx.doi.org/10.5194/tc-10-149-2016.

Nilsen, F., Gjevik, B., Schauer, U., 2006. Cooling of the West Spitsbergen Current: isopycnal diffusion by topographic vorticity waves. J. Geophys. Res. 111 (C8), C08012, http://dx.doi.org/10.1029/2005JC002991.

Nilsen, F., Cottier, F., Skogseth, R., Mattsson, S., 2008. Fjord-shelf exchanges controlled by ice and brine production: the interannual variation of Atlantic Water in Isfjorden, Svalbard. Cont. Shelf Res. 28 (14), 1838—1853, http://dx.doi.org/10.1016/j.csr.2008.04.015.

Nilsen, F., Skogseth, R., Vaardal-Lunde, J., Inall, M., 2016. A simple shelf circulation model — intrusion of Atlantic Water on the West Spitsbergen Shelf. J. Phys. Oceanogr. 46 (4), 1209—1230, http://dx.doi.org/10.1175/JPO-D-15-0058.1.

Pavlov, A.K., Tverberg, V., Ivanov, B.V., Nilsen, F., Falk-Petersen, S., Granskog, M.A., 2013. Warming of Atlantic Water in two Spitsbergen fjords over the last century (1912—2009). Polar Res. 32 (1), 11206, http://dx.doi.org/10.3402/polar.v32i0.11206.

Promińska, A., Falck, E., Walczowski, W., unpublished data. Interannual Variability in Hydrography and Water Mass Distribution in Hornsund, an Arctic Fjord on Svalbard. (unpublished data).

Saloranta, T.M., Haugan, P.M., 2004. Northward cooling and freshening of the warm core of the West Spitsbergen Current. Polar Res. 23 (1), 79—88, http://dx.doi.org/10.3402/polar.v23i1.6268.

Saloranta, T.M., Svendsen, H., 2001. Across the Arctic front west of Spitsbergen: high-resolution CTD sections from 1998—2000. Polar Res. 20 (2), 177—184, http://dx.doi.org/10.3402/polar.v20i2.6515.

Schauer, U., Fahrbach, E., Osterhus, S., Rohardt, G., 2004. Arctic warming through the Fram Strait: oceanic heat transport from 3 years of measurements. J. Geophys. Res. 109 (C6), C06026, http://dx.doi.org/10.1029/2003JC001823.

Svendsen, H., Beszczynska-Møller, A., Hagen, J.O., Lefauconnier, B., Tverberg, V., Gerland, S., Ørbæk, J.B., Bischof, K., Papucci, C., Zajaczkowski, M., Azzolini, R., Bruland, O., Wiencke, C., Winther, J.G., Dallmann, W., 2002. The physical environment of Kongsfjorden—Krossfjorden, an Arctic fjord system in Svalbard. Polar Res. 21 (1), 133—166, http://dx.doi.org/10.3402/polar.v21i1.6479.

Swerpel, S., 1985. The Hornsund Fiord: water masses. Pol. Polar Res. 6 (4), 475—496.

Tverberg, V., Nøst, O.A., Lydersen, C., Kovacs, K.M., 2014. Winter sea ice melting in the Atlantic Water subduction area, Svalbard Norway. J. Geophys. Res. 119 (9), 5945—5967, http://dx.doi.org/10.1002/2014JC010013.

Walczowski, W., 2013. Frontal structures in the West Spitsbergen Current margins. Ocean Sci. 9 (6), 957—975, http://dx.doi.org/10.5194/os-9-957-2013.

Walczowski, W., Piechura, J., 2011. Influence of the West Spitsbergen Current on the local climate. Int. J. Climatol. 31 (7), 1088—1093, http://dx.doi.org/10.1002/joc.2338.

Weslawski, J.M., Koszteyn, J., Zajaczkowski, M., Wiktor, J., Kwasniewski, S., 1995. Fresh water in Svalbard fjord ecosystem. In: Skjoldal, H.R., Hopkins, C., Erikstad, K.E., Leinaas, H.P. (Eds.), Ecology of Fjords and Coastal Waters: Proc. Mare Nor Symposium on the Ecology of Fjords and Coastal Waters, Tromsø, Norway, 5—9 December 1994. 229—241.

Węsławski, J.M., Jankowski, A., Kwaśniewski, S., Swerpel, S., Ryg, M., 1991. Summer hydrology and zooplankton in two Svalbard fiords. Pol. Polar Res. 12 (3), 445—460.

Węsławski, J.M., Kwaśniewski, S., Stempniewicz, L., Błachowiak-Samołyk, K., 2006. Biodiversity and energy transfer to top trophic levels in two contrasting Arctic fjords. Pol. Polar Res. 27 (3), 259—278.

Węsławski, J.M., Szczucka, J., Głuchowska, M., Ormańczyk, M., Hoppe, Ł., Schmidt, B., Promińska, A., Kwaśniewski, S., Berge, J., Deja, K., Fey, D.P., unpublished data. A Comparative Study of the Fish Community in Two Fjords on Svalbard. (unpublished data).

Oceanologia (2017) 59, 413—421

Available online at www.sciencedirect.com

ScienceDirect

journal homepage: www.journals.elsevier.com/oceanologia/

ORIGINAL RESEARCH ARTICLE

Comparison of meteorological conditions in Svalbard fjords: Hornsund and Kongsfjorden

Małgorzata Cisek *, **Przemysław Makuch, Tomasz Petelski**

Institute of Oceanology, Polish Academy of Sciences, Sopot, Poland

Received 11 May 2017; accepted 30 June 2017
Available online 18 July 2017

KEYWORDS
Arctic meteorology;
GAME;
Svalbard

Summary This paper presents the results of a comparison of basic meteorological parameters in two Arctic fjords situated on the west coast of Spitsbergen, the main island of the Svalbard archipelago. Air temperature, wind speed and direction, humidity and cloud cover from the period 2005 to 2016 are described and compared with previous (from 1975) analyses of meteorological conditions in the investigated region. Such a choice of dates coincides with the time the GAME project measurements were carried out. The main goal of this study was to compare meteorological conditions in two fjords: Hornsund and Kongsfjorden, during the time of rapid climate changes. The results are collated with research results available in literature from previous years. We discovered that in the investigated period the climate of the Hornsund region is more oceanic than in Kongsfjorden. The stable level of the difference in climate elements is manifested and is evident mainly through greater amplitudes in air temperatures in Kongsfjorden, and in stronger winds in Hornsund.

* Corresponding author at: Institute of Oceanology, Polish Academy of Sciences, Powstańców Warszawy 55, 81-712 Sopot, Poland. Tel.: +48 587311821; fax: +48 585512130.
E-mail address: gosiak@iopan.gda.pl (M. Cisek).
Peer review under the responsibility of Institute of Oceanology of the Polish Academy of Sciences.

Production and hosting by Elsevier

http://dx.doi.org/10.1016/j.oceano.2017.06.004

1. Introduction

The comparison described in this paper regards two Svalbard fjords: Hornsund and Kongsfjorden. Both are located on the west coast of Spitsbergen, the main island of the Svalbard archipelago. They were both investigated within the GAME project (Growing of the Arctic Marine Ecosystem), which was focused on verifying the hypothesis that the Arctic marine ecosystem is aging due to global warming effects. The selected fjords have a similar area, shape and water circulation. Even though Hornsund is located more southward than Kongsfjorden, the water in this fjord is colder. Warm Atlantic Water reaches Kongsfjorden directly from the West Spitsbergen Current, whereas Hornsund is strongly influenced by the cold Sørkapp Current. Such a system impacts the meteorological conditions in both fjords. As a result, mean temperature values in the Hornsund stations are well correlated with the temperature of the Atlantic Water carried by the West Spitsbergen Current (Walczowski and Piechura, 2011). The climate of the west coast of Spitsbergen, including Hornsund and Kongsfjorden, has been studied for many years and is well described in literature (e.g. Forland et al., 1997; Hanssen-Bauer et al., 1990; Marsz and Styszyńska, 2007, 2013; Kejna, 2002; Kejna and Dzieniszewski, 1993; Kierzkowski, 1996; Przybylak, 2007, 2002). The influence of the atmospheric circulation on the climate of this region has been described by Niedźwiedź (1997), while the problem of precipitation in the Hornsund area was presented by Łupikasza (2009). In this paper, the authors focused on the differences in the main meteorological parameters in the Hornsund and Kongsfjorden fjords. The analyzed parameters included: wind speed and direction, air temperature, humidity and cloud cover, data from the last ten years (2005–2016) was also incorporated. The meteorological parameters that were analyzed are responsible for shaping the conditions of the ecosystems of the studied fjords.

2. Material and methods

Temperature, humidity and cloud cover data comes from the weather stations No. 01003 (Hornsund) and No. 01007 (Ny-Ålesund) of the World Meteorological Organization (WMO) and were taken from http://rp5.kz. This website is provided and supported by Raspisaniye Pogodi Ltd., St. Petersburg, Russia. Databases of meteorology and hydrometeorology are maintained on license from the Russian Federal Service for Hydrometeorology and Environmental Monitoring (Roshydromet). The time period from 2005 to 2016 was chosen to be long enough to allow appropriate comparisons. It also coincides with the time the GAME project measurements were carried out. However, a period longer than the duration of the GAME project was chosen in order to facilitate a comparison which provides more data on climatic impact than a single measurement. Real data from wind measurements at 10 m a.s.l., from stations located in the fjords: from the French-German Arctic Research Base at Ny-Ålesund (AWIPEV) station in Kongsfjorden (Maturilli et al., 2013) and from the Polish Polar Station in Hornsund, was analyzed and compared to winds at 10 m a.s.l. from the NCEP/NCAR reanalysis (Kalnay et al., 1996). Data from the later period (after 2013) was not available. Temperature and salinity values of the Atlantic Water in the West Spitsbergen Current come from the database of the Institute of Oceanology Polish Academy of Sciences (IOPAS) and was collected during the Arctic summer cruises of r/v *Oceania*.

To observe the climatic changes in the studied region the results obtained from the comparison of meteorological conditions in Hornsund and Kongsfjorden in recent years are collated with research results from previous years. However, the main goal of this paper is a comparison of weather conditions in the two fjords and not the study of climate change.

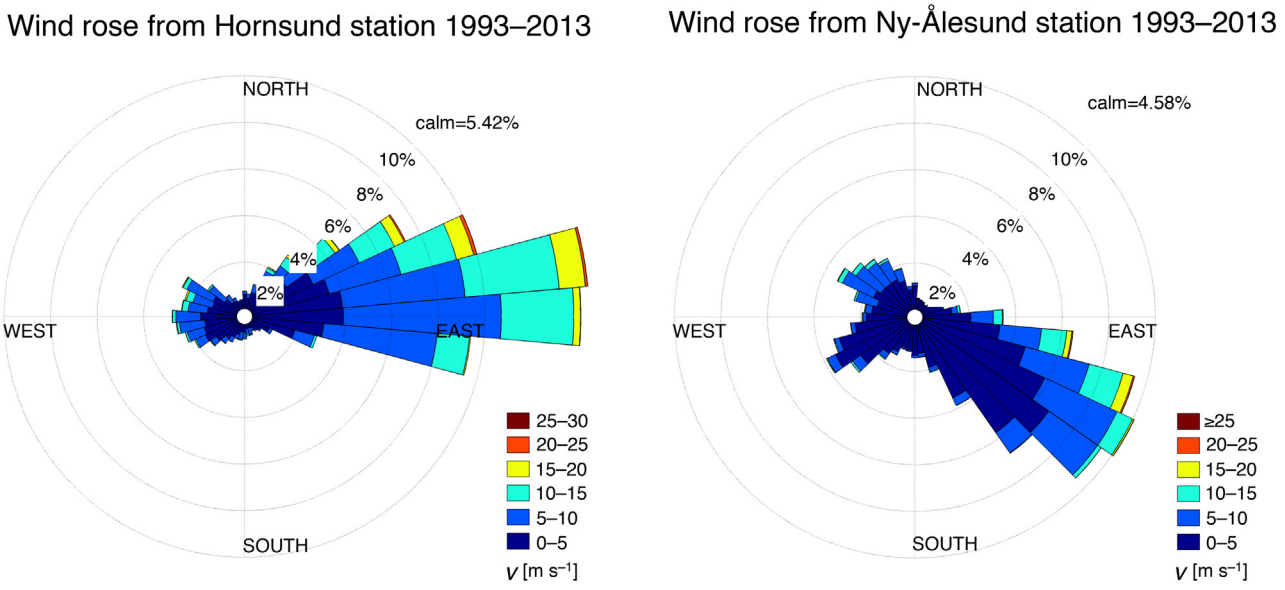

Figure 1 Local wind roses for the Hornsund station (left) and the Ny-Ålesund station (right) for the period from 1993 to 2013.

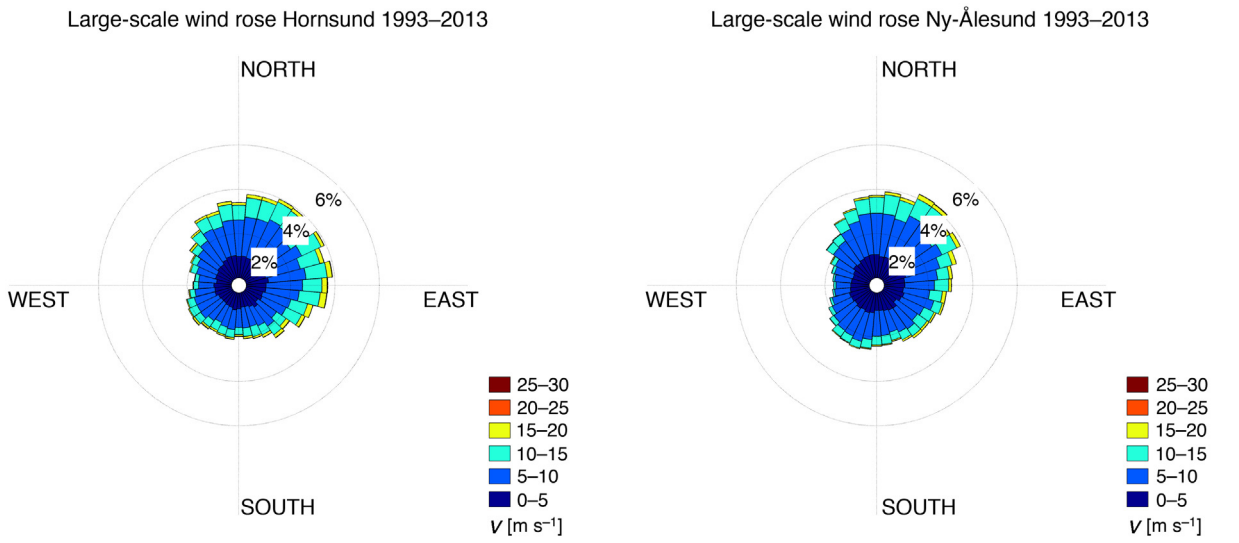

Figure 2 Large-scale wind roses (from NCEP/NCAR reanalysis) for the Hornsund station (left) and the Ny-Ålesund station (right) for the period from 1993 to 2013.

3. Results

3.1. Wind

The wind roses prepared with data from 1993 to 2013 for Ny-Ålesund (Kongsfjorden) and Hornsund are showed in Fig. 1. Fig. 2 shows surface wind directions from the NCEP/NCAR reanalysis data, interpolated for the position of the station. The wind roses of the reanalysis data are similar for both fjords (the pressure field in this area is the same in Hornsund and in Kongsfjorden) but 'in situ' measurements show that the wind is stronger in Hornsund (also Fig. 5) which indicates less friction and a more marine type of climate in the Hornsund region than in Kongsfjorden. Wind directions obtained from the reanalysis are based on a large-scale pressure field. The difference between the station measured winds and the geostrophic winds is distinct. The measurements of surface wind directions and speeds at coastal Arctic stations are often not representative of the neighboring regions. A recent paper on wind climate of the Hornsund station in Svalbard (Marsz and Styszyńska, 2013) states that the "Hornsund station is characterized by a special wind regime. [...] This is caused by a strong influence of local conditions". The situation is similar in other stations based in the Svalbard fjords. The climatology compiled by Hanssen-Bauer et al. (1990) shows that for Kongsfjorden, surface winds usually blow along the axis of the fjord. Esau and Repina (2012) provide a review of literature for the wind climate of Kongsfjorden. However, wind direction tunneling is not the only phenomenon influencing the local wind climatology. Other effects, such as, fen and fall (katabatic) winds are also significant. Using an eddy-resolving model, Esau and Repina (2012) showed that thermal land-sea breeze circulation dominates over katabatic winds in Ny-Ålesund (Kongsfjorden). The terrain orography determines the mean wind directions, and in many cases the horizontal temperature gradient controls its behavior. Cisek et al. (personal communication) reported that the breeze mechanism is one of the most important factors controlling wind directions on the west coast of Spitsbergen.

Calculations and results presented in this paper are based on absolute measured values of wind speed (independent of wind direction) in both fjords, and the differences between them over a period from 2005 to 2016. The mean wind speed values during the studied decade were 5.6 m s^{-1} and 4.1 m s^{-1} in Hornsund and Ny-Ålesund, respectively, while in Ny-Ålesund, the yearly mean for the period from 1975 to 2000 was 2.6 m s^{-1} (Przybylak and Araźny, 2006) and the multiannual yearly mean in Hornsund was 5.5 m s^{-1} (Marsz and Styszyńska, 2007).

Fig. 3 presents monthly mean wind speeds in both fjords. In both cases the trend is similar. It shows that it is very rare for winds in Kongsfjorden to be stronger than in Hornsund. It is even more evident in Fig. 4 where the differences between monthly mean wind speeds in both fjords are displayed. There are only 6 cases (out of over 130) when the monthly mean wind speed is greater in Ny-Ålesund than in Hornsund (shown where the graph of wind differences is below the zero value).

This difference in monthly mean values (Fig. 5) of wind speeds clearly shows that the multiannual monthly mean wind speed in Hornsund is 2.5 m s^{-1} higher than in Kongsfjorden (Fig. 5). The multiannual monthly mean wind speed in both stations reaches maximum values in February and minimum values in the summer months.

Wind patterns presented in Fig. 2 obtained from reanalysis data are similar. It means there are no difference in field pressure between Hornsund and Kongsfjorden and there should not be a great difference in measured wind speed in these fjords. However more marine character of Hornsund area and less air-land friction around cause that wind in Hornsund is stronger what can be noticed in Fig. 5.

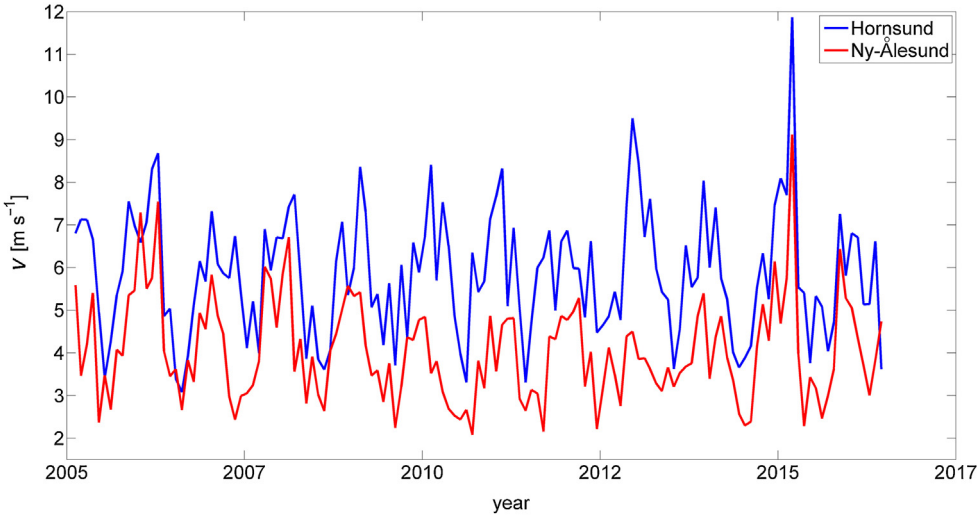

Figure 3 Monthly mean value of wind speed in Hornsund (blue line) and Kongsfjorden (red line) for the period from 2005 to 2016. (For interpretation of the references to color in this figure legend, the reader is referred to the web version of the article.)

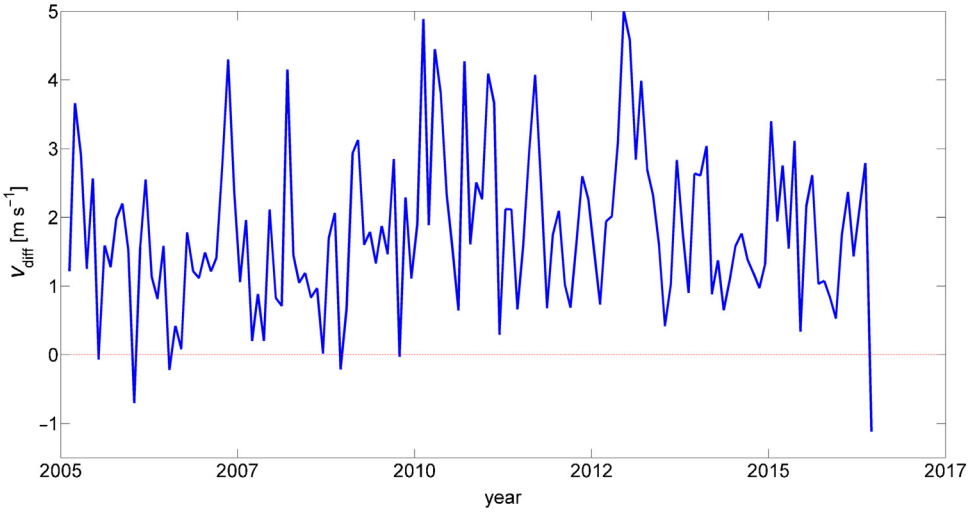

Figure 4 Differences in monthly mean values of wind speed (Hornsund–Kongsfjorden) for the period from 2005 to 2016.

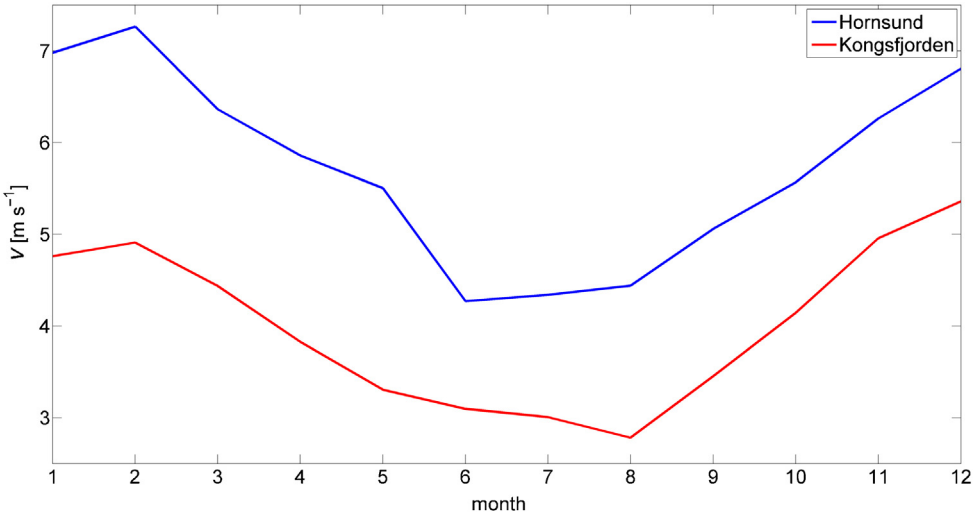

Figure 5 Multiannual monthly mean of wind speed in Hornsund (blue) and Kongsfjorden (red) for the period from 2005 to 2016. (For interpretation of the references to color in this figure legend, the reader is referred to the web version of the article.)

3.2. Temperature

The yearly mean air temperature in Ny-Ålesund for the period from 1975 to 2000 was −5.8°C. July was the warmest month with a mean temperature of 4.9°C, February was the coldest, with a mean temperature of −14.2°C (Przybylak and Araźny, 2006). The multiannual yearly mean air temperature in Hornsund for the period from 1979 to 2006 was −4.4°C. The highest monthly mean was also recorded in July (4.4°C) and the coldest month was January with a monthly mean air temperature of −11.3°C (Marsz and Styszyńska, 2007). Over the period from 2005 to 2016 the multiannual yearly mean air temperature was −2.34°C in Hornsund, and −3.43°C in Ny-Ålesund. The coldest month in Hornsund was March with a multiannual monthly mean temperature of −8.6°C while the warmest month was July with a temperature of 4.8°C. In addition, the lowest multiannual monthly mean air temperature in Ny-Ålesund was recorded in March, −9.9°C and the highest was recorded in July at 5.9°C.

Trends for difference in air temperature between Hornsund and Kongsfjorden for the studied ten-year period were calculated and no significant trends have been found. The trendline is represented by a red line on the graph depicting changes in air temperature differences between both fjords in years 2005–2016, and shows a very slight decrease (the slope coefficient is equal to -1.14×10^{-5}). We can assume that the air temperature difference persists on constant level.

Daily mean air temperatures in both fjords and the differences between them are presented in Figs. 6 and 7. The chart of the differences in temperature has similar features to the ones of the temperature itself and the amplitude of the changes in differences is analogous to that of the temperature but is shifted by about a half a year.

In the cold season, temperatures in Ny-Ålesund are usually lower than in Hornsund, while during the warm season the situation is opposite. This dependency is well presented in Fig. 8, depicting multiannual monthly mean air temperatures in both stations.

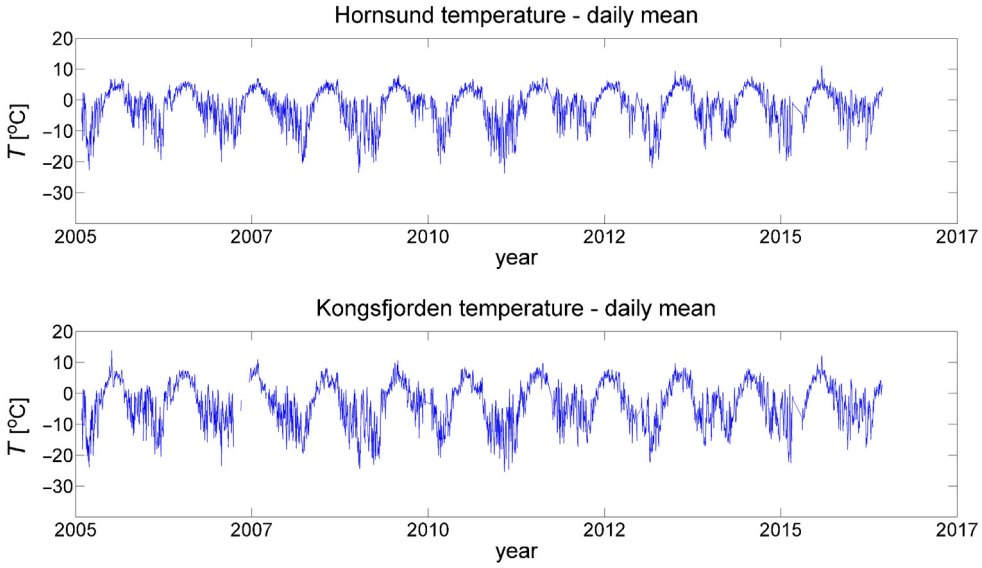

Figure 6 Daily mean air temperature from Hornsund (upper plot) and Kongsfjorden (lower plot) for the period from 2005 to 2016.

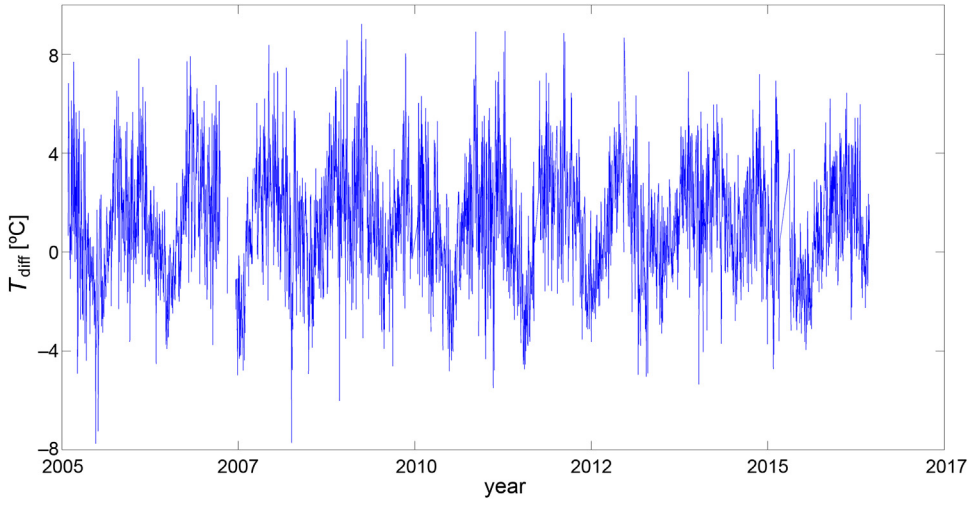

Figure 7 The difference of daily mean air temperatures (Hornsund–Kongsfjorden) for the period from 2005 to 2016.

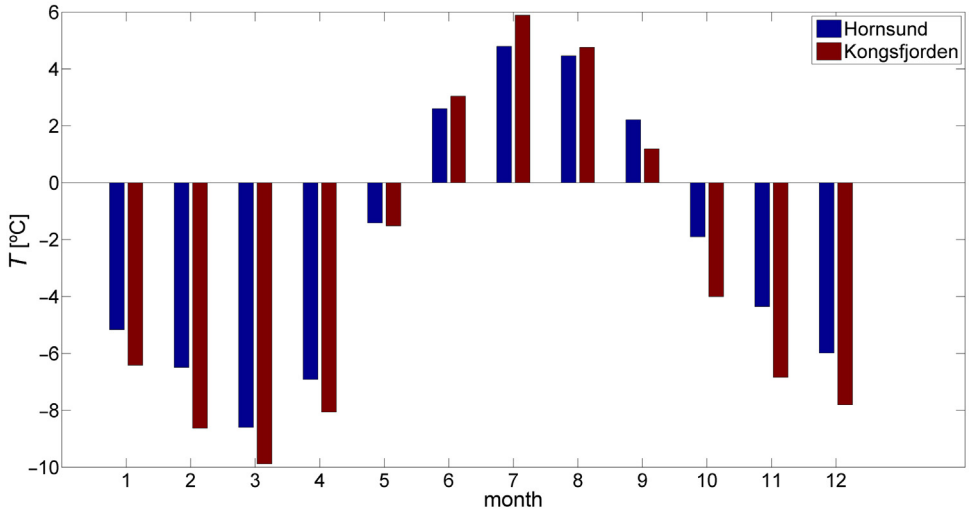

Figure 8 Multiannual monthly mean of air temperatures in Hornsund (blue bars) and Kongsfjorden (red bars) for the period from 2005 to 2016. (For interpretation of the references to color in this figure legend, the reader is referred to the web version of the article.)

Table 1 Climatic conditions at the Hornsund station (H), the Ny-Ålesund station (N) and the difference between them (H-N). T – temperature, v – wind speed, C – cloud cover, RH – relative humidity. The table contains multiannual monthly mean values.

Parameter	Station	I	II	III	IV	V	VI	VII	VIII	IX	X	XI	XII	I-XII
T [°C]	H	−5.2	−6.5	−8.6	−6.9	−1.4	2.6	4.8	4.5	2.2	−1.9	−4.4	−6.0	−2.2
	N	−6.4	−8.6	−9.9	−8.1	−1.5	3.0	5.9	4.8	1.2	−4.0	−6.8	−7.8	−3.2
	H-N	1.2	2.1	1.3	1.1	0.1	−0.4	−1.1	−0.3	1.0	2.1	2.5	1.8	1.0
v [m s^{-1}]	H	6.9	7.3	6.4	5.8	5.5	4.3	4.3	4.4	5.1	5.5	6.3	6.9	5.7
	N	4.8	4.9	4.6	4.0	3.3	3.1	3.0	2.7	3.4	4.2	5.0	5.3	4.0
	H-N	2.1	2.3	1.7	1.8	2.2	1.2	1.3	1.7	1.6	1.3	1.3	1.6	1.7
C [%]	H	71.1	68.3	64.6	66.0	80.5	82.4	83.7	83.5	81.6	75.6	72.6	67.2	74.8
	N	66.9	59.3	61.9	60.1	73.9	76.8	78.1	79.8	78.6	68.7	66.1	58.4	69.1
	H-N	4.2	9.0	2.7	5.9	6.6	5.6	5.6	3.8	3.0	6.9	6.5	8.8	5.7
RH [%]	H	78.4	76.2	74.8	74.2	79.4	80.7	85.2	84.6	82.5	78.4	76.9	75.6	78.9
	N	70.9	68.6	68.5	66.4	69.4	70.7	74.1	75.8	76.1	72.5	70.5	69.1	71.0
	H-N	7.5	7.6	6.3	7.8	10.0	10.1	11.1	8.8	6.4	5.9	6.4	6.5	7.9

During the cold months, the multiannual monthly mean temperature in Ny-Ålesund is lower than in Hornsund. In May, the mean temperatures are almost equal. Beginning in June, Kongsfjorden is warmer and then in September, the temperatures are higher in Hornsund. This corresponds well with the sun path and the sun's relative position (higher above the horizon during summer months). Meteorological parameters from both stations are compiled in Table 1.

The amplitude of multiannual monthly mean air temperatures in Kongsfjorden reaches 15.8°C (between March and July), while in Hornsund it is 13.6°C.

To find out what can significantly influence the local climatic and meteorological conditions, data from ocean hydrographic measurements was analyzed. Walczowski and Piechura (2011) found a high positive correlation of the mean summer temperature of Atlantic Water in the core of the West Spitsbergen Current and the yearly mean temperatures from the Hornsund meteorological station for the period from 1996 to 2007. We also compared IO PAN time series of water temperature data from the transect 'N' along the 76°30′N parallel (close to the mouth of the Hornsund fjord) with the yearly mean air temperatures from Hornsund and Kongsfjorden. The correlation coefficient is r = 0.53 for Hornsund and r = 0.62 for Kongsfjorden for the period from 2005 to 2014.

The glance at Fig. 9 confirms that the air temperature in the investigated area increases. It shows monthly mean air temperature in Kongsfjorden from 1975 to date (41 years). This data set comes from eKlima (weather and climate data base from Norwegian Meteorological Institute). Closely 3°C increase of mean air temperature within last 40 years was presented with trend line (red line in Fig. 9) obtained from mentioned data. Additionally, in Fig. 9 it is apparent that in summer months the air temperature is almost fixed from year to year while in winter it gets unambiguously warmer in Kongsfjorden area. This change proves that this fjord climate is changing to more marine type with warmer winters.

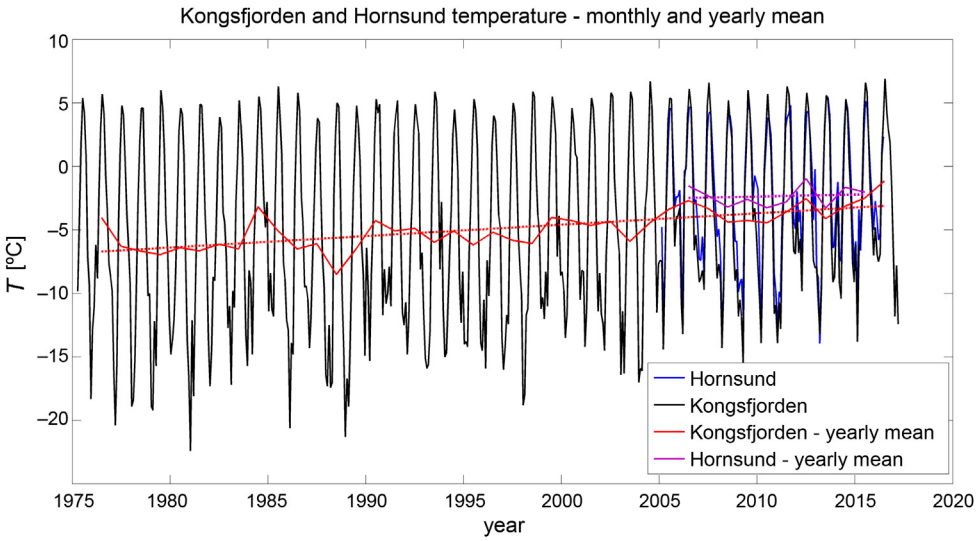

Figure 9 Monthly mean air temperature from Kongsfjorden for years 1975—2016 (black line) and from Hornsund for years 2005—2016 (blue line). Red and purple lines present yearly mean air temperature from Kongsfjorden and Honsund respectively. Dashed red line is trend line of temperature changes in last 40 years and parallel purple dashed line is trend line of temperature changes in Hornsund in last 11 years. (For interpretation of the references to color in this figure legend, the reader is referred to the web version of the article.)

3.3. Relative humidity

The yearly mean relative humidity for the period from 1975 to 2000 was 79.3% in Hornsund, and 77.7% in Ny-Ålesund (Przybylak and Araźny, 2006). The multiannual monthly mean of humidity in Ny-Ålesund during this time oscillated between 72.1% in December and 85.6% in July. During the studied period, the multiannual yearly mean was 70.91% in Ny-Ålesund and 78.83% in Hornsund. The changes in monthly mean values of relative humidity over the last decade in both stations are presented in Fig. 10. In order to emphasize the difference between the fjords, monthly mean values have been plotted instead of daily mean values. Mean relative humidity in Hornsund is almost always higher than in Ny-Ålesund. The difference is significant and reaches up to 16%. The only month during which the mean relative humidity was lower in Hornsund than in Ny-Ålesund was December 2013. A much higher relative humidity in Hornsund may strengthen the infrared cloud radiative effect (CRE) in this region (Cox et al., 2015). This effect could also be the reason behind the mean annual air temperature differences in both fjords because Hornsund has more cloud cover than Kongsfjorden.

3.4. Cloud cover

The multiannual monthly mean of cloud cover in Hornsund and Kongsfjorden is presented in Fig. 11. The mean values are

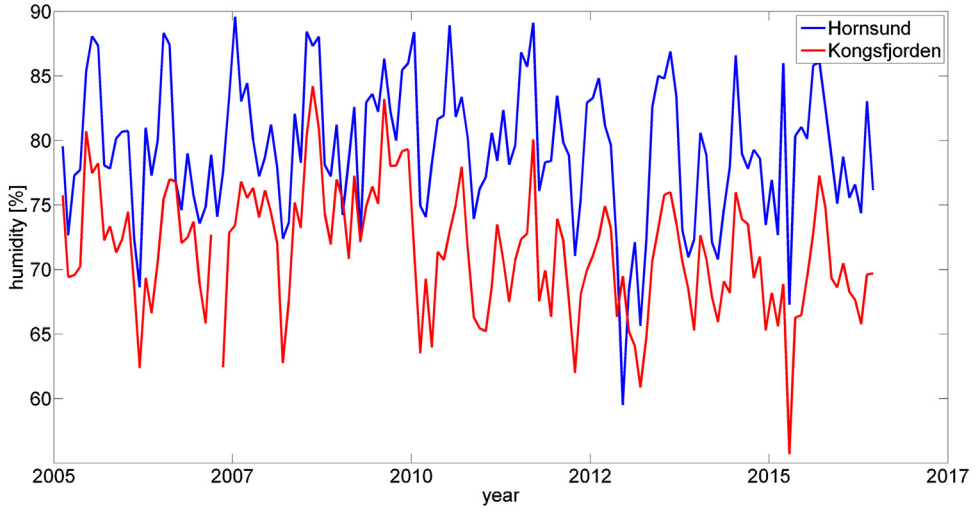

Figure 10 Monthly mean value of relative humidity from Hornsund (blue line) and Kongsfjorden (red line) for the period from 2005 to 2015. (For interpretation of the references to color in this figure legend, the reader is referred to the web version of the article.)

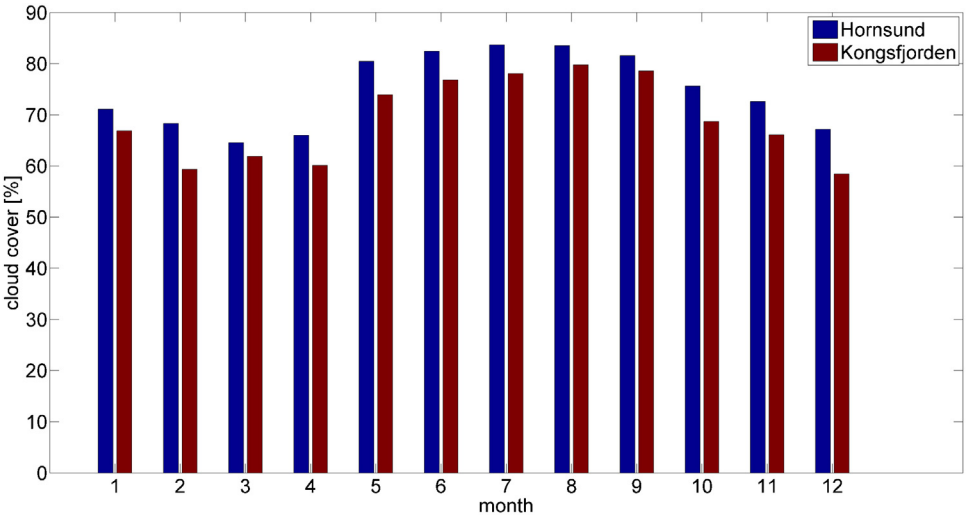

Figure 11 Multiannual monthly cloud cover in Hornsund (blue bars) and Kongsfjorden (red bars) for the period from 2005 to 2016. (For interpretation of the references to color in this figure legend, the reader is referred to the web version of the article.)

similar for both stations, with maximum values of cloud cover during the summer, with a decline in October and November, and a minimum in the spring. In Hornsund, the mean annual cloud cover was 75% during the studied period which indicates a 2% increase, in comparison to years 1978–2009 (Marsz and Styszyńska, 2013). The same pattern was observed in these research stations over a period from 1975 to 2000 (Przybylak and Araźny, 2006). Corresponding plots are true in other Arctic stations (Shupe et al., 2011). Despite the similarity of the observed values of cloud cover in both fjords, there is a key difference between them – the cloud cover is always greater in Hornsund.

All values of the properties analyzed above were tested for statistical significance with one-sided Student's *t*-test and all differences of monthly mean values between Hornsund and Kongsfjorden became statistically significant. The *p*-values are less than 2.2×10^{-16} for wind speed and relative humidity differences, 1.22×10^{-5} for cloud cover differences, and 0.054 for temperature differences. The last *p*-value is slightly greater than 0.05 but it is very close to being statistically significant.

4. Conclusions

The differences in meteorological parameters between the Kongsfjorden and Hornsund fjords are clear and remain on the same level during the studied period, from 2005 to 2016. The comparison of conditions in both fjords for the period from 2005 to 2016 with conditions surveyed before the year 2000 shows some variations. This allows us to reach several conclusions.

Climate change and global warming is clearly present in both fjords, and is manifested by mean air temperature values. Taking long term trends into consideration, the mean annual air temperature has increased by approximately 2°C in both fjords. The difference between the annual amplitude of air temperature in Hornsund and Kongsfjorden has increased. The ocean has more influence on Hornsund than on Kongsfjorden, and it effects air temperature amplitudes, which are smaller in Hornsund.

The air temperature in Kongsfjorden is higher than in Hornsund during the summer and lower in the winter. This relation is probably caused by differences in radiation balance in both fjords. The cloud cover is greater throughout the year in Hornsund than in Kongsfjorden, which enhances the infrared radiative effect (CRE) of the clouds. This is further strengthened by the higher humidity prevailing in Hornsund. Greater cloud cover and humidity as well as a much greater mean wind speed in Hornsund can be explained by the influence of the sea on the climate of Hornsund. The southern part of Spitsbergen, where Hornsund is located, is a narrow area of the island and is surrounded by unfrozen water for most of the year. Kongsfjorden, on the other hand, borders the sea only on its west side. There is more land area east of Kongsfjorden than there is east of Hornsund. In addition, from January to June, sea ice cover occurs west of the latitude of Kongsfjorden. This location, along with the predominant eastward wind direction, makes the climate of Kongsfjorden more continental than in Hornsund. At the same time, Kongsfjorden (as well as the entire region) is under the influence of warm Atlantic Water (AW). The mean temperature of AW carried by the West Spitsbergen Current is slightly better correlated with the mean annual air temperature in Kongsfjorden than with the mean annual air temperature in Hornsund. This is because AW reaches Kongsfjorden directly, while Hornsund is separated from AW by the cold Sørkapp Current.

The relative air humidity in Kongsfjorden decreased considerably over the studied period. The mean value of humidity from the last decade is 11% lower than the multiannual mean from the period from 1975 to 2000. While the humidity in Hornsund increased slightly.

In both fjords, wind direction is conditioned mainly by local orography and the horizontal gradient of air temperature. In both cases the dominant wind direction is determined by the axis of the fjord. The wind speed is often greater in Hornsund than in Ny-Ålesund. Monthly means of wind speed are higher in Hornsund 98% of the time. The differences are significant and reach 5 m s^{-1}. This results in considerably stronger dynamics of air-sea interaction processes in the

Hornsund fjord rather than in Kongsfjorden. The difference is maintained during the studied period with no significant trend found. The authors assume that when the ice cover shrinks, the differences between the climates in these fjords should decrease.

This comparison of basic meteorological parameters in both fjords shows significant differences between them and they are unexpected and not obvious. On the basis of hydrological observations, these differences could be expected to be even greater. This effect is very interesting and needs to be further investigated with special attention given to changes in atmospheric circulation.

Acknowledgements

This study has been supported by the funds from the GAME "Growing of Marine Arctic Ecosystem" project, funded by Narodowe Centrum Nauki grant DEC-2012/04/A/NZ8/00661 and Oceanflux Greenhouse Gases Evolution, a project funded by the European Space Agency, ESRIN contract no. 4000112091/14/ILG. We thank Tomasz Wawrzyniak and the Hornsund Polish Polar Station staff and also Marion Matturilli and the French — German Arctic Research Base at Ny-Ålesund staff for the meteorological data from the station used in the paper.

References

Cox, C.J., Walden, V.P., Rowe, P.M., Shupe, M.D., 2015. Humidity trends imply increased sensitivity to clouds in a warming arctic. Nat. Commun. 6, 8 pp., http://dx.doi.org/10.1038/ncomms10117.

Esau, I., Repina, I., 2012. Wind climate in Kongsfjorden, Svalbard, and attribution of leading wind driving mechanisms through turbulence-resolving simulations. Adv. Meteorol., 568454, 16 pp., http://dx.doi.org/10.1155/2012/568454.

Forland, E.J., Hanssen-Bauer, I., Nordli, P.O., 1997. Climate statistic and longterm series of temperature and precipitation at Svalbard and Jan Mayen, DNMI Rep. No. 21/97 Klima, Oslo.

Hanssen-Bauer, I., Solas, M.K., Steffenson, E.L., 1990. The climate of Spitsbergen, DNMI-Rept. No. 39/90, Klima, Oslo.

Kalnay, E., Kanamitsu, M., Kistler, R., Collins, W., Deaven, D., Gandin, L., Iredell, M., Saha, S., White, G., Woollen, J., Zhu, Y., Chelliah, M., Ebisuzaki, W., Higgins, W., Janowiak, J., Mo, K.C., Ropelewski, C., Wang, J., Leetmaa, A., Reynolds, R., Jenne, R., Joseph, D., 1996. The NCEP/NCAR 40-year reanalysis project. Bull. Am. Meteorol. Soc. 77, 437—471.

Kejna, M., 2002. Warunki meteorologiczne na Kaffiöyra (NW Spitsbergen) w okresie od 13 lipca do 9 września 1999 roku Probl. Klimat. Polar. 10, 93—110.

Kejna, M., Dzieniszewski, M., 1993. Warunki meteorologiczne na Kaffiöyra (NW Spitsbergen) w okresie 26.06—31.08.1985 r. Acta Universitatis N. Copernici, Geografia 24, 43—54.

Kierzkowski, T., 1996. Cechy klimatu lokalnego stacji w Hornsundzie w oparciu o materiał z lat 1978—1995. Probl. Klimatol. Polar. 6, 67—81.

Łupikasza, E., 2009. Zmiany intensywności opadów w Hornsundzie (Spitsbergen) w okresie 1978—2008. Probl. Klimatol. Polar. 19, Gdynia, 169—188.

Marsz, A., Styszyńska, A., 2007. Klimat rejonu Polskiej Stacji Polarnej w Hornsundzie. Maritime University, Gdynia, 71—174.

Marsz, A., Styszyńska, A., 2013. Climate and Climate Change at Hornsund, Svalbard. Gdynia Maritime University, 81—192.

Maturilli, M., Herber, A., König-Langlo, G., 2013. Climatology and time series of surface meteorology in Ny-Ålesund, Svalbard. Earth Syst. Sci. Data 5, 155—163, http://dx.doi.org/10.5194/essd-5-155-2013.

Niedźwiedź, T., 1997. Częstość występowania typów cyrkulacji nad Spitsbergenem (1951—1995). Probl. Klimatol. Polar. 7, VII Seminarium Meteorologii i Klimatologii Polarnej, 9—17.

Przybylak, R., 2002. Changes in seasonal and annual high-frequency air temperature variability in the arctic from 1951 to 1990. Int. J. Climatol. 22 (9), 1017—1032, http://dx.doi.org/10.1002/joc.793.

Przybylak, R., 2007. Recent air-temperature changes in the arctic. Ann. Glaciol. 46 (1), 316—324, http://dx.doi.org/10.3189/172756407782871666.

Przybylak, R., Araźny, A., 2006. Climatic conditions of the north-western part of Oscar II Land (Spitsbergen) in the period between 1975 and 2000. Pol. Polar Res. 27 (2), 133—152.

Shupe, M.D., Walden, V.P., Eloranta, E., Uttal, T., Campbell, J.R., Starkweather, S.M., Shiobara, M., 2011. Clouds at arctic atmospheric observatories. Part I: Occurrence and macrophysical properties. J. Appl. Meteorol. Clim. 50 (3), 626—644, http://dx.doi.org/10.1175/2010JAMC2467.1.

Walczowski, W., Piechura, J., 2011. Influence of the West Spitsbergen Current on the local climate. Int. J. Climatol. 31 (7), 1088—1093, http://dx.doi.org/10.1002/joc.2338.

Oceanologia (2017) 59, 422—430

Available online at www.sciencedirect.com

ScienceDirect

journal homepage: www.journals.elsevier.com/oceanologia/

ORIGINAL RESEARCH ARTICLE

Aerosol Optical Depth variations due to local breeze circulation in Kongsfjorden, Spitsbergen

Malgorzata Cisek*, Tomasz Petelski, Tymon Zielinski, Przemyslaw Makuch, Paulina Pakszys, Anna Rozwadowska, Piotr Markuszewski

Institute of Oceanology, Polish Academy of Sciences, Poland

Received 9 July 2016; accepted 6 April 2017
Available online 24 May 2017

KEYWORDS
Aerosol Optical Depth;
Regional aerosol modifications;
Breeze circulation;
Svalbard

Summary This paper presents the results of Aerosol Optical Depth (AOD) studies which took place in Ny-Ålesund in the spring of 2014 during the iAREA campaign. The measurements were taken using Microtops II hand-held sunphotometers along the Kongsfjorden, on a path leading from the research village to the fjord opening. Local breeze circulation was observed during the measurement campaign which resulted in an evident increase of AOD along the measurement profile towards the open sea. Using the observed AOD, changes over the open sea have been calculated and the location of the breeze front has been determined.

1. Introduction

Aerosol optical properties vary in space and time, and it is especially noticeable in the Arctic. Higher values of Aerosol Optical Depth (AOD) in the spring — the Arctic haze season — and lower values during the summer months have been reported by scientists from various stations around the Arctic region (Tomasi et al., 2007, 2015). The range of AOD deviation at 500 nm varies from 0.12 to over 0.35 (Arctic haze conditions), to values not exceeding 0.1 or even less than 0.05 (clean summer conditions) (Stone et al., 2014; Tomasi et al., 2007). Such a seasonal dependency of AOD values is a result of a wide range of aerosol loads, their composition and size distribution (Herber et al., 2002; Tomasi et al., 2007, 2015) which causes the seasonal chemical composition and the particle size distribution of aerosols to differ considerably. Later into the winter and spring seasons, aged accumulation-mode particles play a dominant role in the number distribution of submicron particles in Spitsbergen. However, in the summer, small particles (Aitken-mode) are prevailing in the Arctic air (Engvall et al., 2008). In the summer, sulfate and sea salt aerosols contribute most to submicron light scattering, while supermicron particle scattering is usually

* Corresponding author at: Institute of Oceanology, Polish Academy of Sciences, Powstańców Warszawy 55, 81-712 Sopot, Poland. Tel.: (+48 58) 73 11 821; fax: (+48 58) 551 21 30.
E-mail address: gosiak@iopan.gda.pl (M. Cisek).
Peer review under the responsibility of Institute of Oceanology of the Polish Academy of Sciences.

Production and hosting by Elsevier

http://dx.doi.org/10.1016/j.oceano.2017.04.005

dominated by sea salt. This phenomenon is most significant in the summer due to broken sea ice (Quinn et al., 2007; Tomasi et al., 2007).

In mesoscale, the advection of anthropogenic aerosols, biomass burning, dust and volcanic aerosols from lower latitudes is significant and has a strong impact on the aerosol load in the Arctic (Generoso et al., 2007; Hirdman et al., 2010; Law and Stohl, 2007; Stohl, 2006; Tomasi et al., 2007, 2015; Treffeisen et al., 2011). In the winter and spring, conditions are best for long-range transport of aerosols and their gaseous precursors. This is due to the southward shift of the polar front, which facilitates the advection of polluted air from mid-latitudes (mainly from Europe and Asia). The effectiveness of the transport of aerosols and their gaseous precursors is additionally enhanced by a stable atmosphere and relatively low scavenging by clouds and precipitation (Quinn et al., 2007).

A potential effect of the increased concentrations of greenhouse gases in the atmosphere is manifested in the 0.6°C rise of the global mean surface temperature since the late 19th century (Nicholls et al., 1996). On a regional scale, the effects such a temperature increase has on precipitation, winds, cloud cover, etc. are not easy to describe (Gjelten et al., 2016), however, the majority of global circulation models show a poleward amplification of climate signals. Such changes result in a warming climate, which may be manifested in the polar regions, through a significant increase in climate variability and increasingly extreme weather situations, deeper cyclones, stronger seasonal cycles and higher precipitation. Until not long ago, no significant surface temperature trends have been observed in Svalbard, while the precipitation level has increased by as much as 25% since the beginning of the XX century (Førland et al., 1997). However, Maturilli et al. (2013, 2015) proved a decadal trend in surface temperature on a level of 1.35°K and 1.3°K.

On a smaller, spatial scale, measurements of wind speed and direction in the Arctic are rarely representative for larger areas surrounding the measurement stations. Many research stations in the Svalbard region have their own, locally typical wind regimes (Mazzola et al., 2012; Rozwadowska et al., 2010; Tomasi et al., 2007). One of the most important issues in the Svalbard fjords is the effect of local orography, which is often manifested by the wind channelling along the fjord axis (Argentini et al., 2003; Beine et al., 2001; Førland et al., 1997; Hanssen-Bauer et al., 1990; Hartmann et al., 1999). Hanssen-Bauer et al. (1990) reported that wind directions along the fjord axis dominate at all Svalbard stations. Additionally, other types of winds such as fens and downfall winds as well as local circulations of the breeze type are observed and they result from horizontal nonuniformity of temperature.

The climatology studies of the Ny-Ålesund and Kongsfjorden areas carried out by Esau and Repina (2012), Hanssen-Bauer et al. (1990) and Maturilli et al. (2013) confirm that for Kongsfjorden, surface winds usually blow along the axis of the fjord. Other types of winds, such as fen and katabatic winds also influence local wind climatology. However, Esau and Repina (2012), using an eddy-resolving model, proved that thermal land-sea breeze circulation is more significant than katabatic winds in Ny-Ålesund (Kongsfjorden). The same was reported by Cisek et al. (unpublished data). They also observed that this effect is true for the entire archipelago, including Hornsund in the south.

2. Study description

The studies were carried out in the area of Kongsfjorden and in Ny-Ålesund itself during the iAREA 2014 (Impact of Absorbing Aerosols on radiating forcing in the European Arctic (iAREA)) campaign which took place in Svalbard between 15 March and 4 May 2014. The iAREA project (http://www.igf.fuw.edu.pl/iAREA) is a part of the Polish-Norwegian Research Programme, and has been realized between 2013 and 2016. For the purpose of this paper, the authors present data from the measurements taken on 6 April 2014 only (Fig. 1).

On 6 April 2014 observations started at 8:55 UTC near the Alfred Wegener Institute (AWI) laboratory in the research

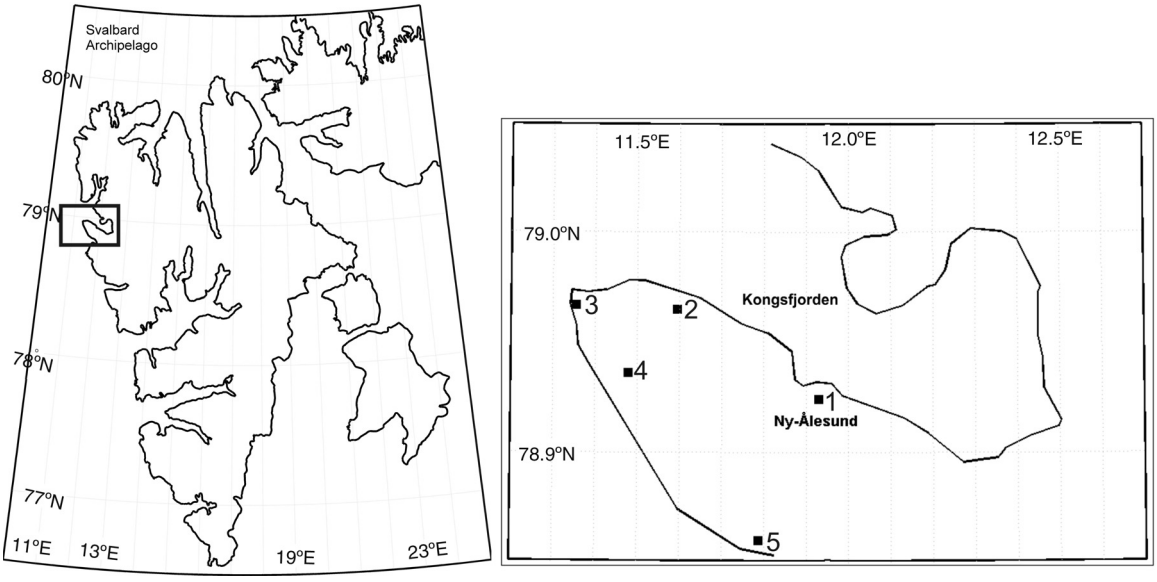

Figure 1 Location of the study area and measurement points in the Kongsfjorden.

village (78.92N, 11.92E). Data collection continued in that location until 10:30 UTC. Then, using a snowmobile, the research team moved north-west along the fjord. Measurements were also taken during relocation. Observations at the fjord opening (78.96N, 11.33E) started at 12:00 and lasted until 12:27 UTC. The subsequent observations were made on the outer side of the fjord, on the other side of the mountains. The very last two measurements were taken in the fjord again at 13:43 UTC. The rationale for such a measurement regime was to prove that breeze circulation is observed in the area and that it has an impact on local AOD levels.

The measurements were taken with two Microtops II sunphotometers (instruments No. 14475 and 15613). The Microtops II sunphotometer (produced by Solar Light Company USA) is a hand-held instrument for measuring Aerosol Optical Depth, water vapor column and direct irradiance at all selected wavelengths. The device is equipped with five wavelength channels. The measurement procedure involves a quick (c. 10 s) scan of a vertical column of the atmosphere. The full specifics regarding the Microtops II sunphotometer and the Langley calibration technique used by the authors have been described in Markowicz et al. (2012), Morys et al. (2001), Strzalkowska et al. (2014), Zielinski et al. (2012).

Aerosol Optical Depth, a dimensionless, wavelength dependent parameter which refers to the reduction of the amount of direct sunlight passing through the atmosphere. It is a function of the concentration of particles, their size distribution and chemical composition. AOD values change with the change of altitude (Smirnov et al., 2009; Strzalkowska et al., 2014; Zawadzka et al., 2014; Zielinski and Zielinski, 2002). The wavelength dependence of Aerosol Optical Depth can be expressed using an empirical formula described by Ängström as follows (Carlund et al., 2005; Eck et al., 1999; Smirnov et al., 1994; Weller and Leiterer, 1988):

$$\mathrm{AOD} = \beta \times \lambda^{-\alpha}. \quad (1)$$

The β coefficient characterizes the degree of atmospheric turbidity due to aerosols and is equal to the AOD for λ = 1 μm. The Ängström Exponent (α) is dimensionless parameter allowing to estimate the aerosol size distribution and is calculated from a minimum of two wavelengths and is calculated from the following formula:

$$\alpha(\lambda_1, \lambda_2) = -\frac{\ln \mathrm{AOD}(\lambda_1) - \ln \mathrm{AOD}(\lambda_2)}{\ln\lambda_1 - \ln\lambda_2}. \quad (2)$$

During our studies, the Microtops II measurements were taken in a series of five "shots". Sets of 5 scans with the smallest standard deviation have been used in data processing. The baud rate of each instrument was set at 32, which allowed the data collection frequency to meet the NASA AERONET standards. Further improvement of the data quality involved the elimination of cloud contamination. This was achieved through a visual inspection of sky conditions during the measurements and the analyses of satellite images.

3. Results and discussion

As a result of our experiment, we obtained a set of varied AOD values. These variations were found to be correlated with the distance from the open sea. The first step in our analyses regards the meteorological situation in the studied region. Fig. 2 shows a local wind rose for (a) Ny-Ålesund station for years 1992–2013 and (b) large-scale wind rose (from NCEP/NCAR reanalysis) interpolated for the Ny-Ålesund station for years 1992–2013.

The presented wind roses show that the phenomenon of wind tunnelling along the fjord axis is the most significant process controlling local wind directions in Kongsfjorden. Local wind frequencies are qualitatively different from large-scale winds calculated in the reanalysis, concentrating along the fjord axis. Maturilli et al. (2013) conducted a

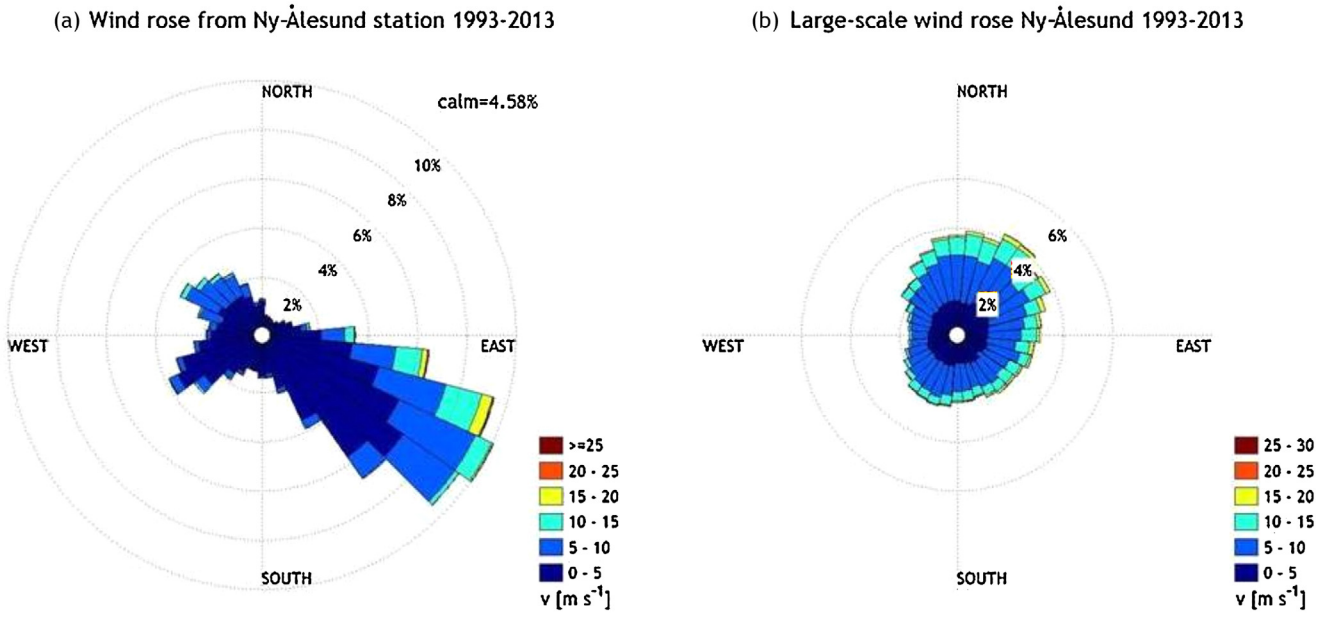

Figure 2 The local wind rose (a) and the large-scale wind rose (b) (from NCEP/NCAR reanalysis) interpolated for the Ny-Ålesund station for years 1992–2013.

Table 1 Averaged, daily wind speed and direction from measurement stations over Spitsbergen on 6 April 2014.

Station	Wind direction [°]			Average wind Speed [m s^{-1}]
	06 UTC	12 UTC	18 UTC	
Hornsund	46	87	48	3.3
Sveagruva	0	57	360	0.8
Ny-Ålesund	143	176	137	2.8
Svalbard Lufthavn	121	117	120	3.6
Pyramiden	262	285	339	2.1
Verlegenhuken	347	333	351	5.6

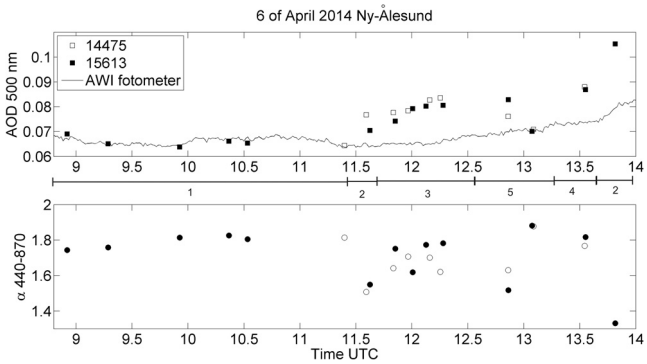

Figure 3 AOD values measured with two Microtops II sunphotometers on 6 April 2014 during the research trip in the Kongsfjorden area. The line in the middle describes consecutive measurement points, from 1 to 5.

long-term analysis of surface meteorology in Ny-Ålesund. The monthly, two-dimensional frequency distribution of wind direction presented by these authors confirms our findings, i.e. that the main wind direction in the area is from the east/south-east throughout the entire year and these conditions are very prominent in April (Maturilli et al., 2013). However, on 6 April 2014, wind situation over Spitsbergen, based on data collected from various stations, looked as presented in Table 1. Wind patterns show eastern direction component.

The results of the AOD measurements during the research trip in the area of Kongsfjorden on 6 April 2014 are presented in Fig. 3.

The measurements were taken using two Microtops II sunphotometers and they have been compared with the results from the AWI sunphotometer located at the AWI laboratory (78.92N, 11.92E). Data collection started at 8:55 UTC in Ny-Ålesund and ended at 13:43 UTC, also in Ny-Ålesund. The AOD values at the beginning of the study were low (below 0.07) for all three instruments. However, the values obtained from the AWI sunphotometer remained stable for a majority of the study period, slightly increasing (to a c. of 0.082) at the end of the study. In the case of the Microtops II measurements taken in different locations on the way to the fjord opening, the AOD values increased to a c. 0.08 close to the fjord opening, reaching the final value of 0.105 when the sunphotometers were taking measurements at the fjord opening, towards the open sea. The Ängström Exponent values remained stable during the entire study period at a level between 1.5 and 1.8, which indicates the presence of relatively small particles in the air and no advection of any other types of particles into the study area.

The spatial picture of the AOD situation on 6 April 2014 in the Svalbard region has been obtained from the NAAPS and MACC models. Fig. 4 presents the Total Optical Depth for 6 April for the entire Arctic obtained from the NAAPS model (Navy Aerosol Analysis and Prediction System, Christensen, 1997; Witek et al., 2007).

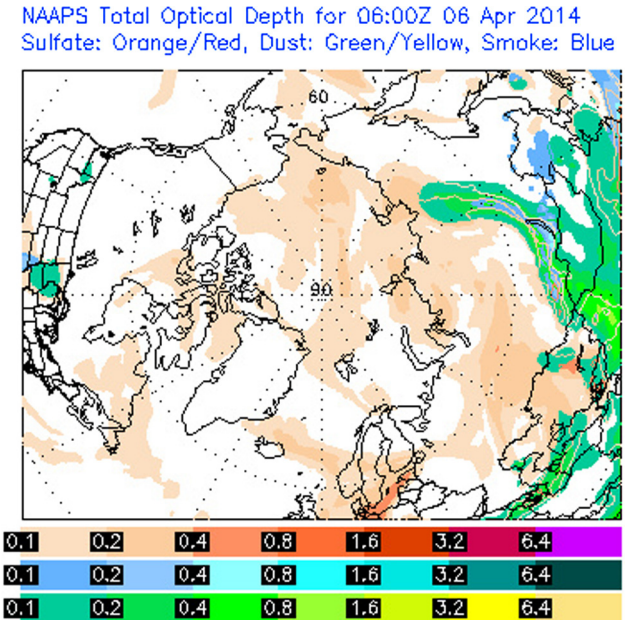

Figure 4 NAAPS derived Total Optical Depth at 06:00 on 6 April 2014 for the Arctic.

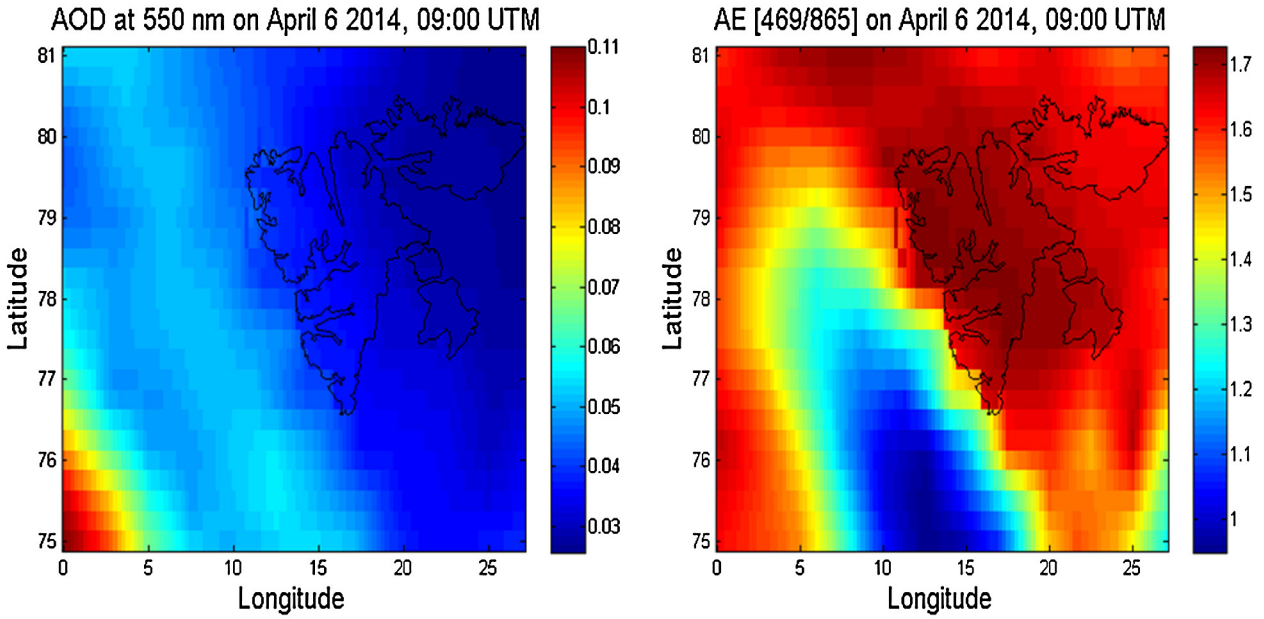

Figure 5 AOD (550 nm) and Ängström Exponent (469/865 nm) over Svalbard at 9:00 UTC on 6 April 2014 modelled using the MACC II system (http://www.gmes-atmosphere.eu).

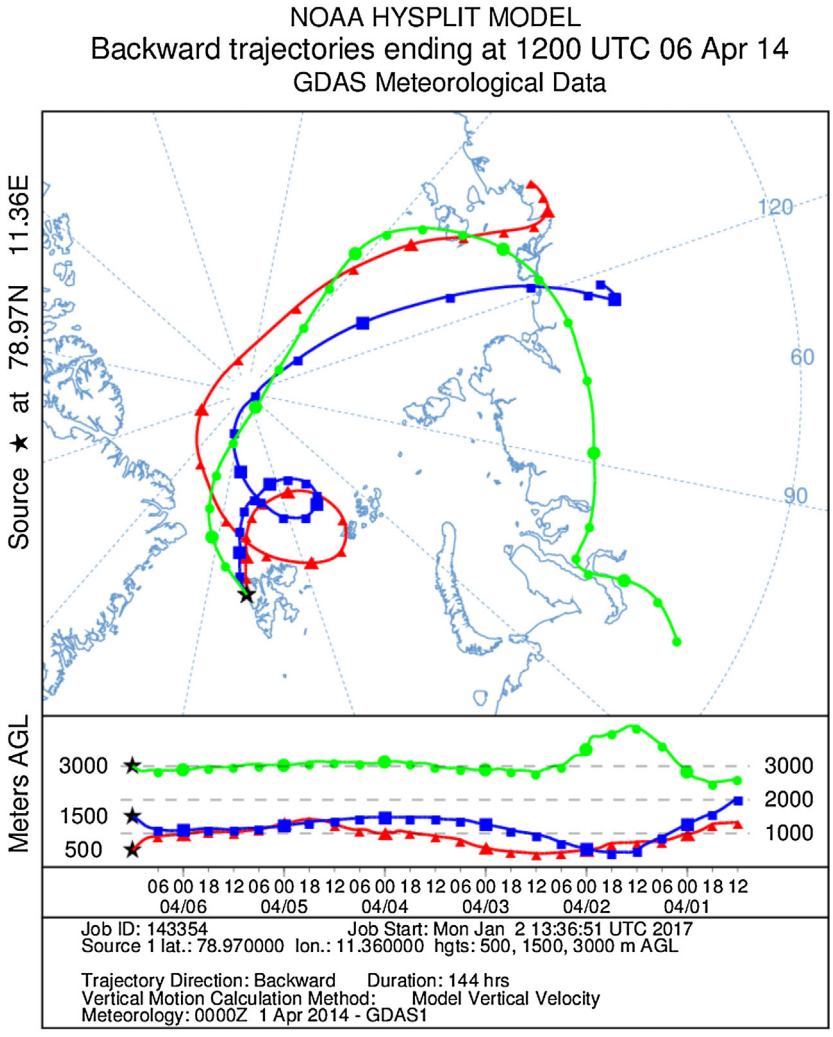

Figure 6 144-h air mass back trajectories obtained from the NOAA HYSPLIT model for 6 April 2014 at 12:00 UTC.

Fig. 4 presents the background situation of air in the Arctic and is in good agreement with the results of the sunphotometer measurements. The picture shows a slightly polluted aerosol situation over the vast area of the Arctic, including the Svalbard region. The majority of the region shows total optical depth values around 0.1 up to 0.2. Higher values (c. 0.4—0.8) are observed over Asia and at higher latitudes in Siberia, these are related to dust plumes. In the marine area of the Arctic some sulfate levels are observed which increase the optical depth to around 0.1—0.2, while off the western coast of Svalbard, these values are roughly around 0.1 and below. Even lower values have been obtained from reanalysis of AOD at 550 nm over the Svalbard region using the Monitoring Atmospheric Composition and Climate-Interim Implementation system (MACC-II) (Fig. 5).

Both graphs have been calculated for 0.25° per pixel at 9:00 UTC. Unfortunately, it is impossible to calculate these values at noon, however, all values before 9:00 UTC and at 3:00 p.m. UTC are consistent on 6 April 2014. The AOD values are in agreement with those obtained from the NAAPS model and those from the Microtops II sunphotometer measurements (Fig. 3). They range from c. 0.03 to 0.06. Additionally, the Ängström Exponent values are comparable with those from Fig. 3. They indicate the presence of mostly smaller particles in the atmosphere. It is also clear that higher values of AOD (reaching 0.07) are observed to the west of the archipelago and the values decrease eastward.

The meteorological situation over this period of time in the Svalbard region explains such a situation. Fig. 6 shows 144-h air mass back trajectories obtained from the NOAA HYSPLIT model for 6 April 2014 at 12:00 UTC.

The air mass back trajectories clearly show that on 6 April air masses were advected to the study area from over the clean Arctic region at all three altitudes above sea level. On the western side of Svalbard, they arrived in the Kongsfjorden area from over the open sea. The same pattern was observed for 4 and 5 April 2014. The NOAA obtained picture of the meteorological situation in the Svalbard region on 6 April 2014 shows wind direction at 10 m a.s.l. and air pressure changes (Fig. 7).

The situation presented in Fig. 7 indicates that the Svalbard archipelago creates a rather unique conditions in terms of wind direction patterns. In the entire region winds blew mostly from the western direction, however, over Svalbard, especially on its western side, the wind pattern was slightly different and turned from the north-west towards the north-east. This was due to a temperature difference between the cold land of the archipelago and the warm water west of the islands. This difference caused a mesoscale distortion of the pressure field in the area of the archipelago.

The observed changes in AOD relative to the distance from the open sea can be explained by greater aerosol concentration over the sea (Fig. 8).

The fact that the AOD variations had been observed at small distance changes confirms the presence of a pronounced barrier which distinguishes two air spaces with different aerosol concentrations. In our opinion, this barrier was simply a border of a breeze-like front, which was connected with convection resulting from the temperature differences between the much warmer water and colder island area. In order to verify this hypothesis, we checked if our

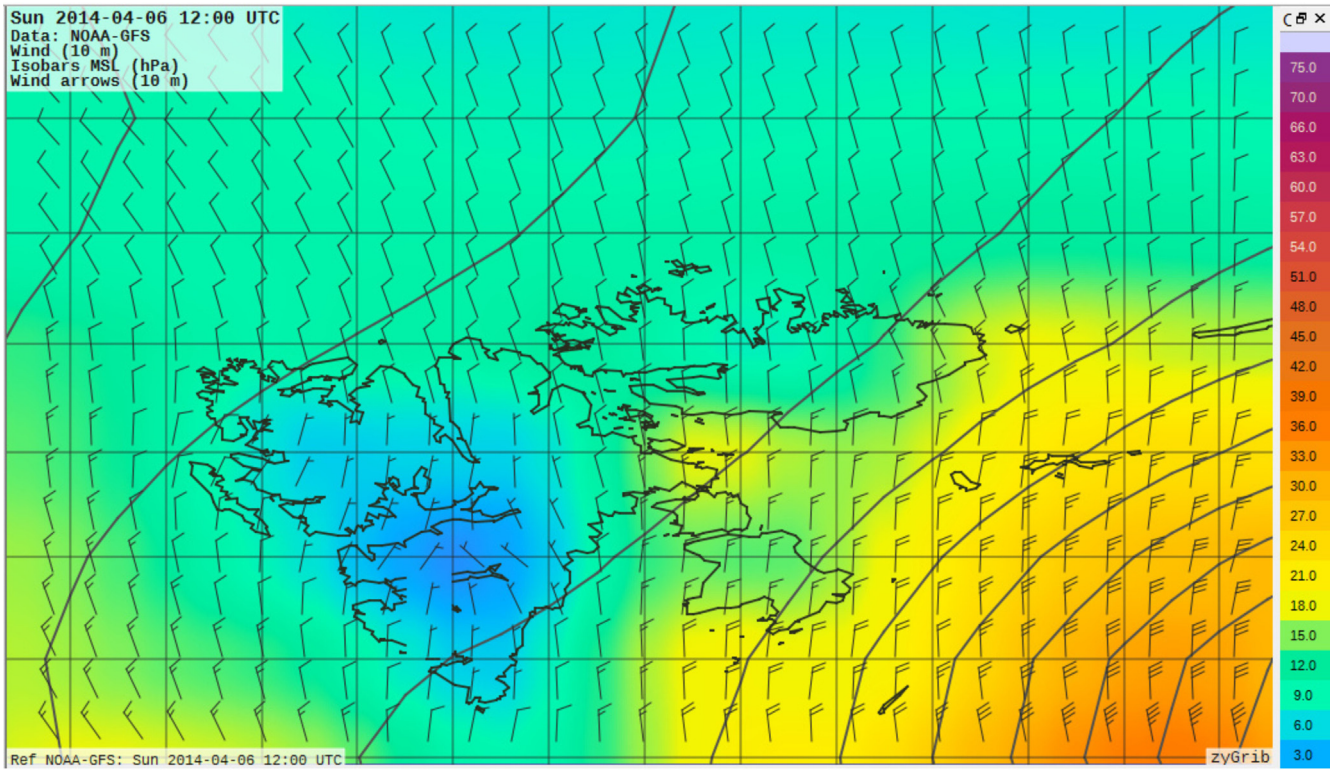

Figure 7 The NOAA — GFS generated wind direction patterns at 12:00 UTC on 6 April 2014 in the Svalbard region.

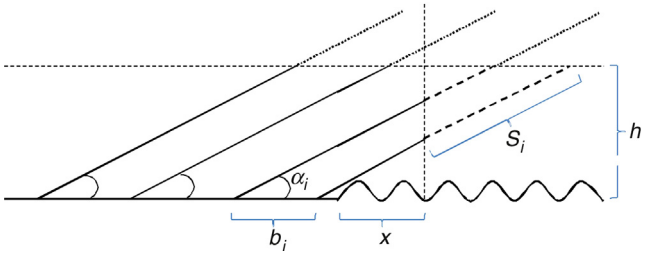

Figure 8 A conceptual picture of geometric assumptions for the result analyses. h denotes height of a breeze front a.s.l., S_i is a length of optical path through layer with higher aerosol concentration, b_i denotes distance between measurement points, while letter x denotes distance between the breeze front and the measurement point closest to the sea, and α_i denotes an angle between measurement path and surface.

results could be explained using the measurement through a layer with a higher aerosol concentration (S_i). The vertical dashed line is the breeze front and to the right (over the sea) the aerosol concentration is higher. The letters b_i denote the distance between measurement points, while the letter x denotes the distance between the breeze front and the measurement point closest to the sea. Despite the fact that we analyzed a 3D case, we decided to present the case study in this 2D form to ensure a clear presentation of the case. Calculations of the S_i distance accounted not only for angle alpha (Solar angle) but also the angles between the breeze front plane and the N–S direction (γ), and the hour angle (β_i). Therefore, the following formula was applied in our calculations:

$$S_i = \frac{h}{\sin\alpha_i} - \frac{x + b_i}{\sin(\beta_i + \gamma)\cos\alpha_i}. \quad (3)$$

During the study time, the increased wind velocity and flow structure were governed by a deep low-pressure system over the Bear Island. Fig. 9 shows vertical changes of air pressure and temperature on 6 April 2014 in Ny-Ålesund.

The radio sounding results show no atmospheric inversions up to c. 8 km a.s.l., and thus we assumed the top vertical limit in the further considerations at a level of 8 km a.s.l. Distance x was derived from the equation for S_i and we found the x value to be x = 5.7 km, which is in agreement with our estimates for the distance between the measurement point and the open sea. Following the assumption that the front plane is parallel to the western coast of the island, we assumed the γ angle to be 20°. The S_i values calculated from Eq. (3) were further correlated with the AOD values at a particular measurement point and the measurements in Ny-Ålesund. The results of such correlations are presented in Fig. 10.

This figure reveals that the AOD changes are correlated with distance S_i, at a statistically significant level, i.e. 0.613. Such a result is satisfactory since the geometry of the front, which prevented aerosol advection towards the island, has been simplified. In reality, it is not a vertical wall which does not change with time. In our opinion, these results confirm the hypothesis that the decreased levels of aerosol concentration inland, on that particular day, result from a mesoscale distortion of the pressure field, caused by a difference in temperatures between cold land and warm waters of the West Spitsbergen Current west of Svalbard.

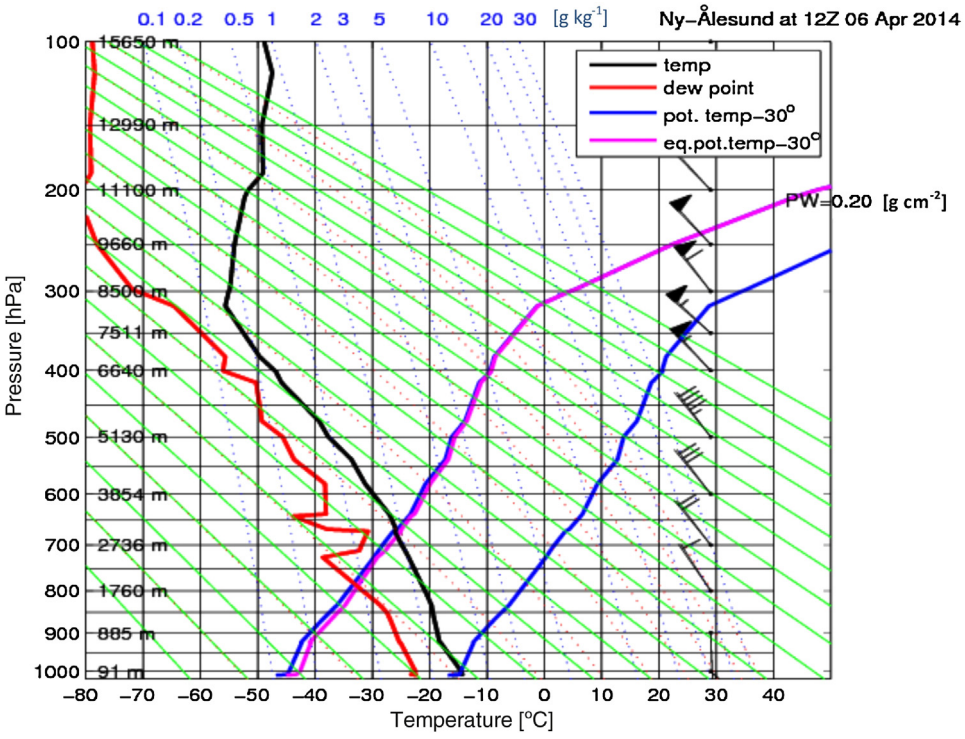

Figure 9 Vertical profile of air pressure and temperature provided by radio sounding in Ny-Ålesund at 12:00 UTC on 6 April 2014.

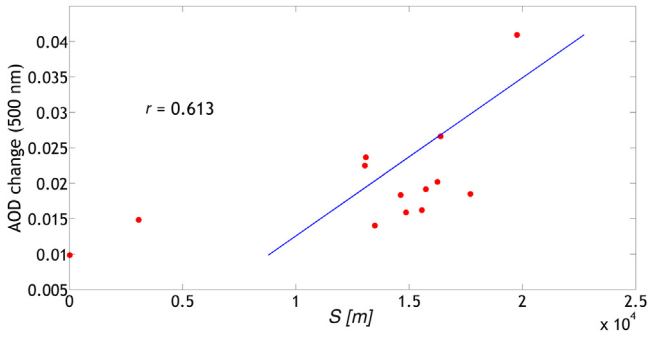

Figure 10 AOD changes versus distance during the sunphotometer study on 6 April 2014.

4. Conclusions

Firstly, these surprising changes of AOD values with the distance from the open sea in the area of Kongsfjorden are in good agreement with the model calculations. The authors are aware of the fact that the data set is not sufficient enough to provide a sound statistical analysis, thus the conclusions of the present study cannot be far-reaching. The described result is presented in a careful way. We realize that a local phenomenon of katabatic winds in one relatively small fjord cannot significantly influence AOD, or its influence is so small that it is not measurable (the impact is smaller than the measurement accuracy). This is clear from the comparison of the AOD data collected at sea level and at the Zeppelin Station (c. 450 m a.s.l). The air is so clean in the area that extinction at several 100 m a.s.l. did not show measurable values. Additionally, radio sounding results show no atmospheric inversions up to c. 8 km a.s.l. Such differences in these optical values between Ny-Ålesund and the fjord opening were most likely a result of the temperature differences between the cold archipelago and the warm waters west of the islands. These differences caused a mesoscale distortion of the pressure field in the entire archipelago area. This phenomenon should be taken into consideration while planning, and further analyzing AOD changes in this area.

Acknowledgments

The authors would like to acknowledge the support of the Polish-Norwegian Research Programme operated by the National Centre for Research and Development under the Norwegian Financial Mechanism 2009—2014 under Project Contract No. Pol-Nor/196911/38/2013 and also project KNOW, Leading National Research Centre received by the Centre for Polar Studies for the period 2014—2018 established by regulation No. 152 (2013, Nov 14) of the Rector of the University of Silesia.

This study also has been supported by funds from the GAME "Growing of Marine Arctic Ecosystem" project, funded by Narodowe Centrum Nauki grant DEC-2012/04/A/NZ8/00661.

The authors would also like to thank D. Westphal from the Naval Research Laboratory in Monterey for providing the NAAPS model input (http://www.nrlmry.navy.mil/aerosol/), and to acknowledge the MACC-II project, funded by the European Union under the 7th Framework Programme FP7 THEME [SPA.2011.1.5-02] under grant agreement no. 283576 for the provided data.

References

Argentini, S., Viola, A.P., Mastrantonio, G., Maurizi, A., Georgiadis, T., Nardino, M., 2003. Characteristics of the boundary layer at Ny-Ålesund in the Arctic during the ARTIST field experiment. Ann. Geofis. 46 (2), 185—196.

Beine, H.J., Argentini, S., Maurizi, A., Mastrantonio, G., Viola, A., 2001. The local wind field at Ny-Ålesund and the Zeppelin mountain at Svalbard. Meteorol. Atmos. Phys. 78 (1—2), 107—113.

Carlund, T., Hakansson, B., Land, P., 2005. Aerosol optical depth over the Baltic Sea derived from AERONET and SeaWiFS measurement. Int. J. Remote Sens. 26 (2), 233—245.

Christensen, J.H., 1997. The Danish Eulerian hemispheric model — a three-dimensional air pollution model used for the Arctic. Atmos. Environ. 31 (24), 4169—4191, http://dx.doi.org/10.1016/S1352-2310(97)00264-1.

Eck, T.F., Holben, B.N., Reid, J.S., Dubovik, O., Smirnov, A., O'Neill, N.T., Slutsker, I., Kinne, S., 1999. Wavelength dependence of the optical depth of biomass burning, urban, and desert dust aerosols. J. Geophys. Res. 104, http://dx.doi.org/10.1029/1999JD900923.

Engvall, A.-C., Krejci, R., Ström, J., Treffeisen, R., Scheele, R., Hermansenand, O., Paatero, J., 2008. Changes in aerosol properties during spring-summer period in the Arctic troposphere. Atmos. Chem. Phys. 8 (3), 445—462.

Esau, I., Repina, I., 2012. Wind climate in Kongsfjorden, Svalbard, and attribution of leading wind driving mechanisms through turbulence-resolving simulations. Adv. Meteorol. 568454, 16 pp, http://dx.doi.org/10.1155/2012/568454.

Førland, E.J., Hansen-Bauer, I., Nordli, P.Ø., 1997. Climate Statistics and Long-term Series of Temperature and Precipitation at Svalbard and Jan Mayen. Den Norske Meteorologiske Institutt (DNMI) Rep. 21/97 KLIMA, Oslo, Norway.

Generoso, S., Bréon, F.-M., Chevallier, F., Balkanski, Y., Schulz, M., Bey, I., 2007. Assimilation of POLDER aerosol optical thickness into the LMDz-INCA model: implications for the Arctic aerosol burden. J. Geophys. Res. 112 (D2), 2156—2202, http://dx.doi.org/10.1029/2005JD006954.

Gjelten, H.M., Nordli, O., Isaksen, K., Førland, E.J., Sviashchennikov, P.N., Wyszynski, P., Prokhorova, U.V., Przybylak, R., Ivanov, B.V., Urazgildeeva, A., 2016. Air temperature variations and gradients along the coast and fjords of western Spitsbergen. Pol. Polar Res. 38 (1), 41—60.

Hanssen-Bauer, I., Solas, M.K., Stefensen, E.L., 1990. The Climate of Spitsbergen. Den Norske Meteorologiske Institutt (DMNI) Rep. 39/90 KLIMA, Oslo, Norway.

Hartmann, J., Albers, F., Argentini, S., Bochert, A., Bonafe, U., Cohrs, W., Conidi, A., Freese, D., Georgiadis, T., Ippoliti, A., Kaleschke, L., Lüpkes, C., Maixner, U., Mastrantonio, G., Ravegnani, F., Reuter, A., Trivellone, G., Viola, A., 1999. Arctic radiation and turbulence interaction study (ARTIST). Report on Polar Research 305/1999. Alfred Wegener Institute for Polar and Marine Research, Bremerhaven, 81 pp.

Herber, A., Thomason, L.W., Gernandt, H., Leiterer, U., Nagel, D., Schulz, K.H., Kaptur, J., Albrecht, T., Notholt, J., 2002. Continuous day and night aerosol optical depth observations in the Arctic between 1991 and 1999. J. Geophys. Res. 107 (D10), 4097, http://dx.doi.org/10.1029/2001JD000536.

Hirdman, D., Burkhart, J.F., Sodemann, H., Eckhardt, S., Jefferson, A., Quinn, P.K., Sharma, S., Strom, J., Stohl, A., 2010. Long-term trends of black carbon and sulphate aerosol in the Arctic: changes in atmospheric transport and source region emissions. Atmos. Chem. Phys. 10 (19), 9351—9368, http://dx.doi.org/10.5194/acp-10-9351-2010.

Law, K.S., Stohl, A., 2007. Long-term trends of black carbon and sulphate aerosol in the Arctic: changes in atmospheric transport and source region emissions. Science 315 (5818), 1537—1540, http://dx.doi.org/10.1126/science.1137695.

Markowicz, K.M., Zielinski, T., Blindheim, S., Gausa, M., Jagodnicka, A.K., Kardas, A.E., Kumala, W., Malinowski, S., Posyniak, M., Petelski, T., Stacewicz, T., 2012. Study of vertical structure of aerosol optical properties by sun photometers and ceilometer during macron campaign in 2007. Acta Geophys. 60 (5), 1308—1337, http://dx.doi.org/10.2478/s11600-011-0056-7.

Maturilli, M., Herber, A., Konig-Langlo, G., 2013. Climatology and time series of surface meteorology in Ny-Ålesund, Svalbard. Earth Syst. Sci. Data 5 (1), 155—163, http://dx.doi.org/10.5194/essd-5-155-2013.

Maturilli, M., Herber, A., König-Langlo, G., 2015. Surface radiation climatology for Ny-Ålesund, Svalbard (78.9°N), basic observations for trend detection. Theor. Appl. Climatol. 120 (1), 331—339, http://dx.doi.org/10.1007/s00704-014-1173-4.

Mazzola, M., Stone, R.S., Herber, A., Tomasi, C., Lupi, A., Vitale, V., Lanconelli, C., Toledano, C., Cachorro, V.E., O'Neill, N.T., Shiobara, M., Aaltonen, V., Stebel, K., Zielinski, T., Petelski, T., Ortiz de Galisteo, J.P., Torres, B., Berjon, A., Goloub, P., Li, Z., Blarel, L., Abboudm, I., Cuevas, E., Stock, M., Schulz, K.-H., Virkkula, A., 2012. Evaluation of sun photometer capabilities for retrievals of aerosol optical depth at high latitudes: the POLAR-AOD intercomparison campaigns. Atmos. Environ. 52, 4—17.

Morys, M., Mims III, F.M., Hagerup, S., Anderson, S.E., Baker, A., Kia, J., Walkup, T., 2001. Design, calibration, and performance of MICROTOPS II handheld ozone monitor and Sun photometer. J. Geophys. Res.-Atmos. 106 (D13), 2156—2202.

Nicholls, N., Gruza, G.V., Jouzel, J., Karl, T.R., Ogallo, L.A., Parker, D. E., 1996. Observed climate variability and change. In: Houghton, J.T., Filho, L.G.M., Callander, B.A., Harris, N., Kattenberg, A., Maskell, K. (Eds.), Climate Change 1995: The Science of Climate Change. Cambridge Univ. Press, Cambridge, UK, 133—192.

Quinn, P.K., Shaw, G., Andrews, E., Dutton, E.G., Ruoho-Airola, T., Gong, S.L., 2007. Arctic haze: current trends and knowledge gaps. Tellus B 59 (1), 99—114.

Rozwadowska, A., Zielinski, T., Petelski, T., Sobolewski, P., 2010. Cluster analysis of the impact of air back-trajectories on aerosol optical properties at Hornsund, Spitsbergen. Atmos. Chem. Phys. 10 (3), 877—893, http://dx.doi.org/10.5194/acp-10-877-2010.

Smirnov, A., Royer, A., O'Neill, N., Tarussov, A., 1994. A study of the link between synoptic air mass type and atmospheric optical parameters. J. Geophys. Res. 99 (D10), 20967—20982.

Smirnov, A., Holben, B.N., Slutsker, I., Giles, D.M., McClain, C.R., Eck, T.F., Sakerin, S.M., Macke, A., Croot, P., Zibordi, G., Quinn, P. K., Sciare, J., Kinne, S., Harvey, M., Smyth, T.J., Piketh, S., Zielinski, T., Proshutinsky, A., Goes, J.I., Nelson, N.B., Larouche, P., Radionov, V.F., Goloub, P., Krishna Moorthy, K., Matarrese, R., Robertson, E.J., Jourdin, F., 2009. Maritime aerosol network as a component of aerosol robotic network. J. Geophys. Res. 114, 1—10, http://dx.doi.org/10.1029/2008JD011257.

Stohl, A., 2006. Characteristics of atmospheric transport into the Arctic troposphere. J. Geophys. Res.-Atmos. 111 (D11), D11306, http://dx.doi.org/10.1029/2005jd006888, 17 pp.

Stone, R.S., Sharma, S., Herber, A., Eleftheriadis, K., Nelson, D.W., 2014. A characterization of Arctic aerosols on the basis of aerosol optical depth and black carbon measurements. Elem. Sci. Anth. 2, 27, http://dx.doi.org/10.12952/journal.elementa.000027.

Strzalkowska, A., Makuch, P., Zawadzka, O., Pakszys, P., 2014. A modern approach to aerosol studies over the Baltic Sea. In: Zielinski, T., Pazdro, K., Dragan-Górska, A., Weydmann, A. (Eds.), Insights on Environmental Changes. Springer, Dordrecht, 49—64.

Tomasi, C., Kokhanovsky, A., Lupi, A., Ritter, C., Smirnov, A., O'Neill, N., Stone, R., Holben, B., Nyeki, S., Wehrli, C., Stohl, A., Mazzola, M., Lanconelli, Ch., Vitale, V., Stebel, K., Aaltonen, V., de Leeuw, G., Rodriguez, E., Herber, A.B., Radionov, V.F., Zielinski, T., Petelski, T., Sakerin, S.M., Kabanov, D.M., Xue, Y., Mei, L., Istomina, L., Wagener, R., McArthur, B., Sobolewski, P.S., Kivi, R., Courcoux, Y., Larouche, P., Broccardoz, S., Piketh, S.J., 2015. Aerosol remote sensing in polar regions. Earth-Sci. Rev. 140, 108—157.

Tomasi, C., Vitale, V., Lupi, A., Di Carmine, C., Campanelli, M., Herber, A., Treffeisen, R., Stone, R.S., Andrews, E., Sharma, S., Radionov, V., von Hoyningen-Huene, W., Stebel, K., Hansen, G.H., Myhre, C.L., Wehrli, C., Aaltonen, V., Lihavainen, H., Virkkula, A., Hillamo, R., Stroem, J., Toledano, C., Cachorro, V.E., Ortiz, P., de Frutos, A.M., Blindheim, S., Frioud, M., Gausa, M., Zielinski, T., Petelski, T., Yamanouchi, T., 2007. Aerosols in polar regions: a historical overview based on optical depth and in situ observations. J. Geophys. Res. 112 (D16), D16205, http://dx.doi.org/10.1029/2007JD008432, 28 pp.

Treffeisen, R., Herber, A., Ström, J., Shiobara, M., Yamanouchi, T., Yamagata, S., Holmén, K., Kriew, M., Schrems, O., 2011. Interpretation of Arctic aerosol properties using cluster analysis applied to observations in the Svalbard area. Tellus B 56 (5), 457—476, http://dx.doi.org/10.3402/tellusb.v56i5.16469.

Weller, M., Leiterer, V., 1988. Experimental data on spectral aerosol optical thickness and its global distribution. Beitr. Phys. Atmos. 61 (1), 1—9.

Witek, M.L., Flatau, P., Quinn, P., Westphal, D., 2007. Global sea-salt modeling: results and validation against multicampaign shipboard measurements. J. Geophys. Res. 112 (D8), D08215, http://dx.doi.org/10.1029/2006JD007779, 14 pp.

Zawadzka, O., Makuch, P., Markowicz, K.M., Zielinski, T., Petelski, T., Ulevicius, V., Strzalkowska, A., Rozwadowska, A., Gutowska, D., 2014. Studies of aerosol optical depth with use of Microtops sun photometers and MODIS detectors in the coastal areas of the Baltic Sea. Acta Geophys. 62 (2), 400—422, http://dx.doi.org/10.2478/s11600-013-0182-5.

Zielinski, T., Petelski, T., Makuch, P., Strzalkowska, A., Ponczkowska, A., Markowicz, K.M., Chourdakis, G., Georgoussis, G., Kratzer, S., 2012. Sudies of aerosols advected to coastal areas with use of remote techniques. Acta Geophys. 60 (5), 1359—1385, http://dx.doi.org/10.2478/s11600-011-0075-4.

Zielinski, T., Zielinski, A., 2002. Aerosol extinction and optical thickness in the atmosphere over the Baltic Sea determined with lidar. J. Aerosol Sci. 33 (6), 47—61.

Oceanologia (2017) 59, 431—444

Available online at www.sciencedirect.com

ScienceDirect

journal homepage: www.journals.elsevier.com/oceanologia/

ORIGINAL RESEARCH ARTICLE

Aerosol optical properties over Svalbard: a comparison between Ny-Ålesund and Hornsund

Paulina Pakszys *, **Tymon Zielinski**

Institute of Oceanology, Polish Academy of Sciences, Sopot, Poland

Received 30 August 2016; accepted 12 May 2017
Available online 22 June 2017

KEYWORDS
Arctic aerosols;
Optical properties;
Spitsbergen fjords;
Regional aerosol modifications;
CAMS model

Summary This paper presents the CAMS model based aerosol optical properties calculated for two Spitsbergen fjords, Kongsfjorden (Ny-Ålesund) and Hornsund (Polish Polar Station in Hornsund) measured between 2010 and 2015. A small decrease in Aerosol Optical Depth (AOD) is shown throughout the study period leading to an alteration of the state of the polar atmosphere. However, the potential differences observed between the stations were not statistically significant. While during the studied period no significant differences in chemical composition between the stations were observed, increasing mean values of Black Carbon (BC) were found to be associated with an increasing number of wild forest fires in remote areas producing smoke plumes, which are further transported over vast distances and reach Spitsbergen.

1. Introduction

It is an unquestionable fact that the Arctic climate is being transformed and as a result of these changes it is being warmed at a rate two to three times higher than the global average (ACIA, 2004; IPCC, 2013). The evidence of climate change can also be observed in the sea, in the reduction of the Arctic Ocean ice cover, in the melting of glaciers and permafrost, and in changes in the functioning of biotic elements. However, the atmosphere and its components play a crucial role in the changes in the Arctic system and the leading position in the context of climate response has been attributed to aerosols (Rodríguez et al., 2012). The Arctic area is very sensitive to any climate shifts due to its lack of

* Corresponding author at: Institute of Oceanology, Polish Academy of Sciences, Powstańców Warszawy 55, 81-712 Sopot, Poland. Tel.: +48 58 7311901.
E-mail address: pakszys@iopan.gda.pl (P. Pakszys).
Peer review under the responsibility of Institute of Oceanology of the Polish Academy of Sciences.

Production and hosting by Elsevier

http://dx.doi.org/10.1016/j.oceano.2017.05.002

local anthropogenic aerosol sources. Rapidly changing weather conditions, seasonal changes in solar radiation, surface albedo and the supply of polluted air masses from continental regions make the Arctic one of the more important targets of research on climate change (Kaufman et al., 2002; Nagel et al., 1998).

The highly variable distribution, chemical composition and concentration of aerosols have a strong impact on the distribution of the radiative balance of the Earth by modifying the amount of energy passing through the atmosphere (Charlson et al., 1992; Rozwadowska and Gorecka, 2012; Tomasi et al., 2007; Treffeisen et al., 2004). Thus, these small particles can significantly alter the state of the atmosphere both directly and indirectly.

The degree of climatic impact is related to the levels of aerosols originating from both marine and continental environments (the contents of which vary significantly) and depends on air mass sources and trajectories (Petelski et al., 2014). These aerosol types are, in general, poorly accounted for in climate models. It has been long established that better quantification methods of the radiative forcing of different types of aerosols are needed to improve the predictions of future climate changes (Brock et al., 2011). Improving our knowledge and understanding of atmospheric processes, including aerosols, has been the subject of interest of international research activities for decades Such research initiatives include, e.g. Aerosol Robotic Network — AERONET, Maritime Aerosol Network — MAN, The Polar Aerosol Optical Depth measurement network project — POLAR-AOD, Aerosol-Cloud Coupling And Climate Interactions in the Arctic — ACCACIA, Polar Study using Aircraft, Remote Sensing, Surface Measurements, and Models of Climate Chemistry, Aerosols, and Transport — POLARCAT, Impact of Absorbing aerosols on Radiative forcing in the European Arctic — iAREA.

The aerosol climate effect balances the surface-atmosphere radiation directly and indirectly by scattering and absorbing sunlight in the shortwave band. This is the intensity of sunlight scattered back to space, absorbed in the atmosphere and arriving to the surface (caused by natural and anthropogenic forces). In the Arctic, the direct effect usually leads to the warming of the atmosphere and cooling of the surface which depends on the amount of solar radiation passing through the atmosphere, on the properties of aerosol particles and also on the reflective state of the surface beneath. The warming effect in polar regions, mostly over ice and snow, causes a warming effect at the surface (caused by its absorption ability and high albedo, which can exceed 0.85 in visible spectroscopy (VIS)) (Engvall et al., 2008; Tomasi et al., 2007). The indirect effect results in cloud evolution patterns which alter the formation process of warm, ice and mixed-phase clouds increasing the number of droplets and the amount of ice particle concentration (Markowicz et al., 2012).

Since small particles scatter more light per mass unit and stay in the atmosphere longer than bigger particles, aerosol size distribution is another key climate criterion alongside aerosol chemical composition and particle size, which influences the number of cloud condensation nuclei.

Both properties (the chemical composition and particle size) together with the changing annual solar cycle and the diverse conditions of the boundary layers make the Arctic a very complicated system to study. Thus, it is crucial for us to understand and to describe the aerosol processes to be able to determine their properties, and therefore their impact on the climate (Stone et al., 2010).

Climate conditions of Spitsbergen are related to its location, i.e. the northern part of the north hemisphere, where both the Norwegian Current and West Spitsbergen Current have a strong influence on local temperatures causing moderate climate conditions. Cold polar air from the north and west (i.e. the high pressure systems around the Greenland and Polar regions) comes into contact with warm, wet marine air from the south (a low pressure system between Greenland and Svalbard) in the Arctic region (Rozwadowska et al., 2010; Treffeisen et al., 2007). Such conditions cause cyclonic circulations with fronts which are responsible for the formation of clouds, rains, and high speed winds. These are key elements which describe the changeable weather in the Spitsbergen region. Such changeability causes unique weather patterns to appear across various areas of the archipelago.

This paper attempts to identify changes in the Arctic atmosphere by determining the horizontal structure of physical, optical and chemical aerosol properties over Spitsbergen using the Copernicus Atmosphere Monitoring Service (CAMS) model reanalysis. It is an atmospheric composition global model, the European Union's flagship Earth-observation programme. The CAMS model is built by EU-funded Global Earth-system Monitoring using Space and in situ data (GEMS) and series of Monitoring atmospheric composition & climate (MACC) projects at European Centre for Medium-Range Weather Forecast (ECMWF) (Inness et al., 2013). Reanalysis of the Atmospheric Composition includes AOD and the particle chemical composition with the following elements: Black Carbon (BC), Organic Matter (OM), Sea Salt (SS), Sulfates (SU) and Dust (DU) at 550 nm (Morcrette et al., 2009).

Two locations were taken into consideration for the analyses of the aerosol properties. These are — Ny-Ålesund, in the north and Hornsund, in the south. Such a choice of geographical locations provides the right conditions to study how significantly different types of air masses over the study area influence aerosol characteristics.

2. Description of the study area

This paper focuses on the comparison of aerosol conditions in two Spitsbergen locations, Ny-Ålesund and Hornsund (Fig. 1).

Ny-Ålesund (NYA) is the northernmost research station located in Kongsfjorden, and thus it is surrounded by mountains and a tundra system. It hosts fifteen permanent research stations run by agencies from ten different countries, which concentrate their research on environmental sciences, mostly atmospheric. Hornsund (HOR), on the other hand, is located in the south of Spitsbergen, and the Polish Polar station, which provides all-year research facilities, is located there.

Such a choice of stations allows us to observe a variety of air masses in both study areas. Both stations conduct continuous aerosol measurements using ground based-techniques, which are common in the study of atmospheric pollutants, including aerosol particles. These are optical methods, which facilitate the collection of data from one

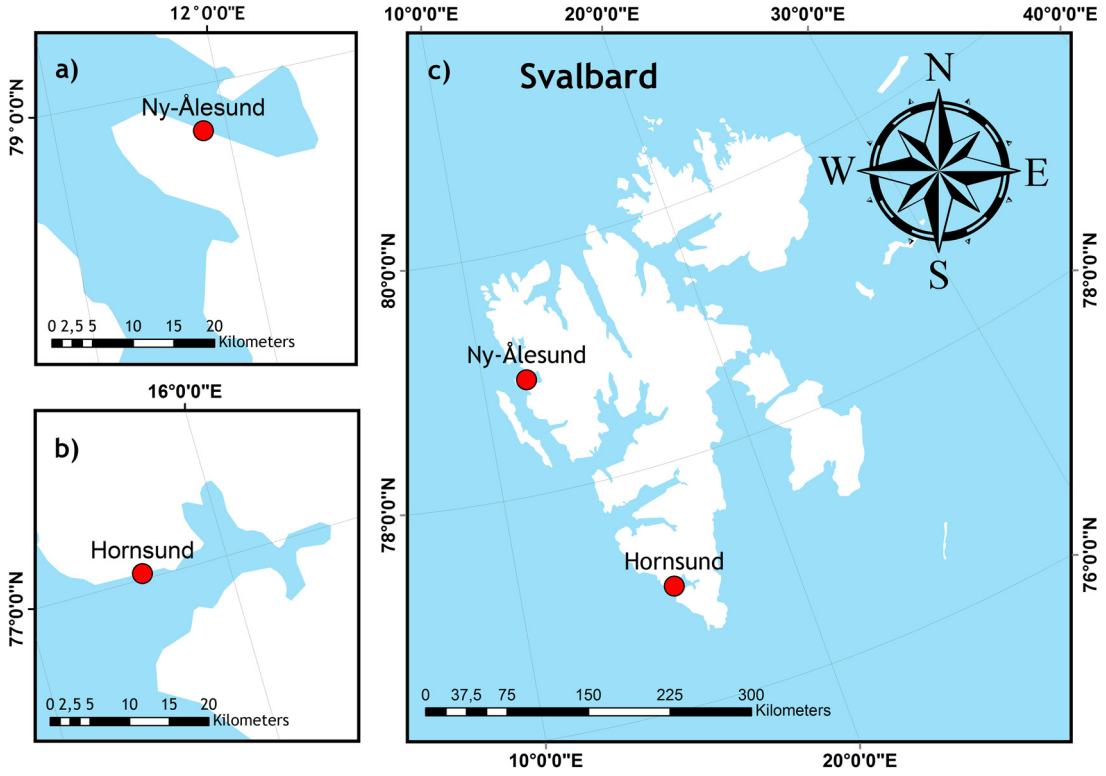

Figure 1 Location of Ny-Ålesund and Hornsund.

location or from a limited area (Dixon, 1998; Drollette, 2000; Labow et al., 1996; Smirnov et al., 2002) and thus, they are very useful in the study of particle optical properties, such as Aerosol Optical Depth (AOD), which is a crucial element in aerosol research (Dubovik et al., 2002; Markowicz et al., 2008; Mazzola et al., 2012; Zielinski, 2004; Zielinski et al., 2012). Satellite remote sensing also facilitates studies of spatial aerosol distribution over a study area, however, it requires the use of good aerosol models.

The comparison of aerosols at both locations for a period between 2010 and 2016 leads to the development of knowledge about temporal and spatial variability of Arctic aerosols through the use of the Copernicus Atmosphere Monitoring Service (CAMS) model reanalysis, which includes in situ datasets.

3. Methodology

Due to the uncertainties in emissions, transport and non-linear physical processes, the modelling and prediction of the state of aerosol particles includes a significant amount of uncertainties (e.g. radiative effects or cloud nuclei formation). Ground-based observation networks, complemented in recent years by satellite sensors which offer a more global view of aerosol distribution, have been crucial in improving our knowledge of this atmospheric component.

ECMWF has been committed to operate the Copernicus Atmosphere Monitoring Service (CAMS) and the Copernicus Climate Change Service (C3S) on behalf of the European Commission until the end of 2020. We used this model for our analyses of the results presented in this article. It includes the ECMWF Integrated Forecasting System (forward model) which was extended by modules of atmospheric chemistry, aerosols and greenhouse gases, and also a data-assimilation module (Bellouin et al., 2008). The forward modules use 12 prognostic variables (11 aerosol mass mixing ratios and one precursor — SO_2) and they include both the satellite and in situ data.

The initial physical parameterizations of aerosol particulate processes mostly used the aerosol approach established by the Laboratoire de Météorologie Dynamique general circulation model (LOA/LMD-Z model) (Boucher et al., 2002; Reddy et al., 2005). Natural particles such as mineral dust and sea salt are set with 3 sizes of bins and for dust, the bin limits are at 0.03, 0.55, 0.9, and 20 μm, while for sea salt — at 0.03, 0.5, 5 and 20 μm (Benedetti and Fisher, 2007).

Dust emissions are based on available characteristics such as winds at 10 m a.s.l., soil moisture, UltraViolet-Visible Spectroscopy (UV-VIS) of the surface albedo or a land area with vegetation during the snow-free conditions. Sea-salt emissions are described by using a source function based on works by Guelle et al. (2001) and Schulz et al. (2004). This approach involves wet sea-salt mass fluxes at 80% relative humidity to be integrated for the three size bins between 2 and 4 μm. Sources for the other aerosol types which are linked to emissions from domestic, industrial, power generation, transport and shipping activities, are taken from the SPEW (Speciated Particulate Emission Wizard; http://www.hiwater.org/spew.htm), and EDGAR (Emission Database for Global Atmospheric Research; http://edgar.jrc.ec.europa.eu/) annual- or monthly-mean climatologies. Emissions of OM, BC and SO_2 linked to fire emissions are obtained using the

GFAS (on MODIS) satellite observations of fire radiative power, as described in Kaiser et al. (2012). Removal processes are also included, and these are: dry deposition with turbulent transfer to the surface, gravitational settling, and wet deposition including rainout by large-scale and convective precipitation as well as wash-out of aerosols within and below clouds (Morcrette et al., 2011). Finally, effects of hygroscopy are described for OM and BC particles (Morcrette et al., 2011).

The CAMS reanalysis of reactive gases (Inness et al., 2013), aerosols and atmospheric composition reanalysis (covers tropospheric and stratospheric reactive gases and aerosols) as well as the meteorological fields are presented in one consistent data set. The meteorological observations assimilation is based on ECMWF RD setup, which include the satellites, sondes and surface measurements. The assimilated observation also includes AODs, recovered from the MODIS instruments onboard the Terra and Aqua satellites over the ocean and dark land surface. The assimilation in the CAMS system is based on satellite atmospheric composition retrievals. The advantages of that is, the subset of trace gases and total aerosol with sufficient accuracy is limited to the place of observations, while satellites cover almost the whole world. Each aerosol type is corrected in relation to the level of its original contribution to the total aerosol mass (Benedetti et al., 2009). These results have been validated by independent observations from the AErosol RObotic NETwork (AERONET).

At the latitude on which Svalbard lies, photometric studies are limited to spring-summer months, since the rest of the year (from late September to early March) is mostly dark or fully dark (polar night). The sunphotometer facilitates the collection of data on cloudless days to avoid cloud contamination. In cases when there are some scattered clouds present, an effort is made to keep at least an angular distance of 30° between the Sun and the closest cloud patch.

Observations are essential in the process of describing the ever changing components of the atmosphere and when it comes to aerosol characteristics, long-term observations are a necessity. In general, particulate optical properties are obtained using ground-based methods. The model database (set to the same parameters) is a supplementary set. This allows us to gather the elements needed to describe aerosol optical parameters, such as AOD and the Ångström Exponent (AE).

The Aerosol Optical Depth is a dimensionless, wavelength dependent parameter which refers to the weakening of direct sunlight passing through the atmosphere. It is a function of the concentration of particles, their size distribution and their chemical composition. AOD is a measure of the state and type of aerosol particles (e.g., urban haze, smoke particles, desert dust, sea salt), which are present in a column of air, measured over a distance between the instrument (Earth's surface) and the top of the atmosphere (WMO, 1994). Thus, the AOD is described as an integrated extinction coefficient τ over a vertical column of unit cross section (see formula (1)). The extinction coefficient is the fractional depletion of radiance per unit path length (also called attenuation, especially in reference to radar frequencies).

$$\mathrm{AOD} = \tau = \int_0^l \epsilon(\lambda, h)\, dh, \tag{1}$$

where ϵ is an extinction coefficient, λ is a wavelength, h is the height ("top") of the atmosphere.

For further interpretations, we used all available AODs from the CAMS model at the following wavelengths: 469, 550, 670, 865 and 1240 nanometers (nm), however, in further analyses we concentrated mostly on AODs at 550 nm.

The AE describes dominating particles in relation to their size. The size distribution of aerosols can be estimated from spectral aerosol optical depth, typically from 440 nm to 870 nm. The negative slope (or first derivative) of AOD with wavelengths in a logarithmic scale is known as the AE. Values of AE greater than 2.0 indicate the presence of fine mode particles (e.g., smoke particles and sulfates), while values of AE near zero indicate the presence of coarse mode particles such as desert dust (Eck et al., 1999). The coefficient characterizes the degree of atmospheric turbidity due to aerosols and is equal to the AOD for a wavelength (λ) equal to 1 μm. The AE is calculated from a minimum of two wavelengths using the following formula:

$$\mathrm{AE}(\lambda_1, \lambda_2) = \frac{\ln \mathrm{AOD}(\lambda_1) - \ln \mathrm{AOD}(\lambda_2)}{\ln \lambda_1 - \ln \lambda_2}. \tag{2}$$

Using the CAMS obtained AODs we calculated AE for two wavelengths: 469 nm and 865 nm, which is the closest proxy to the typical AEs analyzed by other researchers.

The data set was sequenced into analyses of weekly, monthly, seasonal and annual changes in horizontal direction. Distribution, identifying aerosol sources, partial chemical composition, types and size distribution were analyzed with the CAMS model and meteorological data.

Additionally, information on meteorological data (wind speed and direction) has been collected from the weather services of the World Meteorological Organization (WMO) for both stations: Hornsund (01003) and Ny-Ålesund (01007). Wind direction was divided into 16 cases (with a 22.5° step). The main direction, and monthly analyses for the period 2010–2015 are useful when connecting sources of aerosols and in determining local emissions.

4. Results and discussion

The Arctic presents particular challenges when assessing aerosol impact due to large variations in aerosol concentrations, and their varying chemical, physical and optical properties.

Polar aerosols were characterized by Tomasi et al. (2012), who presented a time series of AODs at a number of sites, for the period 1977–2010, including in Ny-Ålesund for the period of 1991–2010. Climatologically, AODs (500 nm) greater than 0.1 during the spring and very low AODs during the summer months persist over the Arctic, and unusually high values of AODs are typically not observed during Arctic summers. Diurnal average AODs (500 nm) varied from 0.12 to 0.25 during the winter-spring time (result of Arctic Haze events) (Rahul et al., 2014). Herber et al. (2002) reported values of AOD (532 nm) during the summer at 0.046 ± 0.012, with over 90% of AODs (532 nm) between 0.022 and 0.070 in summertime. Therefore, the winter-spring AODs of over 0.08 are relatively high due to Arctic Haze episodes, and those below 0.065 characterize clean-air cases. Analyses of time series of AOD measurements carried out in Ny-Ålesund

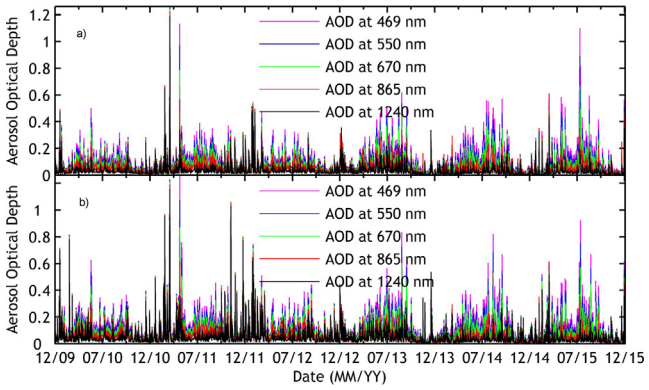

Figure 2 3-hour Aerosol Optical Depth (whole spectrum) at two sites: a) Ny-Ålesund and b) Hornsund based on reanalysis from the CAMS model for the period 2010—2015.

show a noticeable increase in AOD over the last ten years, changing the estimations of the long-term average variability of this parameter from 2.0% per year found by Tomasi et al. (2007) in the 1977—2006 period to nearly zero in the last ten years.

Results from the CAMS model analyses were concentrated on optical and chemical properties. Taking into account the AOD in all spectra, we did not find significant differences between the stations in the period 2010—2015 (Fig. 2). Slight changes in absorption are visible at the beginning of 2010 and in the winter of 2011 but they are mostly concentrated in the water vapor absorption channel — 1240 nm. These changes at longer wavelengths are connected with a low sensitivity to the fine-mode aerosols and relatively well-known absorption properties of dust (almost non-absorbing), given the bigger errors in AOD retrieval. Each peak is almost the same, with small differences in values, which are mostly higher in Hornsund (Fig. 2b).

As mentioned above, there are differences in the water vapor channel, but taking into account the extinction in 550 nm, the higher values of AOD are seen in Hornsund, with exception to 2015, when higher values are observed in Ny-Ålesund (Fig. 3). During the summer of 2015, a very intensive

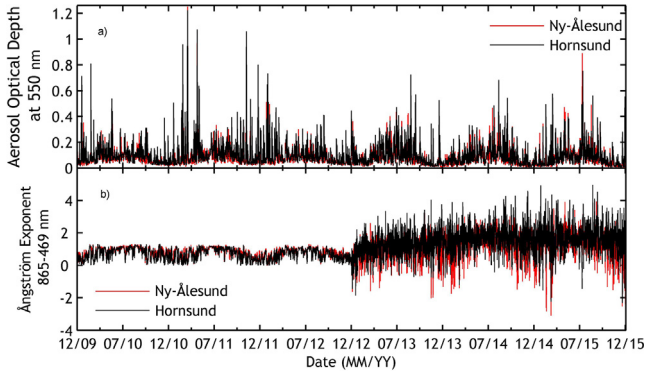

Figure 3 3-hour a) Aerosol Optical Depth at 550 nm and b) Ångström Exponent for 865—469 nm in Hornsund (black line) and Ny-Ålesund (red line) based on reanalysis from the CAMS model during a period 2010—2015. (For interpretation of the references to color in this figure legend, the reader is referred to the web version of this article.)

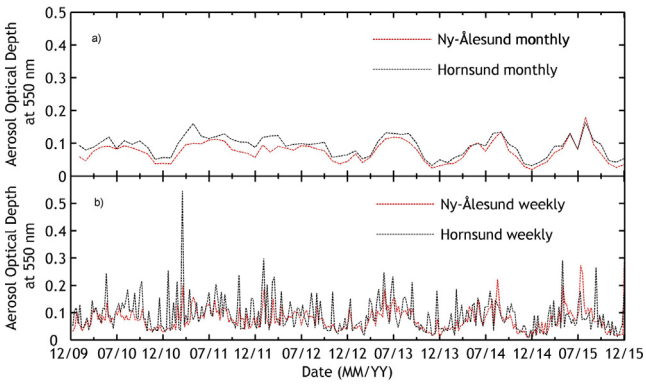

Figure 4 (a) Monthly and (b) weekly means of Aerosol Optical Depth at 550 nm in Ny-Ålesund (red dashed line) and Hornsund (black dashed line) based on reanalysis from the CAMS model during a period 2010—2015. (For interpretation of the references to color in this figure legend, the reader is referred to the web version of this article.)

Arctic Event occurred which was related to massive biomass burning (BB). According to the Canadian Wildland Fire Information System (http://cwfis.cfs.nrcan.gc.ca) forest fires started in late April in Canada. Slight differences seen on the upper plot of Fig. 3 could be explained by the topography of both stations. The event was observed with a delay of several hours between the two stations. This delay was caused by wind circulation, and the speed and direction of winds which transport polluted air-masses. The Ångström Exponent is generally stable during 2010—2012, with a predominance of large particles in the atmosphere. Elevated values of AOD in 2010 and 2011 do not change the composition of the atmosphere (see Fig. 7). After 2012 the Ångström Exponent values changed significantly, increasing in Hornsund and decreasing at the same time in Ny-Ålesund. Sudden, large differences in the extinction in 469 nm and 869 nm, and the resulting differences in the Ångström Exponent, appeared at the beginning of 2012 due to the use of different types of data. From 2010 to 2012 results from reanalysis were used and then, for 2013—2015 — near-real-time data from the CAMS model was applied. The values of the Ångström Exponent above 1.3 in both locations are directly linked to the increasing numbers of recent BB episodes advecting pollution in to the Arctic.

Furthermore, monthly and weekly means of AOD confirm that the mean values are higher in Hornsund than in Ny-Ålesund (Fig. 4). The high values of AOD are mostly related to air-masses from mid-latitudes carrying anthropogenic pollution. From this point, we can conclude that pollution generating events from urbanized areas affect Hornsund more than Ny-Ålesund. It can be confirmed by circulation pathways and local orography. Isaksen et al. (2016) found that during the spring and winter, when polluted air masses are transported mainly from Europe and Asia, the temperature anomaly is more often observed in Hornsund than in Ny-Ålesund. This is strongly connected with anticyclonic types of circulation, which transport air masses from Europe and the Atlantic Ocean. The orography, in addition, has a great impact on the observations of pollution; in Ny-Ålesund during advection from a northern direction a local production of sea-salt is initiated, which could dry-out the polluted air masses.

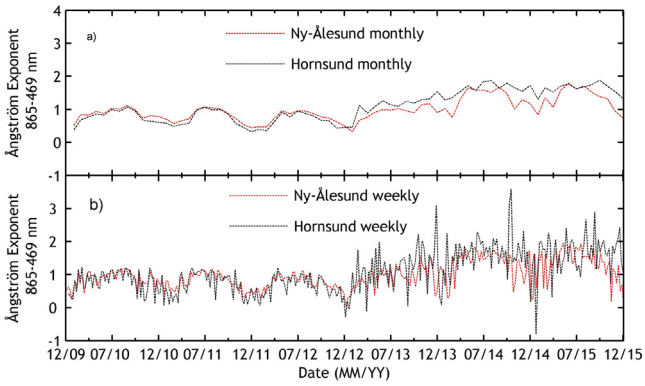

Figure 5 (a) Monthly and (b) weekly means of Ångström Exponent for 865–469 nm in Ny-Ålesund (red dashed line) and Hornsund (black dashed line) and Ny-Ålesund (red dashed line) based on reanalysis from the CAMS model during a period 2010–2015. (For interpretation of the references to color in this figure legend, the reader is referred to the web version of this article.)

Additionally, mountains around the station cause changes in the route of transported air masses (Lisok et al., 2016). Fig. 5 shows weekly and monthly means of AE. The Hornsund station displays higher peaks, with strong a discrepancy especially in 2014. Annual means of this parameter show discrepancy between the stations, higher values in 2010–2012 in Ny-Ålesund, and lower in 2013–2015 (Tables 1 and 2).

Arctic Haze is among most significant phenomena, which occur in the Arctic, however, recent observations of air pollution show that it is mostly related to biomass burning events (Turetsky et al., 2011; Westerling et al., 2006). Over a period of last 10 years, high AODs were observed in particular years (2005, 2006, 2008 and 2011). They occurred as a result of strong aerosol events such as the Arctic Haze or were advected with air masses from BB sources. It is obvious that average AODs show an increasing trend over Svalbard for the period of 2000 and 2012 (Pakszys et al., 2015). This may indicate increasing atmospheric pollution in the region, which may potentially lead to a significant warming at ground level (Tomasi et al., 2015).

Fires influence climate systems on temporal and spatial scales as a result of emissions of trace gases and aerosols (Bowman et al., 2009; Marlon et al., 2008; Power et al., 2008; Ward et al., 2012). Numbers of large biomass burning cases have been increasing over the period of the last 100 years. Unfortunately, it is obvious that anthropogenic activities are the main factor in this process (Brönnimann et al., 2007; Mtetwa and McCormick, 2003). This situation can be related both to climate changes and agricultural fires. These events are a significant global source of atmospheric gases and particles, which influence the chemistry of the atmosphere and thus the climate of the Earth (Beringer et al., 2003; Crutzen et al., 1979; Langenfelds et al., 2002; Page et al., 2002).

Some events in the past have been well described in literature, but they are based on different models and measurements. The Arctic was strongly impacted by aerosol particles from wild fires in Canada in July 2004 (Stohl, 2006; Stohl et al., 2006) and as a result of the Kasatochi and Sarychev volcanic activity, which began in August 2008 (Hoffmann et al., 2010) as well as in July 2009 (Tomasi

Table 1 Annual mean of Aerosol Optical Depth (AOD) at 550 nm, Ångström Exponent for 865–469 nm, five chemical components at 550 nm: Sea Salt, Dust, Organic Matter, Black Carbon and Sulphate in Ny-Ålesund based on reanalysis from the CAMS model.

Ny-Ålesund						
	2010	2011	2012	2013	2014	2015
AOD 550 nm	0.0708	0.0841	0.0747	0.0746	0.0695	0.0743
AE 865–469	0.8696	0.7806	0.7443	0.8959	1.3378	1.3183
SSAOD 550 nm	0.0181	0.0277	0.0250	0.0230	0.0078	0.0102
DUAOD 550 nm	0.0173	0.0188	0.0194	0.0046	0.0010	0.0011
OMAOD 550 nm	0.0041	0.0048	0.0044	0.0089	0.0048	0.0100
BCAOD 550 nm	0.0012	0.0012	0.0009	0.0023	0.0014	0.0015
SUAOD 550 nm	0.0301	0.0315	0.0250	0.0357	0.0545	0.0516

Table 2 Annual mean of Aerosol Optical Depth (AOD) at 550 nm, Ångström Exponent for 865–469 nm, five chemical components at 550 nm: Sea Salt, Dust, Organic Matter, Black Carbon and Sulphate in Hornsund based on reanalysis from the CAMS model.

Hornsund						
	2010	2011	2012	2013	2014	2015
AOD 550 nm	0.0899	0.1113	0.0943	0.0876	0.0804	0.0843
AE 865-469	0.7820	0.7038	0.6594	1.1347	1.6258	1.6194
SSAOD 550 nm	0.0320	0.0481	0.0422	0.0326	0.0143	0.0184
DUAOD 550 nm	0.0174	0.0194	0.0194	0.0049	0.0011	0.0012
OMAOD 550 nm	0.0045	0.0053	0.0044	0.0094	0.0052	0.0085
BCAOD 550 nm	0.0013	0.0013	0.0009	0.0026	0.0015	0.0015
SUAOD 550 nm	0.0348	0.0373	0.0274	0.0382	0.0583	0.0547

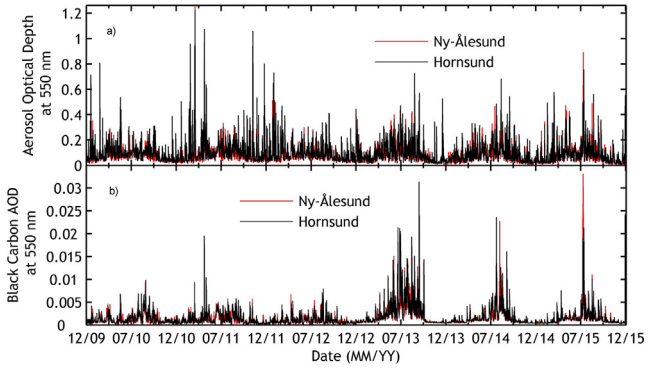

Figure 6 3-hour a) Aerosol Optical Depth at 550 nm and b) Black Carbon Aerosol Optical Depth at 550 nm in Ny-Ålesund (red line) and Hornsund (black line) and Ny-Ålesund (red line) based on reanalysis from the CAMS model during a period 2010—2015. (For interpretation of the references to color in this figure legend, the reader is referred to the web version of this article.)

et al., 2012), respectively. In May 2006, agricultural fires in Eastern Europe resulted in the highest pollution levels in the Arctic region ever recorded (Myhre et al., 2007; Stohl et al., 2007). In July 2015 Markowicz et al. (2016b) reported about intense Canadian fires over the European Arctic, which was one of the most spectacular biomass burning events in the last decade. It also shows greater averages of AOD at 550 nm (during summer) — 0.0843 (0.1222) in Hornsund than 0.0743 (0.1177) in Ny-Ålesund (Tables 1 and 2, 5 and 6). These fires are also visible in Fig. 6. Following high values of AOD, which indicate potential events in the Arctic (above 0.1, but looking for extremes, above 0.6), we can also see changes in Black Carbon (BC) values. BC is very absorptive at all spectrum ranges, and even more so at longer wavelengths. Dust, on the other hand, becomes less absorptive as the wavelength is increased. Strong values of BC are related to the BB events, due to the fact that it is a component of forest fires. Also, values of AE representing smaller particles, correspond with the size of BB particles. These values are three times higher than the multiannual average this year (0.0015, Tables 1 and 2). These small particles can reach high latitudes much easier, and be transported over vast distances.

Emissions of trace gases and aerosols during fires have significant impact on the climate on a temporal and spatial scale. They are related to growing anthropogenic activities and agricultural fires over the world. Such events have an impact on the chemistry of the atmosphere. Variations in increasing anthropogenic emissions of SO_2 from coal-burning events and industrial activity in Europe and Asia since 2000 have led to the formation of sulphate particle loadings, which have been subsequently transported to the Arctic. This increase is clearly seen over the last years (Fig. 7). These strong peaks in 2012 are probably primarily related to the values of AOD in that period in both stations, and thus also to the strong wind blowing through the fjords at the beginning of the year (Tables 3 and 4). BC and dust are clearly major absorbers in the solar spectrum; they both show large seasonal and interannual variability (Fig. 7). However, their participation in the chemistry of the atmosphere has been decreasing significantly since 2013. There are no significant differences in the chemical composition between the stations, though, sharp increases in each individual value is present at both stations. Regarding Tables 1 and 2 as well as Fig. 7, only the sea-salt component shows some visible variations. From 2010 to 2012 its participation is twice as high in Hornsund than in Ny-Ålesund, and then in 2013—2015 the discrepancy is weaker, but there are still higher values in Hornsund than in Ny-Ålesund. SSAOD values show strong seasonal variations due to a strong correlation with wind speed (see Fig. 7, Tables 3 and 4). Dust emissions show differences smaller than an order of magnitude, the biggest

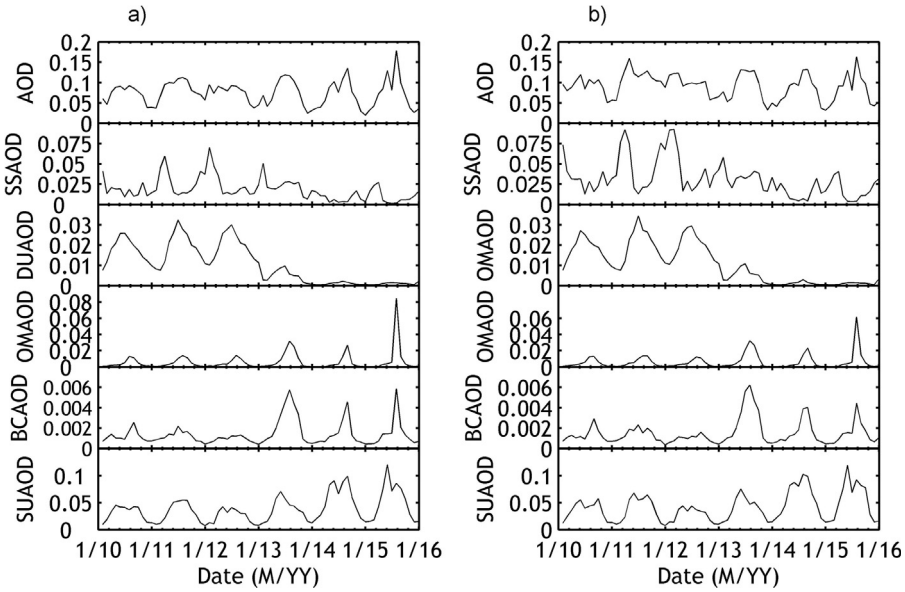

Figure 7 Monthly mean values of AOD at 550 nm, Ångström Exponent for 865—469 nm, 5 chemical components at 550 nm: Sea Salt, Dust, Organic Matter, Black Carbon and Sulphates in (a) Ny-Ålesund and (b) Hornsund from reanalysis from the CAMS model for 2010—2015.

Table 3 Monthly means of wind velocity [m s^{-1}] and direction [0—360°] for Ny-Ålesund, for a period of 2010—2015 based on the WMO database.

Ny-Ålesund mean values wind velocity and direction												
	2010		2011		2012		2013		2014		2015	
	v	Dir.	v	Dir.	v	Dir.	v	Dir.	v	Dir.	v	Dir.
1	4.94	179.01	3.84	173.02	5.71	163.10	4.36	165.83	3.52	180.90	5.07	164.22
2	3.64	158.03	5.14	160.64	5.31	175.15	4.01	162.68	4.53	156.26	5.86	185.21
3	4.11	175.48	5.37	190.00	5.76	163.00	3.83	154.20	4.94	187.68	6.16	169.34
4	3.33	173.42	5.19	172.11	3.37	179.30	3.53	178.94	3.94	200.72	5.31	159.82
5	3.16	188.33	3.33	197.44	4.27	196.90	3.24	196.97	3.53	195.50	2.49	195.13
6	2.67	200.32	2.76	237.49	2.52	214.11	3.84	220.23	2.85	223.72	3.55	211.84
7	2.58	151.07	3.29	157.21	3.21	160.42	3.39	173.96	2.50	178.25	3.44	158.37
8	3.01	183.97	3.42	156.15	4.26	174.73	3.79	159.13	2.47	149.61	2.69	153.42
9	2.55	202.04	2.60	183.89	4.05	165.62	4.13	157.40	4.33	200.73	3.47	189.93
10	4.15	178.09	4.75	170.05	3.24	176.80	3.88	192.81	5.46	161.86	3.88	180.87
11	3.26	177.72	5.04	181.31	4.36	173.38	4.99	180.84	4.46	189.60	6.64	174.85
12	5.06	180.95	5.72	166.23	4.39	172.67	5.34	166.07	6.27	173.97	5.77	154.78

Table 4 Monthly means of wind velocity [m s^{-1}] and direction [0—360°] for Hornsund for a period of 2010—2015 based on the WMO database.

Hornsund mean values of wind velocity and direction												
	2010		2011		2012		2013		2014		2015	
	v	Dir.	v	Dir.	v	Dir.	v	Dir.	v	Dir.	v	Dir.
1	4.94	179.01	3.84	173.02	5.71	163.10	4.36	165.83	3.52	180.90	5.07	164.22
2	3.64	158.03	5.14	160.64	5.31	175.15	4.01	162.68	4.53	156.26	5.86	185.21
3	4.11	175.48	5.37	190.00	5.76	163.00	3.83	154.20	4.94	187.68	6.16	169.34
4	3.33	173.42	5.19	172.11	3.37	179.30	3.53	178.94	3.94	200.72	5.31	159.82
5	3.16	188.33	3.33	197.44	4.27	196.90	3.24	196.97	3.53	195.50	2.49	195.13
6	2.67	200.32	2.76	237.49	2.52	214.11	3.84	220.23	2.85	223.72	3.55	211.84
7	2.58	151.07	3.29	157.21	3.21	160.42	3.39	173.96	2.50	178.25	3.44	158.37
8	3.01	183.97	3.42	156.15	4.26	174.73	3.79	159.13	2.47	149.61	2.69	153.42
9	2.55	202.04	2.60	183.89	4.05	165.62	4.13	157.40	4.33	200.73	3.47	189.93
10	4.15	178.09	4.75	170.05	3.24	176.80	3.88	192.81	5.46	161.86	3.88	180.87
11	3.26	177.72	5.04	181.31	4.36	173.38	4.99	180.84	4.46	189.60	6.64	174.85
12	5.06	180.95	5.72	166.23	4.39	172.67	5.34	166.07	6.27	173.97	5.77	154.78

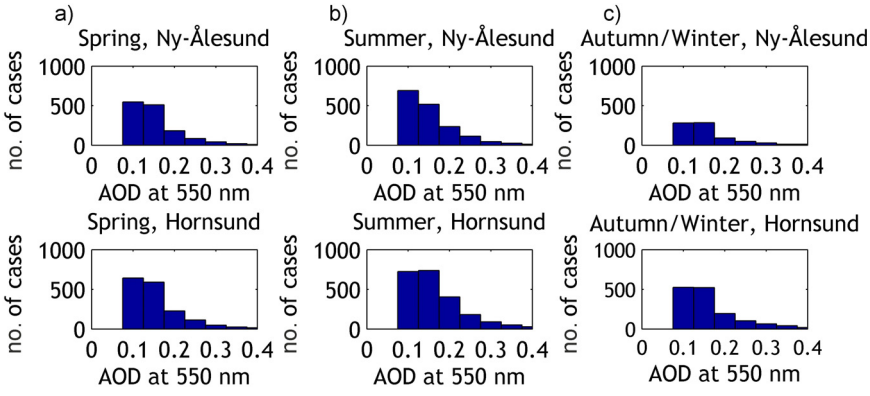

Figure 8 Relative frequency histograms of AOD (550 nm) from CAMS database > 0.1 at Ny-Ålesund (upper plots) and Hornsund (lower plots) from 2010 to 2015 performed into (a) spring, (b) summer and (c) autumn-winter season.

Table 5 Seasonal mean of AOD at 550 nm, Ångström Exponent (440—870 nm or 865—469 nm) from the CAMS database in Ny-Ålesund and Hornsund for a period 2010—2015.

		Ny-Ålesund		Hornsund	
	Season	AOD	AE	AOD	AE
2010	Spring	0.0880	0.9427	0.1036	0.8886
	Summer	0.0885	1.0614	0.1049	1.0099
	Autumn and winter	0.0526	0.7309	0.0750	0.6071
2011	Spring	0.0954	0.9036	0.1220	0.8423
	Summer	0.1040	1.0039	0.1238	0.9780
	Autumn and winter	0.0679	0.6003	0.0993	0.4888
2012	Spring	0.0874	0.9409	0.0957	0.8798
	Summer	0.0828	0.8550	0.1014	0.7735
	Autumn and winter	0.0641	0.5861	0.0900	0.4872
2013	Spring	0.1008	0.9322	0.1139	1.1281
	Summer	0.1048	0.9608	0.1275	1.1811
	Autumn and winter	0.0436	0.8431	0.0532	1.1138
2014	Spring	0.0867	1.5980	0.0910	1.6954
	Summer	0.1070	1.5557	0.1224	1.8074
	Autumn and winter	0.0409	1.0896	0.0528	1.4947
2015	Spring	0.0982	1.6059	0.1034	1.7096
	Summer	0.1177	1.5819	0.1222	1.7185
	Autumn and winter	0.0392	1.0320	0.0545	1.5210

differences (0.006) occur in 2012, DUAOD has a value of 0.0194 in Hornsund and 0.0194 in Ny-Ålesund. Organic matter values have slightly bigger values in 2011 (0.0048) and 2013 (0.0094) in Hornsund, while sulfates — are always greater by about 0.0040 in Hornsund which is about 10% of the value.

Furthermore, a slight increase in stratospheric AODs has recently been observed due to the transfer of sulphate aerosol particles and gases between the troposphere and low stratosphere at tropical latitudes, which has also had impact on polar regions (Tomasi et al., 2015).

Table 6 Seasonal mean of AOD at 550 nm $>$ 0.1, Ångström Exponent (440—870 nm or 865—469 nm) from the CAMS database in Ny-Ålesund and Hornsund for a period 2010—2015.

		Ny-Ålesund		Hornsund	
	Season	AOD	AE	AOD	AE
2010	Spring	0.1491	0.9957	0.1632	0.8645
	Summer	0.1294	1.1089	0.1352	1.0141
	Autumn and winter	0.1657	0.5073	0.1834	0.3967
2011	Spring	0.1569	0.9797	0.1944	0.8354
	Summer	0.1503	1.1177	0.1531	1.0276
	Autumn and winter	0.2056	0.2933	0.2288	0.2653
2012	Spring	0.1360	1.0552	0.1407	0.9116
	Summer	0.1376	0.9517	0.1502	0.7219
	Autumn and winter	0.1893	0.3410	0.2003	0.2942
2013	Spring	0.1604	0.9771	0.1704	1.2195
	Summer	0.1664	0.8934	0.1911	1.2813
	Autumn and winter	0.1460	0.4475	0.1689	0.8721
2014	Spring	0.1517	1.6667	0.1481	1.7560
	Summer	0.1810	1.6359	0.1733	1.9647
	Autumn and winter	0.1371	1.1455	0.1467	1.5996
2015	Spring	0.1631	1.6886	0.1617	1.7825
	Summer	0.2027	1.7255	0.1891	1.9155
	Autumn and winter	0.2002	0.7098	0.1827	1.3137

An Aerosol Optical Depth below 0.1 at 550 nm is usually classified as clean-air in the Arctic, air which was not advected from mid-latitudes. We divided the whole dataset into three seasons: spring, summer and autumn-winter combined. Due to the fact that in situ aerosol measurements can only be carried out during the polar day, these two seasons are mostly statistically irrelevant in comparison to other results. We also wanted to determine where the strongest events occurred, and so we had to single out cases where the AOD was larger than 0.1. AOD $<$ 0.1 in Ny-Ålesund represents 78% of the whole dataset while in Hornsund it is 69%. Then, we divided the AOD values into 13 classes from 0.1 to 1.3. The AODs $>$ 0.4 are not present in Fig. 8, because their percentage is far too low in Ny-Ålesund, where they represent 2.67% of cases without values above 0.1 and in Hornsund it is 2.92%. According to the first paragraph in this chapter, greater AODs persist especially during the spring (Tables 5 and 6). This suggests that the aerosols which are advected to the Artic are

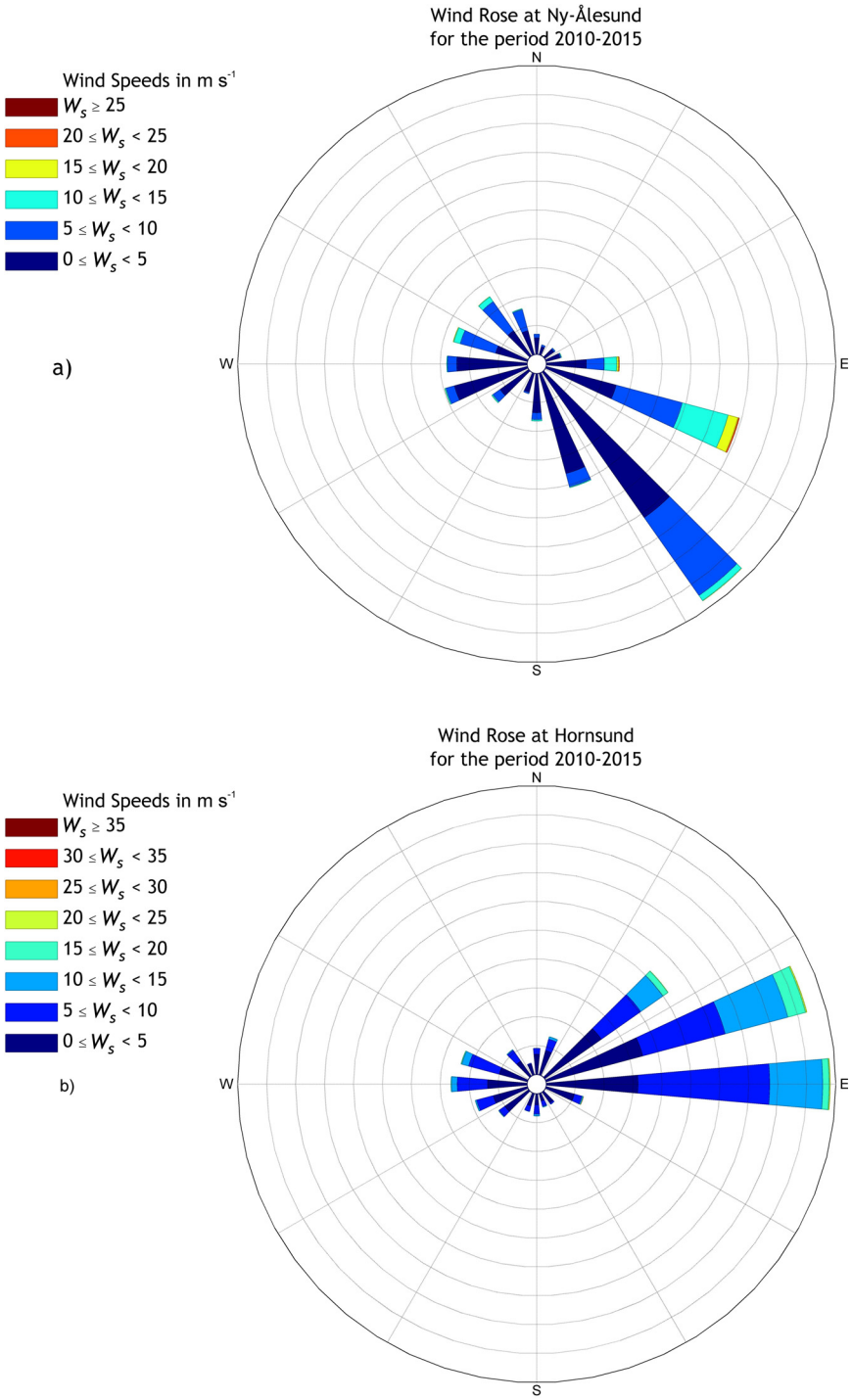

Figure 9 Wind rose (wind speed [m s^{-1}] and direction [0—360°]) for (a) Ny-Ålesund and (b) Hornsund for a period of 2010—2015 based on the WMO database.

enriched by aerosols of continental and anthropogenic origin in midlatitudes. Results without clean-air values explain also higher values in winter and early spring, which result from the haze conditions in the atmosphere, or common BB events. Furthermore, individual year mean values for each season are higher at the Hornsund station. The exception for higher values at the Hornsund station is the instance of small differences in 2014 and 2015 — but only when we take into account the threshold for extreme AODs (AOD $>$ 0.1). We can conclude that during the Haze events differences between the two stations decrease, which is related to the changing conditions of the atmosphere due to transportation of air to the Arctic. In general, seasonal variations of both parameters (AOD and AE) resemble the multi-year pattern.

The main factor regulating the circulation of the atmosphere over the two stations is the orography of the surrounding area. Hornsund receives eastern direction of advection, while the inflow in Ny-Ålesund is from the south-east. It is quite closely related to the influx of aerosols. Strong winds from the south and south-west in Hornsund (i.e. associated mostly with the wind along the fjord) cause the domination of marine aerosols, especially during the period 2011—2012. Due to large areas of open water west of Spitsbergen, emissions of sea-salt and organic aerosols are expected to be dominant. However, the state of the surface waters around Spitsbergen influences the type and the intensity of the regional atmospheric circulation and thus affects the frequency of winds with specific directions, which are recorded at both stations. The presence of a low pressure system west of Spitsbergen causes an increase of eastward winds, particularly on the west coast (Rogers et al., 2005; Tsukernik et al., 2007) (Fig. 9). Although, the frequency of winds from certain directions at the Hornsund station depends on the type and intensity of the regional atmospheric circulation (Marsz and Styszyńska, 2007). In addition, the wind regime, and especially its structure, is heavily influenced by local conditions, especially the position of the station relative to the main elements of the orography. This causes that the wind direction recorded at the stations often does not indicate the actual direction of the flow of air masses.

5. Conclusions

Analyses of the time series of modelled AODs from the CAMS model carried out for Ny-Ålesund and Hornsund show a noticeable decrease in AOD over the study period, leading to the alteration of the state of the polar atmosphere. It is less than 1% (at a linear trend) for each half-year of the model results at both locations. Potential differences observed between the two stations are not statistically significant, it is always a 2% difference between values, and it is always higher in Hornsund for each half-year of observations.

Annual and monthly means of AOD confirm that the mean values are higher in Hornsund than in Ny-Ålesund. The Hornsund station has higher peaks of AE values, with a strong discrepancy in 2014, still, annual means of this parameter represent a big discrepancy between the stations, higher values in 2010—2012 in Ny-Ålesund, and lower in 2013—2015. Results of seasonal means show the highest values in winter and in early spring, which correlates with haze conditions in the atmosphere, or common BB events. Also, individual yearly mean values are higher at the Hornsund station in all seasons.

In general, the increasing values of AOD are related mostly to air masses carrying anthropogenic pollution from midlatitudes. This is most often caused by the Artic Haze, but recently more and more events are related to biomass burning (Markowicz et al., 2016a,b; Moroni et al., 2017; Tomasi et al., 2015). Such events reach both stations at different times, which is related to the circulation and orography of the surrounding area.

There are no significant differences in chemical composition between the stations, although, sharp increases in individual values appear at both stations. Increasing mean values of BC and OM are associated with the increasing number of agricultural forest fires reaching Spitsbergen. During the Haze events differences between the two stations decrease, this is related to the changing conditions of the atmosphere due to the transportation of air to the Arctic. Nevertheless, taking into account the AOD in all spectra we did not find any significant differences between the stations in the period 2010—2015.

Modelling and prediction of aerosol properties is associated with a large degree of uncertainty due to the unpredictable character of the processes which involve aerosols. Nevertheless, the CAMS model is quite successful at reproducing the temporal variability of aerosols and the dominant aerosol types over the two chosen stations, as described in this paper. The results obtained from modelling with the CAMS (Copernicus Atmosphere Monitoring Service) were used to prove that the Arctic model could correctly estimate Arctic events and provide accurate aerosol information for the area of Svalbard. Previous comparisons with the MODIS derived AODs, the NAAPS model and in situ data shows that all models overestimate the values of AOD. However, including the AOD from the MODIS observations significantly increases the consistency between the model and the NAAPS derived AODs. Nevertheless, the CAMS model provides a good reconstruction of real values of AOD, especially during the occurrence of changes in the atmosphere and the subsequent changes in the composition and concentration of aerosols (Markowicz et al., 2016a).

Acknowledgements

This study was partly financially supported by the NCN (National Science Center) project GAME, No. DEC-2012/04/A/NZ8/00661.

The authors would also like to acknowledge the support of this research by the Polish-Norwegian Research Programme operated by the National Centre for Research and Development under the Norwegian Financial Mechanism 2009—2014 as a part of Project Contract No. Pol-Nor/196911/38/2013 and also project KNOW, Leading National Research Centre received by the Centre for Polar Studies for the period 2014—2018 established by regulation No. 152 (2013, Nov 14) of the Rector of the University of Silesia.

We would like to acknowledge CAMS model, contracted by the European Centre for Medium-Range Weather Forecasts, a European Union (Delegation Agreement signed on 11/11/2014) flagship service building on 10 years of monitoring the atmosphere and climate, for data provided. This data

enabled the development of a large range of products dedicated to analysing the composition of the atmosphere and is also an essential asset for a better understanding of climate change.

References

ACIA, 2004. Impacts of a Warming Arctic. Arctic Climate Impact Assessment. Cambridge Univ. Press, 144 pp.

Bellouin, N., Jones, A., Haywood, J., Christopher, S.A., 2008. Updated estimate of aerosol direct radiative forcing from satellite observations and comparison against the Hadley Centre climate model. J. Geophys. Res. 113, D10205, 15 pp., http://dx.doi.org/10.1029/2007JD009385.

Benedetti, A., Fisher, M., 2007. Background error statistics for aerosols. Q. J. R. Meteorol. Soc. 133 (623), 391—405, http://dx.doi.org/10.1002/qj.37.

Benedetti, A., Morcrette, J.-J., Boucher, O., Dethof, A., Engelen, R. J., Fisher, M., Flentje, H., Huneeus, N., Jones, L., Kaiser, J.W., Kinne, S., Mangold, A., Raziner, M., Simmons, A.J., Suttie, M., 2009. Aerosol analysis and forecast in the European Centre for Medium-Range Weather Forecasts Integrated Forecast System: 2. Data assimilation. J. Geophys. Res. 114, D13205, 18 pp., http://dx.doi.org/10.1029/2008JD011115.

Beringer, J., Hutley, L.B., Tapper, N.J., Coutts, A., Kerley, A., O'Grady, A.P., 2003. Fire impacts on surface heat, moisture and carbon fluxes from a tropical savanna in northern Australia. Int. J. Wildl. Fire 12 (4), 333—340, http://dx.doi.org/10.1071/wf03023.

Boucher, O., Pham, M., Venkataraman, C., 2002. Simulation of the Atmospheric Sulfur Cycle in the LMD GCM: Model Description, Model Evaluation, and Global and European Budgets. Note no. 23, Inst. Pierre-Simon Laplace, Paris, France 26 pp. Available at: http://icmc.ipsl.fr/images/publications/scientific_notes/note23.pdf.

Bowman, D.M., Balch, J.S., Artaxo, P., Bond, W.J., Carlson, J.M., Cochrane, M.A., D'Antonio, C.M., DeFries, R.S., Doyle, J.C., Harrison, S.P., Johnston, F.H., Keeley, J.E., Krawchuk, M.A., Kull, C.A., Marston, J.B., Moritz, M.A., Prentice, I.C., Roos, C.I., Scoot, A.C., Swetnam, T.W., van der Werf, G.D., Pyne, S.J., 2009. Fire in the earth system. Science 324 (5926), 481—484, http://dx.doi.org/10.1126/science.1163886.

Brock, C.A., Cozic, J., Bahreini, R., Froyd, K.D., Middlebrook, A.M., McComiskey, A.A., Brioude, J., Cooper, O.R., Stohl, A., Aikin, K. C., de Gouw, J.A., Fahey, D.W., Ferrare, R.A., Gao, R.-S., Gore, W., Holloway, J.S., Hübler, G., Jefferson, A., Lack, D.A., Lance, S., Moore, R.H., Murphy, D.M., Nenes, A., Novelli, P.C., Nowak, J. B., Ogren, J.A., Peischl, J., Pierce, R.B., Pilewskie, P., Quinn, P. K., Ryerson, T.B., Schmidt, K.S., Schwarz, J.P., Sodemann, H., Spackman, J.R., Stark, H., Thomson, D.S., Thornberry, T., Veres, P., Watts, L.A., Warneke, C., Wollny, A.G., 2011. Characteristics, sources, and transport of aerosols measured in spring 2008 during the aerosol, radiation, and cloud processes affecting Arctic Climate (ARCPAC) Project. Atmos. Chem. Phys. 11 (6), 2423—2453, http://dx.doi.org/10.5194/acp-11-2423-2011.

Brönnimann, S., Ewen, T., Luterbacher, J., Diaz, H.F., Stolarski, R.S., Neu, U., 2007. Climate variability and extremes during the past 100 years. In: Brönnimann, S., Luterbacher, J., Ewen, T., Diaz, H. F., Stolarski, R.S., Neu, U. (Eds.), A Focus on Climate During the Past 100 Years. Springer, Dordrecht, 1—25, http://dx.doi.org/10.1007/978-1-4020-6766-2_1.

Charlson, R.J., Schwartz, S.E., Hales, J.M., Cess, R.D., Coakley, J.A., Hansen, J.E., Hofmann, D.J., 1992. Climate forcing by anthropogenic aerosols. Science 255 (5043), 423—430, http://dx.doi.org/10.1126/science.255.5043.423.

Crutzen, P.J., Heidt, L.E., Krasnec, J.P., Pollock, W.H., Seiler, W., 1979. Biomass burning as a source of atmospheric gases CO, H_2 N_2O, NO, CH_3Cl and COS. Nature 282, 253—256, http://dx.doi.org/10.1038/282253a0.

Dixon, G.J., 1998. Laser radars produce three-dimensional pictures. Laser Focus World 4 (08/01/1998), 129—136.

Drollette, D., 2000. Ancient writings come to light. Photon. Spectra 4, 40.

Dubovik, O., Holben, B., Eck, T.F., Smirnov, A., Kaufman, Y.J., King, M.D., Tanré, D., Slutsker, I., 2002. Variability of absorption and optical properties of key aerosol types observed in worldwide locations. J. Atmos. Sci. 59 (3), 590—608, http://dx.doi.org/10.1175/1520-0469(2002)059<0590:VOAAOP>2.0.CO;2.

Eck, T.F., Holben, B.N., Reid, J.S., Dubovik, O., Smirnov, A., O'Neill, N.T., Slutsker, I., Kinne, S., 1999. Wavelength dependence of the optical depth of biomass burning, urban, and desert dust aerosols. J. Geophys. Res. Atmos. (1984—2012) 104 (D24), 31333—31349, http://dx.doi.org/10.1029/1999JD900923.

Engvall, A.-C., Krejci, R., Ström, J., Treffeisen, R., Scheele, R., Hermansen, O., Paatero, J., 2008. Changes in aerosol properties during spring-summer period in the Arctic troposphere. Atmos. Chem. Phys. 8 (3), 445—462, http://dx.doi.org/10.5194/acp-8-445-2008.

Guelle, W., Schulz, M., Balkanski, Y., Dentener, F., 2001. Influence of the source formulation on modeling the atmospheric global distribution of the sea salt aerosol. J. Geophys. Res. 106 (D21), 27,509—27,524, http://dx.doi.org/10.1029/2001jd900249.

Herber, A., Thomason, L.W., Gernandt, H., Leiterer, U., Nagel, D., Schulz, K.H., Kaptur, J., Albrecht, T., Notholt, J., 2002. Continuous day and night aerosol optical depth observations in the Arctic between 1991 and 1999. J. Geophys. Res. Atmos. (1984—2012) 107 (D10), AAC 6, 13 pp., http://dx.doi.org/10.1029/2001JD000536.

Hoffmann, A., Ritter, C., Stock, M., Maturilli, M., Eckhardt, S., Herber, A., Neuber, R., 2010. Lidar measurements of the Kasatochi aerosol plume in August and September 2008 in Ny-Ålesund, Spitzbergen. J. Geophys. Res. 115 (D2), D00L12, 12 pp., http://dx.doi.org/10.1029/2009JD013039.

Inness, A., Baier, F., Benedetti, A., Bouarar, I., Chabrillat, S., Clark, H., Clerbaux, C., Coheur, P., Engelen, R.J., Errera, Q., Flemming, J., George, M., Granier, C., Hadji-Lazaro, J., Huijnen, V., Hurtmans, D., Jones, L., Kaiser, J.W., Kapsomenakis, J., Lefever, K., Leitão, J., Razinger, M., Richter, A., Schultz, M.G., Simmons, A. J., Suttie, M., Stein, O., Thépaut, J.-N., Thouret, V., Vrekoussis, M., Zerefos, C., 2013. The MACC reanalysis: an 8 yr. data set of atmospheric composition. Atmos. Chem. Phys. 13 (8), 4073—4109, http://dx.doi.org/10.5194/acp-13-4073-2013.

IPCC — Intergovernmental Panel on Climate Change, 2013. Climate Change 2013, The Physical Science Basis. Contribution of Working Group I to the Fifth Assessment Report of the Intergovernmental Panel on Climate Change. Cambridge Univ. Press, Cambridge, UK/New York, USA, 1535 pp., http://dx.doi.org/10.1017/CBO9781107415324,

Isaksen, K., Nordli, Ø., Førland, E.J., Łupikasza, E., Eastwood, S., Niedźwiedź, T., 2016. Recent warming on Spitsbergen — influence of atmospheric circulation and sea ice cover. J. Geophys. Res. Atmos. 121 (20), 11,913—11,931, http://dx.doi.org/10.1002/2016JD025606.

Kaiser, J.W., Heil, A., Andreae, M.O., Benedetti, A., Chubarova, N., Jones, L., Morcrette, J.-J., Raziner, M., Schultz, M.G., Suttie, M., van der Werf, G.R., 2012. Biomass burning emissions estimated with a global fire assimilation system based on observed fire radiative power. Biogeosciences 9 (1), 7339—7398, http://dx.doi.org/10.5194/bg-9-527-2012.

Kaufman, Y.J., Tanré, D., Boucher, O., 2002. A satellite view of aerosols in the climate system. Nature 419 (6903), 215—223, http://dx.doi.org/10.1038/nature01091.

Labow, G.J., Flynn, L.E., Rawlins, M.A., Beach, R.A., Simmons, C.A., Schubert, C.M., 1996. Estimation of ozone with total ozone portable spectroradiometer instruments. II. Practical operation

and comparisons. Appl. Opt. 35 (30), 6084—6089, http://dx.doi.org/10.1364/AO.35.006084.

Langenfelds, R.L., Francey, R.J., Pak, B.C., Steele, L.P., Lloyd, J., Trudinger, C.M., Allison, C.E., 2002. Interannual growth rate variations of atmospheric CO_2 and its (^{13}C, H_2, CH_4, and CO between 1992 and 1999 linked to BB. Glob. Biogeochem. Cycles 16 (3), 1048, http://dx.doi.org/10.1029/2001GB001466 21-1—21-22.

Lisok, J., Markowicz, K.M., Ritter, C., Makuch, P., Petelski, T., Chilinski, M., Kaminski, J.W., Becagli, S., Traversi, R., Udisti, R., Rozwadowska, A., Jefimow, M., Markuszewski, P., Neuber, R., Pakszys, P., Stachlewska, I.S., Struzewska, J., Zielinski, T., 2016. 2014 iAREA campaign on aerosol in Spitsbergen — Part 1: Study of physical and chemical properties. Atmos. Environ. 140, 150—166, http://dx.doi.org/10.1016/j.atmosenv.2016.05.051.

Markowicz, K.M., Flatau, P.J., Kardas, A.E., Remiszewska, J., Stelmaszczyk, K., Woeste, L., 2008. Ceilometer retrieval of the boundary layer vertical aerosol extinction structure. J. Atmos. Ocean. Technol. 25 (6), 928—944, http://dx.doi.org/10.1175/2007JTECHA1016.1.

Markowicz, K.M., Chilinski, M.T., Lisok, J., Zawadzka, O., Stachlewska, I.S., Janicka, L., Rozwadowska, A., Makuch, P., Pakszys, P., Zielinski, T., Petelski, T., Posyniak, M., Pietruczuk, A., Szkop, A., Westphal, D.L., 2016a. Study of aerosol optical properties during long-range transport of biomass burning from Canada to Central Europe in July 2013. J. Aerosol Sci. 101, 156—173, http://dx.doi.org/10.1016/j.jaerosci.2016.08.006.

Markowicz, K.M., Pakszys, P., Ritter, C., Zielinski, T., Udisti, R., Cappelletti, D., Mazzola, M., Shiobara, M., Xian, P., Zawadzka, O., Lisok, J., Petelski, T., Makuch, P., Karasiński, G., 2016b. Impact of North American intense fires on aerosol optical properties measured over the European Arctic in July 2015. J. Geophys. Res. Atmos. 121, 14487—14512, http://dx.doi.org/10.1002/2016JD025310.

Markowicz, K.M., Zielinski, T., Blindheim, S., Gausa, M., Jagodnicka, A.K., Kardas, A.E., Kumala, W., Malinowski, S.P., Petelski, T., Posyniak, M., Stacewicz, T., 2012. Study of vertical structure of aerosol optical properties with sun photometers and ceilometer during the MACRON campaign in 2007. Acta Geophys. 60 (5), 1308—1337, http://dx.doi.org/10.2478/s11600-011-0056-7.

Marlon, J.R., Bartlein, P.J., Carcaillet, C., Gavin, D.G., Harrison, P., Higuera, E., Joos, F., Power, M.J., Prentice, I.C., 2008. Climate and human influences on global BB over the past two millennia. Nat. Geosci. 1, 697—702, http://dx.doi.org/10.1038/ngeo313.

Marsz, A.A., Styszyńska, A. (Eds.), 2007. Climate in the Region of Polish Polar Station in Hornsund — State, Changes and its Causes, Gdynia Maritime Univ. Publ., Gdynia, 71—86, (in Polish).

Mazzola, M., Stone, R.S., Herber, A., Tomasi, C., Lupi, A., Vitale, V., Lanconelli, C., Toledano, C., Cachorro, V.E., O'Neill, N.T., Shiobara, M., Aaltonen, V., Stebel, K., Zielinski, T., Petelski, T., Ortiz de Galisteo, J.P., Torres, B., Berjon, A., Goloub, P., Li, Z., Blarel, L., Abboud, I., Cuevas, E., Stock, M., Schulz, K.-H., Virkkula, A., 2012. Evaluation of sun photometer capabilities for retrievals of aerosol optical depth at high latitudes: the POLAR-AOD intercomparison campaigns. Atmos. Environ. 52, 4—17, http://dx.doi.org/10.1016/j.atmosenv.2011.07.042.

Morcrette, J.J., Boucher, O., Jones, L., Salmond, D., Bechtold, P., Beljaars, A., Bededetti, A., Bonet, A., Kaiser, J.W., Razinger, M., Schulz, M., Serrar, S., Simmons, A.J., Sofiev, M., Suttie, M., Tompkins, A.M., Untch, A., 2009. Aerosol analysis and forecast in the ECMWF Integrated Forecast System. Part I: Forward modelling. J. Geophys. Res. 114 (D6), D06206, 17 pp., http://dx.doi.org/10.1029/2008JD011235.

Morcrette, J.J., Kaiser, J.W., Benedetti, A., Jones, L., Razinger, M., Suttie, M., 2011. Prognostic Aerosols in the ECMWF IFS: MACC vs GEMS Aerosols. Tech. Memo. 659. European Centre for Medium-Range Weather Forecasts, Reading, UK 32 pp. Available at: http://www.ecmwf.int/publications/library/do/references/show?id=90354.

Moroni, B., Cappelletti, D., Crocchianti, S., Becagli, S., Caiazzo, L., Traversi, R., Udisti, R., Mazzola, M., Markowicz, K., Ritter, C., Zielinski, T., 2017. Morphochemical characteristics and mixing state of long range transported wildfire particles at Ny-Ålesund (Svalbard Islands). Atmos. Environ. 156, 135—145, http://dx.doi.org/10.1016/j.atmosenv.2017.02.037.

Mtetwa, L., McCormick, M.P., 2003. Development of BB Gaseous and Particulate Emissions Database for Assimilation Into Air Quality Forecast Systems. AGU Fall Meeting Abstracts, B1062.

Myhre, C.L., Toledano, C., Myhre, G., Lihavainen, H., 2007. Regional aerosol optical properties and radiative impact of the extreme smoke event in the European Arctic in spring 2006. Atmos. Chem. Phys. 7 (22), 511—534, http://dx.doi.org/10.5194/acp-7-5899-2007.

Nagel, D., Herber, A., Thomason, L.W., Leiterer, U., 1998. Vertical distribution of the spectral aerosol optical depth in the Arctic from 1993 to 1996. J. Geophys. Res. Atmos. (1984—2012) 103 (D2), 1857—1870, http://dx.doi.org/10.1029/97JD02678.

Page, S.E., Siegert, F., Rieley, J.O., Boehm, H.D.V., Jaya, A., Limin, S., 2002. The amount of carbon released from peat and forest fires in Indonesia during 1997. Nature 420, 61—65, http://dx.doi.org/10.1038/nature01131.

Pakszys, P., Zielinski, T., Markowicz, K.M., Petelski, T., Makuch, P., Lisok, J., Chilinski, M., Rozwadowska, A., Ritter, C., Neuber, R., Udisti, R., Mazzola, M., 2015. Annual changes of aerosol optical depth and Ångström Exponent over Spitsbergen. In: Zielinski, T., Weslawski, M., Kuliński, K. (Eds.), Free Preview Impact of Climate Changes on Marine Environments. Springer, Cham/Heidelberg/New York/Dordrecht/London, 23—36, http://dx.doi.org/10.1007/978-3-319-14283-8_3.

Petelski, T., Markuszewski, P., Makuch, P., Jankowski, A., Rozwadowska, A., 2014. Studies of vertical coarse aerosol fluxes in the boundary layer over the Baltic Sea. Oceanologia 56 (4), 697—710, http://dx.doi.org/10.5697/oc.56-4.697.

Power, M.J., Marlon, J., Ortiz, N., Bartlein, P.J., Harrison, S.P., Mayle, F.E., Ballouche, A., Bradshow, R.H.W., Carcaillet, C., Cordova, C., Mooney, S., Moreno, P.I., Prentice, I.C., Thonicke, K., Tinner, W., Whitlock, C., Zhang, Y., Zhao, Y., Ali, A.A., Anderson, R.S., Beer, R., Behling, H., Briles, C., Brown, K.J., Brunelle, A., Bush, M., Camill, P., Chu, G.Q., Clark, J., Colombaroli, D., Connor, S., Daniau, A.-L., Daniels, M., Dodson, J., Doughty, E., Edwards, M.E., Finsinger, W., Foster, D., Frechette, J., Gaillard, M.-J., Gavin, D.G., Gobet, E., Haberle, S., Hallett, D. J., Higuera, P., Hope, G., Horn, S., Inoue, J., Kaltenrieder, P., Kennedy, L., Kong, Z.C., Larsen, C., Long, C.J., Lynch, J., Lynch, E.A., McGlone, M., Meeks, S., Mensing, S., Meyer, G., Minckley, T., Mohr, J., Nelson, D.M., New, J., Newnham, R., Noti, R., Oswald, W., Pierce, J., Richard, P.J.H., Rowe, C., Sanchez Go-i, M.F., Shuman, B.N., Takahara, H., Toney, J., Turney, C., Urrego-Sanchez, D.H., Umbanhowar, C., Vandergoes, M., Vanniere, B., Vescovi, E., Walsh, M., Wang, X., Williams, N., Wilmshurst, J., Zhang, J.H., 2008. Changes in fire regimes since the Last Glacial Maximum: an assessment based on a global synthesis and analysis of charcoal data. Clim. Dynam. 30 (7), 887—907, http://dx.doi.org/10.1007/s00382-007-0334-x.

Rahul, P.R.C., Sonbawne, S.M., Devara, P.C.S., 2014. Unusual high values of aerosol optical depth evidenced in the Arctic during summer 2011. Atmos. Environ. 94, 606—615, http://dx.doi.org/10.1016/j.atmosenv.2014.01.052.

Reddy, M.S., Boucher, O., Bellouin, N., Schulz, M., Balkanski, Y., Dufresne, J.L., Pham, M., 2005. Estimates of global multicomponent aerosol optical depth and direct radiative perturbation in the Laboratoire de Météorologie Dynamique General Circulation Model. J. Geophys. Res. 110 (D10), D10S16, 16 pp., http://dx.doi.org/10.1029/2004JD004757.

Rodríguez, E., Toledano, C., Cachorro, V., Ortiz, P., Stebel, K., Berjón, A., Blindheim, S., Gausa, M., de Frutos, A.M., 2012. Aerosol characterization at the sub-Arctic site Andenes (69° N, 16° E), by the analysis of columnar optical properties. Q. J. R. Meteorol. Soc. 138 (663), 471—482, http://dx.doi.org/10.1002/qj.921.

Rogers, J.C., Yang, L., Li, L., 2005. The role of Fram Strait winter cyclones on sea ice flux and on Spitsbergen air temperatures. Geophys. Res. Lett. 32, L06709, 4 pp., http://dx.doi.org/10.1029/2004GL022262.

Rozwadowska, A., Zieliński, T., Petelski, T., Sobolewski, P., 2010. Cluster analysis of the impact of air back-trajectories on aerosol optical properties at Hornsund, Spitsbergen. Atmos. Chem. Phys. 10 (3), 877—893, http://dx.doi.org/10.5194/acp-10-877-2010.

Rozwadowska, A., Gorecka, I., 2012. The impact of a non-uniform land surface on the radiation environment over an Arctic fjord — a study with a 3D radiative transfer model for stratus clouds over the Hornsund fjord, Spitsbergen. Oceanologia 54 (4), 509—543, http://dx.doi.org/10.5697/oc.54-4.509.

Schulz, M., de Leeuw, G., Balkanski, Y., 2004. Sea-salt aerosol source functions and emissions. In: Granier, C., Artaxo, P., Reeves, C.E. (Eds.), Emission of Atmospheric Trace Compounds. Advances in Global Change Research, vol. 18. Springer, Dordrecht, 333—354, http://dx.doi.org/10.1007/978-1-4020-2167-1_9.

Smirnov, A., Holben, B.N., Eck, T.F., Slutsker, I., Chatenet, B., Pinker, R.T., 2002. Diurnal variability of aerosol optical depth observed at AERONET (Aerosol Robotic Network) sites. Geophys. Res. Lett. 29 (23), 30-1—30-4, http://dx.doi.org/10.1029/2002GL016305.

Stohl, A., 2006. Characteristics of atmospheric transport into the Arctic troposphere. J. Geophys. Res. -Atmos. 111 (D11), D11306, 17 pp., http://dx.doi.org/10.1029/2005JD006888.

Stohl, A., Andrews, E., Burkhart, J.F., Forster, C., Herber, A., Hoch, S.W., Kowal, D., Lunder, C., Mefford, T., Ogren, J.A., Sharma, S., Spichtinger, N., Stebel, K., Stone, R., Ström, J., Tørseth, K., Wehrli, C., Yttri, K.E., 2006. Pan-Arctic enhancements of light absorbing aerosol concentrations due to North American, boreal forest fires during summer 2004. J. Geophys. Res. 111 (D22), D22214, 20 pp., http://dx.doi.org/10.1029/2006JD007216.

Stohl, A., Berg, T., Burkhart, J.F., Fjæraa, A.M., Forster, C., Herber, A., Hov, Ø., Lunder, C., McMillan, W.W., Oltmans, S., Shiobara, M., Simpson, D., Solberg, S., Stebel, K., Ström, J., Tørseth, K., Treffeisen, R., Virkkunen, K., Yttri, K.E., 2007. Arctic smoke—record high air pollution levels in the European Arctic due to agricultural fires in Eastern Europe in spring 2006. Atmos. Chem. Phys. 7 (2), 511—534, http://dx.doi.org/10.5194/acp-7-511-2007.

Stone, R.S., Herber, A., Vitale, V., Mazzola, M., Lupi, A., Schnell, R. C., Dutton, E.G., Liu, P.S.K., Li, S.-M., Dethloff, K., Lampert, A., Ritter, C., Stock, M., Neuber, R., Maturilli, M., 2010. A three-dimensional characterization of Arctic aerosols from airborne Sun photometer observations: PAM-ARCMIP, April 2009. J. Geophys. Res. Atmos. (1984—2012) 115 (D13), 18 pp., http://dx.doi.org/10.1029/2009JD013605.

Tomasi, C., Kokhanovsky, A., Lupi, A., Ritter, C., Smirnov, A., O'Neill, N.T., Stone, R.S., Holben, B.N., Nyeki, S., Wehrli, C., Stohl, A., Mazzola, M., Lanconelli, C., Vitale, V., Stebel, K., Aaltonen, V., de Leeuw, G., Rodriguez, E., Herber, A.B., Radionov, V.F., Zielinski, T., Petelski, T., Sakerin, S.M., Kabanov, D.M., Xue, Y., Mei, L., Istomina, L., Wagener, R., McArthur, B., Sobolewski, P.S., Kivi, R., Courcoux, Y., Larouche, P., Broccardo, S., Piketh, S., 2015. Aerosol remote sensing in polar regions. Earth Sci. Rev. 140, 108—157, http://dx.doi.org/10.1016/j.earscirev.2014.11.001.

Tomasi, C., Lupi, A., Mazzola, M., Stone, R.S., Dutton, E.G., Herber, A., Radionov, V., Holben, B.N., Sorokin, M., Sakerin, S.M., Tverpugova, S.A., Lanvonelli, C., Petkov, B., Vitale, V., 2012. An update of the long-term trend of aerosol optical depth in the polar regions using POLAR-AOD measurements performed during the International Polar Year. Atmos. Environ. 52, 29—47, http://dx.doi.org/10.1016/j.atmosenv.2012.02.055.

Tomasi, C., Vitale, V., Lupi, A., Di Carmine, C., Campanelli, M., Herber, A., Treffeisen, R., Stone, R.S., Andrews, E., Sharma, S., Radionov, V., von Hoyningen-Huene, W., Stebel, K., Hansen, G.H., Myhre, C.L., Wehrli, C., Aaltonen, V., Lihavainen, H., Virkkula, A., Hillamo, R., Ström, J., Toledano, C., Cachorro, V.E., Ortiz, P., de Frutos, A.M., Blindheim, S., Frioud, M., Gausa, M., Zielinski, T., Petelski, T., Yamanouchi, T., 2007. Aerosols in polar regions: a historical overview based on optical depth and in situ observations. J. Geophys. Res. -Atmos. 112 (D16), D16205, 28 pp., http://dx.doi.org/10.1029/2007JD008432.

Treffeisen, R., Herber, A., Ström, J., Shiobara, M., Yamanouchi, T., Yamagata, S., Kolmén, K., Kriews, M., Schrems, O., 2004. Interpretation of Arctic aerosol properties using cluster analysis applied to observations in the Svalbard area. Tellus B 56 (5), 457—476, http://dx.doi.org/10.3402/tellusb.v56i5.16469.

Treffeisen, R., Tunved, P., Ström, J., Herber, A., Bareiss, J., Helbig, A., Stone, R.S., Hoyningen-Huene, W., Krejci, R., Stohl, A., Neuber, R., 2007. Arctic smoke—aerosol characteristics during a record smoke event in the European Arctic and its radiative impact. Atmos. Chem. Phys. 7 (11), 3035—3053, http://dx.doi.org/10.5194/acp-7-3035-2007.

Tsukernik, M., Kindig, D.N., Serreze, M.C., 2007. Characteristics of winter cyclone activity in the northern North Atlantic: Insights from observations and regional modeling. J. Geophys. Res. 112 (D3), D03101, 19 pp., http://dx.doi.org/10.1029/2006JD007184.

Turetsky, M.R., Kane, E.S., Harden, J.W., Ottmar, R.D., Manies, K.L., Hoy, E., Kasichke, E.S., 2011. Recent acceleration of BB and carbon losses in Alaskan forests and peatlands. Nat. Geosci. 4, 27—31, http://dx.doi.org/10.1038/ngeo1027.

Ward, D.S., Kloster, S., Mahowald, N.M., Rogers, B.M., Randerson, J. T., Hess, P.G., 2012. The changing radiative forcing of fires: global model estimates for past, present and future. Atmos. Chem. Phys. 12 (22), 10857—10886, http://dx.doi.org/10.5194/acp-12-10857-2012.

Westerling, A.L., Hidalgo, H.G., Cayan, D.R., Swetnam, T.W., 2006. Warming and earlier spring increase western U.S. forest wildfire activity. Science 313 (5789), 940—943, http://dx.doi.org/10.1126/science.1128834.

WMO, 1994. Report of the WMO workshop on the measurements of atmospheric optical depth and turbidity. World Meteorol. Org. Rep. GAW-101, 13 pp.

Zielinski, T., 2004. Studies of aerosol physical properties in coastal areas. Aerosol Sci. Technol. 38 (5), 513—524, http://dx.doi.org/10.1080/02786820490466738.

Zielinski, T., Petelski, T., Makuch, P., Strzalkowska, A., Ponczkowska, A., Drozdowska, V., Gutowska, D., Kowalczyk, J., Darecki, M., Piskozub, J., 2012. Studies of aerosols advected to coastal areas with use of remote techniques. Acta Geophys. 60 (5), 1359—1385, http://dx.doi.org/10.2478/s11600-011-0075-4.

Oceanologia (2017) 59, 445—459

Available online at www.sciencedirect.com

ScienceDirect

journal homepage: www.journals.elsevier.com/oceanologia/

ORIGINAL RESEARCH ARTICLE

Monthly dynamics of carbon dioxide exchange across the sea surface of the Arctic Ocean in response to changes in gas transfer velocity and partial pressure of CO_2 in 2010

Iwona Wrobel *

Institute of Oceanology, Polish Academy of Sciences, Sopot, Poland

Received 5 July 2016; accepted 17 May 2017
Available online 7 June 2017

KEYWORDS
Partial pressure of CO_2;
Gas transfer velocity;
Arctic fjord;
Air—sea CO_2 fluxes;
Greenland and Barents seas

Summary The Arctic Ocean (AO) is an important basin for global oceanic carbon dioxide (CO_2) uptake, but the mechanisms controlling air—sea gas fluxes are not fully understood, especially over short and long timescales. The oceanic sink of CO_2 is an important part of the global carbon budget. Previous studies have shown that in the AO differences in the partial pressure of CO_2 (ΔpCO_2) and gas transfer velocity (k) both contribute significantly to interannual air—sea CO_2 flux variability, but that k is unimportant for multidecadal variability. This study combined Earth Observation (EO) data collected in 2010 with the in situ pCO_2 dataset from Takahashi et al. (2009) (T09) using a recently developed software toolbox called FluxEngine to determine the importance of k and ΔpCO_2 on CO_2 budgets in two regions of the AO — the Greenland Sea (GS) and the Barents Sea (BS) with their continental margins. Results from the study indicate that the variability in wind speed and, hence, the gas transfer velocity, generally play a major role in determining the temporal variability of CO_2 uptake, while variability in monthly ΔpCO_2 plays a major role spatially, with some exceptions.

* Correspondence address: Institute of Oceanology Polish Academy of Sciences,Powstańców Warszawy 55, 81-712 Sopot, Poland. Tel.: +48 587311801.
E-mail address: iwrobel@iopan.gda.pl.
Peer review under the responsibility of Institute of Oceanology of the Polish Academy of Sciences.

Production and hosting by Elsevier

http://dx.doi.org/10.1016/j.oceano.2017.05.001

1. Introduction

The global carbon cycle plays an important role in energy and mass exchange in the Earth System and links the components of this system (land, ocean, atmosphere) (Garbe et al., 2014; Thomas et al., 2004). Increases in atmospheric carbon dioxide (CO_2) concentrations caused mainly by the burning fossil fuels, cement production and growing urbanization are directly responsible for 60% of the average global air temperature increase (IPCC, 2013; Kulinski and Pempkowiak, 2011). Half of the CO_2 emitted remains in the atmosphere while the rest is absorbed by the oceans and land biomass (Le Quéré et al., 2010, 2016; Omar et al., 2003; Sabine et al., 2004; Yasunaka et al., 2016). Relevant knowledge of air–sea CO_2 fluxes and their spatial and temporal variability is essential to gain the necessary understanding of the global carbon cycle and to fully resolve the ocean's role in climate variability (Le Quéré et al., 2013; Wanninkhof et al., 2009; Woolf et al., 2013). It is well known that the Arctic Ocean (AO) is an overall sink for CO_2 throughout the year even though continental shelves can either be regional or seasonal sinks or sources of atmospheric CO_2. However, there is a lot of uncertainty in calculating the CO_2 budgets of marginal and coastal shelf seas especially in the Polar Ocean margins (Cai et al., 2006; Doney et al., 2009; Landschützer et al., 2014). At present, the net air–sea CO_2 fluxes in the AO have been estimated at -0.12 ± 0.06 PgC yr^{-1} with net global ocean CO_2 uptake at -2.2 ± 0.5 PgC yr^{-1} (Goddijn-Murphy et al., 2015; Gruber, 2009; Schuster et al., 2013; Takahashi et al., 2009; Wanninkhof et al., 2013). Additionally, Cai et al. (2006) have shown that the average sea–air CO_2 flux for Arctic shelves is estimated as -12 ± 4 gC m^{-1} a^{-1}. Arctic shelves are greatly influenced by sea ice cover and the age of terrestrial inputs resulting in large CO_2 sinks during ice-free periods (Bates and Mathis, 2009; Cai et al., 2006).

Projections of trends in net carbon dioxide air–sea fluxes suggest that, in the future, CO_2 uptake by the ocean will increase because of sea ice loss (IPCC, 2013; Rödenbeck, 2005; Schuster et al., 2013). Reports have also been published, indicating that the seawater partial pressure of CO_2 (pCO_{2W}) in the North Atlantic has increased at a rate higher than the atmospheric pCO_2 (pCO_{2A}) (Lefèvre et al., 2004; Olsen et al., 2003).

Currently, there are several different approaches for estimating air–sea CO_2 fluxes. The first involves measuring direct fluxes using eddy correlation techniques (Else et al., 2011; Kondo and Tsukamoto, 2012; Repina et al., 2007). Another method focuses on calculating net air–sea CO_2 exchange with a mass balance assessment of carbon stocks and the inputs/outputs of carbon or vertical variations in DIC (Dissolved Inorganic Carbon) (Arrigo et al., 2010; MacGilchrist et al., 2014). The third approach takes into account differences in atmospheric and seawater pCO_2 combined with gas transfer velocity parameterizations (k) (Bates and Mathis, 2009; Boutin et al., 2002; Land et al., 2013; Landschützer et al., 2014; Takahashi et al., 2009). This final approach can employ the neural network technique, the advantage of which is that it can "notice" and exploit unpredicted correlations in the data (Lefèvre et al., 2005; Telszewski et al., 2009; Yasunaka et al., 2016).

In this article, the net CO_2 flux across the sea surface is calculated by multiplying ΔpCO_2 by the CO_2 gas transfer velocity coefficient (k), which depends primarily on the degree of turbulence near the interface. The direction and rates of net air–sea CO_2 exchange are determined by the product of the difference in values between pCO_2 in seawater and the atmosphere, and also by the rate of k. Positive ΔpCO_2 values indicate that the sea is a source of atmospheric carbon dioxide, whereas negative values indicate that it is a sink. Choosing the appropriate formula for gas transfer velocity is the key when calculating net air–sea gas fluxes. The main difficulty in quantifying k is its dependence on several physicochemical elements of the environment, such as surfactants, wind speed, sea state, surface roughness and breaking waves (Ho et al., 2006; McGillis et al., 2001; Shutler et al., 2016; Takahashi et al., 2009; Wanninkhof et al., 2009). In the literature, a wide range of different gas transfer parameterizations can be found that were derived using a number of techniques, e.g., Wanninkhof and McGillis (1999), Nightingale et al. (2000), McGillis et al. (2001), Ho et al. (2006), and Wanninkhof et al. (2013). At present, parameterizations with a quadratic wind speed relationship are interchangeable in the Arctic as Wrobel and Piskozub (2016) have shown. Fluxes resulting from using these functions (Ho et al., 2006; Wanninkhof et al., 2013) are only 3–4% higher (Fig. 1), respectively, than the most accurate parameterization applied to the study region, which is Nightingale et al. (2000) (see also Wrobel and Piskozub, 2016). Earlier studies showed that over interannual and shorter timescales, both components of the right hand side of Eq. (1) are significant in controlling air–sea fluxes, with only a few exceptions (Couldrey et al., 2016; Doney et al., 2009). Over longer, interannual to multidecadal timescales, flux variability is controlled only by ΔpCO_2 (Bates, 2012; Couldrey et al., 2016; Doney et al., 2009; Gruber et al., 2003; Le Quéré et al., 2000). The high uncertainty in the size of the net AO sink stems from the lack of coordinated in situ measurements in the winter; data are interpolated for the rest of the year. A potential alternative solution lies in exploiting satellite data from EO techniques (Boutin et al., 2002).

When studying air–sea CO_2 exchange across the sea surface in the AO, one has to remember the important role of extensive ice coverage in this process. Because of this, the monthly dynamics of air–sea interactions were analyzed in this paper during a one year period. Seasonal sea ice cover can reduce the exchange of CO_2 across the sea surface, but it

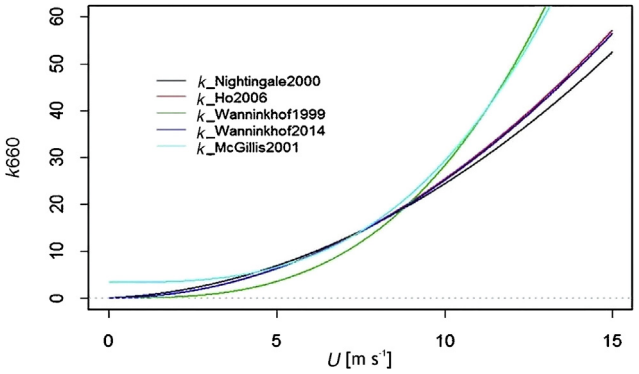

Figure 1 Gas transfer velocity [m s^{-1}] using different parameterizations as a function of wind speed [m s^{-1}].

also influences biogeochemical processes in surface water, especially inside Arctic fjords. The decrease of sea ice cover can result in an increase in outgassing in shallow shelf areas when surface waters are mixed deeper during the spring and winter. As was demonstrated in earlier studies by Olsen et al. (2003), Arrigo et al. (2008), Sejr et al. (2011), and others, sea ice loss in the AO produces a large area of open, ice-free water that is favorable for phytoplankton growth. Thinner seasonal sea ice cover replaces thick multi-year sea ice which makes it a weaker barrier for sea ice exchange, which means that phytoplankton spring blooms can absorb more CO_2 (Arrigo et al., 2008). Decreases of sea ice extent also cause water surface warming and, thus, act to reduce the CO_2 uptake by the ocean (Bates and Mathis, 2009). We do not yet fully understand whether decreased sea ice extent will indirectly affect higher CO_2 uptake by the ocean in the Arctic or not.

Trends and variability in the Arctic CO_2 sink have been studied intensively. Observations suggest its decrease is caused by increased in-water pCO_2 (Ashton et al., 2016; Boutin et al., 2002; Goddijn-Murphy et al., 2016; Lefèvre et al., 2004; MacGilchrist et al., 2014; Schuster et al., 2013). Marine pCO_2 seems to have been rising faster than atmospheric pCO_2, especially in the summer (Couldrey et al., 2016). The results from the FluxEngine-based Earth Observation (EO) data obtained from the European Space Agency OceanFlux Greenhouse Gases (GHG) Evolution project (http://www.oceanflux-ghg.org/) to evaluate how flux variability is controlled on short timescales. The present study examines the following testable hypothesis: air–sea CO_2 fluxes on a one year timeframe are dependent on both ΔpCO_2 and k.

1.1. Study area

The AO (Fig. 2) is relatively small ($\sim 10.7 \times 10^6$ km), and belongs to a class of ocean basins known as Mediterranean seas, with broad, shallow (<200 m deep) continental shelves surrounding a central basin. The AO has limited pathways of communication with Atlantic and Pacific waters, through the Bering Strait, the Canadian Archipelago, the Fram Strait and the Norwegian Sea gateways. Thermohaline forcing is the dominant driver (Piechura and Walczowski, 2009). Seasonal sea ice cover, especially in winter, reduces the exchange of energy, mass, and gases between the atmosphere and the ocean, and it also has a negative effect on sunlight penetration into the ocean that is needed for photosynthesis. Whether the Arctic acts as a sink or a source of CO_2 is controlled by many variables that are, themselves, influenced by climate change, including biological activity (Arrigo et al., 2010), temperature (Polyakov et al., 2004), riverine inputs (Dai et al., 2009), and sea ice melt (Bates and Mathis, 2009).

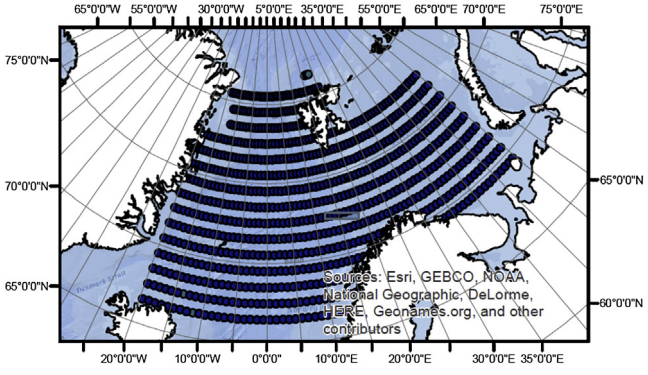

Figure 2 Study area (source: ArcGis basemap) — Greenland Sea and Barents Sea with sampling points.

The Barents Sea (BS) is the largest of the AO seas (1,424,000 km^2 area with a volume of about 316,000 km^3) and covers broad, shallow continental shelves with a maximum depth of ~600 m (average depth ~229 m) (Gurgul, 2002). It is characterized by an inflow of warm, saline Atlantic water via the Norwegian Atlantic Current and minimal freshwater inputs (Omar et al., 2003). Maximum wind speeds over the BS are about 20 m s^{-1}, with an average of approximately 6 m s^{-1} (Gurgul, 2002). Warm, saline Atlantic water is transformed into subsurface water by the process of brine rejection from sea ice formation or the cooling of surface water, and it is then transported to the Kara Sea and the central basin of the AO (Omar et al., 2007).

The Greenland Sea (GS) covers an area of 1,205,000 km^2 with an average depth of 1450 m and a maximum depth of approximately 5500 m. It lies south of the Arctic Basin and is a major pathway for the exchange of Arctic water with warm, saline Atlantic water through the Fram Strait via the deep East Greenland Current. Greenland Sea Deep Water is formed in the central GS, and it aerates the North Atlantic Deep Water (Nakaoko et al., 2006).

2. Methods

2.1. Data sets

Net air–sea CO_2 fluxes were calculated using the FluxEngine toolset (Shutler et al., 2016), which was created as a part of the European Space Agency funded OceanFlux Greenhouse Gases project (http://www.oceanflux-ghg.org) to encourage the use of satellite Earth Observation data. The toolbox allows its users to create their own climatology from the data available. After choosing the relevant data and formulae, users can create monthly global flux datasets. FluxEngine is available publicly on the Ifremer/CERSAT (Centre d'Exploitation et de Recherche Satellitaire) Nephelae Cloud (no specific skills are required to use it), and can be run through a web interface (http://cersat.ifremer.fr/data/collections/oceanflux) or it can also be downloaded. The source code can be downloaded from a GitHub server (Goddijn-Murphy et al., 2015; Shutler et al., 2016; Wrobel and Piskozub, 2016).

The calculations for this study were based on the climatological mean distribution of surface water pCO_2 and salinity values from Takahashi et al. (2009) (T09) climatology, archived at the Carbon Dioxide Information and Analysis Centre (CDIAC, Oak Ride, National Laboratory (Takahashi et al., 2008)) in non-El Niño conditions. T09 data were normalized to 2010 to evaluate seasonal variations in air–sea CO_2 fluxes (the calculations were based on Olsen et al. (2003), Omar et al. (2003), Nakaoko et al. (2006), Goddijn-Murphy et al. (2015) approaches, that assumed the partial CO_2 pressure in seawater has increased at a rate of 1.5 μatm yr^{-1}, on average observed for CO_2 partial pressure

in the air). Wind speed data at 10 m a.s.l. were obtained from the GlobWave project (http://globwave.ifremer.fr/), which produced a 20-plus year time series of global coverage multi-sensor cross-calibrated wave and wind data. The Sea Surface Temperature (SST) data were obtained from Ifremer/CERSAT and produced OceanFlux from ARC/(A)ATRS (Advance Along Track Scanning Radiometer measurements) carried out by the Envisat satellite (Merchant et al., 2012). SST_{skin} data are defined as the *"radiometric temperature of the surface measured by an infrared radiometer operating in the 1–12 μm waveband (10–20 μm depth"* according to definition in The Global Ocean Data Assimilation Experiment (GODAE) high-resolution sea surface temperature pilot project; Minnett and Kaiser-Weiss, 2012). The (A)ATSR is a self-calibrating radiometer that provides estimates of SST and exhibits a very small standard deviation of error. The k coefficient was estimated using the Nightingale et al. (2000) parameterization (hereafter called N2000, Fig. 1), which best fits the AO (Wrobel and Piskozub, 2016). All input data and climatologies were linearly re-interpolated to a $1^\circ \times 1^\circ$ geographical grid from the original resolution, and calculated for 2010 using the FluxEngine toolset. Data were extracted for the AO (north of 66°) from global resolution.

2.2. Parameterizations

The air–sea CO_2 flux is controlled by wind speed, SST, Sea Surface Salinity (SSS), sea state, and biological activity (Goddijn-Murphy et al., 2016). The calculations of CO_2 flux between the air and the sea [F, mgC m^{-2} day^{-1}] are given based the ΔpCO_2 [μatm] across a thin (~10–250 μm) mass boundary layer at the sea surface and the solubility of CO_2 [α, g m^{-3} μatm^{-1}] multiplied by the gas transfer velocity [k, cm h^{-1}] as a function of wind speed. The concentration of CO_2 in the sea water is a function of SSS and SST, its solubility [α, g m^{-3} μatm^{-1}], and its fugacity [fCO_2, μatm]. Hence, the standard bulk formula for the flux (F) was defined as:

$$F = k(\alpha_W pCO_{2W} - \alpha_S pCO_{2A}), \quad (1)$$

where S is the air–sea interface, A is the air, and W is water. We can replace fugacity with partial pressure (their values differ by $< 0.5\%$ over the temperature range considered) (McGillis et al., 2001). So Eq. (1) becomes:

$$F = k(\alpha_W pCO_{2W} - \alpha_S pCO_{2A}), \quad (2)$$

$$F = k\alpha\Delta pCO_2. \quad (3)$$

Gas transfer velocity was mainly parametrized as:

$$k_W = Sc^{-n}(a_0 + a_1 U + a_2 U^2 + a_3 U^3), \quad (4)$$

(Wanninkhof et al., 2009) where ($a_0 \ldots a_n$) are coefficients (one or more of which may be set to zero) of polynomials in wind-speed U [m s^{-1}], Sc is the Schmidt number of dissolved gas. Schmidt numbers at the skin surface (Sc_{skin}) are a function of SST [= (kinematic viscosity of water)/(diffusion coefficient of CO_2 in water)]. The Schmidt number for CO_2 in seawater at 20°C is equal to 660.0. The calculations were based on the Nightingale et al. (2000) parameterization:

$$k = \sqrt{(600.0/Sc_{skin}) * (0.222\,U_{10}^2 + 0.333\,U_{10})}. \quad (5)$$

The parameterization was based on multiple trace experiment conducted in the southern North Sea during one month in 1992 and 1993 and based on data from March and October 1989.

3. Results and discussion

The global monthly air–sea CO_2 flux variability, the partial pressure of CO_2 in seawater (pCO_{2W}), and gas transfer velocity rates (k) were estimated using FluxEngine software. Values were extracted from these for the two study regions – the GS and BS in the AO (north of 66°) (Fig. 2). The periods from October to April were defined as wintertime and from May to September as summertime. Since wind velocity was used to estimate k, Fig. 1 shows a wide range of empirical formulas. The N2000 quadratic dependence of k on wind speed, which fit the best to AO air–sea interaction measurements (Wrobel and Piskozub, 2016), was chosen for this study. In the AO where the average wind speed during the study period was approximately 8 ± 0.7 m s^{-1} (see Table 1), the average gas transfer velocity rate was 13.0 ± 1.9 cm h^{-1} (Fig. 1). For better proof of results, a statistical summary of the data was calculated (Table 1). The area, as a whole, is a sink of CO_2 with an annual average wind speed of approximately 8 ± 0.7 m s^{-1}, an annual average k of 13.0 ± 1.9 cm h^{-1}, and a concentration of pCO_{2W} (332.4 ± 11.8 μatm) lower than the annual partial pressure of CO_2 in the atmosphere for the year 2010 (382 ± 0.6 μatm). The SST was approximately 3.0 ± 1.6°C and salinity was 34.3.

Table 2 shows the mean monthly variability of the estimated variables. Despite the AO acting as a sink for atmospheric CO_2, considerable variability in ΔpCO_2 was observed

Table 1 Statistics of data used for calculations. Descriptions in rows: k – gas transfer coefficient, U_{10} – 10-m wind speed, pCO_{2W} and pCO_{2A} – seawater and atmospheric partial pressure of CO_2, respectively, ΔpCO_2 – difference in partial pressure, SST – sea surface temperature.

	N	Ave.	Min	Max	St. error	Var.	St. dev
F [mgC m^{-2} day^{-1}]	576	−8.0	−15.4	−4.2	0.1	2.6	1.6
k [cm h^{-1}]	576	13.0	7.9	17.9	0.1	3.5	1.9
U_{10} [m s^{-1}]	576	8.3	5.8	9.7	0.0	0.4	0.7
pCO_{2W} [μatm]	576	332.4	292.7	354.6	0.5	139.2	11.8
ΔpCO_2 [μatm]	576	−50.1	−91.1	−27.7	0.5	152.2	12.3
pCO_{2A} [μatm]	576	382.5	381.2	384.1	0.0	0.4	0.6
SST [°C]	576	3.0		6.5	0.1	2.7	1.6

in space and time (Fig. 6 and Table 2). The pCO_{2W} varies considerably, both spatially and temporarily, as has been shown in recent studies, e.g., Olsen et al. (2003), Omar et al. (2003), Nakaoko et al. (2006), Takahashi et al. (2009), and Sejr et al. (2011). The mean values of partial CO_2 pressure in the air range from 372.5 ± 0.6 μatm in August to 389.1 ± 0.6 μatm in May, while values of partial CO_2 pressure in seawater varied from 309.1 ± 11.8 μatm in August to 348.2 ± 11.8 μatm in February. Bates and Mathis (2009) showed that when SST rises by 1°C pCO_{2W} should increase by up to 8 to 12 μatm/°C. Nakaoko et al. (2006) reported that monthly pCO_{2W} values increased proportionately to increasing SST (in 1994–2001), except in May and June. In June, when SST was above 2°C, pCO_{2W} was higher than 250 μatm, while lower pCO_{2W} was observed when SST was about 1°C. The results from FluxEngine show that when SST increased above 2.5°C, pCO_{2W} was lower than 340 μatm, and when SST decreased below 2.5°C, pCO_{2W} was higher than 340 μatm, except in May. Calculations from FluxEngine indicate the opposite relationship to that demonstrated in Bates and Mathis (2009). During the study period, gas transfer velocity varied from 19.9 ± 1.9 cm h^{-1} in December, when values of wind speed were higher than 10 m s^{-1}, to 6.6 ± 1.9 cm h^{-1} in July when wind speed was lower than 5 m s^{-1}. The strongest winds in the AO were from October to April at mean values of 9.0 ± 0.7 m s^{-1}, while from May to September the values were 6.0 ± 0.7 m s^{-1}.

Fig. 3 shows the relationships between annual mean pCO_{2W} concentrations and air–sea CO_2 fluxes to the north. Over spatial scales, the air–sea CO_2 flux values were strongly positively linked to the partial pressure of CO_2 in seawater (much less than with k) (see Table 3). Regions from the Arctic Circle to the North Pole were sinks of CO_2, and all surface pCO_2 values were below atmospheric levels (pCO_2 in the atmosphere was 380 μatm in 2010), although the Arctic Circle regions were close to equilibrium. The calculated oceanic CO_2 uptake varied between −6 to −16 mgC m^{-2} day^{-1}, and pCO_{2W} concentrations varied between 360 and 290 μatm to the northward. Variations in pCO_{2W} mainly stemmed from to biological activity, changes in sea surface temperature, and water mass transport, which are clearly indicated in Fig. 3 (Garbe et al., 2014; Nakaoko et al., 2006). The SST of the GS and BS was dominated by the inflow of warm North Atlantic Ocean water.

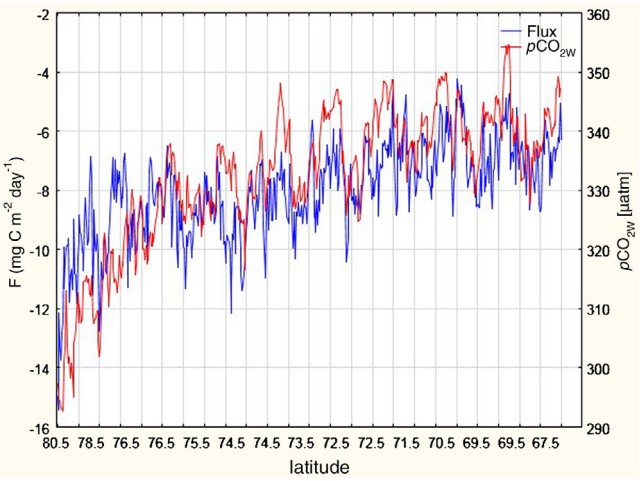

Figure 3 Annual mean pCO_2 in seawater [μatm] and air–sea CO_2 fluxes [mgC m^{-2} day^{-1}].

Fig. 4 illustrates maps of the zonal mean pCO_{2W} in February and August, and Fig. 5 indicates differences between them. In summer, all the pCO_{2W} values in the GS and BS were below atmospheric levels, while in winter pCO_{2W} was close to or higher than atmospheric levels in the BS. These results are in good agreement with those obtained by Cai et al. (2006), Nakaoko et al. (2006) for 1992–2001, and Sejr et al. (2011) for 2006–2009. Calculations from FluxEngine indicate that annual mean values of pCO_{2W} in 2010 were 332.4 ± 11.8 μatm (see Table 1), with mean values in August of 295 ± 11.8 μatm in the GS and 355 ± 11.8 μatm in the BS. Weiss et al. (1992) showed in July 1981 and 1990 that pCO_{2W} concentrations were around 225–230 μatm, while in August 1994–2001 they were around 255 μatm in the GS and 280 μatm in the BS (Nakaoko et al., 2006). During 1995–2003, the annual mean pCO_2 was 313 ± 4.1 μatm in the GS and 292 ± 6.1 μatm in the BS (Arrigo et al., 2010), and in 1995 it was only 282 ± 31 μatm (Takahashi et al., 2002). Generally, the AO is a strong net CO_2 sink; however, there

Table 2 Monthly dynamics of the datasets in the AO. Descriptions in columns: k – gas transfer coefficient, U_{10} – 10-m wind speed, pCO_{2W} and pCO_{2A} – seawater and atmospheric partial pressure of CO_2, respectively, ΔpCO_2 – difference in partial pressure, SST – sea surface temperature.

	F [mgC m^{-2} day^{-1}]	k [cm h^{-1}]	U_{10} [m s^{-1}]	pCO_{2W} [μatm]	ΔpCO_2 [μatm]	pCO_{2A} [μatm]	SST [°C]
Jan	−10.9	18.4	10.6	341.7	−44.2	385.9	2.24
Feb	−8.5	16.6	10	348.2	−39.5	387.8	2.2
Mar	−8.8	16	9.8	346.2	−39.5	385.6	1.92
Apr	−8.4	13.5	8.8	341.5	−44.6	387	1.72
May	−6.9	9.1	7	334.6	−56.5	389.1	2.01
Jun	−4.4	6.8	5.8	328.1	−57.7	384.6	3.44
Jul	−4	6.6	5.2	314.6	−63	377.6	4.99
Aug	−5	7.4	5.9	309.1	−59.4	372.5	4.55
Sep	−6	9.4	6.9	321.3	−52.4	373.11	4.14
Oct	−8.2	16.5	9.4	335.1	−39.1	376.1	3.99
Nov	−11.7	17.5	10	334.2	−48.5	382.7	2.67
Dec	−13.6	19.9	10.9	335	−49	385.2	2.71

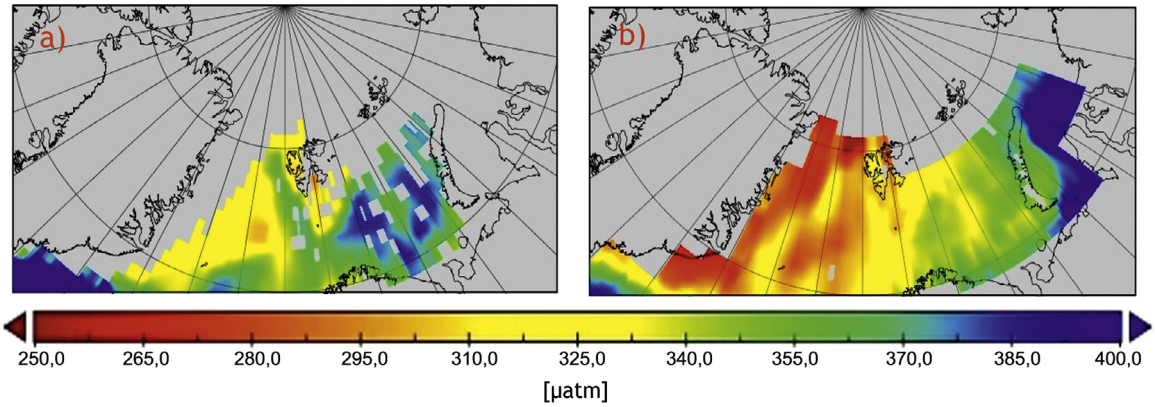

Figure 4 Monthly mean values for pCO_2 in seawater [µatm] in February (a) and August (b).

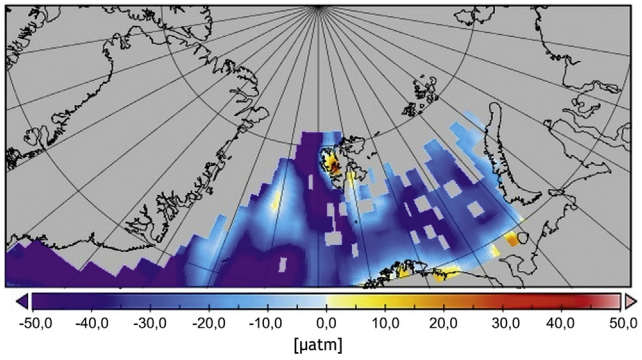

Figure 5 Difference maps for surface water pCO_2 [µatm] values for August–February.

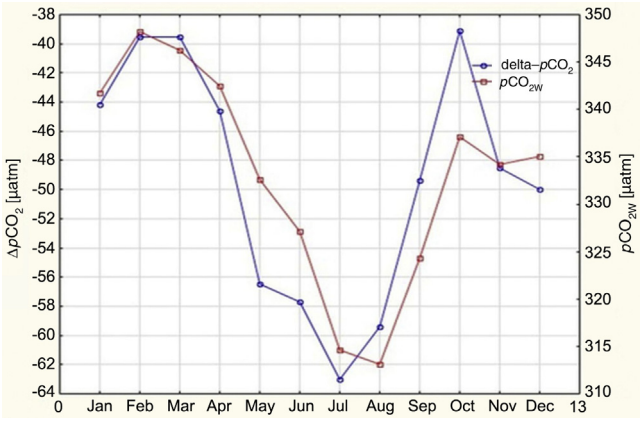

Figure 6 Monthly variability of differences in partial pressure of CO_2 ΔpCO_2 [µatm] and pCO_2 in seawater [µatm].

Table 3 The Pearson linear correlation between datasets in the Arctic Ocean. Descriptions in rows and columns: k – gas transfer coefficient, U_{10} – 10-m wind speed, pCO_{2W} and pCO_{2A} – atmospheric and seawater partial pressure of CO_2, respectively, ΔpCO_2 – difference in partial pressure, SST – sea surface temperature.

	F [mgC m^{-2} day^{-1}]	k [cm h^{-1}]	U_{10} [m s^{-1}]	pCO_{2W} [µatm]	ΔpCO_2 [µatm]	pCO_{2A} [µatm]	SST [°C]
F [mgC m^{-2} day^{-1}]	1.000	0.185	0.042	0.757	0.759	−0.664	0.628
k [cm h^{-1}]	0.185	1.000	0.930	0.636	0.643	−0.663	0.655
U_{10} [m s^{-1}]	0.042	0.930	1.000	0.567	0.570	−0.540	0.457
pCO_{2W} [µatm]	0.757	0.636	0.567	1.000	1.000	−0.833	0.732
ΔpCO_2 [µatm]	0.759	0.643	0.570	1.000	1.000	−0.849	0.745
pCO_{2A} [µatm]	−0.664	−0.663	−0.540	−0.833	−0.849	1.000	−0.878
SST [°C]	0.628	0.655	0.457	0.732	0.745	−0.878	1.000

Table 4 The Pearson linear correlation coefficient between datasets in 2010. Descriptions in columns and rows: k – gas transfer coefficient, U_{10} – 10-m wind speed, pCO_{2W} and pCO_{2A} – seawater and atmospheric partial pressure of CO_2, respectively, ΔpCO_2 – difference in partial pressure, SST – sea surface temperature.

	F [mgC m^{-2} day^{-1}]	k [cm h^{-1}]	U_{10} [m s^{-1}]	pCO_{2W} [µatm]	ΔpCO_2 [µatm]	pCO_{2A} [µatm]	SST [°C]
F [mgC m^{-2} day^{-1}]	1.000	−0.934	−0.928	−0.640	−0.559	−0.475	0.606
k [cm h^{-1}]	−0.934	1.000	0.992	0.761	0.788	0.382	−0.568
U_{10} [m s^{-1}]	−0.928	0.992	1.000	0.826	0.815	0.472	−0.661
pCO_{2W} [µatm]	−0.640	0.761	0.826	1.000	0.877	0.718	−0.858
ΔpCO_2 [µatm]	−0.559	0.788	0.815	0.877	1.000	0.295	−0.562
pCO_{2A} [µatm]	−0.475	0.382	0.472	0.718	0.295	1.000	−0.888
SST [°C]	0.606	−0.568	−0.661	−0.858	−0.562	−0.888	1.000

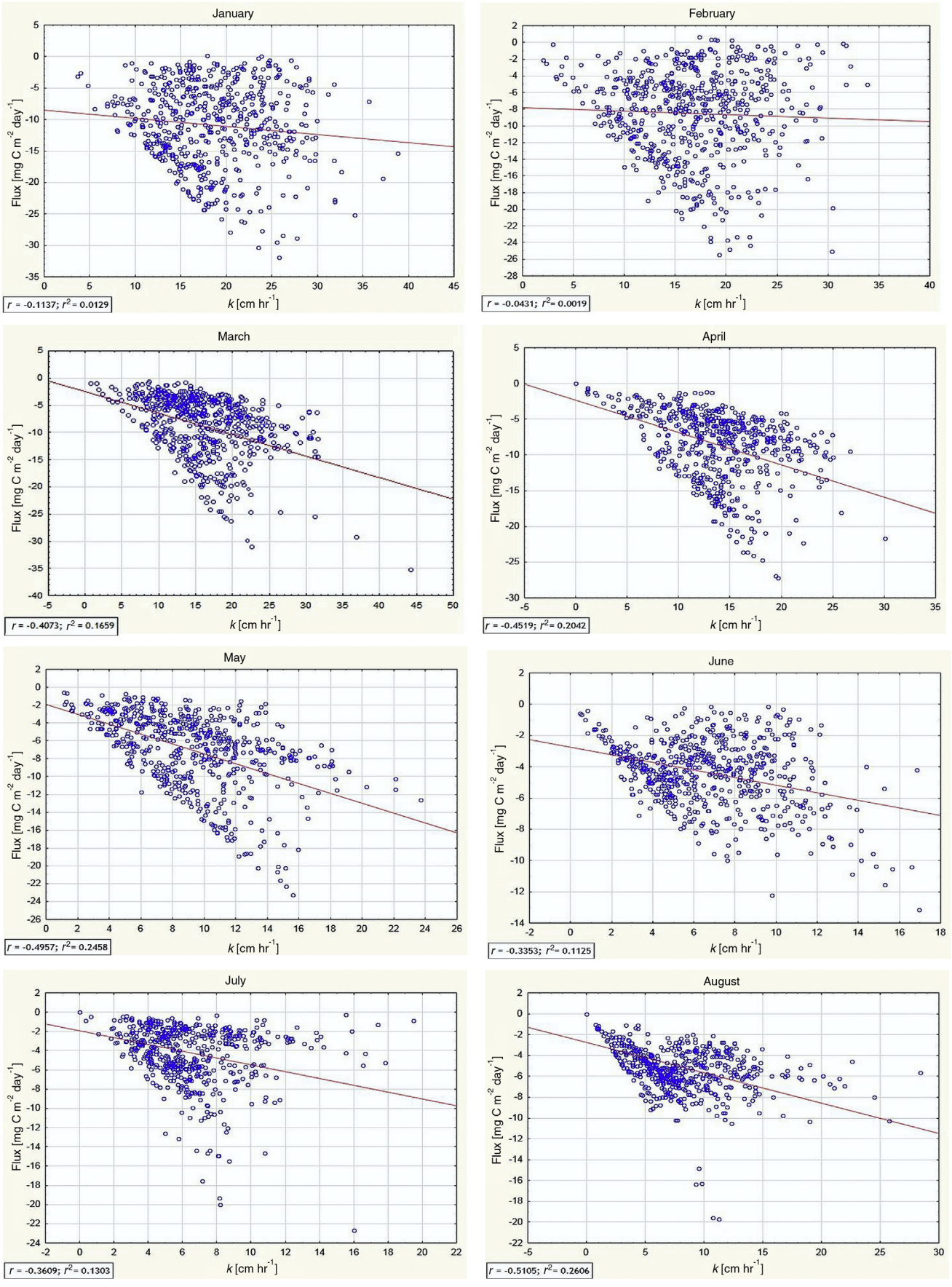

Figure 7 Monthly variations of air—sea CO_2 fluxes [mgC m^{-2} day^{-1}] as a function of gas transfer velocity [cm h^{-1}].

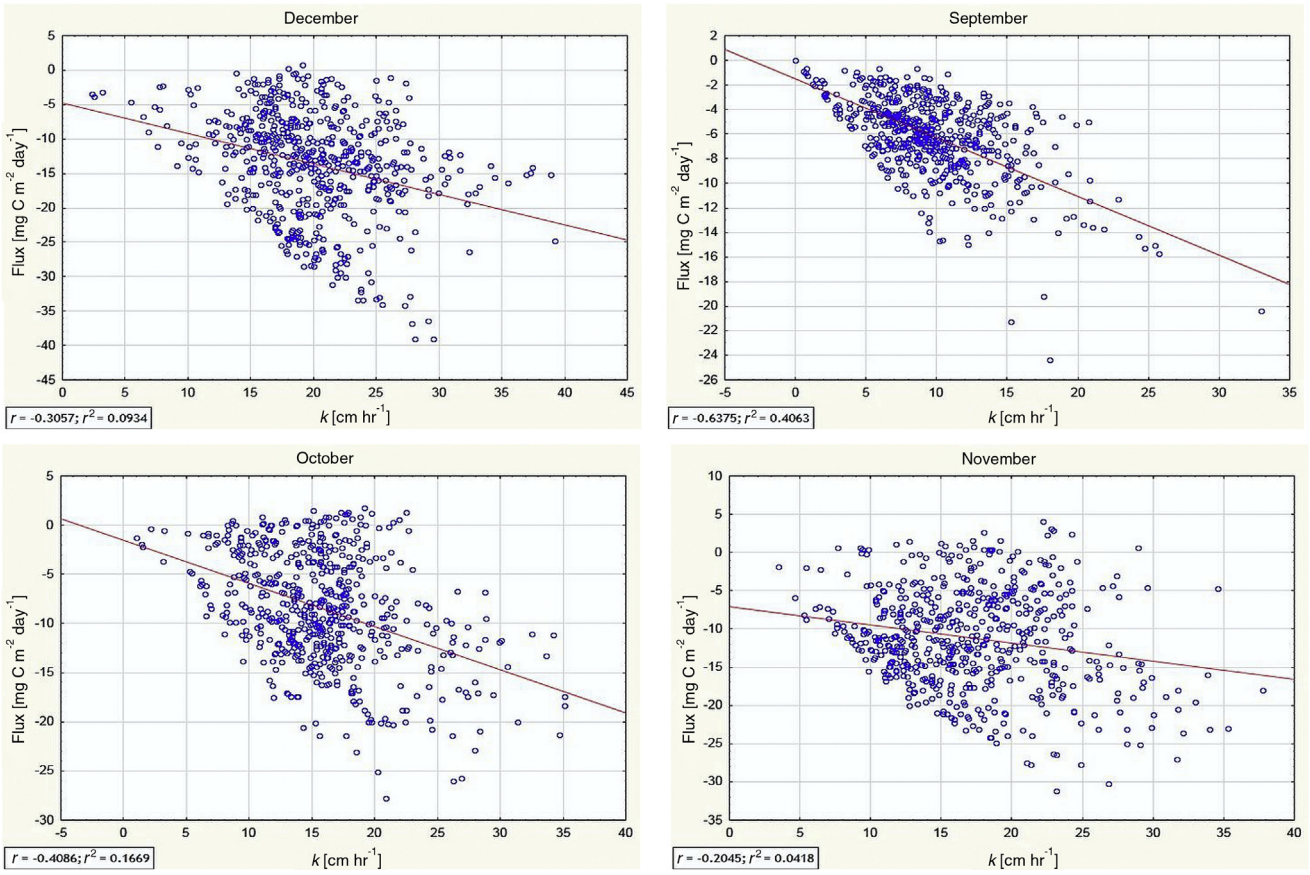

Figure 7. (*Continued*).

are shallow coastal areas where it is a source of CO_2 to the atmosphere, caused by river outputs and sea ice melting (Bates and Mathis, 2009). Seasonal changes in biological activity (phytoplankton primary production, PP), sea water warming and cooling, and the volume of CO_2 exchange caused seasonal changes in surface pCO_2. In wintertime, during the study, when the temperature of sea water was lower than in summer, pCO_{2W} levels were higher in the open water of the GS and BS in February (310—370 and 355—400 μatm, respectively) than in August (250—325 and 325—370 μatm, respectively) (Fig. 4). Additionally, in the GS, in both February and August, the concentration of pCO_{2W} was lower (Fig. 4) with differences in absolute values higher than in the BS (Fig. 5). This observation agrees well with earlier results obtained by Takahashi et al. (2002), Olsen et al. (2003), and Nakaoko et al. (2006). During summertime, surface pCO_{2W} values decreased, in spite of seasonal warming and oceanic CO_2 uptake increased thanks to high CO_2 exchange (Bates and Mathis, 2009). These processes were counterbalanced by the uptake of CO_2 in summertime by phytoplankton that decreased pCO_2.

Fig. 5 shows that inside the Arctic fjord the difference between pCO_2 in the summer and the winter was caused by lower surface-water pCO_2 levels resulting from sea ice melt, dissolution of $CaCO_3$, primary production, and strong stratification of the water column inside the fjord. Melting sea ice in the summer caused low pCO_2 levels, but melt water ponds were also pCO_{2A} sinks (Sejr et al., 2011; Semiletov et al., 2004). The results from estimations contrast with those gathered by Omar et al. (2007) and Sejr et al. (2011), and they show that fjords and nearby lands in the AO are places where physical process do not exceed biological CO_2 uptake because of runoff from lands, but in the open water area of the AO the opposite was found. This could steam from the fjords not being well represented in the data, and it could imply some underestimation of ΔpCO_2 rates. It does indicate, though, that more study of the shallow and marginal areas is required.

Fig. 6 shows the monthly values of pCO_{2W} and ΔpCO_2. Over the temporal scale, of the study period, all surface pCO_2 levels were below atmospheric levels (average 380 μatm) resulting in negative ΔpCO_2. The calculated pCO_{2W} and ΔpCO_2 values show seasonal variation of about 39 and 24 μatm, respectively, with two maxima for pCO_{2W} in February and October and one minima in August, and two minima for ΔpCO_2 in March and October and one maxima in July. These observations agree well with the previous studies (Nakaoko et al., 2006; Takahashi et al., 2009). The ΔpCO_2 values increased (at a rate of 5 μatm) compared to previous results obtained by Takahashi et al. (2009). The seasonal difference in ΔpCO_2 (strong negative values in the summertime) resulted from the biological drawdown of CO_2. Differences in the partial pressure of CO_2 were very strongly correlated with changes in the partial pressure of CO_{2W}, especially in wintertime, when the average water temperature was higher than the air temperature (see also the discussion in Table 2).

Figs. 7 and 8 show regression lines, correlations, and determination coefficients between air—sea CO_2 fluxes,

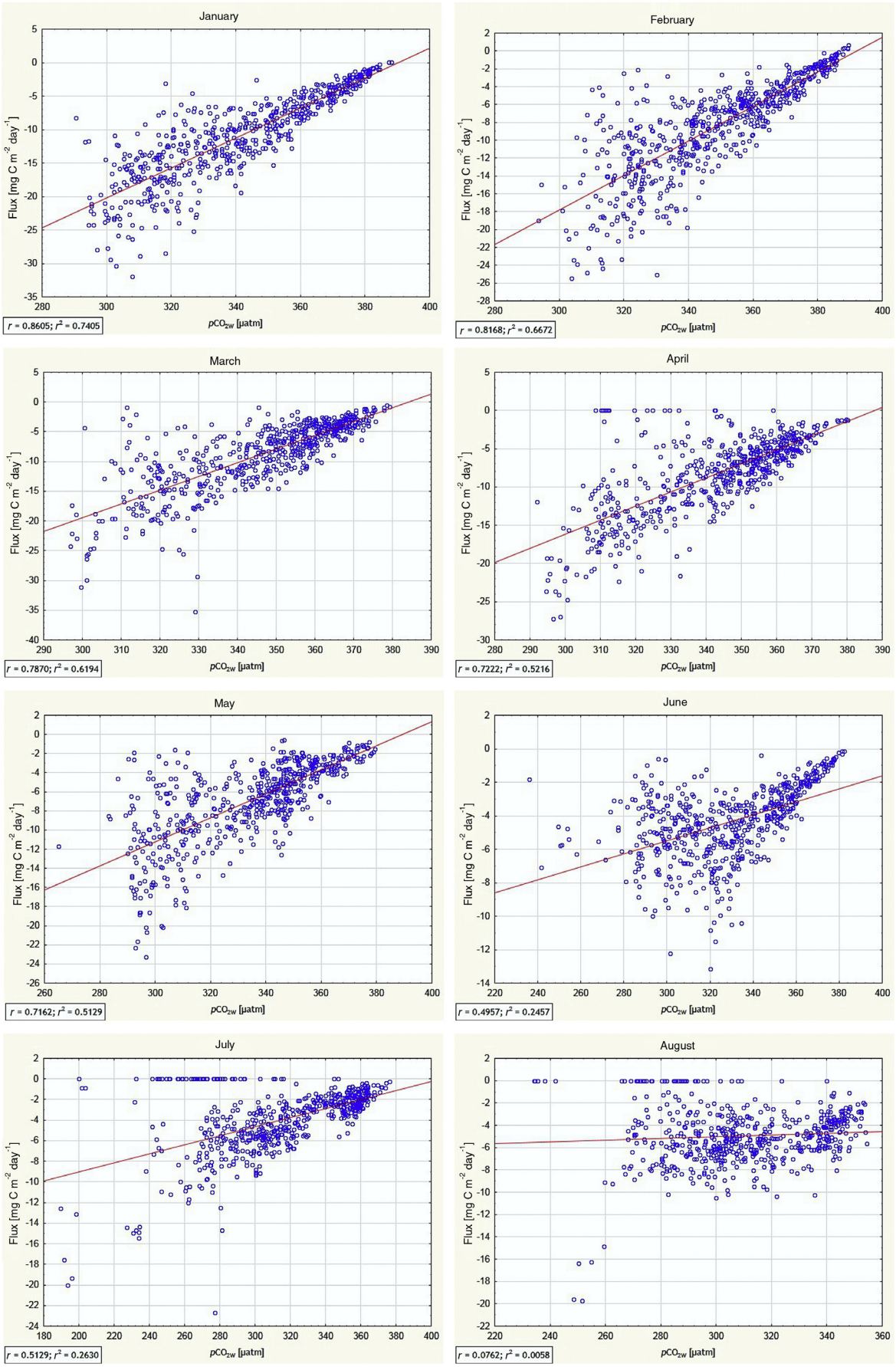

Figure 8 Monthly dynamics of air–sea CO_2 flux [mgC m^{-2} day^{-1}] as a function of pCO_2 in seawater [µatm].

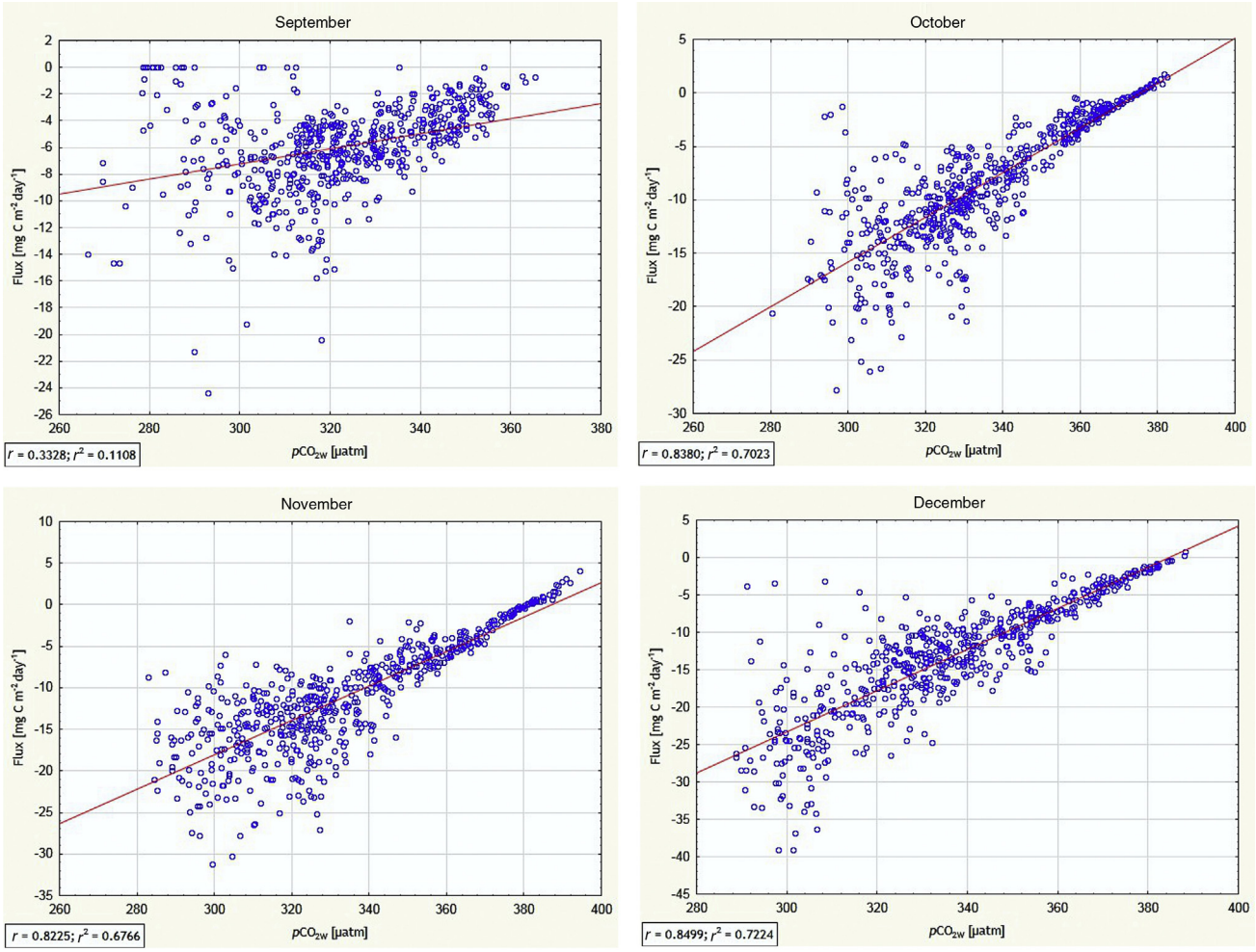

Figure 8. (*Continued*).

pCO_{2W}, and k for individual months. The correlation coefficient (r) represents the linear relationship between two variables and the determination coefficient (r^2) represents the proportion of common variation between the two variables (StatSoft Inc., 2013). Over spatial scales, fluxes were better correlated with pCO_{2W} than with gas transfer velocity during each month. In the relationship between air–sea fluxes and k, in May, August, and September more than 20% of variability in fluxes was explained by k (typically less than 20%; Fig. 7). More than 50% of variability in fluxes was explained by pCO_{2W} (except from June to September, when it was less than 20%; Fig. 8). In summertime, CO_2 flux variability was controlled by k, as a function of sea ice cover. The results reflect those obtained by Doney et al. (2009) and Couldrey et al. (2016). They demonstrated that variability in k contributes to only approximately 35% of the global interannual flux variability, while ΔpCO_2 contributes 60% of total variability.

Fig. 9 shows spatiotemporal mean air–sea CO_2 fluxes in the GS and BS during study period using the Nightingale et al. (2000) k parameterization. Cai et al. (2006) estimated that the continental shelves of the AO were responsible for the total uptake of atmospheric CO_2 of 52 TgC a^{-1}, equivalent to an average air–sea CO_2 flux of −12 gC m^{-2} a^{-1}. The total uptake for the BS was estimated to be about 3.2 TgC a^{-1} or a flux of −4.38 gC m^{-2} a^{-1}. Following the methods described in Table S1 in Cai et al. (2006), the total uptake of atmospheric CO_2 on the continental shelves of the GS and BS was estimated as 3.6 TgC a^{-1} and the average air–sea CO_2 fluxes were estimated about −3.62 gC m^{-2} a^{-1}. As can be seen, the GS was a stronger net sink of CO_2 in winter (approximately −12 mgC m^{-2} day^{-1}), while the BS was a very weak sink for CO_2 that was close to equilibrium. There were seasonal changes throughout the year. The annual mean air–sea CO_2 flux for the whole study area was −8.0 mgC m^{-22} day^{-1} (see Table 1). This is because the BS had higher SST than the GS because of the inflow of warm water via the North Atlantic Current (Land et al., 2013). Additionally, as is shown in Fig. 3, air–sea CO_2 fluxes are strongly positively correlated with pCO_{2W} over spatial scales. Estimates for the central GS are similar to previous results: 52 gC m^{-2} a^{-1} for the 1992–2001 period (Nakaoko et al., 2006), 25 gC m^{-2} a^{-1} for 2006, and 42 gC m^{-2} a^{-1} for 2009 (Sejr et al., 2011). Most areas of the BS became CO_2 sources in summer and fall, which is likely to be from the effect of sea–water temperature changes. During spring, no upward CO_2 flux was observed in the Arctic sector of the Atlantic Ocean. The air–sea CO_2 flux from the atmosphere decreased slightly

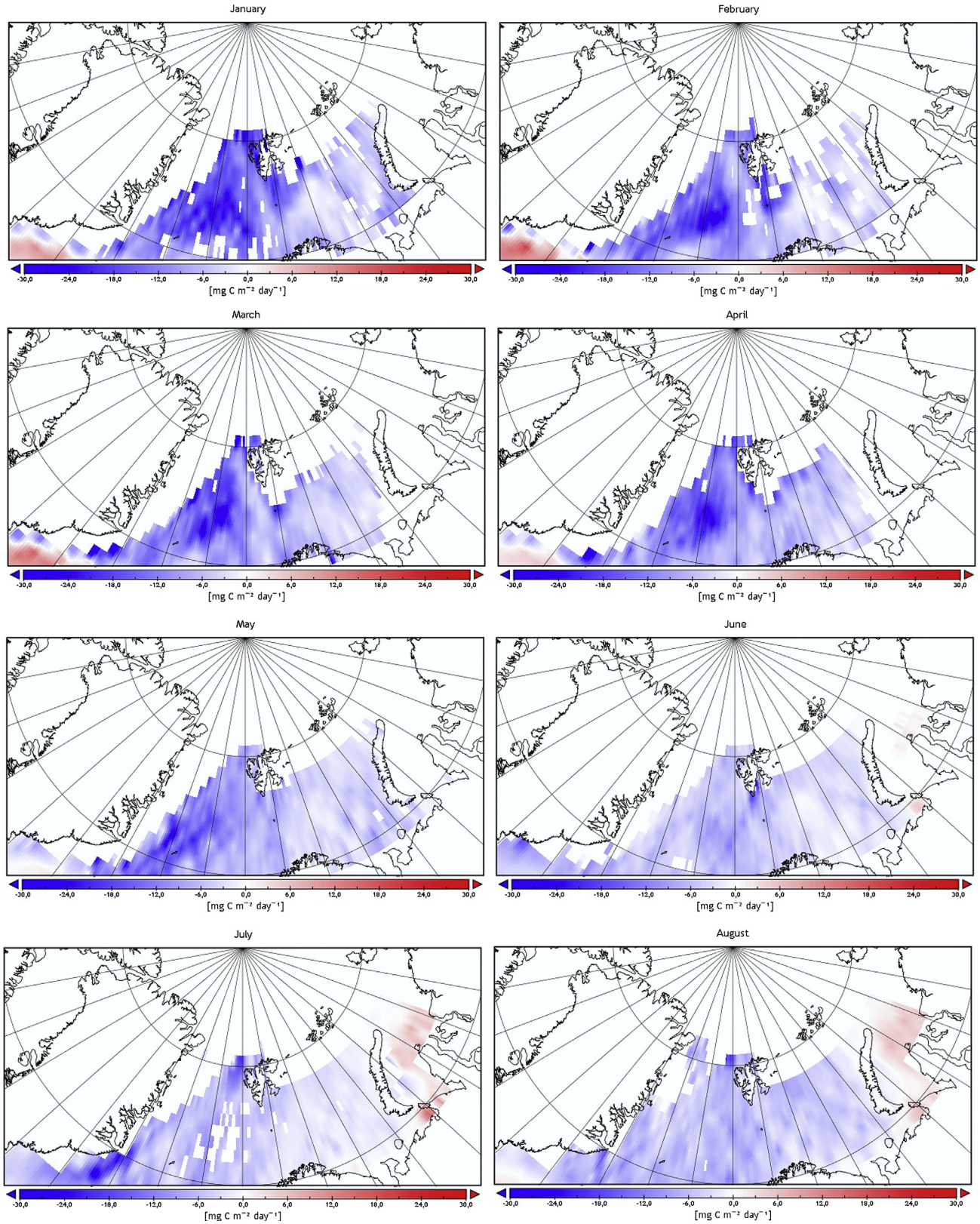

Figure 9 Monthly mean values for air–sea CO_2 fluxes [mgC m^{-2} day^{-1}] combined using *k* parameterization by Nightingale et al. (2000). Blue is absorbing, red is emitting. (For interpretation of the references to color in this figure legend, the reader is referred to the web version of the article.)

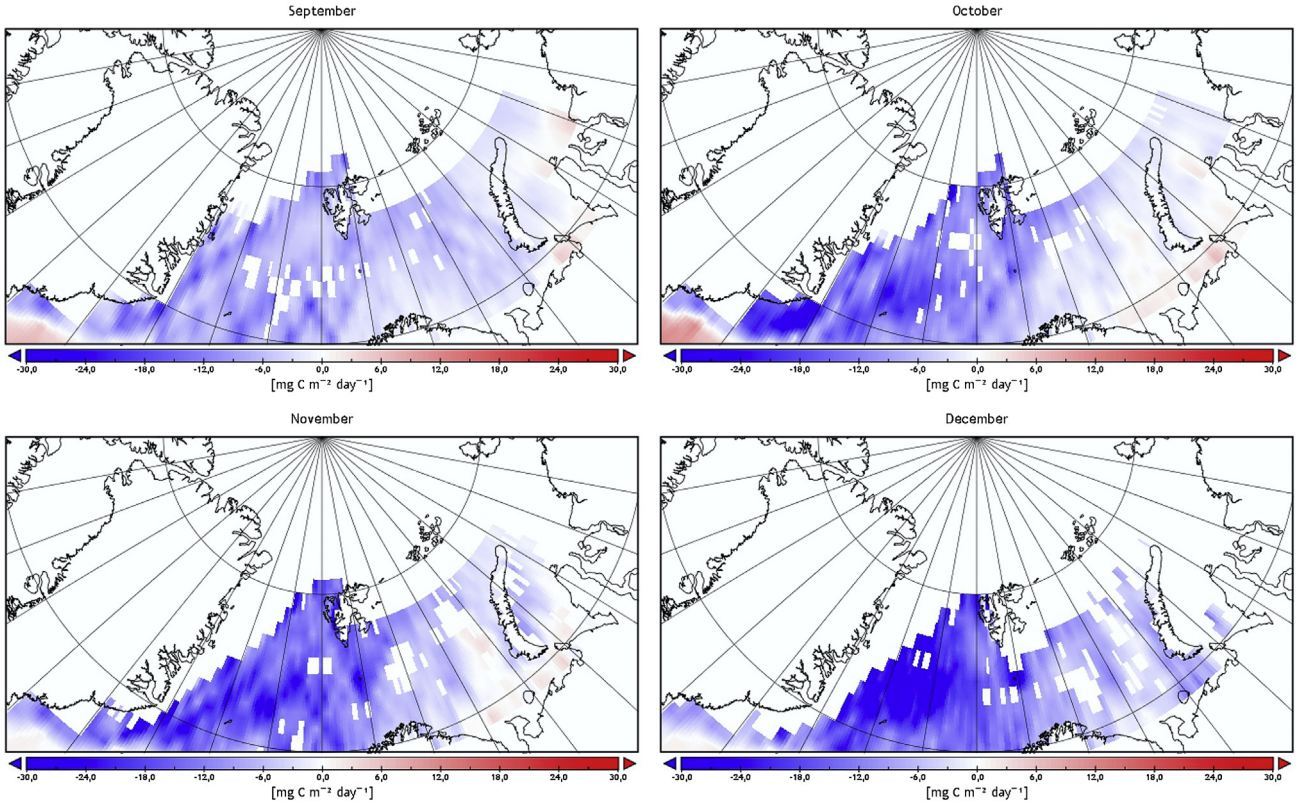

Figure 9. (*Continued*).

during June and July (Fig. 9), which was because of a steep decrease in average wind speed and low pCO_2; these values were in good agreement with results reported by Arrigo et al. (2010).

The relationships among the variables influencing gas fluxes on spatial and temporal scales are shown in Tables 3 and 4. In general, there were very few positive correlations between air–sea CO_2 fluxes and k over spatial scales ($r = 0.185$, $p < 0.05$), and very strong negative correlations over temporal scales ($r = -0.935$, $p < 0.05$) with moderate negative correlations in individual months (Fig. 7). In wintertime, when the wind was stronger (hence higher k), than in summertime, the rates of air–sea CO_2 fluxes were up to -10 mgC m^{-2} day^{-1}. In June and July, the rates of air–sea CO_2 exchange were small (<5 mgC m^{-2} day^{-1}) when compared to the annual average (Table 1). These results match those derived by Nakaoko et al. (2006) for the GS and BS. In summertime, the majority of measurements were much less scattered around the trend line than in wintertime when the values were more scattered (Fig. 7). The fluxes across the air–sea interface were controlled by SST, wave breaking, friction velocity, sea state, turbulence, etc. (Goddijn-Murphy et al., 2016; Nightingale et al., 2000). The rate of transfer across the sea surface is usually a parameter that is a function of wind speed at 10 m. a.s.l. However, there were also other factors that influence air–sea CO_2 fluxes, such as surface films, fetch, and chemical enhancement (McGillis et al., 2001; Wanninkhof et al., 2009). Strong positive correlations between pCO_2 and air–sea fluxes ($r = 0.757$, $p < 0.05$) over spatial scales and quite strong negative correlations over temporal scales ($r = -0.640$, $p < 0.05$) were noted (Fig. 8). In the AO, the spatial variability in pCO_{2W} showed quite strong positive correlations with SST ($r = 0.732$, $p > 0.05$), while temporal variability showed even stronger negative correlations with SST ($r = -0.858$, $p > 0.05$; Tables 3 and 4).

4. Conclusions

This study examined the effect of monthly changes in gas transfer velocity and ΔpCO_2 in controlling air–sea CO_2 fluxes in the Greenland Sea and the Barents Sea, during a one year period. It also examined the following testable hypothesis: air–sea CO_2 fluxes over one year are dependent on both ΔpCO_2 and k. Results from FluxEngine showed that air–sea CO_2 fluxes had fewer positive correlations with gas transfer velocity (k) over spatial scales (Table 3), and almost perfect negative correlations over temporal scales (Table 4) with moderate negative correlations within individual months (Fig. 7). Additionally, there were strong positive correlations between pCO_2 and air–sea fluxes over spatial scales (Table 3) and quite strong negative correlations over temporal scales (Table 4), with strong positive correlations within individual months (Fig. 8). In the relationships between air–sea fluxes and gas transfer velocity in May, August, and September, more than 20% of the variability in fluxes was explained by k (typically it was less than 20%; Fig. 7). More than 50% of variability in fluxes was explained by pCO_{2W} (except from June to September, where it was less than 20%; Fig. 8). The results indicate that the variability in wind speed, and, hence, gas transfer velocity, plays a major role over temporal

scales, while ΔpCO_2, and hence pCO_{2w}, plays a major role over spatial scales in determining the monthly variation of CO_2 uptake in this area. On these timescales it is critical to obtain estimates of pCO_2 and k for accurate flux variability to be derived. We can predict the future state of the global carbon cycle only if we improve understanding the carbon cycle mechanisms of this area by using our ability to diagnose past change and analyze present variability.

As can be seen, even using satellite data is insufficient for specifying the mechanisms controlling carbon uptake in the Arctic Ocean. There are many gaps in the data from this region, and many uncertainties in approaches to estimating air—sea fluxes. We still do not know exactly how sea ice melting influences carbon uptake or how each component of the biological and physical carbon dioxide pumps influence air—sea flux values. Two relatively simple improvements may prevent the data gaps in projecting and evaluating carbon fluxes in this region in the future — a use of new techniques for interpolating data as well as a use of commercial ships for transporting and deploying sampling equipment in the winter.

Acknowledgements

The publication was financed with funds from Leading National Research Centre (KNOW) received by the Centre for Polar Studies for the period 2014—2018; OceanFlux Greenhouse Gases Evolution, a project funded by the European Space Agency, ESRIN Contract No. 4000112091/14/I-LG; and GAME project of National Science Centre No. DEC-2012/04/A/NZ8/00661. I would also like to thank Jacek Piskozub for significant corrections and comments.

References

Arrigo, K.R., van Dijken, G.L., Pabi, S., 2008. Impact of a shrinking Arctic ice cover on marine primary production. Geophys. Res. Lett. 35 (19), L19603, 6 pp., http://dx.doi.org/10.1029/2008GL035028.

Arrigo, K.R., Pabi, S., van Dijken, G.L., Maslowski, W., 2010. Air—sea flux of CO_2 in the Arctic Ocean, 1998—2003. J. Geophys. Res. Biogeosci. 115 (G4), 15 pp., http://dx.doi.org/10.1029/2009JG001224.

Ashton, I.G., Shutler, J.D., Land, P.E., Woolf, D.K., Quartly, G.D., 2016. A sensitivity analysis of the impact of rain on regional and global sea—air fluxes of CO_2. PLOS ONE 11 (9), e0161105, 18 pp., http://dx.doi.org/10.1371/journal.pone.0161105.

Bates, N.R., 2012. Multi-decadal uptake of carbon dioxide into subtropical mode water of the North Atlantic Ocean. Biogeoscience 9 (7), 2649—2659, http://dx.doi.org/10.5194/bg-9-2649-2012.

Bates, N.R., Mathis, J.T., 2009. The Arctic Ocean marine carbon cycle: evaluation of air—sea CO_2 exchanges, ocean acidification impacts and potential feedbacks. Biogeosciences 6 (11), 2433—2459, http://dx.doi.org/10.5194/bg-6-2433-2009.

Boutin, J., Etcheto, J., Merlivat, L., Rangama, Y., 2002. Influence of gas exchange coefficient parameterization on seasonal and regional variability of CO_2 air—sea fluxes. Geophys. Res. Lett. 29 (8), 23-1—23-4, http://dx.doi.org/10.1029/2001GL013872.

Cai, W.-J., Dai, M., Wang, Y., 2006. Air—sea exchange of carbon dioxide in ocean margins: a province-based synthesis. Geophys. Res. Lett. 33 (12), L12603, http://dx.doi.org/10.1029/2006GL026219.

Couldrey, M.P., Oliver, K.I.C., Yool, A., Halloran, P.R., 2016. On which timescales do gas transfer velocities control North Atlantic CO_2 flux variability? Global Biogeochem. Cycl. 30 (5), 787—802, http://dx.doi.org/10.1002/2015GB005267.

Dai, A., Qian, T., Trenberth, K.E., Millimian, J.D., 2009. Changes in continental freshwater discharge from 1948 to 2004. J. Climate 22 (10), 2773—2792, http://dx.doi.org/10.1175/2008JCLI2592.1.

Doney, S.C., Lima, I., Feely, R.A., Glover, D.M., Lindsey, K., Mahowald, N., Moore, J.K., Wanninkhof, R., 2009. Mechanisms governing interannual variability in upper-ocean inorganic carbo system and air—sea CO_2 fluxes: physical climate and atmospheric dust. Deep-Sea Res. Pt. II 56 (8—10), 640—655, http://dx.doi.org/10.1016/j.dsr2.2008.12.006.

Else, B.G.T., Papakyriakou, T.N., Galley, R.J., Drennan, W.M., Miller, L.A., Thomas, H., 2011. Wintertime CO_2 fluxes in an Arctic polynya using eddy covariance: evidence for enhanced air—sea gas transfer during ice formation. J. Geophys. Res. 116 (C9), C00G03, 15 pp., http://dx.doi.org/10.1029/2010JC006760.

Garbe, C.S., Rutgersson, A., Boutin, J., de Leeuw, G., Delille, B., Fairall, C.W., Gruber, N., Hare, J., Ho, D.T., Johnson, M.T., Nightingale, P.D., Pettersson, H., Piskozub, J., Sahlee, E., Tsai, W., Ward, B., Woolf, D.K., Zappa, C.J., 2014. Transfer across the air—sea interface. In: Liss, P.S., Johnson, M.T. (Eds.), Ocean—Atmosphere Interactions of Gases and Particles. Springer-Earth Sys. Sciences, Berlin, Heidelberg, 55—111.

Goddijn-Murphy, L., Woolf, D.K., Land, P.E., Shutler, J.D., Donlon, C., 2015. The OceanFlux Greenhouse Gases methodology for deriving a sea surface climatology of CO_2 fugacity in support of air—sea gas flux studies. Ocean Sci. 11 (4), 519—541, http://dx.doi.org/10.5194/os-11-519-2015.

Goddijn-Murphy, L., Woolf, D.K., Callaghan, A.H., Nightingale, P.D., Shutler, J.D., 2016. A reconciliation of empirical and mechanistic models of the air—sea gas transfer velocity. J. Geophys. Res. 121 (1), 818—835, http://dx.doi.org/10.1002/2015JC011096.

Gruber, N., 2009. Carbon cycle: fickle trends in the ocean. Nature 458 (7235), 155—156, http://dx.doi.org/10.1038/458155a.

Gruber, N., Keeling, C.D., Bates, N.P., 2003. Interannual variability in the North Atlantic Ocean carbon sink. Science 298 (5602), 2374—2378, http://dx.doi.org/10.1126/science.1077077.

Gurgul, H., 2002. Białe Pustynie — Arktyka. Wyd. Kurpisz. Poznań, 4—30.

Ho, D.T., Law, C.S., Smith, M.J., Schlosser, P., Harvey, M., Hill, P., 2006. Measurements of air—sea gas exchange at high wind speeds in the Southern Ocean: implications for global parameterizations. Geophys. Res. Lett. 33 (16), L16611, http://dx.doi.org/10.1029/2006GL026817.

IPCC, 2013. Carbon and other biogeochemical cycles. In: Stocker, T.F., Qun, D., Plattner, G.-K., Tignor, W., Allen, S.K., Boschung, J., Nauels, A., Xia, Y., Bex, V., Midgley, P.M. (Eds.), Climate Change 2013: The Physical Science Basis. Contribution of Working Group I to the Fifth Assessment Report of the Intergovernmental Panel on Climate Change. Cambridge Univ. Press, Cambridge, 470—516.

Kondo, F., Tsukamoto, O., 2012. Comparative CO_2 flux measurements by eddy covariance technique using open- and closed-path gas analysers over the Equatorial Pacific Ocean. Tellus B 64 (17511), 1—12, http://dx.doi.org/10.3402/tellusb.v64i0.17511.

Kulinski, K., She, J., Pempkowiak, J., 2011. Short and medium term dynamics of the carbon exchange between the Baltic Sea and the North Sea. Cont. Shelf Res. 31 (15), 1611—1619, http://dx.doi.org/10.1016/j.csr.2011.07.001.

Land, P.E., Shutler, J.D., Cowling, R.D., Woolf, D.K., Walker, P., Findlay, H.S., Upstill-Goddard, R.C., Donlon, C.J., 2013. Climate change impacts on sea—air fluxes of CO_2 in three Arctic seas: a sensitivity study using Earth observation. Biogeosciences 10 (12), 8109—8128, http://dx.doi.org/10.5194/bg-10-8109-2013.

Landschützer, P., Gruber, N., Bakker, D.C.E., Schuster, U., 2014. Recent variability of the global ocean carbon sink. Global

Biogeochem. Cycl. 28 (9), 927–949, http://dx.doi.org/10.1002/2014GB004853.

Le Quéré, C., Andres, R.J., Boden, T., Conway, T., Houghton, R.A., House, J.I., Marland, G., Peters, G.P., van der Werf, G.R., Ahlström, A., Andrew, R.M., Bopp, L., Canadell, J.G., Ciais, P., Doney, S.C., Enright, C., Friedlingstein, P., Huntingford, C., Jain, A.K., Jourdain, C., Kato, E., Keeling, R.F., Klein Goldewijk, K., Levis, S., Levy, P., Lomas, M., Poulter, B., Raupach, M.R., Schwinger, J., Sitch, S., Stocker, B.D., Viovy, N., Zaehle, S., Zeng, N., 2013. The global carbon budget 1959–2011. Earth Syst. Sci. Data 5, 165–185, http://dx.doi.org/10.5194/essd-5-165-2013.

Le Quéré, C., Andrew, R.M., Canadell, J.G., Sitch, S., Korsbakken, J.I., Peters, G.P., Manning, A.C., Boden, T.A., Tans, P.P., Houghton, R.A., Kelling, R.F., Alin, S., Andrews, O.D., Anthoni, P., Barbero, L., Bopp, L., Chevallier, F., Chini, L.P., Ciais, P., Currie, K., Delire, C., Doney, S.C., Friedlingstein, P., Gkritzalis, T., Harris, I., Hauck, J., Haverd, V., Hoppema, M., Goldewijk, K. K., Jain, A.K., Kato, E., Körtzinger, A., Landschützer, P., Lefèvre, N., Lenton, A., Lienert, S., Lombardozzi, D., Melton, J.R., Metzl, N., Millero, F., Monteiro, P.M.S., Munro, D.R., Nabel, J.E.M.S., Nakaoko, S.I., O'Brien, K., Olsen, A., Omar, A.M., Ono, T., Pierrot, D., Poulter, B., Rödenbeck, C., Salisbury, J., Schuster, U., Schwinger, J., Séférian, R., Skjelvan, I., Stocker, B.D., Sutton, A.J., Takahashi, T., Hanqin, T., Tilbrook, B., van der Laan-Luijkx, I.T., van der Werf, G.R., Viovy, N., Walker, A.P., Wiltshire, A.J., Zaehle, S., 2016. Global Carbon budget 2016. Earth Syst. Sci. Data 8 (2), 605–649, http://dx.doi.org/10.5194/essd-8-605-2016.

Le Quéré, C., Orr, J.C., Monfray, P., Aumont, O., Madec, G., 2000. Interannual variability of the oceanic sink of CO_2 from 1979 through 1997. Global Biogeochem. Cycl. 14 (4), 1247–1265, http://dx.doi.org/10.1029/1999GB900049.

Le Quéré, C., Takahashi, T., Buitenhuis, E.T., Rödenbeck, C., Sutherland, S.C., 2010. Impact of climate change and variability on the global oceanic sink of CO_2. Global Biogeochem. Cycl. 24 (4), GB4007, http://dx.doi.org/10.1029/2009GB003599.

Lefèvre, N., Watson, A.J., Olsen, A., Rios, A.F., Perez, F.F., Johannessen, T., 2004. A decrease in the sink for atmospheric CO_2 in the North Atlantic. Geophys. Res. Lett. 31 (7), L07306, http://dx.doi.org/10.1029/2003GL018957.

Lefèvre, N., Watson, A.J., Watson, A.R., 2005. A comparison of multiple regression an neutral network techniques for mapping in situ pCO_2 data. Tellus B 57 (5), 375–384, http://dx.doi.org/10.1111/j.1600-0889.2005.00164.x.

MacGilchrist, G.A., Naveira Garabato, A.C., Tsubouchi, T., Bacon, S., Torres-Valdés, S., Azetsu-Scott, K., 2014. The Arctic Ocean carbon sink. Deep-Sea Res. Pt. I 86, 39–55, http://dx.doi.org/10.1016/j.dsr.2014.01.002.

McGillis, W.R., Edson, J.B., Hare, J.E., Fairall, C.W., 2001. Direct covariance air–sea CO_2 fluxes. J. Geophys. Res. 106 (C8), 16729–16745, http://dx.doi.org/10.1029/2000JC000506.

Merchant, C.J., Embury, O., Rayner, N.A., Berry, D.I., Corlett, G.K., Lean, K., Veal, K.L., Kent, E.C., Llewellyn-Jones, D.T., Remedios, J.J., Saunders, R., 2012. A 20 year independent record of sea surface temperature for climate from Along-Track Scanning Radiometers. J. Geophys. Res. 117 (C12), C12013, 18 pp., http://dx.doi.org/10.1029/2012JC008400

Minnett, P., Kaiser-Weiss, A., 2012. Discussion Document: Near-surface Oceanic Temperature Gradients, https://www.ghrsst.org/wp-content/uploads/2016/10/SSTDefinitionsDiscussion.pdf.

Nakaoko, S.I., Aoki, A., Nakazawa, T., Hashida, G., Morimoto, S., Yamanouchi, T., Yoshikawa-Inoue, H., 2006. Temporal and spatial variations of oceanic pCO_2 and air–sea CO_2 flux in Greenland Sea and Barents Sea. Tellus B 58 (2), 148–616, http://dx.doi.org/10.1111/j.1600-0889.2006.00178.

Nightingale, P.D., Malin, G., Law, C.S., Watson, A.J., Liss, P.S., Liddicoat, M.I., Boutin, J., Upstill-Goddard, R.C., 2000. In situ evaluation of air–sea gas exchange parameterizations using novel conservative and volatile tracers. Global Biogeochem. Cycl. 14 (1), 373–387, http://dx.doi.org/10.1029/1999GB900091.

Olsen, A., Bellerby, R.G.J., Johannessen, T., Omar, A.M., Skjelvan, I., 2003. Interannual variability in the wintertime air–sea flux of carbon dioxide in the northern North Atlantic 1981–2001. Deep-Sea Res. Pt. I 50 (11), 1323–1338, http://dx.doi.org/10.1016/S0967-0637(03)00144-4.

Omar, A.M., Johannessen, T., Kaltin, S., Olsen, A., 2003. Anthropogenic increase of oceanic pCO_2 in the Barents Sea surface water. J. Geophys. Res. 108 (C12), 18-1–18-8, http://dx.doi.org/10.1029/2002JC001628.

Omar, A.M., Johannessen, T., Olsen, A., Kaltin, S., Rey, F., 2007. Seasonal and interannual variability of the air–sea CO_2 flux in the Atlantic sector of the Barents Sea. Mar. Chem. 104 (3), 203–213, http://dx.doi.org/10.1016/j.marchem.2006.11.002.

Piechura, J., Walczowski, W., 2009. Warming of the West Spitsbergen Current and sea ice north of Svalbard. Oceanologia 51 (2), 147–164, http://dx.doi.org/10.5697/oc.51-2.147.

Polyakov, I.V., Alekseev, G.V., Timokhov, L.A., Bhatt, U.S., Colony, R. L., Simmons, H.L., Walsh, D., Walsh, J.E., Zakharov, V.F., 2004. Variability of the Intermediate Atlantic Water of the Arctic Ocean over the last 100 years. J. Climate 17 (23), 4485–4497, http://dx.doi.org/10.1175/JCLI-3224.1.

Repina, I.A., Semiletov, I.P., Smirnov, A.S., 2007. Eddy correlation measurements of air–sea CO_2 fluxes in the Laptev Sea in the summer period. Doklady Earth Sci. 413 (2), 452–456, http://dx.doi.org/10.1134/S1028334X07030300.

Rödenbeck, C., 2005. Estimating CO_2 Sources and Sinks From Atmospheric Mixing Ratio Measurements Using a Global Inversion of Atmospheric Transport. Max-Planck Institute for Biogeochemistry, Jena, 53 pp.

Sabine, C.L., Feely, R.A., Gruber, N., Key, R.M., Lee, K., Bullister, J. L., Wanninkhof, R., Wong, C.S., Wallace, D.W.R., Tilbrook, B., Millero, F.J., Peng, T.-H., Kozyr, A., Ono, T., Ríos, A.F., 2004. The oceanic sink for anthropogenic CO_2. Science 305 (5682), 367–371, http://dx.doi.org/10.1126/science.1097403.

Schuster, U., McKinley, G.A., Bates, N., Chevallier, F., Doney, S.C., Fay, A.R., González-Dávila, M., Gruber, N., Jones, S., Krijnen, J., Landschützer, P., Lefèvre, N., Manizza, M., Mathis, J., Metzl, N., Olsen, A., Ríos, A.F., Rödenbeck, C., Santana-Casiano, J.M., Takahashi, T., Wanninkhof, R., Watson, A.J., 2013. An assessment of the Atlantic and Arctic sea–air CO_2 fluxes, 1990–2009. Biogeosciences 10 (1), 607–627, http://dx.doi.org/10.5194/bg-10-607-2013.

Sejr, M.K., Krause-Jensen, D., Rysgaard, R., Sørensen, L.L., Christensen, P.B., Glud, R.N., 2011. Air–sea flux of CO_2 in arctic coastal waters influenced by glacial melt water and sea ice. Tellus B 63 (5), 815–822.

Semiletov, I.P., Makshtas, A., Akasofu, S.-I., Andreas, L.A., 2004. Atmospheric CO_2 balance: the role of the Arctic sea ice. Geophys. Res. Lett. 31 (5), L05121, 4 pp., http://dx.doi.org/10.1029/2003GL017996.

Shutler, J.D., Piolle, J.-F., Land, P.E., Woolf, D.K., Goddijn-Murphy, L., Paul, F., Girard-Ardhuin, F., Chapron, B., Donlon, C.J., 2016. FluxEngine: a flexible processing system for calculating atmosphere–ocean carbon dioxide gas fluxes and climatologies. J. Atmos. Ocean. Technol. 33 (4), 741–756, http://dx.doi.org/10.1175/JTECH-D-14-00204.1.

StatSoft Inc., 2013. Electronic Statistical Textbook. StatSoft. WEB, Tulsa, OK, http://www.statsoft.com/textbook/.

Takahashi, T., Sutherland, S.C., Sweeney, C., Poisson, A., Metzl, N., Tilbrook, B., Bates, N., Wanninkhof, R., Feely, R.A., Sabine, C., Olafsson, J., Nojiri, Y., 2002. Global sea–air CO_2 flux based on climatological surface ocean pCO_2, and seasonal biological and temperature effects. Deep-Sea Res. Pt. II 49 (9–10), 1601–1622, http://dx.doi.org/10.1016/S0967-0645(02)00003-6.

Takahashi, T., Sutherland, S.C., Kozyr, A., 2008. Global Ocean Surface Water Partial Pressure of CO_2 Database: Measurements

Performed during 1968—2006 (Version 1.0). ORNL/CDIAC-152, NDP-088, Carbon Dioxide Information Analysis Center, Oak Ridge National Laboratory. U.S. Department of Energy, Oak Ridge, TN, p. 37831.

Takahashi, T., Sutherland, S.C., Wanninkhof, R., Sweeney, C., Feely, R.A., Chipman, D.W., Hales, B., Friederich, G., Chavez, F., Sabine, C., Watson, A., Bakker, D.C.E., Schuster, U., Metzl, N., Yoshikawa-Inoue, H.Y., Ishii, M., Midorikawa, T., Nojiri, Y., Köertzinger, A., Steinhoff, T., Hoppema, M., Olafsson, J., Arnarson, T. S., Tilbrook, B., Johannessen, T., Olsen, A., Bellerby, R., Wong, C. S., Delille, B., Bates, N.R., de Baar, H.J.W., 2009. Climatological mean and decadal change in surface ocean pCO_2 and net sea—air CO_2 flux over the global oceans. Deep-Sea Res. II 56 (8—10), 554—577, http://dx.doi.org/10.1016/j.dsr2.2008.12.009.

Telszewski, M., Chazottes, A., Schuster, U., Watson, A.J., Moulin, C., Bakker, D.C.E., González-Dávila, M., Johannessen, T., Körtzinger, A., Lüger, H., Olsen, A., Omar, A., Padin, X.A., Ríos, A.F., Steinhoff, T., Santana-Casiano, M., Wallace, D.W.R., Wanninkhof, R., 2009. Estimating the monthly pCO_2 distribution in the North Atlantic using a self-organizing neural network. Biogeosciences 6 (10), 1405—1421, http://dx.doi.org/10.5194/bg-6-1405-2009.

Thomas, H., Bozec, Y., Elkalay, K., de Baar, H.J.W., 2004. Enhanced open ocean storage of CO_2 from Shelf Sea pumping. Science 304 (5673), 1005—1008, http://dx.doi.org/10.1126/science.1095491.

Wanninkhof, R., McGillis, W.R., 1999. A cubic relationship between air—sea CO_2 exchange and wind speed. Geophys. Res. Lett. 26 (13), 1889—1892.

Wanninkhof, R., Asher, W.E., Ho, D.T., Sweeney, C.S., McGillis, W.R., 2009. Advances in quantifying air—sea gas exchange and environmental forcing. Ann. Rev. Mar. Sci. 1, 213—244, http://dx.doi.org/10.1146/annurev.marine.010908.163742.

Wanninkhof, R., Park, G.-H., Takahashi, T., Sweeney, C., Feely, R., Nojiri, Y., Gruber, N., Doney, S.C., McKinley, G.A., Lenton, A., Le Quéré, C., Heinze, C., Schwinger, J., Graven, H., Khatiwala, S., 2013. Global ocean carbon uptake: magnitude, variability and trends. Biogeosciences 10 (3), 1983—2000, http://dx.doi.org/10.5194/bg-10-1983-2013.

Weiss, R.F., Van Woy, F.A., Salameh, P.K., 1992. Surface Water and Atmospheric Gas Chromatography: Results From Expeditions Between 1977 and 1990. Scripps Institute of Oceanography. Carbon Dioxide Information Analysis, Centre Oak Ridge National Laboratory, NDP-044.

Woolf, D.K., Goddijn-Murphy, L.M., Prytherch, J., Yelland, M.J., Nightingale, P.D., Shutler, J.D., Piolle, J.-F., Hanafin, J., Chapron, B., 2013. Appropriate treatment of uncertainty and ambiguity; a flexible system for climatological calculations in response to an on-going debate on the transfer velocity. Proc. 'ESA Living Planet Symposium 2013', Edinburgh, 9—13 September 2013, 8 pp., http://www.oceanflux-ghg.org/content/download/75643/973537/file/Woolf_etal_LivingPlanet_2013.pdf.

Wrobel, I., Piskozub, J., 2016. Effect of gas-transfer-velocity parameterizations choice on air—sea CO_2 fluxes in the North Atlantic and the European Arctic. Ocean Sci. 12 (5), 1091—1103, http://dx.doi.org/10.5194/os-12-1091-2016.

Yasunaka, S., Murata, A., Watanabe, E., Chierici, M., Fransson, A., van Heuven, S., Hoppema, M., Ishii, M., Johannessen, T., Kosugi, N., Lauvset, S.V., Mathis, J.T., Nishino, S., Omar, A.M., Olsen, A., Sasano, D., Takahashi, T., Wanninkhof, R., 2016. Mapping of the air—sea CO_2 flux in the Arctic Ocean and its adjacent seas: basin-wide distribution and seasonal to interannual variability. Polar Sci. 10 (3), 323—334, http://dx.doi.org/10.1016/j.polar.2016.03.006.

Oceanologia (2017) 59, 460—472

Available online at www.sciencedirect.com

ScienceDirect

journal homepage: www.journals.elsevier.com/oceanologia/

ORIGINAL RESEARCH ARTICLE

Aerosol physical properties in Spitsbergen's fjords: Hornsund and Kongsfjorden during AREX campaigns in 2014 and 2015

Piotr Markuszewski [a,b,*], **Anna Rozwadowska** [a], **Malgorzata Cisek** [a], **Przemysław Makuch** [a], **Tomasz Petelski** [a]

[a] *Institute of Oceanology, Polish Academy of Sciences, Sopot, Poland*
[b] *Centre for Polar Studies National Leading Research Centre, Sosnowiec, Poland*

Received 11 July 2016; accepted 1 March 2017
Available online 25 May 2017

KEYWORDS
Arctic aerosol;
Sea spray;
Black carbon concentration;
Scattering coefficient;
Ångström exponent

Summary We present results of measurements of aerosol physical properties conducted on board of r/v *Oceania* during two cruises to the Spitsbergen region in 2014 (AREX 2014) and 2015 (AREX 2015). Measurements of aerosol size distribution, aerosol scattering coefficient and black carbon concentrations were made in two different Spitsbergen fjords: Hornsund and Kongsfjorden. The aerosol size distribution was measured in the size range from 0.09 μm to 47 μm using two aerosol size distribution spectrometers and a standard condensation particle counter. For the scattering coefficient an integrating nephelometer was used. Black carbon concentration was measured by an aethalometer. Temporal variabilities in physical properties of aerosol observed during the AREX 2014 and AREX 2015 campaigns were much higher than the differences between both fjords. The basic factors influencing aerosol conditions were advection and local generation of marine aerosol. In 2015 an episode of smoke advection was observed in both fjords causing an increase in the mean black carbon concentration from 7—12 ng m^{-3} to about 60 ng m^{-3}, and an aerosol scattering coefficient at 550 nm from 2—4 Mm^{-1} to 12—17 Mm^{-1}. Moreover, under certain conditions statistically significant gradients in aerosol optical properties were observed along the fjord axis reflecting an impact of mountains surrounding the fjords.

* Corresponding author at: Institute of Oceanology, Polish Academy of Sciences, Powstańców Warszawy 55, 81-712 Sopot, Poland. Tel.: +48 (58) 7311901; fax: (+48 58) 551 21 30.
E-mail address: pmarkusz@iopan.gda.pl (P. Markuszewski).
Peer review under the responsibility of Institute of Oceanology of the Polish Academy of Sciences.

ELSEVIER Production and hosting by Elsevier

http://dx.doi.org/10.1016/j.oceano.2017.03.012

1. Introduction

The study of atmospheric aerosols in the marine boundary layer is significant for a variety of climatic issues. Among others, aerosol particles take part in heat, moisture and mass exchange processes. Without understanding the mechanics of aerosol emission and transport it is practically impossible to properly model regional and global weather or climate. Study of aerosol properties in Polar Regions is of particular importance for two reasons, firstly because of very low anthropogenic perturbations there, and secondly because of the strong effect climate changes have on the Arctic. Recent years have seen several measurement campaigns concentrated on aerosol physical properties and transport (Lisok et al., 2016; McFarquhar et al., 2011; Ritter et al., 2016; Tunved et al., 2013). However, only few experiments addressed the differences in aerosol properties between different stations/fjords in the Spitsbergen region.

The study of polar aerosols is always a big challenge, not only because of the isolation of the researched region, but also because of the variety of phenomena occurring in this area. The presence of "Arctic Haze", partially explained by several authors (Quinn et al., 2007; Sharma et al., 2006; Shaw, 1995), and advections of continental air masses containing smoke from forest fires which contributes to enhanced soot concentrations in the Arctic area (Damoah et al., 2004; Stohl et al., 2006) belong to them. Apart from smoke, Asian dust transport has also been observed, mainly in spring (Stone et al., 2010). A comprehensive analysis of atmospheric composition in polar regions was presented by Tomasi et al. (2015). This paper comprises up-to-date knowledge about remote sensing measurements in both Arctic and Antarctic areas.

The challenge of identifying the source regions of Arctic aerosol was taken up by several authors. Large events such as boreal forest fires in Alaska and Canada during the summer of 2004 and its influence on aerosol optical parameters have been studied among others by Stohl et al. (2006). Myhre et al. (2007) and Treffeisen et al. (2007) dealt with another event of pollution and a special meteorological situation in the European Arctic which occurred in 2006. A thorough analysis of the relations between aerosol composition and aerosol optical properties with air masses was presented by Stock et al. (2014). They presented that aerosol optical depth in Ny-Alesund did not depend on the North Atlantic Oscillation.

The comparison of the aerosol optical thickness and the Ångström exponent between northern Norway and Hornsund was presented by Chen et al. (2013). Based on data from AERONET (Aerosol Robotic Network) they found that the four-year annual mean values for the aerosol optical thickness at 500 nm $\tau(500)$ at Andenes and Hornsund were equal to 0.10. Based on analysis of changes in the Ångström exponent (AE) the study concludes that fine-mode particles dominated at both sites. Furthermore, both sites had similar seasonal variations of the aerosol size distribution despite one site being located in the Arctic while the other in a sub-arctic area.

Comprehensive analyses of the optical properties in Hornsund are provided by Rozwadowska et al. (2010) and Rozwadowska and Sobolewski (2010). The authors found that in spring, the changes in AOT values over the station were strongly influenced by long-range advection, mainly from Europe and Asia. The phenomenon of AOT variability in summer was explained by the local direction and speed of advection (1-day trajectories). The impact of distant sources on AOT was strongly modified by cleansing processes en route to Hornsund. However, the highest AOT cases in summer were also associated with long-range transport from Europe, Asia and North America.

Lisok et al. (2016) and Ritter et al. (2016) presented results of measurement of aerosol physical and chemical properties during the iAREA2014 campaign that took place on Svalbard in three stations (Ny—Ålesund, Longyearbyen and Hornsund). The authors' aim was to investigate in situ passive and active remote sensing observations as well as numerical simulations to describe the temporal variability of aerosol single-scattering properties during the spring season on Spitsbergen.

This study presents results of aerosol properties' measurements performed during two Arctic campaigns on board of r/v *Oceania*, AREX (ARctic EXperiment), conducted in 2014 and 2015. The AREX campaign is an annual three-month cruise to the Northern Atlantic, the Nordic Seas and fjords of Spitsbergen. This paper compares aerosol physical properties in Hornsund and Kongsfjorden during the 2014 and 2015 campaigns and relates the differences in these properties to variations in air mass advections and meteorological conditions. The issue of spatial variability of aerosol optical properties in the fjords is also addressed.

2. Area of study

The measurements were carried out in order to investigate variability of aerosol physical properties in two different fjords of Spitsbergen: Hornsund and Kongsfjorden. Hornsund is located in the south of the Spitsbergen area. Kongsfjorden is situated in the northern part of the island (Fig. 1).

The fjords differ from each other with respect to their hydrographic conditions. The Hornsund fjord is cooler than Kongsfjorden because of limited inflow of warm waters from the West Spitsbergen Current (WSC). The mouth of Hornsund is much more often occupied by much lighter and fresher water from of shelf Sorkapp Current which flows from the Barents Sea. The topographical structure of Kongsfjorden, on the other hand, allows for larger injections of warm water from the WSC due to the wide trough of the fjord. Moreover, the shelf current is not influential in this area. A more detailed description of current structures in this area is presented by Walczowski (2013). Differences in locations and hydrographic conditions of the fjords are reflected in differences in local meteorological conditions in the fjords which are discussed with Cisek (personal communication). In both fjords the wind direction is determined mainly by local orography and a horizontal gradient of air temperature, thus in each fjord the dominant wind direction is determined by the axis of the fjord (Svendsen et al., 2002). Moreover, Hornsund has higher wind speeds, humidity and cloud cover than Kongsfjorden. The air temperature, however, is higher in Hornsund only in winter. In summer, the air temperature over Kongsfjorden is higher.

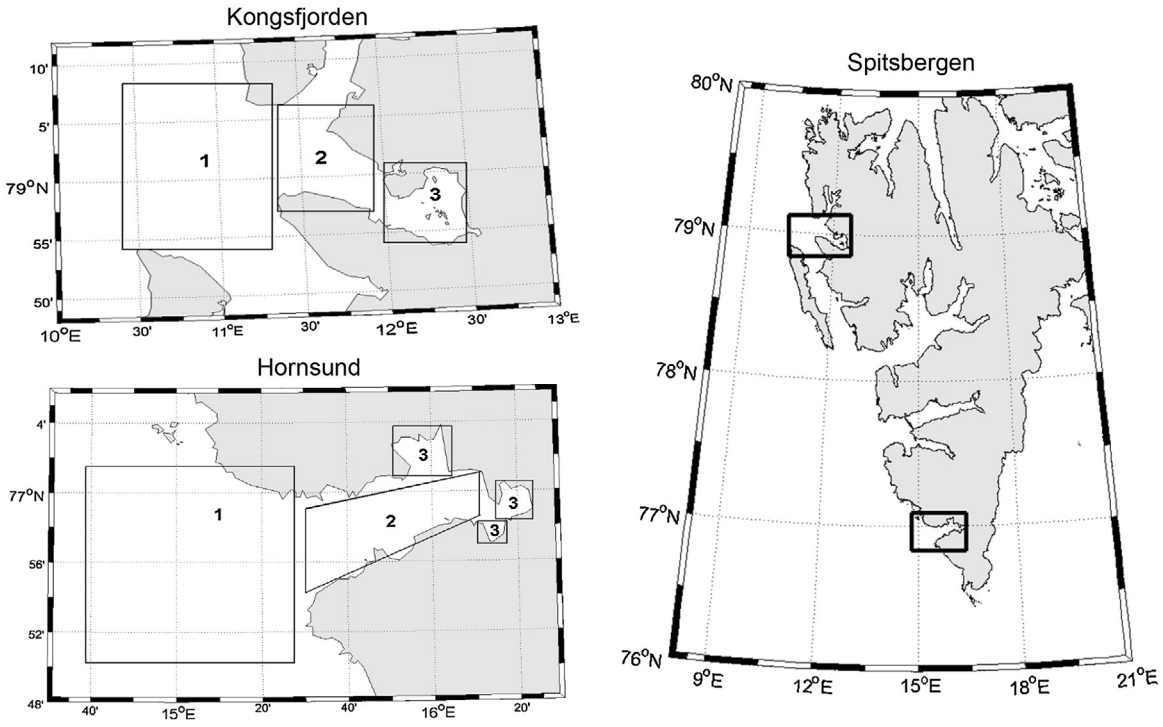

Figure 1 Location of Hornsund and Kongsfjorden and fjords' subregions where the measurements were performed during the AREX campaigns in 2014 and 2015. Numbers represent the fjord subregions: 1 — innermost part of the fjord, 2 — central part, 3 — fjord mouth and the sea outside the fjord.

3. Methods

3.1. Measurements

Measurements of aerosol size distribution, aerosol scattering coefficient and black carbon (BC) concentration were performed during the AREX 2014 and 2015 cruises. In 2014, the measurements in Hornsund were carried out from 25 July (the 206th day of the year) to 1 August (213). In Kongsfjorden, the measurement period lasted from 5 August (217) to 10 August (222). In 2015, the measurements took place in similar periods: from 26 July (207) to 1 August (213) in Hornsund and from 3 August (215) to 9 August (221) in Kongsfjorden.

Aerosol size distribution was assessed by the CSASP-100-HV aerosol spectrometer (manufactured by Particle Measuring System) and a TSI laser aerosol spectrometer 3340 (LAS). The CSASP counts aerosol particles in a diameter range from 0.5 μm to 47 μm in 36 channels. The device was successfully used and described well in several earlier papers (e.g. Petelski et al., 2014; Petelski, 2005; Savelyev et al., 2014; Zieliński, 2004). The LAS counts aerosol particles from diameter size of 0.09 μm up to 7.5 μm in 99 channels. Both instruments use a He—Ne Laser beam. However, thanks to a more sophisticated optical system, the LAS ensures a wider measurement range (Hämeri et al., 2010). In order to compare and check the results from the LAS, a TSI Condensation Particle Counter (CPC) was also used (TSI 3771). The CPC estimates the total aerosol concentration in a diameter range from 0.01 μm to 4.5 μm. However, an analysis of the CPC's measurements is beyond the scope of the present paper.

Equivalent black carbon concentration was measured by a Magee Scientific Company AE-31 aethalometer (e.g. Arnott et al., 2005; Hansen et al., 1984). Equivalent black carbon concentration is the black carbon concentration which—accumulated on a filter — would give the same light attenuation as the actual aerosol accumulated there. However, except for strong mineral dust advections, black carbon is the main aerosol absorber of light. The AE-31 operates in 7 spectral channels: 370, 470, 520, 590, 660, 880 and 950 nm. We used the 520 nm channel for our research. The aerosol accumulation time was set to 1 h and the flow to 65 $cm^3\ s^{-1}$ (3.9 l min^{-1}). Such a long accumulation time was necessary due to the very small aerosol load in the Arctic. The BC concentration is based on measurements of light attenuation by aerosol accumulated on a quartz filter. However, this method is prone to errors due to loading effect. The measurements require correction for this effect when the attenuation of the aerosol accumulated on the filter exceeds 10 (Schmid et al., 2006). During the AREX experiments the filters were changed frequently and the attenuation rarely reached this threshold value. The correction based on Virkkula et al. (2005) was applied in those cases.

Aerosol scattering properties were measured by the TSI nephelometer 3563 (Anderson et al., 1996). The instrument operates on 3 wavelengths: 450, 550 and 700 nm. The measured scattering coefficients were corrected for the effects of non-Lambertian illumination and truncation of scattering in near-forward and near-backward angles using the Anderson and Ogren (1998) method. The scattering coefficients for this research have been averaged to 1 h resolution to match the BC concentration measurements. Detailed descriptions

of the nephelometer and aethalometer are given by Lisok et al. (2016).

During the cruise, all particle counters were situated on a special measurement platform mounted on the fore-mast, 8 m above sea level. The common inlet of the aethalometer and nephelometer was located near the fore-mast, 1 m below the measurement platform.

Meteorological observations from the WMO stations at Ny-Alesund (01007) and Hornsund (01003) were also used in this study for the fjord measurement periods. The meteorological data is available at www.rp5.kz. The standards of WMO meteorological stations are presented by Jarraud (2008).

3.2. Backward trajectories

Six-day backward trajectories (144 h) of the air masses advecting towards the fjords were computed by the NOAA HYSPLIT model (Hybrid Single—Particle Lagrangian Integrated Trajectory Model, Draxler and Hess, 1998) using the GDAS meteorological dataset (Rolph, 2016; Stein et al., 2015). The trajectories were computed for air mass arrival times of 0 and 12 UTC and arrival heights of 500, 1500 and 3000 m. However, only the 500 m trajectories were used in this study.

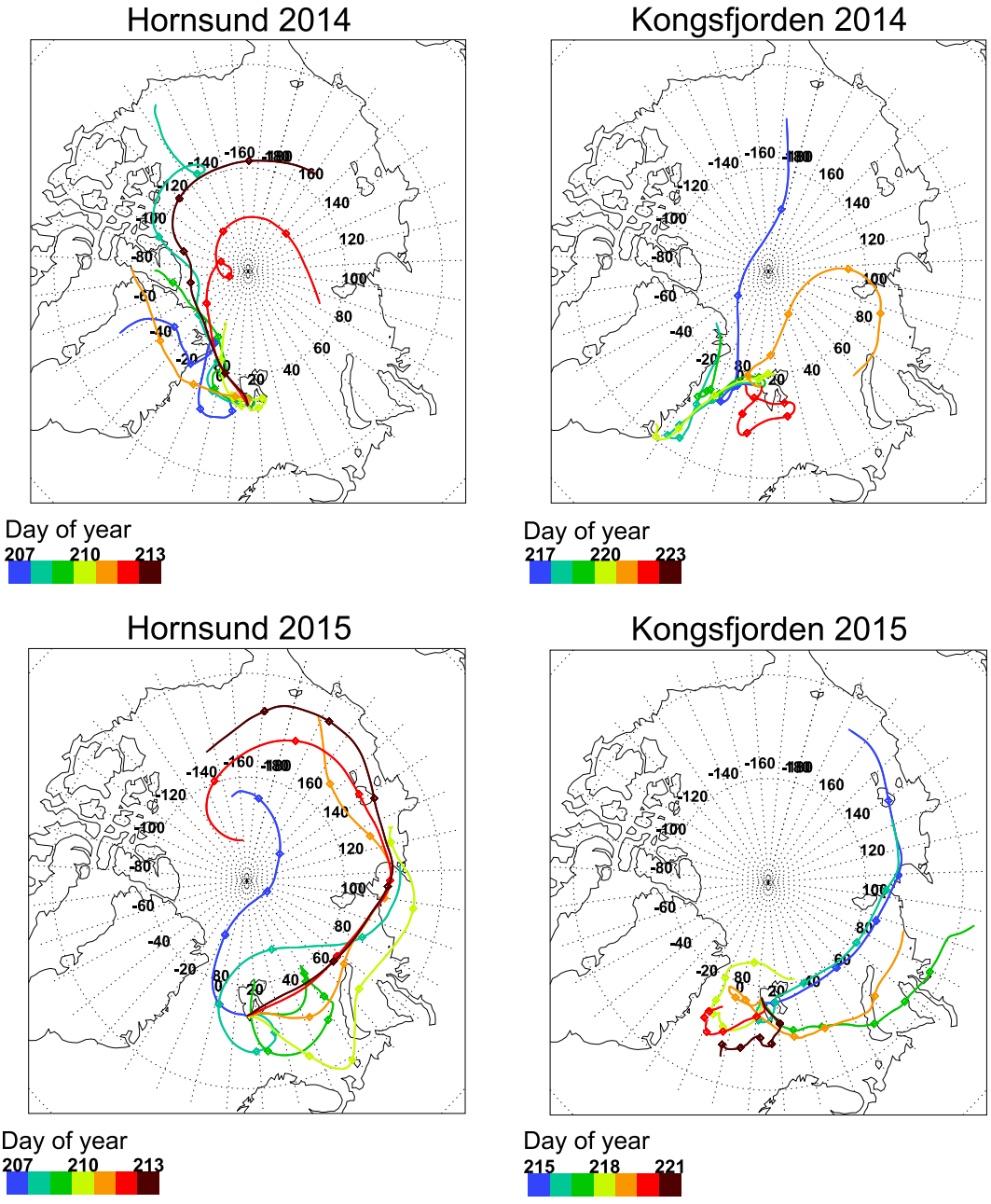

Figure 2 Back-trajectories of air masses arriving at 500 m above Hornsund (left) and Kongsfjorden (right) during aerosol measurements in the fjords. The trajectories were computed for 12 UTC on a day indicated by the trajectory colour. (For interpretation of the references to color in this figure legend, the reader is referred to the web version of this article.)

3.3. Definitions of physical quantities used in this work

The basic aerosol size distribution parameters used in this paper are: zero moment M_0 (mean aerosol concentration), first moment M_1, mean particle diameter $\overline{D_p}$ and effective radius r_e. These parameters are defined as follows:

$$M_0 = \sum_{i=1}^{k} N_i, \tag{1}$$

$$M_1 = \sum_{i=1}^{k} N_i D_{p_i}, \tag{2}$$

$$\overline{D_p} = M_1 M_0^{-1}, \tag{3}$$

$$r_e = \left(\sum_{i}^{k} r_i^3 N_i\right)\left(\sum_{i}^{k} r_i^2 N_i\right)^{-1}, \tag{4}$$

where N_i is the aerosol concentration in the interval (instrument channel) i with the diameter D_{pi} and the $r_i = D_{pi}$*0.5 which is the particle radius.

In the paper, aerosol scattering properties are characterized by scattering coefficient at light wavelength of 550 nm, b, and Ångström exponent, AE, of the scattering coefficient spectrum $b(\lambda)$ representing the slope of the scattering coefficient spectrum in a log-log scale:

$$b(\lambda) = b(\lambda_0)e^{-AE}, \tag{5}$$

where λ_0 is a selected wavelength, usually λ_0 = 1 μm resolution. In this work, AE was estimated using linear fitting in log-log scale for the spectral range of 450–700 nm. In this paper, we discuss hourly means of b and AE.

4. Results and discussion

4.1. Air-mass advection and meteorological conditions during measurement period

The campaign periods of 2014 and 2015 differ distinctively in both advection directions and meteorological conditions. In 2014, air masses from northern Greenland, the Canadian Arctic Islands and the Arctic Ocean dominated in the atmospheric boundary layer (trajectory arrival height of 500 m over the station) over both Hornsund and Kongsfjorden (Fig. 2) with 9 August 2014 (221) as an exception when the

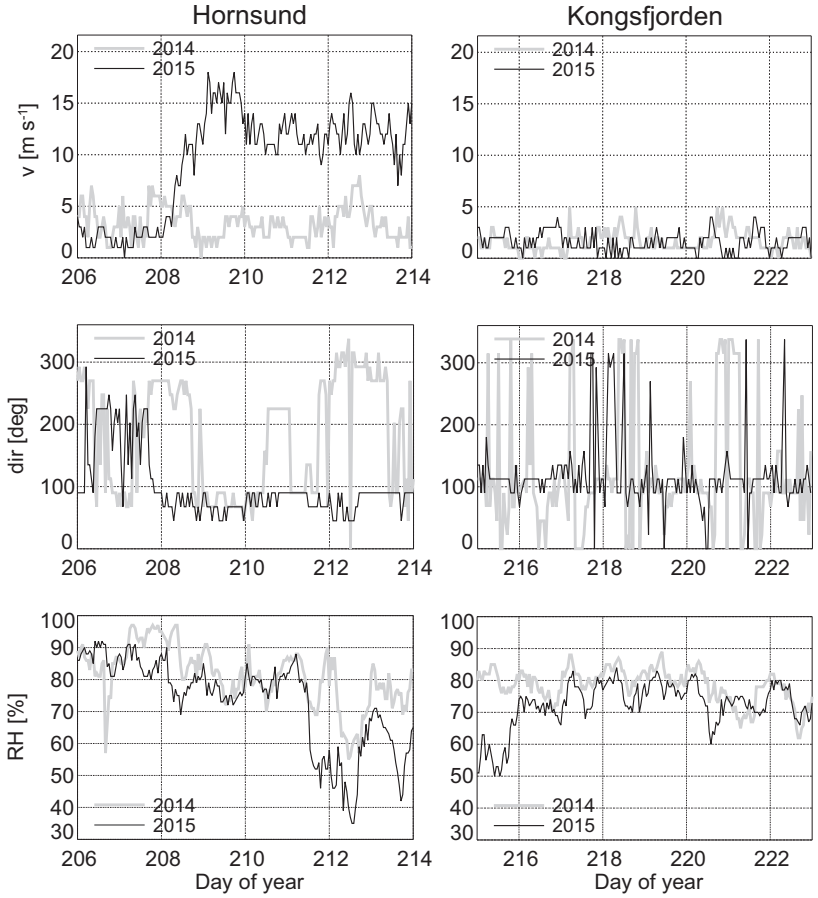

Figure 3 Meteorological conditions at the Hornsund (Hornsund fjord) and the Ny Ålesund (Kongsfjorden) WMO stations: wind speed (v), wind direction (dir) and relative humidity (RH during aerosol measurements in the fjords (AREX 2014 and 2015). Wind direction angles are determined clockwise starting from the North, i.e. 0° is N, 90°E, 180°S and 270°W.

air-mass back-trajectories led from the vicinity of Nova Zemlya over the Arctic Ocean to Kongsfjorden.

In 2014 meteorological conditions in both fjords did not change significantly during the experiment (Fig. 3). During the campaign, wind speeds, *v*, in both fjords were typically < 5 m s^{-1} with values slightly higher in Hornsund than in Kongsfjorden. In Hornsund *v* exceeded 5 m s^{-1} during the analyzed time period. Wind directions (at 10 m) close to the main axis of the fjords dominated regardless of the direction of winds in the free troposphere. Hornsund stretches from West to East, while Kongsfjorden lies along a NW-SE direction. This was reflected in dominant wind directions: E and W in Hornsund and from E, ESE and N in Kongsfjorden. Relative humidity (RH) fluctuated around 80% with a negative trend. The RH fluctuations were stronger in Hornsund than in Kongsfjorden. In Hornsund RH $>$ 90% was observed on 26 and 27 July 2014 (207 and 208) and RH $<$ 70% on 31 July (212); in Kongsfjorden on 9 and 10 August 2014 (221 and 222).

In 2015 advection patterns were more variable (Fig. 2). From 25 to 27 July (206—208) the air masses over Hornsund came from the Arctic Ocean with the exception of the short period on 26 July (207, 0 UTC) when the trajectory originated over the Siberian coast, near the Taymyr and Yamal Peninsulas. Starting on 27 July (208) the advection pattern began to gradually change. On 27 (208, 12 UTC) and 28 July (209, 0 UTC) the trajectories lead from the vicinity of the Taymyr Peninsula, went around Spitsbergen from the north side and reached Hornsund from the south-east. From 28 July (209, 12 UTC) to 29 July (210, 0 UTC) Hornsund was under inflow from the Barents Sea. After that, the air masses from the Siberian coast affected the Spitsbergen area. Six-day trajectories originated near the Taymyr Peninsula, passed Nova Zemlya and reached Hornsund from the south. Starting from 30 July (211) air masses from the Arctic Ocean near the Chukotka Peninsula and Alaska advected to Hornsund, crossing the Taymyr Peninsula. The air mass movement was fast and the air reached Hornsund from the east. This circulation pattern was also observed for Kongsfjorden and continued up to 4 August (216, 0 UTC) at which time the trajectories gradually shortened, indicating slower air-mass movement, and reached Kongsfjorden from the southwest (4 August, 216) and south (5 August, 217). On 6 August (218), Kongsfjorden was influenced by local air masses from the Greenland Sea. On 7 August (219), the air masses arriving over Kongsfjorden again originated over the Taymyr Peninsula. Loops on the trajectories indicated that the advection was associated with low pressure systems. Starting from 8 August 220) to the end of the measuring period, the air masses in Kongsfjorden advected from the Greenland Sea.

Meteorological conditions in Hornsund in 2015 were more dynamic than in 2014 (Fig. 3). During the measuring cam-

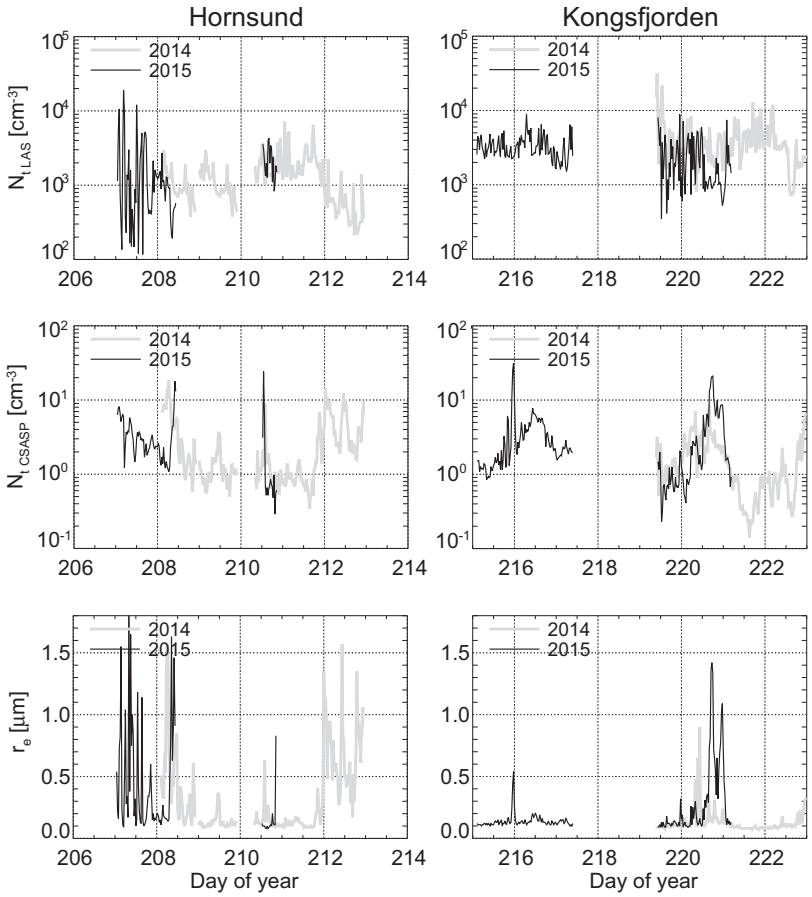

Figure 4 Time series of total aerosol concentration from the particle counters used during the measurements in Hornsund and Kongsfjorden in 2014 and 2015: LAS ($N_{t\,LAS}$, particle radius range: 0.09—7.5 μm) and CSASP ($N_{t\,CSASP}$, particle radius range 0.5—47 μm), and aerosol effective radius (r_e) computed on the basis of the particle counters' measurements (Eq. (4)).

paign, winds from the East (Hornsund) and ESE (Kongsfjorden) dominated. From 28 July to 1 August (209–213) strong eastern winds occurred (with their speed greater than 10 m s^{-1}) in Hornsund. However, wind speed was <5 m s^{-1} throughout the whole Kongsfjorden's part of the campaign. The advection from Siberia was also associated with small RH values. From 30 July to 1 August (211–213) RH < 60% (Hornsund) was observed. In Kongsfjorden RH < 60% was found on 3 August (216).

4.2. Aerosol size distribution observations

Table 1 presents total aerosol concentration characteristic for each particle counter, such as mean aerosol concentration M_0, mean standard deviation, minimum and maximum values for each fjord and the whole period of measurements. Additionally, basic aerosol size distribution parameters are presented such as zero moment M_0 (mean aerosol concentration, Eq. (1)), first moment M_1 (Eq. (2)) and the mean particle diameter (Eq. (3)). Fig. 4 presents time series of total aerosol particle concentrations from all three particle counters.

During the campaign in 2015 for the CSASP size range of measurements higher total aerosol particle concentrations were observed in both fjords. For Hornsund, the mean concentration values were 2.9 cm^{-3} in 2014 and 7.4 cm^{-3} in 2015. A similar situation was observed in Kongsfjorden but with smaller differences. Furthermore, in Hornsund the medium particle diameter was higher than in 2015 (where values changed from 3.07 μm in 2014 up to 3.50 μm in 2015). In Kongsfjorden the situation was opposite to Hornsund, smaller particles dominated in 2014 ($\overline{D_p}$ varied from 3.55 μm in 2014 up to 2.82 μm in 2015). The case was different for smaller particles measured using the LAS. M_0 in 2015 were lower than in 2014 for both fjords. The mean diameters of particles in Kongsfjorden were larger by approximately 0.7 μm.

4.3. Aerosol optical properties observations

In 2014 during both parts of the cruise very low black carbon concentrations in the atmosphere was recorded, with mean BC concentrations lower than 8 ng m^{-3}, and low scattering coefficient b(550 nm) (≥2–3 Mm^{-1}). Low values of these parameters were associated with dominant western advections (Fig. 2). Fig. 5 shows the time series of these properties. The measurements reveal that local aerosol generation from the fjord surface or marine aerosol advection from the sea in the vicinity of Spitsbergen have a significant impact on aerosol optical properties for both fjord regions during the 2014 campaign. This is indicated by a considerable correlation between AE and b(550 nm) (R = −0.58 and −0.51 in Hornsund and Kongsfjorden respectively) and between AE and v (R = −0.42 and −0.54). A high positive correlation coefficient between the scattering coefficient and the effective radius of aerosol particles (R = 0.55 and 0.84 in Hornsund and Kongsfjord respectively) also suggest that an increase in aerosol scattering is caused by large particles. All the correlation coefficients showed in this paper are statistically significant at the level of 0.001. The measurements performed during the campaigns did not allow us to observe any impact of RH on aerosol optical properties. Even though

Table 1 Basic characteristics of mean aerosol size distributions from measurements with CSASP (particle radius range of 0.5–47 μm), LAS (0.09–7.5 μm) and CPC (0.01–4.5 μm) in Hornsund (H) and Kongsfjorden (K) during the 2014 and 2015 AREX cruises. M_0 is the zero moment (mean total aerosol concentration), M_1 is the first moment and $\overline{D_p}$ is the mean particle diameter defined as in Eqs. (1)–(3). σ is the standard deviation and Min, Max are respectively the minimum and maximum values of the total aerosol concentrations.

	CSASP						LAS						CPC			
	M_0 [cm^{-3}]	M_1 [cm^{-3} μm^{-1}]	$\overline{D_p}$ [μm]	σ [cm^{-3} μm^{-1}]	Min [cm^{-3}]	Max [cm^{-3}]	M_0 [cm^{-3}]	M_1 [cm^{-3} μm^{-1}]	$\overline{D_p}$ [μm]	σ [cm^{-3} μm^{-1}]	Min [cm^{-3}]	Max [cm^{-3}]	M_0 [cm^{-3}]	σ [cm^{-3} μm^{-1}]	Min [cm^{-3}]	Max [cm^{-3}]
H 2014	2.9E+00	1.0E+01	3.1E+00	2.1E+00	7.3E−01	1.0E+01	2.0E+03	2.4E+02	1.3E−01	1.1E+03	7.5E+02	4.9E+03	8.9E+02	2.2E+03	3.6E+02	5.4E+04
H 2015	7.4E+00	2.7E+01	3.5E+00	4.4E+00	3.0E+00	2.1E+01	1.4E+03	1.6E+02	1.3E−01	1.3E+03	2.8E+02	6.5E+03	1.9E+03	6.7E+03	6.0E+01	9.1E+04
K 2014	1.7E+00	5.8E+00	3.6E+00	1.2E+00	4.5E−01	9.1E+02	4.4E+03	4.3E+02	1.4E−01	3.3E+03	1.2E+03	1.6E+04	1.1E+03	1.1E+03	1.4E+02	6.3E+04
K 2015	3.2E+00	9.6E+00	2.8E+00	3.0E+00	9.8E−01	1.6E+01	3.0E+03	4.1E+02	1.7E−01	1.6E+03	1.2E+03	7.7E+03	1.9E+07	3.2E+03	2.7E+02	5.8E+04

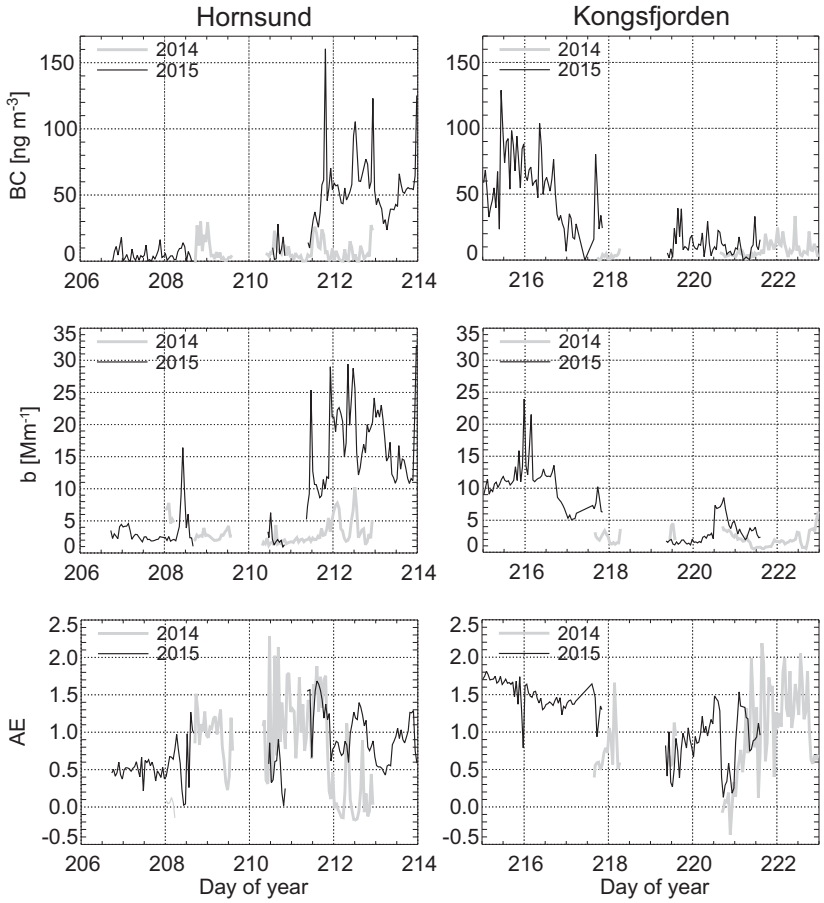

Figure 5 Time series of aerosol optical properties measured during the campaign in Hornsund and Kongsfjorden in 2014 and 2015: black carbon concentration (BC), scattering coefficient (b) and the dimensionless Ångström exponent (AE).

ambient RH was high enough to affect particle size, and thus the scattering coefficient, RH in the nephelometer chamber was below 57%, so the impact of RH on measured b(550 nm) can be deemed negligible or small during the fjord periods of both AREX campaigns.

In 2015, variability in aerosol optical properties was mainly caused by smoke advection. Distinct periods of elevated BC concentrations and scattering coefficient were observed in both fjords, which caused increased values of the mean aerosol scattering coefficient and BC concentrations. Correlation between b and BC was high in both Hornsund (R = 0.76) and Kongsfjorden (R = 0.79). It must be noted, however, that the simultaneous occurrence of large BC values and high wind speeds in Hornsund strengthened this correlation for Hornsund. Elevated BC and b(550 nm) values occurred during fast advection of air masses from the Siberian coast and the Arctic Ocean near the Chukotka Peninsula and Alaska. Smoke brought by this advection could come from fires occurring at that time in Canada (near the Great Slave Lake) and in Alaska (https://firms.modaps.eosdis.nasa.gov/firemap/). They could also be remnants of smoke from strong forest fires in Canada from the beginning of July, still present in the Arctic atmosphere. Moreover, during the fjord stage of the AREX 2015 campaign, fires were also reported in Siberia (Yamalo-Nenetskiy Avtonomyy Okrug — northern part of the West Siberian Plain, and on the Chukotka Peninsula). The elevated BC concentration and scattering coefficient lasted from noon on 30 July to 5 p.m. on 4 August (211—216). Further in this paper, this period is referred to as “advection period” or “smoke advection period”. The periods with small values of BC and b are referred to as 'background'. When the ship was in Hornsund in 2015, the background period lasted from 25 July to 29 July (206—210). It was also observed from 8 to 9 August 2015 (220—221) during the ship's stay in Kongsfjorden. Measurements from 2014 were also treated as “background” measurements.

During the smoke advection period in 2015 the respective mean values (±standard deviation) of BC, b(550 nm) and AE were 56.6 ± 24.2 ng m^{-3}, 17.08 ± 5.70 Mm^{-1} and 0.96 ± 0.32 in Hornsund, and 67.5 ± 21.2 ng m^{-3}, 12.16 ± 2.86 Mm^{-1} and 1.55 ± 0.19 in Kongsfjorden. In spite of a lower BC concentration in Hornsund than in Kongsfjorden, the scattering coefficient was higher in Hornsund. This was due to high winds in Hornsund during the smoke advection period (up to 15 m s^{-1}). When the ship moved to Kongsfjorden the wind speed decreased drastically ($v < 4$ m s^{-1}). A considerable contribution of sea spray aerosol in Hornsund are indicated by high correlation coefficients: R = 0.47 for b versus v, −0.61 for AE versus b. Outside the advection period (background period), BC, b and AE values in both fjords were similar to each other and comparable with values measured in 2014 (Table 2).

Table 2 Means and standard deviations of aerosol scattering coefficient (b), Ångström exponent (AE) and black carbon concentration (BC) measured in Hornsund (H) and Kongsfjorden (K) during the 2014 and 2015 AREX cruises. The index "s" stands for "smoke advection" and "b" means "background" periods. Both periods are defined in Section 4.3.

	Nephelometer		AE-31
	b(550 nm) [Mm^{-1}]	AE	BC [ng m^{-3}]
H 2014	3.10 ± 1.83	0.78 ± 0.64	7.7 ± 7.8
H 2015	10.20 ± 8.26	0.77 ± 0.37	31.9 ± 31.4
K 2014	2.12 ± 1.16	0.92 ± 0.57	6.9 ± 6.0
K 2015	7.02 ± 4.67	1.20 ± 0.42	29.1 ± 23.2
H_s 2015	17.08 ± 5.70	0.96 ± 0.32	56.6 ± 24.2
K_s 2015	12.16 ± 2.86	1.55 ± 0.19	67.5 ± 21.2
H_b 2015	3.29 ± 2.51	0.53 ± 0.24	4.8 ± 4.6
K_b 2015	3.73 ± 1.97	0.92 ± 0.38	10.5 ± 7.3

4.4. Long-range advection and local aerosol generation — their impact on aerosol optical properties

A typical approach in the study of aerosols over oceans is to relate aerosol properties, e.g. b or AE, to wind speed being a proxy of local aerosol generation (e.g. O'Dowd et al., 2010; Smirnov et al., 2003; Vaishya et al., 2012). However, the measurements performed in the Kongsfjorden and Hornsund fjords show that the effects of advections should not be neglected in such relationships even in remote Arctic sites. Fig. 6 compares the impacts of marine aerosol generation, represented by wind speed, and smoke advection on b and AE in Hornsund and Kongsfjorden during the AREX 2015 campaign. In Fig. 6, "H" and "K" stand for Hornsund and Kongsfjorden respectively, and indices "s" and "b" denote smoke advection and background periods. Separate plots are given for measurements from the interior of the respective fjord (regions 2 and 3 defined in Fig. 1) and the fjord mouth and the adjacent ocean area (region 1). The low-wind ($v < 5$ m s^{-1}) background values of b for the fjords were the same inside Hornsund and Kongsfjorden (subregions 2 and 3; 3 ± 1 Mm^{-1}). In Kongsfjorden the smoke advection caused an increase in scattering coefficient by about 10 Mm^{-1} with respect to the non-advection period (an increase to 12.8 ± 3.0 Mm^{-1}). This difference is statistically significant at the level of 0.05. Given a nearly constant b with v within the range of 0–10 m s^{-1}, we may assume a similar increase in b in Hornsund due to smoke advection alone during that period. Further increase in b, up to 30 Mm^{-1}, was due to marine aerosol generation and was observed when wind speeds exceeded 10 m s^{-1}. Smoke advection also influenced AE, causing its statistically significant increase from AE = 1.05 ± 0.22 to AE = 1.49 ± 0.19 in Kongsfjorden (subregions 2 and

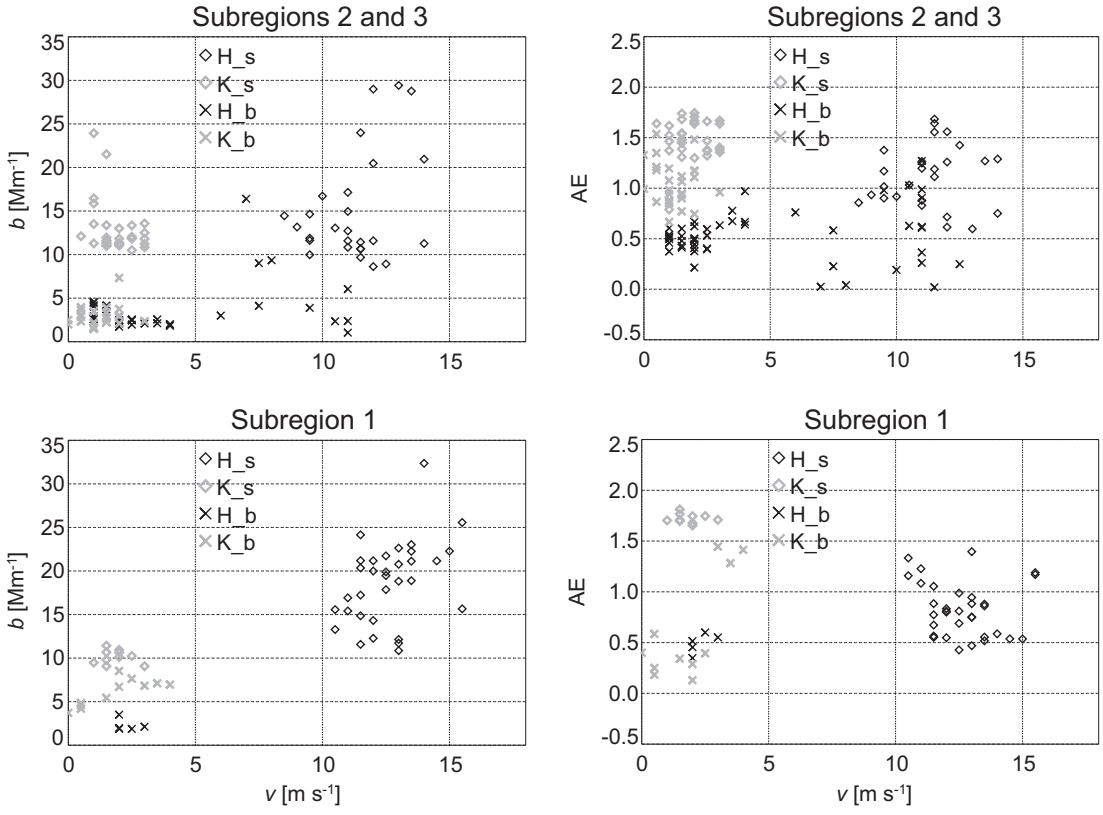

Figure 6 Dependency of aerosol scattering coefficient b(550 nm) and Ångström exponent (AE) on marine aerosol generation, represented by wind speed, and smoke advection in 2015. H and K denote respective measurements from Hornsund and Kongsfjorden, "s" stands for "smoke advection" and "b" means "background", i.e. non-smoke advection period. Fjord regions are defined in Fig. 1.

3; $v < 5$ m s^{-1}). A similar value of an increase in the Angstrom coefficient is also expected in Hornsund (from 0.53 ± 0.14 to about 1.00). Given the limited data the impact of wind speeds on AE cannot be precisely determined in the fjords. However, based on Fig. 6, AE seems to be less sensitive to local wind generation than to smoke advection.

Measurements performed in the fjords in 2015 reveal that long-range advection can considerably affect optical properties of aerosols in the Arctic. Further, negligence of its impact may lead to false conclusions. An example is shown in Fig. 6. A negligence of advection impact would result, for example, in a false, positive correlation between AE and v for Hornsund. This is because the smoke advection occurred simultaneously with strong winds in Hornsund and the smoke and marine aerosol had the opposite impact on AE. While the presence of fine smoke particles increased AE by about 0.5—1, the coarse mode sea spray aerosols reduced it. When the impact of the smoke aerosol on AE dominates, we obtain a positive correlation coefficient between v and AE.

4.5. Spatial variability of aerosol properties in a fjord

The last issue addressed in this paper is the dependence of aerosol optical properties on the location of the sampling site in a fjord. For this purpose, three subregions were selected in both Hornsund and Kongsfjorden (Fig. 1): the mouth of a given fjord and the adjacent ocean area (subregion 1), the central part of the fjord (subregion 2) and the innermost part of the fjord including lateral fjords (subregion 3). Measurements from subregion 3 are expected to be most affected by the land surrounding a given fjord, while the measurements from region 1 should be closest to oceanic conditions. Measurements from region 2 can be treated as representative of a given fjord. Furthermore, for each fjord we selected cases of meteorological conditions for which measurements were performed in all the fjord subregions. For Hornsund, the following cases were selected: the smoke advection period with winds from the fjord interior (N-E-S wind directions; 350—170°) and v within the range of 11—13 m s^{-1} (Hornsund, case 1) as well

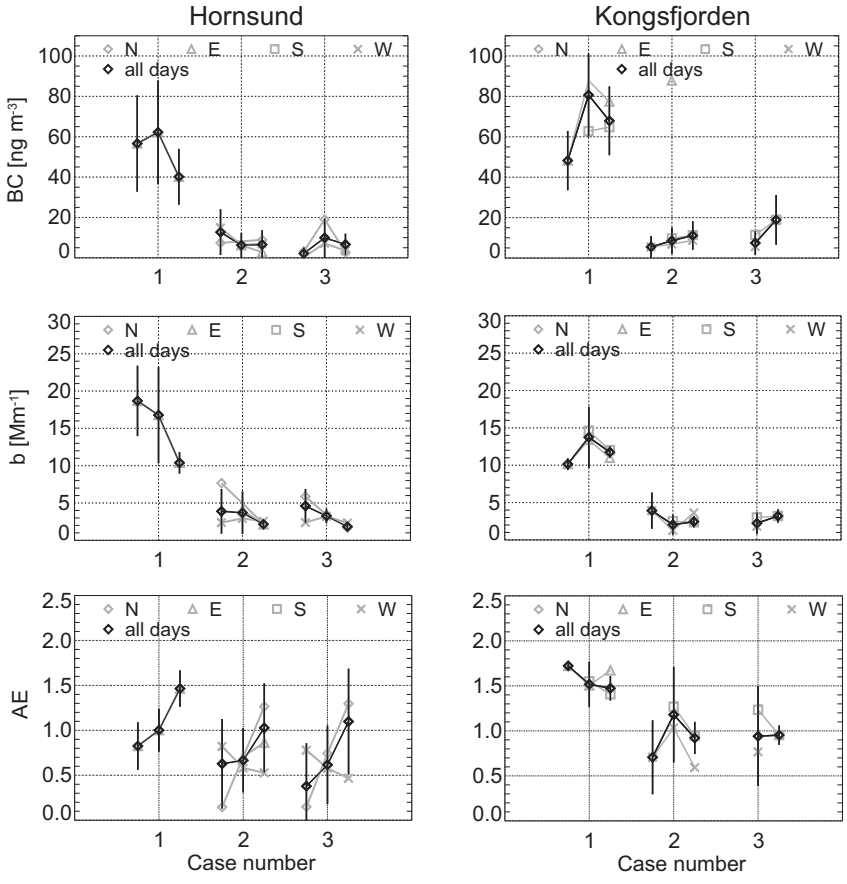

Figure 7 Dependency of black carbon concentration (BC), scattering coefficient (b) and the dimensionless Ångström exponent (AE) on the location of measurement sites in Hornsund and Kongsfjorden. The location is expressed as a respective fjord subregion defined in Fig. 1. Numbers below the plot for BC (Hornsund, case 1) are subregion numbers and show the order of subregions in all the plots. Cases are defined as follows: Hornsund 1 — smoke advection period, wind direction of 350°—170°, v = 11—13 m s^{-1}, Hornsund 2 — background period, wind direction of 350°—170°, $v < 4$ m s^{-1}, Hornsund 3 — background period, wind direction of 170°—350°, $v < 4$ m s^{-1}, Kongsfjorden 1 — smoke advection period, wind direction of 5°—180°, $v < 4$ m s^{-1}, Kongsfjorden 2 — background period, wind direction of 20°—200°, $v < 4$ m s^{-1}, Kongsfjorden 3 — background period, wind direction of 20°—200°, $v < 4$ m s^{-1}. Black symbols and lines show the means and standard deviations for all the measurements within a given case. Grey symbols represent means for selected directions of air mass arrival at a given fjord (E — east, W — west, S — south, N — north).

as winds from the fjord interior (N-E-S; Hornsund, case 2) and the ocean (S-W-N 170–350°; Hornsund, case 3) with $v < 4$ m s^{-1} during the background periods in 2015 and in 2014. Wind speeds less than 4 m s^{-1} ensure a lack of local aerosol generation in the fjord. The cases selected for Kongsfjorden are as follows: smoke advection with winds from the fjord interior (NNE-SSW, 20–220°) with $v < 4$ m s^{-1} (Kongsfjorden, case 1) as well as background periods (2014 and 2015) with wind speeds < 4 m s^{-1} and wind directions from the fjord (Kongsfjorden, case 2) and ocean (Kongsfjorden, case 3). Additionally, within each case the data was divided into subcases with respect to the direction of air mass advection to a given fjord, just before the air mass reached the fjord. The mean values of BC, *b* and AE for each case and each sector are shown in Fig. 7. Locations of points for each case in the plot are in agreement with the geographical position of the respective fjord subregions, i.e. from east (subsection 1, leftmost point) to west (subsection 3, rightmost point).

For all the Hornsund cases an increase in AE is observed in the inner part of the fjord with respect to the fjord mouth while BC and *b* usually decrease (cases 1 and 2 for BC, and 1 and 3 for *b*). The differences between the respective values for subregion 1 and 3 are statistically significant at the level of 0.05. In Kongsfjorden, BC increases moving from the fjord mouth to its innermost part (all cases) while for *b* and AE the changes are less pronounced. Moreover, in Hornsund the main differences between the optical properties of aerosols are found for the central and inner parts of the fjord; in Kongsfjorden the largest differences were typically observed between subregion 1 (the fjord mouth and the adjacent ocean) and the central part of the fjord (subregion 2).

In the case of the fast advection along a fjord axis (Hornsund case 1, easterly winds; 30 July, 211 day of the year, to 1 August, 213) relatively strong gradients in aerosol optical properties were observed. The scattering coefficient decreased from the outside of the fjord to the innermost part of the fjord (from 19 to 10 Mm^{-1}), while AE increased (from 0.83 to 1.46) indicating the smaller contribution of coarse mode marine aerosols inside the fjord at the time. The differences in *b* and AE between subregions 1 and 3 are statistically significant at the level of 0.05. In Hornsund similar tendencies were also observed in the cases of weak winds ($v < 4$ m s^{-1}) regardless of their direction (cases 2 and 3), especially in the case of advection from the north (grey diamonds in Fig. 7). The separation of data with respect to advection direction indicates that gradients of aerosol properties in Hornsund largely depend on the direction of large scale wind fields in the vicinity of the fjord with respect to the axis of the fjord (compare subcases of case 2 and 3 for Hornsund). It must be remembered, however, that the measurement in different parts of the fjords and in different fjords we not performed simultaneously; they are displaced in time with respect to each other. Moreover, the number of measurements is very limited and the time period of the measurements is very short. Therefore, the results presented in this section must be treated as preliminary. The problem requires further study.

5. Conclusions

The temporal variability in physical properties of aerosols observed during the AREX 2014 and AREX 2015 campaigns was much higher than the differences between the Hornsund and Kongsfjorden fjords. Outside the smoke advection period in 2015, BC, *b* and AE values in both fjords were similar to each other. The mean values of the aerosol characteristics analyzed in this study are given in Tables 1 and 2 for each of the fjord and different periods.

The important factor influencing aerosol conditions during the AREX 2014 and 2015 campaigns was the generation of marine aerosols. This conclusion is supported with high correlations between the Angstrom exponent AE and scattering coefficient *b*, and between AE and wind speed.

In 2015, an episode of smoke advection was observed in both fjords causing an increase in BC concentrations from 7–12 ng m^{-3} to about 60 ng m^{-3}, and scattering coefficient from 2–4 Mm^{-1} to 12–17 Mm^{-1}. Its significantly increased BC concentration, *b* and AE values in both fjords (compare Table 2).

Under certain conditions statistically significant gradients in aerosol optical properties were observed along the fjord axis reflecting an impact of mountains surrounding the fjord on aerosol distribution in a fjord. In Hornsund, a statistically significant increase in the Ångström exponent and reduction in the scattering coefficient were found (moving from the fjord mouth and adjacent ocean to the fjord innermost regions) for fast easterly advection of biomass burning aerosol (wind speed in the fiord of 11–13 m s^{-1}) and northerly advection (wind speed in a fjord of <4 m s^{-1}) (compare Fig. 7).

In Hornsund the main differences between the optical properties of aerosols were found for the central and inner parts of the fjord; in Kongsfjorden the largest differences were usually observed between subregion 1 (the fjord mouth and the adjacent ocean) and the central part of the fjord (subregion 2).

In this study we show complexity of phenomena influencing spatial variability of aerosol properties such as orography or meteorological conditions. However, these phenomena need further comprehensive studies.

Acknowledgments

This work was supported through the National Science Centre grant id. number: 2015/17/N/ST10/02396, by funds from the GAME "Growing of the Arctic Marine Ecosystem" project funded by the National Science Centre grant DEC-2012/04/A/NZ8/00661, and the Polish-Norwegian Research Programme operated by the National Centre for Research and Development under the Norwegian Financial Mechanism 2009–2014 as part of Project Contract No Pol-Nor/196911/38/2013.

References

Anderson, T.L., Covert, D.S., Marshall, S.F., Laucks, M.L., Charlson, R.J., Waggoner, A.P., Ogren, J.A., Caldow, R., Holm, R.L., Quant, F.R., Sem, G.J., Wiedensohler, A., Ahlquist, N.A., Bates, T.S., 1996. Performance characteristics of a high-sensitivity, three-wavelength, total scatter/backscatter nephelometer. J. Atmos. Ocean. Technol. 13, 967–986, http://dx.doi.org/10.1175/1520-0426(1996)013<0967:PCOAHS>2.0.CO;2.

Arnott, W.P., Hamasha, K., Moosmüller, H., Sheridan, P.J., Ogren, J. A., 2005. Towards aerosol light-absorption measurements with a

7-wavelength aethalometer: evaluation with a photoacoustic instrument and 3-wavelength nephelometer. Aerosol Sci. Technol. 39, 17—29, http://dx.doi.org/10.1080/027868290901972.

Anderson, T.L., Ogren, J.A., 1998. Determining aerosol radiative properties using the TSI 3563 integrating nephelometer. Aerosol Sci. Technol. 29, 57—69.

Chen, Y.-C., Hamre, B., Frette, Ø., Blindheim, S., Stebel, K., Sobolewski, P., Toledano, C., Stamnes, J.J., 2013. Aerosol optical properties in Northern Norway and Svalbard. Atmos. Meas. Tech. Discuss. 6, 10761—10795, http://dx.doi.org/10.5194/amtd-6-10761-2013.

Damoah, R., Spichtinger, N., Forster, C., James, P., Mattis, I., Wandinger, U., Beirle, S., Wagner, T., Stohl, A., 2004. Around the world in 17 days — hemispheric-scale transport of forest fire smoke from Russia in May 2003. Atmos. Chem. Phys. 4 (5), 1311—1321, http://dx.doi.org/10.5194/acp-4-1311-2004.

Draxler, R.R., Hess, G.D., 1998. An overview of the HYSPLIT_4 modelling system for trajectories. Aust. Meteorol. Mag. 47 (4), 295—308.

Hansen, A.D., Rosen, H., Novakov, T., 1984. The aethalometer—an instrument for the real-time measurement of optical absorption by aerosol particles. Sci. Total Environ. 36, 191—196, http://dx.doi.org/10.1016/0048-9697(84)90265-1.

Hämeri, K., Koivisto, A., Järvelä, M., Lyyranen, J., Auvinen, A., Jokiniemi, J., 2010. Optical Diameter of Mobility Classified Aerosol. American Association for Aerosol Research. Oregon Convention Center, Portland, OR, USA.

Jarraud, M., 2008. Guide to Meteorological Instruments and Methods of Observation (WMO-No. 8). World Meteorological Organisation, Geneva, Switzerland, 681 pp.

Lisok, J., Markowicz, K.M., Ritter, C., Makuch, P., Petelski, T., Chilinski, M., Kaminski, J.W., Becagli, S., Traversi, R., Udisti, R., Rozwadowska, A., Jefimow, M., Markuszewski, P., Neuber, R., Pakszys, P., Stachlewskaa, I.S., Struzewska, J., Zielinski, T., 2016. 2014 iAREA campaign on aerosol in Spitsbergen — Part 1: Study of physical and chemical properties. Atmos. Environ. 140, 150—166, http://dx.doi.org/10.1016/j.atmosenv.2016.05.051.

McFarquhar, G.M., Ghan, S., Verlinde, J., Korolev, A., Strapp, J.W., Schmid, B., Tomlinson, J.M., Wolde, M., Brooks, S.D., Cziczo, D., Dubey, M.K., Fan, J., Flynn, C., Gultepe, I., Hubbe, J., Gilles, M. K., Laskin, A., Lawson, P., Leaitch, W.R., Liu, P., Xiaohong, L., Lubin, D., Mazzoleni, C., MacDonald, A.M., Moffet, R.C., Morrison, H., Ovchinnikov, M., Shupe, M.D., Turner, D.D., Xie, S., Zelenyuk, A., Bae, K., Freer, M., Glen, A., 2011. Indirect and semi-direct aerosol campaign: the impact of Arctic aerosols on clouds. B. Am. Meteorol. Soc. 92 (2), 183—201.

Myhre Lund, C., Toledano, C., Myhre, G., Stebel, K., Yttri, K.E., Aaltonen, V., Johnsrud, M., Frioud, M., Cachorro, V., de Frutos, A., Lihavainen, H., Campbell, J.R., Chaikovsky, A.P., Shiobara, M., Welton, E.J., Tørseth, K., 2007. Regional aerosol optical properties and radiative impact of the extreme smoke event in the European Arctic in spring 2006. Atmos. Chem. Phys. 7 (22), 5899—5915, http://dx.doi.org/10.5194/acp-7-5899-2007.

O'Dowd, C., Monahan, C., Dall'Osto, M., 2010. On the occurrence of open ocean particle production and growth events. Geophys. Res. Lett. 37 (19), L19805, http://dx.doi.org/10.1029/2010GL044679.

Petelski, T., 2005. Coarse aerosol concentration over the North Polar Waters of the Atlantic. Aerosol Sci. Technol. 39 (8), 695—700, http://dx.doi.org/10.1080/02786820500182362.

Petelski, T., Markuszewski, P., Makuch, P., Jankowski, A., Rozwadowska, A., 2014. Studies of vertical coarse aerosol fluxes in the boundary layer over the Baltic Sea. Oceanologia 56 (4), 697—710, http://dx.doi.org/10.5697/oc.56-4.697.

Quinn, P.K., Shaw, G., Andrews, E., Dutton, E.G., Ruoho-Airola, T., Gong, S.L., 2007. Arctic haze: current trends and knowledge gaps. Tellus B 59 (1), 99—114.

Ritter, C., Neuber, R., Schulz, A., Markowicz, K.M., Stachlewska, I.S., Lisok, J., Makuch, P., Pakszys, P., Markuszewski, P., Rozwadowska, A., Petelski, T., Zielinski, T., Becagli, S., Traversi, R., Udisti, R., Gausa, M., 2016. 2014 iAREA campaign on aerosol in Spitsbergen — Part 2: Optical properties from Raman-lidar and in-situ observations at Ny-Ålesund. Atmos. Environ. 141, 1—19, http://dx.doi.org/10.1016/j.atmosenv.2016.05.053.

Rolph, G.D., 2016. Real-time Environmental Applications and Display sYstem (READY). NOAA Air Resources Laboratory, Silver Spring, MD Website (http://ready.arl.noaa.gov).

Rozwadowska, A., Sobolewski, P., 2010. Variability in aerosol optical properties at Hornsund, Spitsbergen. Oceanologia 52 (4), 599—620, http://dx.doi.org/10.5697/oc.52-4.599.

Rozwadowska, A., Zieliński, T., Petelski, T., Sobolewski, P., 2010. Cluster analysis of the impact of air back-trajectories on aerosol optical properties at Hornsund, Spitsbergen. Atmos. Chem. Phys. 10 (3), 87—893, http://dx.doi.org/10.5194/acp-10-877-2010.

Savelyev, I.B., Anguelova, M.D., Frick, G.M., Dowgiallo, D.J., Hwang, P.A., Caffrey, P.F., Bobak, J.P., 2014. On direct passive microwave remote sensing of sea spray aerosol production. Atmos. Chem. Phys. 14 (21), 11611—11631, http://dx.doi.org/10.5194/acp-14-11611-2014.

Schmid, O., Artaxo, P., Arnott, W.P., Chand, D., Gatti, L.V., Frank, G. P., Hoffer, A., Schnaiter, M., Andreae, M.O., 2006. Spectral light absorption by ambient aerosols influenced by biomass burning in the Amazon Basin. I: Comparison and field calibration of absorption measurement techniques. Atmos. Chem. Phys. 6 (11), 3443—3462, http://dx.doi.org/10.5194/acp-6-3443-2006.

Sharma, S., Andrews, E., Barrie, L.A., Ogren, J.A., Lavoue, D., 2006. Variations and sources of the equivalent black carbon in the high Arctic revealed by long-term observations at Alert and Barrow: 1989—2003. J. Geophys. Res. Atmos. 111 (D14), http://dx.doi.org/10.1029/2005JD006581.

Shaw, G.E., 1995. The Arctic haze phenomenon. B. Am. Meteorol. Soc. 76 (12), 2403—2413, http://dx.doi.org/10.1175/1520-0477(1995)076<2403:TAHP>2.0.CO;2.

Smirnov, A., Holben, B.N., Eck, T.F., Dubovik, O., Slutsker, I., 2003. Effect of wind speed on columnar aerosol optical properties at Midway Island. J. Geophys. Res. 108 (D24), 4802, http://dx.doi.org/10.1029/2003JD003879.

Stein, A.F., Draxler, R.R., Rolph, G.D., Stunder, B.J.B., Cohen, M.D., Ngan, F., 2015. NOAA's HYSPLIT atmospheric transport and dispersion modeling system. B. Am. Meteorol. Soc. 96, 2059—2077, http://dx.doi.org/10.1175/BAMS-D-14-00110.1.

Stock, M., Ritter, C., Aaltonen, V., Aas, W., Handorff, D., Herber, A., Treffeisen, R., Dethloff, K., 2014. Where does the optically detectable aerosol in the European Arctic come from? Tellus B 66, http://dx.doi.org/10.3402/tellusb.v66.21450.

Stohl, A., Andrews, E., Burkhart, J.F., Forster, C., Herber, A., Hoch, S.W., Kowal, D., Lunder, C., Mefford, T., Ogren, J.A., Sharma, S., Spichtinger, N., Stebel, K., Stone, R., Ström, J., Tørseth, K., Wehrli, C., Yttri, K.E., 2006. Pan-Arctic enhancements of light absorbing aerosol concentrations due to North American boreal forest fires during summer 2004. J. Geophys. Res. Atmos. 111 (D22), http://dx.doi.org/10.1029/2006JD007216.

Stone, R.S., Herber, A., Vitale, V., Mazzola, M., Lupi, A., Schnell, R. C., Dutton, E.G., Liu, P.S.K., Li, S.-M., Dethloff, K., Lampert, A., Ritter, C., Stock, M., Neuber, R., Maturilli, M., 2010. A three-dimensional characterization of Arctic aerosols from airborne Sun photometer observations: PAM-ARCMIP. J. Geophys. Res. Atmos. 115 (D13), http://dx.doi.org/10.1029/2009JD013605.

Svendsen, H., Beszczynska-Møller, A., Hagen, J.O., Lefauconnier, B., Tverberg, V., Gerland, S., Børre Ørbøk, J., Bischof, K., Papucci, C., Zajaczkowski, M., Azzolini, R., Bruland, O., Wiencke, C., Winther, J.-G., Dallmann, W., 2002. The physical environment of Kongsfjorden—Krossfjorden, an Arctic fjord system in Svalbard. Polar Res. 21 (1), 133—166, http://dx.doi.org/10.1111/j.1751-8369.2002.tb00072.x.

Tomasi, C., Kokhanovsky, A.A., Lupi, A., Ritter, C., Smirnov, A., O'Neill, N., Robert, T., Stone, S., Holben, B.N., Nyeki, S., Wehrli,

C., Stohl, A., Mazzola, M., Lanconelli, C., Vitale, V., Stebel, K., Aaltonen, V., de Leeuw, G., Rodriguez, E., Herber, A.B., Radionov, V.F., Zielinski, T., Petelski, T., Sakerin, S.M., Kabanov, D.M., Xue, Y., Mei, L., Istomina, L., Wagener, R., McArthur, B., Sobolewski, P. S., Kivi, R., Courcoux, Y., Larouche, P., Broccardo, S., Piketh, S. J., 2015. Aerosol remote sensing in polar regions. Earth-Sci. Rev. 140, 108—157.

Treffeisen, R., Tunved, P., Ström, J., Herber, A., Bareiss, J., Helbig, A., Stone, R.S., Hoyningen-Huene, W., Krejci, R., Stohl, A., Neuber, R., 2007. Arctic smoke—aerosol characteristics during a record smoke event in the European Arctic and its radiative impact. Atmos. Chem. Phys. 7 (11), 3035—3053, http://dx.doi.org/10.5194/acp-7-3035-2007.

Tunved, P., Ström, J., Krejci, R., 2013. Arctic aerosol life cycle: linking aerosol size distributions observed between 2000 and 2010 with air mass transport and precipitation at Zeppelin station. Ny-Ålesund. Svalbard., 2013. Atmos. Chem. Phys. 13 (7), 3643—3660, http://dx.doi.org/10.5194/acp-13-3643-2013.

Vaishya, A., Jennings, S.G., O'Dowd, C., 2012. Wind-driven influences on aerosol light scattering in north-east Atlantic air. Geopys. Res. Lett. 39 (5), L05805, http://dx.doi.org/10.1029/2011GL050556.

Virkkula, A., Ahlquist, N.C., Covert, D.S., Arnott, W.P., Sheridan, P. J., Quinn, P.K., Coffman, D.J., 2005. Modification, calibration and a field test of an instrument for measuring light absorption by particles. Aerosol Sci. Technol. 39 (1), 68—83, http://dx.doi.org/10.1080/027868290901963.

Walczowski, W., 2013. Frontal structures in the West Spitsbergen Current margins. Ocean Sci. 9 (6), 957—975, http://dx.doi.org/10.5194/os-9-957-2013.

Zieliński, T., 2004. Studies of aerosol physical properties in coastal areas. Aerosol Sci. Technol. 38 (5), 513—524, http://dx.doi.org/10.1080/02786820490466738.

Oceanologia (2017) 59, 473—495

Available online at www.sciencedirect.com

ScienceDirect

journal homepage: www.journals.elsevier.com/oceanologia/

ORIGINAL RESEARCH ARTICLE

Modelling of the Svalbard fjord Hornsund

Jaromir Jakacki [a,*], **Anna Przyborska** [a], **Szymon Kosecki** [a], **Arild Sundfjord** [b], **Jon Albretsen** [c]

[a] *Institute of Oceanology, Polish Academy of Sciences, Sopot, Poland*
[b] *Norwegian Polar Institute, Tromsø, Norway*
[c] *Institute of Marine Research, Bergen, Norway*

Received 14 July 2016; accepted 5 April 2017
Available online 20 May 2017

KEYWORDS
Hydrodynamic model;
Fjord circulation;
Heat and salt content and anomalies;
Hornsund model

Summary The Arctic Ocean is currently in transition towards a new, warmer state. Understanding the regional variability of oceanographic conditions is important, since they have a direct impact on local ecosystems. This work discusses the implementation of a hydrodynamic model for Hornsund, the southernmost fjord of western Svalbard. Despite its location, Hornsund has a stronger Arctic signature than other Svalbard fjords. The model was validated against available data, and the seasonal mean circulation was obtained from numerical simulations. Two main general circulation regimes have been detected in the fjord. The winter circulation represents a typical closed fjord system, while in summer the fresh water discharge from the catchment area generates a surface layer with a net flow out of Hornsund. Also described are the local hydrographic front and its seasonal variability, as well as the heat and salt content in Hornsund. The integration of salt and heat anomalies provides additional information about the

Abbreviations: A4, 4-km resolution Pan-Arctic model (based on ROMS); ADCP, Acoustic Doppler current profiler; AO, Arctic Ocean; AW, Atlantic Water; AWAKE, Projects (including the AWAKE-2 — Arctic Climate System Study of Ocean, Sea Ice and Glaciers Interactions in Svalbard Area); GAME, Growing of the Arctic Marine Ecosystem project; GLAERE, Glaciers as Arctic Ecosystem Refugia project; ERAi, ERA-Interim — a global atmospheric reanalysis; HOBO, temperature and pressure sensor; HRM, high resolution numerical model of the Hornsund; HYCOM, Hybrid Coordinate Ocean Model; SCA, Salt Content Anomaly; KNOW, The Leading National Research Centre; MIKE, MIKE by DHI — software from the Danish Hydrological Institute; MIKE HD, Mike Flow Model, Hydrodynamic module; NavSim, NavSim Polska sp. z o.o. — Polish Dealer of the Canadian branch of this marine software company; ModOIE, Mesoscale modelling of Ice, Ocean and Ecology of the Arctic Ocean; NPI, Norway Polar Institute; ROMS, Regional Ocean Modelling System; S800, 800 m Svalbard area model (based on ROMS); SC, Sorkapp Current; TOPEX/POSEIDON, Ocean Surface Topography from Space — NASA; TOPAZ4, an ocean-sea ice data assimilation system for the North Atlantic and Arctic global TPXO model of ocean tides; WSC, West Spitsbergen Current.

* Corresponding author at: Institute of Oceanology, Polish Academy of Sciences, Powstańców Warszawy 55, Sopot, Poland. Tel.: +48 587311903.
E-mail address: jjakacki@iopan.gda.pl (J. Jakacki).

Peer review under the responsibility of Institute of Oceanology of the Polish Academy of Sciences.

Production and hosting by Elsevier

http://dx.doi.org/10.1016/j.oceano.2017.04.004

salt flux into the innermost basin of the fjord - Brepollen during the summer. Extensive *in situ* observations have been collected in Hornsund for the last two decades but our hydrodynamic model is the first ever implemented for this area. While at the moment *in situ* observations better represent the state of this fjord's environment and the location of measurements, a numerical model, despite its flaws, can provide a more comprehensive image of the entire fjord's physical state. *In situ* observations and numerical simulations should therefore be regarded as complementary tools, with models enabling a better interpretation and understanding of experimental data.

1. Introduction

Hornsund is a fjord in the south-west of the Svalbard archipelago. Its position and wide opening to Greenland Sea shelf waters (Fig. 1), as well as the large area of contact between the coastal waters and tidewater glacier fronts, expose it to the strong influence of the shelf waters. The fjord's 12 km wide mouth faces west towards the Greenland Sea. Hornsund is 30 km long with a maximum depth of about 260 m (average *ca* 90 m) (Frankowski and Zioła-Frankowska, 2014), an estimated surface area of 275 km^2 and a volume of 23 km^3. The fjord's coastline is very diverse, with a number of small bays, which are the mouths of valleys with glaciers flowing into the sea. Some of these small bays appeared as late as the beginning of the 20th century as a result of glacier recession. The area and coastline of Hornsund have been expanding gradually since the retreat of glaciers. The total area of glacier cover in Hornsund diminished from 1899 to 2010 by

Figure 1 Location of the study area — the Hornsund fjord.
Source: https://en.wikipedia.org/wiki/Svalbard (Oona Räisänen).

approximately 172 km^2, the average loss of area being 1.6 km^2 $year^{-1}$. The recession rate increased from ~1 km^2 $year^{-1}$ in the first decades of the 20th century up to ~3 km^2 $year^{-1}$ in 2001—2010 (Błaszczyk et al., 2013).

Atlantic Water (AW) supplies the biggest volume flux to the Arctic Ocean (AO) and is one of the most important factors shaping the region's climate (Walczowski, 2007, 2013). The West Spitsbergen Current (WSC) is the AW branch that has the greatest influence on conditions in Hornsund. The AW carried by this current is characterized as warm and saline (temperature *ca* 3.5—6.0°C and salinity > 35 in the surface layer off the entrance to Hornsund). But there is another current in the Hornsund area that also has a strong influence on the fjord's state. This is the Sorkapp Current (SC), which carries cold, and fresher water from the western part of the Svalbard Archipelago and the Barents Sea (temperature −1.5 to +1.5°C, salinity 34.3—34.8) (Cottier et al., 2005; Gluchowska et al., 2016). It is a typical fjord with an internal Rossby deformation radius representing the ratio of the internal wave speed to the Coriolis parameter. In the case of Hornsund we can assume that the maximum water depth is 200 m, with a surface layer (T = 4—7°C and S = 30—32) that is *ca* 20 m thick and lower layers (T = 0—4°C and S = 34—35) having an internal Rossby deformation radius between 3.5 and 6 km (Cottier et al., 2005; Nilsen et al., 2008). When the internal Rossby radius is smaller than the width of the fjord, the influence of the Earth's rotation is not insignificant. This means that variations in the flow are driven by rotational dynamics; such fjords are often called “broad”.

Tides are another process that have a strong influence on the fjord. Generally, tides are the main hydrodynamic driver in the fjord: water circulation in the fjord is governed mainly by tides and shelf currents. Tides and currents have a strong influence on the heat, salt and fresh water budgets in the fjord. The amplitude of the tidal components varies between ±0.75 m and the main component of tidal forcing in this area is the semi-diurnal (M2) constituent (Kowalik et al., 2015). Other tidal components are considered in the section on validation.

The study area has been examined previously and many experiments have been done there; indeed, much *in situ* research is still in progress (mostly Polish-Norwegian cooperative ventures), for example, AWAKE-2 (*Arctic Climate System Study of Ocean, Sea Ice and Glacier Interactions in Svalbard Area*) project, GAME (*Growing of the Arctic Marine Ecosystem*) and GLAERE (*Glaciers as Arctic Ecosystem Refugia*). Although these projects usually focus on interdisciplinary studies, *in situ* measurements do not provide a complete picture of the fjord's physical state. Typically, the observations are carried out over short timescales (for example, observations performed from a research vessel) or as long-term *in situ* measurements based on moorings. Direct measurements provide the most accurate results, but making measurements that would be representative of the whole fjord area would be very expensive and logistically difficult (apart from satellite measurements, but these cover only the surface). Another approach that could provide a complete image of the fjord's physical state is modelling. There are already many models embracing Hornsund: the Hybrid Coordinate Ocean Model (HYCOM) (Chassignet et al., 2006), which has a spatial resolution of 1/12deg; TOPAZ4 (Counillon et al., 2010; Sakov et al., 2012), which has a horizontal resolution of 10—16 km and does not take into consideration all the most important factors for studies of water circulation inside fjords (like tides); the Nordic Seas HYCOM model, which has a horizontal resolution of about 4 km, to name but three. Their domains cover much larger areas and their horizontal resolutions are insufficient for studying hydrodynamic processes in Hornsund. To conclude, we could say that although modelling tools are developing rapidly, no high-resolution hydrodynamic model focused on Hornsund has yet been developed. Both the models supplying lateral boundary data cover the Hornsund area (Hattermann et al., 2016), but the fjord is covered by only a few cells, which are insufficient for providing appropriate results.

The model that we implemented for the fjord is of high resolution, but as boundary condition we used data from another (covering a larger geographical area), lower resolution model. Our high-resolution model thus extends the existing model of the Arctic by a fjord, which in the larger model is not correctly represented. In our study, we decided to use software from the Danish Hydrological Institute (MIKE by DHI, MD) as an additional tool in order to acquire a better understanding of the processes that govern the behaviour of the fjord's physical state. With the MD software one can use an unstructured grid (also known as a mesh grid) that allows a model domain of variable spatial resolution to be created, which has advantages in areas with a wide range of depths.

This paper focuses on the implementation of MD for Hornsund and is divided into five main sections. The *Introduction* is followed by the *Model description* and *Implementation*. General information, such as the horizontal and vertical grids, the model domain and bathymetry, are presented here, and all the parameters used (including parameterizations) are listed in the table. The *Boundaries* section describes the implementation of lateral boundary conditions and applied atmospheric forcing. A separate subsection addresses the inclusion of fresh water sources from glaciers and the catchment area. The validation procedures are then described in the next three subsections. Each compares model results with available data for different areas. Because of the extensive lateral boundaries, the shelf area and fjord interior are taken into account separately. Also, because of the different nature of the driving mechanism, tidal flow is dealt with in a separate validation subsection. The main findings, including a description of typical summer and winter circulation patterns, and the hydrographic front, are presented in *Results and discussion*. This section concludes with an analysis of the heat and salt anomalies. Integrated over time, these anomalies reveal that circulation in Brepollen is relatively stable and can only be disturbed by the fresh water discharged from its catchment area.

2. Model description and implementation

2.1. General information

The numerical model of Hornsund (HRM) was set up based on MIKE HD 3D software (Mike Flow Model, Hydrodynamic module, MH). This model solves Reynolds-averaged Navier—Stokes (MIKE and Doc, 2010—2014) equations (RANS) for an incompressible medium with the Boussinesq assumption and

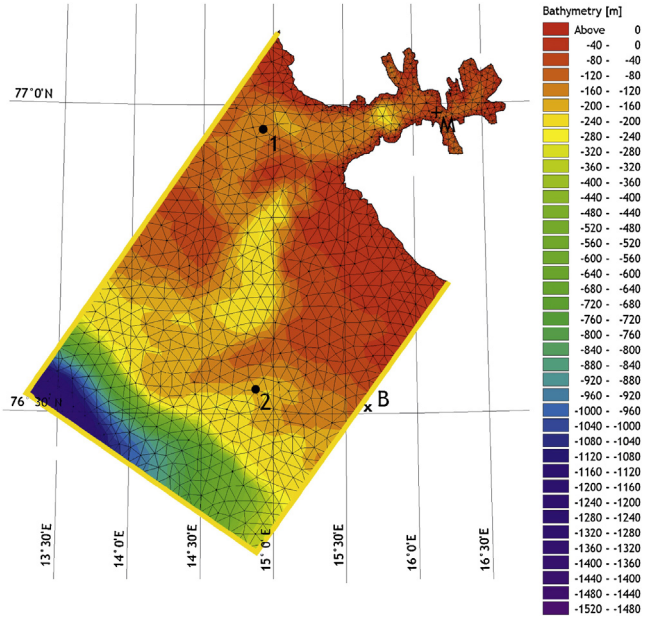

Figure 2 Model domain and bathymetry. The mesh grid, two validation points (1 and 2), the location of the thermistor string and upward looking Acoustic Doppler Current Profiler (ADCP, marked as 'M') have been marked. The solid yellow line delineates the lateral boundary and point 'B' has been inserted as a validation boundary point. (For interpretation of the references to color in this figure legend, the reader is referred to the web version of this article.)

shallow water approximation. The main parts of the model are the domain, grid and bathymetry (Fig. 2). The model's bathymetry was derived on the basis of electronic charts developed by Primar (international collaboration) and distributed by NavSim Polska sp. z o.o. (the Polish dealer of the Canadian branch of this marine software company). The above-mentioned unstructured grid enables a variable horizontal resolution to be used. The model grid consists of 2087 elements and 1293 nodes (an element is defined as a rectangle corner, and a node is the centre of the rectangle, equivalent to the grid centre in a structured grid). The smallest cell in our domain has a horizontal resolution of *ca* 300 m and the largest cell has a dimension of *ca* 3000 m. The vertical dimension of an average cell in the Hornsund area is *ca* 2.6 m (the average depth of Hornsund is about 90 m). Smaller nodes cover parts of the domain that consist of shallower water areas. The mesh grid is also shown in Fig. 2. This figure shows two validation points (points 1 and 2), and the location of the thermistor string and upward looking Acoustic Doppler Current Profiler (ADCP, the point marked 'M'). The model time step is set to 30 s (the solution technique was selected as a low-order fast algorithm). The model is based on the sigma coordinates system with 35 vertical levels. The initial temperature and salinity conditions were constant, and velocity and sea level were set to zero.

2.2. Model setup and numerical parameters

As mentioned earlier, the model solves the well-known RANS equations. However, although these equations are well known, some of the numerical features can vary and are therefore presented here. Mike by DHI is very well documented (MIKE and Doc, 2010—2014), so we provide only a table (Table 1) with the parameters used in the model.

2.3. Boundaries

The lateral boundary condition is one of the most important components of the model. It has to combine tidal forces (the internal representation does not provide the correct amplitude of sea level variation, so it has to be applied as the external sea level variation), velocity, salinity and temperature. The line of the lateral boundary is shown by the thick yellow lines in Fig. 2.

In our case three sources of data were used. Tidal forces in the Hornsund model were applied as sea level from the global tidal model (data represent the major diurnal (K1, O1, P1 and Q1) and semidiurnal tidal constituents (M2, S2, N2 and K2)) with a spatial resolution of $0.25^\circ \times 0.25^\circ$ based on TOPEX/POSEIDON altimeter data (MIKE_DHI, 2014). Barotropic velocities together with respective sea level and active tracers (temperature and salinity) were taken from two Norwegian model simulations (Hattermann et al., 2016). The coupled ocean and sea ice model is a version of the Regional Ocean Modelling System (ROMS) (www.myroms.org; Budgell, 2005; Haidvogel et al., 2008; Shchepetkin and McWilliams, 2009) with two different horizontal resolutions. The first one, the A4 model, covers a pan-Arctic domain with a 4 km resolution, while the second one (high-resolution model (S800, Albretsen et al., 2017)) is a one-way nested simulation with an 800 m resolution of the domain covering Svalbard and a large part of the Fram Strait. Both models (A4 and S800) were forced by atmospheric fields derived from ERA interim reanalysis (ERAi, Dee et al., 2011). In addition, A4 and S800 (Hattermann et al., 2016) used tidal forces retrieved from the global TPXO model of ocean tides (Egbert and Erofeeva, 2002).

The barotropic part of the boundary was specified using Flather's boundary condition (Flather, 1976):

Table 1 Parameters used in the model.

Parameter	Value	Model option or comments (if needed)
General information		
Horizontal resolution	Size of cell (max, min) = (300, 3000)	Mesh grid presented in Fig. 2
Vertical coordinates	35 vertical levels, min = ~0.2 m, max = ~40 m	Sigma coordinates
Simulation periods	01.2005–06.2010	
Maximum time step	30 s	
Bathymetry source	NavSim (based on **E**lectronic Navigational Charts – ENC)	
Flood and dry	Included	
Horizontal turbulence model	Smagorinsky	
Vertical turbulence model	$k-\varepsilon$	
Bed friction	Constant in domain, but depends on cell thickness	
Flood and dry	Included	
Density	Salinity and temperature dependent	
Coriolis forcing	Included	
Atmospheric forcing	Included	Based on ERAi: – Mean sea level pressure – Wind speed and direction – 2 m potential temperature – Cloudiness – Precipitation – Wind speed
Ice thickness and concentration	Included	Based on S800 model
Critical CFL value	0.8	Courant–Friedrichs–Lewy number
Initial conditions		Initialization from cold start
Surface level	0 m	
Velocities	0 m s^{-1}	

$$\overline{u} = \overline{u}^{ext} - \sqrt{\frac{g}{D}}(\xi - \xi^{ext}). \quad (1)$$

Computed from the Sommerfeld wave equation and the continuity equation, this condition is one of the most efficient open boundary conditions (Jeżowiecka-Kabsch and Szewczyk, 2001; Kantha and Clayson, 2000). In Eq. (1) $\overline{u}$ denotes depth-averaged velocity, D is the local depth and ξ represents sea level. The superscript *ext* links external data. The barotropic velocities in Eq. (1) were extracted and interpolated based on an 800 m ROMS setup that covers the Nordic Seas (Hattermann et al., 2016). In addition, the Dirichlet boundary was applied to temperature and salinity. The data for those variables were taken from the Nordic Seas ROMS model (4 km horizontal resolution; Lien et al., 2013).

The 2D field was interpolated for the top boundary layer. The model does not require any atmospheric data, but in order to replicate realistic conditions, we applied the following atmospheric data:

- Mean sea level pressure,
- Wind speed and direction,
- 2 m potential temperature,
- Cloudiness,
- Precipitation,
- Sea ice concentration,
- Sea ice thickness.

Atmospheric fields were prepared on the basis of the ERA Interim reanalysis data set (from the European Centre for Medium-Range Weather Forecasts) and ice coverage was taken from the S800 model.

2.4. Fresh water sources

Fresh water sources are an important part of the fjord ecosystem. The main ones include direct precipitation on to the fjord surface (taken into account as atmospheric forcing), tidewater glacier ablation and calving, melting of fast ice and sea ice, and land/riverine outflow. The fresh water sources for the Hornsund area and a compilation of the available data were presented at the Mare Nor Symposium on the Ecology of Fjords and Coastal waters (Węsławski et al., 1995). This is summarized in Fig. 3. The percentages and quantitative contributions of all fresh water components (ablation, precipitation, snow and rivers) were estimated on the basis of Fig. 3a and b. Next, the percentage contribution of each source was estimated on the basis of that report and Fig. 3b. Then, the quantitative contribution of the fresh water component for each location shown in Fig. 3b was adopted from Węsławski's results (Węsławski et al., 1995; Fig. 3a). We also introduced a time shift between the western and eastern parts of the fjord, because of the melting processes that occur in the catchment area. Moving the time period of ice melt is based on an observation provided by the Polish Polar Station in Hornsund. Melting always begins in the shelf area and then moves eastwards. The time shift between the eastern and western parts is about one month and it is not visible in the figure (Fig. 3c). Although the AWAKE2 project run by the Institute of Oceanology, Sopot, had one work

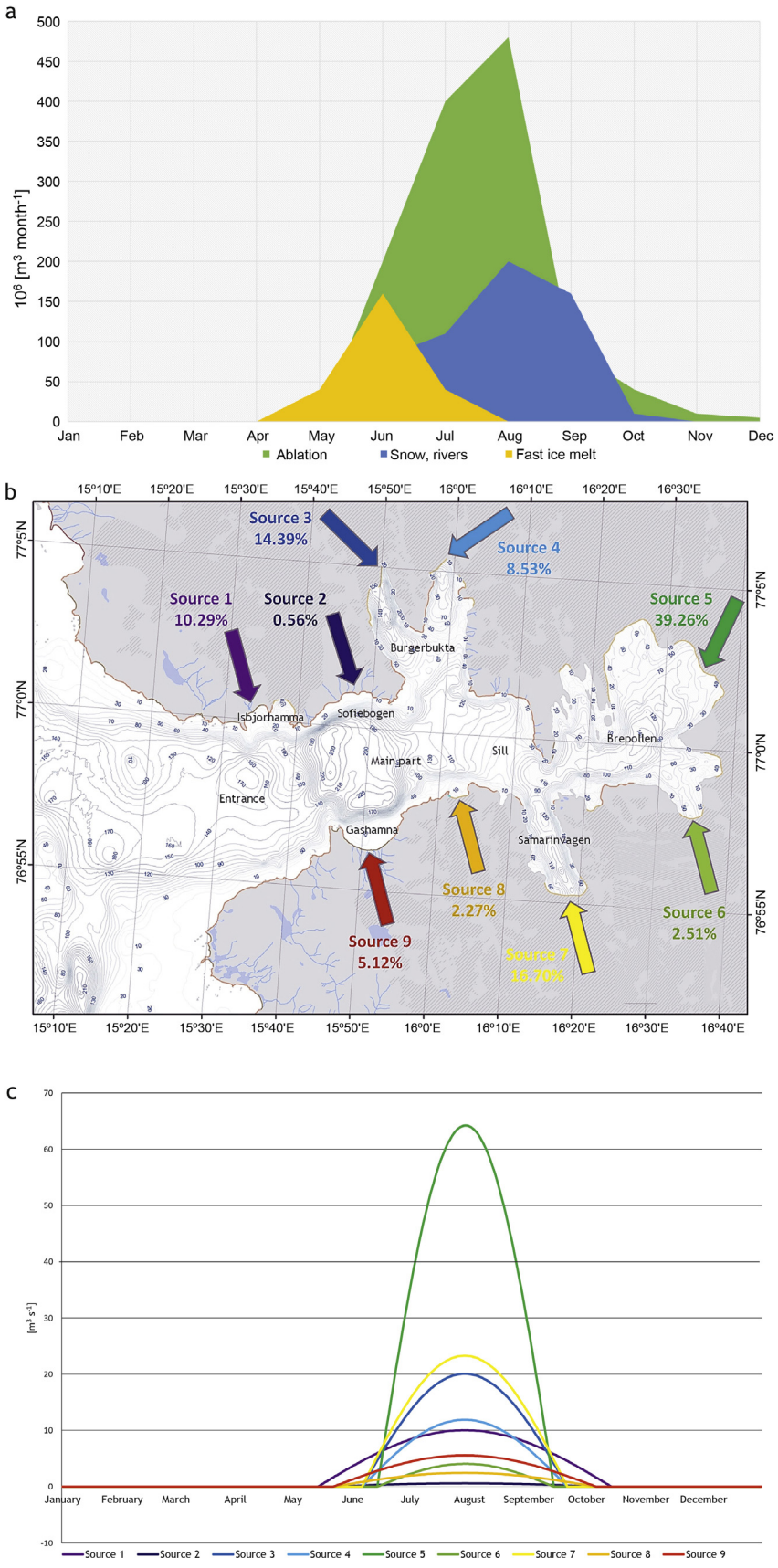

Figure 3 Sources of fresh water and their time dependence in Hornsund based on Węsławski, 1995 (a); the version implemented for the model (b) represents the estimated percentage contribution of each source; the time variability of each source (c).

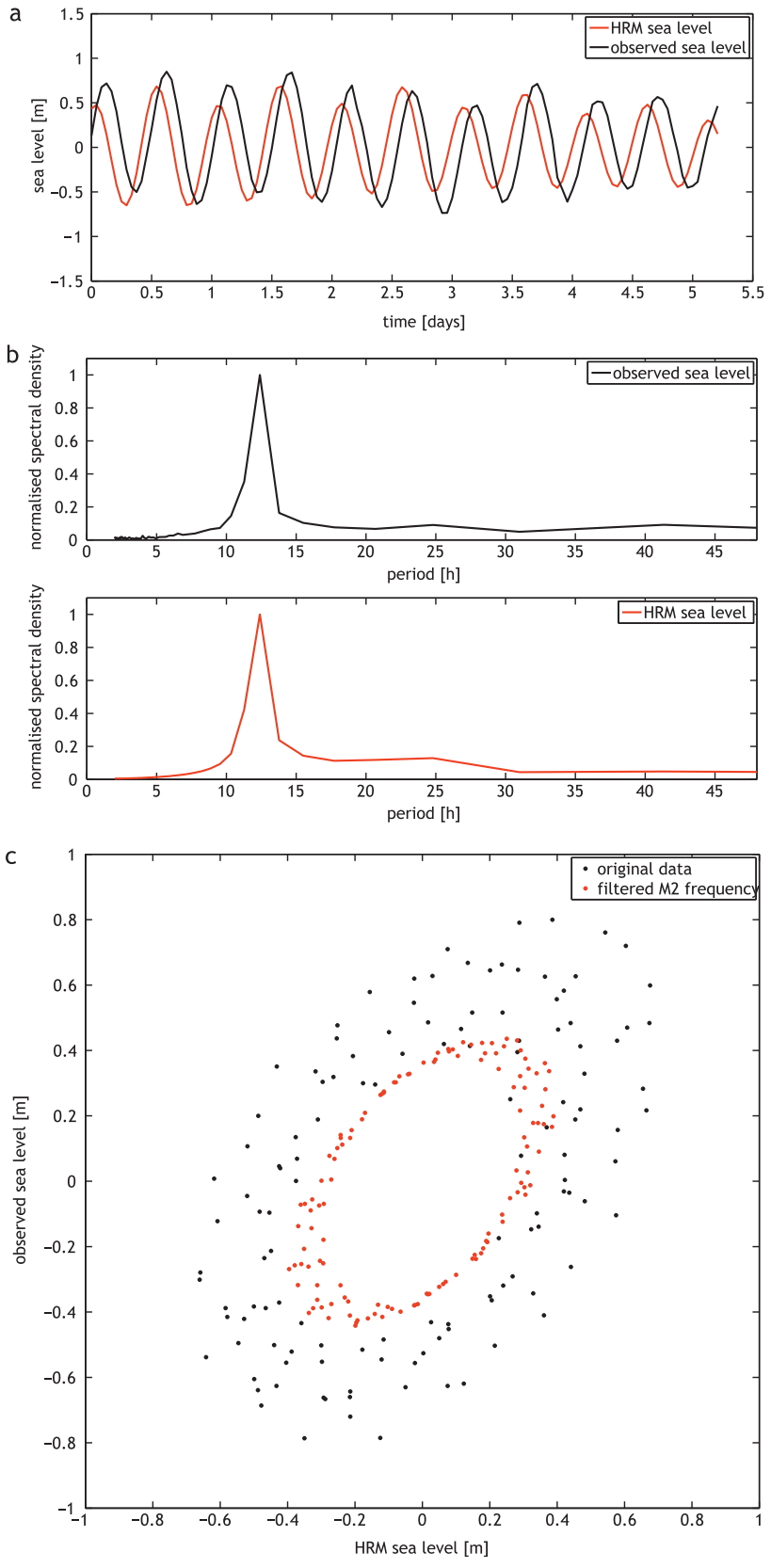

Figure 4 (a) Time series of the modelled (HRM, red line) and measured (black line) sea surface level, (b) power spectrum density derived from the time series shown in (a). The upper, black line image stands for the experimental results and the lower, red line represents the spectrum of HRM sea level; (c) comparison between measured (vertical axis) and HRM (horizontal axis) sea levels with a filtered M2 (semi-diurnal, red points) component. (For interpretation of the references to color in this figure legend, the reader is referred to the web version of this article.)

package focused on estimating fresh water sources in that area, the results are still not available. Because there are no other data that could represent fresh water from the Hornsund drainage basin, we decided to utilize the sources from Fig. 3 (Węsławski et al., 1995) in the model for the whole simulation.

3. Model validation

The validation procedure depends on the area and local forces. As validation of tidal forces requires different methods from temperature or salinity variation, it was divided into three parts:

- Tides;
- The shelf area;
- The fjord's interior.

3.1. Tide validation

The lack of experimental data does not permit long-term validation, so we used short-term measurements from the

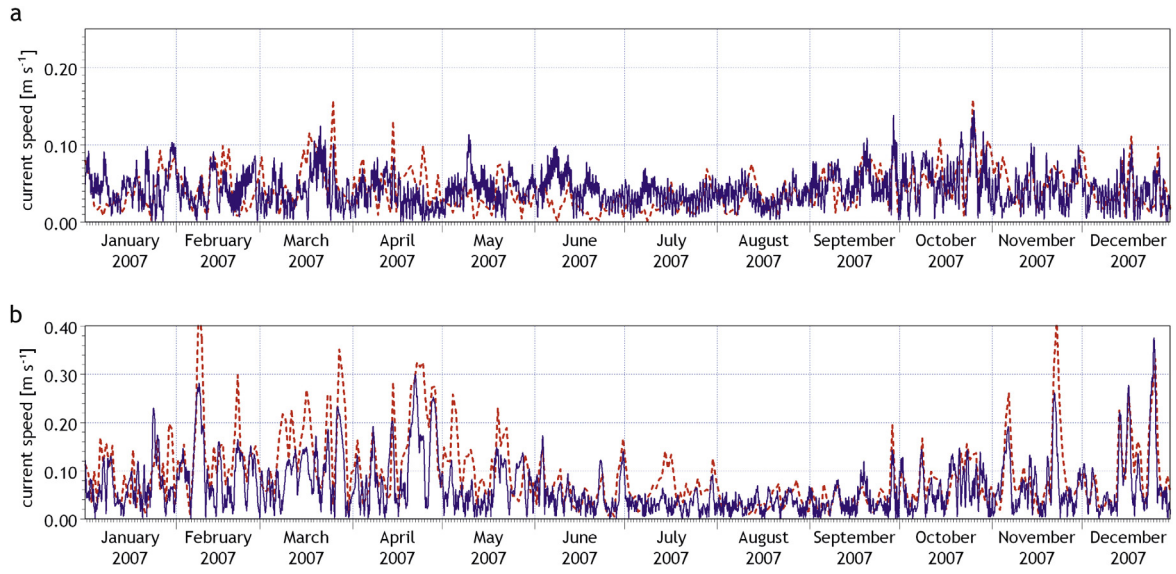

Figure 5 Comparison of barotropic current velocity at the two locations in the shelf area shown in Fig. 2 (the upper image represents point 1 (a) and the lower one point 2 (b); the blue and red lines represent the HRM and S800 models respectively). (For interpretation of the references to color in this figure legend, the reader is referred to the web version of this article.)

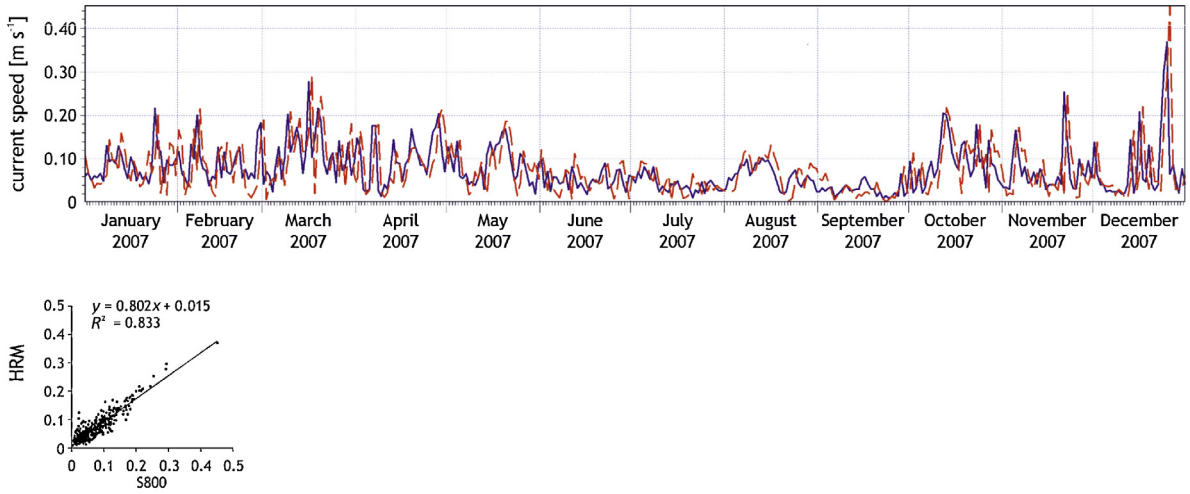

Figure 6 Comparison of the current velocity for one point located on the boundary (south-east, yellow boundary line — point 'B' in Fig. 2). The blue and red lines represent the HRM and S800 models respectively. The linear regression for this series is shown on the lower panel. Correlation coefficient $R \approx 0.91$. (For interpretation of the references to color in this figure legend, the reader is referred to the web version of this article.)

area in front of the Hansbreen Glacier measured by the Institute of Geophysics of the Polish Academy of Sciences (IGF). The *in situ* measurements were made between 9 and 15 August 2011 using a Schlumberger Mini-Diver. This instrument was equipped with a pressure sensor, and the duration of measurements was limited by its memory capacity. Our model does not provide results for those dates, but in the case of tides there will only be a phase shift between the data. Fig. 4a shows a sea level time series as measured by the Mini-Diver and the modelled one. The spectral analysis of these signals is shown in Fig. 4b. The power spectral density was normalized to the maximum of both signals (in this case to the measured maximum sea level) for better clarity. Sea levels with a filtered M2 component are compared in Fig. 4c.

Because of the different time series, the phase shift is visible in Fig. 4c as a circle (or ellipse) formed by the red points. Despite the short period covered by the *in situ* data, the results provide quite a good comparison between the measured and modelled amplitudes and frequencies. One maximum shown in Fig. 4b (period close to 12 h) represents the semidiurnal tidal constituent (M2, although there are also other semidiurnal constituents in this area), the other (close to 24 h) relates to diurnal components. However, for a short time series it is impossible to separate all the semidiurnal and diurnal constituents.

3.2. The shelf area

In the second step of the validation we compared our model data with the data provided by the S800 and A4 models. For this purpose we compared the barotropic current velocity, salinity and temperature derived from our Hornsund model with the results of models implemented as lateral boundary conditions (the comparison was performed for the two points shown in Fig. 2). Fig. 5 compares the temporal variability of the current speed derived from S800 model with that from the HRM model. The main differences can be explained by the bathymetry. All the models use different sources of bottom topography; in the case of the barotropic velocity it is the main reason for these differences. Linear correlation between these series yields low values of the coefficient that are close to 0.3. This might suggest that the lateral boundary condition has been implemented incorrectly. Except for the point located on the south-east boundary line (point 'B') on the yellow line in Fig. 2, the correlation is much better. The value of the coefficient is about 0.91 and is shown in Fig. 6. This confirms the earlier suggestion that the differences between S800 and HRM in the shelf area mostly result from differences in bathymetries.

Fig. 7 shows a time series of surface salinity and temperature derived from the HRM and A4 models. The solid lines

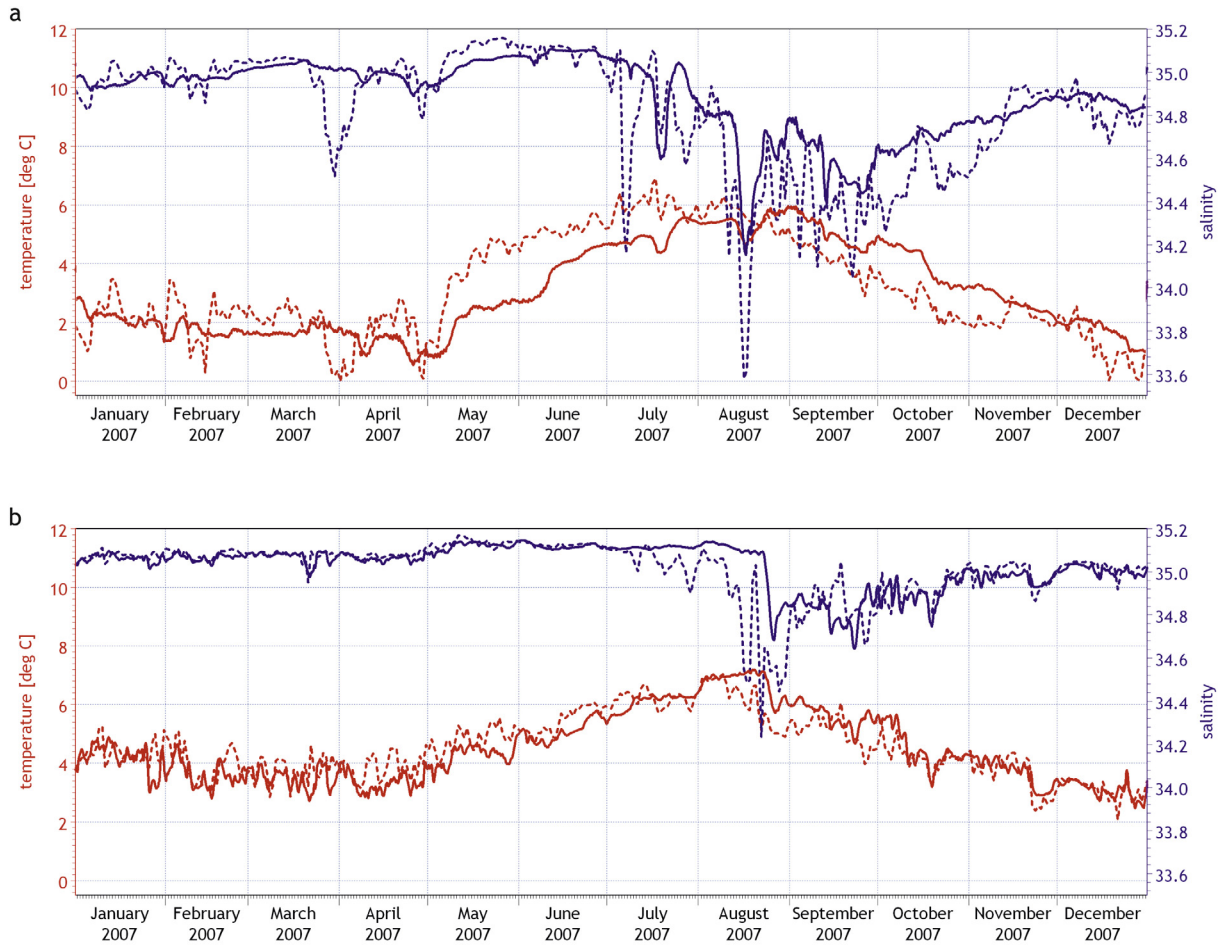

Figure 7 Comparison of temperature and salinity in the surface layer (the upper graph represents point 1 (a), the lower graph point 2 (b); the red and blue lines represent temperature and salinity respectively; the dashed lines represent model A4, the solid lines HRM). (For interpretation of the references to color in this figure legend, the reader is referred to the web version of this article.)

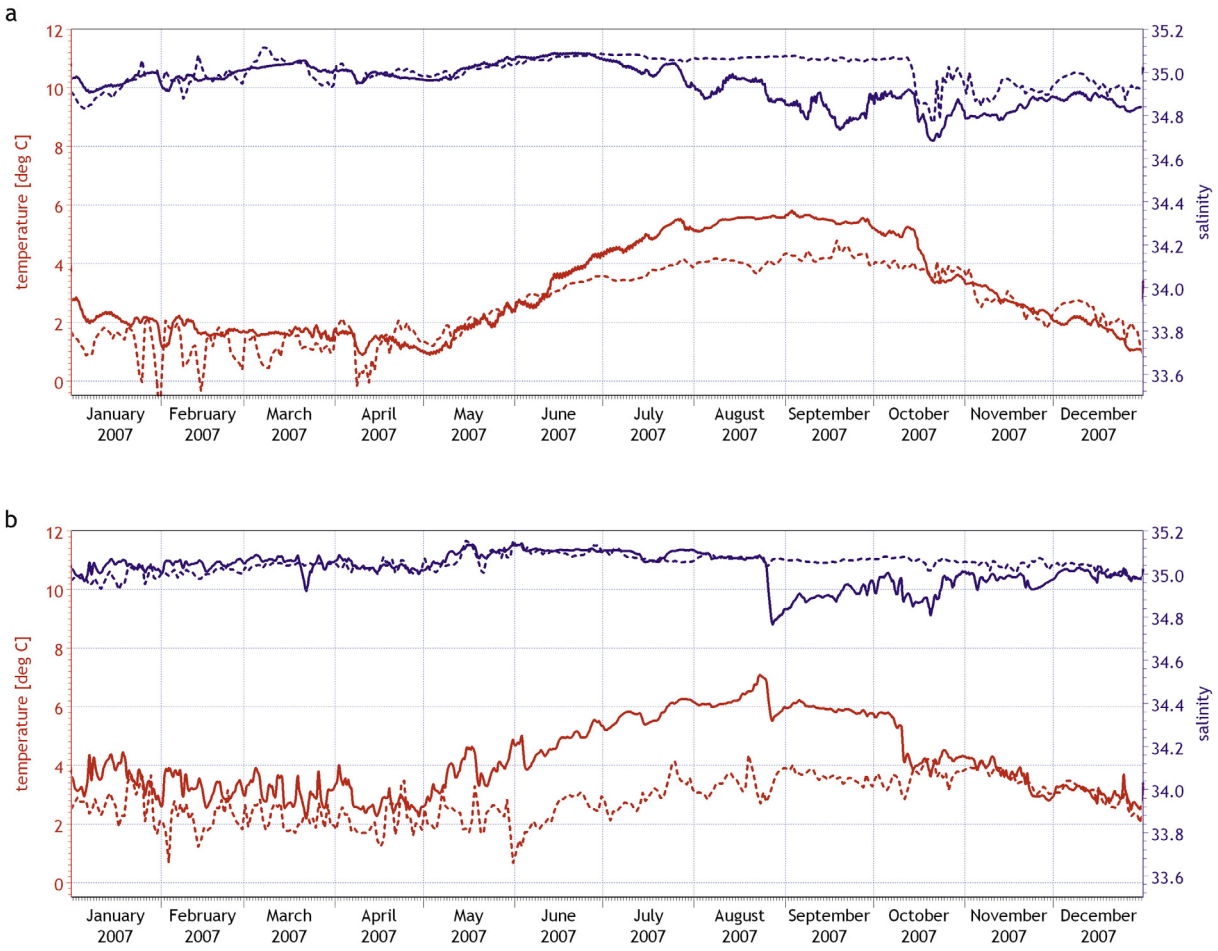

Figure 8 Comparison of temperature and salinity in the bottom layer (the upper graph represents point 1 (a), the lower graph point 2 (b); the red and blue lines represent temperature and salinity respectively; the dashed lines represent model A4, the solid lines HRM). (For interpretation of the references to color in this figure legend, the reader is referred to the web version of this article.)

refer to our HRM model. The comparison for the surface layer looks quite good. Model A4 has a 4 km resolution, so the fjord has only several points in it. In our case the main differences are between May and October, when fresh water sources were active throughout the fjord. Moreover, it is plainly evident that the model reproduces the seasonal variability of the shelf area. Fig. 8 shows a similar graph, but for the bottommost layer. Here, there is also good agreement between the results of the two models, although the temperature is a little higher for the second point in summer.

Table 2 Correlation coefficient calculated for temperature and salinity for points 1 and 2.

	Point 1	Point 2
Surface layer		
Temperature	0.80	0.88
Salinity	0.85	0.65
Bottom layer		
Temperature	0.91	0.49
Salinity	0.43	0.22

Both models (A4 and HRM) are quite different, so a comparison between them yields different results for the bottom layers. Nonetheless, HRM still reproduces seasonal variability (which is stronger in this case) and except for the summer, the time series are very close. In summer there is a visible influence of the fresh water sources on the shelf area, but in the other seasons the variability from both models is very similar. A simple linear correlation yields the coefficients shown in Table 2.

The best correlation coefficients are for the surface layer. This is the result of the similar atmospheric fluxes implemented in both models (S800, A4 and HRM used the same source of atmospheric forces, so we had expected to get a good correlation) and also because the forcing at the open boundaries is similar (HRM uses boundary conditions from S800 and S800 from A4). The influence of the fjord is also clear in summer. The differences, visible mostly on the temperature curves, are driven by fresh water sources.

3.3. The fjord interior

The limited availability of experimental data does not help to carry out a detailed validation of the fjord interior. Most data

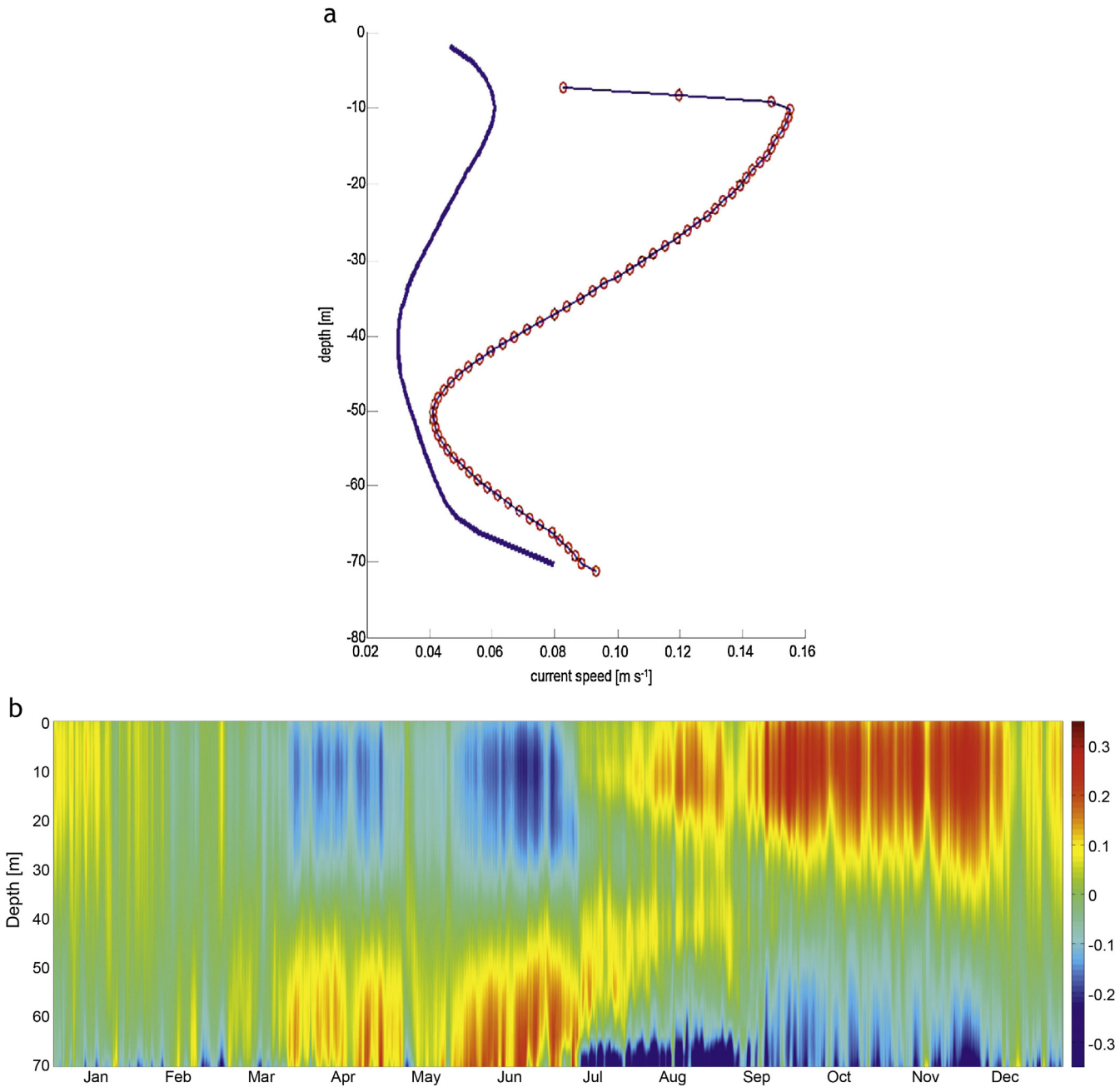

Figure 9 (a) Depth profile of the average current magnitude measured by ADCP (thin blue line with red circles) and HRM model data (thick blue line). (b) Average (for 2006—2009) temporal variability of vertical profile of current directed into Brepollen (positive value means 'into'). (For interpretation of the references to color in this figure legend, the reader is referred to the web version of this article.)

are available from the AWAKE projects (including the AWAKE-2 — Arctic Climate System Study of Ocean, Sea Ice and Glacier Interactions in the Svalbard Area) managed by the Institute of Oceanology and implemented within the framework of Polish-Norwegian collaboration. The most important time series are provided by the Norway Polar Institute's (NPI) instrument mooring located at the silled entrance to Brepollen (76.9850N 16.1728E, see Fig. 2). They were collected between September 2013 and June 2014. The mooring, equipped with a profiling current metre and a string of thermistors, was deployed at a depth of 76 m on the sill at the entrance to Brepollen and was in operation from 5 September 2013 to 5 July 2014. An AADI RDCP600 Acoustic Doppler Current Profiler was used to measure 3D currents. This instrument was mounted in a bottom frame and covered the range from ~72 m upwards with 1 m vertical resolution. It is important to add that the signal-to-noise ratio of individual current measurements decays with distance from the instrument and the upper part of the data shown in the following has large uncertainty and is included only for

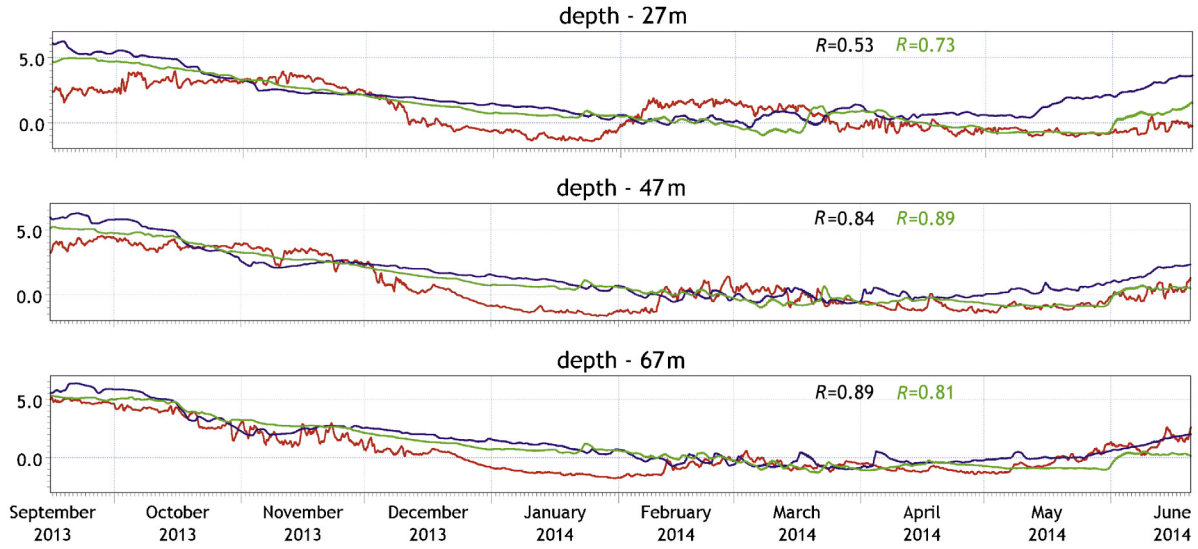

Figure 10 Temporal variability of temperature from *in situ* measurements and model simulations: red — from the thermistor string, blue and green — the HRM model (2006—2007 and 2007—2008 respectively). The location of the mooring is marked in Fig. 2 by 'M'. Linear correlation coefficients are inserted on each figure. The correlation coefficients between temperatures from the thermistors and HRM for 2006—2007 are marked in blue, and the correlation coefficients between temperatures from the thermistors and HRM for 2007—2008 in green. (For interpretation of the references to color in this figure legend, the reader is referred to the web version of this article.)

illustrational purposes. The RDCP600 was also equipped with a pressure sensor and a temperature sensor. TinyTag Aquatic2 thermistors were installed at 5 m intervals from 27 to 67 m depth. On the same rope, a HOBO U20-001-03 temperature and pressure sensor was attached at 22 m depth. The pressure sensor showed modest variation during the deployment, indicating that the thermistor chain was not seriously subducted by strong currents. Because we had no model integrations for that year, we will make a comparison for different years.

Fig. 9a shows a comparison between the average modelled current magnitude (HRM model, thick blue line) and that measured by the ADCP (left) for different depths recorded during this experiment. The result shows good compatibility between the measured and modelled velocity profile. It shows the minimum current velocity located at around 40—50 m depth. This minimum exists because of the internal tide oscillations.

In order to obtain a broader image of inflows and outflows at this location we calculated the three-year average temporal variability of currents into Brepollen (Fig. 9b — a positive velocity means 'into Brepollen'). Two main regimes are visible. The first one is between March and July. During this time the inflow into Brepollen is in the lower layer and the outflow in the upper layer. In the second one (between August and December) the inflow into Brepollen takes place in the upper layers (mostly below 30 m). The first regime ensues from the typical circulation when lighter fresh water is flowing out in the upper layers. The second one comes into existence when the volume of fresh water is negligible. This situation is typical of narrow fjords, *i.e.* when the internal Rossby deformation radius is bigger than the width of the fjord. In a such situation, water flows into the fjord in the upper layers and out in the lower layers or *vice versa*. At middle depths, the internal tidal motion is bidirectional and its average constitutes the local minimum of the magnitude.

Fig. 10 illustrates the 9 months' variability of temperature for three depths: 27, 47 and 67 m. Although the differences between the modelled and measured temperatures sometimes exceed 2 degrees, the model appears to reproduce seasonal variability quite well. Correlation coefficients are mostly over 0.8; they are smaller only for the shallowest depths. The lower correlation coefficients for 27 m depth can be explained by the low-resolution atmospheric data focused on large-scale variability (ERAi). In addition, large scale reanalysis such as ERAi does not focus on local scale processes.

4. Results and discussion

4.1. General circulation

As mentioned before, rotational effects influence the general circulation in Hornsund: this is presented in Fig. 11 as two typical circulation regimes. The figures represent the average circulation for the whole domain (temporal and depth mean) for January and July 2008, which is equivalent to the winter and summer states. For greater clarity we have used streamlines instead of vectors.

The main circulation pattern (shown in Fig. 11) represents the residual current that enters the fjord on the southern side and then recirculates along its northern part. In summer, waters of shelf origin penetrate much farther into the fjord's main basin and reach the entrance of the inner basin called Brepollen. In winter, fresh water sources are limited to

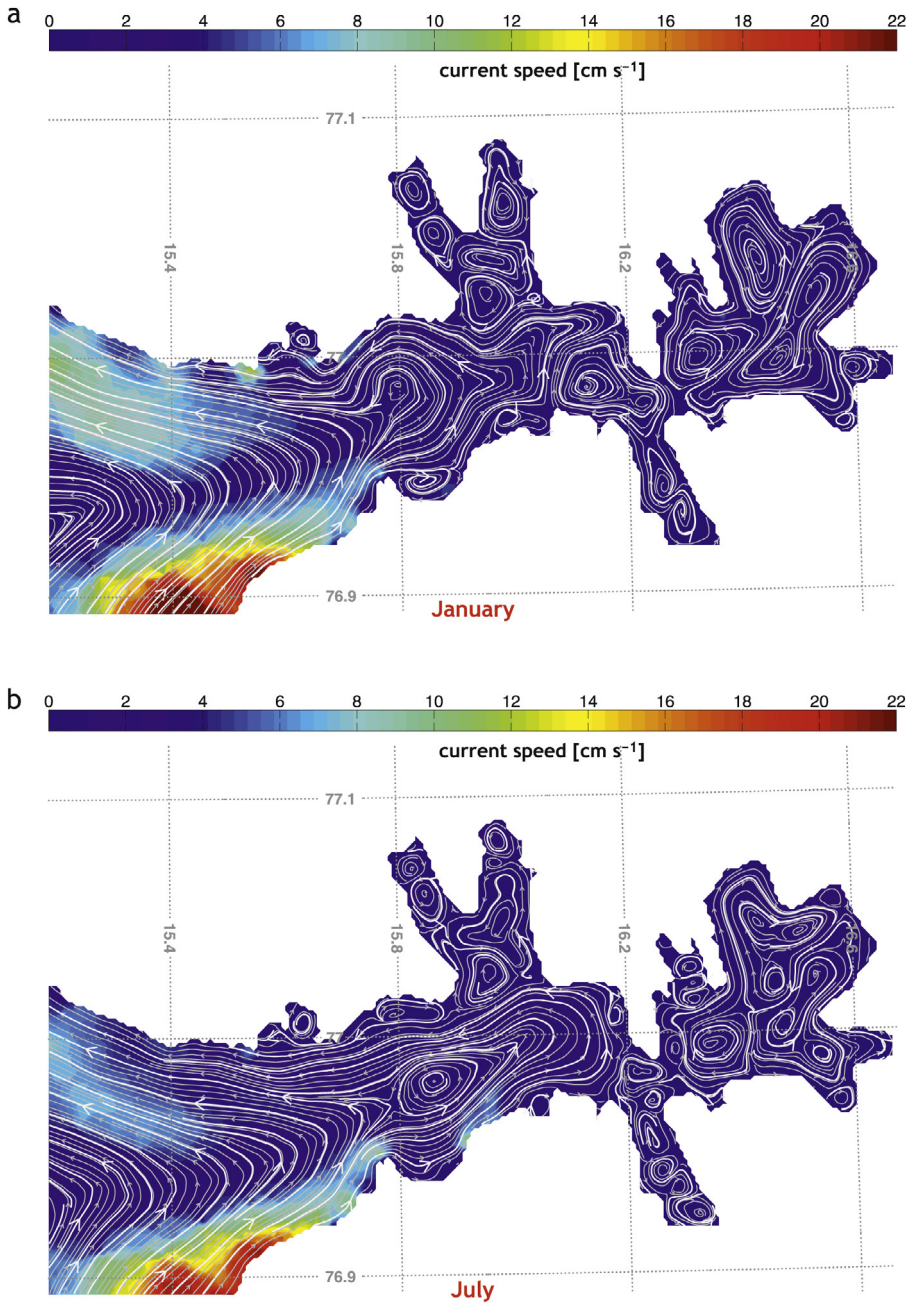

Figure 11 Streamlines (white lines) and current speed (colour-coded) over domain and time averaged in Hornsund for January (a) and July 2008 (b).

meltwater from marine terminating glaciers, thus the residual circulation pattern is similar but the volume exchange between the fjord and the shelf is much smaller than in summer (MIKE DHI does not have any assimilation data module or parameterization of ocean-glacier interaction such as surface melting or submerged plume discharge, so the representation of underwater glaciers is not possible). A cyclonic circulation is observed in the central area of the fjord mostly during the periods when fresh water inputs are the smallest. In summer this cyclonic flow is disrupted by an intense circulation driven by fresh water from terrestrial and glacial sources. The circulation in Brepollen, the easternmost part of the fjord, is also characterized by seasonal variability, with the main winter circulation pattern significantly different from that in July. Small-scale eddies in Brepollen, Samarinvagen and Burgerbukta are also more abundant in July. Increased fresh water discharge in summer results in stronger stratification in the fjord; as a consequence, submesoscale eddies are generated owing to the internal Rossby deformation radius.

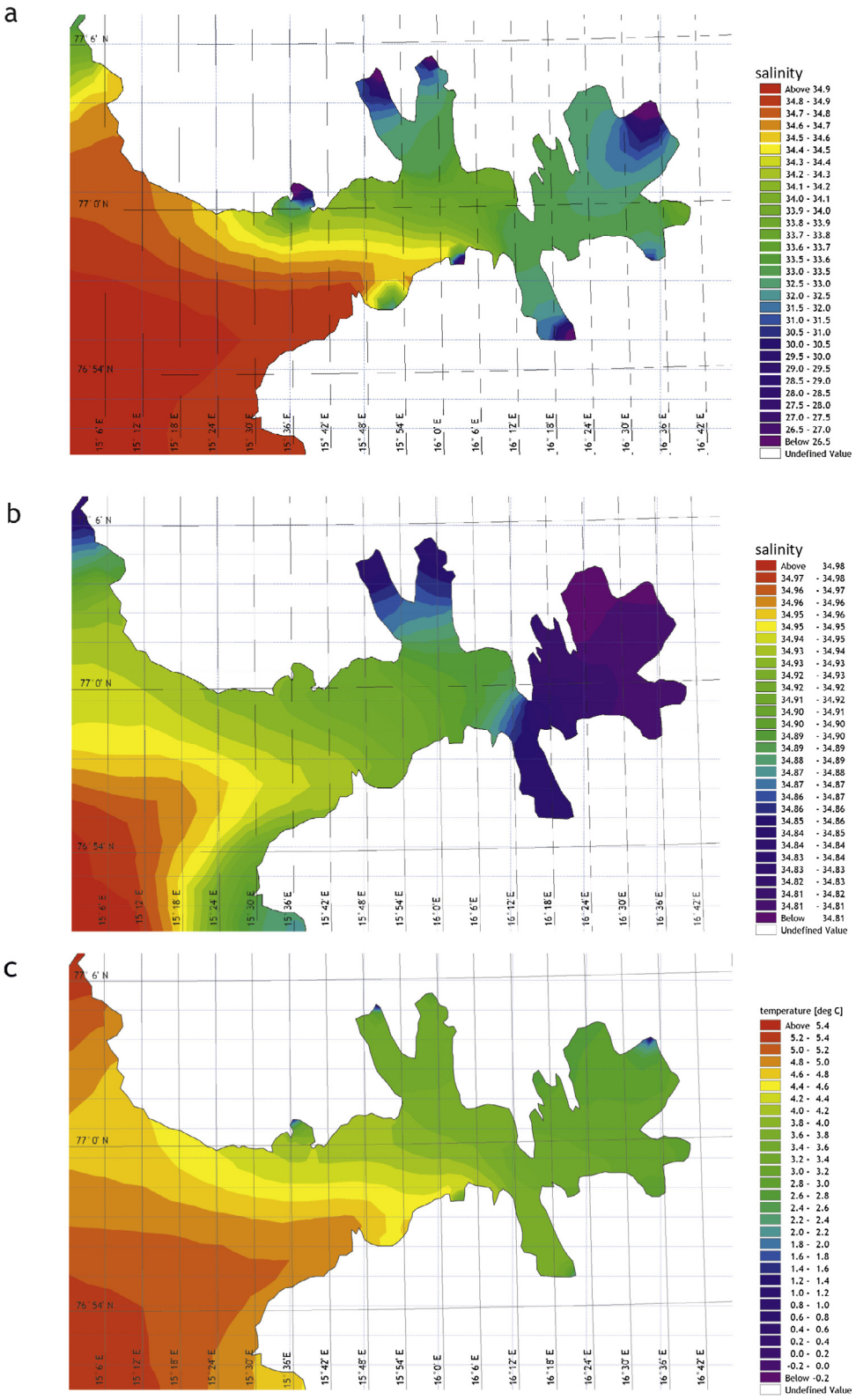

Figure 12 Average sea surface salinity (a and b) and temperature (c and d) retrieved for January (c and d) and July (a and b) 2009.

d

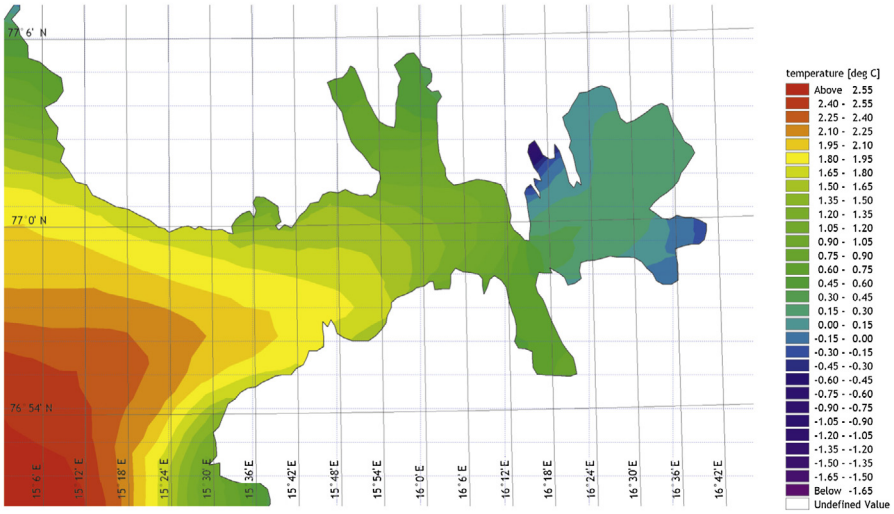

Figure 12. (*Continued*).

4.2. Hydrological front

The fjord's dynamics and fresh water from the catchment area (including the underwater glaciers, which are not included in the model) generate a hydrological front mostly at the mixed layer depth. Fronts, natural boundaries between waters of different properties, affect mixing processes, which occur in the water in both the horizontal and vertical. Dramatic changes in the properties of waters can result in the formation of various eddies, which affect local wind conditions, coastal upwelling, intrusions of intermediate waters and sea ice. The fronts may be visible on the surface as demarcation lines, colour changes, foam accumulation or choppy waters. The best indicators of the spread of riverine waters in the sea are density and salinity (Fedorov, 1986; Ginzburg and Kostianoy, 2009), but here we use temperature and salinity.

The front is represented by strong temperature and salinity gradients (Fig. 12). Fresh water from the catchment area leaves the northern area of the main fjord and oceanic water enters the fjord through the southern part of the mouth. The shape and gradient of the front depends mostly on the fresh water content in the surface layers of the fjord.

In winter this front also exists but the salinity and temperature gradients are much weaker and they are clearly symmetrical. The temperature and salinity distributions in the fjord are more homogeneous at that time and the fjord waters are generally separated from the AW of the WSC by the front, yet its shape, location and physical properties strongly depend on the season. The shape of the surface temperature and salinity fields result from the dynamic impact of the Earth's rotation on the fjord. The typical baroclinic Rossby deformation radius is 3.5–6 km for the Svalbard fjords (Cottier et al., 2010). The outer part of Hornsund is 30 km wide, which is 5–10 times greater than the internal deformation radius. The effect of rotation is better visible in the summer months, since in the warm season the strongly, vertically stratified waters tend to reduce the internal Rossby deformation radius, so the Coriolis force is more pronounced and can act more effectively in the narrower parts of the fjord as well. Fig. 13b–f shows the sections marked in Fig. 13a. The first one (IP1-IP2-IP3-IP4-IP5) is along the fjord (we call it the along-fjord section (HS)), while the second one is across the fjord entrance (A-A′, the cross-section (VS)). At the HS an area is visible in the middle depths with a strong salinity and temperature gradient (at about 20 m depth) – above this depth the fresh water from the catchment area flows out in the surface layers of the fjord. The waters are mixed, and the degree of mixing depends on the distance from the source and local dynamic conditions. The VSs show that the main core of the shelf waters enters the southern mouth area. Moreover, the image showing the velocities of VS (which represents the velocity of inflow – a positive value means that the flow is directed into the fjord) confirms that the main outflow area is in the upper and lower layers and is closer to the northern part of the fjord. As mentioned earlier, the shape of the front depends on the fresh water content in the fjord and could be very useful for estimating the amount of fresh water from glaciers and the catchment area. We will be able to formulate more general conclusions about the hydrological front and the impact of other factors on front formation following a detailed analysis of the front over a longer period of time; this is planned for the near future.

4.3. Salt and heat content and its anomaly of the main fjord and Brepollen

The fjord's dynamics strongly depend on the season. The annual variability could be represented by the fjord's heat and salt content. Furthermore, the fjord is known to be under the strong influence of shelf waters consisting of WSC and SC, and it is impossible to separate them because these two currents mix at the fjord's mouth (Gluchowska et al., 2016; Walczowski, 2013). Analysis of the salt and

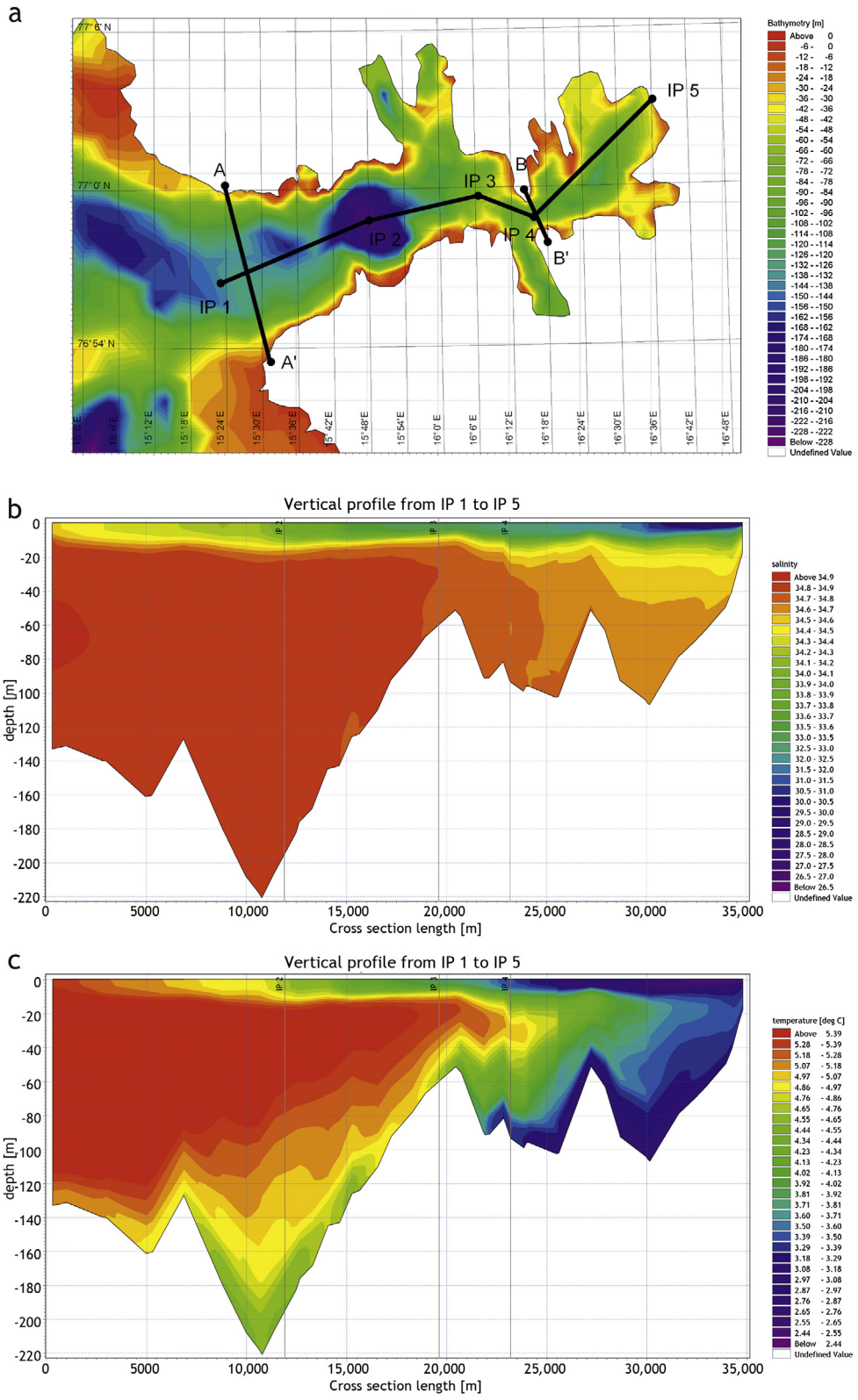

Figure 13 Vertical sections of salinity, temperature and velocity towards the fjord for July; (a) locations of the sections; section IP1-IP2-IP3-IP4-IP5 of salinity (b) and temperature (c); sections A-A′ of salinity (d), temperature (e) and velocity directed towards the fjord (f). Section IP1-IP2-IP3-IP4-IP5 is called along-fjord (HS), sections A-A′ and B-B′ are called cross-sections (VS). Cross-sections are shown with north on the left-hand side (i.e.points A or B from panel a)). Positive velocity on the subplot (f) is directed into the fjord. Sections A-A′ and B-B′ are also presented for discussion in the subsection 'Salt and heat content and its anomaly in the main fjord and Brepollen' and in Fig. 16.

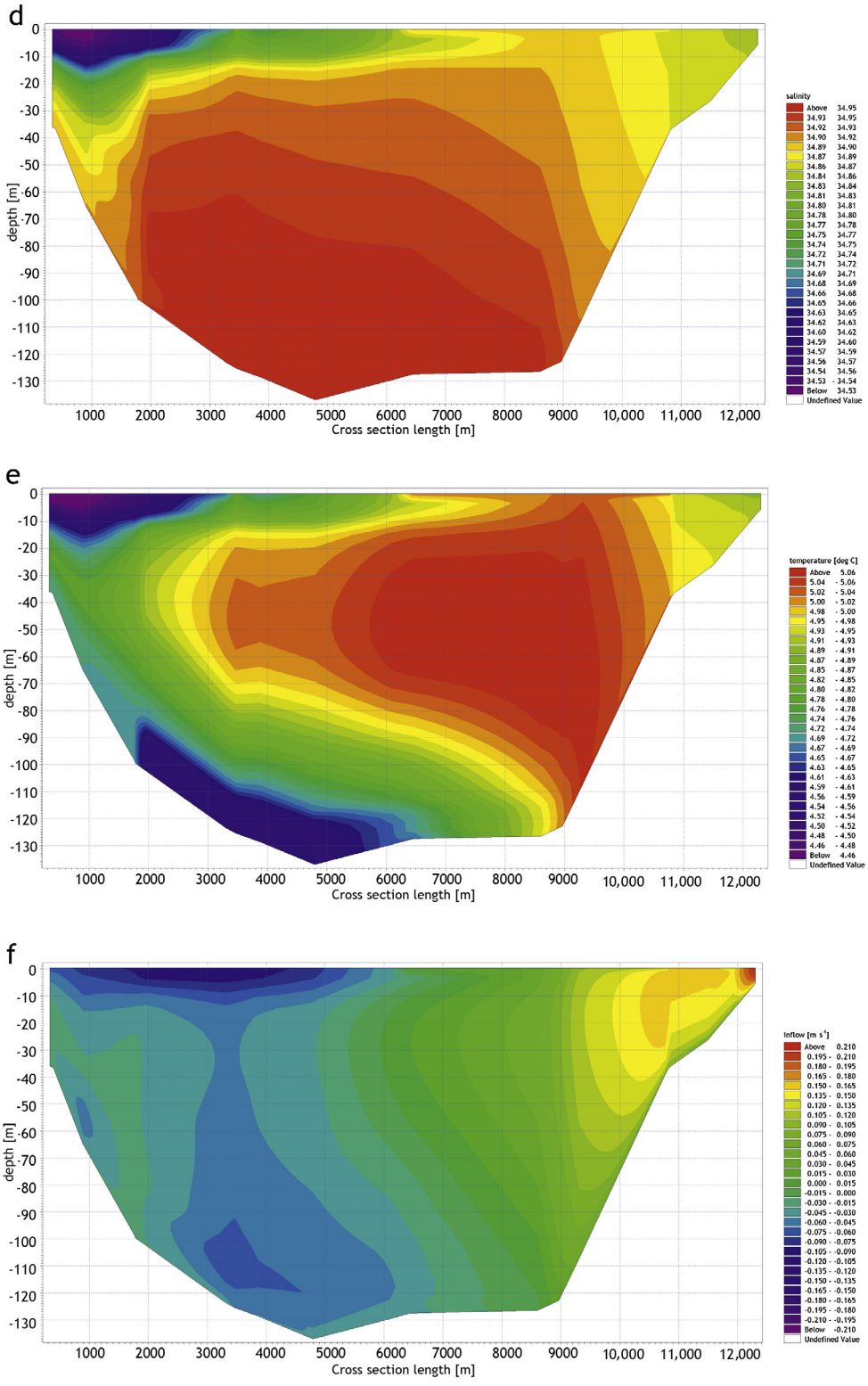

Figure 13. (*Continued*).

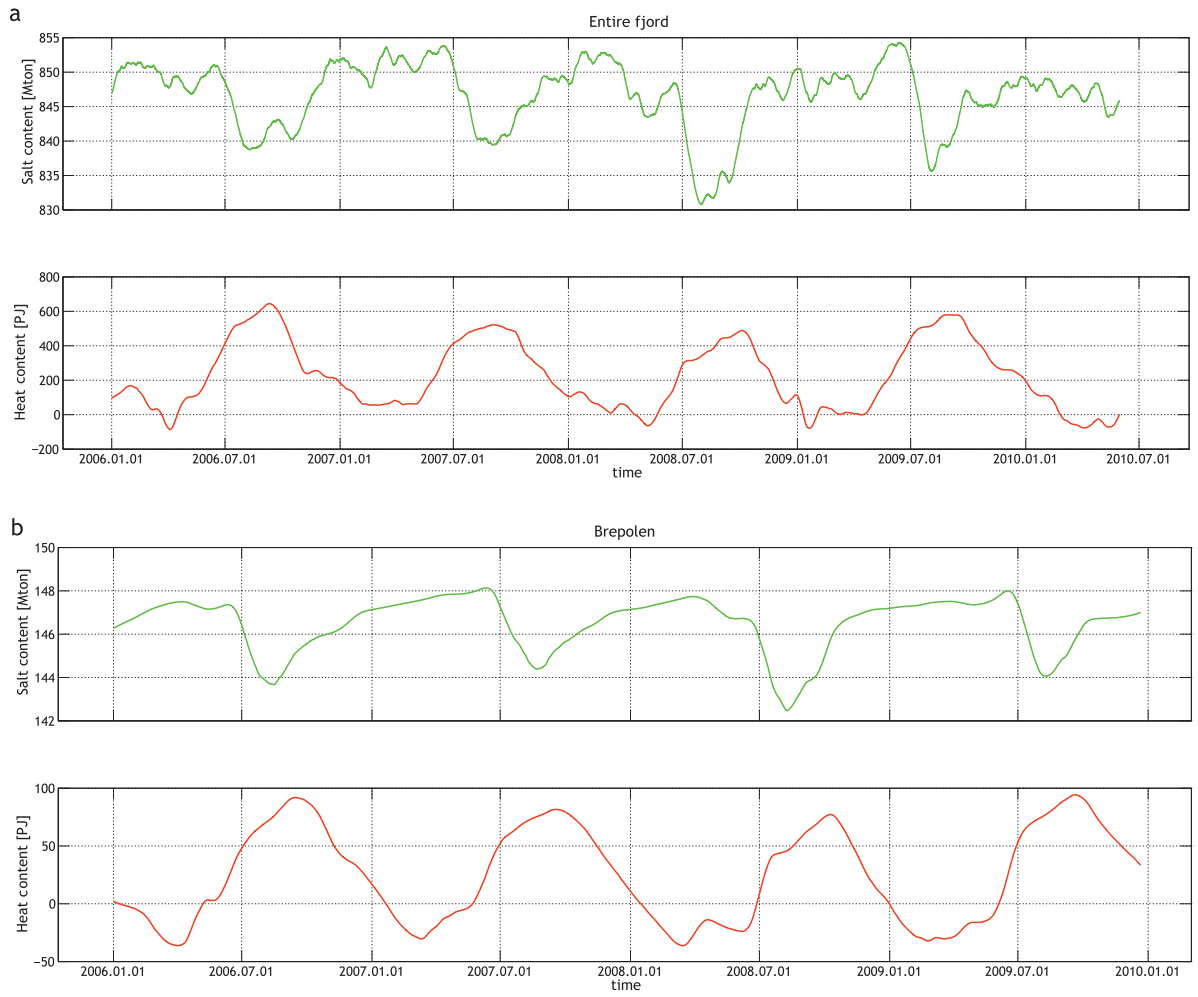

Figure 14 Heat and salt content for the entire fjord (a) and Brepollen (b) for the period 01.01.2006—31.12.2009.

heat content in the whole fjord shows the clearly visible seasonal variability in the heat and salt content of the entire fjord and Brepollen (Fig. 14) (note: the reference temperature for the heat content was taken to be 0.1°C). Moreover, any increase in the salt content during any part of the year, except during periods of decreasing catchment area activity, which begins in mid-July (see Fig. 4c), means that it is mostly under the influence of WSC. Fig. 15 shows the salt content anomaly (SCA) integrated over time. The anomaly was integrated because this process removes all small oscillations. For example, if the anomaly is represented by a simple sine function, through oscillation, the time integrated sine will yield zero in the long-term. On the other hand, it works like a low pass filter. The salt anomaly integrated over time (and its derivative — Eqs. (2) and (3) for the entire fjord provides no evidence that only WSC or only SC (Fig. 15) exert an influence there. However, Fig. 16 shows that the method detects inflows of more saline or fresher water into the fjord or Brepollen, but it is still difficult to say whether Hornsund is under the influence of only one of them.

$$\Theta_A(t) = \int_0^t (\Theta(t') - \overline{\Theta}) dt', \tag{2}$$

$$\Theta'_A(t) = \frac{d\Theta_A}{dt}, \tag{3}$$

where Θ is the tracer, t the time, and $\overline{\theta}$ the time averaged tracer.

Separating the inflows of WSC and SC in Hornsund appears to be impossible. But for Brepollen the anomalies are very stable and there is a strong seasonal variability. The inference is that the circulation is stable but that it can be disturbed by fresh water from the catchment area and glaciers. Consequently, at this time scale, the circulation supplies additional heat and transfers salt from the shelf area into Brepollen and the entire fjord. Furthermore, it transfers additional salt and heat to the main fjord area, but this is small compared to the short time scale of natural variability associated with inflows from the shelf. As shown in Fig. 15, the variability in the

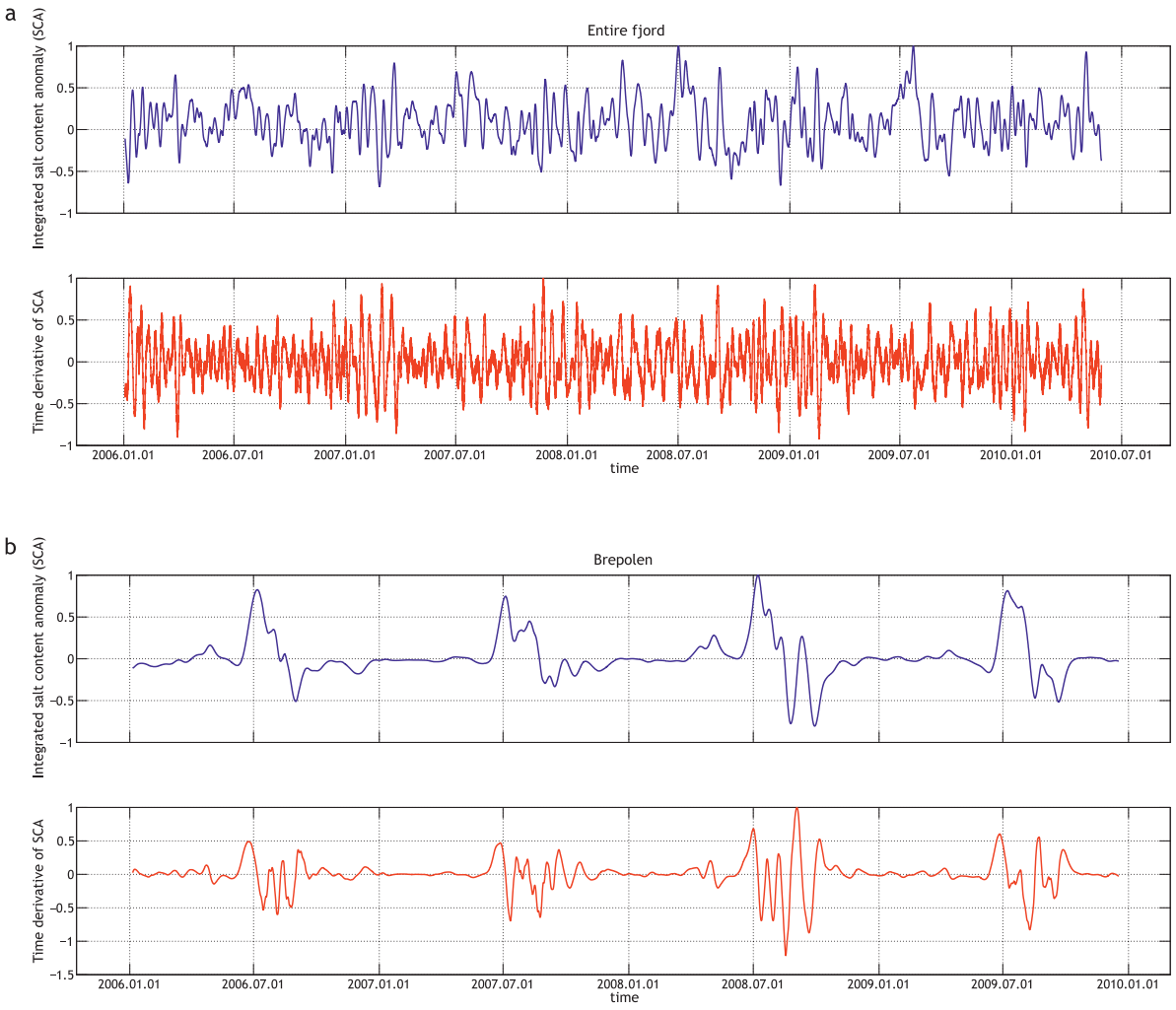

Figure 15 The SCA (over time) and its derivative for the entire fjord (a) and the Brepollen area (b) for the period 01.01.2006–31.12.2009.

salt content is related to inflows of more saline or fresher water into Brepollen. The atmospheric influence on the salt content can be neglected. Precipitation represents a very small amount of the fresh water from the catchment area, and other atmospheric factors are unrelated to the integrated salt content. Other factors that could have some influence on the salt content are underwater glaciers. But as we stated above, we are unable to construct even a simple representation of the glacier, so we should not analyze the influence of heat content. SCA in the Brepollen shows a strong seasonal variability which depends strongly on fresh water discharge. Although the fresh water discharge for every year is identical, the SCAs are different (Fig. 15). As mentioned above, we do not think that atmospheric factors could have a strong influence on this. Only shelf waters consisting of mixed WSC and SC could change the shape of SCA. Fig. 16 shows sections B-B′ (shown in Fig. 13a) on the positive and negative representation of SCA (also for the positive and negative time derivative of SCA). It is clear that increasing (as well as decreasing) SCA is caused by inflows of more saline waters from the main fjord to Brepollen. The time derivative of SCA is more sensitive than SCA and it is much easier to detect inflows of more saline (or fresher) water into Brepollen.

5. Concluding remarks

A hydrodynamic model has been implemented for the west Svalbard fjord Hornsund. HRM reproduces seasonal variability of the fjord properly. Validation of the model shows quite good agreement between the available data and the model results. The general circulation is shown, based on the model integrations. Generally, the fjord circulation can be divided into two regimes, one representing the winter circulation, the other being related to summer and strongly linked to fresh water discharges. Furthermore, the fjord's hydrodynamic front has been documented. Seasonal variability is also presented for the heat and salt content. Analysis of the integrated salt content anomaly suggests that apart from the strong seasonal periodicity driven by shelf waters, rela-

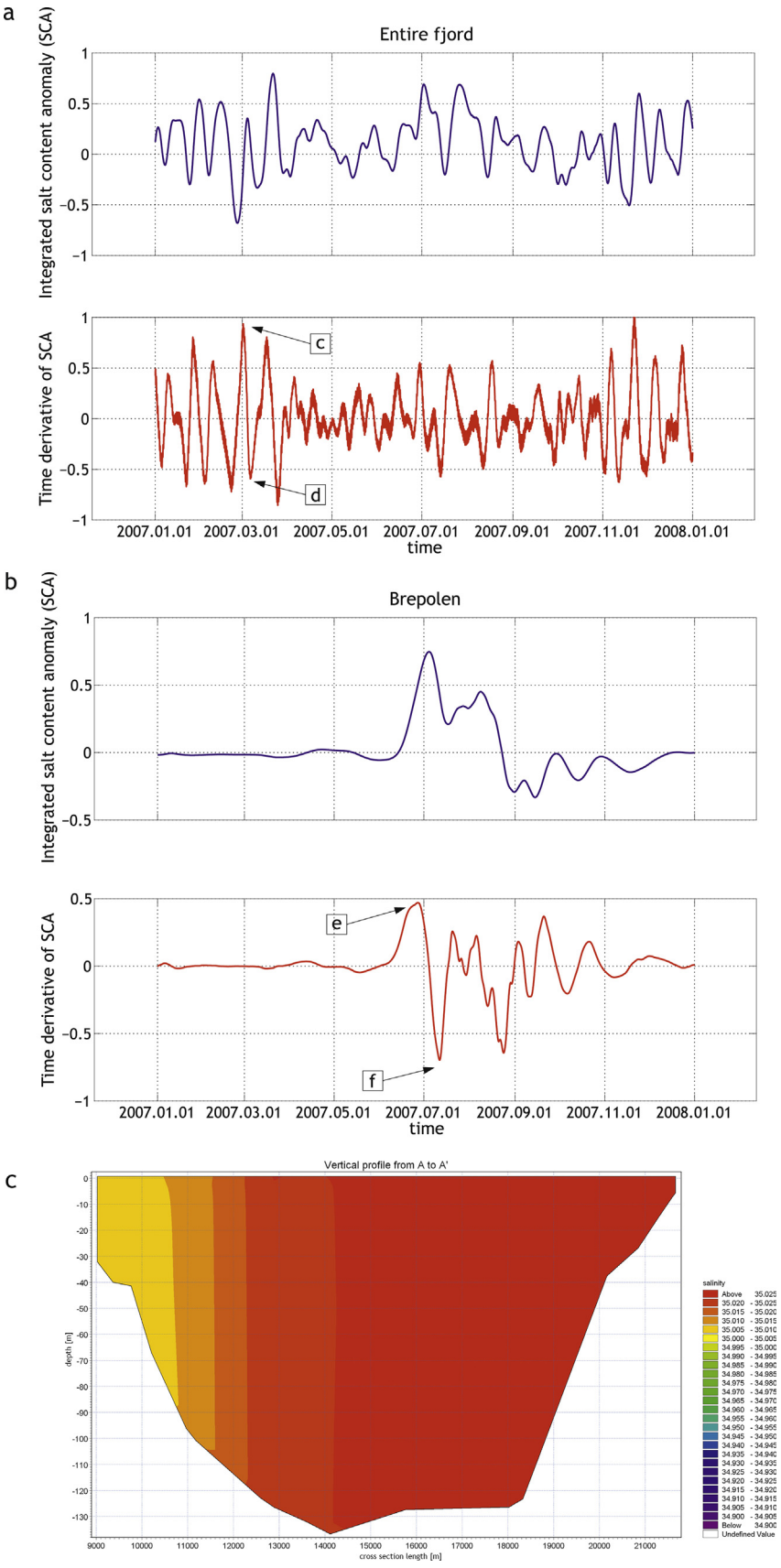

Figure 16 Zoomed, time-integrated salt anomaly for the entire fjord and the Brepollen area, and sections (c, d, e, f) representing the inflows of saline and fresh water (the time location on the chart is also marked on subplots (a) and (b)), sections are marked in Fig. 13a (A-A′ and B-B′). The results are for 2007.

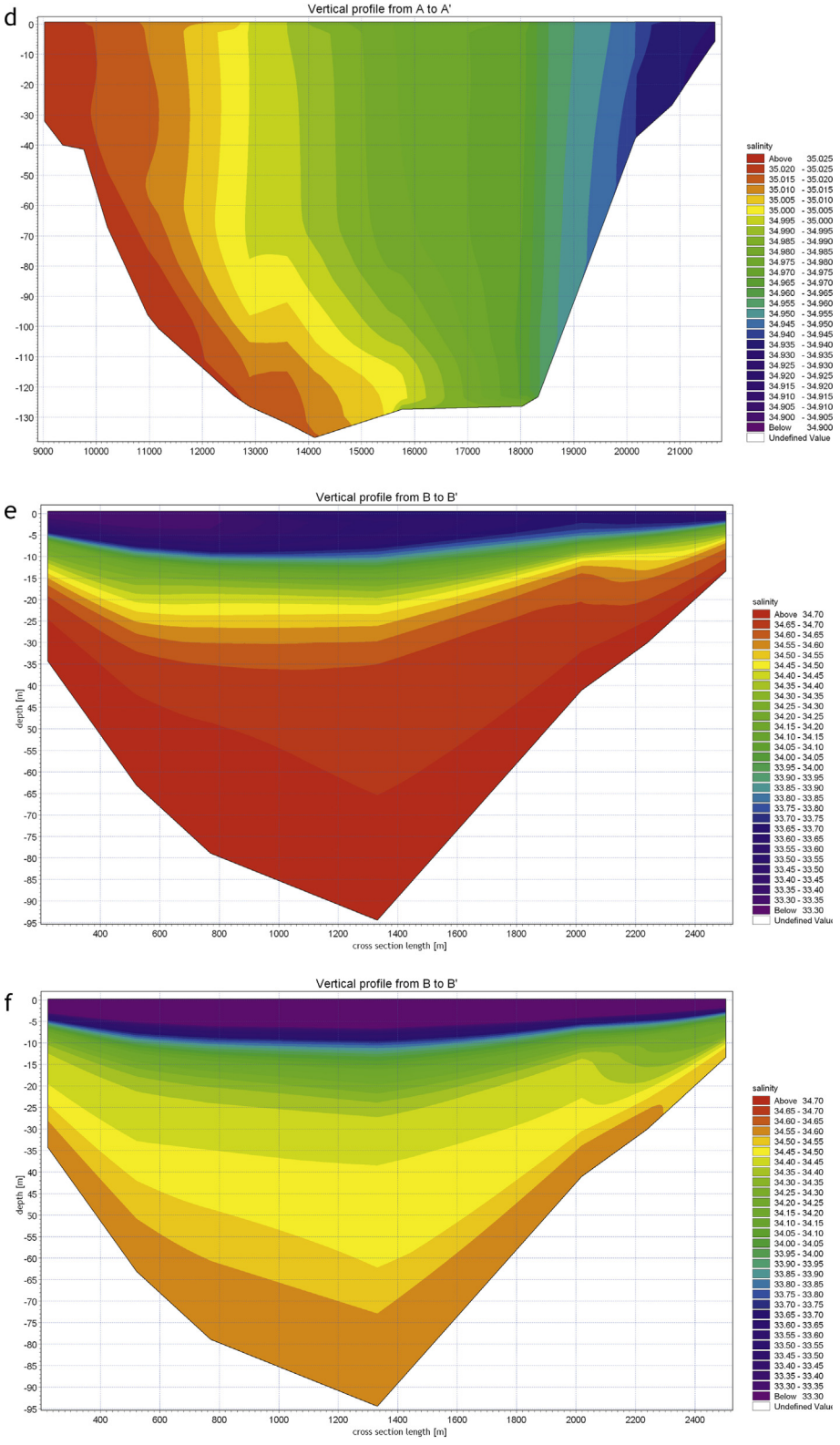

Figure 16. (*Continued*).

tively large amounts of salt and heat are transported into Brepollen when water from the catchment area is carried into the fjord.

The model has also some drawbacks. It does not incorporate any ice model, so it uses only external data. This means there is no fresh water generated during ice melting. The same problem also arises when ice forms. Freezing does not introduce any saline water into the fjord. Ice cover in the model is treated only as a barrier between atmospheric forces and the fjord surface, modifying only momentum and heat fluxes. Furthermore, in an Arctic fjord it is important to include underwater glaciers. But DHI does not provide any module that could help create such glacier walls in the model. The inclusion of these processes would probably decrease heat content in the fjord and would increase salt content. We think that it could also have some influence on the general circulation of the fjord as well as on the shape, salinity and temperature gradient in the hydrological front.

We are planning to include in our future work underwater glaciers (in the first step in basic form as an underwater wall that has no salinity or freezing temperature). After that we intend to investigate the hydrological front more deeply, include more realistic winds (data from ECMWF are close to the geostrophic wind, but the main wind in the Hornsund area approximates a sea breeze) and analyze the influence of factors affecting climate change.

Acknowledgements

We are very grateful to Prof. Andrzej Jankowski for his advice and the helpful, stimulating discussion.

The project was co-financed from the funds of the Leading National Research Centre (KNOW) received by the Centre for Polar Studies for the period 2014—2018.

This work was also partially carried out within the framework of projects GAME (DEC-2012/04/A/NZ8/00661) and AWAKE2 (Pol-Nor/198675/17/2013).

Data from the A4 and S800 models were made available through the Fram Centre 'Arctic Ocean' flagship project 'ModOIE'.

References

Albretsen, J., Hattermann, T., Sundfjord, A., 2017. Ocean and sea ice circulation model results from Svalbard area (ROMS) [Data set]. Norwegian Polar Institute, http://dx.doi.org/10.21334/npolar.2017.2f52acd2.

Błaszczyk, M., Jania, J., Kolondra, L., 2013. Fluctuations of tidewater glaciers in Hornsund Fjord (Southern Svalbard) since the beginning of the 20th century. Pol. Polar Res. 34 (4), 327—352, http://dx.doi.org/10.2478/popore-2013-0024.

Budgell, W.P., 2005. Numerical simulation of ice-ocean variability in the Barents Sea region: towards dynamical downscaling. Ocean Dynam. 55 (3), 370—387, http://dx.doi.org/10.1007/s10236-005-0008-3.

Chassignet, E.H., Hurlburt, H.E., Smedstad, O.M., Halliwell, G.R., Hogan, P.J., Wallcraft, A.P., Bleck, R., 2006. Ocean prediction with the hybrid coordinate ocean model (HYCOM). In: Chassignet, E.P., Verron, J. (Eds.), Ocean Weather Forecasting. Springer, Dordrecht, 577 pp., http://dx.doi.org/10.1007/1-4020-4028-8.

Cottier, F.R., Nilsen, F., Skogseth, R., Tverberg, V., Skarthhamar, J., Svendsen, H., 2010. Arctic fjords: a review of the oceanographic environment and dominant physical processes. Geol. Soc. London, Spec. Publ. 344 (1), 35—50, http://dx.doi.org/10.1144/SP344.4.

Cottier, F., Tverberg, V., Inall, M., Svendsen, H., Nilsen, F., Griffiths, C., 2005. Water mass modification in an arctic fjord through cross-shelf exchange: the seasonal hydrography of kongsfjorden, Svalbard. J. Geophys. Res. 110 (C12), 18 pp., http://dx.doi.org/10.1029/2004JC002757.

Counillon, F., Sakov, P., Bertino, L., 2010. Development of TOPAZ4 prototype. In: EGU General Assembly Conference Abstracts.

Dee, D.P., Uppala, S.M., Simmons, A.J., Berrisford, P., Poli, P., Kobayashi, S., Andrae, U., Balmaseda, M.A., Balsamo, G., Bauer, P., Bechtold, P., Beljaars, A.C.M., van de Berg, L., Bidlot, J., Bormann, N., Delsol, C., Dragani, R., Fuentes, M., Geer, A.J., Haimberger, L., Healy, S.B., Hersbach, H., Hólm, E.V., Isaksen, L., Kållberg, P., Köhler, M., Matricardi, M., McNally, A.P., Monge-Sanz, B.M., Morcrette, J.J., Park, B.K., Peubey, C., de Rosnay, P., Tavolato, C., Thépaut, J.N., Vitart, F., 2011. The ERA-Interim reanalysis: configuration and performance of the data assimilation system. Quarter. J. R. Meteorol. Soc. 137 (656), 553—597, http://dx.doi.org/10.1002/qj.828.

Egbert, G.D., Erofeeva, S.Y., 2002. Efficient inverse modeling of barotropic ocean tides. J. Atmos. Ocean. Technol. 19, 183—204, http://dx.doi.org/10.1175/1520-0426(2002)019<0183:EIMOBO>2.0.CO;2.

Fedorov, K.N., 1986. The Physical Nature and Structure of Oceanic Fronts. Springer-Verlag, New York, 333 pp.

Flather, R.A., 1976. A tidal model of the northwest European continental shelf. Mem. Soc. Roy. Sci. Liege 6 (10), 141—164.

Frankowski, M., Zioła-Frankowska, A., 2014. Analysis of labile form of aluminum and heavy metals in bottomsediments from Kongsfjord, Isfjord, Hornsund fjords. Environ. Earth Sci. 71 (3), 1147—1218, http://dx.doi.org/10.1007/s12665-013-2518-5.

Ginzburg, A.I., Kostianoy, A.G., 2009. Front and mixing processes. Oceanography 1, 7 pp.

Gluchowska, M., Kwasniewski, S., Prominska, A., Olszewska, A., Goszczko, I., Falk-Petersen, S., Hop, H., Weslawski, J.M., 2016. Zooplankton in Svalbard fjords on the Atlantic-Arctic boundary. Polar Biol. 39 (10), 1—18, http://dx.doi.org/10.1007/s00300-016-1991-1.

Haidvogel, D.B., Arango, H., Budgell, W.P., Cornuelle, B.D., Curchitser, E., Di Lorenzo, E., Fennel, K., Geyer, W.R., Hermann, A.J., Lanerolle, L., Levin, J., McWilliams, J.C., Miller, A.J., Moore, A. M., Powell, T.M., Shchepetkin, A.F., Sherwood, C.R., Signell, R.P., Warner, J.C., Wilkin, J., 2008. Ocean forecasting in terrain-following coordinates: formulation and skill assessment of the Regional Ocean Modeling System. J. Comp. Phys. 222 (7), 3595—3624, http://dx.doi.org/10.1016/j.jcp.2007.06.016.

Hattermann, T., Isachsen, P.E., von Appen, W.-J., Albretsen, J., Sundfjord, A., 2016. Eddy-driven recirculation of Atlantic Water in Fram Strait. Geophys. Res. Lett. 43 (7), 3406—3414, http://dx.doi.org/10.1002/2016GL068323.

Jeżowiecka-Kabsch, K., Szewczyk, H., 2001. Mechanika płynów. Oficyna Wyd. Politech. Wroc., Wrocław, 386 pp.

Kantha, L.H., Clayson, C.A., 2000. Numerical Models of Oceans and Oceanic Processes. Acad. Press, San Diego, 750 pp.

Kowalik, Z., Marchenko, A., Brazhnikov, D., Marchenko, N., 2015. Tidal currents in the western Svalbard Fjords. Oceanologia 57 (4), 318—332, http://dx.doi.org/10.1016/j.oceano.2015.06.003.

Lien, V.S., Vikebø, F.B., Skagseth, Ø., 2013. One mechanism contributing to co-variability of the Atlantic inflow branches to the Arctic. Nat. Commun., http://dx.doi.org/10.1038/ncomms2505 Art No. 1488.

MIKE_DHI, 2014. MIKE 21 Toolbox. Global Tide Model — Tidal Prediction. DHI, Hørsholm, 20 pp.

MIKE and Doc. 2010—2014. MIKE 21 & MIKE 3 Flow Model FM. Hydrodynamic Module, Sci. Doc., DHI, Hørsholm, 14 pp.

Nilsen, F., Cottier, F., Skogseth, R., Mattsson, S., 2008. Fjord—shelf exchange controlled by ice and brine production: the interannual

variation of Atlantic Water in Isfjorden, Svalbard. Cont. Shelf Res. 28 (14), 1838—1853, http://dx.doi.org/10.1016/j.csr.2008.04.015.

Sakov, P., Counillon, F., Bertino, L., Lisæter, K.A., Oke, P.R., Korablev, A., 2012. TOPAZ4: an ocean-sea ice data assimilation system for the North Atlantic and Arctic. Ocean Sci. 8 (4), 633—656, http://dx.doi.org/10.5194/os-8-633-2012.

Shchepetkin, A.F., McWilliams, J.C., 2009. Correction and commentary for "Ocean forecasting in terrain-following coordinates: formulation and skill assessment of the regional ocean modeling system" by Haidvogel et al. J. Comp. Phys. 228 (24), 8985—9000, http://dx.doi.org/10.1016/j.jcp.2009.09.002.

Węsławski, J.M., Koszteyn, J., Zajaczkowski, M., 1995. Fresh water in Svalbard fjord ecosystems. In: Skjodal, H.R., Hopking, C., Erikstad, K.E., Leinaa, H.P. (Eds.), Ecology of Fjords and Coastal Waters. Elsevier, Amsterdam, 229—241.

Walczowski, W., 2007. Warm anomalies propagation in the west spistbergen current. Probl. Klimatol. Polar. 17, 71—76, (in Polish with English summary).

Walczowski, W., 2013. Frontal structures in the West Spitsbergen Current margins. Ocean Sci. 9 (6), 957—975, http://dx.doi.org/10.5194/os-9-957-2013.

Oceanologia (2017) 59, 496–507

Available online at www.sciencedirect.com

ScienceDirect

journal homepage: www.journals.elsevier.com/oceanologia/

ORIGINAL RESEARCH ARTICLE

Comparison of bacterial production in the water column between two Arctic fjords, Hornsund and Kongsfjorden (West Spitsbergen)

Anetta Ameryk [a], **Katarzyna M. Jankowska** [b,*], **Agnieszka Kalinowska** [b], **Jan M. Węsławski** [c]

[a] *National Marine Fisheries Research Institute, Gdynia, Poland*
[b] *Gdańsk University of Technology, Gdańsk, Poland*
[c] *Institute of Oceanology, Polish Academy of Sciences, Sopot, Poland*

Received 15 August 2016; accepted 10 June 2017
Available online 1 July 2017

KEYWORDS
Bacterial production;
Arctic fjords;
Spitsbergen;
Hornsund;
Kongsfjorden

Summary Bacterial production and the accompanying environmental factors were measured in the water columns of two Arctic fjords during the cruise in July and August 2013. Water samples were collected at six stations located in the central part of Hornsund and Kongsfjorden. In Hornsund, where average water temperatures were 1.25-fold lower than in Kongsfjorden, the bacterial production was twice as high (0.116 ± 0.102 vs 0.05 ± 0.03 mg C m^{-3} h^{-1}). Statistical analysis indicated that chlorophyll *a* concentration itself was not a significant factor that affected bacterial production, in contrast to its decomposition product, pheophytin, originating from senescent algal cells or herbivorous activity of zooplankton. Single and multiple regression analysis revealed that water temperature, dissolved organic carbon (DOC), and pheophytin concentration were the main factors affecting bacterial production in both fjords.

* Corresponding author at: Gdańsk University of Technology, Narutowicza 11/12 Street 80-233 Gdańsk, Poland. Fax: +58 347 20 44.
E-mail addresses: aameryk@mir.gdynia.pl (A. Ameryk), kjank@pg.gda.pl (K.M. Jankowska), agnieszka.kalinowska@poczta.onet.pl (A. Kalinowska), weslaw@iopan.gda.pl (J.M. Węsławski).
Peer review under the responsibility of Institute of Oceanology of the Polish Academy of Sciences.

Production and hosting by Elsevier

http://dx.doi.org/10.1016/j.oceano.2017.06.001

1. Introduction

Polar regions are extremely important research fields because of their unique vulnerability to climate change. One of the already visible and predicted signs of global warming is intensive retreat of glaciers. Due to glacial meltwater inflow, and therefore particulate matter (Urbański et al., 2017) and freshwater introduction, changes were observed in the microbial community composition in the Arctic fjords (Piquet et al., 2010, 2016).

Fjords of Hornsund (located on the south-west coast of Spitsbergen, Fig. 1) and Kongsfjorden (located on the north-west coast of Spitsbergen) were selected as sites where monitoring of the implications of climate change is possible (Warwick et al., 2003) due to their location in the area of increasing air temperature as well as inflow of Atlantic Waters (AW) (Serreze et al., 2000; Walczowski and Piechura, 2006, 2007, 2011; Walczowski et al., 2012). Kongsfjorden remains under strong influence of warm and saline West Spitsbergen Current. It follows the deeper part of the Fram Strait, and often enters the fjord, causing warming of its environment (Cottier et al., 2005; Svendsen et al., 2002). The South West coast of Spitsbergen is more affected by coastal Arctic waters from the Barents Sea which are less saline (Skagseth et al., 2008). This so called Sørkapp Current has great influence on the Hornsund Fjord (Cottier et al., 2005; Swerpel, 1985).

Research carried out in recent years in the polar regions shows that low temperature is not a limiting factor of bacterial activity (Kirchman et al., 2005; Rivkin et al., 1996). Many authors highlight the need to combine conventional techniques of determining bacterial production (based on the incorporation of ^{3}H-thymidine or ^{3}H-leucine) (Fuhrman and Azam, 1982; Kirchman et al., 1985; Simon and Azam, 1989) with single-cell analysis to identify the capability for assimilation of dissolved organic matter (DOM) by individual groups of bacteria (Elifantz et al., 2007).

The total abundance, biomass, and morphological structure of bacterioplankton can be evaluated by means of the direct cell counting technique, without the need of bacteria cultivation (Amann et al., 1995). In recent years, intensive development of non-cultivating techniques has contributed significantly to the expansion of knowledge on microbial diversity and community composition in the environment (Piquet et al., 2010, 2016; Zengler, 2009).

Although Kongsfjorden BP data are available for several seasons and years (Engel et al., 2013; Iversen and Seuthe, 2011; Motegi et al., 2013; Piquet et al., 2016; Wängberg et al., 2008), no information is to date available on BP in Hornsund. Experiments regarding the impact of climate change on microorganisms also were conducted in Isfjorden, under the influence of the Atlantic Waters (Lara et al., 2013).

Despite this multi-annual overview on the functioning of West Spitsbergen fjords, the details of microbial processes are still not fully understood. An interdisciplinary approach, combining hydrology, chemical composition of glacial and surface runoff, as well as and metagenomic data, is necessary to establish the scale of impact of biotic and abiotic factors

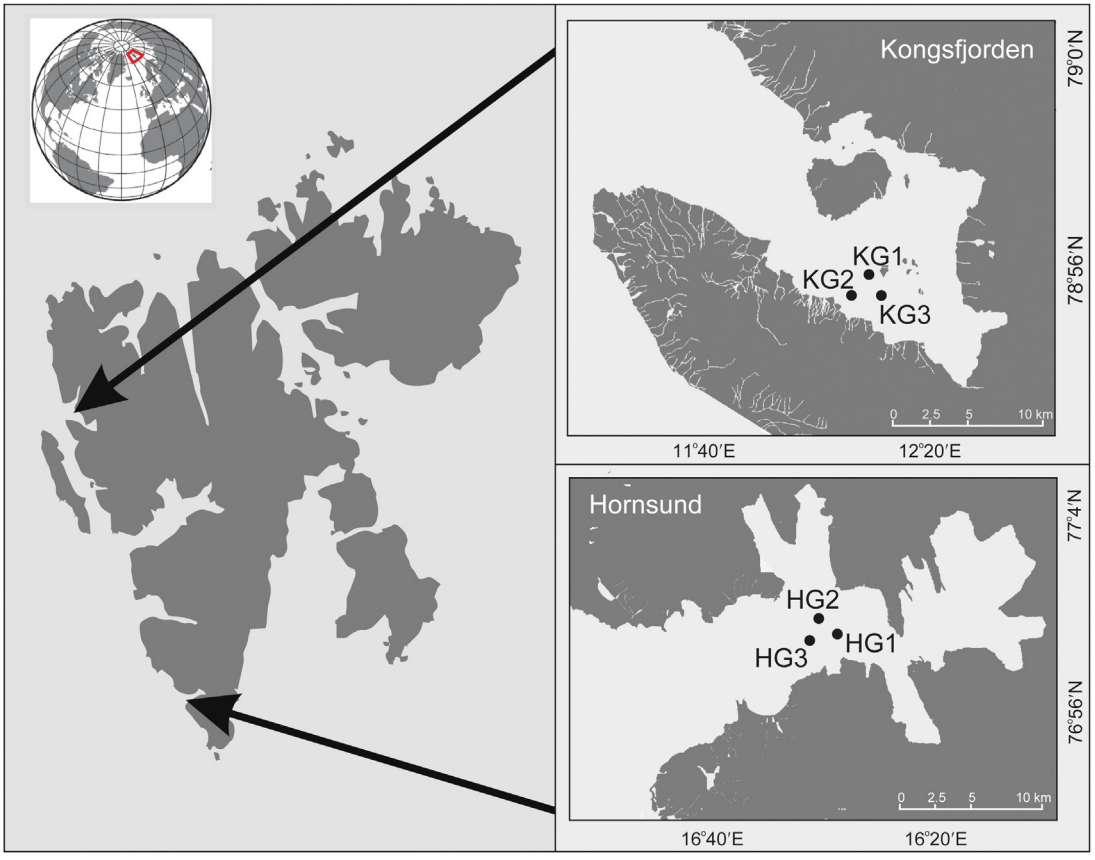

Figure 1 Maps of sampling points (GAME data).

on microbial life in marine ecosystems. Therefore, the primary objective of the study was to compare bacterial production in two Arctic fjords, and to determine the factors influencing it.

2. Material and methods

2.1. Study area and sampling

Marine water was sampled in the scope of GAME project on 29–30.07.2013 in Hornsund, and on 7–9.08.2013 in Kongsfjorden during a cruise of *r/v Oceania* (Institute of Oceanology, Polish Academy of Sciences). Samples were taken at three stations in each of the two fjords, HG1, HG2, and HG3 in Hornsund, and KG1, KG2, and KG3 in Kongsfjorden (Fig. 1). Separate samples were collected for measurements of bacterial production (BP) and determination of total bacterial number (TBN), biomass (BBM), average cell volume (ACV), and morphological form (MF).

Samples for the determination of bacterial production were collected at 4–5 depths in the water column: surface, 10 m, 25 m, 75 m (HG1 at 50 m instead of 75 m), and bottom in Hornsund; surface (0 m), 10 m, 15 m, 35 m, 75 m, and bottom in Kongsfjorden. Total bacterial number, biomass, and cell volume were determined in samples from 5 to 8 depths (see Tables 1 and 2). Surface water samples were collected by means of a bucket, and the others by Niskin bottles.

2.2. Bacterial production

For all the samples, four 10 ml subsamples were prepared: triplicates and one blank. To avoid any bacterial growth in the blank, 100 μl of 36% formaldehyde was added immediately after sampling. 200 μl leucine was then added to the samples (final solution of 20 nM). 100 nM leucine was added to the bottom water sample. Leucine reagent was a mixture of ^{3}H-leucine (SA = 54.1 Ci mmol^{-1}) and L-leucine in ratio 1:9. Incubation held in in situ temperature (range between 1.7 and 5.4°C) lasted for 3 h. To finish the incubation, 100 μl of formaldehyde was added to samples. Samples were filtered through 0.2 μm nitrocellulose filters. Prior to filtration, chimneys were cooled in the freezer. Filters were rinsed with 10× 1 ml of cold (0°C) trichloroacetic acid and 10× 1 ml of 80% ethanol. They were stored in scintillation vials, dried, and frozen at −20°C until further processing. Unfrozen filters were dissolved in 0.5 ml ethyl acetate, and 6 ml of scintillation cocktail was added to the vials. Well mixed samples were counted on a scintillation counter Beckmann LS 6000IC twice: after one and after four days after the addition of the scintillation cocktail.

Table 1 Values of all measured bacterial parameters in the waters of Hornsund (total bacterial number (TBN) and bacterial biomass (BBM) already published by Kalinowska et al., 2015).

	Depth	BP [mg C m^{-3} h^{-1}]	ACV [μm^3]	MF [%]			TBN [10^5 cells cm^{-3}]	BBM [mg C m^{-3}]
				R	C	O		
HG1	0 m	0.319	0.27	48	49	3	3.46	14.73
	5 m	n.d.	0.07	75	19	6	4.11	8.06
	10 m	0.123	0.10	68	27	5	3.16	7.28
	15 m	n.d.	0.04	67	30	3	2.15	3.15
	25 m	0.160	0.27	36	63	1	2.94	12.09
	35 m	n.d.	0.02	73	26	1	2.23	2.20
	50 m	0.032	n.d.	n.d.	n.d.	n.d.	n.d.	n.d.
	75 m	n.d.	0.03	70	29	1	1.71	2.08
	Bottom (77 m)	0.085	n.d.	n.d.	n.d.	n.d.	n.d.	n.d.
HG2	0 m	0.330	0.16	60	34	6	3.94	12.06
	5 m	n.d.	0.04	68	25	7	2.14	2.99
	10 m	0.051	0.33	44	52	4	3.21	14.01
	15 m	n.d.	0.16	43	53	4	2.55	7.96
	25 m	0.127	0.31	38	58	4	3.62	16.14
	35 m	n.d.	0.12	47	49	4	3.19	8.24
	75 m	0.023	0.27	41	55	4	3.56	14.62
	Bottom (103 m)	0.022	0.10	48	49	3	2.11	4.85
HG3	0 m	0.118	0.26	46	50	4	2.36	9.74
	5 m	n.d.	n.d.	n.d.	n.d.	n.d.	n.d.	n.d.
	10 m	0.037	0.24	52	44	4	3.03	11.83
	15 m	n.d.	n.d.	n.d.	n.d.	n.d.	n.d.	n.d.
	25 m	0.215	0.22	52	44	4	3.29	12.33
	35 m	n.d.	0.07	64	30	6	3.36	6.48
	75 m	0.027	0.20	47	50	3	3.62	12.73
	Bottom (105 m)	0.065	0.25	42	56	2	2.60	10.17

HG1, HG2, HG3 name of stations in Hornsund; BP, bacterial production; ACV, average cell volume; MF, morphological form; R, rods; C, cocci; O, others; n.d., not determined.

Table 2 Values of all measured bacterial parameters in the waters of Kongsfjorden (total bacterial number (TBN) and bacterial biomass (BBM) already published by Kalinowska et al., 2015).

	Depth	BP [mg C m^{-3} h^{-1}]	ACV [μm^3]	MF [%]			TBN [10^5 cells cm^{-3}]	BBM [mg C m^{-3}]
				R	C	O		
KG1	0 m	0.055	0.31	42	37	21	1.55	7.72
	5 m	n.d.	0.29	49	42	9	1.67	6.75
	10 m	0.030	0.21	42	50	8	1.55	5.76
	15 m	0.048	0.30	31	66	3	1.84	8.16
	25 m	n.d.	0.07	63	32	5	1.09	2.02
	35 m	0.015	0.03	76	21	3	1.16	1.36
	75 m	0.012	0.05	66	29	5	1.55	2.30
	Bottom (105 m)	0.015	0.23	38	60	2	2.02	7.66
KG2	0 m	0.041	0.21	50	44	6	1.21	4.49
	5 m	n.d.	n.d.	n.d.	n.d.	n.d.	n.d.	n.d.
	10 m	0.047	0.18	47	48	5	2.70	8.87
	15 m	0.141	0.15	51	46	3	4.25	12.42
	25 m	n.d.	n.d.	n.d.	n.d.	n.d.	n.d.	n.d.
	35 m	0.039	0.14	47	50	3	1.76	4.83
	75 m	0.013	0.10	53	44	3	1.53	3.50
	Bottom (118 m)	0.117	n.d.	n.d.	n.d.	n.d.	n.d.	n.d.
KG3	0 m	0.052	0.20	48	41	11	1.86	6.79
	5 m	n.d.	n.d.	n.d.	n.d.	n.d.	n.d.	n.d.
	10 m	0.106	0.45	17	81	2	1.52	8.47
	15 m	0.082	0.16	44	52	4	1.81	5.53
	25 m	n.d.	n.d.	n.d.	n.d.	n.d.	n.d.	n.d.
	35 m	0.021	0.34	28	64	8	1.77	8.13
	75 m	0.012	0.16	30	68	2	1.81	5.53
	Bottom (96 m)	0.060	n.d.	n.d.	n.d.	n.d.	n.d.	n.d.

KG1, KG2, KG3 name of stations in Kongsfjorden; BP, bacterial production; ACV, average cell volume; MF, morphological form; R, rods; C, cocci; O, others; n.d., not determined.

Due to the lack of access to the scintillation counter during the cruise, the concentration of leucine applied in the study was chosen based on literature data. In order to verify the value of the concentration, a saturation curve was prepared. Water samples used for that purpose were from 10 m, HG1 station. Several leucine concentrations were added to the consecutive sub-samples: 2.5 nM, 5 nM, 10 nM, 20 nM, 40 nM, and 80 nM. The water saturation curve shows that 20 nM was the appropriate concentration of leucine. 3.1 kg C mol Leu^{-1} conversion factor (Kirchman, 1992) was applied.

2.3. Total bacterial number, biomass, average cell number, and morphological structure

Water samples were fixed immediately after collection with particle-free formaldehyde solution to a final concentration of 2%. The samples were kept at +4°C until further analyses. The DAPI (4′,6-diamidino-2-phenylindole) direct count method (Porter and Feig, 1980) was used for microscopic analysis: the samples were stained for 10–15 min with DAPI solution to a final concentration of 1 $\mu g\ ml^{-1}$ and filtered on 25 mm polycarbonate filters (Millipore, 0.2 μm pore diameter).

Microscopic slides were observed under an epifluorescence microscope Nikon Eclipse 80i under 1000-fold magnification (HBO-103W high pressure mercury burner, 330–380 nm excitation filter, 420 nm barrier filter, and 400 nm dichroic mirror). A PC coupled with high resolution CCD digital camera Nikon DS-5 Mc-U2 and MultiScan v.14.02 counting program with the modification of Świątecki (1997) were used for the image analysis.

Total bacterial number, biomass, average cell volume, and morphological structure were obtained based on the mean value from 2 series of photos (10 fields each). Bacterial cells were classified to three morphological types: cocci, rods, and others (vibrio). Total bacterial number and biomass were calculated after Norland (1993), as presented in Kalinowska et al. (2015).

2.4. Additional analyses

Analyses of chlorophyll *a*, pheophytin, nutrients, and dissolved organic and inorganic carbon (DOC and DIC) concentrations were also performed in the scope of the GAME project. The detailed methodology was described by Wiktor et al. (2017) and Zaborska et al. (2016). Salinity and water temperature were measured by means of a CTD probe SEA-BIRD SBE 49.

For statistical calculations, the majority of the data, apart from temperature and salinity, were converted by a natural logarithm. DIC values were transformed by an exponential function: *e* to the power *x*. For the comparison of the mean values between the fjords Student's *t*-test was applied.

3. Results

Bacterial production values determined in Hornsund were higher than in Kongsfjorden. In Hornsund, bacterial production ranged from 0.022 to 0.33 mg C m^{-3} h^{-1}, whereas in Kongsfjorden BP varied from only 0.012 to 0.141 mg C m^{-3} h^{-1}, and averaged 2× higher (av. = 0.116 ± SD 0.102 mg C m^{-3} h^{-1} in Hornsund vs. 0.050 ± 0.038 mg C m^{-3} h^{-1} in Kongsfjorden). The coefficient variation (CV = SD/Av) in Hornsund exceeded 88%. This suggests a larger fluctuation in bacterial production than in the Kongsfjorden, where CV is 76.4%.

Depth profiles of bacterial production in the water column show two maxima in Hornsund: at the surface and at a depth of 25 m, and at 10—15 m in Kongsfjorden (Fig. 2a, Tables 1 and 2). These depths correspond to fluorescence maxima and location of the thermocline. Bacterial production decreased to the minimum at a depth of 50—75 m. In the bottom layer, bacterial production usually slightly increased. The values corresponding to the surface water layer on stations HG1 and HG2 clearly diverged from the remaining data, as seen in detail in Fig. 2a. Student's *t*-test results showed a statistically significant difference between bacterial production in both fjords (Fig. 3). Despite the observed difference between the fjords in terms of bacterial abundance (Kalinowska et al., 2015), no correlation was found between the abundance and average cell volume.

Temperature ranged from 1.63 to 5.43°C, av. 2.90 ± 1.02°C in the colder Hornsund Fjord. In the warmer Kongsfjorden, it varied from 1.78 to 5.48°C, av. 3.63 ± 0.88°C. CV in Hornsund was higher (35.2%) than in Kongsfjorden (24.1%), again showing a higher fluctuation of the parameter in the colder fjord. Temperature was rising with depth, reaching its maximum at approximately 25 m in Hornsund, and at approximately 20 m in Kongsfjorden, and then dropping till the bottom (Fig. 2b).

Salinity ranged from 30.17 to 31.02 (av. 33.8 ± 1.33 SD) in Hornsund, and from 34.79 to 34.86 (av. 34.2 ± 0.91) in the more saline Kongsfjorden. The coefficient variation was low, and showed no considerable difference between the fjords, amounting to 3.94% in the southern fjord, and 2.66% in the northern one. Salinity was constantly increasing with depth in the water column (Fig. 2c).

Detailed values of chlorophyll *a*, pheophytin, DIC, DOC, and nutrients are published in Zaborska et al. (2016) and Wiktor et al. (2017).

The analysis of single regression equations of bacterial production with other parameters (Table 3) showed that BP variability was accounted for to the greatest extent by the concentration of pheophytin and dissolved organic carbon, whether each fjord was considered separately or together. Pheophytin, which is a product of chlorophyll decay, accounted for 47% of bacterial production variability in Hornsund, 52% in Kongsfjorden, and 56% for samples from both fjords combined (Fig. 4). No significant differences were observed between the fjords in terms of average pheophytin concentrations, but the highest values of bacterial production in the surface layer at HG1 and HG2 stations correspond to very high pheophytin concentrations.

Chlorophyll *a*, indicating the presence of living phytoplankton, accounted for only 20% of bacterial production variation. The strong correlation of BP and DIC (R^2 = 0.52 for Hornsund; R^2 = 0.33 for Kongsfjorden; and R^2 = 0.45 for all the data) is inversely proportional (Fig. 5). At the same time, differences in the average concentrations of DIC between the fjords were not statistically significant (Table 3). Dissolved

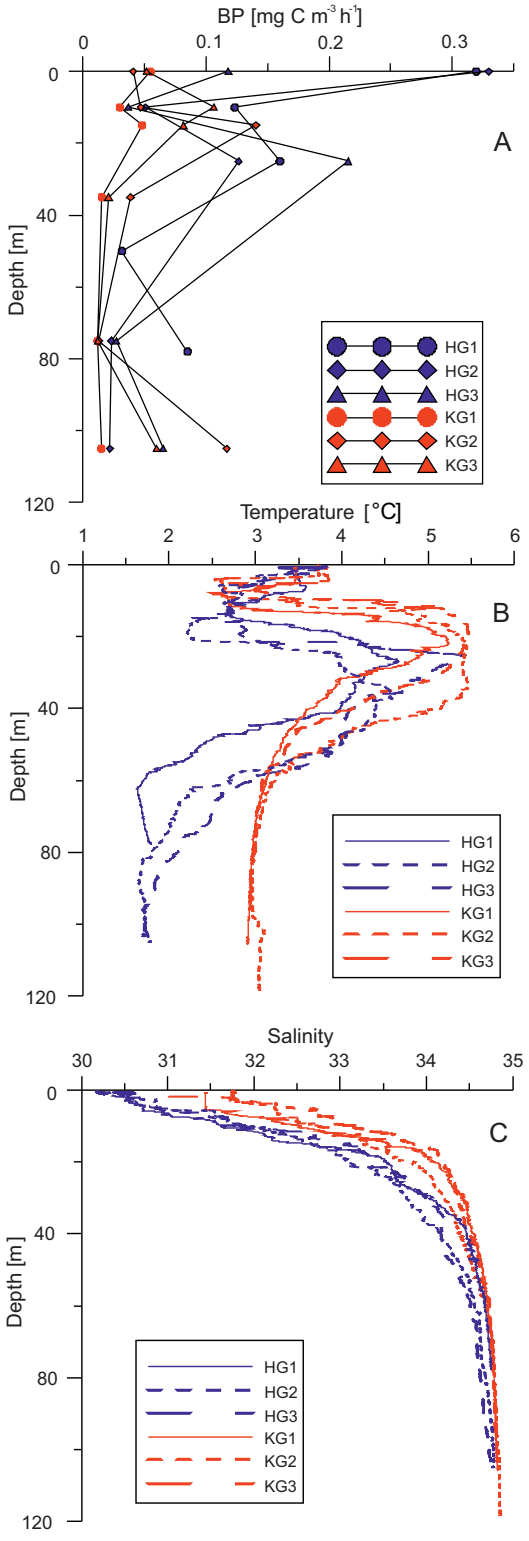

Figure 2 Depth profiles of bacterial production (a), salinity and (b) temperature in (c) Hornsund (HG1, HG2, HG3) and Kongsfjorden (KG1, KG2, KG3) waters.

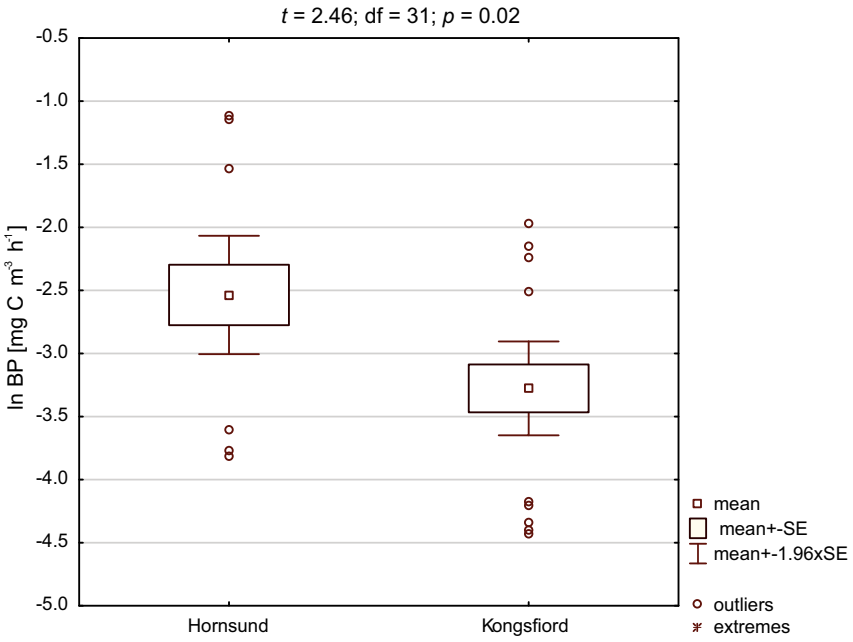

Figure 3 Difference between bacterial production in the water columns of Hornsund and Kongsfjorden (Student's *t*-test for equal variance).

organic carbon had no statistically significant effect on the BP in each of the fjords separately, but significantly accounted for 14% of the variation in the total set of data. Nutrients in the form of phosphate, nitrate, and ammonium were inversely proportional, and significant only for bacterial production in Hornsund.

Temperature accounted for 13% of the variability in bacterial production in both fjords simultaneously. However, based on the scatter plot, a regression line for each of the fjords can be plotted separately (Fig. 6). At a lower temperature, BP is higher in Hornsund. Temperature in Hornsund accounts for 57% of bacterial production variation, and is statistically significant. In Kongsfjorden, no statistical significance of temperature was found. Both temperature and salinity played a greater role in explaining the variability of BP in Hornsund, as well as in the data from both fjords combined. BP was directly proportional to temperature and inversely proportional to salinity.

Table 3 Single regression in separate fjords and in combined material — bacterial production [mg C m^{-3} h^{-1}] (ln transformed) versus different variables.

Parameter	Hornsund $N = 15$		Kongsfjorden $N = 18$		Both fjords $N = 33$	
	R^2 R^{-2}_{adj}	p	R^2 R^{-2}_{adj}	p	R^2 R^{-2}_{adj}	p
ln Pheoph	0.47/0.43	**	0.52/0.48	**	0.56/0.54	***
eDIC	0.52/0.48	**	0.33/0.28	**	0.45/0.43	***
ln Chlor		ns		ns	0.20/0.17	*
Temperature	0.57/0.54	**		ns	0.13/0.10	*
Salinity	0.37/0.32	*		ns	0.30/0.27	**
ln DOC		ns		ns	0.14/0.11	*
ln PO_4	0.32/0.27	*		ns		ns
ln NO_3	0.55/0.52	**		ns		ns
ln NH_4	0.55/0.52	**		ns		ns
ln TBN		ns		ns	0.30/0.27	**
ln BBM		ns	0.39/0.35	**	0.37/0.35	***

Pheoph, concentration of pheophytin [mg m^{-3}]; DIC, conc. of dissolved inorganic carbon [mg C dm^{-3}]; Chlor, conc. of chlorophyll *a* [mg m^{-3}]; DOC, conc. of dissolved organic carbon [mg C dm^{-3}]; PO_4, conc. of phosphates [mmol m^{-3}]; NO_3, conc. of nitrates [mmol m^{-3}]; NH_4, conc. of ammonium [mmol m^{-3}]; TBN, total bacterial number [10^5 cells cm^{-3}]; BBM, bacterial biomass [mg C m^{-3}]; ln, natural log transformed; *e*, transformed by an exponential function: *e* to the power *x*. *N*, number of measurements; R^2 R^{-2}_{adj}, determination coefficient/adjusted determination coefficient; *p*, level of significance; ns, not significant.

* $p < 0.05$.
** $p < 0.01$.
*** $p < 0.001$.

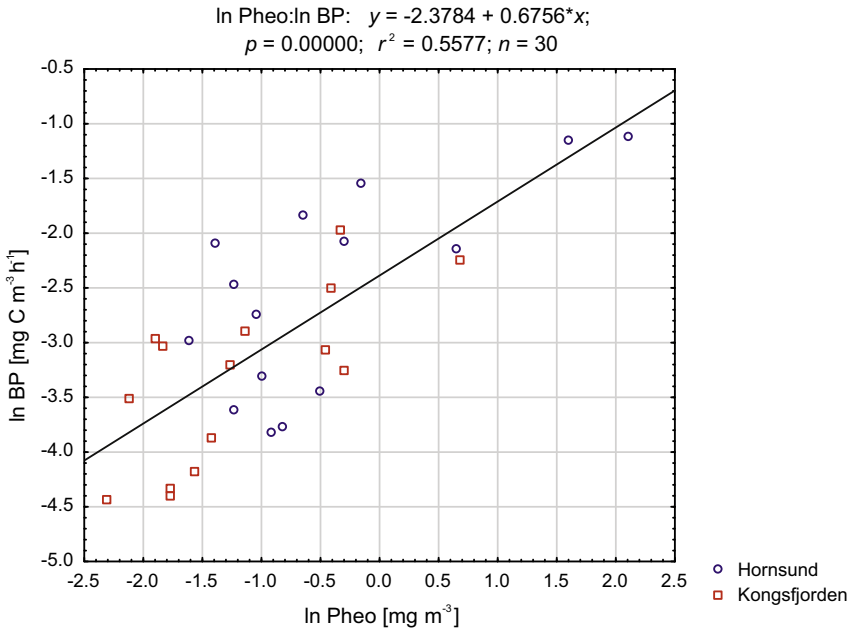

Figure 4 Relationship between bacterial production (BP) and concentrations of pheophytin in both fiords (different colours and shapes show values in each fiord).

Bacterial production showed no statistically significant dependence on bacterial abundance in each of the fjords separately. Considering all the data together, however, TBN accounted for 30% of BP variation. Higher bacterial production in Hornsund is followed by higher bacterial abundance in the fjord, and analogically: lower production corresponds to lower abundance in Kongsfjorden (Fig. 7). Bacterial biomass partially accounted for bacterial production variability in Kongsfjorden (39%) and in all the data (37%) (Fig. 8).

The results of multiple regression analysis for BP values from both fjords suggested that temperature, salinity, dissolved organic carbon, chlorophyll *a* concentrations, and total bacterial number combined account for 92% of bacterial production variability in both fjords (Table 4). Three regression factors: TBN, temperature, and pheophytin accounted for 69% of BP variability, while variables independent from bacterial number, namely temperature, pheophytin, and DOC explained a comparable value of 68% of results.

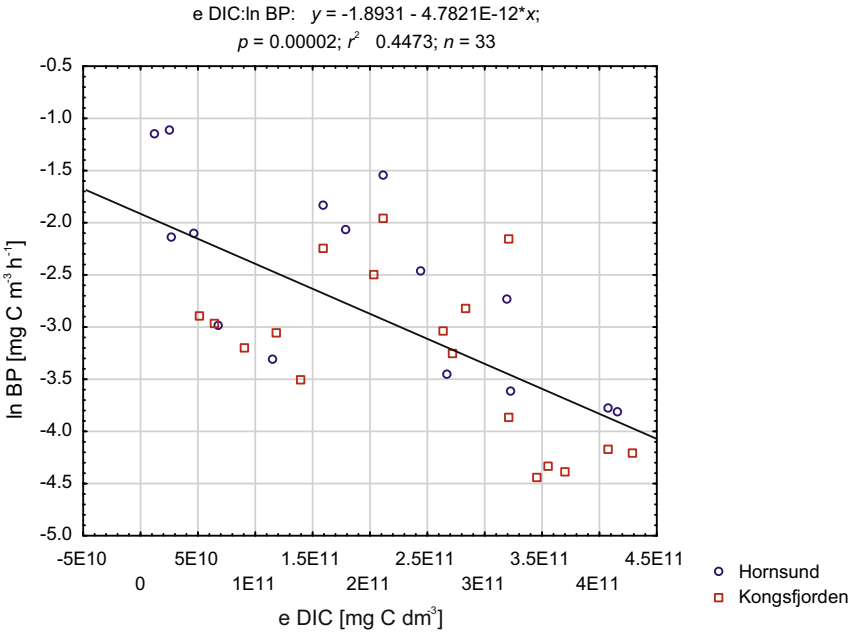

Figure 5 Relationship between bacterial production (BP) and concentrations of dissolved inorganic carbon (DIC) in both fiords (different colours and shapes show values in each fiord).

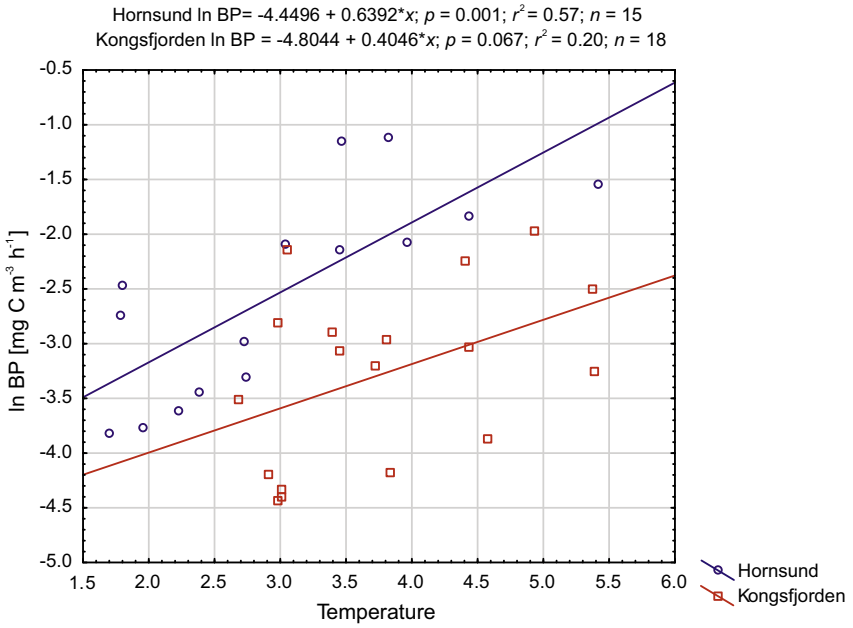

Figure 6 Dependence between bacterial production (BP) and water temperature in Hornsund and Kongsfjorden.

4. Discussion

It should be mentioned that the regression analyses shown in this study are based on a limited amount of data. Our results present temporary conditions, "a snapshot", and do not necessarily depict the general or multi-annual dependencies in the study environment. In the context of the comprehensive and simultaneous analysis of multiple biological and physicochemical parameters (GAME project), an attempt was made to estimate the relationship between bacterial production and environmental factors. In both fjords described in this study, sampling was carried out on three reference stations best characterising the areas of interest, and permitting mutual comparison (Węsławski et al., 2017).

The Kongsfjorden is strongly influenced by warm and saline waters of the West Spitsbergen Current (WSC) (Hop et al., 2002; Piquet et al., 2010, 2016; Svendsen et al., 2002; Wiencke and Hop, 2016). It shows hydrographic characteristics specific for both Arctic and broad fjords, related to water temperature, most frequent wind directions, freshwater inflow, and Coriolis effect, affecting the dynamics in the fjord (Svendsen et al., 2002). Water entering the

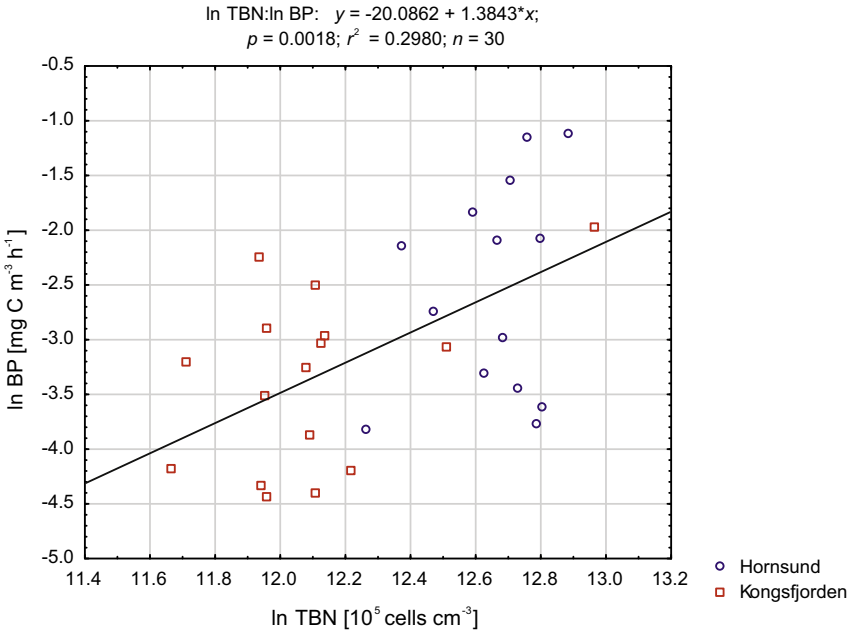

Figure 7 Relationship between bacterial production (BP) and total bacterial numbers (TBN) in water in both fiords (different colours and shapes show values in each fiord).

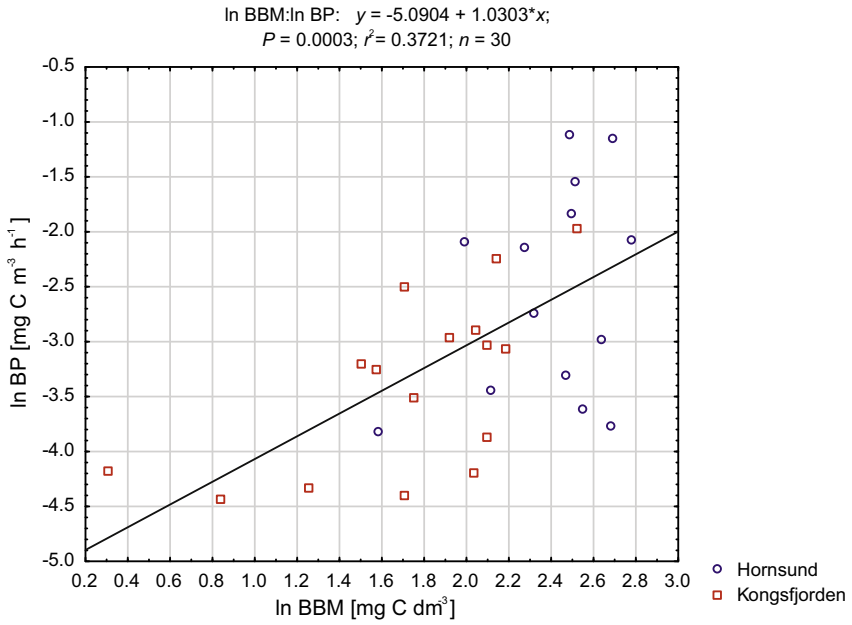

Figure 8 Relationship between bacterial production (BP) and bacterial biomass (BBM) in water in both fiords (different colours and shapes show values in each fiord).

Hornsund fjord will tend to inflow along the southern coast, and outflow along the northern coast of the basin (Cottier et al., 2007). Water of Atlantic origin (modified by mixing with Arctic Water) is usually observed as a bottom inflow. All of the water formations found in the fjord depend on Atlantic, Arctic, and glacial water mixing, and show seasonal variability (Cottier et al., 2005; Drewnik et al., 2016; Svendsen et al., 2002). Seasonal occurrence of local upwellings has been observed at glacier faces in both fjords (Węsławski et al., 1991). Upwelling processes were also clearly reported in Kongsfjorden in winter, during the occurrence of northern winds (Cottier et al., 2007). According to Divya and Krishnan (2017) and Promińska (unpublished data), summer 2013 was extraordinary in terms of hydrographic

Table 4 Multiple regression between ln BP [mg C m^{-3} h^{-1}] and physical and biological variables in the water column in both of the fjords.

	Term	<beta>	R^2 R^{-2}_{adj}	*p*	*N*
A					
ln BP	Intercept	−5.561	0.94/0.92	<0.00001	24
	Temp	0.746			
	Salinity	−0.346			
	ln DOC	1.268			
	ln Chlor	−0.267			
	ln TBN	0.852			
B					
ln BP	Intercept	−14.564	0.72/0.68	<0.00001	29
	ln TBN	0.885			
	Temp	0.298			
	ln Pheoph	0.453			
C					
ln BP	Intercept	−4.448	0.71/0.67	<0.00001	30
	Temp	0.352			
	ln Pheoph	0.378			
	ln DOC	1.362			

A, the best equation to all of the factors; *B*, the second best equation; *C*, the third best equation; Temp., temperature; DOC, conc. of dissolved organic carbon [mg C dm^{-3}]; Chlor, conc. of chlorophyll *a* [mg m^{-3}]; Pheoph, concentration of pheophytin [mg m^{-3}]; TBN, total bacterial number [10^5 cells cm^{-3}]; ln, natural log transformed; <beta> standardised coefficient of regression; R^2 R^{-2}_{adj}, determination coefficient/adjusted determination coefficient; *p*, level of significance; *N*, number of measurements.

conditions in West Spitsbergen fjords. Driven by climate change, high inter-annual variabilities in water masses in Kongsfjorden suggest that in the era of ongoing global warming, Hornsund might also soon become more influenced by the Atlantic Waters, and reveal hydrographic patterns similar to those of Kongsjforden.

Bacterial production values presented in this study do not deviate from the values representative of Svalbard, presented in other studies (Boras et al., 2010; Iversen and Seuthe, 2011; Lara et al., 2013; Piquet et al., 2016; Wängberg et al., 2008). However, statistically significant differences were observed between the two fjords. Both BP values (presented in this article) as well as bacterioplankton abundance and biomass values (Kalinowska et al., 2015) were higher in Hornsund than in Kongsfjorden. Higher values of microbiological parameters in the colder fjord raise a question about the reason of this phenomenon, especially that statistical analysis also shows a faster increase of bacterial production at lower temperature.

The answer might be the adaptation ability of typical arctic bacterioplankton to lower temperatures, and/or higher availability of organic matter (OM) supplied from the land (especially from bird colonies, numerously localised in Hornsund), which is more widely discussed by Kalinowska et al. (2015). Although low salinity differences do not influence bacterial physiology, they can be an indicator of freshwater inflow of glacial or land origin. In our study, bacterial production was inversely proportional to salinity. Therefore, we speculate that bacteria might have developed owing to the organic matter coming from such runoff, especially that Zaborska et al. (2016) reported a significantly greater share of OM of terrestrial origin in the waters of Hornsund (50–70% C_{org}) than in those of Kongsfjorden (20–40% C_{org}). Dissolved organic carbon (DOC) values, measured in the same samples as microbiological parameters, were also significantly higher in Hornsund than Kongsfjorden (Zaborska et al., 2016).

According to De Corte et al. (2011), the high particle load associated with the melting of ice from the surrounding glaciers, and high radiation conditions during the summer might play a key role in the structuring of the microbial food web in the coastal Arctic regions. Jankowska et al. (2005) suggests that higher organic matter concentrations in the inshore areas corresponded with higher bacterial biomass and abundance. Piquet et al. (2010) also suggested that freshwater originating from melting glaciers might introduce non-marine species, and simultaneously displace typical marine microorganisms to deeper water layers, where they receive less light. That, in turn, could limit primary production, similarly as high sediment input reducing the transparency of the water column. Urbański et al. (2017) points out extremely high suspended particulate matter concentrations at the glacier front, correlating with the feeding birds aggregation. This may indicate both high ecosystem richness and biodiversity in that spot, as well as possible introduction of large amounts of bird faeces to the waters in front of glaciers which may constitute a highly important food source for microorganisms. All of the above suggests that the activity of glaciers may significantly influence marine microbial communities. The exact scale of the phenomenon and detailed processes, however, are still unknown.

According to Maranger et al. (2015), next to temperature, bacterioplankton abundance and chlorophyll *a* concentration are also parameters affecting bacterial production in the Arctic. Among 720 samples collected throughout the Arctic, these parameters accounted for the variability of bacterial production in 57%. Phytoplankton growth is directly related to light availability, i.e. the depth of the euphotic zone where photosynthesis is possible. Bacterioplankton, in turn, is related to phytoplankton abundance, and the possibility to use its secretions as a food source.

Because phytoplankton utilises dissolved inorganic carbon, the correlation between primary production and DIC is expected to be inversely proportional. On the other hand, an increase in primary production results in increased bacterial production. Because the inverse proportion between BP and DIC reported in this study was considered as mediated by phytoplankton and therefore as an indirect relationship, DIC was not taken into account in the multiple regressions.

The range of the euphotic zone (1% PAR) is different in both fjords. It averages 16.21 m in Kongsfjorden, and 9.56 m in Hornsund (Smoła et al., 2017). Literature data show that primary production is higher by an order of magnitude in Kongsfjorden than in Hornsund. This is directly related to the turbulence and depth of the euphotic zone (Piwosz et al., 2009). While the species composition for planktonic protists differs between fjords, a higher number of taxa and biomass were recorded in Hornsund (Wiktor et al., 2017).

Bertilsson et al. (2004) suggests that solar radiation exerted a minor influence on the bioavailability of total DOM of the Southern Ocean. In this study, the analysis of bacterial production at all sampled depths from both fjords (N = 30) showed that the content of chlorophyll *a*, combined in the equation with temperature and total bacterial number (TBN), was not statistically significant. Instead of chlorophyll, pheophytin concentration was added to the regression with temperature and TBN. Pheophytin is a chlorophyll decomposition product derived from senescent algal cells, or released from phytoplankton cells due to the herbivorous activity of zooplankton (Welschmeyer et al., 1984). Together, temperature, TBN and pheophytin concentration accounted for 68% of the variability of BP. Also, the maximum BP values detected in the surface layer in Hornsund (stations HG1 and HG2) were followed by the maximum values of pheophytin concentrations. In the case of this study, the dependence of BP on phytoplankton could have only occurred in samples from the two most shallow layers. The deeper ones were already below the range of euphotic layer.

Although bacterial production is much higher in the euphotic zone, the microbial processes in the aphotic zone play a greater role in the entire ecosystem. The primary role in the intensity of microbial processes in the aphotic zone is played by the accessibility of organic matter (OM) derived from the decomposition of faecal pellets of zooplankton feeding on phytoplankton, and decomposition of phytoplankton itself. In the euphotic zone, however, organic matter comes from secretions of living phytoplankton.

Better understanding of the impact of the environmental conditions on marine microbial communities in polar ecosystems requires long-term monitoring. The interdisciplinary approach, combining data regarding glacial meltwater inflow, hydrological parameters, and co-functioning of microorganisms, phytoplankton, and zooplankton in the Arctic fjords, should be applied.

5. Conclusions

The study results show higher bacterial production in the waters of the colder Hornsund Fjord, compared to the waters of Kongsfjorden, considered as a warmer fjord. A similar trend has been reported in the case of bacterioplankton abundance and biomass. Apart from temperature, the waters of both fjords differ in the amount and availability of dissolved organic matter (DOM). It may originate from primary production or surface runoff from land during the polar summer. High amounts of biogenic compounds can originate from the tundra, melting glaciers and numerous bird colonies, and are flushed out to the waters of the Hornsund Fjord.

The results show that in both fjords, the most important factors influencing marine bacterioplankton production include temperature, pheophytin (the product of phytoplankton degradation) concentration, and the content of dissolved organic carbon. DOM can be either originating from faecal pellets of herbivorous zooplankton, or from surface runoff.

Acknowledgements

This study was funded by two National Science Centre projects: MAESTRO — Growing of the Arctic Marine Ecosystem — GAME (DEC-2012/04/A/NZ8/00661) and OPUS — From benthos-dominated to zooplankton-dominated mode: two faces of the Arctic fjords in the changing world — FACE2FACE (NCN-2012/05/B/ST10/01908).

We want to express special thanks to Agata Zaborska, Anna Kubiszyn and Grzegorz Siedlewicz for providing the chemical data, as well as Jakub Kowalczyk and Agnieszka Promińska for providing hydrographic data (IO PAN archives). We are grateful to the crew of the r/v *Oceania* who participated in the work at sea, and to other cruise participants for help, support, and cooperation.

References

Amann, R.I., Ludwig, W., Schleifer, K.H., 1995. Phylogenetic identification and in situ detection of individual microbial cells without cultivation. Microbiol. Rev. 59 (1), 143—169.

Bertilsson, S., Carlsson, P., Granéli, W., 2004. Influence of solar radiation on the availability of dissolved organic matter to bacteria in the Southern Ocean. Deep-Sea Res. Pt. II 51 (22), 2557—2568, http://dx.doi.org/10.1016/j.dsr2.2000.07.001.

Boras, J.A., Sala, M.M., Arrieta, J.M., Sà, E.L., Felipe, J., Agusti, S., Duarte, C.M., Vaqué, D., 2010. Effect of ice melting on bacterial carbon fluxes channeled by viruses and protists in the Arctic Ocean. Polar Biol. 33 (12), 1695—1707, http://dx.doi.org/10.1007/s00300-010-0798-8.

Cottier, F.R., Nilsen, F., Inall, M.E., Gerland, S., Tverberg, V., Svendsen, H., 2007. Wintertime warming of an Arctic shelf in response to large-scale atmospheric circulation. Geophys. Res. Lett. 34 (10), L10607, 5 pp., http://dx.doi.org/10.1029/2007GL029948.

Cottier, F., Tverberg, V., Inall, M., Svendsen, H., Nilsen, F., Griffiths, C., 2005. Water mass modification in an Arctic fjord through cross-shelf exchange: the seasonal hydrography of Kongsfjorden, Svalbard. J. Geophys. Res. 110 (C12), C12005, 18 pp., http://dx.doi.org/10.1029/2004JC002757.

De Corte, D., Sintes, E., Yokokawa, T., Herndl, G.J., 2011. Changes in viral and bacterial communities during the ice-melting season in the coastal Arctic (Kongsfjorden, Ny-Ålesund). Environ. Microbiol. 13 (7), 1827—1841, http://dx.doi.org/10.1111/j.1462-2920.2011.02497.x.

Divya, D.T., Krishnan, K.P., 2017. Recent variability in the Atlantic water intrusion and water masses in Kongsfjorden, an Arctic fjord. Polar Sci. 11, 30—41, http://dx.doi.org/10.1016/j.polar.2016.11.004.

Drewnik, A., Węsławski, J.M., Włodarska-Kowalczuk, M., Łącka, M., Promińska, A., Zaborska, A., Głuchowska, M., 2016. From the worm's point of view. I: Environmental settings of benthic ecosystems in Arctic fjord (Hornsund, Spitsbergen). Polar Biol. 39 (8), 1411—1424, http://dx.doi.org/10.1007/s00300-015-1867-9.

Elifantz, H., Dittel, A.I., Cottrell, M.T., Kirchmann, D.L., 2007. Dissolved organic matter assimilation by heterotrophic bacterial groups in the western Arctic Ocean. Aquat. Microb. Ecol. 50 (1), 39—49, http://dx.doi.org/10.3354/ame01145.

Engel, A., Borchard, C., Piontek, J., Schulz, K.G., Riebesell, U., Bellerby, R., 2013. CO_2 increases ^{14}C primary production in an Arctic plankton community. Biogeoscience 10 (3), 1291—1308, http://dx.doi.org/10.5194/bg-10-1291-2013.

Fuhrman, J.A., Azam, F., 1982. Thymidine incorporation as a measure of heterotrophic bacterioplankton production in marine surface waters—evaluation and field results. Mar Biol. 66 (2), 109—120, http://dx.doi.org/10.1007/BF00397184.

Hop, H., Pearson, T., Hegseth, E.N., Kovacs, K.M., Wiencke, C., Kwasniewski, S., Eiane, K., Mehlum, F., Gulliksen, B., Włodarska-Kowalczuk, M., Lydersen, C., Węsławski, J.M., Cochrane, S., Gabrielsen, G.W., Leakey, R.J.G., Lønne, O.J., Zajaczkowski, M., Falk-Petersen, S., Kendall, M., Wängberg, S.-Å., Bischof, K., Voronkov, A.Y., Kovaltchouk, N.A., Wiktor, J., Poltermann, M., di Prisco, G., Papucci, C., Gerland, S., 2002. The marine ecosystem of Kongsfjorden, Svalbard. Polar Res. 21, 167—208.

Iversen, K.R., Seuthe, L., 2011. Seasonal microbial processes in a high-latitude fjord (Kongsfjorden, Svalbard): I. Heterotrophic bacteria, picoplankton and nanoflagellates. Polar Biol. 34 (5), 731—749, http://dx.doi.org/10.1007/s00300-010-0929-2.

Jankowska, K., Włodarska-Kowalczuk, M., Wieczorek, P., 2005. Abundance and biomass of bacteria in two Arctic glacial fjords. Pol. Polar Res. 26 (1), 77—84.

Kalinowska, A., Ameryk, A., Jankowska, K., 2015. Microbiological survey in two arctic fjords: total bacterial number and biomass comparison of Hornsund and Kongsfjorden. In: Impact of Climate Changes on Marine Environments. Springer, Cham/Heidelberg/New York/Dordrecht/London, 115—126, http://dx.doi.org/10.1007/978-3-319-14283-8_9.

Kirchman, D.L., 1992. Incorporation of thymidine and leucine in the subarctic Pacific: application to estimating bacterial production. Mar. Ecol.-Prog. Ser. 82, 301—309.

Kirchman, D.L., K'ness, E., Hodson, R., 1985. Leucine incorporation and its potential as a measure of protein synthesis by bacteria in natural waters. Appl. Environ. Microbiol. 49, 599—607.

Kirchman, D.L., Malmstrom, R.R., Cottrell, M.T., 2005. Control of bacterial growth by temperature and organic matter in the Western Arctic. Deep-Sea Res. Pt. II 52 (24), 3386—3395, http://dx.doi.org/10.1016/j.dsr2.2005.09.005.

Lara, E., Arrieta, J.M., Garcia-Zarandona, I., Boras, J.A., Duarte, C.M., Agusti, S., Wassmann, P.F., Vaqué, D., 2013. Experimental evaluation of the warming effect on viral, bacterial and protistan communities in two contrasting Arctic systems. Aquat. Microb. Ecol. 70, 17—32, http://dx.doi.org/10.3354/ame01636.

Maranger, R., Vaqué, D., Nguyen, D., Hébert, M.-P., Lara, E., 2015. Pan-Arctic patterns of planktonic heterotrophic microbial abundance and processes: controlling factors and potential impacts of warming. Progr. Oceanogr. 139, 221—232, http://dx.doi.org/10.1016/j.pocean.2015.07.006.

Motegi, C., Tanaka, T., Piontek, J., Brussaard, C.P.D., Gattuso, J.-P., Weinbeuer, M.G., 2013. Effect of CO_2 enrichment on bacterial

metabolism in an Arctic fjord. Biogeosciences 10, 3285—3296, http://dx.doi.org/10.5194/bg-10-3285-2013.

Norland, S., 1993. The relationship between biomass and volume of bacteria. In: Kemp, P.F., Sherr, B.F., Sherr, E.B., Cole, J.J. (Eds.), Handbook of Methods in Aquatic Microbial Ecology. Lewis Publ., New York, 303—308.

Piquet, A.M.T., Maat, D.S., Confurius-Guns, V., Sintes, E., Herndl, G. J., van de Poll, W.H., Wiencke, C., Buma, A.G.J., Bolhuis, H., 2016. Springtime dynamics, productivity and activity of prokaryotes in two Arctic fjords. Polar Biol. 39 (10), 1749—1763, http://dx.doi.org/10.1007/s00300-015-1866-x.

Piquet, A.M.T., Scheepens, J.F., Bolhuis, H., Wiencke, C., Buma, A.G. J., 2010. Variability of protistan and bacterial communities in two Arctic fjords (Spitsbergen). Polar Biol. 33, 1521—1536, http://dx.doi.org/10.1007/s00300-010-0841-9.

Piwosz, K., Walkusz, W., Hapter, R., Wieczorek, P., Hop, H., Wiktor, J., 2009. Comparison of productivity and phytoplankton in a warm (Kongsfjorden) and a cold (Hornsund) Spitsbergen fjord in midsummer 2002. Polar Biol. 32 (4), 549—559, http://dx.doi.org/10.1007/s00300-008-0549-2.

Porter, K.G., Feig, Y.S., 1980. The use of DAPI for identifying and counting aquatic microflora. Limnol. Oceanogr. 25 (5), 943—948.

Rivkin, R.B., Anderson, M.R., Lajzerowicz, C., 1996. Microbial processes in cold oceans. I. Relationship between temperature and bacterial growth rate. Aquat. Microb. Ecol. 10 (3), 243—254, http://dx.doi.org/10.3354/ame010243.

Serreze, M.C., Walsh, J.E., Chapin III, F.S., Osterkamp, T., Dyurgerov, M., Romanovsky, V., Oechel, W.C., Morison, J., Zhang, T., Barry, R. G., 2000. Observational evidence of recent change in the northern high-latitude environment. Clim. Change 46 (1), 159—207, http://dx.doi.org/10.1023/A:1005504031923.

Simon, M., Azam, F., 1989. Protein-content and protein-synthesis rates of planktonic marine-bacteria. Mar. Ecol.-Prog. Ser. 51, 201—213.

Skagseth, Ø., Furevik, T., Ingvaldsen, R., Loeng, H., Mork, K.A., Orvik, K.A., Ozhigin, V., 2008. Volume and heat transports to the Arctic Ocean via the Norwegian and Barents Seas. In: Dickson, B., Meincke, J., Rhines, P. (Eds.), Arctic-Subarctic Ocean Fluxes: Defining the Role of the Northern Seas in Climate. Springer, Dordrecht, 45—64, http://dx.doi.org/10.1007/978-1-4020-6774-7_3.

Smoła, Z.T., Tatarek, A., Wiktor, J., Wiktor Jr., J.M., Hapter, R., Kubiszyn, A., Węsławski, J.M., 2017. Primary producers and production in two West Spitsbergen fjords — comparison of two fjord systems (Hornsund and Kongsfjorden). Pol. Pol. Res. (accepted for publication).

Svendsen, H., Beszczyńska-Möller, A., Hagen, J.O., Lefauconnier, B., Tverberg, V., Gerland, S., Ørbæk, J.B., Bischof, K., Papucci, C., Zajączkowski, M., Azzolini, R., Bruland, O., Wiencke, C., Winther, J., Dallmann, W., 2002. The physical environment of Kongsfjorden — Krossfjorden, an Arctic fjord system in Svalbard. Polar Res. 21 (1), 133—166, http://dx.doi.org/10.1111/j.1751-8369.2002.tb00072.x.

Swerpel, S., 1985. The Hornsund fjord: water masses. Pol. Polar Res. 6, 475—496.

Świątecki, A., 1997. Zastosowanie wskaźników bakteriologicznych w ocenie wód powierzchniowych. (Application of Bacteriological Indicators in Surficial Water Quality Assessment). WSP, Olsztyn, 105 pp.

Urbański, J.A., Stempniewicz, L., Węsławski, J.M., Dragańska-Deja, K., Wochna, A., Goc, M., Iliszko, L., 2017. Subglacial discharges create fluctuating foraging hotspots for sea birds in tidewater glacier bays. Sci. Rep. 7, 43999, http://dx.doi.org/10.1038/srep43999.

Walczowski, W., Piechura, J., 2006. New evidence of warming propagating toward the Arctic Ocean. Geophys. Res. Lett. 33 (12), 5 pp., http://dx.doi.org/10.1029/2006GL025872.

Walczowski, W., Piechura, J., 2007. Pathways of the Greenland Sea warming. Geophys. Res. Lett. 34 (10), L10608, http://dx.doi.org/10.1029/2007GL029974.

Walczowski, W., Piechura, J., 2011. Influence of the West Spitsbergen Current on the local climate. Int. J. Climatol. 31 (7), 1088—1093, http://dx.doi.org/10.1002/joc.2338.

Walczowski, W., Piechura, J., Goszczko, I., Wieczorek, P., 2012. Changes of the Atlantic Water properties as an important factor of the European Arctic marine climate. ICES J. Mar. Sci. 69 (5), 864—869, http://dx.doi.org/10.1016/j.jmarsys.2016.11.005.

Wängberg, S.-Å., Andreasson, K.I.M., Gustavson, K., Reinthaler, T., Henriksen, P., 2008. UV-B effects on microplankton communities in Kongsfjord, Svalbard — a mesocosm experiment. J. Exp. Mar. Biol. Ecol. 365 (2), 156—163, http://dx.doi.org/10.1016/j.jembe.2008.08.010.

Warwick, R.M., Emblow, C., Feral, J.P., Hummel, H., Van Avesaath, P., Heip, C., 2003. European marine biodiversity research sites. Report of the European Concerted Action: BIOMARE. NIOO-CEME, Yerseke, The Netherlands, 136 pp.

Welschmeyer, N.A., Coping, M., Vernet, M., Lorenzen, C.J., 1984. Diel fluctuation in zooplankton grazing rate as determined from the downward vertical flux of pheopigments. Mar. Biol. 83 (3), 263—270, http://dx.doi.org/10.1007/BF00397458.

Węsławski, J.M., Bucholz, F., Głuchowska, M., Weydmann, A., Huenterlage, K., 2017. Ecosystem maturation follows the warming of Arctic fjords. Oceanologia 59 (4), 592—602, http://dx.doi.org/https://doi.org/10.1016/j.oceano.2017.02.002.

Węsławski, J.M., Jankowski, A., Kwaśniewski, S., Swerpel, S., Ryg, M., 1991. Summer hydrology and zooplankton in two Svalbard fjords. Pol. Polar Res. 12 (3), 445—460.

Wiencke, C., Hop, H., 2016. Ecosystem Kongsfjorden: new views after more than a decade of research. Polar Biol. 39 (10), 1679—1687, http://dx.doi.org/10.1007/s00300-016-2032-9.

Wiktor, J., Kosakowska, A., Łotocka, M., Zaborska, A., Szymczycha, B., Kwaśniewski, S., Wiktor Jr., J.M., Kubiszyn, A., 2017. Planktonic Protists of two fjords of West Spitsbergen: similarities and differences. (unpublished data).

Zaborska, A., Włodarska-Kowalczuk, M., Legeżyńska, J., Jankowska, E., Winogradow, A., Deja, K., 2016. Sedimentary organic matter sources, benthic consumption and burial in west Spitsbergen fjords — signs of maturing of Arctic fjordic systems? (in press), J. Mar. Syst., http://dx.doi.org/10.1016/j.jmarsys.2016.11.005.

Zengler, K., 2009. Central role of the cell in microbial ecology. Microbiol. Mol. Biol. Rev. 73 (4), 712—729, http://dx.doi.org/10.1128/MMBR.00027-09.

Oceanologia (2017) 59, 508—524

Available online at www.sciencedirect.com

ScienceDirect

journal homepage: www.journals.elsevier.com/oceanologia/

ORIGINAL RESEARCH ARTICLE

Zooplankton structure in high latitude fjords with contrasting oceanography (Hornsund and Kongsfjorden, Spitsbergen)

Mateusz Roman Ormańczyk *, **Marta Głuchowska, Anna Olszewska, Slawomir Kwasniewski**

Institute of Oceanology, Polish Academy of Sciences, Sopot, Poland

Received 6 September 2016; accepted 19 June 2017
Available online 13 July 2017

KEYWORDS
Zooplankton;
Arctic;
Taxonomic composition;
Size structure;
Biogeographic and trophic affinity;
Atlantic water influence

Summary Zooplankton inhabiting the Hornsund and Kongsfjorden fjords on Spitsbergen (Svalbard) were investigated in summer 2013. The goal of the study was to determine how the zooplankton communities vary in environments functioning under different oceanographic regimes. Sampling was conducted with nets of different mesh size and selectivity (56 μm WP-2, 180 μm MultiNet, and 1000 μm Tucker Trawl), which permitted comparing a wide size spectrum of zooplankton components. Species composition did not differ substantially between the fjords, but the zooplankton in Hornsund was almost two times less numerous, and it had lower biomass per unit volume. The highest abundance at both sites was in the smallest zooplankton size fraction found only in samples taken with 56 μm mesh WP-2 net. These comprised as much as 71% and 58% of the total zooplankton abundance in Hornsund and Kongsfjorden, respectively. The communities in both fjords had comparable contributions of Arctic and boreo-Arctic species biomass in the year of the study. However, the comparison of zooplankton characteristics over several years showed changes in abundance and biogeographic structure that corresponded with variations in the physical environments of the fjords. The results of the study permit predicting the possible effects of the increasing influence of Atlantic waters on zooplankton communities inhabiting Arctic marine pelagic ecosystems.

* Corresponding author at: Institute of Oceanology, Polish Academy of Sciences, Powstańców Warszawy 55, 81-712 Sopot, Poland. Tel.: +48 587311786; fax: +48 585512130.
E-mail address: ormanczyk@iopan.gda.pl (M.R. Ormanczyk).
Peer review under the responsibility of Institute of Oceanology of the *Polish* Academy of Sciences.

ELSEVIER | Production and hosting by Elsevier

http://dx.doi.org/10.1016/j.oceano.2017.06.003

1. Introduction

The west coast of Spitsbergen is a region of complex oceanography where different parts function under more Arctic or more Atlantic influences (Cottier et al., 2010; Nilsen et al., 2008; Svendsen et al., 2002). This results in coexisting of marine biota of Atlantic and Arctic affinity, representing the Atlantic Subarctic Province and the Boreal Polar Province according to Longhurst (2007) (Gluchowska et al., 2016; Hop et al., 2006). The marine environments of the fjords are considered to be a balance between Atlantic, Arctic, brine and freshwater inputs, and are potentially sensitive indicators of environmental change (Cottier et al., 2005, 2010; Nilsen et al., 2008). Because of this, they also provide pseudo-mesocosm experimental setups that facilitate investigations of, for example, responses of biota to environmental variations, including those induced by climate change.

In recent years, the Atlantic water (AW) range in the eastern Fram Strait has been observed to shift northward and with it there have been pronounced increases in water temperature and salinity (Walczowski and Piechura, 2011; Walczowski et al., 2012). Consequently, the advection of AW and associated zooplankton into Kongsfjorden (Willis et al., 2006, 2008), the appearance of the blue mussel in Isfjorden (Berge et al., 2006), or decreasing sea ice cover north of Spitsbergen have all been observed (Walczowski et al., 2012). The growing influence of the AW in Fram Strait and the Arctic Ocean are recognized as symptoms of "Atlantification" (Årthun et al., 2012; Polyakov et al., 2010) and the most consequential results of this include the extension of the ice-free water period in the Arctic shelf seas, decreases in the extent and thickness of perennial sea ice, and the warming and mixing of the Arctic Ocean surface layer (ACIA, 2005; IPCC, 2007; Rodrigues, 2009). In pelagic systems, earlier studies on the West Spitsbergen Shelf (WSS) found influence of Atlantic water on plankton communities with respect to species composition, age structure, and biomass (Gluchowska et al., 2016; Kwasniewski et al., 2013; Rokkan Iversen and Seuthe, 2011; Trudnowska et al., 2014), with studies focusing mainly on mesozooplankton. It is anticipated, however, that the northern expansion of Atlantic boreal species will entail a shift toward a smaller size spectrum of zooplankton in Arctic regions (Beaugrand et al., 2002; Grebmeier, 2012; Hop et al., 2006). Zooplankton of small size are important link between microbial and classical (phytoplankton based) trophic levels (Calbet et al., 2000; Roff et al., 1995; Wickham, 1995). At present, the role of small zooplankton in Spitsbergen fjords and its possible modifications as a result of Atlantic influence are still not well known. Given the observed speed of environmental change, the acquisition of the missing knowledge seems necessary.

The aim of this study was to describe the differences between zooplankton communities from Hornsund and Kongsfjorden, two fjords on the WSS that are influenced by different oceanographic regimes. The novelty of the study is that evaluating of the zooplankton composition and structure took into account broad zooplankton size spectrum, based on data from parallel sampling with different nets, performed in the two fjords in the same year and season. Additionally, holo-mesozooplankton was assessed according to trophic preferences and biogeographic affiliations of the species comprising the community for both, the year of the study and interannually. The leading hypothesis was that the zooplankton in Kongsfjorden, the fjord strongly influenced by AW, would support higher concentrations of smaller/boreal taxa, in comparison to Hornsund.

2. Material and methods

2.1. Sampling area

Hornsund and Kongsfjorden are glacial fjords on the west coast of Spitsbergen, separated by a distance of about 250 km (Fig. 1) in a south-north direction. Both fjords have complex bottom topographies with depressions and coastlines with numerous bays. They also have well-marked inner parts, but neither of the fjords has a sill at its entrance. The depressions reach 150—250 m in Hornsund and 250—350 m in Kongsfjorden, and the inner areas are about 90—120 m deep (Prominska et al., 2017a). The number of surging glaciers varies between the fjords: there are 13 glaciers entering Hornsund (Swerpel, 1985) and four entering Kongsfjorden (Svendsen et al., 2002). The fjords are occupied by water masses of local origin and two remote water masses—Atlantic water (AW) carried by the West Spitsbergen Current (WSC) and Arctic-type waters (ArW) of the Sørkapp Current (SC), which fill the fjords in varied proportions (Cottier et al., 2005; Svendsen et al., 2002; Swerpel, 1985). The physical properties and biota of the remote water masses undergo transformations before or while entering the fjord, and the degree of the transformations depends on, among others, the distance from the source region and the complexity of the hydrographic processes the water masses encounter as they move (Cottier et al., 2005, 2010; Nilsen et al., 2008). As a result, the fjords receive different amounts of remote input, and they function under more Arctic-type (Hornsund) or more Atlantic-type (Kongsfjorden) regimes (Piwosz et al., 2009).

2.2. Field methods and samples processing

Zooplankton was sampled from r/v *Oceania* in 2013 at stations situated along the main axes of the fjords (Fig. 1, Table 1) with three different zooplankton nets: WP-2 net (Tranter, 1968) with 0.25 m^2 opening area and 0.056 mm mesh; MPS MultiNet Type *Midi* (HYDRO-BIOS Apparategebau GmBH) with 0.25 m^2 opening area and 0.180 mm mesh; Tucker Trawl net (Clarke, 1969) with 1 m^2 opening area and 1.0 mm mesh. The nets were towed vertically from near the bottom to the surface. After collection, the zooplankton were immediately preserved in a 4% formaldehyde solution in sea water buffered with borax. Water temperature and salinity were measured in vertical profiles at all zooplankton stations prior to net sampling with a Sea-Bird SBE 49 FastCAT conductivity-temperature-depth probe.

In the laboratory, the zooplankton samples were analyzed qualitatively and quantitatively following standard procedures described in Postel et al. (2000) and Kwasniewski et al. (2010). For the purposes of biomass estimations based on length-mass relationships, measurements of total length or another appropriate dimension were taken of randomly selected animals for which there was no information on size

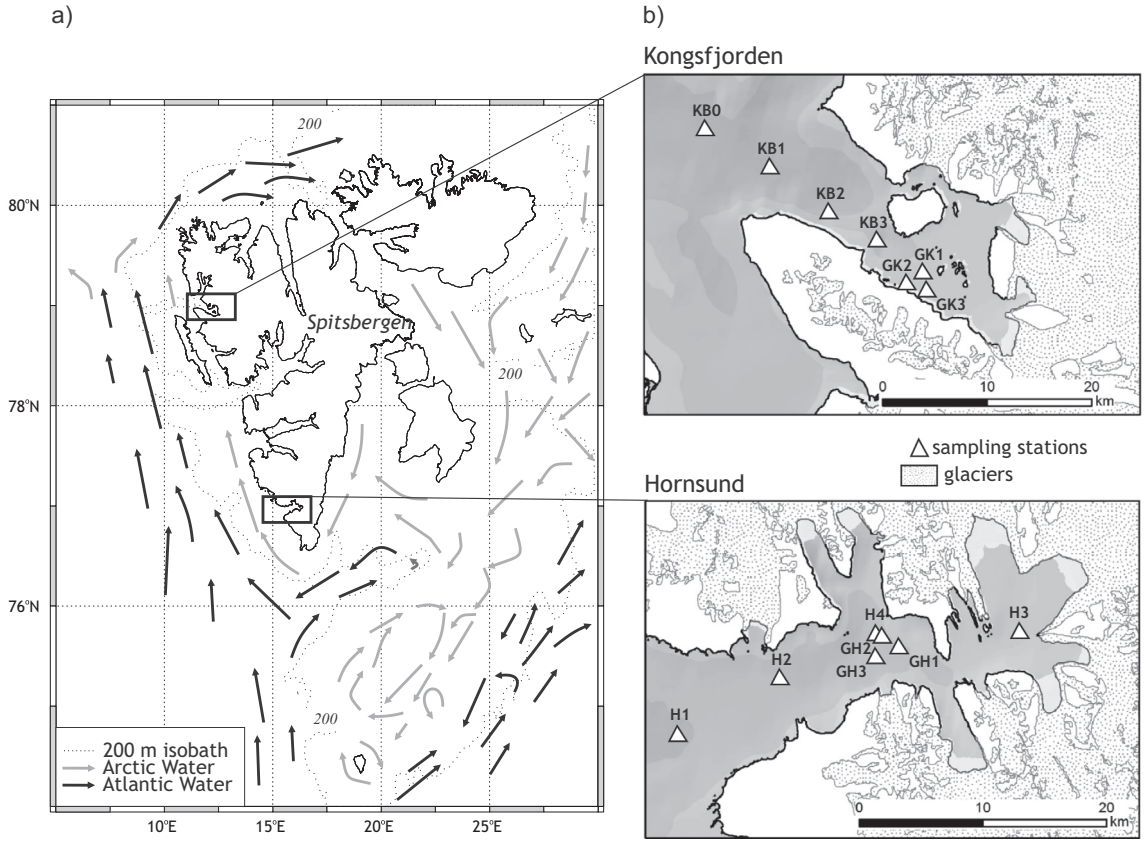

Figure 1 Map of the Spitsbergen region with surface current patterns (after Sakshaug et al. (2009), simplified) (a), and sampling station locations (b).

in literature (at least ten specimens per sample, except in cases when fewer specimens were available). With taxa for which there are no length-mass relationships published (*Pagurus pubescens* zoëa and megalopa, *Hyas* sp. zoëa, and fish larvae), a known number of specimens was collected from a sample, dried for 48 h at 50°C, weighed, and the mean dry mass of an individual, considered as nominal, was calculated.

2.3. Data analysis

The characteristics of the zooplankton communities compared were calculated for estimated abundances of zooplankton in a standard water volume unit [ind m^{-3}]. This was done to focus the comparison between the fjords more on the qualitative characteristics of zooplankton community, rather than on the quantitative ones. The basic information on the zooplankton

Table 1 Zooplankton sampling metadata in the studied fjords in summer 2013.

Fjord	Station	Date	Latitude [N]	Longitude [E]	Depth [m]	Gear type
Hornsund	H1	27.07.2013	76°56.313′	15°22.577′	150	MPS
Hornsund	H2	27.07.2013	76°58.767′	15°42.300′	140	MPS; TT
Hornsund	H3	27.07.2013	77°0.586′	16°28.935′	125	MPS; TT
Hornsund	H4	27.07.2013	77°0.617′	16°1.059′	95	MPS; TT
Hornsund	GH1	29.07.2013	77°0.021′	16°5.439′	70	WP-2; MPS; TT
Hornsund	GH2	29.07.2013	77°0.497′	16°2.233′	95	WP-2; MPS; TT
Hornsund	GH3	29.07.2013	76°59.624′	16°0.930′	100	WP-2; MPS; TT
Kongsfjorden	KB0	05.08.2013	79°2.543′	11°7.842′	310	MPS
Kongsfjorden	KB1	05.08.2013	79°0.788′	11°25.969′	340	MPS
Kongsfjorden	KB2	05.08.2013	78°58.684′	11°42.365′	300	MPS; TT
Kongsfjorden	KB3	06.08.2013	78°57.362′	11°55.688	350	MPS; TT
Kongsfjorden	GK1	07.08.2013	78°55.851′	12°8.367′	95	WP-2; MPS; TT
Kongsfjorden	GK2	08.08.2013	78°55.237′	12°4.131′	115	WP-2; MPS; TT
Kongsfjorden	GK3	08.08.2013	78°54.932′	12°9.652	85	WP-2; MPS; TT

characteristics calculated for the total zooplankton stock was summarized additionally in Section 3.3.1.

2.3.1. Size fraction division

In order to better estimate the quantitative characteristics of a zooplankton community considered for its wide size range, it was decided to use the abundance estimates of species and taxa representing particular size fractions based on data from samples collected with different nets. This method for calculating abundance took into account the limitations of zooplankton net sampling (Tranter, 1968) that are related to the differences in the sizes of zooplankton organisms and the different selectivity of the plankton nets used. Every organism identified was initially assigned to one of three operational size categories: 1 – small zooplankton (SZ); 2 – medium zooplankton (MZ); 3 – large zooplankton (LZ).

Small zooplankton (SZ). This size fraction included, first of all, metazoans with nominal body sizes <0.2 mm, caught with the WP2/0.056 net. Additionally, a few other organisms with larger nominal sizes were classified to this size fraction. These organisms had small widths or diameters, which precluded them from being efficiently retained on the 0.180 mm mesh of the MPS net. The abundance of emblematic SZ representative *Microsetella norvegica* was evaluated based only on WP2/0.056 net catches since this species was found exclusively in samples from this net. The abundances of other SZ species/taxa were calculated by subtracting from the abundances estimated based on the WP2/0.056 net catches, the abundances based on the MPS/0.180 catches. This was done for the following species/taxa: *Triconia borealis*, *Oncaea* spp., Cyclopoida, Harpacticoida, copepod nauplii, *Limacina helicina* veligers, gastropod larvae, bivalve larvae, polychaete larvae, *Fritillaria borealis*, and *Oikopleura* spp. Consequently, it was assumed that the SZ fraction included individuals of, for example, *T. borealis* and *Oncaea* spp., or bivalve veligers, comprising only younger copepodid stages or smaller specimens of taxa that were not caught by the coarser MPS/0.180 net.

Medium zooplankton (MZ). This size fraction comprised organisms with nominal body sizes in the range of 0.2–10.0 mm, predominantly all those caught with the MPS/0.180 net, including copepods and copepod nauplii (except those of smaller sizes included in SZ), ostracods, isopods; larval cirripedes, gastropods, echinoderms and bryozoans; polychaetes and their larvae; hydrozoans, chaetognaths, and appendicularians <10 mm length; as well as hyperiid amphipods, plus euphausiid and decapod larvae with body sizes <5 mm. The hyperiid amphipods and larval euphausiids and decapods with body sizes 5–10 mm were caught in higher abundances in the TT/1.0 net samples most probably because of their mobility, which increased their chances of escaping the net with a smaller opening area that was towed vertically. Therefore, these zooplankters were considered as contributions to the LZ and not the MZ size fraction.

Large zooplankton (LZ). The LZ size fraction comprised hyperiid amphipods, euphausiids, and decapods, mysids, hydrozoans, appendicularians, chaetognaths and fish larvae with nominal body sizes >10 mm, and hyperiid amphipods, larval euphausiids, and decapods with body sizes of 5–10 mm. The abundances of the representatives of this size fraction were calculated based on TT/1.0 net catches, except for the abundances of chaetognaths with body sizes of 10–20 mm, which were based on MPS/0.180 net catches. These were usually higher most probably because 10–20 mm chaetognaths were narrow in cross section, and that allowed them to escape effectively through the width of the coarse mesh on the TT net (Tranter, 1968).

The results of the abundance estimates for the three size fractions were summed to determine the values of total zooplankton community abundance.

2.3.2. Biomass estimation

Stage, species, or taxon-specific biomasses used in this study were either obtained earlier (for details see Kwasniewski et al., 2010) or were calculated using the length-mass relationships published in Böer et al. (2005), Gannefors et al. (2005), Lundberg et al. (2006), and Pérez-Camacho et al. (1994) and nominal mean lengths for species determined from our own measurements. The nominal mean lengths used in the formulas were the geometrical mean values calculated from measurements of particular taxa or developmental stages. The way the animals were measured reflected the requirements of the relationships used. Zooplankton biomass (dry mass) was calculated based on the zooplankton abundances per cubic meter and is expressed as mg DM m^{-3}.

2.3.3. Interannual comparison of zooplankton

The interannual comparison of zooplankton from the fjords focused on the taxonomic community structure, considered in terms of abundance and biomass, and also on the biogeographic and trophic community structures, considered in terms of biomass. The comparisons were done for the summer seasons of 2002, 2007, 2012, and 2013 using published (Gluchowska et al., 2016; Trudnowska et al., 2012; Walkusz et al., 2003) and unpublished (IO PAN, Marine Ecology Department) data. The community biogeographic and trophic structures were assessed by calculating the contributions to the biomass of species representing affinity in their main distribution for particular geographic ranges or trophic groups to the total community biomass. The evaluations were done for a subset of holozooplankton species and for the biomass estimates calculated based on MPS/0.180 net samples, which were the only samples available for the years compared other than 2013. The biogeographic affinity of the species followed that in Gluchowska et al. (2016), and the classification of species according to dietary preferences (herbivorous, omnivorous, carnivorous) was based on data from Blachowiak-Samolyk et al. (2008).

2.4. Statistical analyses

To compare the hydrography and the zooplankton characteristics between Hornsund and Kongsfjorden, a number of univariate and multivariate characteristics was used. To test for differences in zooplankton community taxonomic structure, one-way ANOSIM with two a priori sets of samples, each representing one of the studied fjords, was performed. The SIMPER (similarity percentages) procedure was used to determine the contribution of species to group similarities (Clarke and Warwick, 2001). The resemblance between the fjords of the zooplankton structure for each size category was

measured using the Bray–Curtis similarity index that was calculated based on the relative abundance or biomass of species and taxa. The differences between the fjords in univariate characteristics, including water temperature and salinity, and zooplankton abundance and biomass of each of the three size categories, as well as of the dominant species, were tested with the non-parametric Mann–Whitney *U*-test. The χ^2 test for independence was used to compare the proportions of *Calanus finmarchicus* and *Calanus glacialis* copepodid stages and the zooplankton size fraction proportions in the total zooplankton abundance and biomass. The interannual variability in holozooplankton abundance and biomass were compared using the Kruskal–Wallis test. All specified statistical analyses were performed using PRIMER 6 (Clarke and Warwick, 2001) and STATISTICA 10 (StatSoft Inc.). The significance level for all of the statistical tests was 0.05.

3. Results

3.1. Hydrography

In 2013, the mean water column salinity was lower in Hornsund (34.09; range: 33.72–34.59) than in Kongsfjorden (34.59; range: 34.28–34.84; Mann–Whitney *U*-test: $Z_{7,7} = 2.30$, $p = 0.021$), while the mean water column temperature was in the same range in both fjords (Hornsund: 1.12–3.72°C, Kongsfjorden: 2.69–3.78°C; $Z_{7,7} = 0.76$, $p = 0.443$). With regard to the occurrence of water masses in the years compared (2002, 2007, 2012 and 2013), Hornsund was regularly filled with intermediate water and surface water, with varying amounts of winter cooled water found in the inner basin and both Atlantic transformed water and AW in the front part of the fjord (Prominska et al., 2017a). In contrast, Kongsfjorden was typically occupied by transformed Atlantic water along with varying admixtures of AW, intermediate water, and local water. Characteristic AW occurred in Hornsund in the largest amounts in 2013, but it was not observed at all in 2007 and 2012. However, AW was present in Kongsfjorden in the largest amounts in 2013 and 2007, but it was not found at all in 2012.

3.2. Zooplankton composition

During the present study, a total of 69 taxa were recorded in Hornsund and Kongsfjorden, including 50 species and genera and 19 taxa identified to higher levels in Hornsund and 45 and 24, respectively, in Kongsfjorden. Among the taxa recorded, 52 occurred in both fjords, eight were identified only in Hornsund (including species and genera such as *Bougainvillia superciliaris*, *Dimophyes arctica*, *Halitholus cirratus*, *Hyas araneus*, *Hyperia galba*, *Myrianida* sp., *Sarsia* sp., *Velutina* sp.), and nine only in Kongsfjorden (*Boreomysis arctica*, *Erythrops erythrophthalma*, *Meganyctiphanes norvegica*, *Mesaiokeras spitsbergensis*, *Neoscolecithrix farrani*, *Pelagobia* sp. and *Cyanea capillata*, plus *Protomedeia grandimana*, and larval Appendicularia).

3.3. Zooplankton abundance and biomass

The zooplankton community was almost two times less numerous and had nearly two times lower biomass per unit volume [m^3] in Hornsund than in Kongsfjorden. The mean abundance in Hornsund and Kongsfjorden was as follows, respectively: 5840 ind m^{-3} (range: ~3800–8500 ind m^{-3}) and 9832 ind m^{-3} (range: ~4900–14,100 ind m^{-3}); the mean biomass was: 59 mg DM m^{-3} (range: ~42–93 mg DM m^{-3}) and 121 mg DM m^{-3} (range: ~65–188 mg DM m^{-3}). The contribution of particular size fractions to overall community abundance and biomass also differed between the fjords ($\chi^2 = 551.3$, $p < 0.05$ and $\chi^2 = 15.150$, $p < 0.05$ for abundance and biomass, respectively). The majority of community abundance (Table 2) consisted of SZ in both Hornsund (71%) and Kongsfjorden (58%), while MZ comprised less of the abundance in Hornsund than in Kongsfjorden (29% versus 42%). The contribution of LZ to overall community abundance was of much less importance (<1% in both fjords).

The bulk of the zooplankton biomass (Table 3) was composed of MZ, with 72% and 65% shares in Hornsund and Kongsfjorden, respectively. This was followed by LZ (26% in Hornsund and 32% in Kongsfjorden), while the SZ contribution to total zooplankton biomass was negligible (2% and 3%, respectively). When comparing the amounts of zooplankton in the particular size fractions, there was no difference between the fjords in SZ abundance, but there was a difference in its biomass (Mann–Whitney *U* test: $Z_{3,3} = 0.873$, $p = 0.383$; $Z_{3,3} = 1.746$, $p = 0.031$). There were significant differences in MZ abundance and biomass between Hornsund and Kongsfjorden, with higher values for both in the latter fjord ($Z_{7,7} = 2.811$, $p = 0.005$ and $Z_{7,7} = 2.900$, $p = 0.009$). No significant differences in LZ abundance or biomass were noted between the fjords ($Z_{5,6} = 0.639$, $p = 0.523$; $Z_{5,6} = 0.274$, $p = 0.784$), but the values showed high variability, particularly with regard to biomass.

3.3.1. Zooplankton stock size

The zooplankton stock size in terms of numbers per m^2 was, on average, 524,878 ind m^{-2} (range: ~428,700–596,600 ind m^{-2}) and 1,340,252 ind m^{-2} (range: ~657,900–1,981,100 ind m^{-2}) in Hornsund and Kongsfjorden, respectively. The main components were copepods nauplii (42% and 38% in Hornsund and Kongsfjorden, respectively), *Oithona similis* (12% and 28%), and bivalve veligers (27% and 11%). A high share (10%) of *Pseudocalanus* spp. was recorded in Hornsund, while in Kongsfjorden *F. borealis* and *L. helicina* veligers contributed considerably to the stock size (both 5%). *Calanus finmarchicus* comprised 3% and 4% in Hornsund and Kongsfjorden, respectively. The contribution of *C. glacialis* to the total mean zooplankton abundance in the water column was 1% in each fjord.

The zooplankton stock biomass was 5.17 g DM m^{-2} (range: ~0.94–8.04 g DM m^{-2}) in Hornsund and 23.37 g DM m^{-2} (range: ~7.72–44.82 g DM m^{-2}) in Kongsfjorden. The main contributors to zooplankton biomass in both fjords were *C. glacialis* (31% and 29% in Hornsund and Kongsfjorden, respectively) and *C. finmarchicus* (21% and 23%). Other species that contributed substantially to zooplankton biomass in Hornsund were *Parasagitta elegans* (9%), *Calanus hyperboreus* (6%), *Eukrohnia hamata* (6%), *Metridia longa* (5%), and *Pseudocalanus* spp. (3%), while in Kongsfjorden they were *C. hyperboreus* (13%), *Thysanoessa inermis* (5%), *L. helicina veligers* (5%), and *O. similis* (4%).

Table 2 Most abundant zooplankton species [ind m^{-3}] in different size fractions.

	Small Zooplankton (SZ)		Medium Zooplankton (MZ)		Large Zooplankton (LZ)	
	Hornsund	Kongsfjorden	Hornsund	Kongsfjorden	Hornsund	Kongsfjorden
N samples	3	3	7	7	6	5
Total mean zooplankton [ind m^{-3}]	4164	5688	1671	4131	5	13
Min.–max. [ind m^{-3}]	2735–5614	3039–7066	1108–2886	1894–7016	4–7	3–23
Microsetella norvegica	7–9	3–19				
Triconia borealis	0–23	46–49	7–62	15–80		
Copepoda nauplii	2259–2996	2462–6524	47–204	21–121		
Limacina helicina veligers	1–4	17–352	<1–5	37–275		
Bivalvia veligers	427–2975	213–400	<1–20	106–810		
Fritillaria borealis	0–8	0–229	<1–27	54–490		
Calanus finmarchicus			113–311	152–322		
Calanus glacialis			28–74	30–105		
Calanus hyperboreus			3–14	1–46		
Microcalanus spp.			8–62	32–194		
Pseudocalanus spp.			220–934	97–560		
Metridia longa			8–28	<1–20		
Acartia longiremis			8–43	<1–7		
Oithona similis			340–1249	945–4621		
Themisto abyssorum			0–1	<1–1	0–1	0–11
Themisto libellula			0 to <1	0–0	<1	>1
Meganyctiphanes norvegica						0 to <1
Thysanoessa inermis					<1–1	<1–6
Thysanoessa longicaudata					0 to <1	<1
Thysanoessa raschii					0 to <1	<1–1
Eukrohnia hamata			0–4	0–4	<1–3	0 to <1
Parasagitta elegans			1–11	<1–3	2–4	2–10

3.4. Zooplankton community structure

The zooplankton community structure, considered in terms of abundance, differed between Hornsund and Kongsfjorden within each of the size fractions: SZ (ANOSIM test: $R = 0.519$; $p = 0.050$), MZ (ANOSIM test: $R = 0.978$; $p = 0.001$), and LZ (ANOSIM test: $R = 0.448$; $p = 0.015$). The overall comparison of the Bray–Curtis index showed that the zooplankton community differed the least between the fjords in the SZ fraction and the most for LZ, while the differences in MZ were intermediate based on this metric (Kruskal–Wallis test $H_{2,72} = 17.04$; $p < 0.001$). The results of SIMPER analysis indicated that the Hornsund and Kongsfjorden communities differed in the contributions to total abundance of, for example, bivalve veligers and copepod nauplii in the SZ fraction, *O. similis* and *Pseudocalanus* spp. in that of MZ, and *Themisto abyssorum*, *T. libellula*, and *E. hamata* in the LZ fraction (Table 2, Fig. 2).

The zooplankton community structure in terms of biomass also differed between Hornsund and Kongsfjorden within the size fractions: SZ (ANOSIM test: $R = 0.378$; $p = 0.051$), MZ (ANOSIM test: $R = 0.561$; $p = 0.020$), and LZ (ANOSIM test: $R = 0.704$; $p = 0.020$). SIMPER analysis results indicated that the main species responsible for differences in the community biomass structure were, among others, *L. helicina* and bivalve veligers in the SZ fraction, *C. finmarchicus* CV, *C. glacialis* CV, and *M. longa* (all stages) in MZ, and *T. libellula*, *T. inermis*, and *E. hamata* in the LZ size fraction (Table 3, Fig. 2).

3.4.1. Small zooplankton (SZ)

The main components of SZ (Fig. 2a) in both fjords were copepod nauplii (57% of SZ abundance in Hornsund and 88% in Kongsfjorden) and bivalve veligers (42% and 5%, respectively). A notable component of SZ in Kongsfjorden was also small *L. helicina* veligers (3%), which were two orders of magnitude more abundant than they were in Hornsund. The highest contribution to the SZ biomass (Fig. 2a) was made by bivalve veligers (64% and 33% in Hornsund and Kongsfjorden, respectively) followed by copepod nauplii (21% and 18%). The contribution of *L. helicina* was also substantial in Kongsfjorden. The contribution of copepods to SZ biomass in both fjords was very small (approximately 3%) in the present study (Table 3).

3.4.2. Medium zooplankton (MZ)

MZ (Fig. 2b) was dominated by copepods, among which the prevailing taxa were *O. similis*, *Pseudocalanus* spp., and *C. finmarchicus* at 39%, 32%, and 9% of MZ abundance in Hornsund and 55%, 7%, and 6% in Kongsfjorden, respectively. The copepods *C. glacialis* (3% and 2%), *Microcalanus* spp. (2% in both fjords), *C. hyperboreus* (<1% and 1%), *M. longa* (1% and <1%), and *Acartia longiremis* (1% and <1%) were less numerous but still important. Populations of *C. finmarchicus* had a different copepodid structure in Hornsund than in Kongsfjorden ($\chi^2 = 46.119$, $p < 0.001$), with higher contributions of younger copepodids in the former fjord. Populations of *C. glacialis* did not differ significantly between the fjords in this respect, ($\chi^2 = 6.153$, $p = 0.292$). Notable MZ components

Table 3 Main zooplankton biomass species [mg DM m^{-3}] in different size fraction.

	Small Zooplankton (SZ)		Medium Zooplankton (MZ)		Large Zooplankton (LZ)	
	Hornsund	Kongsfjorden	Hornsund	Kongsfjorden	Hornsund	Kongsfjorden
N samples	3	3	7	7	6	5
Total mean zooplankton [mg DM m^{-3}]	1.482	3.597	42.671	78.289	15.199	39.172
Min.–max. [mg DM m^{-3}]	1.042–2.035	2.378–5.421	32.536–66.218	58.022–98.717	8.889–24.249	4.358–83.885
Microsetella norvegica	0.007–0.009	0.003–0.020				
Triconia borealis	0.000–0.046	0.095–0.099	0.015–0.126	0.031–0.163		
Copepoda nauplii	0.294–0.338	0.320–0.848	0.211–0.909	0.093–0.540		
Limacina helicina veligers	0.008–0.024	0.145–2.972	0.003–0.073	0.537–4.023		
Bivalvia veligers	0.233–1.606	0.823–1.545	0.002–0.077	0.409–3.124		
Calanus finmarchicus			7.435–16.367	15.224–35.900		
Calanus glacialis			10.965–31.057	13.482–47.508		
Calanus hyperboreus			1.412–6.587	0.432–19.573		
Microcalanus spp.			0.057–0.433	0.226–1.355		
Pseudocalanus spp.			0.815–3.339	0.571–2.356		
Metridia longa			1.662–4.251	0.004–1.582		
Acartia longiremis			0.081–0.426	0.001–0.074		
Oithona similis			0.842–3.097	2.345–11.461		
Fritillaria borealis			0.001–0.039	0.077–0.701		
Themisto abyssorum			0.000–0.016	0.068–0.375	0.000–0.928	0.000–16.107
Themisto libellula			0.000–0.012		0.115–1.408	0.035–1.736
Meganyctiphanes norvegica						0.000–14.701
Thysanoessa inermis					0.000–3.889	0.341–27.248
Thysanoessa longicaudata					0.000–0.052	0.008–0.185
Thysanoessa raschii					0.000–0.247	0.220–24.431
Eukrohnia hamata			0.006–0.074	0.000–0.383	2.685–15.151	0.000–0.631
Parasagitta elegans			0.042–0.249	0.005–0.054	2.012–8.275	0.674–13.543

in both fjords also included appendicularians, first of all, *F. borealis* (1% and 5% of MZ abundance), bivalve veligers (1% and 11%), and chaetognaths <10 mm (<1% in both fjords). Some taxa contributed notably to the MZ fraction only in one fjord, for example, cirripede larvae in Hornsund (1% share) and echinoderm larvae in Kongsfjorden (1%). Copepods comprised 97% and 90% of the MZ biomass in Hornsund and Kongsfjorden, respectively. *Calanus finmarchicus*, *C. glacialis*, and *C. hyperboreus* contributed the highest proportions to the biomass in both Hornsund (25%, 46%, 8%), and in Kongsfjorden (31%, 34%, 13%). The remaining portions of the MZ biomass were of *O. similis* (4% and 7%), *Pseudocalanus* spp. (5% and 2%), *M. longa* (6% and 1%), *Microcalanus* spp. (<1% and 1%), and *A. longiremis* (1% and <1%), in Hornsund and Kongsfjorden, respectively. Except for the copepods, a significant portion of the MZ biomass in Kongsfjorden was of *L. helicina* veligers and juveniles (7%), and bivalve veligers (2%). In absolute values, *C. finmarchicus*, *C. hyperboreus*, *Microcalanus* spp., and *O. similis* biomass was higher in Kongsfjorden, whereas that of *Pseudocalanus* spp., *M. longa*, and *A. longiremis* was higher in Hornsund (Table 3). *Calanus glacialis* biomass was, however, comparable in the two fjords (Mann–Whitney *U* test: $Z_{7,7} = 0.767$, $p = 0.443$). Two Hydrozoa species also contributed markedly to the MZ biomass – *B. superciliaris* in Hornsund and *Aglantha digitale* in Kongsfjorden.

3.4.3. Large zooplankton (LZ)

Numerically, LZ (Table 2) made a very small contribution to total zooplankton abundance, which is why the taxonomic structure of this fraction is presented more specifically only for the biomass of LZ (Table 3).

The main biomass components among LZ (Fig. 2c) were chaetognaths (66% in Hornsund and 16% in Kongsfjorden), euphausiids (17% and 61%), amphipods (6% and 27%), and larval fishes (3% and 6%). Moreover, decapods (4% of LZ) and hydrozoans (7%) were the remarkable biomass components in Hornsund. Two species of chaetognaths – *E. hamata* and *P. elegans* – were found in both fjords; in Hornsund their shares of the biomass of chaetognaths were similar (52% and 48% for *E. hamata* and *P. elegans*, respectively), whereas in Kongsfjorden the latter was clearly more important than the former (9% and 91%). Among euphausiids, the most important species was *T. inermis*, which was 79% of the euphausiid biomass in Hornsund and 48% in Kongsfjorden. The second euphausiid present in both fjords was *Thysanoessa raschii* (9% and 23% of the euphausiid biomass in Hornsund and Kongsfjorden, respectively), while *M. norvegica* was noted only in Kongsfjorden, where it constituted 24% of the euphausiid biomass. Two important species of hyperiid amphipods were noted – *T. abyssorum*, which constituted 40% and 91% of the hyperiid biomass in Hornsund and Kongsfjorden, and *T. libellula* (60% and 9%). In Hornsund decapods were represented first by *P. pubescens* (53% of the decapods biomass) followed by *Sabinea septemcarinata* (21%) and *Pandalus borealis* (15%), while in Kongsfjorden the same species constituted 24%, 67%, and 9%, respectively, of the decapod biomass. *Clione limacina* (2%) was also a notable LZ biomass component in Hornsund.

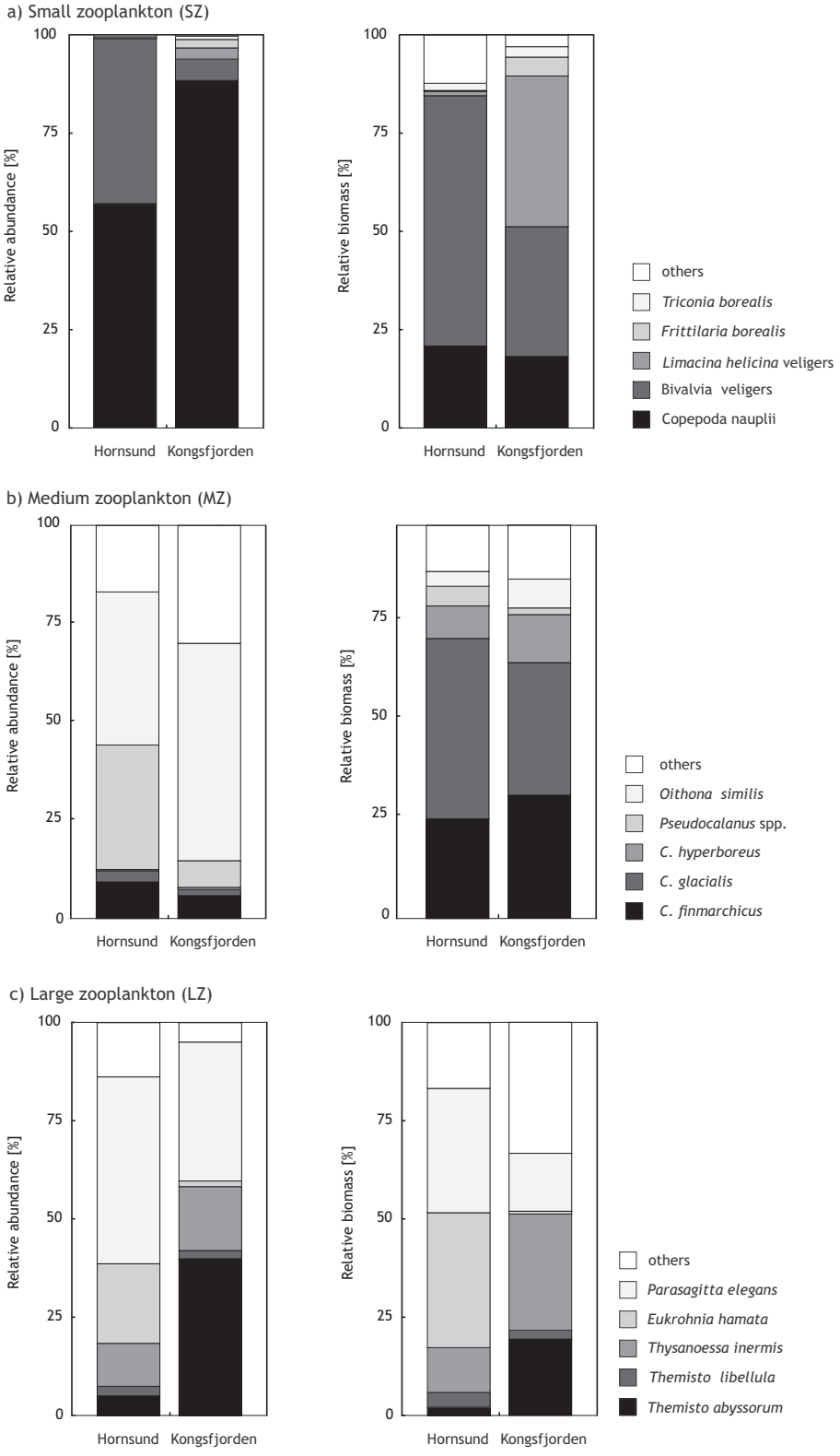

Figure 2 Relative water column mean abundance [ind m^{-3}] and biomass [mg DM m^{-3}] of zooplankton in Hornsund and Kongsfjorden in each size category: Small Zooplankton, SZ (a), Medium Zooplankton, MZ (b), and Large Zooplankton, LZ (c).

The large zooplankton Hydrozoa were remarkable only in Hornsund, and they were predominantly represented by *H. cirratus* (93%).

3.5. Zooplankton interannual variability

The comparison of interannual (2002, 2007, 2012, 2013) changes in holozooplankton abundance and biomass showed clear variability. The differences were not statistically significant among the years compared in Hornsund, while the differences in abundance and biomass among the years in Kongsfjorden were statistically significant (Fig. 3).

When zooplankton composition was assessed for holozooplankton species biogeographic affinity and biomass, Arctic and boreo-Arctic species together comprised nearly the same portion of the biomass in both regions in the year of the study (Fig. 4). The comparison among years showed that in 2002, 2007, and 2012 the biomass of Arctic species was higher in Hornsund than in Kongsfjorden. Even in 2012, when there was a biomass peak in Kongsfjorden caused by the very high biomass of Arctic *C. glacialis*, the contribution of Arctic species to biomass was still higher in Hornsund (Fig. 3b). In turn, the absolute biomass of Arctic species was higher in Hornsund in comparison to Kongsfjorden in 2002 and 2007 (48 vs. 25 mg DM m^{-3} in 2002, and 66 vs. 36 mg DM m^{-3} in 2007), while in 2012 and in 2013 the opposite was observed (53 vs. 109 mg DM m^{-3}, and 20 vs. 52 mg DM m^{-3}) (Fig. 3b). A comparable pattern was observed in total holozooplankton biomass changes, which were higher in Hornsund in 2002 and 2007 and lower in 2012 and 2013. The biomass in Hornsund in 2013 was the lowest in our records (Fig. 3b).

The zooplankton biomass composition assessment of holozooplankton species for trophic affinity indicated that the predominant trophic group in both fjords was the pelagic herbivores comprised mainly of *Calanus* spp. regardless of year (Fig. 5). The percentage of carnivorous zooplankton was higher in Hornsund compared to Kongsfjorden in 2002, 2007, and 2012. In 2013, the contributions of the different trophic categories to the total holozooplankton biomass were more similar between the fjords.

4. Discussion

4.1. Hydrography

The comparison of the interannual data on temperature, salinity, and water masses distribution in Hornsund and Kongsfjorden showed considerable interannual variability in fjord hydrography (Prominska et al., 2017a,b). Recently, it was suggested that the impact of AW on these environments

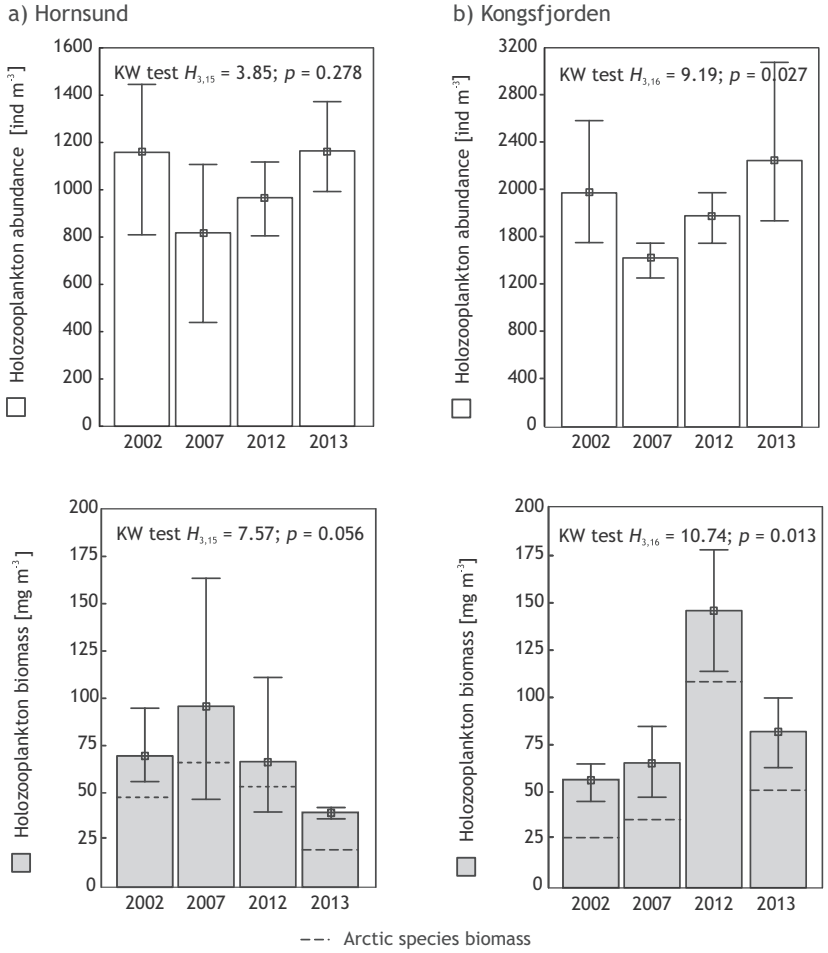

Figure 3 Interannual variability in abundance [ind m^{-3}] and biomass [mg DM m^{-3}] of holozooplankton in Hornsund (a) and Kongsfjorden (b). Calculations are for zooplankton collected with an MPS/0.180 net. Bars denote ranges between min. and max.

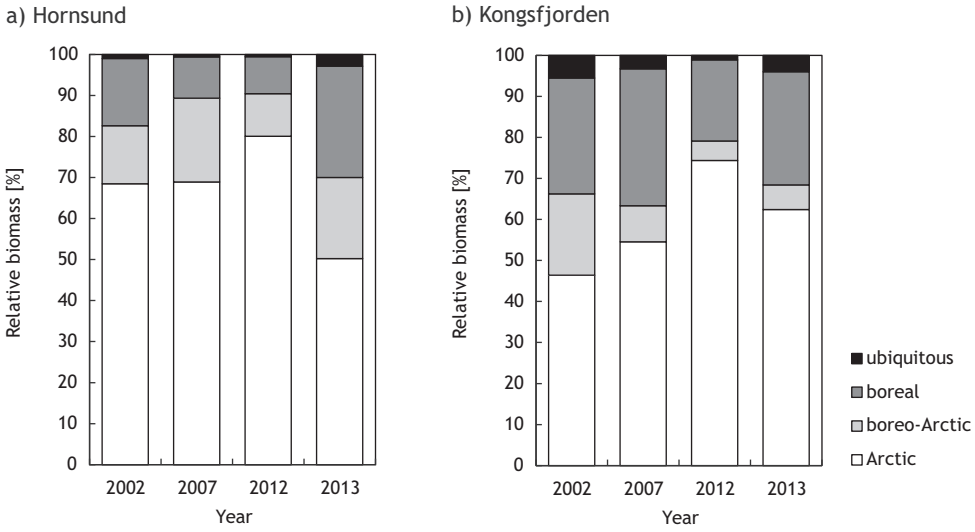

Figure 4 Biogeographic composition of holozooplankton in Hornsund (a) and Kongsfjorden (b). Calculations are for zooplankton biomass collected with an MPS/0.180 net.

is stronger in Kongsfjorden than in Hornsund. This concurs with earlier observations based on less intense, more loosely coordinated investigations (Piwosz et al., 2009; Swerpel, 1985; Weslawski et al., 1991). However, in 2013, when this study was conducted, the influence of AW in Hornsund was stronger than in previous years, and the highest water temperature since 2001 was measured there (Prominska et al., 2017b). This explains the results of the comparison of fjord hydrography done for this study which indicated that in summer 2013 there was no difference in the mean sea water temperature in the fjords, while, simultaneously, the mean salinity was still, as expected, lower in Hornsund.

4.2. Zooplankton communities in Hornsund and Kongsfjorden

Despite the lack of pronounced differences in hydrography, the 2013 zooplankton community in Hornsund can still be considered to be more of a cold-water, Arctic character, while that in Kongsfjorden was of a mixed Arctic-Atlantic character. Earlier research suggests a similar plankton diversity pattern on the West Spitsbergen Shelf and in fjords (Gluchowska et al., 2016; Kwasniewski et al., 2010; Piwosz et al., 2009; Trudnowska et al., 2014; Weydmann and Kwasniewski, 2008). This study, however, was the first that attempted to evaluate fjord zooplankton diversity using parallel sampling with different nets done in the same year and season. Based on this unique study material, a wider size spectrum of zooplankton community components was compared for the first time in the two fjords. All of the zooplankton species and taxa recorded during this study had been observed previously in the area (Gluchowska et al., 2016; Hop et al., 2006; Koszteyn and Kwasniewski, 1989; Weslawski et al., 1991), and most of them had been noted in both locations, with a few only observed in one fjord. This agrees with earlier reports that the zooplankton communities

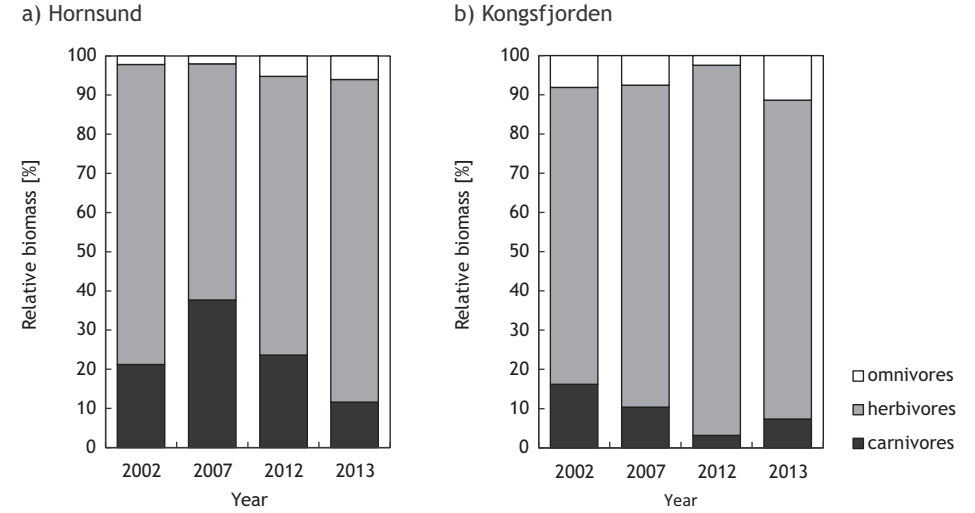

Figure 5 Trophic composition of holozooplankton in Hornsund (a) and Kongsfjorden (b). Calculations are for zooplankton biomass collected with an MPS/0.180 net.

from different Spitsbergen fjords and shelf waters do not vary as much in faunal composition as they do in community structure (Gluchowska et al., 2016; Kwasniewski et al., 2010; Trudnowska et al., 2015). The differences in the presence of taxa suggest that the occurrence in Hornsund of the hydromedusae *H. cirratus* and *B. superciliaris*, which are considered common in the Arctic (Kramp, 1959; Manko, 2015), confirm the assumption that the environment of this fjord is of a more Arctic character. The presence of the boreal Atlantic euphausiid *M. norvegica* in Kongsfjorden indicates the stronger influence of AW (Buchholz et al., 2012), which could be facilitated by the narrower shelf and deeper trench there (Prominska et al., 2017a; Svendsen et al., 2002). On the other hand, a reason for the differences observed in zooplankton composition could be the imbalanced sampling of all the specific microhabitats in the fjords, such as glacier embayments or near-bottom waters where rare species, such as the benthopelagic copepods *M. spitsbergensis* and *N. farrani*, are typically found (Schulz and Kwasniewski, 2004).

The quantitative assessment of the zooplankton communities revealed that zooplankton was less numerous and its biomass was lower per m^3 and in the overall standing stock (m^2) in Hornsund. This agrees with findings of other studies, for example Gluchowska et al. (2016), Kwasniewski et al. (2010), Piwosz et al. (2009), and Weslawski et al. (1991), even if the comparison of results is not always straightforward. Possible explanations for the lower zooplankton concentration in Hornsund than in Kongsfjorden could be either better living conditions in a more hydrographically diverse environment, which is the situation in the frontal zones that are typically considered to favor higher plankton productivity (Munk et al., 2003; Skarðhamar et al., 2007), or the more intense influx of AW into Kongsfjorden that transports biota in from the more productive adjacent shelf (Willis et al., 2006, 2008), or both.

Zooplankton is composed of a wide spectrum of organism types and sizes (Lenz, 2000), and every net used to collect it is selective (Sameoto et al., 2000; Skjoldal et al., 2013; Tranter, 1968). Studies show that a significant zooplankton part is omitted in surveys using standard mesozooplankton nets because of the limited retention of small-sized organisms (Gallienne and Robins, 2001; Pasternak et al., 2008; Turner, 2004). Choosing to use three net types in the present study was based on the experience of earlier zooplankton research in the region and on general methodological recommendations (Sameoto et al., 2000; Skjoldal et al., 2013; Tranter, 1968). This approach increased the chances of catching a wider spectrum of plankton organisms and allowed for a more complete description of the communities studied. In terms of abundance, the most numerous metazoan zooplankton components in the studied fjords were those in the SZ size fraction. These comprised as much as 71% and 58% of the total zooplankton abundance in Hornsund and Kongsfjorden, respectively. MZ organisms were generally two times less numerous, although occasionally some of them reached abundances as high as those of SZ, whereas LZ was two orders of magnitude less abundant. In terms of biomass, the main community components were MZ (53–86%) with a marked contribution of LZ (11–45%) and a minor one of SZ (3%). The comparisons of the relative contribution of different size classes to zooplankton communities in other studies showed comparable results (Arashkevich et al., 2002; Hirche et al., 1994) and concurred with the inherent pattern of organism size distribution in pelagic environments (Platt and Denman, 1977; Sheldon et al., 1972; Zhou and Huntley, 1997).

In Hornsund, the SZ size fraction consisted mainly of small (<0.2 mm in nominal size) copepod nauplii and small bivalve veligers, whereas in Kongsfjorden this size fraction included predominantly small copepod nauplii. Presumably, most of these were *Oithona* spp. nauplii measuring from 132 μm to 218 μm (Castellani et al., 2007), and the high concentrations of small copepod nauplii in Kongsfjorden corresponded with higher concentrations of *O. similis* in this fjord. This was observed during the present study and previously (Gluchowska et al., 2016; Lischka and Hagen, 2005; Piwosz et al., 2009). The higher abundances of bivalve veligers in Hornsund in comparison to those in Kongsfjorden were, however, a new finding. Gluchowska et al. (2016) found higher concentrations of bivalve veligers in Kongsfjorden, but this was based on data from a 0.180 mm mesh net. The present study showed that in addition to the bivalve veligers sampled with the MPS/0.180 net, there was a numerous group of smaller-sized veligers (0.146 mm mean total length) that were found predominantly in Hornsund. Bivalve veligers appear to be the most abundant meroplankton in Svalbard fjords during summer (this study, Gluchowska et al., 2016; Koszteyn and Kwasniewski, 1989; Stübner et al., 2016), but this group is not homogenous in its size structure, or, most probably, in taxonomy. Additionally, *L. helicina* veligers were important SZ organisms in Kongsfjorden. The occurrence of this holoplankton component in large amounts in summer was reported in earlier studies from this fjord (Hop et al., 2006; Weslawski et al., 2000), and it corresponds with the life cycle of this species (Gannefors et al., 2005). Presumably, the differences in the contribution of predominating small zooplankton taxa between Hornsund and Kongsfjorden could have resulted from differences in the seasonal development of zooplankton in these fjords (Gluchowska et al., 2016), but it could also be a consequence of the different impacts AW has on the fjord's marine environment, for example, by influencing the species composition of the fjord biota.

The MZ size fraction distinguished in this study can be considered the equivalent of mesozooplankton, which is probably the most studied category of zooplankton in Svalbard marine ecosystems (Gluchowska et al., 2016; Hop et al., 2002; Kwasniewski, 1990; Lischka and Hagen, 2005; Piwosz et al., 2009; Trudnowska et al., 2014; Walkusz et al., 2009) and elsewhere. The present results correspond with earlier findings (Gluchowska et al., 2016; Kwasniewski et al., 2003; Trudnowska et al., 2014; Walkusz et al., 2009; Weydmann et al., 2014), with respect to both taxonomic composition and the quantity characteristics of this zooplankton size fraction from the fjords studied. The most important mesozooplankton taxa in Hornsund and Kongsfjorden were the copepods *O. similis*, *Pseudocalanus* spp., *C. finmarchicus*, *C. glacialis*, and *C. hyperboreus*. Based on this study, it was also estimated that, overall, MZ constituted 29–50% of the total zooplankton abundance, and 53–86% of the total zooplankton biomass. This indicated that, in a simplified approach, mesozooplankton represent the main part of the zooplankton component of the Svalbard marine ecosystem. In Hornsund, which is considered to be a more Arctic system, *Pseudocalanus* spp. was more numerous and its contribution to total MZ abundance was higher, while in Kongsfjorden,

which is influenced more by AW, the most important species was *O. similis*, which corresponds with earlier findings (Gluchowska et al., 2016; Walkusz et al., 2009; Weslawski et al., 1991). The main factors responsible for the species distribution patterns observed in the two fjords with differing environments are not fully explained by this single study. However, the suggestion that *O. similis* benefits from higher concentrations of organic particles, which are its food source (González and Smetacek, 1994; Walkusz et al., 2009) and also that it probably takes advantage of the higher water temperatures found in Kongsfjorden seem plausible. This is also in agreement with the scenarios of pelagic food web modification from increasing temperature, which suggests that smaller boreal species will have increasingly important roles in the higher latitudes (Beaugrand et al., 2002, 2010; Hays et al., 2005; Wassmann et al., 2011). The abundances of other important medium-sized copepods did not differ significantly between the studied fjords; however, the slightly higher abundances of *T. borealis*, *Microcalanus* spp., and *C. hyperboreus* observed in Kongsfjorden were probably related, first of all, to the greater depths in this fjord. Characteristically, these species avoid the upper layers of the water column (Darnis and Fortier, 2014; Østvedt, 1955). In addition to copepods, taxa that made a marked contribution to the MZ fraction, but only in Kongsfjorden, were *F. borealis* and medium-sized bivalve veligers. Differences in the number of veligers could have resulted from the different seasonality in the ecosystem functioning of the two fjords; however, the higher number of *F. borealis* probably fits in with the proposed scenario of the increasing role of small particles in pelagic ecosystems experiencing warming (e.g., Beaugrand et al., 2002; Morán et al., 2010). *Oithona similis* and *Pseudocalanus* spp. were the most numerous copepods, but they were of minor importance to MZ biomass, the majority of which was comprised of three *Calanus* species: *C. finmarchicus*, *C. glacialis*, and C. *hyperboreus*. The biomass per cubic meter of these three copepods was 79% and 78% of the total MZ biomass in Hornsund and Kongsfjorden, respectively. Overall, their contribution to the total zooplankton standing stock biomass was 58% and 65%, which confirms that these copepods are the most important species in the marine ecosystems of Svalbard (e.g., Daase et al., 2007; Hop et al., 2006). The lower biomass of *C. finmarchicus* in Hornsund (10.71 mg DM m^{-3}) than in Kongsfjorden (24.19 mg DM m^{-3}) corresponds to the anticipated more Atlantic character of the latter fjord. However, some of this difference could be caused by differences in population stage composition that result from differences in seasonality between the fjords (this study, Gluchowska et al., 2016). On the other hand, higher amounts of *C. finmarchicus* in Kongsfjorden could stem from the advection of a probably more developed oceanic population (Willis et al., 2006, 2008).

The constituents of the LZ size fraction were about two orders of magnitude less numerous than the constituents of SZ and MZ, yet their abundances were about the same as those found in earlier studies on macrozooplankton in Svalbard waters (Buchholz et al., 2010; Dalpadado et al., 2016; Weslawski et al., 2000). The abundances of LZ in the present study could have been underestimated as sampling with the TT was not done in trawling mode but in vertical tow mode at the stations and also because approximately the 10 m layer above the seabed was omitted during sampling to avoid damaging the net and contaminating the catch with bottom sediments. Recently euphausiids and amphipods were found to aggregate close to the seabed in fjords (Hirche et al., 2015), so parts of their populations could have been omitted by the sampling method. Large zooplankton organisms can be good indicators of different water masses, even if they are not very diverse (e.g., Buchholz et al., 2010). The higher abundance of *T. abyssorum* in Kongsfjorden concurred with the findings of Dalpadado et al. (2016) and was also in line with observations of Atlantic euphausiid species such as *M. norvegica* and *N. megalops* in this fjord, which suggests that AW has a marked impact on the pelagic environment of Kongsfjorden (Buchholz et al., 2010; Weslawski et al., 1991, 2000). In turn, the higher relative abundance of *T. libellula* among hyperiid amphipods and of *T. inermis* among euphausiids could be a manifestation of the more cold water character of the Hornsund environment (Buchholz et al., 2010; Dalpadado et al., 2016; Koszteyn et al., 1995). Another observation that also supports this was the higher abundance of hermit crab (*P. pubescens*) larvae in this fjord. Balazy et al. (2015) showed that this species inhabits the shallow rocky bottom south of Hornsund, from where its larvae could be transported to the fjord with the cold, coastal Sørkapp Current. This species is not as abundant on the AW-influenced coasts in the vicinity of Kongsfjorden. Hydromedusae were generally more important and diverse in Hornsund, probably because this fjord preserved a more coastal character, in contrast to the more oceanic one in Kongsfjorden, which was subjected to stronger advective flushing. Hydromedusae fauna can be richer in coastal rather than in open sea waters in this region. The finding of the Arctic-associated *H. cirratus* (Kramp, 1959; Manko, 2015) only in Hornsund and the Atlantic-associated *A. digitale* (Kramp, 1959; Manko, 2015) predominating among the hydromedusae in Kongsfjorden, adds more evidence in support of the overarching conclusion of this study which is that the pelagic ecosystem in Hornsund is of a more Arctic character while that of Kongsfjorden is more Atlantic. This concurs with the hypothesized "Atlantification" of the Kongsfjorden ecosystem (Dalpadado et al., 2016; Prominska et al., 2017a).

4.3. Zooplankton interannual variability

This study found that the zooplankton communities in Hornsund and Kongsfjorden were composed of species of Arctic, boreo-Arctic, boreal, and ubiquitous biogeographic affinities that contributed different proportions in the two fjords in different years, which is an observation that corroborates the results of earlier research (Gluchowska et al., 2016; Kwasniewski et al., 2003; Piwosz et al., 2009; Trudnowska et al., 2014; Walkusz et al., 2009). The comparison of the interannual changes in the composition of mesozooplankton suggests that in Hornsund between 2002 and 2012 the contribution of Arctic and boreo-Arctic species was higher than in Kongsfjorden, whereas it diminished substantially in 2013. Simultaneously, in previous years the contribution of Arctic and boreo-Arctic species was lower in Kongsfjorden than in Hornsund on account of the important admixture of boreal (Atlantic) and ubiquitous species, while in the year of the study it was equal to that in Hornsund. The changes observed in zooplankton biogeographic composition are supported by hydrographic observations (Prominska et al., 2017b).

The high percentages of Arctic and boreo-Arctic species in Hornsund between 2002 and 2012 occurred during a time when AW inflows into the fjord were low, while the lowest contribution of these species in 2013 coincided with the highest influx of AW masses observed during the hydrographic time series (2001–2013). An analogous relationship was observed between the biogeographic composition of the zooplankton and the hydrography in Kongsfjorden. In years when the contribution of Arctic and boreo-Arctic species was relatively low, the presence of AW in the fjord was low. When an exceptionally high proportion of Arctic species represented mainly by *C. glacialis* was noted in 2012, the hydrographic data showed the lowest amount of AW in Kongsfjorden. The return to an increased proportion of boreal (Atlantic) and ubiquitous species in 2013 was associated with the marked presence of AW in the fjord.

Changes in total zooplankton abundance and biomass in the years studied oscillated somewhat and were statistically significant only in the very dynamic environment of Kongsfjorden. Variations in total biomass could suggest decreasing biomass in Hornsund and increasing in Kongsfjorden. These fluctuations were mainly associated with variations in the biomass of Arctic species. The general reason for increasing zooplankton biomass in Kongsfjorden could be its higher phytoplankton productivity (Hop et al., 2002; Piwosz et al., 2009; Smola et al., in press). Arctic species could benefit from increased food availability or from increased temperature if it remained within their range of tolerance, so they could perform at higher rates (Weydmann et al., 2015) and achieve higher productivity. In contrast, the strongest AW influx in 2013 in Hornsund coincided with decreased total zooplankton biomass and also the lower biomass of Arctic species. This could be interpreted as a short term effect of disturbance (Lindahl and Perissinotto, 1987), which was manifested as the removal of the original, Hornsund, Arctic fauna and the replacement of it with advected, WSC Atlantic fauna, followed by a lack of acclimation allowing the components of one or both of the biota to take advantage of the new circumstances, such as increased productivity, similar to that suggested for the Kongsfjorden ecosystem (Piwosz et al., 2009).

In polar marine ecosystems, in which food webs can comprise fewer components, but in which the key species are highly specialized, changes in species composition can have cascading effects and impact various trophic levels (Drinkwater, 2006; Falk-Petersen et al., 1990, 2007; Frank et al., 2005; Grebmeier, 2012; Jackson et al., 2001). The shift toward a higher contribution of boreal *C. finmarchicus* would directly alter the feeding conditions of the little auk, *Alle alle* (Jakubas et al., 2011; Kwasniewski et al., 2010). Another important effect of changes in the taxonomic composition of the zooplankton community associated with changes in hydrography, appears to be the increase in the proportion of ubiquitous species, mainly small *O. similis* that is linked with a higher admixture of AW. Small-sized copepods do not contribute as much to the zooplankton biomass in high latitude regions as do the larger species of the genus *Calanus* and *Metridia* (Ashjian et al., 2003; Hopcroft et al., 2005; Svensen et al., 2011; present study); however, this is expected to change along with the warming of Arctic ecosystems. Studies suggest the role of small copepods in ecosystem functioning is essential (e.g., Gallienne and Robins, 2001). The advantage of small taxa in future warmer systems, in addition to the general rule of biota responding positively to temperature (Huntley and Lopez, 1992), is their high fecundity and fast growth rates, which are possible because of their effective feeding on small-sized particles and omnivory. These features mean small species are less affected by rapid changes in environmental conditions (Ward and Hirst, 2007), which would favor an increase in their importance in warming, Arctic seas. Changes in size structure of zooplankton communities are suggested to be of greater importance to ecosystem functioning than changes in the zooplankton biomass (Lane et al., 2008; Richardson and Schoeman, 2004). One of the reasons for this could be the potential role of small copepods, like *O. similis*, as mediators between microbial and classical food webs (Svensen et al., 2011). Hence, more focus should be put on determining the roles of the small size fraction of zooplankton since their role in future Arctic ecosystem functioning would increase.

The trophic composition of the zooplankton communities in both the fjords was predominated by herbivorous species. In Hornsund, a somewhat higher contribution of carnivores represented by the chaetognaths *P. elegans* and *E. hamata* was observed. In contrast, carnivores were less abundant in Kongsfjorden, and they were mainly represented by *P. elegans* and *T. abyssorum*. Blachowiak-Samolyk et al. (2007) and Hirche et al. (1994) found chaetognaths and hyperiid amphipods to be the most numerous carnivores in Arctic pelagic ecosystems. Comparisons of holozooplankton trophic composition over the years suggest decreasing contributions of carnivorous taxa in both of the fjords studied. This could suggest a modification toward the growing importance of smaller, omnivorous zooplankton and, as a consequence, the greater dissipation of carbon in the environment (e.g. Wassmann et al., 2011; Weslawski et al., 2011).

5. Conclusions

The results of our study corroborate with earlier findings and confirm that historically the zooplankton communities in Hornsund and Kongsfjorden have been formed by a mixture of organisms originating from the Atlantic Subarctic Province and the Boreal Polar Province. In recent years, however, the faunal composition, abundance, and biomass of zooplankton have undergone changes linked to variations in hydrographic conditions. This study indicates the possible directions of modifications in zooplankton communities in Arctic shelf seas impacted by 'Atlantification', a phenomenon related to increasing advection of Atlantic-origin waters and their biota to Arctic systems. The observed differences between zooplankton communities from Hornsund and Kongsfjorden were substantial and concerned every zooplankton size fraction. We conclude that the results of this study confirm the working hypothesis that Atlantic water influence supports higher concentrations of small and medium zooplankton, mainly of boreal and ubiquitous affinity, a feature observed primarily in Kongsfjorden. The study also found an increase of the biomass of zooplankton in Atlantic influenced Kongsfjorden, possibly because of positive effect on Arctic fauna of increasing temperature, which changed within the species tolerance range. In case of Hornsund, the strong impact of waters of Atlantic origin in 2013 left a visible mark on the pelagic environment and the zooplankton community,

weakening its typical Arctic character and decreasing biomass, most likely due to disturbance effect.

The results of the study do not signal that the environmental changes observed as a consequence of the increasing impact of Atlantic waters on Arctic shelf ecosystems will have immediate negative effects on Arctic zooplankton. However, scales of these effects most likely depend on extent of the temperature increase, rate of water mass exchange, and perseverance of the phenomena. The effects can also have a tendency to accumulate, leading to a tipping point and changes which will be irreversible and negative.

Acknowledgments

This study is part of the GAME (2012/04/A/NZ8/00661) and Face2Face (2012/05/B/ST10) projects funded by the Polish National Science Centre.

References

ACIA, 2005. Arctic Climate Impact Assessment. Cambridge Univ. Press, New York, 1042 pp.

Arashkevich, E., Wassmann, P., Pasternak, A., Wexeles Riser, C., 2002. Seasonal and spatial changes in biomass, structure, and development progress of the zooplankton community in the Barents Sea. J. Mar. Syst. 38 (1—2), 125—145, http://dx.doi.org/10.1016/S0924-7963(02)00173-2.

Årthun, M., Eldevik, T., Smedsrud, L.H., Skagseth, Ø., Ingvaldsen, R. B., 2012. Quantifying the influence of Atlantic heat on Barents Sea ice variability and retreat. J. Climate 25, 4736—4743, http://dx.doi.org/10.1175/JCLI-D-11-00466.1.

Ashjian, C.J., Campbel, R.G., Welch, H.E., Butler, M., Van Keuren, D., 2003. Annual cycle in abundance, distribution, and size in relation to hydrography of important copepod species in the western Arctic Ocean. Deep-Sea Res. Pt. I 50 (10—11), 1235—1261, http://dx.doi.org/10.1016/S0967-0637(03)00129-8.

Balazy, P., Kuklinski, P., Włodarska-Kowalczuk, M., Barnes, D., Kędra, M., Legeżynska, J., Weslawski, J.M., 2015. Hermit crabs (*Pagurus* spp.) at their northernmost range: distribution, abundance and shell use in the European Arctic. Polar Res. 34 (1), http://dx.doi.org/10.3402/polar.v34.21412 18 pp.

Beaugrand, G., Reid, P.C., Ibañez, F., Lindley, J.A., Edwards, M., 2002. Reorganization of North Atlantic marine copepod biodiversity and climate. Science 296 (5573), 1692—1694, http://dx.doi.org/10.1126/science.1071329.

Beaugrand, G., Edwards, M., Legendre, L., 2010. Marine biodiversity, ecosystem functioning, and carbon cycles. Proc. Natl. Acad. Sci. U. S. A., http://dx.doi.org/10.1073/pnas.0913855107.

Berge, J., Johnsen, G., Nilsen, F., Gulliksen, B., Slagstad, D., Pampanin, D.M., 2006. The *Mytilus edulis* population in Svalbard: how and why. Mar. Ecol.-Prog. Ser. 309, 305—306.

Blachowiak-Samolyk, K., Kwasniewski, S., Dmoch, K., Hop Haakon, Falk-Petersen, S., 2007. Trophic structure of zooplankton in the Fram Strait in spring and autumn 2003. Deep-Sea Res. Pt. II 54, 2716—2728, http://dx.doi.org/10.1016/j.dsr2.2007.08.004.

Blachowiak-Samolyk, K., Søreide, J.E., Kwasniewski, S., Sundfjord, A., Hop, H., Falk-Petersen, S., Hegseth, E.N., 2008. Hydrodynamic control of mesozooplankton abundance and biomass in northern Svalbard waters (79—81°N). Deep-Sea Res. Pt. II 11 (55), 2210—2224, http://dx.doi.org/10.1016/j.dsr2.2008.05.018.

Böer, M., Gannefors, C., Kattner, G., Graeve, M., Hop, H., Falk-Petersen, S., 2005. The Arctic pteropod *Clione limacina*: seasonal lipid dynamics and life-strategy. Mar. Biol. 147 (3), 707—717, http://dx.doi.org/10.1007/s00227-005-1607-8.

Buchholz, F., Buchholz, C., Weslawski, J.M., 2010. Ten years after: krill as indicator of changes in the macro-zooplankton communities of two Arctic fjords. Polar Biol. 33 (1), 101—113, http://dx.doi.org/10.1007/s00300-009-0688-0.

Buchholz, F., Werner, T., Buchholz, C.M., 2012. First observation of krill spawning in the high Arctic Kongsfjorden, west Spitsbergen. Polar Biol. 35 (8), 1273—1279, http://dx.doi.org/10.1007/s00300-012-1186-3.

Calbet, A., Landry, M.R., Scheinberg, R.D., 2000. Copepod grazing in a subtropical bay. Species-specific responses to a midsummer increase in nanoplankton standing stock. Mar. Ecol.-Prog. Ser. 193, 75—84.

Castellani, C., Irigoien, X., Harris, R.P., Holliday, N.P., 2007. Regional and temporal variation of *Oithona* spp., biomass, stage structure and productivity in the Irminger Sea, North Atlantic. J. Plankton Res. 29 (12), 1051—1070, http://dx.doi.org/10.1093/plankt/fbm079.

Clarke, M.R., 1969. A new midwater trawl for sampling discrete depth horizons. J. Mar. Biol. Assoc. U.K. 49, 945—960.

Clarke, K.R., Warwick, R.M., 2001. Change in Marine Communities: An Approach to Statistical Analysis and Interpretation, 2nd edn. PRIMER-E, Plymouth, 176 pp.

Cottier, F., Tverberg, V., Inall, M., Svendsen, H., Nilsen, F., Griffiths, C., 2005. Water mass modification in an Arctic fjord through cross-shelf exchange: the seasonal hydrography of Kongsfjorden, Svalbard. J. Geophys. Res. 110 (C12), C12005, http://dx.doi.org/10.1029/2004JC002757 18 pp.

Cottier, F., Nilsen, F., Skogseth, R., Tverberg, V., Skarðhamar, J., Svendsen, H., 2010. Arctic fjords: a review of the oceanographic environment and dominant physical processes. J. Geol. Soc. Lond. Spec. Publ. 344, 35—50.

Daase, M., Vik, J.O., Bagøien, E., Stenseth, N.C., Eiane, K., 2007. The influence of advection on Calanus near Svalbard: statistical relations between salinity, temperature and copepod abundance. J. Plankton Res. 29 (10), 903—911, http://dx.doi.org/10.1093/plankt/fbm068.

Dalpadado, P., Hop, H., Rønning, J., Pavlov, V., Sperfeld, E., Buchholz, F., Rey, A., Wold, A., 2016. Distribution and abundance of euphausiids and pelagic amphipods in Kongsfjorden, Isfjorden and Rijpfjorden (Svalbard) and changes in their relative importance as key prey in a warming marine ecosystem. Polar Biol. 39 (10), 1765—1784, http://dx.doi.org/10.1007/s00300-015-1874-x.

Darnis, G., Fortier, L., 2014. Temperature, food and the seasonal vertical migration of key arctic copepods in the thermally stratified Amundsen Gulf (Beaufort Sea, Arctic Ocean). J. Plankton Res. 36 (4), 1092—1108, http://dx.doi.org/10.1093/plankt/fbu035.

Drinkwater, K.F., 2006. The regime shift of the 1920s and 1930s in the North Atlantic. Prog. Oceanogr. 68 (2—4), 134—151.

Falk-Petersen, S., Hopkins, C.C.E., Sargent, J.R., 1990. Trophic relationships in the pelagic food web. In: Barnes, M., Gibson, R.N. (Eds.), Trophic Relationships in the Marine Environment. Aberdeen Univ. Press, Aberdeen, 315—333.

Falk-Petersen, S., Pavlov, V., Timofeev, S., Sargent, J.R., 2007. Climate variability and possible effects on arctic food chains: the role of Calanus. In: Ørbæk, J.B., Kallenborn, R., Tombre, I., Hegseth, E.N., Falk-Petersen, S., Hoel, A.H. (Eds.), Arctic Alpine Ecosystems and People in a Changing Environment. Springer-Verlag Berlin Heidelberg, New York, 147—166.

Frank, K.T., Petrie, B., Choi, J.S., Leggett, W.C., 2005. Trophic cascades in a formerly cod-dominated ecosystem. Science 308 (5728), 1621—1623, http://dx.doi.org/10.1126/science.1113075.

Gallienne, C.P., Robins, D.B., 2001. Is *Oithona* the most important copepod in the world's oceans? J. Plankton Res. 23 (12), 1421—1432, http://dx.doi.org/10.1093/plankt/23.12.1421.

Gannefors, C., Böer, M., Kattner, G., Graeve, M., Eiane, K., Gulliksen, B., Hop, H., Falk-Petersen, S., 2005. The Arctic sea butterfly *Limacina helicina*: lipids and life strategy. Mar. Biol. 147 (1), 169—177, http://dx.doi.org/10.1007/s00227-004-1544-y.

Gluchowska, M., Kwasniewski, S., Prominska, A., Olszewska, A., Goszczko, I., Falk-Petersen, S., Hop, H., Weslawski, J.M., 2016. Zooplankton in Svalbard fjords on the Atlantic-Arctic boundary. Polar Biol. 39 (10), 1785—1802, http://dx.doi.org/10.1007/s00300-016-1991-1.

González, H.E., Smetacek, V., 1994. The possible role of the cyclopoid copepod *Oithona* in retarding vertical flux of zooplankton faecal material. Mar. Ecol.-Prog. Ser. 113, 233—246.

Grebmeier, J.M., 2012. Shifting patterns of life in the pacific arctic and sub-arctic seas. Ann. Rev. Mar. Sci. 4, 63—78, http://dx.doi.org/10.1146/annurev-marine-120710-100926.

Hays, G.C., Richardson, A.J., Robinson, C., 2005. Climate change and marine plankton. Trends Ecol. Evol. 20 (6), 337—344, http://dx.doi.org/http://10.1016/j.tree.2005.03.004.

Hirche, H.-J., Hagen, W., Mumm, N., Richter, C., 1994. The Northeast Water Polynya, Greenland Sea, III. Meso- and macrozooplankton distribution and production of dominant herbivorous copepods during spring. Polar Biol. 14 (7), 492—503, http://dx.doi.org/10.1007/BF00239054.

Hirche, H.-J., Laudien, J., Buchholz, F., 2015. Near-bottom zooplankton aggregations in Kongsfjorden: implications for pelagebenthic coupling. Polar Biol. 39 (10), http://dx.doi.org/10.1007/s00300-15-1799-4.

Hop, H., Falk-Petersen, S., Svendsen, H., Kwasniewski, S., Pavlov, V., Pavlova, O., Søreide, J.E., 2006. Physical and biological characteristics of the pelagic system across Fram Strait to Kongsfjorden. Prog. Oceanogr. 71 (2—4), 182—231, http://dx.doi.org/10.1016/j.pocean.2006.09.007.

Hop, H., Pearson, T., Hegseth, E.N., Kovacs, K.M., Wiencke, C., Kwasniewski, S., Eiane, K., Mehlum, F., Gulliksen, B., Wlodarska-Kowalczuk, M., Lydersen, C., Weslawski, J.M., Cochrane, S., Gabrielsen, G.W., Leakey, R.J.G., Lønne, O.J., Zajaczkowski, M., Falk-Petersen, S., Kendall, M., Wängberg, S.-Å., Bischof, K., Voronkov, A.Y., Kovaltchuk, N.A., Wiktor, J., Poltermann, M., di Prisco, G., Papucci, C., Gerland, S., 2002. The marine ecosystem of Kongsfjorden, Svalbard. Polar Res. 21 (1), 167—208.

Hopcroft, R.R., Clarke, C., Nelson, R.J., Raskoff, K.A., 2005. Zooplankton communities of the Arctic's Canada Basin: the contribution by smaller taxa. Polar Biol. 28 (3), 198—206, http://dx.doi.org/10.1007/s00300-004-0680-7.

Huntley, T.L., Lopez, M.D.G., 1992. Temperature-dependent production of marine copepods: a global synthesis. Am. Nat. 140 (2), 201—242, http://dx.doi.org/10.1086/285410.

IPCC (Intergovernmental Panel on Climate Change), 2007. Climate Change 2007: The Physical Science Basis. Contribution of Working Group I to the Fourth Assessment Report of the Intergovernmental Panel on Climate Change, 996 pp.

Jackson, J.B.C., Kirby, M.X., Berger, W.H., Bjorndal, K.A., Botsford, L.W., Bourque, B.J., Bradbury, R.H., Cooke, R., Erlandson, J., Estes, J.A., Hughes, T.P., Kidwell, S., Lange, C.B., Lenihan, H.S., Pandolfi, J.M., Peterson, C.H., Steneck, R.S., Tenger, M.J., Warner, R.R., 2001. Historical overfishing and the recent collapse of coastal ecosystems. Science 293 (5530), 629—637, http://dx.doi.org/10.1126/science.1059199.

Jakubas, D., Gluchowska, M., Wojczulanis-Jakubas, K., Karnovsky, N. J., Keslinka, L., Kidawa, D., Walkusz, W., Boehnke, R., Cisek, M., Kwasniewski, S., Stempniewicz, L., 2011. Foraging effort does not influence body condition and stress level in little auks. Mar. Ecol.-Prog. Ser. 432, 277—290, http://dx.doi.org/10.3354/meps09082.

Koszteyn, J., Kwasniewski, S., 1989. Comparison of fjord and shelf mesozooplankton communities of the southern Spitsbergen region. Rapp. P.-V. Reun. Cons. Int. Explor. Mer. 188, 164—169.

Koszteyn, J., Timofeev, S.F., Weslawski, J.M., Malinga, B., 1995. Size structure *of Themisto abyssorum* Boeck and *Themisto libellula* (Mandt) populations in European Arctic seas. Polar Biol. 15 (2), 85—92, http://dx.doi.org/10.1007/BF00241046.

Kramp, P.L., 1959. The hydromedusae of the Atlantic Ocean and Adjacent waters, Dana Report No. 46. 1—283.

Kwasniewski, S., 1990. A note on zooplankton of the Hornsund Fjord and its seasonal change. Oceanografia 12, 7—27.

Kwasniewski, S., Hop, H., Falk-Petersen, S., Pedersen, G., 2003. Distribution of Calanus species in Kongsfjorden, a glacial fjord in Svalbard. J. Plankton Res. 25 (1), 1—20, http://dx.doi.org/10.1093/plankt/25.1.1.

Kwasniewski, S., Gluchowska, M., Jakubas, D., Wojczulanis-Jakubas, K., Walkusz, W., Karnovsky, N., Blachowiak-Samolyk, K., Cisek, M., Stempniewicz, L., 2010. The impact of different hydrographic conditions and zooplankton communities on provisioning Little Auks along the West coast of Spitsbergen. Prog. Oceanogr. 87 (1—4), 72—82, http://dx.doi.org/10.1016/j.pocean.2010.06.004.

Kwasniewski, S., Walkusz, W., Cottier, F.R., Leu, E., 2013. Mesozooplankton dynamics in relation to food availability during spring and early summer in high latitude glaciated fjord (Kongsfjorden), with focus on Calanus. J. Mar. Syst. 111, 83—96, http://dx.doi.org/10.1016/j.jmarsys.2012.09.012.

Lane, P.V., Llinás, L., Smith, S.L., Pilz, D., 2008. Zooplankton distribution in the western Arctic during summer 2002: hydrographic habitats and implications for food chain dynamics. J. Mar. Syst. 70 (1—2), 87—133, http://dx.doi.org/10.1016/j.jmarsys.2007.04.001.

Lenz, J., 2000. Introduction. In: Harris, R.P., Wiebe, P.H., Lenz, J., Skjoldal, H.R., Huntley, M. (Eds.), ICES Zooplankton Methodology Manual. Academic Press, San Diego, 684 pp.

Lindahl, O., Perissinotto, R., 1987. Short-term variations in the zooplankton community related to water exchange processes in the Gullmar fjord, Sweden. J. Plankton Res. 9 (6), 1113—1132, http://dx.doi.org/10.1093/plankt/9.6.1113.

Lischka, S., Hagen, W., 2005. Life histories of the copepods *Pseudocalanus minutus*, *P. acuspes* (Calanoida) and *Oithona similis* (Cyclopoida) in the arctic Kongsfjorden (Svalbard). Polar Biol. 28 (12), 910—921, http://dx.doi.org/10.1007/s00300-005-0017-1.

Longhurst, A.R., 2007. Ecological Geography of the Sea, 2nd ed. Elsevier, 542 pp.

Lundberg, M., Hop, H., Eiane, K., Gulliksen, B., Falk-Petersen, S., 2006. Population structure and accumulation of lipids in the ctenophore *Mertensia ovum*. Mar. Biol. 149 (6), 1345—1353, http://dx.doi.org/10.1007/s00227-006-0283-7.

Manko, M., 2015. Pelagic coelenterates in the Atlantic sector of the Arctic Ocean — species diversity and distribution as water mass indicators. Oceanol. Hydrobiol. St. 44 (4), 466—479, http://dx.doi.org/10.1515/ohs-2015-0044.

Morán, X.A., López-Urrutia, A., Calvo-Díaz, A., Li, W.K.W., 2010. Increasing importance of small phytoplankton in a warmer ocean. Glob. Chang. Biol. 16 (3), 1137—1144, http://dx.doi.org/10.1111/j.1365-2486.2009.01960.x.

Munk, P., Hansen, B.W., Nielsen, T.G., Thomsen, H.A., 2003. Changes in plankton and fish larvae communities across hydrographic fronts off West Greenland. J. Plankton Res. 25 (7), 815—830, http://dx.doi.org/10.1093/plankt/25.7.815.

Nilsen, F., Cottier, F., Skogseth, R., Mattsson, S., 2008. Fjord — shelf exchanges controlled by ice and brine production: the interannual variation of Atlantic Water in Isfjorden, Svalbard. Cont. Shelf Res. 28 (14), 1838—1853, http://dx.doi.org/10.1016/j.csr.2008.04.015.

Østvedt, O.J., 1955. Zooplankton investigations from weather ship M in the Norwegian Sea, 1948—1949, Det Norske Videnskaps-Akademi i Oslo (Oslo). Hvalrådets Skrifter 40 93 pp.

Pasternak, A., Arashkevich, E., Reigstad, M., Wassmann, P., Falk-Petersen, S., 2008. Dividing mesozooplankton into upper and lower size groups: applications to the grazing impact in the Marginal Ice Zone of the Barents Sea. Deep-Sea Res. Pt. II 55 (20—21), 2245—2256, http://dx.doi.org/10.1016/j.dsr2.2008.05.002.

Pérez-Camacho, A., Beiras, R., Albentosa, M., 1994. Effects of algal food concentration and body size on the ingestion rates of

Ruditapes decussatus (Bivalvia) veliger larvae. Mar. Ecol.-Prog. Ser. 115 (1—2), 87—92.http://www.jstor.org/stable/24849733.

Piwosz, K., Walkusz, W., Hapter, R., Wieczorek, P., Hop, H., Wiktor, J., 2009. Comparison of productivity and phytoplankton in a warm (Kongsfjorden) and cold (Hornsund) Spitsbergen fjord in mid-summer 2002. Polar Biol. 32 (4), 549—559, http://dx.doi.org/10.1007/s00300-008-0549-2.

Platt, T., Denman, K., 1977. Organisation in the pelagic ecosystem. Helgol. wiss. Meeresunters. 30, 575—581.

Polyakov, I.V., Timokhov, L.A., Alexeev, V.A., Bacon, S., Dmitrenko, I. A., Fortier, L., Frolov, I.E., 2010. Arctic Ocean warming contributes to reduced polar ice cap. J. Phys. Oceanogr., http://dx.doi.org/10.1175/2010JPO4339.1.

Postel, L., Fock, H., Hagen, W., 2000. Biomass and abundance. In: Harris, R.P., Wiebe, P.H., Lenz, J., Skjoldal, H.R., Huntley, M. (Eds.), ICES Zooplankton Methodology Manual. Acad. Press, London, 83—192.

Prominska, A., Cisek, M., Walczowski, W., 2017a. Kongsfjorden and Hornsund hydrography — comparative study based on a multiyear survey in fjords of west Spitsbergen. Oceanologia 59 (4), 397—412, http://dx.doi.org/10.1016/j.oceano.2017.07.003.

Prominska, A., Falck, E., Walczowski, W., 2017b. Interannual variability in hydrography and water mass distribution in Hornsund, an Arctic fjord on Svalbard. Polar Res. (submitted for publication).

Richardson, A.J., Schoeman, D.S., 2004. Climate impact on plankton ecosystems in the Northeast Atlantic. Science 305 (5690), 1609—1612, http://dx.doi.org/10.1126/science.1100958.

Rodrigues, J., 2009. The increase in the length of the ice-free season in the Arctic. Cold Reg. Sci. Technol. 59 (1), 78—101, http://dx.doi.org/10.1016/j.coldregions.2009.05.006.

Roff, J.C., Turner, J.T., Webber, M.K., Hopcroft, R.R., 1995. Bacteriovory by tropical copepod nauplii: extent and possible significance. Aquat. Microb. Ecol. 9 (2), 165—175, http://dx.doi.org/10.3354/ame009165.

Rokkan Iversen, K., Seuthe, L., 2011. Seasonal microbial processes in a high-latitude fjord (Kongsfjorden, Svalbard): I. Heterotrophic bacteria, picoplankton and nanoflagellates. Polar Biol. 34 (5), 731—749, http://dx.doi.org/10.1007/s00300-010-0929-2.

Sakshaug, E., Johnsen, G.H., Kovacs, K.M., 2009. Ecosystem Barents Sea. Tapir Academic Press, Trondheim.

Sameoto, D., Wiebe, P., Runge, J., Postel, L., Dunn, J., Miller, C., Coombs, S., 2000. Collecting zooplankton. In: Harris, R., Wiebe, P., Lenz, J., Skjoldal, H.R., Huntley, M. (Eds.), ICES Zooplankton Methodology Manual. Acad. Press, New York, 55—81.

Schulz, K., Kwasniewski, S., 2004. New species of benthopelagic calanoid copepods from Kongsfjorden (Spisbergen, Svalbard Archipelago). Sarsia 89 (3), 143—159, http://dx.doi.org/10.1080/00364820410005214.

Sheldon, R.W., Prakash, A., Sutcliffe Jr., W.H., 1972. The size distribution of particles in the ocean. Limnol. Oceanogr. 17 (3), 327—340, http://dx.doi.org/10.4319/lo.1972.17.3.0327.

Skarðhamar, J., Slagstad, D., Edvardsen, A., 2007. Plankton distributions related to hydrography and circulation dynamics on a narrow continental shelf of Northern Norway. Estuar. Coast. Shelf Sci. 75 (3), 381—392, http://dx.doi.org/10.1016/j.ecss.2007.05.044.

Skjoldal, H.R., Wiebe, P.H., Postel, L., Knutsen, T., Kaartvedt, S., Sameoto, D.D., 2013. Intercomparison of zooplankton (net) sampling systems: results from the ICES/GLOBEC sea-going workshop. Prog. Oceanogr. 108, 1—42, http://dx.doi.org/10.1016/j.pocean.2012.10.006.

Smola, Z., Tatarek, A., Wiktor, J.M., Wiktor Jr., J.M.W., Kubiszyn, A., Weslawski, J.M., in press. Primary producers and production in two West Spitsbergen fjords — comparison of two fjord systems (Hornsund and Kongsfjorden). Pol. Polar Res. (in press).

Stübner, E.I., Søreide, J.E., Reigstad, M., Marquardt, M., Blachowiak-Samolyk, K., 2016. Year-round meroplankton dynamics in high-Arctic Svalbard. J. Plankton Res. 38 (3), 522—536, http://dx.doi.org/10.1093/plankt/fbv124.

Svendsen, H., Beszczynska-Möller, A., Hagen, J.O., Lefauconnier, B., Tverberg, V., Gerald, S., Ørbæk, J.B., Bischof, K., Papucci, C., Zajaczkowski, M., Azzolini, R., Bruland, O., Wiencke, C., Winther, J., Dallmann, W., 2002. The physical environment of Kngsfjorden—Krossfjorden, an Arctic Fjord system in Svalbard. Polar Res. 21 (1), 133—166.

Svensen, C., Seuthe, L., Vasilyeva, Y., Pasternak, A., Hansen, E., 2011. Zooplankton distribution across Fram Strait in autumn: are small copepods and protozooplankton important? Prog. Oceanogr. 91 (4), 534—544, http://dx.doi.org/10.1016/j.pocean.2011.08.001.

Swerpel, S., 1985. The Hornsund Fiord: water masses. Pol. Polar Res. 6 (4), 475—496.

Tranter, D.J. (Ed.), 1968. Monographs on Oceanographic Methodology 2. Zooplankton Sampling. UNESCO, Imprimerie Rolland, Paris, 27—56.

Trudnowska, E., Szczucka, J., Hoppe, Ł., Boehnke, R., Blachowiak-Samolyk, K., 2012. Multidimensional zooplankton observations on the northern West Spitsbergen Shelf. J. Marine Syst. 89—99, 18—25, http://dx.doi.org/10.1016/j.jmarsys.2012.03.001.

Trudnowska, E., Basedow, S.L., Blachowiak-Samolyk, K., 2014. Mid-summer mesozooplankton biomass, its size distribution, and estimated production within a glacial Arctic fjord (Hornsund, Svalbard). J. Marine Syst. 137, 55—66, http://dx.doi.org/10.1016/j.jmarsys.2014.04.010.

Trudnowska, E., Sagan, S., Kwasniewski, S., Darecki, M., Blachowiak-Samolyk, K., 2015. Fine scale zooplankton vertical distribution in relation to hydrographic and optical characteristics of the surface Arctic waters. J. Plankton Res. 37 (1), 120—133, http://dx.doi.org/10.1093/plankt/fbu087.

Turner, J.T., 2004. The importance of small planktonic copepods and their roles in pelagic marine food webs. Zool. Stud. 43 (2), 255—266.

Walczowski, W., Piechura, J., 2011. Influence of the west spitsbergen current on the local climate. Int. J. Climatol. 31 (7), 1088—1093, http://dx.doi.org/10.1002/joc.2338.

Walczowski, W., Piechura, J., Goszczko, I., Wieczorek, P., 2012. Changes in Atlantic water properties: an important factor in the European Arctic marine climate. ICES J. Mar. Sci. 69 (5), 864—869, http://dx.doi.org/10.1093/icesjms/fss068.

Walkusz, W., Storemark, K., Skau, T., Gannefors, C., Lundberg, M., 2003. Zooplankton community structure: a comparison of fjords, open water and ice stations in the Svalbard area. Pol. Polar Res. 24 (2), 149—165.

Walkusz, W., Kwasniewski, S., Falk-Petersen, S., Hop, H., Tverberg, V., Wieczorek, P., Weslawski, J.M., 2009. Seasonal and spatial changes in the zooplankton community of Kongsfjorden, Svalbard. Polar Res. 28, 254—281.

Ward, P., Hirst, A.G., 2007. *Oithona similis* in a high latitude ecosystem: abundance, distribution and temperature limitation of fecundity rates in a sac spawning copepod. Mar. Biol. 151 (3), 1099—1110, http://dx.doi.org/10.1007/s00227-006-0548-1.

Wassmann, P., Duarte, C.M., Agustí, S., Sejr, M.K., 2011. Footprints of climate change in the Arctic marine ecosystem. Glob. Change Biol. 17 (2), 1235—1249, http://dx.doi.org/10.1111/j.1365-2486.2010.02311.x.

Weslawski, J.M., Jankowski, A., Kwasniewski, S., Swerpel, S., Ryg, M., 1991. Summer hydrology and zooplankton in two Svalbard fiords. Pol. Polar Res. 12 (3), 445—460.

Weslawski, J.M., Pedersen, G., Falk-Petersen, S., Porazinski, K., 2000. Entrapment of macroplankton in an Arctic fjord basin, Kongsfjorden, Svalbard. Oceanologia 42 (1), 57—69.

Weslawski, J.M., Kendall, M.A., Wlodarska-Kowalczuk, M., Iken, K., Kedra, M., Legezynska, J., Sejr, M.K., 2011. Climate change effects on Arctic fjord and coastal microbenthic diversity-

—observations and predictions. Mar. Biodiv. 41 (1), 71—85, http://dx.doi.org/10.1007/s12526-010-0073-9.

Weydmann, A., Kwasniewski, S., 2008. Distribution of Calanus populations in a glaciated fjord in the Arctic (Hornsund, Spitsbergen) — the interplay between biological and physical factors. Polar Biol. 31 (9), 1023—1035, http://dx.doi.org/10.1007/s00300-008-0441-0.

Weydmann, A., Søreide, J.E., Kwasniewski, S., Leu, E., Falk-Petersen, S., Berge, J., 2014. Ice-related seasonality in zooplankton community composition in a high Arctic fjord. J. Plankton Res. 35 (4), 831—842, http://dx.doi.org/10.1093/plankt/fbt031.

Weydmann, A., Zwolicki, A., Muś, K., Kwaśniewski, S., 2015. The effect of temperature on egg development rate and hatching success in *Calanus glacialis* and *C. finmarchicus*. Polar Res. 34 (1), 23947, http://dx.doi.org/10.3402/polar.v34.23947.

Wickham, S.A., 1995. Trophic relations between cyclopoid copepods and ciliated protists: complex interactions link the microbial and classic food webs. Limnol. Oceanogr. 40 (6), 1173—1181, http://dx.doi.org/10.4319/lo.1995.40.6.1173.

Willis, K.J., Cottier, F.R., Kwasniewski, S., 2008. Impact of warm water advection on the winter zooplankton community in an Arctic fjord. Polar Biol. 31 (4), 475—482, http://dx.doi.org/10.1007/s00300-007-0373-0.

Willis, K.J., Cottier, F., Kwasniewski, S., Wold, A., Falk-Petersen, S., 2006. The influence of advection on zooplankton community composition in an Arctic fjord (Kongsfjorden, Svalbard). J. Mar. Syst. 61, 39—54.

Zhou, M., Huntley, M.E., 1997. Population dynamics theory of plankton based on biomass spectra. Mar. Ecol.-Prog. Ser. 159, 61—73, http://dx.doi.org/10.3354/meps159061.

Oceanologia (2017) 59, 525—540

Available online at www.sciencedirect.com

ScienceDirect

journal homepage: www.journals.elsevier.com/oceanologia/

ORIGINAL RESEARCH ARTICLE

Impact of shelf-transformed waters (STW) on foraminiferal assemblages in the outwash and glacial fjords of Adventfjorden and Hornsund, Svalbard

Natalia Szymańska*, Joanna Pawłowska, Małgorzata Kucharska, Agnieszka Kujawa, Magdalena Łącka, Marek Zajączkowski

Institute of Oceanology, Polish Academy of Sciences, Sopot, Poland

Received 11 July 2016; accepted 11 April 2017
Available online 30 May 2017

KEYWORDS
Arctic;
Fjords;
Foraminifera

Summary A new dataset of benthic foraminiferal assemblages from Adventfjorden (tributary fjord of Isfjorden, West Spitsbergen) was compared with the results of a study conducted by Zajączkowski et al. (2010) in Hornsund (West Spitsbergen). According to Nilsen et al. (2016), Atlantic water inflow to the Isfjorden Trough occurs more readily than to anywhere else along the shelf of Spitsbergen; thus, we compared the foraminiferal assemblages of the outwash Adventfjorden fjord, located in the Isfjorden system, with glacial Hornsund, located in southwest Spitsbergen. Despite the juxtaposition of Adventfjorden and Hornsund the data revealed varying impacts of shelf-transformed water (STW) on the benthic foraminiferal assemblages. Outer and central Adventfjorden was dominated by *Adercotryma glomerata*, *Recurvoides turbinata* and *Spiroplectammina* sp., reflecting the presence of STW, while abundant *Melonis barleeanus* in the central area of the fjord indicated a large flux of unaltered organic matter. Only the head of the fjord was dominated by the glaciomarine taxa *Cassidulina reniforme* and *Elphidium clavatum*. Foraminiferal fauna characteristic of STW-influenced environments (i.e., *Nonionellina labradorica* and *R. turbinata*) were also observed in outer Hornsund. However, the glacier-proximal taxa *E. clavatum* and *C. reniforme* were dominant throughout the fjord, demonstrating the impacts of meltwater and high sedimentation. Therefore, it is likely that in Hornsund, glacial impact is a major environmental factor, which is stronger than the influence of STW.

* Corresponding author at: Institute of Oceanology, Polish Academy of Sciences, Powstańców Warszawy 55, 81-712 Sopot, Poland. Tel.: +48 (58) 7311661.
E-mail address: natalia@iopan.gda.pl (N. Szymańska).
Peer review under the responsibility of Institute of Oceanology of the Polish Academy of Sciences.

ELSEVIER Production and hosting by Elsevier

http://dx.doi.org/10.1016/j.oceano.2017.04.006

1. Introduction

Foraminifera are widely used in micropaleontology in the reconstruction of diverse past and present marine ecosystems owing to their sensitivity to environmental parameters and the preservation of their hard shells throughout geological time (Murray, 2006). The geochemical composition (e.g., $\delta^{13}C$, $\delta^{18}O$) of foraminifera tests and the changes in foraminiferal assemblages, abundance and diversity are used as proxies of temperature, salinity, oxygen availability and water mass properties (e.g., Hald et al., 2007; Rasmussen et al., 2012; Ślubowska-Woldengen et al., 2008).

The climate and oceanography of West Spitsbergen are shaped primarily by Atlantic water (AW) inflow. A recent study conducted by Nilsen et al. (2016) found that AW flows into the Isfjorden Trough more easily than anywhere else along the shelf of Spitsbergen. They conclude that barotropic water movement in the Spitsbergen shelf depends on January–February wind stress, which accelerates and expands the WSC over its average flow layer of 500-m-long isobaths. Further transport of warm and saline water to Isfjorden is topographically guided. Therefore, Isfjorden is potentially the most AW-impacted fjord of West Spitsbergen, and AW may reach its innermost inlets, including Adventfjorden. Fjords south of Isfjorden, such as Hornsund, receive less AW and thus experience Arctic-like conditions. According to Nilsen et al. (2016), the inflow of AW to Hornsund is limited by the depth of the mouth of the fjord and wind stress that is weaker than that in Isfjorden Trough. In contrast, Adventfjorden is the outwash arm of Isfjorden, with a wide and relatively deep entrance; thus, rapid water exchange with the Spitsbergen shelf occurs.

In the recent years, a growing influence of Atlantic Water on the hydrographic regime of the European Arctic was observed (Arthun et al., 2012). This phenomenon, so-called 'atlantification', affects the functional properties of the Arctic ecosystems (Carmack and Wassmann, 2006). In the light of the latest findings of Nilsen et al. (2016), Adventfjorden may serve as a fjord model for studying the correlation between foraminiferal assemblages and the outreach of STW. Despite the fact that foraminiferal assemblages in the fjords of European Arctic have been widely studied (e.g., Hald and Korsun, 1997; Korsun and Hald, 2000; Skirbekk et al., 2016), there is a need to validate and refine the results of these studies, in the context of contemporary hydrographic and environmental changes.

Previous studies conducted in Adventfjorden have revealed high sensitivity of the fjord to climatic (Zajączkowski et al., 2004) and ecological changes (Pawłowska et al., 2011) and have shown that benthic foraminiferal assemblages reflect past and present environmental variability, largely steered by the inflow of AW (Majewski and Zajączkowski, 2007). However, according to Beszczyńska-Möller et al. (1997), water formed over the Spitsbergen shelf is a mixture of AW, Arctic water (ArW) transported from the Barents Sea and local glacial meltwater that has reached the shelf area, termed shelf-transformed water (STW). Recent changes in AW inflow and associated heat transport to West Spitsbergen have resulted in the creation of large ice-free areas in northern and western Svalbard (Cottier et al., 2007), leading to changes in the productivity and biodiversity of the Arctic ecosystems (Pawłowska et al., 2011). Therefore, linking faunal changes with local oceanographic data may aid in understanding and predicting environmental responses to the changing climate. The aim of this study is to investigate the impact of STW inflow on the foraminiferal assemblages in a glacial (Hornsund) and an outwash (Adventfjorden) fjord. In these two types of fjords, the location of glacial or glaciofluvial outflow in the inner fjord causes environmental gradients in turbidity, suspended organic matter concentration and sediment stability (Syvitski et al., 1987). According to Zajączkowski (2008), the sedimentological regime is consistent between these two types of fjords, however, outwash fjords exhibit more pronounced horizontal gradients in water density than do glacial fjords. Herein, we have compared a new dataset of foraminiferal assemblages from Adventfjorden with the results of a study conducted by Zajączkowski et al. (2010) in Hornsund. Analysed were datasets from late summer (August), for which there are recent, well-developed foraminiferal tests, representing the average conditions of the studied fjords.

2. Study area

The oceanographic regime off West Spitsbergen is shaped by two coastal currents: the West Spitsbergen Current (WSC), carrying AW and the East Spitsbergen Current (ESC), carrying a mixture of Arctic (ArW) and Polar waters (PW; e.g., Cottier et al., 2005). The classification of water masses proposed by Swift (1986) and Hopkins (1991) defines the temperature and salinity of AW as $>3^{\circ}C$ and >34.9, respectively. The ArW is fresher and colder than AW; however, its temperature and salinity vary according to the outflow from land. In the shelf off West Spitsbergen, AW, ArW and glacial water converge and mix, forming STW over the AW and ArW mixing line (Cottier et al., 2005). Based on the intensities of AW and ArW inflow, the waters on the shelf and in the adjacent fjords shift from Arctic to Atlantic dominance in annual cycles (e.g., Aagard et al., 1987; Svendsen et al., 2002).

This study was conducted in Adventfjorden, one of the southern arms of Isfjorden located on the west coast of Spitsbergen (Svalbard; Fig. 1). The wide and more than 100 m deep entrance of Adventfjorden allows for water exchange with the central part of Isfjorden, the largest fjord system on Spitsbergen. Adventfjorden is 8.3 km long and 3.4 km wide and is located between 78°13′ and 78°17′N and 15°25′ and 15°46′E. In the innermost area, there is a 0.7-km-wide tidal flat. The tides are semidiurnal and have a range of 159 cm (Zajączkowski and Włodarska-Kowalczuk, 2007).

The fjord is a marine coastal system, receiving freshwater and terrigenous material of primarily glacial origin. The Adventelva and Longyearelva rivers are the greatest contributors of sediment and freshwater. Freshwater discharge in summer is 3.18 $m^3 s^{-1}$, with a sediment load of 131–151 mg dm^{-3}. Because the rivers remain frozen in winter, this water supply is cut off for 243 days of the year. Sediment accumulation decreases down-fjord from 1.87 to 0.87 cm $year^{-1}$ (Węsławski et al., 1999; Zajączkowski et al., 2004).

The water salinity is approximately 6 near the tidal flat, and at 1.5 km from the flat, it reaches 28. Since 2005, the fjord has remained ice-free during the winter (Zajączkowski et al., 2010). The climate of the region is warmer than expected from its high latitude owing to the influence of

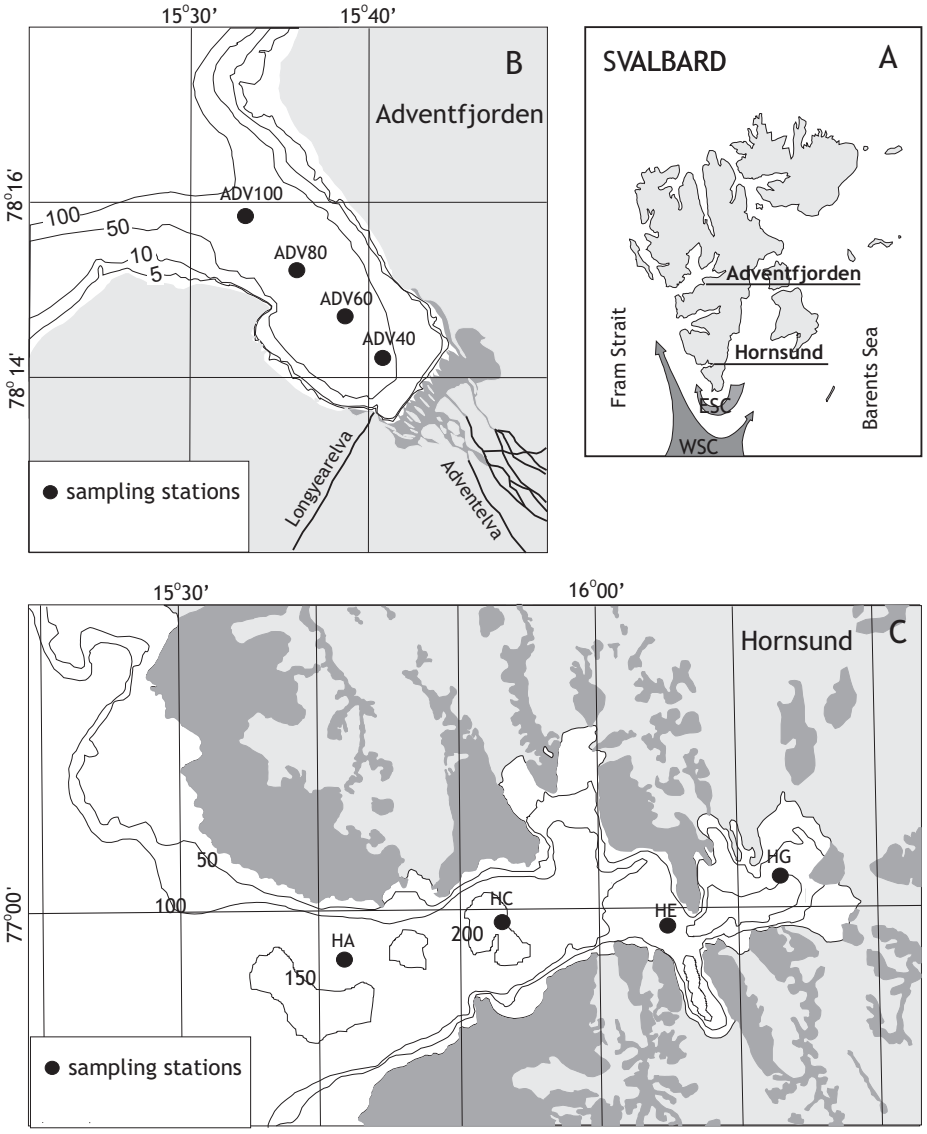

Figure 1 Location of studied fjords (A) and sampling stations in Adventfjorden (B) and Hornsund (C). Sampling stations in Hornsund are from Zajączkowski et al. (2010). WSC — West Spitsbergen Current, ESC — East Spitsbergen Current.

WSC, which transports warm and saline AW northwards. Progressive warming of the WSC over the last decade, as reported by Walczowski and Piechura (2007), has increased the temperature of the STW. In the Isfjorden system, the influence of STW is strongly related to coastal wind stress and the occurrence of winter cyclones in the Fram Strait (Nilsen et al., 2016).

Hornsund is the southernmost fjord of Spitsbergen, located between 77°05′ and 76°53′N and 15°27′ and 16°38′E. The coastline of the fjord encompasses several glacier-proximal basins with depths ranging from 55 to 180 m (Görlich et al., 1987). The fjord is under the influence of STW, with a temperature and salinity of 1°C and 34.7, respectively. STW primarily occupies the central and outer areas of the fjord, whereas the innermost basins are occupied by cold (below 0°C) and saline (35) winter-cooled water (WCW). WCW is produced by salt rejection during sea-ice formation in winter (Beszczyńska-Möller et al., 1997). Hornsund is the most glaciated of the Spitsbergen fjords, as almost 70% of its drainage area is covered by glaciers and 13 tidewater glaciers enter the fjord (Błaszczyk et al., 2013; Hagen et al., 1993). According to Węsławski et al. (1991), up to 12% of the water mass in Hornsund originates from glacial meltwater runoff. Sediment enters through meltwater discharge from the tidewater glaciers. The suspended sediment concentration is the highest in the innermost parts of the glacial bays (Brepollen, Burgerbukta, Isbjörhnamna and Samarinvågen). Sediment accumulation rates vary from 0.5 cm year^{-1} in the inner fjord to 0.7 cm year^{-1} in the mouth of the fjord (Szczuciński et al., 2006).

3. Benthic foraminiferal assemblages in Hornsund

Zajączkowski et al. (2010) investigated the foraminiferal assemblages and modern oceanography of Hornsund. The spatial variation in the foraminiferal assemblages reveals a

zonation stemming from the impact of STW in the area surrounding the mouth of the fjord and glacial meltwater at the head of the fjord.

Outer Hornsund is dominated by a *Nonionellina labradorica* assemblage, with two accessory species, *Recurvoides turbinata* and *Elphidium selseyensis*. The greatest living foraminifera abundance in this part of the fjord is found 3–6 cm below the sediment surface.

In the centre of Hornsund, the boreal *E. selseyensis* is replaced by *Elphidium clavatum*, which is an opportunistic species well-adapted to unstable environments characterised by high sedimentation (Hald and Korsun, 1997). In this part of Hornsund, the *N. labradorica* assemblage is slightly less prevalent; however, it is still abundant in the sediment surface. The numbers of species and agglutinated specimens slightly decreases compared to those in the outer fjord; however, 20 species are still identified, with agglutinated species accounting for 7–30% of the total foraminiferal fauna. The greatest abundance of living foraminifera is found in the upper part of the sediment.

Two sediment cores from the head of Hornsund present proximal glacier conditions. Close to the glacier fronts, agglutinated species disappears completely, and the numbers of foraminiferal individuals and species decreased significantly. *E. clavatum* is dominant; however, the presence of *Cassidulina reniforme* and *N. labradorica* indicates seasonal STW inflow. Furthermore, the presence of *Bucella frigida* indicates sea ice formation during the winter. Most of the living specimens are found in the upper part of the sediment.

4. Methods

This study is based on the analysis of four sediment cores collected from the ship r/v *Oceania* during a sampling campaign in August 2015. A small gravity corer with a 7-cm diameter was used. The temperature and salinity of the water column were measured in 1-s intervals using a Mini CTD Sensordata SD202.

The sampling stations ADV40, ADV60, ADV80 and ADV100 were located along the fjord axis at depths of 40, 60, 80 and 100 m, respectively (Fig. 1). After collection, the 10-cm-long sediment cores were carefully transported to the laboratory in a vertical position and were then cut into 1-cm slices. Sediment was extruded using the piston. Samples were preserved with 70% ethanol solution with Rose Bengal. Rose Bengal allows differentiation between living and dead foraminifera by staining the living individuals. The study by Zajączkowski et al. (2010) of Hornsund found the majority of living foraminiferal individuals in the upper 10 cm of sediment. Therefore, in the present study, foraminiferal fauna from 10-cm-thick sediment was analysed. Next, samples were transported to the Institute of Oceanology PAN in Sopot. In the laboratory, samples were wet-sieved using 500- and 100-μm sieves and dried at 60°C. Samples containing a large number of specimens were divided using a dry microsplitter. When possible, at least 300 foraminiferal specimens were selected and placed on micropaleontological slides. Samples were quantitatively and qualitatively analysed using a microscope for species identification and counting of specimens. Species were identified according to Loeblich and Tappan (1987), and the collection of specimens was stored at the Institute of Oceanology PAN. According to Darling et al. (2016), the morphs traditionally identified as *Elphidium excavatum* f. *clavata* and *E. excavatum* f. *selseyensis* are of two distinct genetic types. Therefore, in the present dataset, the name *E. clavatum* refers to the previously termed *E. excavatum* f. *clavata*. *E. selseyensis* (formerly, *E. excavatum* f. *selseyensis*) is not present in the studied material. Foraminiferal counts are reported as the number of individuals per 10 cm^3 of sediment [ind. 10 cm^{-3}] and as a percent [%] of the total assemblage. Species composition was analysed using Q-mode principal component (PC) analysis of the quantity of living and dead foraminifera specimens. For this purpose, the SYSTAT 11 statistical package was used, and only taxa with an abundance of >1% in at least one sample was considered. Each PC is referred to as a foraminiferal assemblage (FA), named according to the taxa with highest PC scores. PC loadings exceeding 0.4 were regarded as statistically significant (Malmgren and Haq, 1982). Additionally, Shannon–Wiener Index (*H*) was used to express biodiversity. The index was calculated according to the following formula:

$$H = -\sum_{i=1}^{n} p_i \ln p_i,$$

where p_i is the proportion of each specimen belonging to the *i*th species, to the sum of all individuals (Spellerberg and Fedor, 2003).

5. Results

5.1. Adventfjorden oceanography

In the inner fjord (station ADV40), the salinity was lowest on the surface and steadily increased to a depth of 4 m. Four metres from the bottom, the salinity was 33. At the centre of the fjord, the thickness of the brackish surface layer decreased to 2 m and eventually 1 m, but the salinity of the layer was never less than 10. The water temperature exhibited smaller fluctuations than that of the salinity. The surface temperature oscillated around approximately 10°C at all the stations and fell below 3°C at the bottom of the fjord. At the head of the fjord, the temperature reached 5°C at the bottom (Fig. 2).

5.2. Foraminiferal assemblages

In the 40 samples, a total of 8886 specimens were counted, representing 38 species of both living and dead foraminifera. Agglutinated taxa were more abundant than calcareous taxa in the two outermost stations (ADV80 and ADV100; Figs. 3 and 4). At the same stations, dead specimens were dominant over living ones, while the opposite was true for the inner stations (ADV40 and ADV60, Fig. 5). The total counts and percentages of all foraminifera are presented in Appendix 1. The most abundant genus was *Spiroplectammina* sp. (3079 individuals in total), except for at station ADV40, where *E. clavatum* was dominant. *Spiroplectammina biformis* and *Cribrostomoides crassimargo* were the only two species to exceed 1000 specimens in the analysed material (Fig. 6). Clear increasing trends of the sum of living and dead foraminifera specimen

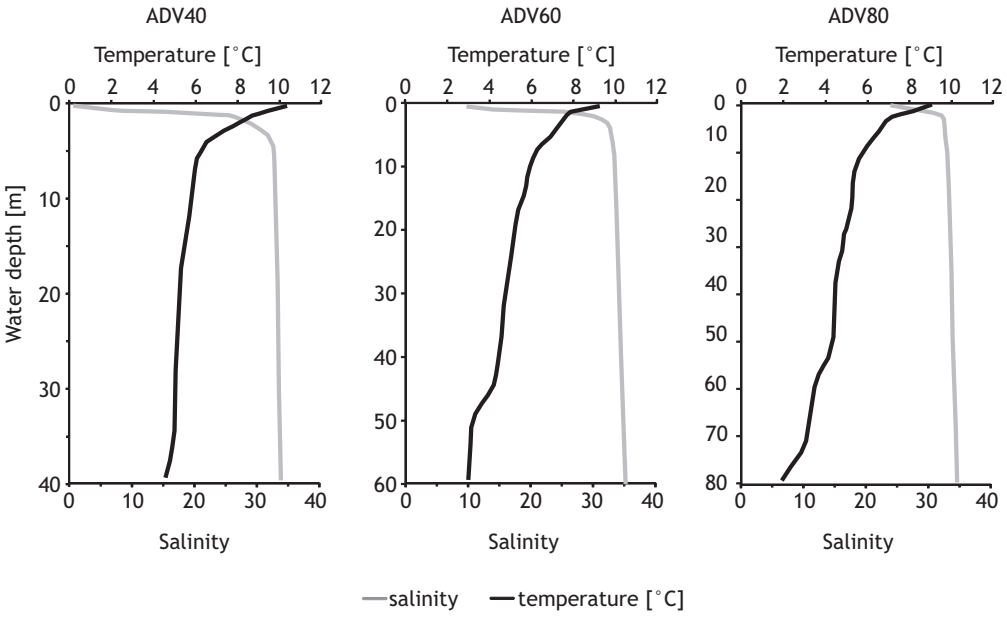

Figure 2 Salinity and temperature of Adventfjorden water in August 2015 measured at stations ADV40, ADV60 and ADV80.

and species richness towards the mouth of the fjord were observed (Figs. 3 and 6). The maximum number of specimens in each station was observed below 4 cm of sediment depth (Fig. 3). The sediment cores revealed great variability in biodiversity. The diversity varied between stations, as well as sediment depths at each station. Station ADV100 was characterised by high species diversity, with a maximum of 16 species found (at a sediment depth of 3 cm), and the Shannon—Wiener diversity index varied between 2 and 2.5 (Figs. 4 and 7). The highest species count of all cores was at station ADV80 at 10 cm in sediment depth, where the Shannon—Wiener diversity index reached its maximum of all samples at 2.8 (Fig. 7). A small number of species were found in stations at the head of the fjord (ADV40, ADV60; Fig. 4).

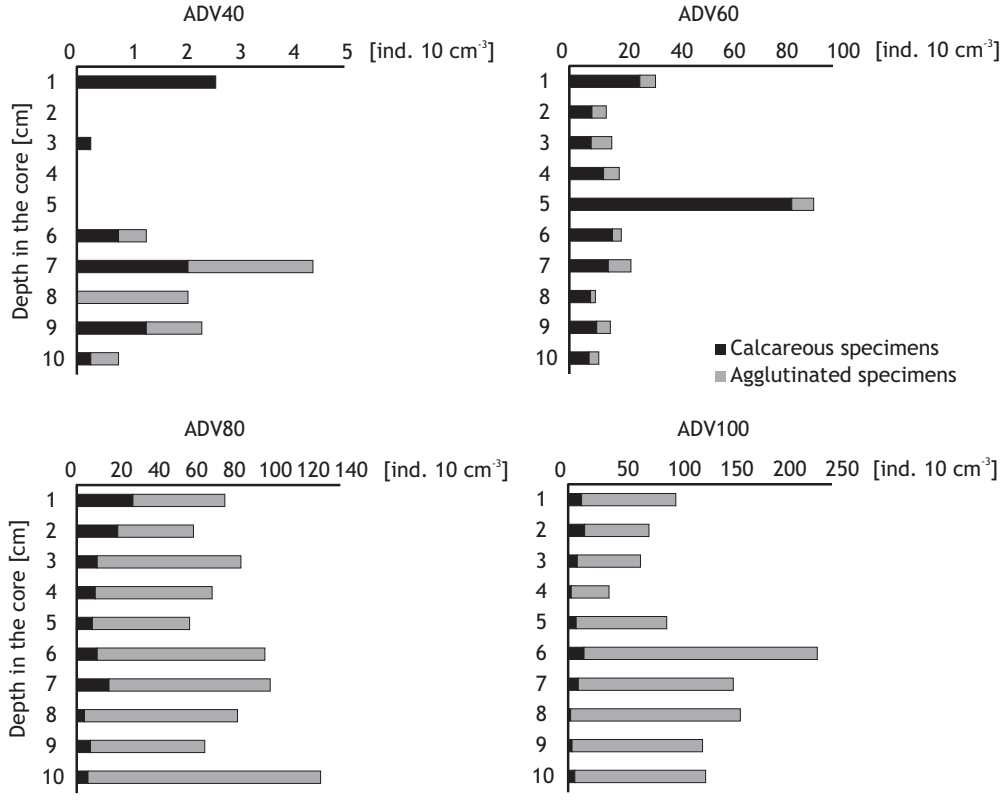

Figure 3 Distribution and quantity of foraminifera individuals, presented as specimens per 10 cm^3.

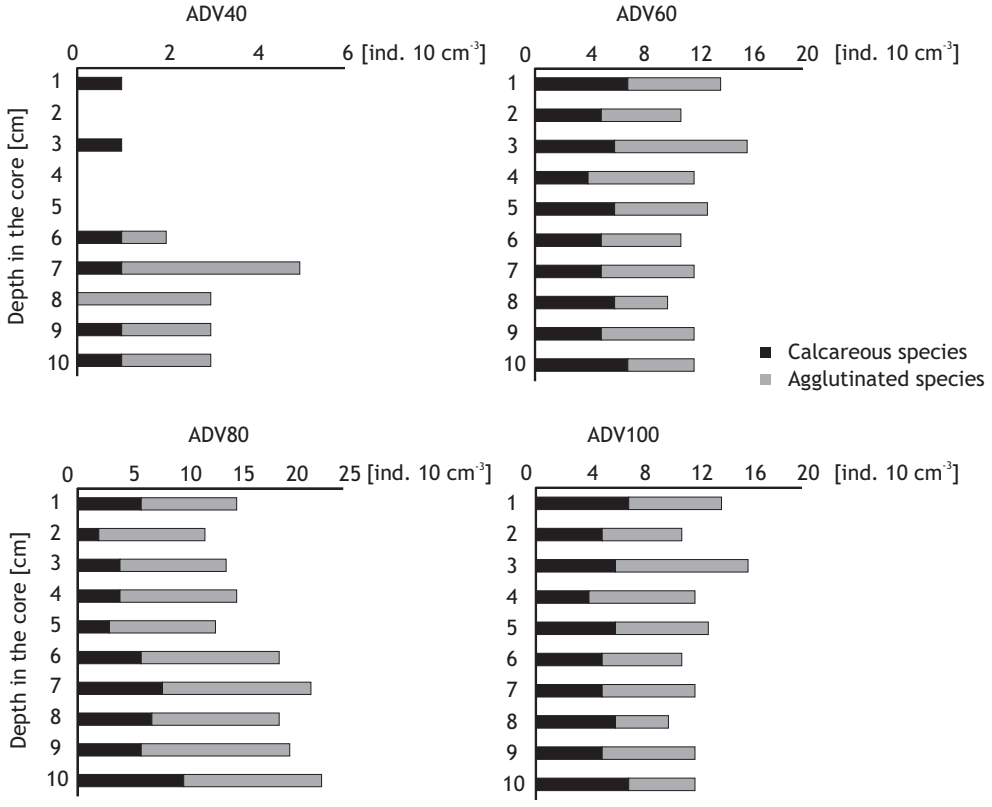

Figure 4 Distribution and quantity of foraminifera species, presented as species per 10 cm^3.

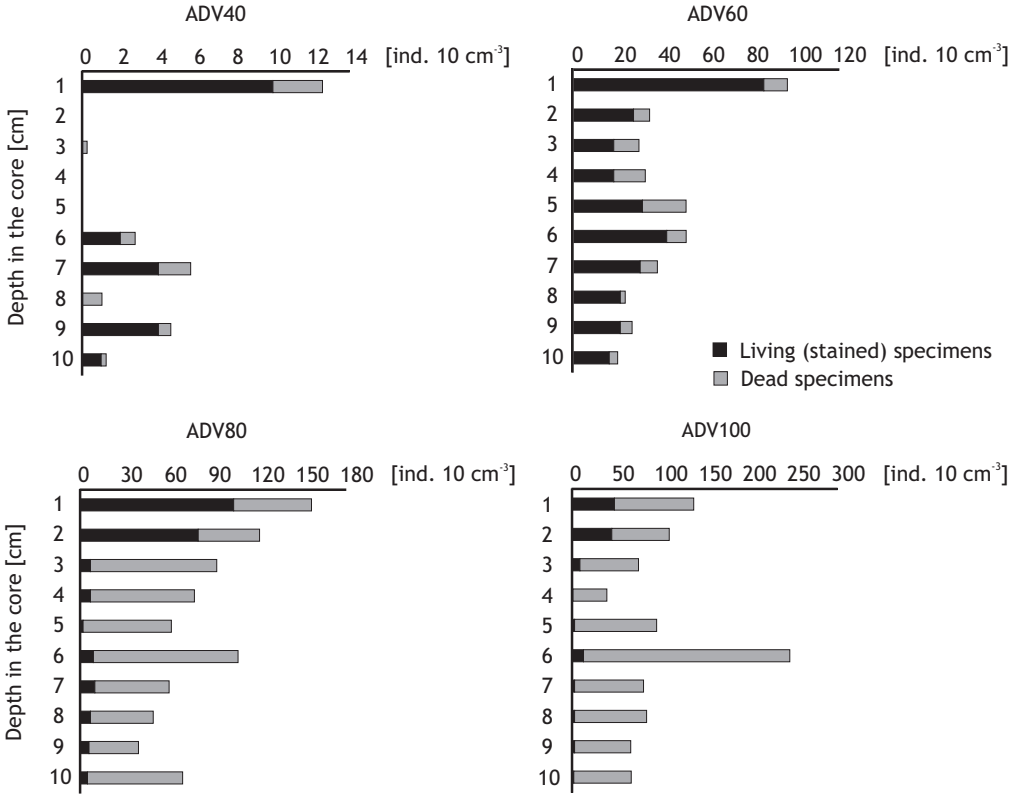

Figure 5 Distribution of living (stained) and dead (unstained) foraminifera specimens, presented as specimens per 10 cm^3.

The foraminiferal assemblage of station ADV100, located at the mouth of the fjord, was characterised by the greatest abundance of individuals, as well as noticeably high species diversity (Figs. 3 and 4). Altogether, 3475 individuals were counted in the core. The most abundant species, *S. biformis*, reached 37 specimens per 10 cm^3 (Fig. 6). Agglutinated taxa were more abundant than calcareous taxa in the two outermost stations (at depths of 80 and 100 m; Figs. 3 and 4). At the same stations, dead specimens were dominant over living ones, while the opposite was true for the inner stations (ADV 40 and ADV 60, Fig. 5). The foraminiferal assemblage at the station ADV 100 was also characterised by high number of living (stained) representatives of *N. labradorica*, especially in the two upper centimetres of sediment depth. Specimens of other species were in large majority found dead (Fig. 8). Most of the agglutinated individuals belonged to the genus

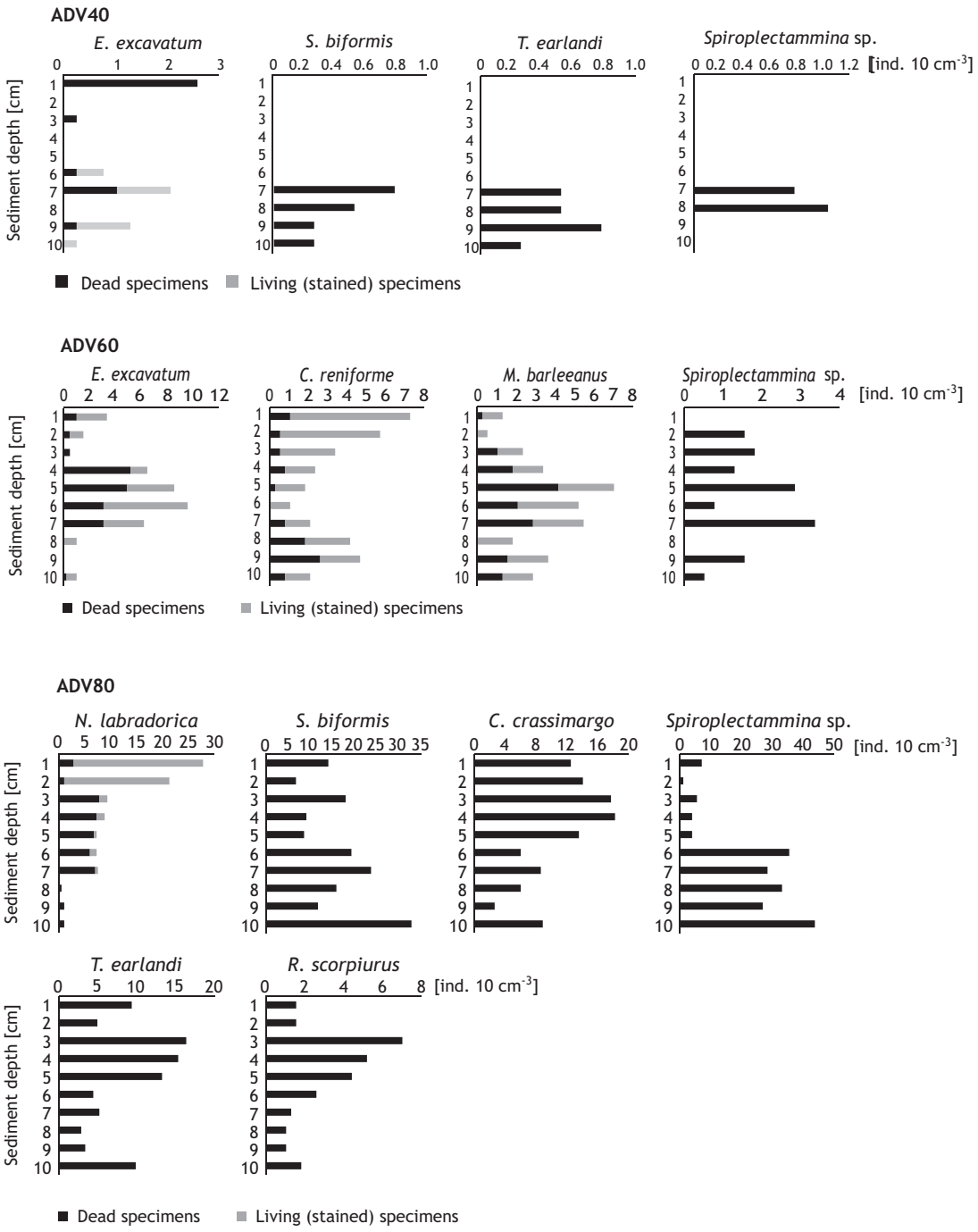

Figure 6 Occurrence of living and dead foraminiferal specimens of dominant foraminiferal taxa (*Elphidium excavatum*, *Spiroplectammina biformis*, *Textularia earlandi*, *Spiroplectammina sp.*, *Cassidulina reniforme*, *Melonis barleeanus*, *Nonionellina labradorica*, *Cribrostomoides crassimargo*, *Reophax scorpiurus*, *Recurvoides turbinata*, *Adercotryma glomerata*, *Ammotium cassis*, *Verneuilina advena*) at the four stations, presented as specimens per 10 cm^3. Taxa comprising more than 2% of total are presented.

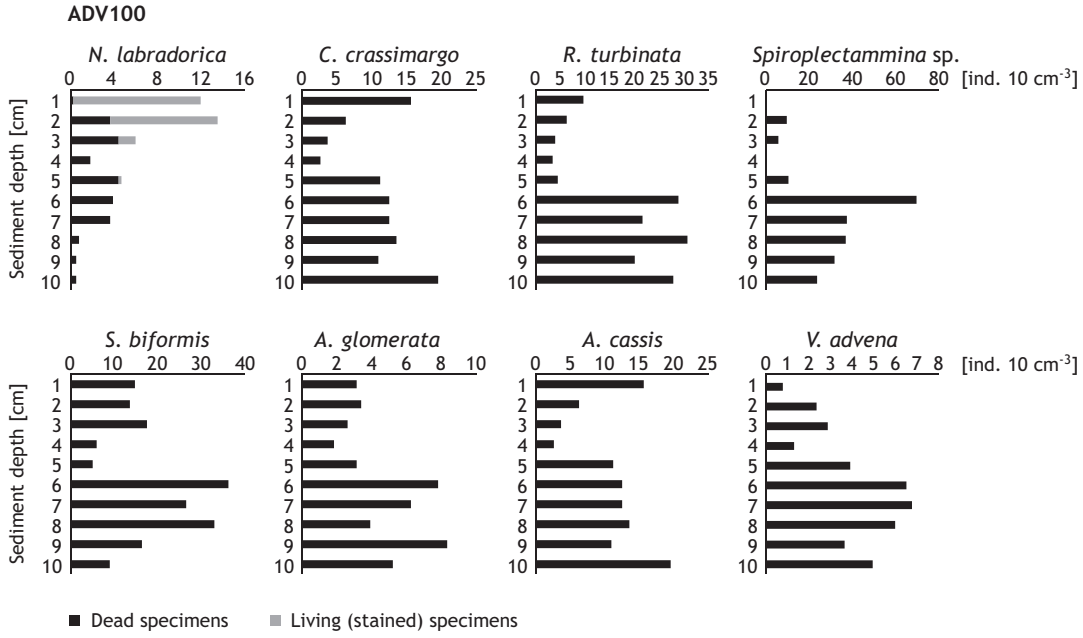

Figure 6 (*Continued*).

Spiroplectammina. The dominant calcareous species was *N. labradorica*, at more than 10 specimens per 10 cm^3 (Figs. 6 and 7). The Shannon—Wiener index was relatively stable, varying between 2 and 2.5 throughout the core (Fig. 7).

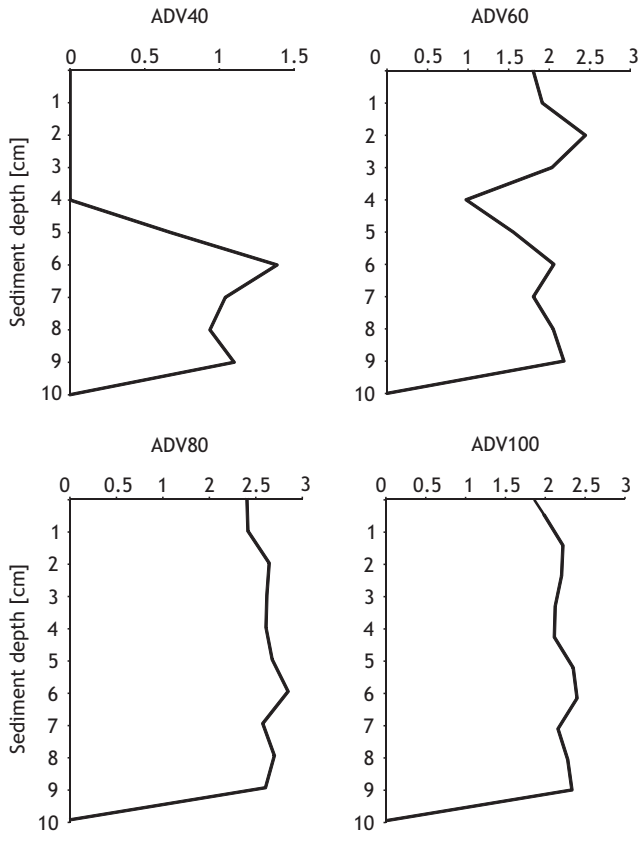

Figure 7 Shannon—Wiener index for foraminiferal assemblages at each station.

At sampling station ADV80, the genus *Spiroplectammina* was also highly abundant, especially at depths below 6 cm, and *S. biformis* reached 40 ind. 10 cm^{-3}. The second most abundant species, *N. labradorica*, reached almost 30 ind. 10 cm^{-3} and was the only calcareous species among the dominant species in ADV80. Generally, the quantity of foraminifera specimens peaked in the deepest part of the core (9—10 cm). The abundance of another calcifying foraminifera species, *E. clavatum*, was noticeably smaller than that of ADV40 and ADV60 (Fig. 3). Station ADV80 was characterised by the highest species Shannon—Wiener index, which reached 2.8 in 6 cm of sediment depth (Fig. 7). The number of living specimens was relatively low, with the exception of the representatives of *N. labradorica* on the sediment depth of 10 cm (100%, Fig. 8).

At sampling station ADV60 revealed a less diverse foraminiferal assemblage compared with those of ADV100 and ADV80. The quantity of specimens was noticeably smaller, although the abundance of *E. clavatum* increased (Fig. 6). The most abundant species in the ADV60 core was *Melonis barleeanus*, which reached 75 ind. 10 cm^{-3} at the depth of 5 cm (Fig. 6). The quantity of foraminifera clearly peaked at 5 cm, exceeding 90 ind. 10 cm^{-3} (Fig. 6). *C. reniforme* reached two abundance maxima at depths of 1 and 8 cm (up to 6 ind. 10 cm^{-3}). At 4 cm, *C. reniforme* abundance dropped noticeably in favour of *M. barleeanus* and *E. clavatum* (Fig. 6). Generally, station ADV60 had the highest percentage of living specimens (Fig. 6). The number of living (stained) specimens of *M. barleeanus* clearly exceeded the number of dead individuals (Fig. 8). The proportion of living specimens of *E. clavatum* reached almost 50% in 6 cm of depth (Fig. 8). Of the dominant calcareous species, *N. labradorica* had the highest percentage of living specimens at 100% at a depth of 2 cm (Figs. 6 and 8).

At the station located near the tidal flat (ADV40), the quantity of foraminifera was distinctly lower than at the other stations, and calcareous taxa were dominant over

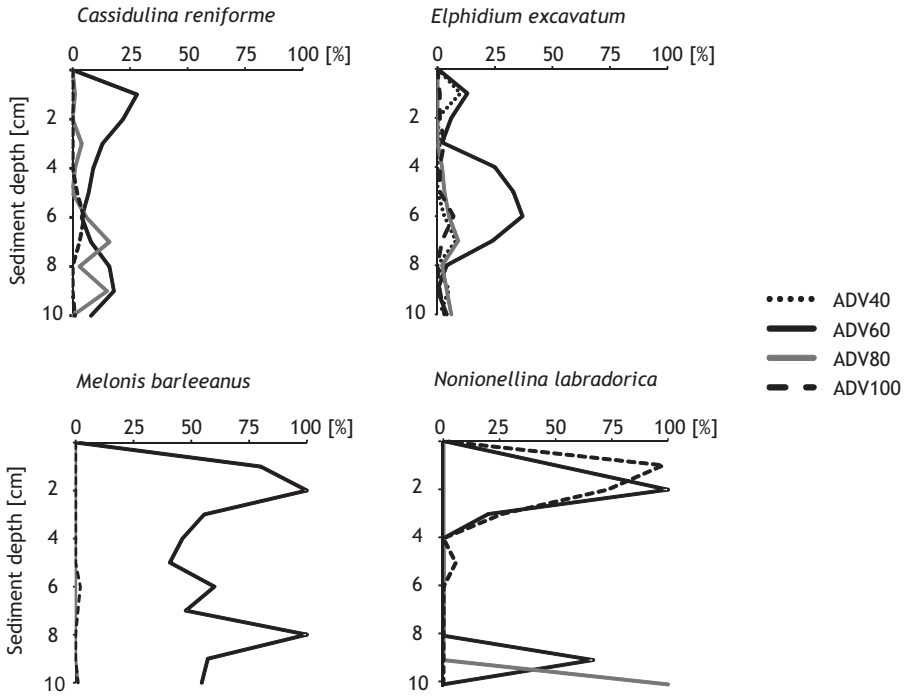

Figure 8 Distribution of the most abundant foraminiferal species as the percent of living (stained) specimens.

agglutinated (Fig. 4). The maximum quantity of foraminifera (5 ind. 10 cm^{-3}) was observed at a depth of 5 cm (Fig. 3). In the ADV40 core, only four species were present: *Cuneata arctica*, *E. clavatum*, *S. biformis* and *Textularia earlandi*. This resulted in the lowest species diversity of all stations and the Shannon—Wiener index peaking at only 1.5 (Fig. 7). *E. clavatum* was the most abundant species (2.5 ind. 10 cm^{-3}) and comprised 50% of the total count in most samples. Living (stained) specimens comprised 10% of the total count (Fig. 8), and these were almost exclusively

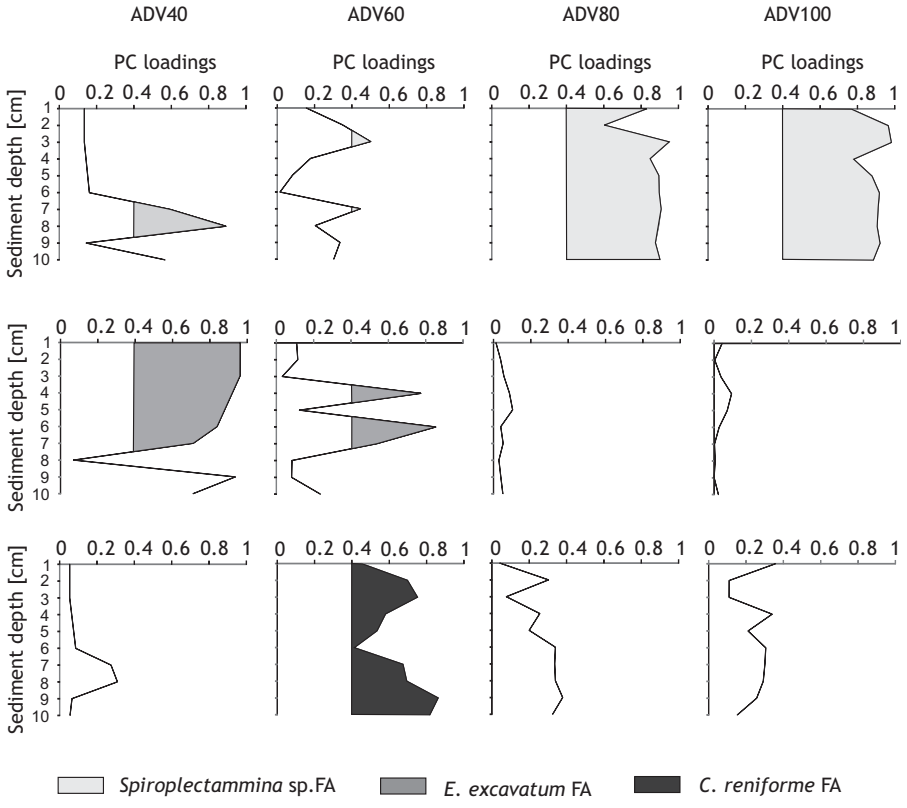

Figure 9 PC loading values for three foraminiferal assemblages. Statistically significant PC loadings are marked in shades of grey.

Table 1 PC scores and percentage of total variance explained by three-factor principal component analysis performed on the sum of living (stained) and dead foraminifera. The dominant taxa are underlined, and accessory species are bolded.

	PC1	PC2	PC3
Percent of total variance explained	48.4	16.8	16.4
Adercotryma glomerata	−0.14137	−0.30133	−0.38282
Ammotium cassis	0.235285	−0.27195	−0.71136
Cassidulina reniforme	−0.64349	−0.54897	**2.699978**
Cibicides lobatulus	−0.40159	−0.29933	−0.2124
Cribrostomoides crassimargo	**1.356035**	−0.02195	**−1.65839**
Cuneata arctica	−0.40037	0.192224	0.344879
Dentalina ittai	−0.42097	−0.2908	−0.24813
Elphidium clavatum	−0.64512	**4.614105**	0.257083
Guttulina dawsoni	−0.42028	−0.28976	−0.2512
Islandiella spp.	−0.42123	−0.29069	−0.24877
Melonis barleeanus	−0.71041	0.057422	**2.314409**
Nonionellina labradorica	0.590668	−0.2811	−0.81346
Quinqueloculina stalkeri	−0.38628	−0.26969	−0.16972
Recurvoides turbinata	0.292502	−0.3727	−0.00953
Reophax scorpiurus	−0.08445	−0.29288	−0.26008
Reophax spp.	−0.37996	−0.32396	−0.02342
Robertina arctica	−0.41299	−0.28574	−0.26516
Spiroplectammina sp.	**4.131051**	0.166076	**1.832678**
Stainforthia feylingi	−0.52469	−0.2965	0.592858
Stainforthia loeblichi	−0.40112	−0.28981	−0.26252
Textularia earlandi	**1.026791**	**0.867865**	**−1.64783**
Textularia torquata	−0.34442	−0.25739	−0.13618
Triloculina frigida	−0.4209	−0.29084	−0.24788
Trochammina nana	−0.35618	−0.32509	−0.17942
Verneuilina advena	−0.11651	−0.29721	−0.31362

representatives of the species *E. clavatum*. Three samples barren of foraminifera were noted at depths of 1–2 and 3–5 cm (Fig. 3).

5.3. Principal component analysis

The principal component analysis explained 89.17% of the total variance in the foraminifera data using a three-factor solution. Each PC was characterised by a dominant and an accessory species. Each PC was referred to as an FA. The assemblages were named after the dominant species (Fig. 9, Table 1).

The *Spiroplectammina* sp. FA with *C. crassimargo* and *T. earlandi* as accessory species explained 48.4% of the foraminiferal variance. All species were agglutinated taxa. The FA *Spiroplectammina* sp. was statistically significant throughout the ADV80 and ADV100 cores and at selected depths in the ADV40 and ADV60 cores (Fig. 9, Table 1).

The second assemblage was named after *E. clavatum*, with accessory species *T. earlandi*. It explained 16.8% of the foraminiferal variance and was abundant in the innermost stations (ADV40 and ADV60). It had a major impact on the sediment surface down to 7 cm in depth (Fig. 9, Table 1).

The *C. reniforme* FA with accessory species *M. barleeanus*, *T. earlandi* and *C. crassimargo* explained 16.4% of the total foraminiferal variance. This was the only FA that was significant at only one station (ADV60), and it was dominant throughout the core (Fig. 9, Table 1).

6. Discussion

6.1. The impact of STW on foraminiferal fauna

In the fjords of Svalbard, the foraminiferal assemblages impacted by STW have been primarily characterised by (i) relatively high biodiversity, (ii) a high abundance of agglutinated taxa and (iii) the presence of *N. labradorica* (e.g., Hald and Korsun, 1997; Zajączkowski et al., 2010). In the Spitsbergen fjords, the presence of *N. labradorica* is positively correlated with the presence of STW (Hald and Korsun, 1997). In the Barents Sea, *N. labradorica* is especially abundant near the highly productive frontal zones and the sea-ice edge (Hald and Steinsund, 1996). Moreover, the presence of *M. barleeanus* may reflect the influence of AW, as observed in the Spitsbergen shelf (Jernas et al., 2013) and modern Norwegian fjords (Husum and Hald, 2004).

In the outermost parts of Adventfjorden (i.e. stations ADV80 and ADV100), the foraminiferal assemblages match all the characteristics of STW-influenced assemblages. An overall increase in foraminiferal abundance and diversity towards the mouth of the fjord was observed. However, this may have resulted from a combination of the impact of STW in the outer fjord with the diminishing impact of the rivers (i.e. decreasing freshwater flux and suspension concentrations). Moreover, *N. labradorica* occurs abundantly in the outer parts of Adventfjorden, matching its general distribution in Arctic fjords. In Svalbard and Novaya Zemlya, peaks of

N. labradorica are characteristic of glacier-distal settings influenced by STW (Hald and Korsun, 1997; Korsun and Hald, 1998; Pogodina, 2005).

Generally, total and agglutinated foraminiferal abundance increased towards the mouth of the fjord, supporting previous findings for Adventfjorden (Majewski and Zajączkowski, 2007). Agglutinated specimens made up to 90% of all foraminiferal specimens in the outermost part of Adventfjorden. Majewski and Zajączkowski (2007) proposed several explanations for such high abundance of agglutinated foraminifera in Adventfjorden. This may partly be explained by a naturally low proportion of calcareous species, which is typical for seasonally ice-free areas (Wollenburg and Kuhnt, 2000). In addition, the dissolution of calcareous tests resulting from lowered pH due to a decay of organic matter may explain the high percentage of agglutinated specimens. The latter explanation is in accordance with the results of Pawłowska et al. (unpublished data – *under review*), which indicate that in Adventfjorden, an organic matter decay in sediments is more intensive in summer than in other seasons, and may possibly have an effect on carbonate preservation in the sediments.

Outer Adventfjorden was dominated by the *Spiroplectammina* sp. FA. The genus *Spiroplectammina* is present in Norwegian and Spitsbergen fjords, as well as on the shelf of Spitsbergen and in the Barents Sea, and it has been reported as the innermost and most shallow-dwelling agglutinated taxa in the shelf regions of the Canadian Arctic (Schröder-Adams et al., 1990) and fjords of Svalbard (Korsun and Hald, 2000). *S. biformis* is also abundantly found in the shallowest parts of northern Norwegian fjords (Murray, 2006). Moreover, the occurrence of *T. earlandi* and *S. biformis* is typical of glaciomarine habitats in the region, while other arenaceous taxa are absent or rare (Hald and Korsun, 1997; Korsun and Hald, 1998). However, data on the modern distribution of *Spiroplectammina* are scarce and geographically patchy and cannot be correlated with certain environmental conditions. For example, Hald and Korsun (1997) did not find a statistically significant correlation between the occurrence of *S. biformis* and any of the analysed environmental parameters.

The high abundance of *R. turbinata* and *Adercotryma glomerata* in outer Adventfjorden may have been related to the presence of STW. Both species are positively correlated with higher temperature and salinity, and their dominance increases towards the outer parts of the Spitsbergen fjords (Hald and Korsun, 1997).

In the inner fjord, the influence of STW on the foraminiferal assemblage was less pronounced and may be reflected by the presence of *N. labradorica*. Moreover, at station ADV60, a great abundance of *M. barleeanus* was noted. The species may be considered an indicator of STW (Jernas et al., 2013); however, its abundance at the other stations was low. The presence of *M. barleeanus* likely results from a large flux of unaltered organic matter on which the species feeds or from the presence of persistent currents at the bottom of the sampling station (Caralp, 1989; Jennings et al., 2004).

Adventfjorden is located relatively far from the Isfjorden Trough, which is the major pathway of water exchange between the Spitsbergen shelf and the central basin of Isfjorden. Because the STW penetrates Isfjorden more deeply than any other fjord along the Spitsbergen coast (Nilsen et al., 2016), the influence of STW is pronounced in Adventfjorden, especially in the outer areas. However, in the innermost part of the fjord, the influence of riverine input prevails over the STW influence on the environment, resulting in the presence of foraminiferal assemblages dominated by *E. clavatum* and *C. reniforme* (Fig. 5). Both taxa are so-called 'glaciomarine' species that thrive in settings with high turbidity and sediment accumulation rates. In Adventfjorden, *E. clavatum* and *C. reniforme* are dominant near the delta slope, which is characterised by high sedimentation rates and subsequent gravity flows and turbidity currents (Zajączkowski and Włodarska-Kowalczuk, 2007), creating environmental stressors that may affect benthic fauna (Wlodarska-Kowalczuk and Pearson, 2004).

Foraminiferal fauna characteristic of STW-influenced environments were also observed in the outer Hornsund. Łącka and Zajączkowski (2016) noted that increased inflow of STW to Hornsund resulted in greater biodiversity and a greater number of rare species. Moreover, they concluded that the presence of *N. labradorica* may be indicative of both STW and high foraminiferal biodiversity. According to Zajączkowski et al. (2010), the species richness was greatest in the outermost part of the fjord. *N. labradorica* and *R. turbinata* were present throughout the fjord, and their abundance decreased towards the head of the fjord. Moreover, the outer and central areas of the fjord were characterised by the presence of *N. labradorica* FA, whereas in the inner fjord, this FA was nearly absent. However, the foraminiferal assemblages in Hornsund were dominated by *C. reniforme* and *E. clavatum* throughout. *E. clavatum* and *C. reniforme* are commonly found in the Barents Sea and in the eastern Greenland shelf, and their occurrence is related to the presence of cold waters with variable salinity (Hald and Steinsund, 1996; Jennings and Helgadóttir, 1994). In the fjords of Svalbard, *C. reniforme* and *E. clavatum* are considered indicative of the influence of meltwater and high sedimentation rates (Hald and Korsun, 1997; Knudsen et al., 2012; Pogodina, 2005). In the Spitsbergen shelf and Nordic Seas, these species are used as ArW indicators (e.g., Ślubowska-Woldengen et al., 2008); however, in Hornsund, their presence may be connected to the presence of cold WCW, which forms in the inner glacial bays (Węsławski et al., 1991).

Hornsund is directly connected to the Spitsbergen shelf, and a wide, no-sill outlet enables direct water exchange. However, the foraminiferal fauna revealed the influence of STW only in the outermost part of the fjord. Central and inner Hornsund were dominated by calcareous, glaciomarine taxa, reflecting the strong influence of glacial meltwater and local waters (Zajączkowski et al., 2010). Therefore, the Hornsund environment is likely shaped by glaciers rather than STW.

6.2. The downcore distribution of foraminiferal fauna

The sampling depth most commonly advised for modern foraminifera studies is the upper 1–2 cm of sediment (Schonfeld et al., 2012), as the majority of living foraminifera is thought to be found there (Murray, 2006). However, according to recent studies, in the Hornsund fjord, living (Rose Bengal-stained) foraminifera appear in depths up to 21 cm, with natural abundance several centimetres below the sedi-

ment surface. This may be attributable to the vertical migration of foraminifera in search of food or oxygen, for example. On the other hand, sediment accumulation, which is relatively high in fjords, may influence the vertical distribution of foraminiferal fauna via the rapid burial of specimens.

The results of this study support the findings of Zajączkowski et al. (2010), as foraminiferal abundance maxima were observed below 4–5 cm in sediment depth. Moreover, previous studies on foraminiferal distribution concluded that there is no universal vertical distribution of species (Murray, 2006). In the case of certain species in the Spitsbergen fjords, the favourable sediment depth is likely fixed. For example, the maximum abundance of *E. clavatum* in both fjords occurred at 4–6 cm in depth, while the majority of *N. labradorica* specimens occurred in the upper 2 cm (see Zajączkowski et al., 2010, for comparison). However, further studies are needed to confirm this assumption.

7. Conclusion

Despite the juxtaposition of an outwash fjord-Adventfjorden and a glaciated fjord-Hornsund, the foraminiferal data revealed varying severity of STW impact on fjord environments. Outwash fjords filled with STW due to their deep entrance, reveal strong influence of STW even far from the inlet. In glacial fjords, the environment is mainly influenced by turbid meltwater and the impact of STW is recorded only in the outer parts of the fjords. Considering these findings, we conclude that studies on both horizontal and vertical distribution of foraminiferal assemblages can provide information on the intensity of STW impact on the fjord environment. Our results confirmed previous assumptions, that foraminiferal assemblages provide information on water mass inflows into fjord systems and thus may serve as a reference for studies on both past and present environmental changes.

Acknowledgements

This work was supported by the National Science Center (grant number 2012/04/A/NZ8/00661) and by the QUAL project funded by the Academy of Finland (grant number 259343).

Appendix 1. Table containing all counted foraminifera species with their abundance and percentage at each sampling station

Sample	ADV40 0–1	ADV40 1–2	ADV40 2–3	ADV40 3–4	ADV40 4–5	ADV40 5–6	ADV40 6–7	ADV40 7–8	ADV40 8–9	ADV40 9–10	Sum in ADV40	% of ADV40 total sum
Astrononion gallowayi (Loeblich and Tapan, 1953)	0	0	0	0	0	0	0	0	0	0	0	0.0
Bolivinellina pseudopunctata (Höglund, 1947)	0	0	0	0	0	0	0	0	0	0	0	0.0
Buccella frigida (Cushman, 1922)	0	0	0	0	0	0	0	0	0	0	0	0.0
Buccella tenerrima (Bandy, 1950)	0	0	0	0	0	0	0	0	0	0	0	0.0
Cassidulina reniforme (Nørvag, 1945)	0	0	0	0	0	0	0	0	0	0	0	0.0
Cibicides lobatulus (Walker and Jacob, 1798)	0	0	0	0	0	0	0	0	0	0	0	0.0
Cornuspira involvens (Reuss, 1850)	0	0	0	0	0	0	0	0	0	0	0	0.0
Cornuspira spp.	0	0	0	0	0	0	0	0	0	0	0	0.0
Dentalina ittai (Loeblich and Tappan, 1953)	0	0	0	0	0	0	0	0	0	0	0	0.0
Elphidium clavatum (Terquem, 1875)	10	0	1	0	0	3	8	0	5	1	28	52.8
Elphidium spp.	0	0	0	0	0	0	0	0	0	0	0	0.0
Elphidium subarcticum (Weiss, 1954)	0	0	0	0	0	0	0	0	0	0	0	0.0
Fissurina marginata (Montagu, 1803)	0	0	0	0	0	0	0	0	0	0	0	0.0
Globobulimina spp.	0	0	0	0	0	0	0	0	0	0	0	0.0
Guttulina dawsoni (Cushman and Ozawa, 1930)	0	0	0	0	0	0	0	0	0	0	0	0.0
Guttulina lactea (Walker and Jacob, 1798)	0	0	0	0	0	0	0	0	0	0	0	0.0
Islandiella helenae (Feyling–Hanssen and Buzas, 1976)	0	0	0	0	0	0	0	0	0	0	0	0.0
Islandiella spp.	0	0	0	0	0	0	0	0	0	0	0	0.0
Lagena gracillima (Seguenza, 1862)	0	0	0	0	0	0	0	0	0	0	0	0.0
Lagena mollis (Cushman, 1944)	0	0	0	0	0	0	0	0	0	0	0	0.0
Melonis barleeanus (Williamson, 1858)	0	0	0	0	0	0	0	0	0	0	0	0.0
Miliolina oblonga (Montagu, 1803)	0	0	0	0	0	0	0	0	0	0	0	0.0
Nonionellina labradorica (Dowson, 1860)	0	0	0	0	0	0	0	0	0	0	0	0.0
Quinqueloculina seminulum (Linnaeus, 1758)	0	0	0	0	0	0	0	0	0	0	0	0.0
Robertinoides charlottensis (Cushman, 1925)	0	0	0	0	0	0	0	0	0	0	0	0.0
Silicosigmoilina groenlandica (Loeblich and Tappan, 1953)	0	0	0	0	0	0	0	0	0	0	0	0.0
Stainforthia feylingi (Knudsen and Seidenkrantz, 1994)	0	0	0	0	0	0	0	0	0	0	0	0.0
Stainforthia loeblichi (Feyling-Hanssen, 1954)	0	0	0	0	0	0	0	0	0	0	0	0.0
Triloculina frigida (Lagoe, 1977)	0	0	0	0	0	0	0	0	0	0	0	0.0
Uvigerina peregrina (Cushman, 1923)	0	0	0	0	0	0	0	0	0	0	0	0.0
Adercotryma glomerata (Brady, 1878)	0	0	0	0	0	0	0	0	0	0	0	0.0
Ammotium cassis (Parker, 1870)	0	0	0	0	0	0	0	0	0	0	0	0.0
Cribrostomoides crassimargo (Norman, 1892)	0	0	0	0	0	0	0	0	0	0	0	0.0
Cuneata arctica (Brady, 1881)	0	0	0	0	0	2	1	0	0	0	3	5.7
Quinqueloculina stalkeri (Loeblich and Tappan, 1953)	0	0	0	0	0	0	0	0	0	0	0	0.0
Recurvoides turbinata (Brady, 1881)	0	0	0	0	0	0	0	0	0	0	0	0.0

Appendix 1. (*Continued*)

Sample	ADV40 0–1	ADV40 1–2	ADV40 2–3	ADV40 3–4	ADV40 4–5	ADV40 5–6	ADV40 6–7	ADV40 7–8	ADV40 8–9	ADV40 9–10	Sum in ADV40	% of ADV40 total sum
Reophax scorpiurus (Montfort, 1808)	0	0	0	0	0	0	0	0	0	0	0	0.0
Reophax spp.	0	0	0	0	0	0	0	0	0	0	0	0.0
Spiroplectammina biformis (Parker and Jones, 1865)	0	0	0	0	0	0	3	2	1	1	7	13.2
Spiroplectammina sp.	0	0	0	0	0	0	3	4	0	0	7	13.2
Textularia earlandi (Parker, 1952)	0	0	0	0	0	0	2	2	3	1	8	15.1
Textularia torquata (Parker, 1952)	0	0	0	0	0	0	0	0	0	0	0	0.0
Trochammina nana (Brady, 1881)	0	0	0	0	0	0	0	0	0	0	0	0.0
Verneuilina advena (Cushman, 1922)	0	0	0	0	0	0	0	0	0	0	0	0.0
Total sum	10	0	1	0	0	5	17	8	9	3	53	100.0

Sample	ADV60 0–1	ADV60 1–2	ADV60 2–3	ADV60 3–4	ADV60 4–5	ADV60 5–6	ADV60 6–7	ADV60 7–8	ADV60 8–9	ADV60 9–10	Sum in ADV60	% of total sum in ADV 60
Astrononion gallowayi (Loeblich and Tapan, 1953)	0	0	0	0	0	0	0	0	0	0	0	0.0
Bolivinellina pseudopunctata (Höglund, 1947)	0	0	0	0	0	0	0	0	0	0	0	0.0
Buccella frigida (Cushman, 1922)	0	0	1	0	0	1	1	0	0	1	4	0.4
Buccella tenerrima (Bandy, 1950)	0	0	0	0	0	0	0	0	1	1	2	0.2
Cassidulina reniforme (Nørvag, 1945)	28	22	13	9	7	4	8	16	18	8	133	13.6
Cibicides lobatulus (Walker and Jacob, 1798)	0	0	0	0	0	0	0	1	0	0	1	0.1
Cornuspira involvens (Reuss, 1850)	0	0	0	0	0	0	0	1	0	0	1	0.1
Cornuspira spp.	0	0	0	0	0	0	0	0	0	0	0	0.0
Dentalina ittai (Loeblich and Tappan, 1953)	0	0	0	0	0	0	0	0	0	0	0	0.0
Elphidium clavatum (Terquem, 1875)	13	6	2	25	33	37	24	4	0	4	148	15.1
Elphidium spp.	1	0	0	0	0	0	0	0	0	0	1	0.1
Elphidium subarcticum (Weiss, 1954)	0	0	0	0	0	0	0	0	0	0	0	0.0
Fissurina marginata (Montagu, 1803)	0	0	0	0	0	0	0	0	0	0	0	0.0
Globobulimina spp.	0	0	0	0	0	0	0	0	0	0	0	0.0
Guttulina dawsoni (Cushman and Ozawa, 1930)	0	0	0	0	0	0	0	0	0	0	0	0.0
Guttulina lactea (Walker and Jacob, 1798)	0	0	0	0	0	0	0	0	0	0	0	0.0
Islandiella helenae (Feyling–Hanssen and Buzas, 1976)	0	0	0	0	0	0	0	0	0	0	0	0.0
Islandiella spp.	0	0	0	0	0	0	0	0	0	0	0	0.0
Lagena gracillima (Seguenza, 1862)	1	0	0	0	1	0	0	0	0	0	2	0.2
Lagena mollis (Cushman, 1944)	0	0	0	0	0	0	0	0	0	0	0	0.0
Melonis barleeanus (Williamson, 1858)	5	2	9	13	277	20	21	7	14	11	379	38.7
Miliolina oblonga (Montagu, 1803)	0	0	0	0	0	0	0	0	0	0	0	0.0
Nonionellina labradorica (Dowson, 1860)	2	1	5	0	5	0	0	2	3	1	19	1.9
Quinqueloculina seminulum (Linnaeus, 1758)	0	0	0	0	0	0	0	0	0	0	0	0.0
Robertinoides charlottensis (Cushman, 1925)	0	0	0	0	0	0	0	0	0	0	0	0.0
Silicosigmoilina groenlandica (Loeblich and Tappan, 1953)	0	0	0	0	0	0	0	0	0	0	0	0.0
Stainforthia feylingi (Knudsen and Seidenkrantz, 1994)	53	2	2	3	2	1	3	0	4	3	73	7.4
Stainforthia loeblichi (Feyling-Hanssen, 1954)	0	0	0	0	0	0	0	0	0	0	0	0.0
Triloculina frigida (Lagoe, 1977)	0	0	0	0	0	0	0	0	0	0	0	0.0
Uvigerina peregrina (Cushman, 1923)	0	0	0	0	0	0	0	0	0	0	0	0.0
Adercotryma glomerata (Brady, 1878)	0	0	0	0	0	0	0	0	1	0	1	0.1
Ammotium cassis (Parker, 1870)	0	0	0	0	0	0	0	0	0	0	0	0.0
Cribrostomoides crassimargo (Norman, 1892)	0	3	2	2	3	2	0	0	0	0	12	1.2
Cuneata arctica (Brady, 1881)	10	1	7	5	2	1	5	0	2	3	36	3.7
Quinqueloculina stalkeri (Loeblich and Tappan, 1953)	1	0	1	1	3	0	2	1	0	0	9	0.9
Recurvoides turbinata (Brady, 1881)	1	6	0	2	0	2	2	3	5	1	22	2.2
Reophax scorpiurus (Montfort, 1808)	0	3	3	0	5	1	0	1	2	0	15	1.5
Reophax spp.	4	0	4	0	3	0	3	0	0	0	14	1.4
Spiroplectammina biformis (Parker and Jones, 1865)	4	2	2	4	5	4	6	0	3	5	35	3.6
Spiroplectammina sp.	0	6	7	5	11	3	13	0	6	2	53	5.4
Textularia earlandi (Parker, 1952)	2	0	2	1	0	0	0	0	1	3	9	0.9
Textularia torquata (Parker, 1952)	0	0	0	3	0	0	2	0	0	0	5	0.5
Trochammina nana (Brady, 1881)	0	0	1	0	0	0	0	0	0	0	1	0.1
Verneuilina advena (Cushman, 1922)	1	0	1	0	0	0	0	2	0	0	4	0.4
Total sum	126	55	62	73	357	76	90	38	60	43	980	100.0

Sample	ADV80 0–1	ADV80 1–2	ADV80 2–3	ADV80 3–4	ADV80 4–5	ADV80 5–6	ADV80 6–7	ADV80 7–8	ADV80 8–9	ADV80 9–10	Sum in ADV80	% of total sum ADV80
Astrononion gallowayi (Loeblich and Tapan, 1953)	1	0	0	0	0	0	0	0	0	2	3	0.1
Bolivinellina pseudopunctata (Höglund, 1947)	0	0	0	0	0	0	0	0	0	1	1	0.0
Buccella frigida (Cushman, 1922)	0	0	0	0	0	1	2	3	1	1	8	0.2
Buccella tenerrima (Bandy, 1950)	0	0	0	0	0	0	4	0	0	4	8	0.2
Cassidulina reniforme (Nørvag, 1945)	1	0	4	1	0	6	16	2	15	0	45	1.4
Cibicides lobatulus (Walker and Jacob, 1798)	0	0	0	0	0	0	4	2	3	2	11	0.3
Cornuspira involvens (Reuss, 1850)	0	2	0	0	0	0	0	0	0	0	2	0.1
Cornuspira spp.	0	0	0	0	0	0	0	0	0	0	0	0.0
Dentalina ittai (Loeblich and Tappan, 1953)	0	0	0	0	0	0	0	0	0	1	1	0.0
Elphidium clavatum (Terquem, 1875)	0	0	0	2	3	5	9	2	4	6	31	1.0
Elphidium spp.	0	0	0	0	0	0	0	0	0	0	0	0.0
Elphidium subarcticum (Weiss, 1954)	0	0	0	0	0	0	0	0	0	0	0	0.0
Fissurina marginata (Montagu, 1803)	0	0	0	0	0	0	0	0	0	0	0	0.0
Globobulimina spp.	1	0	1	0	0	0	0	0	0	0	2	0.1
Guttulina dawsoni (Cushman and Ozawa, 1930)	0	0	0	0	0	0	0	0	0	0	0	0.0
Guttulina lactea (Walker and Jacob, 1798)	0	0	0	0	0	0	0	0	0	1	1	0.0
Islandiella helenae (Feyling–Hanssen and Buzas, 1976)	0	0	0	0	0	0	0	0	0	0	0	0.0

Appendix 1. (*Continued*)

Sample	ADV80 0–1	ADV80 1–2	ADV80 2–3	ADV80 3–4	ADV80 4–5	ADV80 5–6	ADV80 6–7	ADV80 7–8	ADV80 8–9	ADV80 9–10	Sum in ADV80	% of total sum ADV80
Islandiella spp.	0	0	0	0	0	0	0	0	0	0	0	0.0
Lagena gracillima (Seguenza, 1862)	0	0	0	0	0	0	0	0	0	0	0	0.0
Lagena mollis (Cushman, 1944)	0	0	0	0	0	1	1	0	0	0	2	0.1
Melonis barleeanus (Williamson, 1858)	0	0	0	0	0	0	0	0	0	1	1	0.0
Miliolina oblonga (Montagu, 1803)	0	0	0	0	0	1	0	0	0	0	1	0.0
Nonionellina labradorica (Dowson, 1860)	104	82	36	34	28	28	29	2	4	4	351	10.8
Quinqueloculina seminulum (Linnaeus, 1758)	2	0	1	0	0	0	0	0	0	0	3	0.1
Robertinoides charlottensis (Cushman, 1925)	0	0	0	0	0	0	0	0	0	0	0	0.0
Silicosigmoilina groenlandica (Loeblich and Tappan, 1953)	0	0	0	0	0	0	0	0	0	0	0	0.0
Stainforthia feylingi (Knudsen and Seidenkrantz, 1994)	0	0	0	0	0	0	0	4	0	0	4	0.1
Stainforthia loeblichi (Feyling-Hanssen, 1954)	6	0	0	1	1	0	0	0	1	0	9	0.3
Triloculina frigida (Lagoe, 1977)	0	0	0	0	0	0	1	0	0	0	1	0.0
Uvigerina peregrina (Cushman, 1923)	0	0	0	0	0	0	0	1	0	0	1	0.0
Adercotryma glomerata (Brady, 1878)	0	8	11	1	3	1	3	3	4	8	42	1.3
Ammotium cassis (Parker, 1870)	5	20	5	7	4	3	8	17	6	9	84	2.6
Cribrostomoides crassimargo (Norman, 1892)	48	54	68	70	52	23	33	23	10	34	415	12.7
Cuneata arctica (Brady, 1881)	0	0	0	6	2	19	16	8	9	16	76	2.3
Quinqueloculina stalkeri (Loeblich and Tappan, 1953)	2	2	4	2	0	0	2	0	2	4	18	0.6
Recurvoides turbinata (Brady, 1881)	9	14	12	8	10	14	8	25	6	21	127	3.9
Reophax scorpiurus (Montfort, 1808)	6	6	27	20	17	10	5	4	4	7	106	3.3
Reophax spp.	0	0	0	0	0	19	11	2	5	8	45	1.4
Spiroplectammina biformis (Parker and Jones, 1865)	54	26	69	35	33	74	91	61	45	126	614	18.9
Spiroplectammina sp.	27	4	21	15	15	136	109	127	103	168	725	22.3
Textularia earlandi (Parker, 1952)	36	19	63	59	51	17	20	11	13	38	327	10.0
Textularia torquata (Parker, 1952)	0	0	0	0	0	6	9	20	13	25	73	2.2
Trochammina nana (Brady, 1881)	0	0	0	0	0	10	10	0	6	0	26	0.8
Verneuilina advena (Cushman, 1922)	1	2	14	16	12	11	5	12	8	12	93	2.9
Total sum	303	239	336	277	231	385	396	329	262	499	3257	100.0

Sample	ADV100 0–1	ADV100 1–2	ADV100 2–3	ADV100 3–4	ADV100 4–5	ADV100 5–6	ADV100 6–7	ADV100 7–8	ADV100 8–9	ADV100 9–10	Sum in ADV100	% of total sum ADV100	Total sum of specimens in all samples	% of total sum of specimens in all samples
Astrononion gallowayi (Loeblich and Tapan, 1953)	0	0	0	0	0	3	0	0	0	0	3	0.1	6	0.1
Bolivinellina pseudopunctata (Höglund, 1947)	0	0	0	0	0	0	0	0	0	0	0	0.0	1	0.0
Buccella frigida (Cushman, 1922)	0	0	2	1	2	11	6	1	4	2	29	0.6	41	0.5
Buccella tenerrima (Bandy, 1950)	0	0	0	0	0	2	6	3	2	1	14	0.3	24	0.3
Cassidulina reniforme (Nørvag, 1945)	0	0	0	0	2	5	3	0	0	1	11	0.2	189	2.1
Cibicides lobatulus (Walker and Jacob, 1798)	0	0	4	1	1	2	0	2	3	3	16	0.3	28	0.3
Cornuspira involvens (Reuss, 1850)	0	0	0	0	0	1	0	0	0	0	1	0.0	4	0.0
Cornuspira spp.	0	0	0	0	0	0	1	0	0	0	1	0.0	1	0.0
Dentalina ittai (Loeblich and Tappan, 1953)	0	0	0	0	0	0	0	0	1	1	2	0.0	3	0.0
Elphidium clavatum (Terquem, 1875)	1	1	3	1	1	7	2	0	1	3	20	0.4	227	2.6
Elphidium spp.	0	0	0	0	0	0	0	0	0	0	0	0.0	1	0.0
Elphidium subarcticum (Weiss, 1954)	0	0	0	0	0	0	1	0	0	0	1	0.0	1	0.0
Fissurina marginata (Montagu, 1803)	0	0	0	0	0	0	0	0	0	1	1	0.0	1	0.0
Globobulimina spp.	0	0	0	0	0	0	0	0	0	0	0	0.0	2	0.0
Guttulina dawsoni (Cushman and Ozawa, 1930)	0	0	0	0	1	0	0	0	0	1	2	0.0	2	0.0
Guttulina lactea (Walker and Jacob, 1798)	0	0	0	0	0	0	0	0	0	1	1	0.0	2	0.0
Islandiella helenae (Feyling–Hanssen and Buzas, 1976)	0	0	0	0	0	0	0	0	1	0	1	0.0	1	0.0
Islandiella spp.	0	0	0	0	0	0	0	0	0	2	2	0.0	2	0.0
Lagena gracillima (Seguenza, 1862)	0	0	0	0	1	0	0	0	0	0	1	0.0	3	0.0
Lagena mollis (Cushman, 1944)	0	0	0	0	0	0	0	0	0	1	1	0.0	3	0.0
Melonis barleeanus (Williamson, 1858)	0	0	0	0	0	2	1	0	0	1	4	0.1	384	4.3
Miliolina oblonga (Montagu, 1803)	0	0	0	0	0	0	0	0	0	0	0	0.0	1	0.0
Nonionellina labradorica (Dowson, 1860)	46	52	23	7	18	15	14	3	2	2	182	4.0	552	6.2
Quinqueloculina seminulum (Linnaeus, 1758)	0	0	0	0	0	0	0	0	0	0	0	0.0	3	0.0
Robertinoides charlottensis (Cushman, 1925)	2	0	0	1	0	1	0	0	0	0	4	0.1	4	0.0
Silicosigmoilina groenlandica (Loeblich and Tappan, 1953)	0	0	0	0	0	1	0	0	0	0	1	0.0	1	0.0
Stainforthia feylingi (Knudsen and Seidenkrantz, 1994)	0	6	1	0	3	8	1	0	0	1	20	0.4	97	1.1
Stainforthia loeblichi (Feyling-Hanssen, 1954)	0	1	0	0	0	0	1	0	0	2	4	0.1	13	0.1
Triloculina frigida (Lagoe, 1977)	0	0	0	0	0	0	1	0	0	1	2	0.0	3	0.0
Uvigerina peregrina (Cushman, 1923)	0	0	0	0	0	0	0	0	0	0	0	0.0	1	0.0
Adercotryma glomerata (Brady, 1878)	12	13	10	7	12	30	24	15	32	20	175	3.8	218	2.5
Ammotium cassis (Parker, 1870)	60	24	14	10	43	48	48	52	42	75	416	9.1	500	5.6

Appendix 1. (*Continued*)

Sample	ADV100 0–1	ADV100 1–2	ADV100 2–3	ADV100 3–4	ADV100 4–5	ADV100 5–6	ADV100 6–7	ADV100 7–8	ADV100 8–9	ADV100 9–10	Sum in ADV100	% of total sum ADV100	Total sum of specimens in all samples	% of total sum of specimens in all samples
Cribrostomoides crassimargo (Norman, 1892)	86	42	49	32	101	87	52	52	63	80	644	14.0	1071	12.1
Cuneata arctica (Brady, 1881)	0	0	0	0	0	21	12	19	2	2	56	1.2	171	1.9
Quinqueloculina stalkeri (Loeblich and Tappan, 1953)	1	0	0	2	0	7	4	1	2	2	19	0.4	46	0.5
Recurvoides turbinata (Brady, 1881)	37	24	15	13	17	111	83	118	77	107	602	13.1	751	8.5
Reophax scorpiurus (Montfort, 1808)	6	7	14	7	3	9	13	6	8	10	83	1.8	204	2.3
Reophax spp.	0	0	0	0	0	11	7	5	4	1	28	0.6	87	1.0
Spiroplectammina biformis (Parker and Jones, 1865)	64	59	76	26	22	157	115	143	71	39	772	16.8	1428	16.1
Spiroplectammina sp.	0	37	22	0	40	268	144	142	122	91	866	18.8	1651	18.6
Textularia earlandi (Parker, 1952)	75	20	20	36	78	44	9	22	14	11	329	7.2	673	7.6
Textularia torquata (Parker, 1952)	0	0	0	0	0	9	14	9	11	11	54	1.2	132	1.5
Trochammina nana (Brady, 1881)	0	0	0	0	0	25	15	13	15	10	78	1.7	105	1.2
Verneuilina advena (Cushman, 1922)	3	9	11	5	15	25	26	23	14	19	150	3.3	247	2.8
Total sum	393	295	264	149	360	910	603	629	491	502	4596	100.0	8886	100.0

References

Aagard, K., Foldvik, A., Hillman, S.R., 1987. The West Spitsbergen current: disposition and water mass transformation. J. Geophys. Res. 92 (C4), 3778–3784, http://dx.doi.org/10.1029/JC092iC04p03778.

Årthun, M., Eldevik, T., Smedsrud, L.H., Skagseth, Ø., Ingvaldsen, R. B., 2012. Qunatifying the influence of Atlantic heat on Barents Sea ice variability and retreat. J. Climate 25 (13), 4736–4743, http://dx.doi.org/10.1175/JCLI-D-11-00466.1.

Beszczyńska-Möller, A., Węsławski, J.M., Walczowski, W., Zajączkowski, M., 1997. Estimation of glacial meltwater discharge into Svalbard coastal waters. Oceanologia 39 (3), 289–298.

Błaszczyk, M., Jania, J., Kolondra, L., 2013. Fluctuations of tidewater glaciers in Hornsund Fjord (Southern Svalbard) since the beginning of the 20th century. Pol. Polar Res. 34 (4), 327–352, http://dx.doi.org/10.2478/popore-2013-0024.

Caralp, M.H., 1989. Size and morphology of the benthic foraminifer *Melonis barleeanum*; relationships with marine organic matter. J. Foramin. Res. 19 (3), 235–245, http://dx.doi.org/10.2113/gsjfr.19.3.235.

Carmack, E., Wassmann, P., 2006. Food webs and physical–biological coupling on pan-Arctic shelves: unifying concepts and comprehensive perspectives. Progr. Oceanogr. 71 (2–4), 446–477, http://dx.doi.org/10.1016/j.pocean.2006.10.004.

Cottier, F.R., Nilsen, F., Inall, M.E., Gerland, S., Tverberg, V., Svendsen, H., 2007. Wintertime warming of an Arctic shelf in response to large-scale atmospheric circulation. Geophys. Res. Lett. 34 (10), L10607, http://dx.doi.org/10.1029/2007GL029948.

Cottier, F.R., Tverberg, V., Inall, M.E., Svendsen, H., Nilsen, F., Griffiths, C., 2005. Water mass modification in an Arctic fjord through cross-shelf exchange: the seasonal hydrography of Kongsfjorden. Svalbard. J. Geophys. Res. 110, C12005, http://dx.doi.org/10.1029/2004JC002757.

Darling, K.F., Schweizer, M., Knudsen, K.L., Evans, K.M., Bird, C., Roberts, A., Filipsson, H.L., Kim, J.H., Gudmundsson, G., Wade, C.M., Sayer, M.D.J., William, A.E.N., 2016. The genetic diversity, phylogeography and morphology of Elphidiidae (Foraminifera) in the Northeast Atlantic. Mar. Micropaleontol. 129, 1–23, http://dx.doi.org/10.1016/j.marmicro.2016.09.001.

Görlich, K., Węsławski, J.M., Zajączkowski, M., 1987. Suspension settling effect on macrobenthos biomass distribution in the Hornsund fjord. Spitsbergen. Polar Res. 5, 175–192.

Hagen, J.O., Liestøl, R.E., Jørgensen, T., 1993. Glacier atlas of Svalbard and Jan Mayen. Meddelelser 129, PDF 169 pp., http://hdl.handle.net/11250/173065.

Hald, M., Andersson, C., Ebbesen, H., Jansen, E., Klitgaared-Kristensen, D., Risebrobakken, B., Salomonsen, G.R., Sarntheim, H. P., Sejrup, H.P., Telford, R.J., 2007. Variations in temperature and extent of Atlantic Water in the northern North Atlantic during the Holocene. Quat. Sci. Rev. 26 (25–28), 3423–3440, http://dx.doi.org/10.1016/j.quascirev.2007.10.005.

Hald, M., Korsun, S., 1997. Distribution of modern benthic foraminifera from fjords of svalbard, European Arctic. J. Foramin. Res. 27 (2), 101–122.

Hald, M., Steinsund, P.I., 1996. Benthic foraminifera and carbonate dissolution in the surface sediments of the Barents and Kara Seas. Ber. Polarforsch. 212, 285–307.

Hopkins, T.S., 1991. The GIN Sea-A synthesis of its physical oceanography and literature review 1972–1985. Earth Sci. Rev. 30, 175–318.

Husum, K., Hald, M., 2004. A continuous marine record 8000-1600 cal yr BP from the Malangenfjord, north Norway: foraminiferal and isotopic evidence. Holocene 14 (6), 877–887.

Jennings, A.E., Helgadóttir, G., 1994. Foraminiferal assemblages from the fjords and shelf of eastern Greenland. J. Foramin. Res. 24 (2), 123–144, http://dx.doi.org/10.2113/gsjfr.24.2.123.

Jennings, A.E., Weiner, N.J., Helgadottir, G., Andrews, J.T., 2004. Modern foraminiferal faunas of the southwestern to northern Iceland Shelf; oceanographic and environmental controls. J. Foramin. Res. 34 (3), 180–207, http://dx.doi.org/10.2113/34.3.180.

Jernas, P., Klitgaard Kristensen, D., Husum, K., Wilson, L., Koç, N., 2013. Palaeoenvironmental changes of the last two millennia on the western and northern Svalbard shelf. Boreas 42 (1), 236–255, http://dx.doi.org/10.1111/j.1502-3885.2012.00293.x.

Knudsen, L.K., Eiríksson, J., Bartels-Jónsdóttir, H.B., 2012. Oceanographic changes through the last millennium off North Iceland, temperature and salinity reconstructions based on foraminifera and stable isotopes. Mar. Micropaleontol. 84–85, 54–73, http://dx.doi.org/10.1016/j.marmicro.2011.11.002.

Korsun, S., Hald, M., 1998. Modern benthic foraminifera off Novaya Zemlya tidewater glaciers, Russian Arctic. Arc. Alp. Res. 30 (1), 61–77.

Korsun, S., Hald, M., 2000. Seasonal dynamics of benthic foraminifera in a glacially fed fjord of Svalbard, European Arctic. J. Foramin. Res. 30 (4), 251–271, http://dx.doi.org/10.2113/0300251.

Łącka, M., Zajączkowski, M., 2016. Does the recent pool of benthic foraminiferal tests in fjordic surface sediments reflect interannual environmental changes? The resolution limit of the foraminiferal record. Ann. Soc. Geol. Pol. 86 (1), 59–71, http://dx.doi.org/10.14241/asgp.2015.019.

Loeblich, A.R., Tappan, H., 1987. Foraminiferal Genera and their Classification. Van Nostrand Rienhold Co., New York.

Majewski, W., Zajączkowski, M., 2007. Benthic foraminifera in Adventfjorden, Svalbard: last 50 years of local hydrographic changes. J. Foramin. Res. 37 (2), 15—32, http://dx.doi.org/10.2113/gsjfr.37.2.107.

Malmgren, B.A., Haq, B.U., 1982. Asessment of quantitative techniques in paleobiogeography. Mar. Micropaleontol. 7 (3), 269—285.

Murray, J., 2006. Ecology and Applications of Benthic Foraminifera. Cambridge Univ. Press, Cambridge, UK, p. 440.

Nilsen, F., Skogseth, R., Vaardal-Lunde, J., Inall, M., 2016. A simple shelf circulation model — intrusion of Atlantic water on the West Spitsbergen Shelf. J. Phys. Oceanogr. 46, 1209—1230, http://dx.doi.org/10.1175/JPO-D-15-0058.1.

Pawłowska, J., Włodarska-Kowalczuk, M., Zajączkowski, M., Nygård, H., Berge, J., 2011. Seasonal variability of meio- and macrobenthic standing stocks and diversity in an Arctic fjord (Adventfjorden, Spitsbergen). Polar Biol. 34 (6), 833—845, http://dx.doi.org/10.1007/s00300-010-0940-7.

Pogodina, I.A., 2005. Benthic foraminifera in Hornsund fjord (West Spitsbergen). Oceanology 45 (4), 528—535.

Rasmussen, T.L., Forwick, M., Mackensen, A., 2012. Reconstruction of inflow of Atlantic Water to Isfjorden, Svalbard during the Holocene: correlation to climate and seasonality. Mar. Micropaleontol. 94—95, 80—90, http://dx.doi.org/10.1016/j.marmicro.2012.06.008.

Schönfeld, J., Alve, E., Spezzaferri, S., 2012. The FOBIMO (FOraminiferal BIo-MOnitoring) initiative—Towards a standardised protocol for soft-bottom benthic foraminiferal monitoring studies. Marine Micropaleontol. 9495, 1—13.

Schröder-Adams, C.J., Cole, F.E., Medioli, F.S., Mudie, P.J., Scott, D., Dobbin, L., 1990. Recent Arctic shelf foraminifera: seasonally ice covered vs. perennially ice covered areas. J. Foramin. Res. 20 (1), 8—36, http://dx.doi.org/10.2113/gsjfr.20.1.8.

Skirbekk, K., Hald, M., Marchitto, T.M., Junttila, J., Klitgaard Kristensen, D., Aaagaard Sørensen, S., 2016. Benthic foraminiferal growth seasons implied from Mg/Ca-temperature correlations for three Arctic species. Geochem. Geophys. Geosyst. 17 (11), 4684—4704.

Spellerberg, I.F., Fedor, P.J., 2003. A tribute to Claude Shannon (1916—2001) and a plea for more rigorous use of species richness, species diversity and the 'Shannon—Wiener' Index. Global Ecol. Biogeogr. 12 (3), 177—179, http://dx.doi.org/10.1046/j.1466-822X.2003.00015.x.

Svendsen, H., Beszczyńska-Möller, A., Hagen, J.O., Lefauconnier, B., Tverberg, V., Gerland, S., Ørbek, J.B., Bischof, K., Pappucci, C., Zajączkowski, M., Azzolini, R., Bruland, O., Wiencke, C., Winther, J.-G., Dallmann, W., 2002. The physical environment of Kongsfjorden—Krossfjorden, an Arctic fjord system in Svalbard. Polar Res. 21 (1), 133—166.

Swift, J.H., 1986. The Arctic waters. In: Hurdle, B.G. (Ed.), The Nordic Seas. Springer—Verlag, New York, 124—153.

Syvitski, J.P.M., Burrel, D.C., Skei, J.M., 1987. Fjords: processes and products. J. Quart. Sci. 4 (3), 277—278, http://dx.doi.org/10.1002/jqs.3390040311.

Szczuciński, W., Schellter, G., Zajączkowski, M., 2006. Sediment accumulation rates, geochemistry and provenance in complex High Arctic fjord, Hornsund, Svalbard. In: SEDIBUD: Source-to-Sink-Fluxes and Sediment Budgets in Cold Environments, NGF Abstracts Proc. Geol. Soc. Norway, vol. 4. p. 65.

Ślubowska-Woldengen, M., Koç, N., Rasmussen, T.L., Klitgaard-Kristensen, D., Hald, M., Jennings, A.E., 2008. Time-slice reconstructions of ocean circulation changes on the continental shelf in the Nordic and Barents Seas during the last 16,000 cal yr B.P. Quat. Sci. Rev. 27, 1476—1492, http://dx.doi.org/10.1016/j.quascirev.2008.04.015.

Walczowski, W., Piechura, J., 2007. Pathways of the Greenland Sea Warming. Geophys. Res. Lett. 34 (10), L10608, http://dx.doi.org/10.1029/2007GL029974 PDF 5 pp.

Węsławski, J.M., Jankowski, A., Kwaśniewski, S., Swerpel, S., Ryg, M., 1991. Summer hydrology and zooplankton in two Svalbard fjords. Pol. Polar Res. 12 (3), 445—460.

Węsławski, J.M., Zajączkowski, M., Szymelfenig, M., Keck, A., 1999. Influence of salinity and suspended matter on benthos of an Arctic tidal flat. ICES J. Mar. Sci. 56, 194—202.

Wlodarska-Kowalczuk, M., Pearson, T., 2004. Soft-bottom macrobenthic faunal associations and factors affecting species distributions in an Arctic glacial fjord (Kongsfjord, Spitsbergen). Polar Biol. 27, 155—167.

Wollenburg, J.E., Kuhnt, W., 2000. The response of benthic foraminifers to carbon flux and primary production in the Arctic Ocean. Mar. Micropaleontol. 40 (3), 189—231, http://dx.doi.org/10.1016/S0377-8398(00)00039-6.

Zajączkowski, M., 2008. Sediment supply and fluxes in glacial and outwash fjords: Kongsfjorden and Adventfjorden, Svalbard. Polish Polar Res. 29 (1), 59—72.

Zajączkowski, M., Szczuciński, W., Plessen, B., Jernas, P., 2010. Benthic foraminifera in Hornsund, Svalbard: Implications for paleoenvironmental reconstructions. Pol. Polar Res. 31 (4), 349—375, http://dx.doi.org/10.2478/v10183-010-0010-4.

Zajączkowski, M., Włodarska-Kowalczuk, M., 2007. Dynamic sedimentary environments of an Arctic glacier-fed river estuary (Adventfjorden, Svalbard). I. Flux, deposition, and sediment dynamics. Estuar. Coast. Shelf Sci. 74 (1—2), 285—296, http://dx.doi.org/10.1016/j.ecss.2007.04.015.

Zajączkowski, M., Szczuciński, W., Bojanowski, R., 2004. Recent changes in sediment accumulation rates in Adventfjorden, Svalbard. Oceanologia 46 (2), 217—231.

Oceanologia (2017) 59, 541—564

Available online at www.sciencedirect.com

ScienceDirect

journal homepage: www.journals.elsevier.com/oceanologia/

ORIGINAL RESEARCH ARTICLE

The malacostracan fauna of two Arctic fjords (west Spitsbergen): the diversity and distribution patterns of its pelagic and benthic components

Joanna Legeżyńska *, Maria Włodarska-Kowalczuk, Marta Gluchowska, Mateusz Ormańczyk, Monika Kędra, Jan Marcin Węsławski

Institute of Oceanology, Polish Academy of Sciences, Sopot, Poland

Received 14 July 2016; accepted 6 January 2017
Available online 9 March 2017

KEYWORDS
Malacostraca;
Arctic;
Svalbard;
Diversity;
Distribution

Summary This study examines the performance of pelagic and benthic Malacostraca in two glacial fjords of west Spitsbergen: Kongsfjorden, strongly influenced by warm Atlantic waters, and Hornsund which, because of the strong impact of the cold Sørkapp Current, has more of an Arctic character. The material was collected during 12 summer expeditions organized from 1997 to 2013. In all, 24 pelagic and 116 benthic taxa were recorded, most of them widely distributed Arctic-boreal species. The advection of different water masses from the shelf had a direct impact on the structure of the pelagic Malacostraca communities, resulting in the clear dominance of the sub-arctic hyperiid amphipod *Themisto abyssorum* in Kongsfjorden and the great abundance of Decapoda larvae in Hornsund. The taxonomic, functional and size compositions of the benthic malacostracan assemblages varied between the two fjords, and also between the glacier-proximate inner bays and the main fjord basins, as a result of the varying dominance patterns of the same assemblage of species. There was a significant drop in species richness in the strongly disturbed glacial bays of both fjords, but only in Hornsund was this accompanied by a significant decrease in density and diversity, probably due to greater isolation and poorer quality of sediment organic matter in its innermost basin. Our results suggest that the diversity and distribution of benthic malacostracans in these two fjords are only distantly related to the different hydrological regimes; rather, they are governed by

* Corresponding author at: Institute of Oceanology, Polish Academy of Sciences, Powstańców Warszawy 55, 81-712 Sopot, Poland. Tel.: +48 5877311779; fax: +48 585512130.
E-mail address: zosia@iopan.gda.pl (J. Legeżyńska).
Peer review under the responsibility of Institute of Oceanology of the Polish Academy of Sciences.

Production and hosting by Elsevier

http://dx.doi.org/10.1016/j.oceano.2017.01.004

locally acting factors, such as depth, sediment type, the variety of microhabitats and the availability and quality of food.

1. Introduction

Malacostracan crustaceans are widespread across a broad range of Arctic habitats from intertidal (Węsławski et al., 1993) and sea ice (Macnaughton et al., 2007) to deep ocean basins (Brandt, 1997). They can locally dominate the benthic (Conlan et al., 2013; Grebmeier et al., 1989) and plankton (Hirche et al., 2015; Huenerlage et al., 2015) biomass. The total number of bottom-dwelling malacostracan species noted in the Arctic Ocean surpasses 800, while about 50 planktonic forms are known (Sirenko, 2001). They contain both mobile and sessile forms, exhibit a variety of life strategies and hold crucial positions within food-webs, acting as conduits of nutrients and energy to higher trophic levels such as fish, birds and mammals (e.g. Highsmith and Coyle, 1990). The wide functional diversity exhibited by polar crustaceans results from the large species pool, but also from the considerable potential of ontogenetic niche shifts due to the relatively long life cycles and distinct size differences between juveniles and adults (Węsławski et al., 2010). Functional roles within populations are dynamic since different age or sex cohorts may vary considerably in terms of motility, microhabitat choice and food preferences (Carey and Boudrias, 1987; Hopkins et al., 1993; Legeżyńska, 2008; Sainte-Marie, 1986).

Svalbard crustaceans have been studied extensively over the last 150 years and are known to have the greatest species diversity of all the macrozoobenthic taxa (Palerud et al., 2004). Planktonic malacostracans being relatively large and mobile, are not target organisms of standard zooplankton sampling nets (WP-2, mesh 180-μm), therefore they are rarely included in routine plankton surveys. Sampling with specialized equipment (e.g. Tucker trawl or Isaacs-Kidd net with mesh size >1 mm) has shown that euphausiids (*Thysanoessa inermis*, *Thysanoessa raschii* and *Thysanoessa longicaudata*) and amphipods (*Themisto libellula* and *Themisto abyssorum*) are prominent members of the zooplankton communities in Svalbard fjords (Buchholz et al., 2010; Dalpadado et al., 2016; Hirche et al., 2015; Hop et al., 2002). Identification of the epifaunal components of Svalbard benthic communities is still not comprehensive, but investigations using dredges, baited traps and materials collected by SCUBA divers have recorded dense populations of malacostracan crustaceans, especially in the littoral (Nygård et al., 2010; Węsławski et al., 1993) and shallow sublittoral (Berge et al., 2009; Kaczmarek et al., 2005; Laudien et al., 2007; Legeżyńska, 2001; Nygård, 2011; Voronkov et al., 2013). Estimating their density, however, is complicated because of their motility and also the difficulty of taking quantitative samples on the heterogeneous substrates overgrown with macroalgae often found in shallow waters. Grabs operated from on board ship are suitable for catching infauna and small epifauna on soft sediments below 30 m but are much less efficient in the case of large, mobile and rare epifaunal species. Typically, therefore, crustaceans are poorly represented in grab samples and have been overlooked in the majority of subtidal benthic studies from Spitsbergen (e.g. Włodarska-Kowalczuk and Pearson, 2004; Włodarska-Kowalczuk et al., 2012; Włodarska-Kowalczuk and Węsławski, 2008).

Understanding ongoing processes in the Arctic ecosystem requires a better knowledge of the specific life-histories and functional traits of the available species pool (Cochrane et al., 2012; Węsławski et al., 2011). Here we summarize knowledge of planktonic and benthic Malacostraca based on samples collected during 12 summer expeditions organized from 1997 to 2013 by the Institute of Oceanology PAN to two Spitsbergen fjords: Kongsfjorden and Hornsund. The fjords have been frequently used as model oceans (Buchholz et al., 2010), because they have the same physical and biological processes as the adjacent seas, but are ecosystems of manageable size. The two fjords compared are eminently suitable for observations on the possible effects of climate change on the functioning of the Arctic ecosystem. Because of the sea currents on the Spitsbergen shelf they are differently exposed to present-day warming and can be regarded as representing two phases in the course of global warming: a cold one (Hornsund) and a warm one (Kongsfjorden). Furthermore, both fjords have secluded inner glacial bays, which are strongly influenced by the surrounding glaciers. One of the key effects of glacier activity is the considerable accumulation of fine-grained sediments, which is causing bottom habitat heterogeneity in the glacial bays to decline. It has been predicted, however, that glacier retreat in the coming decades will cause the homogenization of the seafloor over large areas of the coastal Arctic and will pose a major threat to species richness, diversity and the trophic structure of bottom communities in the Arctic (Węsławski et al., 2011). Therefore, surveys in the glacial bays may help to assess the changes that, in the future, are likely to take place across seafloor biota on a larger scale.

Our main aims were to update the checklist of malacostracan taxa from Hornsund and Kongsfjorden, and to explore and compare the distribution, abundance and diversity patterns of species in both fjords and their glacial bays and outer basins. We also examined the functional roles and size structure within the crustacean community. Our results provide baseline information for further monitoring research on climate-change-induced effects on the crustacean fauna of the European Arctic.

2. Study area

Hornsund and Kongsfjorden are similarly-sized glacial fjords situated on the west coast of Spitsbergen (Svalbard archipelago; Fig. 1). Both fjords are open to the Greenland Sea

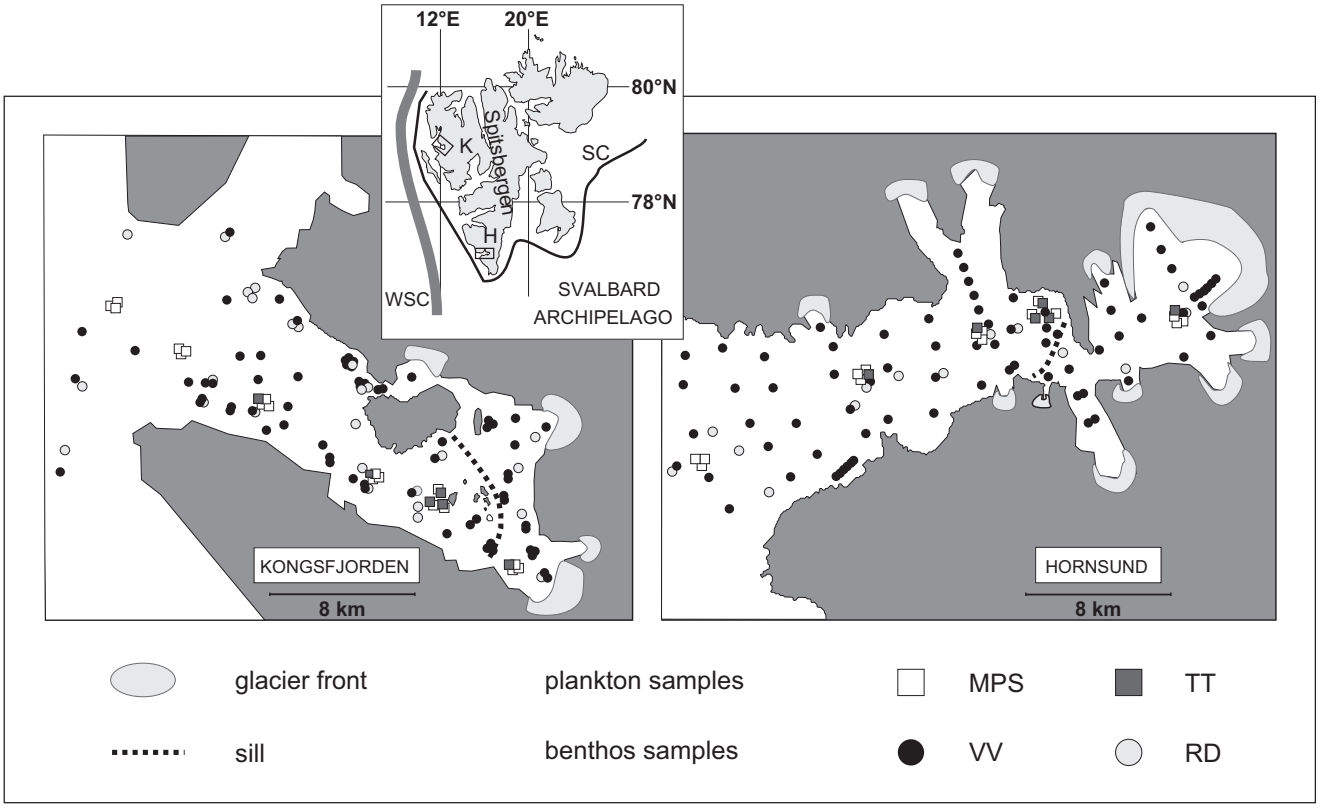

Figure 1 Sampling stations in Kongsfjorden (K) and Hornsund (H); WSC — West Spitsbergen Current; SC — Sørkapp Current; gear used: MPS — multinet; TT — Tucker trawl; VV — van Veen grab; RD — rectangular dredge.

(no entrance sills), but contain well-marked and partially isolated shallower inner basins. The water mass composition in the fjords results from the balance between the Atlantic and Arctic waters flowing along the shelf of west Spitsbergen (West Spitsbergen Current, WSC; $T > 3.0^{\circ}C$ and Sørkapp Current, SC; $-1.5^{\circ}C < T < 1.0^{\circ}C$, respectively) and varies seasonally and year-on-year (Cottier et al., 2005; Svendsen et al., 2002). The bottom topography of northernmost Kongsfjorden (79°N) favours the inflow of Atlantic waters, so this fjord has a more Atlantic-like character than Hornsund (77°N) (Walczowski, 2013). The Hornsund mouth area is shallower, and the strong polar front between the WSC stream and the Sørkapp Current reduces the influence of warm Atlantic waters in that fjord (Walczowski, 2013). The numerous glaciers terminating in the fjords have a great impact on their hydrography. In Kongsfjorden the main disturbance is due to the front formed by the three glaciers situated at the head of the fjord (Kongsvegen, Kronebreen and Kongsbreen); a fourth glacier on the northern coast is less active. In Hornsund the shoreline of the innermost bay (Brepollen) is formed almost entirely by the cliffs of five tidal glaciers; another eight glaciers terminate in the lateral bays on either side of the fjord. The glacial inflows peak in summer, creating steep gradients in turbidity, salinity and mineral sedimentation along the fjords' axes (Svendsen et al., 2002; Włodarska-Kowalczuk et al., 2005; Włodarska-Kowalczuk and Węsławski, 2008). The high concentrations of suspended mineral particles severely limit the depth of the euphotic zone, thereby reducing primary production in the innermost parts of the fjords (Piwosz et al., 2009; Svendsen et al., 2002). With increasing distance from the active glaciers the magnitude of the glacial effects diminishes: concentrations of suspended mineral particles and accumulation rates decline, while sediment stability, the extent of the euphotic zone and primary production all display considerable increases (Piwosz et al., 2009; Svendsen et al., 2002; Włodarska-Kowalczuk and Pearson, 2004; Zajaczkowski, 2008). Subtidal sediments throughout the fjords are dominated by glacio-marine deposits, which are mostly silt and clay (Włodarska-Kowalczuk et al., 2005; Włodarska-Kowalczuk and Węsławski, 2008), but the shallow bottom boasts a diversity of substrata (Kaczmarek et al., 2005; Tatarek et al., 2012; Włodarska-Kowalczuk, 2007; Włodarska-Kowalczuk et al., 2009). The organic carbon concentration in Kongsfjorden sediments decreases significantly with distance up the fjord (Kędra et al., 2010; Włodarska-Kowalczuk and Pearson, 2004), but in Hornsund a clear pattern of change in organic carbon concentration along the fjord axis has not emerged (Drewnik et al., 2016). The environmental characteristics of both fjords are summarized in Table 1.

3. Material and methods

The material was collected during 12 summer expeditions of r/v *Oceania* to the Spitsbergen fjords (1997—2013). Zooplankton was sampled with two different types of sampling gear: a multi plankton sampler (MPS, Hydro-Bios) consisting of five closing nets with a 0.25 m^2 square opening and a

Table 1 Characteristics of the environmental conditions in Kongsfjorden and Hornsund.

	Kongsfjorden		Hornsund	
Location	78°58′–79°03′N 11°23′–11°36′E		76°54′–76°59′N 15°14′–15°23′E	
Length [km]	26		27	
Width [km]	10		12	
Surface [km^2]	231		275	
Volume [km^3]	29.4		23	
	Kongsfjorden		Hornsund	
	Inner basin	Outer basin	Inner basin	Outer basin
Max depths [m]	100	394	180	260
Summer bottom temperature [°C]	−1.3 to 0.5	−0.5 to 3.5	−1.6 to 0.5	−0.8 to 3.5
Summer bottom salinity	34.10–34.50	34.1–34.90	34.30–34.55	34.10–34.85
Sediment accumulation rate [cm y^{-1}]	Up to 10[3] 6–9[4]	0.4[2]	0.7[1]	0.5[1] 0.22[2]
Summer primary production [mgC m^{-2} h^{-1}]	2.47[5]	4.48[5]	<14.00[5]	86.65[5]
Organic carbon content [%]	0.1–1.2[9] 0.2–1.8[10] 0.28[11]	1–3.4[9] 0.5–2.9[10] 1.25[11] 1.38[8]	0.8–1.8[6] 2[7]	0.8–1.8[6] 1.4[7] 1.65[8]

References in superscripts: 1, Szczuciński et al. (2006); 2, Zaborska et al. (2016); 3, Elverhøi et al. (1983); 4, Trusel et al. (2011); 5, Piwosz et al. (2009); 6, Drewnik et al. (2016); 7, Koziorowska et al. (2016); 8, Winkelmann and Knies (2005); 9, Zaborska et al. (2006); 10, Kędra et al. (2010); 11, Kuliński et al. (2014).

180 μm mesh size to collect mesozooplankton, and a Tucker trawl (TT) net (1 m^2 opening area) equipped with a 1 mm mesh net to catch macrozooplankton. Both types of nets were hauled vertically from the bottom to the surface. The samples were preserved with 4% formaldehyde solution in seawater buffered with borax. In the laboratory they were analyzed qualitatively and quantitatively, following the standard procedure described in Postel et al. (2000). All zooplankton abundances are given as water column averages expressed by the number of individuals per 100 m^3. The material consisted of 34 samples collected at 15 stations (Fig. 1, Table 2).

Benthic samples were taken with a van Veen grab (VV, catching area: 0.1 m^2) and a rectangular dredge (RD, opening: 0.8 m × 0.3 m, 1 mm net mesh size, hauled at a speed of 1.5–1.8 kn for 15 min). A total of 323 samples were collected at 202 stations (Fig. 1, Table 2). On board ship, the samples were rinsed carefully with seawater through a 500 μm mesh screen and preserved in 4% formaldehyde solution. In the laboratory the animals were sorted, identified under a stereoscopic microscope to the lowest possible taxonomic level and counted. Benthic densities are stated as the number of individuals per 0.1 m^2 (VV samples) or the number of specimens per sample (RD samples).

The specific names and taxonomic classification follow the World Register of Marine Species (http://www.marinespecies.org/index.php). In some cases, correct identification to species level was not possible. This applied particularly to tiny cumaceans and tanaids: only some of the specimens belonging to the genus *Leucon* and the order Tanaidacea were identified to species level, so we combined them as *Leucon* spp. and Tanaidacea indet. in the subsequent analyses. Nevertheless, it is worth noting that *Leucon* spp. contained at least four species: *Leucon (Leucon) nasica*, *L(L). fulvus*, *L(L). nasicoides* and *L(L). nathorstii* (our own data), whereas tanaids were represented by at least three species, identified by Prof. M. Błażewicz-Paszkowycz (University of Łódź) as *Typhlotanais mixtus*, *Pseudotanais (Pseudotanais) forcipatus* and *Akanthophoreus gracilis* (Błażewicz-Paszkowycz and Sekulska-Nalewajko, 2004; our own data).

To compare the benthic species richness between the fjords, the species accumulation curves for the number of observed species (S_{obs}) and *Chao2* estimator were computed with 95% confidence intervals (Chao, 2004; Colwell, 2013) and plotted as a function of the sampling effort (pooled for VV and RD samples, presence/absence data). *Chao2* is a non-parametric estimator that is calculated on the basis of presence/absence data. Taking into account rare species and the total number of species observed in the sample ($Chao2 = S_{obs} + Q_1^2/2Q_2$, where Q_1 is the number of species recorded in just one sample and Q_2 is the number of species that occurred in exactly two samples), it is used to predict species richness under the assumption that not every species present has been captured.

All benthic taxa were assigned to a size class and functional traits (containing information on their motility, food sources and feeding modes) according to published records (e.g. Błażewicz-Paszkowycz et al., 2012; Enequist, 1949; Hessler and Stromberg, 1989; Legeżyńska et al., 2012; Macdonald et al., 2010; Sainte-Marie and Brunel, 1985). Seven size classes were distinguished on the basis of published information on the maximum size of species: 1 – 0–5 mm, 2 – 6–10 mm, 3 – 11–15 mm, 4 – 16–20 mm, 5 – 21–25 mm, 6 – 26–30 mm and 7 – >30 mm. The guilds considered were combinations of two mobility types (discretely motile – the species can move, but movement is not necessary for feeding; motile – the species moves actively, especially while feeding), two food sources (surface, subsurface pool) and four feeding modes (suspension feeder, deposit feeder, microalgae grazer and carnivore) (Cochrane et al.,

Table 2 Sampling effort.

	Years	N/N_M	Depth [m]
Kongsfjorden			
Plankton MPS	2007, 2012, 2013	16/16	0–320
Plankton TT	2013	6/6	0–350
Benthos VV	1997, 1998, 2006, 2011	136/125	27–380
Benthos RD	1997, 1999, 2000, 2011	27/27	35–350
Hornsund			
Plankton MPS	2007, 2012, 2013	15/15	0–170
Plankton TT	2013	6/6	0–220
Benthos VV	2002, 2003, 2005, 2007, 2011	145/122	50–244
Benthos RD	2003, 2005, 2011	15/13	79–203

N, number of samples taken; N_M, number of samples containing Malacostraca; MPS, multinet; TT, Tucker trawl; VV, van Veen grab; RD, rectangular dredge.

2012; Macdonald et al., 2010). Taxa were coded on the basis of the prevailing feeding type: species employing two types of feeding were coded with both, and species with more possible feeding types as omnivores.

The dataset was divided a priori according to the sampling gear used (i.e. MPS, TT, VV and RD) and station position (two fjords: Hornsund and Kongsfjorden). The large number of samples collected with VV permitted subdivision of the VV dataset containing samples collected in two zones of the fjords (the inner and outer basins of each fjord). The frequency of occurrence and dominance were calculated for each taxon. The number of rare species (i.e. unique taxa occurring in just one sample and singletons – taxa represented by just one specimen) was assessed in each dataset. All statistical analyses were performed with the PRIMER v. 6 software package and PERMANOVA (Anderson et al., 2008; Clarke and Gorley, 2006). Calculations of the pseudo-F and p values were based on 999 permutations of the residuals under a reduced model. The significance level for all the statistical tests was $p = 0.05$.

The univariate descriptors – the number of individuals (N), number of species (S), Shannon–Wiener $\log_e$-based index (H) and Hurlbert index [ES(50)] – were assessed in each sample and the differences were analyzed using two-way (VV dataset) or one-way (MPS, TT and RD datasets) PERMANOVA on a Euclidean similarity matrix. Taxonomic distinctness indices (avTD – average taxonomic distinctness and varTD – variation in taxonomic distinctness) were also compared in the case of the quantitative benthic samples (VV). The average taxonomic distinctness describes the average taxonomic distance (the "path length" between two species following Linnean taxonomy) of all the species in the association. Variation in taxonomic distinctness is defined as the variance of the taxonomic distances between all pairs of species in the association. Five taxonomic levels were used in calculations: species, genus, family, suborder, order and superorder, and equal step levels between successive taxonomic levels were assumed (Clarke and Gorley, 2006). The multivariate differences in taxonomic composition, size structure and functional traits (percentages of individuals representing a certain species, size class or functional guild in the total number of specimens in each sample) were tested using one-way (RD dataset) or two-way (VV dataset) PREMANOVA on a Bray–Curtis similarity matrix based on square-root-transformed data. Constrained analysis of principal coordinates (CAP) was used to visualize the differences in the taxonomic composition of malacostracan assemblages between the two fjords (MPS, TT, RD datasets) or among the four basins distinguished (inner Kongsfjorden, outer Kongsfjorden, inner Hornsund, outer Hornsund, VV sets). Spearman's rank correlation vectors of taxonomic composition with two canonical axes were overlain on the CAP plots. SIMPER analysis was applied to identify the species that were the most important in creating the observed patterns.

4. Results

4.1. Plankton

Members of 5 malacostracan orders were recorded in the plankton samples (Fig. 2). Isopoda represented only by parasitic forms (numerous in MPS samples) were excluded from the subsequent analyses. Nineteen taxa were identified to species/genus level and five to a higher taxonomic level. Data on dominance and frequency for each taxon are listed in Table 3. The material included larvae of six Decapoda species and three juvenile stages of Euphausiacea, of which the furcilla was by far the most abundant and frequent (Table 3). The composition of the taxa varied significantly in both plankton datasets (MPS and TT) between the fjords (one-way PERMANOVA, MPS: pseudo-F 3.40, $p = 0.001$; TT pseudo-F 2.39, $p < 0.05$) (Fig. 3). The Kongsfjorden planktonic fauna was dominated by the amphipod *T. abyssorum* (MPS: 63.1% and TT: 67.9% of total abundance) and Euphausiacea larvae (20.3% and 15.3%, respectively). In Hornsund Euphausiacea larvae (MPS: 48.8%; TT: 29.4%) and *Pagurus pubescens* larvae (25.2% and 27.4%, respectively) were the most numerous. *Themisto libellula* was frequently noted (in 73–100% of all samples depending on the gear and the fjord), but generally, it did not contribute much to the total abundance, making up only 3–8% of a total number of specimens. Other commonly recorded but less abundant species included *T. inermis*, *T. abyssorum* and *Hyas araneus* larvae in Hornsund and *T. inermis* and *T. raschii* in Kongsfjorden (Table 3, Fig. 3). MPS samples from Kongsfjorden and Hornsund did not differ significantly with respect to the average number of species per sample (Kongsfjorden: 5.4 ± 2.2, Hornsund: 6.0 ± 2.4) or

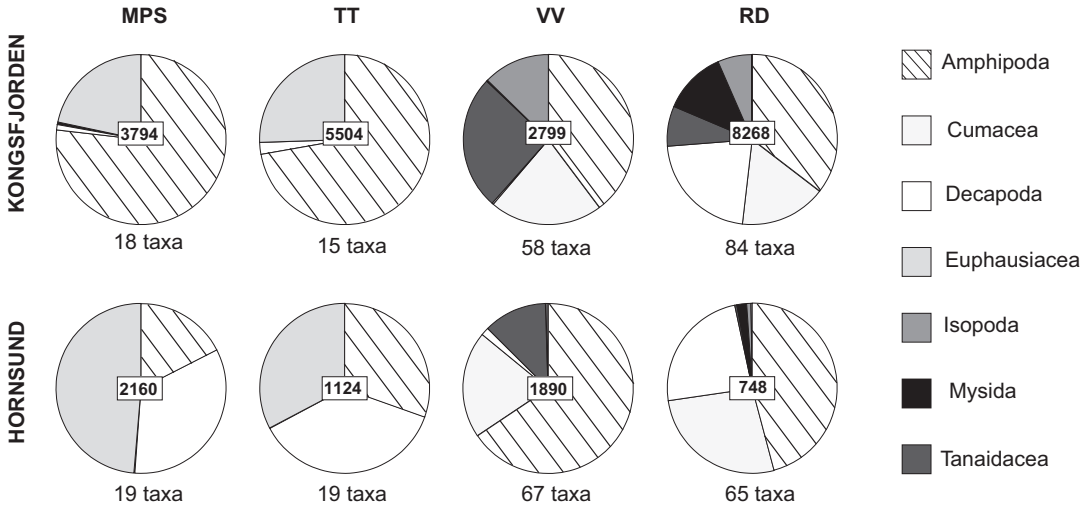

Figure 2 Percentages of malacostracan taxa in the total number of animals collected with four types of sampling gear in Kongsfjorden and Hornsund: MPS – multinet, TT – Tucker trawl, VV – van Veen grab, and RD – rectangular dredge. The numbers of taxa collected in each fjord and with each type of sampling gear are given below the pie charts, while the total numbers of malacostracans collected are shown in the centre of the charts.

the number of individuals per sample (237.1 ± 222.7 and 144.1 ± 100.3, respectively). Mean values of the Shannon–Wiener index and Hurlbert index were significantly higher in Hornsund (1.2 ± 0.4 and 5.2 ± 1.7, respectively) than in Kongsfjorden (0.8 ± 0.4 and 3.9 ± 1.4, respectively) (one-way PERMANOVA, pseudo-*F* 5.5, $p < 0.05$). TT samples did not differ between the fjords with respect to species richness (Kongsfjorden: 9.2 ± 0.8, Hornsund: 10 ± 2.9) or Hurlbert indices (7.4 ± 1.7 and 5.4 ± 1.6, respectively). Higher numbers of individuals per sample were noted in Kongsfjorden than in Hornsund (879.2 ± 662.1 and 174 ± 64, respectively) (one-way PERMANOVA, pseudo-*F* 2.6, $p < 0.05$), while values

Table 3 Planktonic Malacostraca of Kongsfjorden and Hornsund.

	Kongsfjorden MPS			Hornsund MPS			Kongsfjorden TT		Hornsund TT	
	avN	min–max	*F*	avN	min–max	*F*	avN	*F*	avN	*F*
Amphipoda indet.	**4.4**	0–21	38	**7.1**	0–97	20	**0.3**	33	**0.2**	17
Boreomysis arctica	**0.8**	0–12	13				**0.2**	17		
Caridion sp. zoea									**0.2**	17
Decapoda larva indet.	**0.3**	0–3	19	**0.2**	0–3	7			**4.0**	83
Eualus gaimardi zoea							**0.5**	17	**0.2**	17
Euphausiacea calyptopsis				**2.8**	0–38	13				
Euphausiacea furcilla	**43.3**	0–336	75	**48.7**	0–184	80	**134.2**	100	**51.2**	100
Euphausiacea nauplii	**4.9**	0–40	13	**18.7**	0–193	20				
Hyas araneus megalopa				**0.4**	0–3	20				
Hyas araneus zoea				**5.4**	0–25	60			**8.5**	83
Hyperia galba				**0.3**	0–5	7			**0.2**	17
Hyperoche medusarum	**17.1**	0–232	13	**1.2**	0–18	7			**0.5**	33
Meganyctiphanes norvegica	**0.4**	0–7	6	**0.1**	0–2	7	**6.8**	50		
Mysis oculata	**0.1**	0–2	6	**0.2**	0–3	7				
Pagurus pubescens megalopa	**1.3**	0–14	19	**0.3**	0–4	7	**6.5**	83	**0.8**	33
Pagurus pubescens zoea	**0.2**	0–1	19	**36.0**	0–104	93	**6.0**	67	**46.8**	83
Pandalus borealis zoea	**0.6**	0–6	25	**0.5**	0–3	27	**8.0**	100	**1.7**	67
Pseudomma truncatum	**0.2**	0–1	19	**0.0**	0–0	0	**0.3**	33	**0.3**	33
Sabinea septemcarinata zoea	**0.1**	0–1	6	**2.4**	0–15	40	**0.2**	17	**2.3**	67
Thysanoessa longicaudata	**0.5**	0–5	19				**3.7**	100	**1.2**	67
Thysanoessa raschii	**0.4**	0–2	31	**0.3**	0–4	7	**22.8**	100	**0.3**	33
Themisto abyssorum	**149.6**	51–447	100	**10.9**	0–70	60	**596.8**	83	**32.7**	100
Themisto libellula	**11.1**	0–59	81	**5.9**	0–23	73	**23.5**	100	**14.0**	100
Thysanoessa inermis	**1.8**	0–17	44	**2.5**	0–13	47	**69.5**	100	**9.0**	83

MPS, multinet samples; TT, Tucker trawl samples; avN, average number of ind. 100 m^{-3}; min, minimum abundance; max, maximum abundance; *F*, frequency of occurrence.

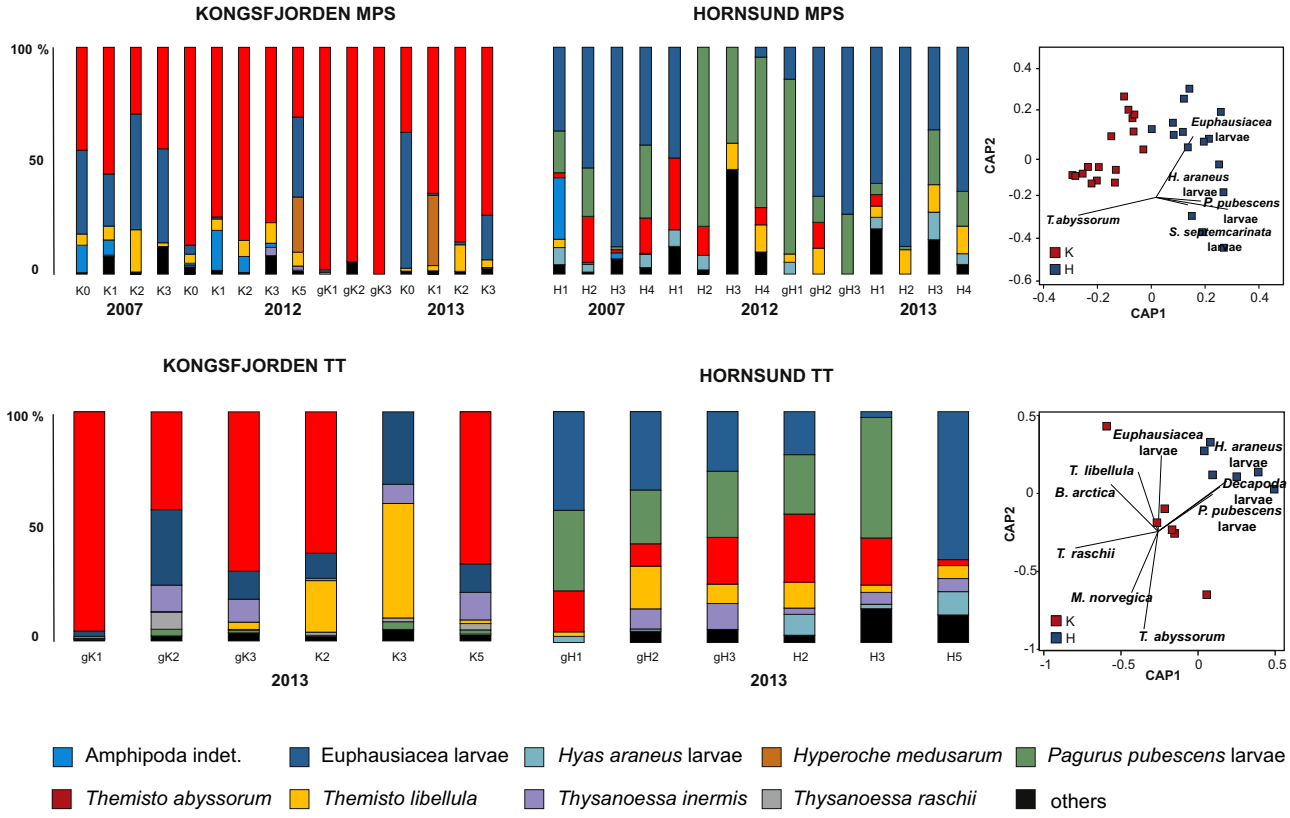

Figure 3 Species composition in pelagic samples collected with MPS — multinet and TT — Tucker trawl in Kongsfjorden and Hornsund. Results of CAP analysis based on Bray–Curtis similarity of species composition in pelagic samples. Taxa with Spearman rank correlations with CAP axes >0.6 are shown. Full species names can be found in Table 4.

of the Shannon–Wiener index were higher in Hornsund than in Kongsfjorden (1.0 ± 0.4 and 1.5 ± 0.2, respectively) (one-way PERMANOVA, pseudo-F 2.7, $p < 0.01$).

4.2. Benthos

Benthic sampling in Kongsfjorden and Hornsund yielded 13 706 specimens belonging to seven orders of Malacostraca (Fig. 2). Typical planktonic elements such as hyperiids, euphausiids, mysids and Decapoda larvae were not included in the analysis of the VV material. A total of 116 benthic taxa were identified in both fjords (Table 4). Species-accumulation curves failed to approach asymptotes for the observed number of species (S_{obs}), but tended to stabilize in the case of the *Chao2* estimators (Fig. 4). The total numbers of species recorded were lower than the estimated ones, but 0.95 CI values overlapped slightly with 0.95 CI of the *Chao2* estimator. After analysing approximately 160 samples from each

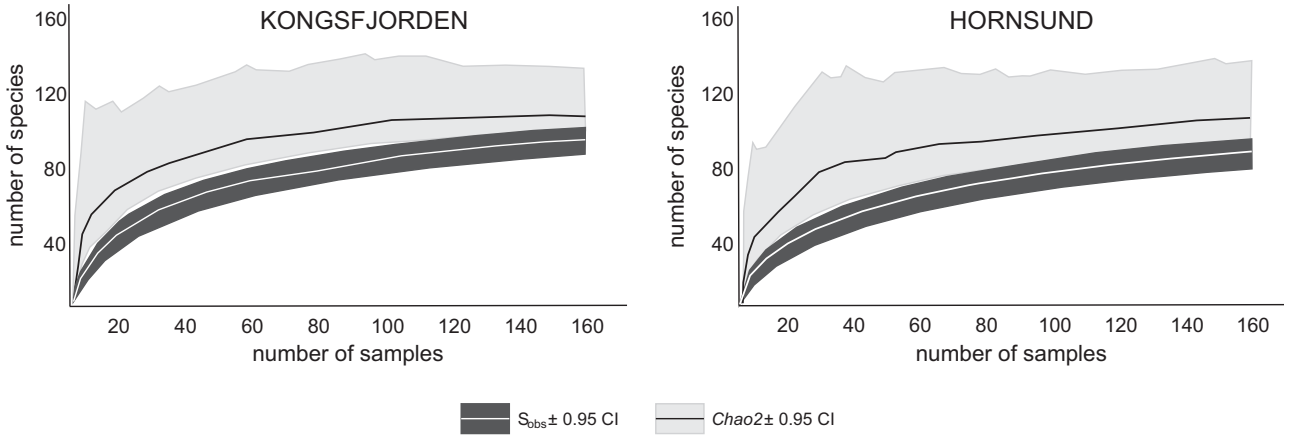

Figure 4 Species accumulation curves plotted for the number of species observed (S_{obs}) and the true number of species estimated with *Chao2* based on VV and RD presence/absence data sets. S_{obs} and *Chao2* are plotted with 0.95 confidence intervals.

Table 4 List of Malacostraca species recorded in Kongsfjorden and Hornsund.

Taxon		Order	Group	Distribution										Habitat of occurrence									
				Large scale distribution				Kongsfjorden and Hornsund records						Depth [m]					Bottom type			Fjord basins	
				I	II	III	IV	K_L	K_C	K_T	H_L	H_C	H_T	<50	50–100	100–200	200–300	>300	Soft	Hard	Algae	In	Out
Acanthonotozoma inflatum	(Krøyer, 1842)	A	B			x	x		x	x		x	x		11	11	11						11
Acanthonotozoma serratum	(Fabricius, 1780)	A	B	x	x	x	x		x	x		x	x			11	11	11					11
Acanthostepheia malmgreni	(Goës, 1866)	A	B		x	x	x				1, 2	x	x	1, 7	1, 11				1, 11			1, 11	
Aceroides (Aceroides) latipes	(Sars, 1883)	A	B	x	x	x	x					x	x	7	11	11							11
Aeginina longicornis	(Krøyer, 1843)	A	B	x	x	x	x				2		x										
Ampelisca eschrichtii	Krøyer, 1842	A	B	x	x	x	x	2	x	x	1, 2	x	x		1, 11	1, 11	11	11	1, 11				1, 11
Amphilochidae indet.	Boeck, 1871	A	B									x	x			11			11				11
Andaniexis lupus	Berge & Vader, 1997	A	B	x		x	x	2		x													
Anonyx laticoxae	Gurjanova, 1962	A	B			x	x	6		x	1, 3		x	3, 6	1				1, 6				6
Anonyx nugax	(Phipps, 1774)	A	B	x	x	x	x	7, 8, 6	x	x	1, 2, 3	x	x	1, 3, 7, 8, 6	1, 3, 11		11		1, 3, 7, 8, 6, 11		1, 7	1, 3, 11	1, 3, 7, 8, 6, 11
Anonyx sarsi	Steele & Brunel, 1968	A	B	x		x	x	7, 6	x	x	1, 2, 3		x	1, 3, 7, 6, 9	3, 11				1, 3, 7, 6		1, 3, 7, 6	7, 6, 9	3, 7, 6, 9, 11
Apherusa bispinosa	(Bate, 1857)	A	B	x	x	x						x	x				11						11
Apherusa corbeli	Lagardère, 1968	A	B				x	9		x				9						9		9	9
Apherusa glacialis	(Hansen, 1888)	A	C		x	x	x	7, 9, 11		x	1, 2	x	x	1, 9		11			11	9		11	11
Apherusa jurinei	Milne Edwards, 1830	A	B	x		x		5, 9		x				5							5		5
Apherusa megalops	(Buchholz, 1874)	A	B			x			x	x				11									11
Apherusa sarsi	Shoemaker, 1930	A	B	x		x	x	7, 9	x	x	1, 2		x	1, 7, 9	11					1, 7, 9	1		1, 9, 11
Apherusa sp.	Walker, 1891	A	B									x	x										
Aristias tumidus	(Krøyer, 1846)	A	B	x	x	x	x				2		x										
Arrhinopsis longicornis	Stappers, 1911	A	B			x	x		x	x				7		11			11				11
Arrhis phyllonyx	(Sars, 1858)	A	B	x	x	x	x	7, 2	x	x	1, 2	x	x	1, 7, 11	11	11	11	11	1, 7, 11			1, 11	1, 11
Atylus carinatus	(Fabricius, 1793)	A	B	x		x		9		x	1, 2		x	1, 9					1	9	1		1, 9
Bathymedon obtusifrons	(Hansen, 1883)	A	B	x	x	x	x	9	x	x		x	x	9		11			11	9			9, 11
Byblis gaimardii	(Kröyer, 1846)	A	B	x	x	x	x	2		x	1, 2	x	x	1	11	11			1, 11				1, 11
Calliopius laeviusculus	(Krøyer, 1838)	A	B	x		x	x	9, 2		x	1, 2, 3		x	1, 9						9	1		1, 9
Caprella septentrionalis	Krøyer, 1838	A	B	x		x	x	7, 5, 9	x	x	1, 2, 3		x	1, 7, 5, 9, 11					7, 9	7, 9	1, 7, 5, 9	9	1, 5, 9, 11
Centromedon productus	(Goës, 1866)	A	B			x	x		x	x				11									11
Centromedon pumilus	(Lilljeborg, 1865)	A	B	x		x	x	2		x													
Crassicorophium crassicorne	(Bruzelius, 1859)	A	B	x		x	x	7, 8		x	2		x	7, 8					8				8
Deflexilodes norvegicus	(Boeck, 1860)	A	B	x		x	x	9		x				9						9		9	9
Deflexilodes tesselatus	(Schneider, 1884)	A	B	x		x	x	9, 2		x				9						9			9
Deflexilodes tuberculatus	(Boeck, 1871)	A	B	x		x	x	9		x				9							9	9	9
Gammarellus homari	(Fabricius, 1779)	A	B	x		x	x	7, 5, 9		x	1, 2, 3		x	1, 3, 7, 5, 9							1, 7, 5, 9	9	1, 7, 5, 9
Gammaropsis melanops	G.O. Sars, 1883	A	B	x		x						x	x			*			11				11
Gammarus oceanicus	Segerstråle, 1947	A	B	x		x	x	9		x	1, 2, 3	x	x	1, 3, 7, 9					1	1, 9	1		1, 9, 11
Gammarus setosus	Dementieva, 1931	A	B	x		x	x	7, 6, 9		x	1, 2, 3		x	1, 3, 7, 6, 9					1, 9	1, 9	1	1, 6, 9	1, 6, 9
Gammarus wilkitzkii	Birula, 1897	A	C			x	x	9		x	1, 2	x	x	1, 7, 9			11			9		9	9, 11
Gitanopsis arctica	Sars, 1895	A	B	x	x	x	x	9		x				9						9			9
Gitanopsis inermis	(Sars, 1883)	A	B	x	x	x	x	5, 9		x		x	x	5, 9	11					9, 11	5	9	5, 9, 11
Goesia depressa	(Goës, 1866)	A	B			x	x		x	x	1, 2	x	x	7	1, 11	1, 11		11	1, 11				1, 11
Gronella lobata	(Chevreux, 1907)	A	B			x	x	2		x													
Guernea (Prinassus) nordenskioldi	(Hansen, 1888)	A	B					9		x				9						9			9
Halirages fulvocinctus	(M. Sars, 1858)	A	B	x	x	x	x	7, 5, 9, 2	x	x	1, 2	x	x	1, 7, 5, 9, 11	1, 11	11	11	11	7, 9		1, 7, 5, 9	1, 7, 9	1, 7, 5, 9, 11
Haploops tubicola	Liljeborg, 1856	A	B	x	x	x	x	2	x	x	1, 2	x	x		1, 11	1, 11	11	11	1, 11				1, 11

Table 4 (*Continued*)

Taxon		Order	Group	Distribution										Habitat of occurrence									
				Large scale distribution				Kongsfjorden and Hornsund records						Depth [m]					Bottom type			Fjord basins	
				I	II	III	IV	K_L	K_C	K_T	H_L	H_C	H_T	<50	50–100	100–200	200–300	>300	Soft	Hard	Algae	In	Out
Harpinia plumosa	(Krøyer, 1842)	A	B	x	x	x	x				2		x										
Harpinia propinqua	Sars, 1891	A	B	x	x	x	x																
Harpinia serrata	G.O. Sars, 1879	A	B	x	x	x	x				1, 2		x		1	1			1				1
Harpinia sp.	Boeck, 1876	A	B						x	x								11					11
Hippomedon holbolli	(Linnaeus, 1758)	A	B	x	x	x	x	2		x													
Hyperia galba	(Kröyer, 1838)	A	P			x	x					x	x										
Hyperoche medusarum	(G.O. Sars, 1877)	A	P			x	x		x	x		x	x										
Idunella aequicornis	Sars, 1870	A	B	x	x	x	x	2, 11		x					11		11	11	11				11
Ischyrocerus anguipes	(Boeck, 1871)	A	B	x		x	x	5, 9, 2		x	1, 2, 3		x	1, 7, 5, 9					9	9	1, 5, 9	1, 9	1, 5, 9
Ischyrocerus megacheir	Sars, 1894	A	B	x	x	x	x	9		x				9						9			9
Ischyrocerus megalops	Krøyer, 1838	A	B	x		x	x	8		x		x	x	8		11			8			11	8
Ischyrocerus sp.	Leach, 1814	A	B						x	x		x	x	7, 9, 11	11	11			7, 9	7, 9	7, 9	7, 9, 11	7, 9, 11
Lepidepecreum umbo	Sars, 1869	A	B	x	x	x	x		x	x	1, 2	x	x	11	1, 11	1, 11	1, 11		1, 11			11	11
Liljeborgia fissicornis	(Sars, 1858)	A	B	x	x	x	x		x	x							11	11					11
Maera danae	Stimpson, 1853	A	B					9		x				9						9			9
Megamoera dentata	(Krøyer, 1842)	A	B	x		x	x	7, 9	x	x	1, 2		x	1, 7, 9, 11		7, 11	11		1, 9		7, 9, 11	9	1, 9, 11
Melphidippa goesi	Stebbing, 1899	A	B	x	x	x	x		x	x	1, 2	x	x		11		11	11					11
Melphidippa sp.	Boeck, 1871	A	B						x	x		x	x										
Menigrates obtusifrons	(Boeck, 1861)	A	B	x		x	x		x	x	1, 2	x	x	1		11			11	1	1	11	11
Metopa spp.	Boeck, 1871	A	B					7		x		x	x	7		11							11
Metopa boeckii	Sars, 1892	A	B	x	x	x	x		x	x		x	x		11	11						11	11
Metopa bruzelii	(Goës, 1866)	A	B	x		x	x				1, 2		x	1	1	1	1	1	1		1		1
Metopa glacialis	(Krøyer, 1842)	A	B			x	x	9, 2		x	2		x	9									9
Metopa pusilla	Sars, 1892	A	B	x		x	x	9		x				9						9			9
Metopa robusta	Sars, 1892	A	B	x	x	x			x	x							11		11				11
Metopa sinuata	Sars, 1892	A	B	x		x	x	9		x				9						9			9
Monoculodes latimanus	(Goës, 1866)	A	B	x	x	x	x	9, 2	x	x		x	x	9, 11	11	11			9	9		9	9, 11
Monoculodes packardi	Boeck, 1871	A	B	x	x	x	x	2	x	x	1, 2	x	x	11	1, 11	1, 11	11	11	1			11	11
Monoculodes sp.	Stimpson, 1853	A	B					8	x	x		x	x	7, 8					8		7		7, 8
Munna sp. 1	Krøyer, 1839	A	B						x	x							11	11	11		7		11
Munna sp. 2	Krøyer, 1839	A	B					7		x				7					7		7		
Neohela monstrosa	(Boeck, 1861)	A	B	x		x	x				1, 2	x	x		1, 11	1, 11	11		1				1, 11
Neopleustes pulchellus	(Krøyer, 1846)	A	B	x		x	x				1, 2		x	1					1				
Odius carinatus	(Bate, 1862)	A	B	x		x	x	9		x	2		x	9						9			9
Onisimus brevicaudatus	Hansen, 1887	A	B			x	x				1, 3	x	x		11				1				11
Onisimus caricus	Hansen, 1887	A	B			x	x	7, 6		x	1, 2, 3		x	1, 3, 7, 6	1, 3				1, 3, 7, 6			1, 3, 6	
Onisimus edwardsi	Krøyer, 1846	A	B	x		x	x	7, 8, 6, 9	x	x	1, 2, 3	x	x	3, 7, 8, 6, 9	3, 11				8, 6, 11		1, 3, 7, 6, 9	1, 9, 11	1, 3, 7, 8, 6, 9, 11
Onisimus glacialis	(Sars, 1900)	A	B			x	x					x	x				*						11
Onisimus litoralis	(Krøyer, 1845)	A	B	x		x	x	6, 9		x	1, 2, 3	x	x	1, 3, 6, 9					1, 3, 6	9	1, 3	1, 3, 9, 11	1, 3, 6, 9, 11
Onisimus plautus	Krøyer, 1845	A	B	x		x	x	6		x	1, 2	x	x	1, 6, 11					6			6, 11	
Onisimus spp.	Boeck, 1871	A	B						x	x		x	x		11	11	11					11	11
Orchomene serratus	(Boeck, 1861)	A	B	x		x			x	x							11						11
Orchomenella minuta	(Krøyer, 1846)	A	B	x		x	x	7, 6	x	x	1, 2, 3	x	x	1, 3, 7, 6, 11	3, 11	11	11	11	1, 3, 7, 6, 11	7	3, 7, 6	3, 11	1, 3, 6, 11
Parapleustes assimilis	(Sars, 1882)	A	B	x	x	x	x	7, 5, 9		x				7, 5, 9							7, 9	9	5, 9
Parapleustes bicuspis	(Krøyer, 1838)	A	B	x		x	x	7, 5, 9		x	1, 2	x	x	1, 7, 5, 9	11				7, 9, 11	1	1, 7, 5, 9	9	1, 5, 9, 11
Parapleustes gracilis	(Buchholz, 1874)	A	B	x		x	x	9		x				9					9	9	9	9	
Parapleustes monocuspis	(Sars, 1893)	A	B			x		7	x	x				7, 1							7		11
Pardalisca cuspidata	Krøyer, 1842	A	B	x	x	x	x		x	x				11	11	11	11						11
Pardalisca tenuipes	Sars, 1893	A	B	x	x	x	x		x	x					11	11							11
Paroediceros lynceus	(Sars, 1858)	A	B	x	x	x	x	7, 8, 6, 9	x	x	1, 2, 3	x	x	1, 7, 8, 6, 9, 11	11	11	11		1, 7, 8, 9	9	7	7, 9, 11	7, 8, 11

Table 4 (*Continued*)

Taxon		Order	Group	Distribution										Habitat of occurrence									
				Large scale distribution				Kongsfjorden and Hornsund records						Depth [m]					Bottom type			Fjord basins	
				I	II	III	IV	K_L	K_C	K_T	H_L	H_C	H_T	<50	50–100	100–200	200–300	>300	Soft	Hard	Algae	In	Out
Photis reinhardi	Krøyer, 1842	A	B	x		x	x					x	x			11		11					11
Phoxocephalus holbolli	(Krøyer, 1842)	A	B	x		x	x		x	x		x	x			11	11		11				11
Pleustes (Pleustes) panoplus	(Krøyer, 1838)	A	B	x		x	x	7, 9, 2	x	x	1, 2		x	1, 7, 9, 11					1, 7, 9	1	1, 7, 9	9	1, 9, 11
Pleustomesus medius	(Goës, 1866)	A	B			x	x				1, 2	x	x	1	1	1, 11					11		1, 11
Pleusymtes glaber	(Boeck, 1861)	A	B	x		x	x	5, 9		x				5, 9					9	9		9	5, 9
Pleusymtes glabroides	(Dunbar, 1954)	A	B			x	x	7, 9		x	1, 2		x	1, 7, 9						7, 9	1		1, 7
Pleusymtes pulchella	(Sars, 1876)	A	B	x		x	x	9, 2		x				9						9			9
Pontoporeia femorata	Krøyer, 1842	A	B	x	x	x	x	7	x	x	1, 2	x	x	1, 7, 11	1, 11	1, 11	1		1, 11				1, 11
Priscillina armata	(Boeck, 1861)	A	B			x		8		x				8					8				8
Protomedeia sp.	Krøyer, 1842	A	B					8		x		x	x	8		11							8, 11
Protomedeia fasciata	Krøyer, 1842	A	B	x		x	x	9	x	x		x	x	9	11					9			9, 11
Protomedeia grandimana	Brüggen, 1906	A	B	x		x	x		x	x	1, 2		x	1	1, 11	1			1, 11				1, 11
Quasimelita formosa	(Murdoch, 1885)	A	B	x		x	x	7, 2	x	x	1, 2	x	x	1, 7, 11	11	1, 11			1, 7		7	11	1, 11
Quasimelita quadrispinosa	(Vosseler, 1889)	A	B		x	x	x		x	x		x	x	11	11	11	11	11	11				11
Rhachotropis aculeata	(Lepechin, 1780)	A	B	x	x	x	x	9	x	x	1, 2	x	x	1, 11	11	11	11	11		1	1		1, 11
Rhachotropis helleri	(Boeck, 1871)	A	B	x	x	x	x	2	x	x							11	11					11
Rhachotropis inflata	(Sars, 1883)	A	B	x	x	x	x	7, 9	x	x				7, 9, 11	11	11				7, 9			9, 1
Rhachotropis macropus	Sars, 1893	A	B	x	x	x	x	2	x	x								11					11
Rostroculodes borealis	(Boeck, 1871)	A	B	x	x	x	x	7	x	x	1, 2		x	1, 7, 11	11	11	11	11	1, 7, 11		1, 9, 7	9	9, 11
Rostroculodes longirostris	(Goës, 1866)	A	B		x	x	x	7	x	x	1, 2	x	x	1, 7	11	11			1, 7				11
Rozinante fragilis	(Goës, 1866)	A	B			x	x	9		x	1	x	x	1, 9		11				9		9	1, 11
Schisturella pulchra	(Hansen, 1887)	A	B	x	x	x	x		x	x							11		11				11
Socarnes bidenticulatus	(Bate, 1858)	A	B	x		x	x				1, 2		x	1	1	1	1		1				1
Socarnes vahlii	(Krøyer, 1838)	A	B	x		x	x	9	x	x				9, 11								9	9, 1
Stegocephalus inflatus	Krøyer, 1842	A	B	x	x	x	x		x	x	1, 2	x	x	1	1, 11	11	11	11	1, 11			11	11
Stenopleustes latipes	(Sars, 1858)	A	B	x	x	x	x		x	x		x	x		11								11
Stenothoidae indet.	Boeck, 1871	A	B						x	x		x	x	11	11	11	11						11
Syrrhoe crenulata	Goës, 1866	A	B	x	x	x	x	7, 9, 2	x	x	1, 2	x	x	7, 9, 11	1, 11	1, 11	11	11	1, 11	7, 9, 11	7, 9		1, 9, 11
Themisto abyssorum	Boeck, 1870	A	P	x	x	x	x	2, 12	x	x	1, 2	x	x	11	11	11	11					11	11
Themisto libellula	Goës, 1865	A	P	x		x	x	2, 12	x	x	1, 2	x	x		11	11	11					11	11
Tiron spiniferus	(Stimpson, 1853)	A	B	x		x	x					x	x			11			11				11
Tryphosinae indet.	Lowry & Stoddart, 1997	A	B									x	x				11						11
Tryphosella horingi	(Boeck, 1871)	A	B	x		x	x				2		x										
Tryphosella schneideri	(Stephensen, 1921)	A	B	x		x	x	9		x		x	x	9		11			11	9			9, 11
Tryphosella spitzbergensis	(Chevreux, 1926)	A	B	x		x	x					x	x		11		11						11
Unciola leucopis	(Krøyer, 1845)	A	B	x		x	x	7	x	x	1, 2	x	x	7	1, 11	1, 11	11	11	1, 7, 11				1, 11
Westwoodilla caecula	(Bate, 1857)	A	B	x	x	x	x	9, 2	x	x		x	x	9, 11	11	11							9, 11
Weyprechtia pinguis	Krøyer, 1838	A	B			x	x	7, 5, 9, 2	x	x	1, 2		x	1, 7, 5, 9, 11	11				7, 9		1, 7, 9	9, 11	1, 5, 9, 11
Brachydiastylis resima	(Krøyer, 1846)	C	B	x	x	x	x	1	x	x		x	x	7	11				7				11
Campylaspis rubicunda	(Liljeborg, 1855)	C	B	x	x	x	x	2	x	x	1	x	x	1	1, 11	1, 11	1, 11	1, 11	1, 11			1, 11	1, 11
Diastylis edwardsii	(Krøyer, 1841)	C	B	x		x	x	2		x													
Diastylis goodsiri	(Bell, 1855)	C	B	x	x	x	x	7, 2	x	x	1	x	x	1, 7, 11	1, 11	1, 11	1, 11	1, 11	1, 7, 11			1, 11	1, 11
Diastylis lucifera	(Krøyer, 1837)	C	B	x	x		x	7	x	x	1	x	x	1, 7, 11	1, 11	1	1	1, 11	1, 7, 11			11	1, 11
Diastylis rathkei	(Krøyer, 1841)	C	B	x	x	x	x	7	x	x	1, 2	x	x	1, 7, 11	1, 11	1, 11	1, 11		1, 7, 11	7		1, 11	1, 11
Diastylis scorpioides	(Lepechin, 1780)	C	B	x	x	x	x		x	x	1, 2	x	x	1	1, 11	1, 11	1, 11	11	11	11		11	1, 11
Diastylis spinulosa	Heller, 1875	C	B	x	x	x	x				1		x	1	1	1			1			1	1
Diastylis sulcata	Calman, 1912	C	B			x						x	x			11							11
Ektonodiastylis nimia	(Hansen, 1920)	C	B		x	x						x	x		11								11
Eudorella emarginata	(Krøyer, 1846)	C	B	x	x	x	x	2	x	x	1	x	x	1, 11	1, 11	1, 11	1, 11	1, 11	1, 11			1, 11	1, 11
Hemilamprops cristatus	(Krøyer, 1846)	C	B	x		x	x					x	x		11	11							11
Lamprops fuscatus	(Sabine, 1824)	C	B	x		x	x	7, 9	x	x				7, 9, 11	11				7, 9	9	7	9	9, 1

Table 4 (*Continued*)

Taxon		Order	Group	Distribution										Habitat of occurrence									
				Large scale distribution				Kongsfjorden and Hornsund records						Depth [m]					Bottom type			Fjord basins	
				I	II	III	IV	K_L	K_C	K_T	H_L	H_C	H_T	<50	50–100	100–200	200–300	>300	Soft	Hard	Algae	In	Out
Leptostylis villosa	(Krøyer, 1841)	C	B	x	x	x	x		x	x		x	x			11	11						11
Leucon spp.	Krøyer, 1846	C	B					2, 9	x	x		x	x	9, 11	11	11	11	11	11	9			9, 1
Caridion gordoni	(Spence Bate, 1858)	D	P	x		x						x	x										
Eualus gaimardii gaimardii	(H. Milne Edwards, 1837)	D	B/P_l	x		x	x	7, 6, 9	x	x	1, 3	x	x	1, 7, 5, 6, 9, 11	1, 11	11	11		1, 6, 11	1, 7, 6, 9, 11	7, 5, 11	1, 6	1, 5, 6, 9, 11
Hyas araneus	Leach, 1816	D	B/P_l	x		x	x	7, 6, 9, 2	x	x	1, 2, 3	x	x	1, 7, 5, 6, 9, 11	1, 3, 11	1, 11	1, 11	1	3, 7, 6, 9, 11	7, 9, 11	7, 5	1, 9	1, 3, 5, 6, 9, 11
Hyas coarctatus	(Montagu, 1815)	D	B	x		x	x	2		x													
Lebbeus polaris	(Goës, 1866)	D	B/P_l	x		x	x	9, 2	x	x	1, 2		x	1, 7, 9, 11	1, 11	1, 11	1, 11	1, 11	7, 9, 11	1, 7, 9	1, 7	9, 11	1, 9, 11
Pagurus pubescens	Krøyer, 1838	D	B/P_l	x		x	x	7, 6, 9, 2	x	x	1, 2, 3	x	x	1, 7, 6, 9, 11	1, 3, 11	1, 11	1, 11	1	1, 3, 6, 11	1, 7, 6, 9	7	1, 9	1, 3, 6, 9, 11
Pandalus borealis	Krøyer, 1838	D	B	x		x	x	7, 2	x	x	1, 2	x	x	7	1, 11	1, 11	1, 11	1, 11	1	7		11	1, 11
Sabinea septemcarinata	(Sabine, 1824)	D	B/P_l	x		x	x	2	x	x	1, 2	x	x	1, 5, 11	1, 11	1, 11	1, 11	1, 11	1, 11		5	1, 11	1, 5, 11
Sclerocrangon boreas	(Phipps, 1774)	D	B/P_l	x		x	x	7, 8, 9, 2	x	x	1, 2		x	1, 7, 8, 9, 11	1, 11	1	1	1	1, 8, 11	1, 7, 9	1, 7		1, 8, 9, 11
Sclerocrangon ferox	(Sars G.O., 1877)	D	B	x		x	x				1		x	1	1	1	1	1	1	1	1	1	
Spirontocaris phippsii	(Krøyer, 1841)	D	B	x		x	x	9		x				9						9			9
Spirontocaris spinus	(Sowerby, 1805)	D	B/P_l	x		x	x	7, 2	x	x	1	x	x	1, 7, 5, 11	1, 11	1, 11	1, 11	1, 11	7	1, 7	1, 7, 5	11	1, 5, 11
Meganyctiphanes norvegica	(M. Sars, 1857)	E	P			x	x	4, 12	x	x		x	x										
Nematoscelis megalops	G.O. Sars, 1883	E	P					4, 12		x													
Thysanoessa inermis	(Krøyer, 1846)	E	P	x		x	x	4, 2, 12	x	x	1, 2, 4	x	x	1, 12	1, 11, 12	1, 4, 11, 12	1, 11, 12	1				1, 4, 11	1, 4, 4, 11
Thysanoessa longicaudata	(Krøyer, 1846)	E	P	x		x	x	4, 12	x	x	1, 4	x	x	1	1	1, 4	1, 11	1					1, 4
Thysanoessa raschii	(M. Sars, 1864)	E	B	x		x	x	4, 12	x	x	1, 4	x	x	1	1	1, 4						1, 4	1, 4
Eugerda sp.	Meinert, 1890	I	B						x	x		x	x	11	11	11	11	11	11			11	11
Eurycope cornuta	Sars, 1864	I	B	x		x	x	2	x	x		x	x	11	11	11	11	11	11			11	11
Gnathia sp.	Leach, 1814	I	B						x	x							11						11
Ilyarachna hirticeps	Krøyer, 1838	I	B	x	x	x	x				1		x	1	1	1			1				1
Janira maculosa	(Krøyer, 1847)	I	B	x		x	x	7	x	x					11		11					11	11
Janiralata tricornis	Sars, 1865	I	B			x	x	9		x				9						9		9	9
Munna fabricii	Krøyer, 1846	I	B	x		x	x	9	x	x	1		x	1, 9, 11	1	1	1	1	1	9	11	1, 9	1, 9, 11
Munna groenlandica	Hansen, 1916	I	B		x			9		x													
Munna kroyeri	Goodsir, 1842	I	B	x				9		x													
Munna pellucida	Gurjanova, 1930	I	B			x		9		x													
Munna spitzbergensis	Gurjanova, 1930	I	B			x	x	5, 9		x				5, 9						9	5		5, 9
Munnopsis typica	M. Sars, 1861	I	B	x	x	x	x	7, 2	x	x	1	x	x	1, 7	1, 11	1, 11	1, 11	1, 11	1, 7, 11		11	1, 11	1, 11
Pleurogonium spinosissimum	(Sars G.O., 1866)	I	B	x		x			x	x		x	x			11							11
Synidotea nodulosa	(Krøyer, 1846)	I	B			x	x	8		x	1, 2		x	1, 8	1	1	1	1	1, 8		1		1
Boreomysis arctica	(Krøyer, 1861)	M	P	x	x	x	x	2	x	x													
Erythrops erythrophthalma	(Goës, 1864)	M	P	x	x	x	x	7	x	x	1	x	x	1, 7	1, 11	1, 11	1, 11	1	11				1, 11
Mysis mixta	Liljeborg, 1853	M	P	x		x	x				1, 3		x	1									1
Mysis oculata	(Fabricius, 1780)	M	P	x	x	x	x	7, 9	x	x	1, 2	x	x	1, 7, 5, 9, 11	11	11			7, 9	9	7, 5	1, 11	1, 5, 9, 11
Parerythrops obesa	(Sars G.O., 1864)	M	P	x		x	x	2		x													
Pseudomma truncatum	S.I. Smith, 1879	M	P	x	x	x	x	2	x	x	1	x	x	1	1, 11	1, 11	1, 11	1, 11				11	1, 11
Stilomysis grandis	(Goës, 1864)	M	P	x		x	x	7	x	x	1	x	x	7	11	11			7			11	11
Tanaidacea indet.	Dana, 1849	T	B	x	x	x	x	7	x	x	2	x	x	7, 10, 11	10, 11	10, 11	10, 11	10, 11	10, 7			10.11	10.11

Order: A – Amphipoda, C – Cumacea, D – Decapoda, E – Euphausiacea, I – Isopoda, M – Mysida, T – Tanaidacea. *Group:* B – benthic, P – pelagic, C – cryopelagic, P_l – planktonic larvae. *Distribution:* I – Norwegian coast (Brattegard and Holthe, 2001), II – deep Greenland Sea (Brandt, 1997), III – Barents Sea (Sirenko, 2001), IV – Svalbard Archipelago (Palerud et al., 2004), K_L – literature records for Kongsfjorden, K_C – current study record for Kongsfjorden, K_T – all records for Kongsfjorden, H_L – literature records for Hornsund, H_C – current study record for Hornsund, H_T – all records for Hornsund. *Habitat of occurrence:* depth ranges, bottom types and fjord basins. References in superscripts: 1, Węsławski (1990); 2, Gulliksen et al. (1999); 3, Legeżyńska et al. (2000); 4, Buchholz et al. (2010); 5, Lippert et al. (2001); 6, Legeżyńska (2001); 7, Kaczmarek et al. (2005); 8, Laudien et al. (2007); 9, Voronkov et al. (2013); 10, Błażewicz-Paszkowycz and Sekulska-Nalewajko; 11, current study; 12, Dalpadado et al. (2016).

fjord, S_{obs} reached 89 (with 0.95 CI intervals from 81 to 97) in Hornsund and 96 (with 0.95 CI intervals from 89 to 103) in Kongsfjorden. *Chao2* gave very similar results for Hornsund (109 species, with 0.95 CI intervals from 96 to 141) and Kongsfjorden (110 species, with 0.95 CI intervals from 100 to 136).

Overall, Amphipoda followed by Cumacea were the most abundant and represented by the highest numbers of species in the benthic samples (Fig. 2). In Hornsund, they constituted 86% of specimens in the VV samples and 73% in the RD samples; in Kongsfjorden the respective values were 61% and 52%. Decapoda were abundant only in the RD samples (24% in Hornsund and 22% in Kongsfjorden). Tanaidacea and Isopoda contributed more to the total number of specimens collected in Kongsfjorden (VV samples: 38%, RD samples: 14%) than in Hornsund (12% and 1.2%, respectively). Mysids were frequent and numerically important only in the RD samples from Kongsfjorden (F = 65.4%, D = 12.1%) (Fig. 2). Among the 44 families, Oedicerotidae (Amphipoda) comprised the highest number of species (13) followed by Lysianassidae (Amphipoda, 9 species), Uristidae (Amphipoda, 8 species), Calliopidae (Amphipoda, 8 species) and Diastylidae (Cumacea, 8 species). As regards abundance, the 10 most dominant species made up between 69% and 89% of the total number of individuals collected in each fjord, depending on the sampling gear. Across the entire data set, there was a high proportion of rare taxa. Thirty species occurred in just one sample and only 16 species were noted with a frequency of >10%. The cumacean *Eudorella emarginata* was the most frequent (F = 69%) and most abundant species (D = 11%) in the benthic material.

4.2.1. Grab samples (VV)

Hornsund and Kongsfjorden shared several frequent and numerically important species, but the results of the PERMANOVA tests showed differences in species composition between the two fjords, between the glacial bays and outer basins within the fjords, and between the respective basins of the both fjords (Table 5). The separation of infauna between fjords and basins is illustrated in the fjord-basin oriented CAP ordination (Fig. 5). The 10 most dominant species respectively made up 81% and 89% of the total number of individuals collected in Hornsund and Kongsfjorden. In both fjords, the glacial basins were dominated by small-bodied tanaids and the cumacean *E. emarginata*, which, however, were much more abundant in Kongsfjorden (Fig. 6). Melitid amphipods, despite their moderate frequency, exhibited a substantial dominance in the outer parts of the fjords, reaching the highest densities noted in the whole material (*Quasimelita formosa* up to 166 ind. 0.1 m^{-2}; *Quasimelita quadrispinosa* up to 225 ind. 0.1 m^{-2}). A number of rare taxa were recorded in all the basins. In Brepollen 12 taxa (67% of all the taxa recorded) were found in just one sample and 9 (50% of all the taxa recorded) were represented by just one specimen, while in the inner Kongsfjorden 3 species among 13 taxa (27% of all the taxa recorded) were noted as individual specimens and in just one sample. Singletons made up 26% (out of 51 species recorded) and 18% (out of 62 species recorded) and unique specimens 31% and 26% in the outer Kongsfjorden and Hornsund, respectively. Species richness, diversity and variation in taxonomic distinctness did not differ significantly between Hornsund and Kongsfjorden. The average taxonomic distinctness and numbers of individuals per sample were significantly higher in Kongsfjorden than in Hornsund. In Hornsund, species richness, density and diversity were significantly higher in the fjord's main basin than in the glacial bays. In Kongsfjorden, the central basin and glacial bay did not differ with regard to density or the diversity of crustacean fauna, but species richness, Hurlbert index and variance of taxonomic distinctness were lower in the inner bay. Comparison of the main basins of the two fjords showed the average species richness, Shannon–Wiener and Hurlbert diversity indices and variances of taxonomic distinctness to be higher in Hornsund than in Kongsfjorden, whereas density and average taxonomic distinctness did not differ significantly. The glacial bay of Kongsfjorden had

Table 5 Results of two-way PERMANOVA comparisons of density and diversity indices (VV samples) and one-way PERMANOVA (RD, MPS, TT samples).

Gear	Source	*N*	*S*	*H*	ES(50)	avTD	varTD	TAX	SIZE	FUN
VV	F	5.96*	0.00	0.00	0.18	16.1***	2.15	8.26***	12.29***	14.14***
	B	3.50	35.05***	29.69***	0.22	24.2***	37.50***	11.76***	18.45***	24.71***
	F × B	6.12*	4.9*	7.8**	21.32***	28.6***	11.73***	3.82***	3.54**	9.51***
	Post hoc pairwise tests for F × B	Hi < Ki** Hi < Ho**	Hi < Ki** Ki < Ko** Hi < Ho***	Ho > Ko** Hi < Ho***	Hi < Ki** Ho > Ko*** Hi < Ho** Ki < Ko***	Hi < Ki*** Hi < Ho***	Ho > Ko*** Hi < Ho*** Ki < Ko*	Hi < Ki*** Ho > Ko*** Hi < Ho*** Ki < Ko***	Hi > Ki*** Ho > Ko*** Hi < Ho*** Ki < Ko***	Hi < Ki*** Ho > Ko*** Hi < Ho*** Ki < Ko***

Gear	Source	*N*	*S*	*H*	ES(50)	TAX	SIZE	FUN
RD	F	6.68**	0.36	1.09	2.57	2.63**	0.43	1.63
MPS	F	2.2	0.47	5.52*	5.00*			
TT	F	0.46	6.74*	7.18**	4.27			

N, number of specimens per sample; *S*, number of taxa per sample; *H*, Shannon–Wiener index; ES(50), Hurlbert index; avTD, average taxonomic distinctness; varTD, variance of taxonomic distinctness; TAX, taxonomic composition; SIZE, size structure; FUN, functional traits.
* $p < 0.05$.
** $p < 0.01$.
*** $p < 0.001$.

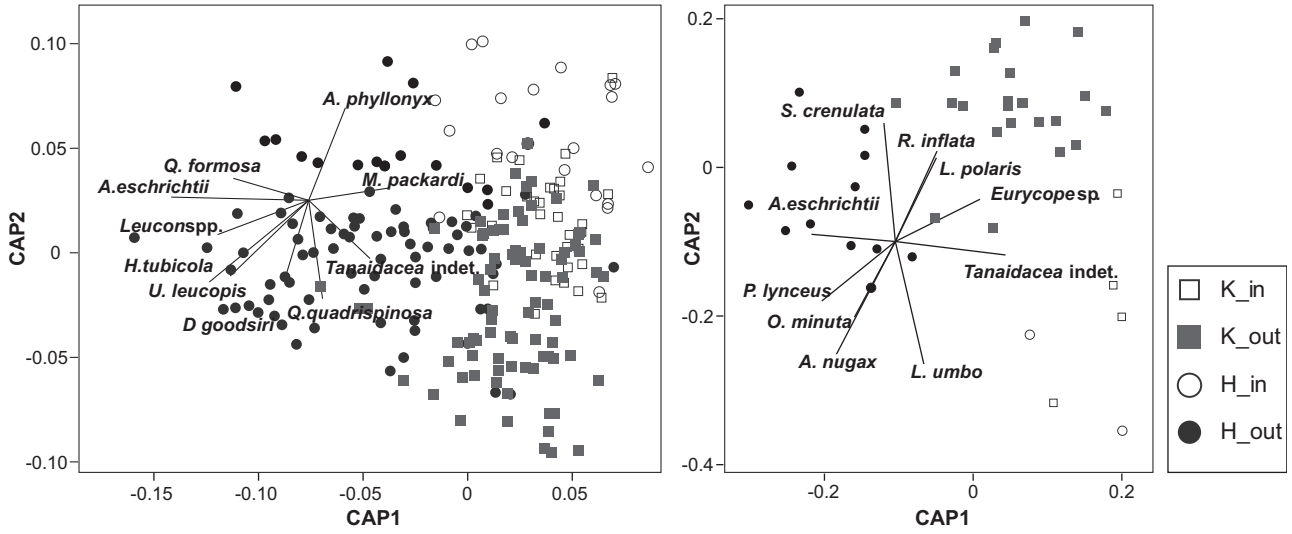

Figure 5 Results of CAP analysis based on the Bray–Curtis similarity of species composition in the benthic samples from Kongsfjorden (K) and Hornsund (H), and their inner glacial bays (in) and outer basins (out); square root transformed VV data (left-hand panel); presence/absence RD data (right-hand panel). Taxa with Spearman rank correlations with CAP axes >0.35 for VV samples and >0.45 in RD samples are shown. Full species names can be found in Table 4.

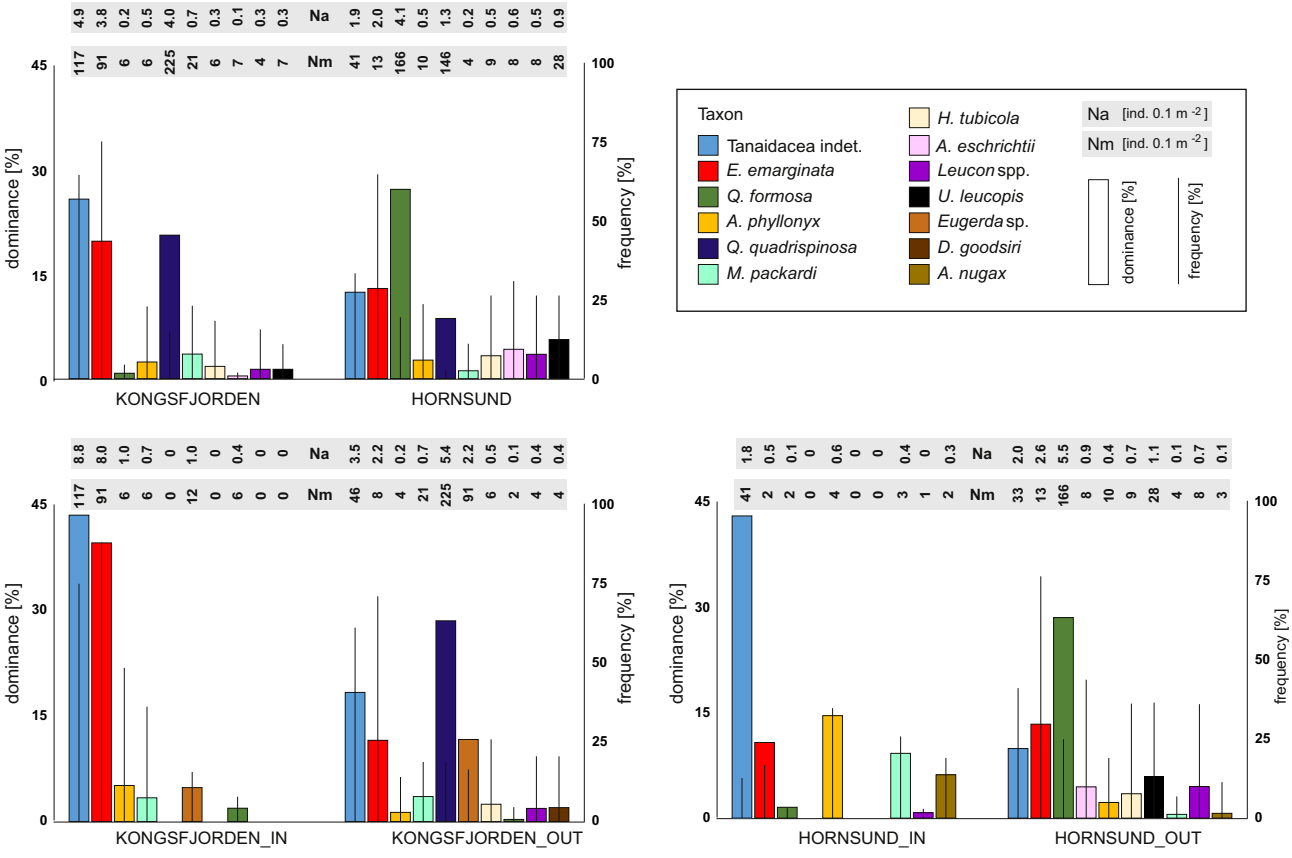

Figure 6 Dominance, frequency and density of the species that contributed most to the dissimilarity between the malacostracan communities of Kongsfjorden and Hornsund and their inner glacial bays (in) and outer basins (out) based on SIMPER analysis of VV samples. Ten species with the highest contribution to the overall dissimilarity are shown for each comparison. The average density (Na; ind. 0.1 m^{-2}) and maximum density (Nm; ind. 0.1 m^{-2}) are shown for each taxon above the dominance/frequency graphs. Full species names can be found in Table 4.

higher densities, species richness, Shannon–Wiener and Hurlbert diversity indices and the average taxonomic distinctness than the glacial bays of Hornsund (Fig. 7, Table 5).

The results of PERMANOVA indicated that the functional structure and size composition of the infaunal communities (explored with VV sampling) differed among the two fjords, the inner and outer basins within each fjord and the respective basins of both fjords (Table 5). Eleven functional groups were recorded, detritus-feeders being predominant. Discretely motile detritus feeders (Kongsfjorden: 51%, Hornsund: 43%) and motile subsurface detritus feeders (Kongsfjorden: 38%, Hornsund: 11%) were dominant in the glacial bays, whereas mobile surface deposit feeders were typical of the outer fjords (Kongsfjorden: 34%, Hornsund: 39%). Numbers of motile and discretely motile suspension feeders increased towards the open sea, comprising 21% of the individuals in outer Hornsund and 10% in outer Kongsfjorden. The proportions of facultative and obligate carnivores ranged from 8 to 40% in the glacial bays of Kongsfjorden and Hornsund, respectively (Fig. 8). The Kongsfjorden fauna was numerically dominated by the smallest species, whereas in Hornsund the size composition was more even. In both fjords organisms belonging to the two smallest size classes (<10 mm) were dominant in the glacial bays (Kongsfjorden: 93%, Hornsund 73%). Crustaceans up to 15 mm comprised 55% and 91% of all individuals collected in the outer parts of Hornsund and Kongsfjorden, respectively. The proportion of species longer than 20 mm was distinctly higher in both the inner (10%) and outer (37%) basins of Hornsund than in Kongsfjorden (3% in each basin) (Fig. 9).

4.2.2. Dredge samples (RD)

The species composition in the RD samples differed significantly between the two fjords (Fig. 5). The ten most dominant species made up 69% and 74% of the total number of individuals collected in Hornsund and Kongsfjorden, respectively (Table 6). The number of species in the dredge samples was variable but on average much higher in Kongsfjorden (306.5 ± 342.8 ind. per sample) than in Hornsund (57.5 ± 55.0 ind. per sample) (one-way PERMANOVA, pseudo-*F*

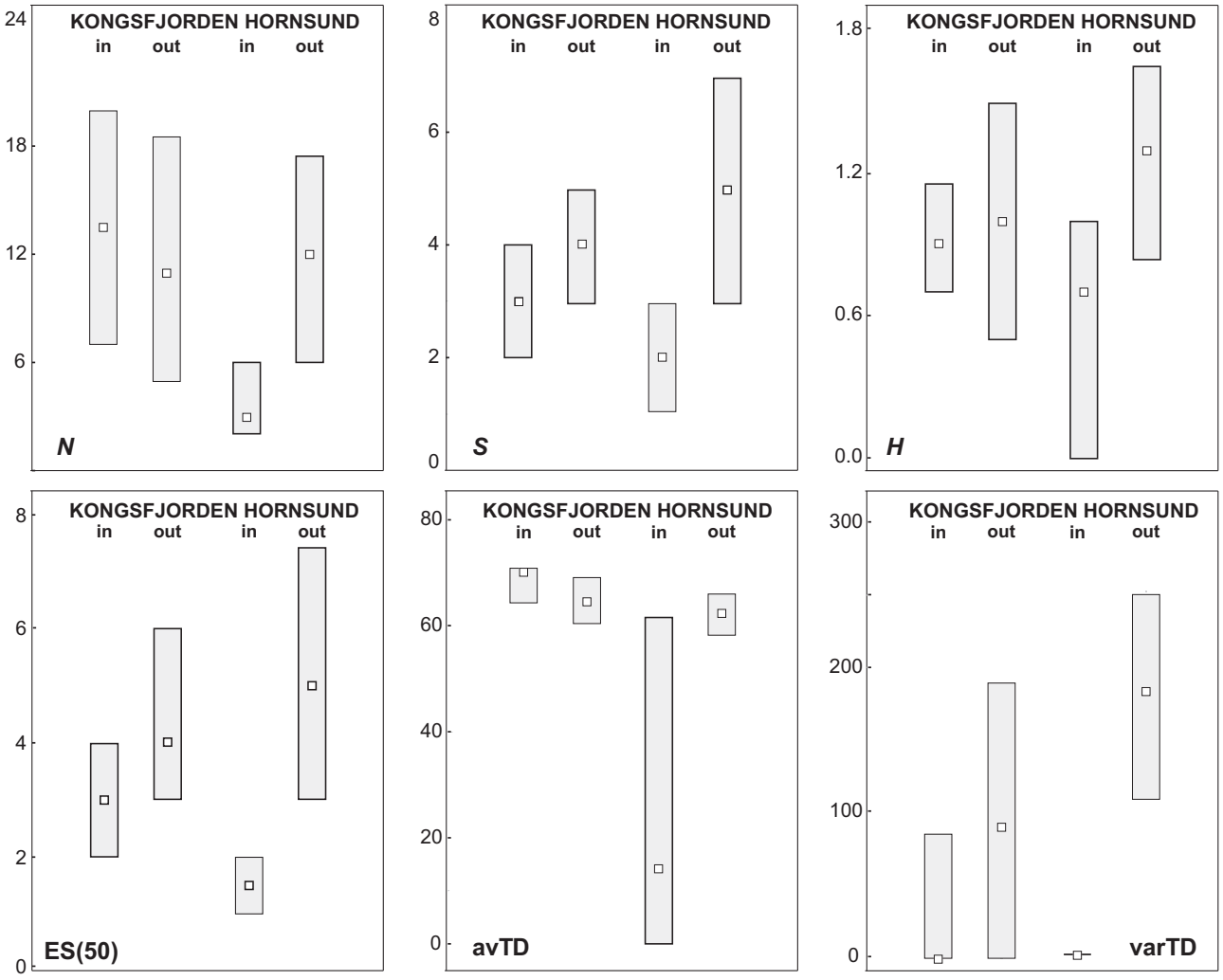

Figure 7 Density (*N* – number of specimens per 0.1 m^{-2}) and diversity [*S* – number of species per sample; *H* – Shannon–Wiener index; ES(50) – Hurlbert index; avTD – average taxonomic distinctness; varTD – variance of taxonomic distinctness] for VV samples. The boxes represent the interquartile range from the 25th to the 75th percentile, while the white squares represent the median value; in – inner glacial bays; out – outer basins.

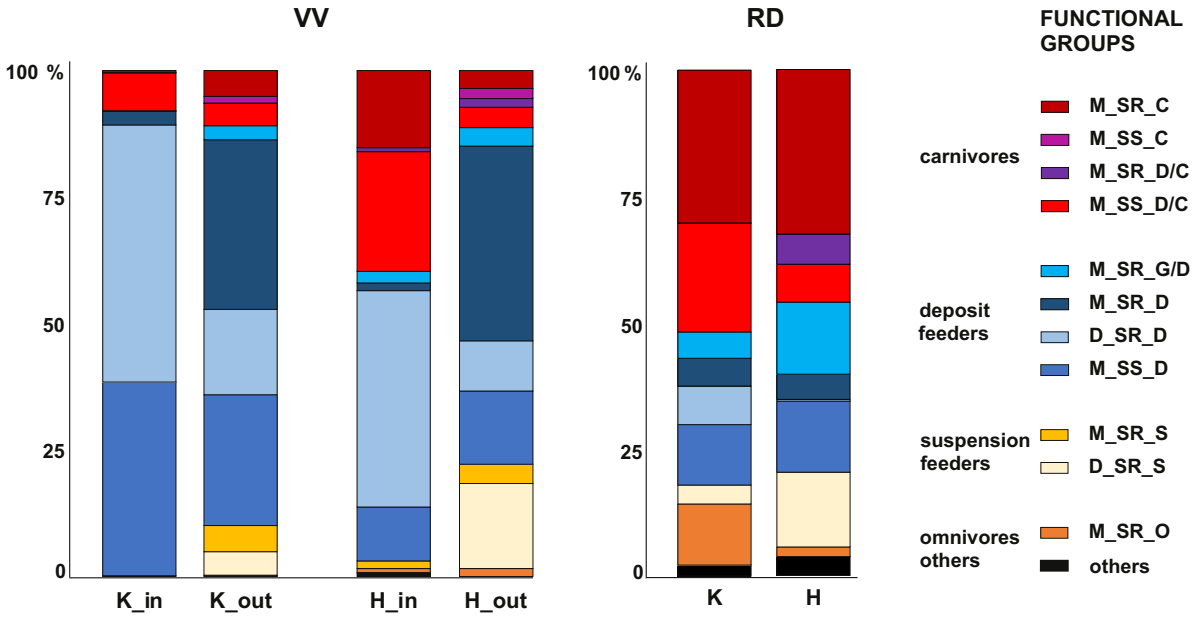

Figure 8 Percentages of individuals belonging to certain functional groups in the total number of specimens taken with a grab (VV) or a dredge (RD) in Kongsfjorden (K) and Hornsund (H), and their inner glacial bays (in) and outer basins (out). Functional group codes: M — motile; D — discretely mobile; SR — surface feeder; SS — subsurface feeder; C — carnivore; D/C — deposit feeder/facultative carnivore; G/D — microalgae grazer/deposit feeder; D — deposit feeder; S — suspension feeder; O — omnivore.

Table 6 The ten most dominant species collected with a dredge in Hornsund and Kongsfjorden.

Kongsfjorden				Hornsund			
Taxon	D	F	Tn	Taxon	D	F	Tn
Monoculodes packardi (A)	14	44	1116	*Sabinea septemcarinata* (D)	16	54	122
Lebbeus polaris (D)	10	48	792	*Diastylis goodsiri* (C)	9	62	68
Eudorella emarginata (C)	9	70	775	*Eudorella emarginata* (C)	9	54	65
Tanaidacea indet. (T)	8	41	630	*Orchomenella minuta* (A)	6	54	44
Arrhis phyllonyx (A)	7	70	616	*Haploops tubicola* (A)	5	46	40
Spirontocaris spinus (D)	5	52	439	*Ampelisca eschrichtii* (A)	4	54	32
Pseudomma truncatum (M)	5	44	402	*Diastylis scorpioides* (C)	4	46	31
Eurycope sp. (I)	4	52	330	*Arrhis phyllonyx* (A)	4	61	31
Syrrhoe crenulata (A)	4	56	321	*Eualus gaimardi* (D)	4	46	29
Mysis oculata (M)	4	11	296	*Unciola leucopis* (A)	4	46	28
Eualus gaimardi (D)	4	37	291	*Leucon* spp. (C)	4	46	27

D, dominance; F, frequency of occurrence; Tn, total number of specimens; A, Amphipoda; C, Cumacea; D, Decapoda; T, Tanaidacea.

12.1, $p < 0.001$, PERMDISP: $t = 1.9$, $p > 0.1$). There were no differences between the two fjords in average species richness (Kongsfjorden: 16.3 ± 6.4; Hornsund: 14.8 ± 8.5) and Shannon—Wiener (1.9 ± 0.5 and 2.1 ± 0.9, respectively) or Hurlbert indices (10.5 ± 3.9 and 13.5 ± 8.2, respectively). Fifteen functional groups were found in both fjords. Mobile forms were in the overwhelming majority, accounting for 81—86% of the fauna. In terms of feeding mode, facultative and obligate carnivores were dominant, making up 60% and 52% of the samples from Hornsund and Kongsfjorden, respectively, and there were 19% of deposit feeders in Hornsund and 25% in Kongsfjorden. The relative abundance of suspension-feeding organisms was much higher in Hornsund (19%) than in Kongsfjorden (4%) (Fig. 8). The Kongsfjorden fauna was dominated by individuals smaller than 20 mm (75%), whereas in Hornsund approximately half the specimens were smaller than and half were larger than 20 mm. However, the PERMANOVA results indicated that neither the functional structure nor the size composition differed between two fjords (Fig. 9).

5. Discussion

5.1. Sampling efficiency

Each type of sampling gear has specific advantages and limitations, and its optimal performance also depends upon the depth and type of substrate. This results in little consistency among datasets obtained using different types of gear, in terms not only of taxonomic composition but also of

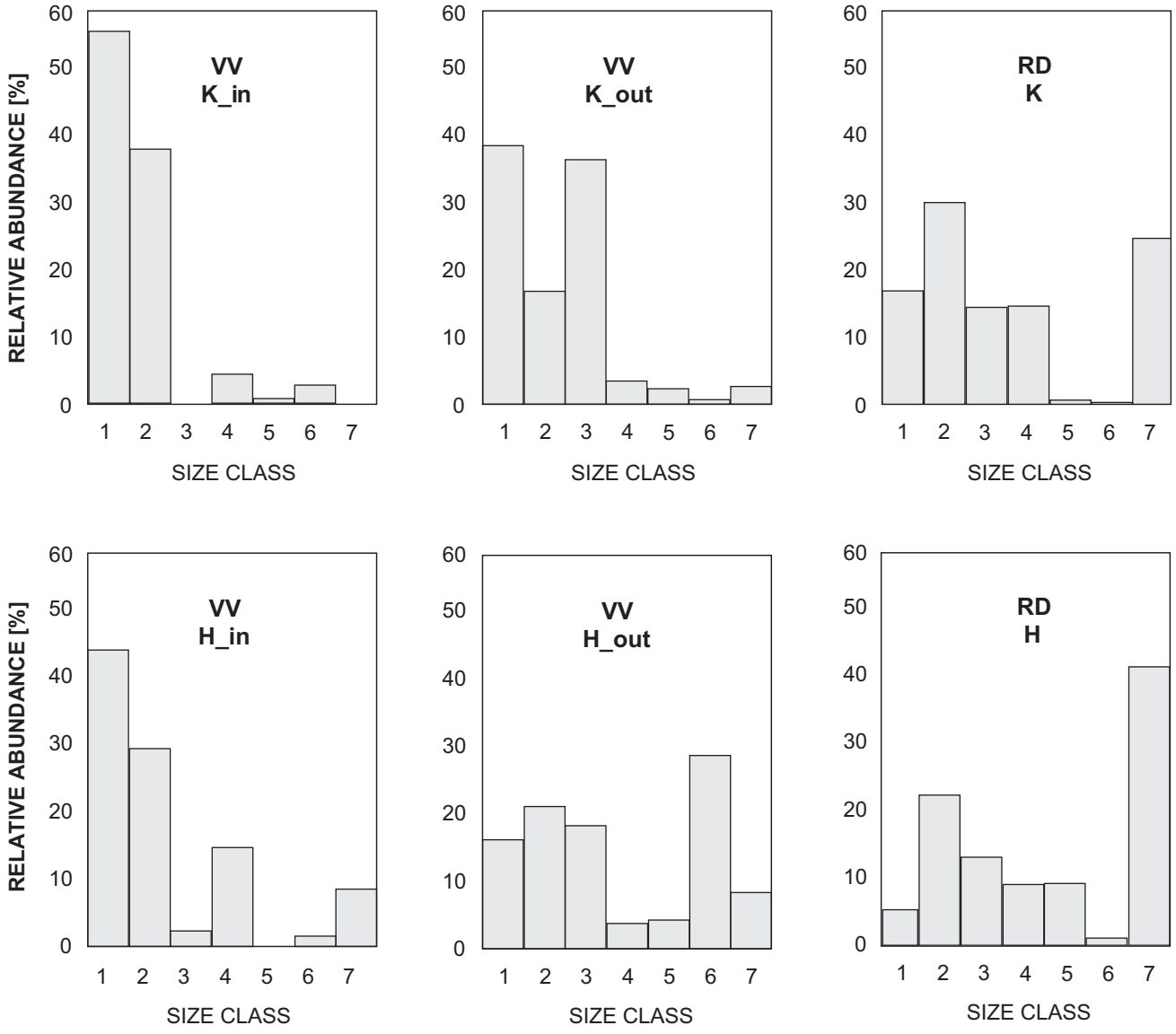

Figure 9 Percentages of individuals belonging to particular size classes in the total number of specimens taken with a grab (VV) or a dredge (RD) in Kongsfjorden (K) and Hornsund (H), and their inner glacial bays (in) and outer basins (out). Size class codes: 1: 0—5 mm; 2: 6—10 mm; 3: 11—15 mm; 4: 16—20 mm; 5: 21—25 mm; 6: 26—30 mm; 7: >30 mm.

functional groups (Brandt and Schnack, 1999; Flannery and Przeslawski, 2015; Jørgensen et al., 2011; Fig. 8). The application of different samplers is, therefore, essential for obtaining a comprehensive synthesis of the community as a whole (Jørgensen et al., 2011). This is particularly evident in the case of the ecologically diversified Malacostraca, characterized as they are by a patchy distribution and abundance. Moreover, some aspects of crustacean behaviour, such as high mobility, the formation of swarms or aggregations and the active avoidance of sampling gear (Hirche et al., 2015; Sainte-Marie and Brunel, 1985), can severely limit sampling effectiveness. Thus, the van Veen grab with its relatively small catching area (0.1 m^2) was less effective (on average 4 species per sample) than a dredge (on average 15—16 species per sample) employed in similar habitats and depth ranges. However, among the gear used the grab was the only type suitable for infauna sampling (Flannery and Przeslawski, 2015), and the large number of samples taken seemed to compensate for this limitation, since the total number of species collected with it (88 species) was comparable to that collected with the dredge (100 species). Dredging accumulates organisms over a long distance and covers mobile as well as scarce forms. Besides epibenthic taxa, the dredged material also contains considerable numbers of infauna that are swirled up in front of the gear (Brandt and Schnack, 1999). However, neither the grab nor the dredge used in this study was able to provide sufficient coverage of the highly mobile hyperbenthos and scavenging Crustacea, known to form aggregations on carcasses (Brandt and Barthel, 1995; Sainte-Marie, 1986). Estimating the composition and densities of such taxa is dependent on specialized equipment, such as sledges with epi- and suprabenthic samplers (Brandt and Barthel, 1995) or baited traps (Legeżyńska, 2001; Nygård, 2011).

The majority of benthic samples in current study came from the subtidal zone (average sampling depth 129 m in Hornsund and 165 m in Kongsfjorden) with a uniformly soft bottom, which is not the type of substrate preferred by most crustacean species. In this habitat, 89 species were recorded in Hornsund and 96 in Kongsfjorden. A similar species richness has been reported for Polychaeta in Hornsund (86 species recorded between 100 and 250 m; Kędra et al., 2013) and for Mollusca in Kongsfjorden (87 species recorded between 5 and 390 m; Włodarska-Kowalczuk, 2007). Shallow (>50 m) bottom areas, which host rich communities of small vagile invertebrates, are still relatively poorly studied because they are not accessible to research vessel operations. A scuba-diving investigation of hard-bottom benthos between 0 and 30 m in Kongsfjorden recorded the occurrence of at least 60 malacostracan species, 37 of which were not found in this study (Voronkov et al., 2013). Dredging in the same fjord on a variety of bottom substrata between 5 and 50 m yielded 49 malacostracan taxa (Kaczmarek et al., 2005). It is, therefore, clear that a broad survey across the entire range of depths and habitats based on the concurrent use of different gear types to cover infauna, epifauna and hyperbenthos is needed in order to obtain a realistic species inventory.

5.2. Species richness

Despite the considerable number of samples taken, the species accumulation curves for S_{obs} of benthic taxa in Kongsfjorden and Hornsund were not asymptotic, suggesting that some species remained undetected in both fjords. The *Chao2* estimator indicated that a larger number of species could be present. S_{obs} may be downward biased owing to the large percentages of rare species. The overlapping values of 0.95 CI of both S_{obs} and *Chao2* suggest that a generally similar richness of malacostracan species may be expected in both fjords.

Combining our data with published records of species richness in Kongsfjorden and Hornsund revealed the presence of around 190 malacostracan taxa: this is about 50% of the species known from the whole Svalbard archipelago area within latitudes 74°—81°N and longitudes 10°—35°E (Palerud et al., 2004). This is a surprisingly high percentage, given the limited area and depth range available in the fjords compared with the whole archipelago. Comparison of our data with other published assessments from the European Arctic is problematic, since sampling effort, collecting methods and depth coverage differ among them. Although a substantial drop in Arthropoda species richness with increasing latitude has been recorded along the Norwegian coast (Narayanaswamy et al., 2010), no obvious poleward pattern exists in the Arctic Ocean (Brandt, 1997; Weisshappel and Svavarsson, 1998). The highest diversity of Malacostraca has been reported from the thoroughly studied Barents Sea (68—81°N), east of Svalbard, the highly heterogeneous ecosystem of which hosts a rich mixture of Arctic and North Atlantic taxa (>500 species) (Sirenko, 2001). A diversity of malacostracan fauna is also characteristic of the western part of the Greenland Sea, west of Svalbard: even a small number of samples (31 epibenthic sledge samples) at three localities from the shelf down to deep waters (67—81°N; 45—2681 m) yielded over 200 species of peracarid crustaceans (i.e. amphipods, isopods, cumaceans and tanaidaceans) (Brandt, 1997). Just five short trawls with the same gear along the eastern Greenland shelf revealed 181 peracarid species between 158 and 251 m (Stransky and Brandt, 2010). Even based on these limited data, a huge difference in malacostracan biodiversity between the eastern and western sides of the Greenland Sea can be assumed and is probably related to differences in primary water masses, ice cover and primary productivity in these two areas (Narayanaswamy et al., 2010).

5.3. Factors determining the distribution and composition of pelagic and benthic malacostracan communities

While the regional species pool is the upshot primarily of evolutionary history, numerous environmental factors, including the properties and distribution of water masses, sedimentation regime, type of available substrata, quality and quantity of food may determine malacostracan distributions (Brandt, 1993, 1995, 1997; Weisshappel and Svavarsson, 1998). Moreover, certain aspects of their biology (e.g. direct vs. larval development) and ecology (pelagic vs. benthic habitat, sessile vs. vagile lifestyle, food and habitat preferences) (Brandt et al., 2012) may be important in creating distribution patterns.

The data on large-scale distribution, summarized in Table 4, indicate that the majority of malacostracan species hitherto recorded in Kongsfjorden and Hornsund show remarkably wide depth ranges and are widely distributed in the North Atlantic and the Arctic. 72% of all 186 taxa were noted along the north coast of Norway and 87% in the Barents Sea. The current species richness and taxonomic composition clearly reflect the glacial history of the Arctic Ocean. At the last glacial maximum, the entire shelf of the Atlantic Arctic was covered with glacial ice that extended beyond the shelf-break and would have precluded the existence of a shallow-water fauna (Jakobsson et al., 2014). Recolonization of the Spitsbergen fjords by species originating from the North Atlantic and deep Arctic Ocean started only 10 000 years ago, after the ice sheet had retreated. Most benthic taxa do not have a planktonic larval stage; this may limit their potential for dispersal and delay colonization of the fjords (Jażdżewski et al., 1995). As a result, the fjord fauna is impoverished and dominated by widespread boreal-Arctic taxa, with a high faunal affinity to the North Atlantic.

Lying at the boundary between the Barents and Greenland Seas, Svalbard is exposed to a variety of hydrological regimes (Walczowski, 2013). Advection of shelf waters has been considered a major factor shaping the pelagic community in the fjords (Dalpadado et al., 2016; Gluchowska et al., 2016). The list of planktonic taxa obtained in our samples is typical of coastal Svalbard waters and consists of a mixture of boreal-Arctic and boreal-Atlantic elements (Węsławski et al., 2000). Their relative contribution to the total abundance in each fjord mirrors the different influences of Atlantic and Arctic waters (see the next section).

The broad distribution of benthic species across the latitudinal and depth gradients may suggest that hydrological conditions and depth have a negligible influence on their presence in these two fjords. Nonetheless, the small depth range in them may be unfavourable to some taxa. For

example, species numbers of tanaids and isopods tend to rise with increasing depth in the Greenland Sea (Brandt, 1997). Similarly, Svavarsson (1997) observed that the species diversity of isopods in the Arctic Ocean peaks in the 320–1100 m depth zone. On the other hand, in contrast to the open sea, fjords contain shallow, structurally complex microhabitats (Kaczmarek et al., 2005; Tatarek et al., 2012; Włodarska-Kowalczuk, 2007; Włodarska-Kowalczuk et al., 2009) that may be species-rich 'hot spots' of benthic crustaceans. Indeed, there is a gradual decrease of species richness with increasing depth in Kongsfjorden and Hornsund: 125 species were reported from waters shallower than 50 m, the number of species fell from 89 to 68 between 50 and 200 m, and only 46 species were found to be living at depths greater than 300 m. A similar depth-related species richness pattern was recorded in gammarid amphipods from the Barents Sea (Bryazgin, 1997). However, the dominant shallow water species in the Spitsbergen fjords are known to be associated with macroalgae vegetation (Kaczmarek et al., 2005; Legeżyńska, 2008; Lippert et al., 2001; Ronowicz et al., 2013), others, such as scavenging lysianassoid amphipods, may benefit from the pelagic and benthic food abundant in this depth zone (Legeżyńska, 2001). Thus, one can assume that substrate heterogeneity rather than depth itself may be responsible for the observed high species richness. This assumption is further supported by the results of soft-bottom studies from shallow Kongsfjorden waters: only 10 species of Crustacea were found between 5 and 30 m on the uniform sand-clay sediment of the outer fjord (Laudien et al., 2007), the same number of species within the same depth zone was collected from the unconsolidated muddy bottom in the Kongsbreen glacial bay (Kaczmarek et al., 2005).

Bottom type is generally considered an important factor structuring entire benthic communities. Jażdżewski et al. (1995) highlighted the low heterogeneity of substrata as one of the main reasons for the poor amphipod diversity in the Arctic. One of the results of glacial activity is the prevalence of fine-grained sediments. Subtidal sediments (>50 m) throughout the fjords are dominated by glacio-marine deposits, which are mostly silt and clay (Drewnik et al., 2016; Włodarska-Kowalczuk and Pearson, 2004). The sediments in the inner and outer basins are similar in their granulometry, but differ in stability (Włodarska-Kowalczuk and Pearson, 2004). A muddy bottom obviously favours the occurrence of burrowing taxa, such as oedicerotid amphipods, cumaceans and tanaids, which are dominant in the inner basins of Kongsfjorden and Hornsund. These taxa can persist on the sediment surface because of their negligible weight (tanaids) or can actively move through or over the soft substratum (*E. emarginata*, oedicerotids). On the other hand, homogeneous fine-grained sediments are regarded as the least favourable habitat for most highly specialized amphipods (Buhl-Mortensen, 1996). For example, relatively large domiculous amphipods, such as *Ampelisca*, *Haploops* and *Unciola*, require a compact bottom and do not colonize the loose sediments in the inner bays (this study). Similarly, Buhl-Mortensen (1996) observed the decreasing dominance of tube-dwelling amphipods from offshore to the inner fjord in southern Norway. As already mentioned, the richest malacostracan community inhabits a diverse shallow water substrata which provide good foraging opportunities and shelter from predators and environmental stressors.

Another factor regulating species distribution may be food availability. Fjords provide benthic fauna with relatively good feeding opportunities; pelagic production is supplemented by other sources, not available in the open sea, such as macro- and microphytobenthos and terrestrial organic matter (Hop et al., 2002; Renaud et al., 2015; Zaborska et al., 2016). Because of their surprisingly variable and flexible feeding behaviours (Dauby et al., 2001; Huenerlage et al., 2015; Legeżyńska et al., 2012), crustaceans can exploit a variety of food sources, adjusting their diet according to local conditions. Fjord morphology, high rates of organic matter fluxes and inorganic sedimentation (Zajaczkowski, 2008) enhance sediment accumulation and inhibit extensive organic matter mineralization (Smith et al., 2015). The surplus of organic matter settled on the bottom in the form of detritus can persist long-buried in the sediments, supporting local benthic communities and releasing them from the dependence on highly seasonal fluctuations of primary production fluxes (Dunton and Schell, 1987; Kędra et al., 2013; McMeans et al., 2013; Renaud et al., 2015). Indeed, detritus has been shown to be an important all-year-round source of food for amphipod communities in the Spitsbergen fjords (Legeżyńska et al., 2012). However, while the food supply seems to be assured in the outer fjord basins, the fauna of the glacial bays may suffer from both a scarcity and the poor quality of food. Typically, organic matter availability diminishes towards the glacial bays (Włodarska-Kowalczuk and Pearson, 2004; Kędra et al., 2010) owing to a number of factors related to glacier activity: decrease in primary production (Piwosz et al., 2009) and dilution of the sedimenting organic matter by the high inorganic sediment load (Görlich et al., 1987).

The pronounced decline of infauna species richness from the outer to the inner basins of Hornsund (62–18 species) and Kongsfjorden (52–15 species) is in accordance with general trends observed in both soft-bottom (Kędra et al., 2013; Włodarska-Kowalczuk et al., 2005, 2012) and hard-bottom benthic communities (Voronkov et al., 2013). Two explanations for the lower faunal diversity in the fjords have usually been put forward: 'the barrier hypothesis', which assumes that geomorphological barriers such as sills or habitat fragmentation may prevent colonization by an offshore species pool, and the 'habitat hypothesis', which attributes the lower diversity of the fjord fauna to the less favourable environmental conditions relative to offshore habitats (Buhl-Mortensen, 1996; Włodarska-Kowalczuk et al., 2012). Both Hornsund and Kongsfjorden lack entrance sills, which should facilitate the penetration of shelf fauna into the fjords. The inner basins, however, are separated from the main fjords by shallow (20–50 m) sills, that may act as a barrier to dispersal. If sills really do act as barriers preventing benthos dispersal, one would expect a different performance of taxa with various dispersal modes in the inner basins (Buhl-Mortensen, 1996). However, a drop in species richness has also been reported in polychaetes with a pelagic larval stage (Kędra et al., 2013; Włodarska-Kowalczuk and Kędra, 2007). Therefore, it can be assumed that the observed trends of diversity are not directly connected with the presence of sills, but rather with the environmental settings characteristic of the outer and inner fjords.

The decline in benthic fauna diversity along the offshore-inner fjord gradient in the Arctic is most commonly attrib-

uted to chronic physical disturbances generated by the activity of tidal glaciers (Kędra et al., 2013; Włodarska-Kowalczuk et al., 2005, 2012; Włodarska-Kowalczuk and Węsławski, 2008). Environmental stressors, i.e. high rates of mineral sedimentation, the substantial turbidity of water, unconsolidated muddy sediments and reduced amounts of organic matter, have a detrimental effect on the macrofauna, which may manifest itself in a biodiversity decline, lower abundance and taxonomic distinctness, reduced biomass and simplification of the functional structure (Kędra et al., 2013; Włodarska-Kowalczuk, 2007; Włodarska-Kowalczuk et al., 2005). Nonetheless, major benthic taxa tend to respond differently to glacier-induced disturbances. The diversity and abundance of polychaetes drop considerably with increasing proximity to the glaciers, both in Hornsund (Kędra et al., 2013) and Kongsfjorden (Włodarska-Kowalczuk and Kędra, 2007), while the species richness of molluscs does not change much along the Kongsfjorden axis and their density is significantly higher in the glacial bays than in other basins of the fjord (Włodarska-Kowalczuk, 2007). Crustaceans do not respond to the proximity of glaciers in Kongsfjorden, which is why Włodarska-Kowalczuk and Kędra (2007) stated that other factors must be responsible for their spatial variability. Current results from Kongsfjorden support their conclusion: there has been a decline in the total number of species, but otherwise the malacostracan communities of the inner and outer basins have not varied in average density and diversity. A totally different picture emerged for Hornsund, where the malacostracans of the innermost glacial basin (Brepollen) were clearly less diversified and much poorer in both species and numbers compared to the outer basin community (see the next section). This suggests that the crustaceans' response may be highly variable and difficult to account for. The lack of a clear response to glacier-induced disturbances has also been observed in Antarctic cumaceans (Pabis and Błażewicz-Paszkowycz, 2011).

Environmental conditions in the inner fjord basins may lead to simplification of the functional structure of the faunal associations (Włodarska-Kowalczuk et al., 2005). The benthic communities of the inner fjords are usually dominated numerically by small, mobile, surface detritus feeders represented by several species that cope well with glacial sedimentation disturbances (Włodarska-Kowalczuk, 2007; Włodarska-Kowalczuk et al., 2005, 2012). The same trend holds true in the case of crustaceans. Two taxa that are predominant in the inner bays of both fjords were tanaids and the cumacean *E. emarginata*. Tanaids are elongated crustaceans that are usually less than 2 mm long and most often occur within the surface sediment layer. Their ecology is still poorly known. According to Błażewicz-Paszkowycz and Sekulska-Nalewajko (2004), they prefer sites with unstable sediments. All the species identified by Błażewicz-Paszkowycz and Sekulska-Nalewajko (2004) from the Kongsfjorden samples (included in our material) belong to the suborder Tanaidomorpha, which are assumed to be tubicolous (Błażewicz-Paszkowycz et al., 2012); some species, however, may be free-living inside delicate corridors made of mud particles (Błażewicz-Paszkowycz, 2007). Most tanaids are regarded as non-selective deposit feeders, but the representatives of Pseudotanaidea found in our material may be micropredators feeding on harpacticoida and foraminifera (Prof. M. Błażewicz-Paszkowycz, personal communication). The cumacean *E. emarginata* is a widely distributed eurybathic Arctic-boreal burrowing species. It was the most frequent taxon in our benthic materials, recorded throughout the depth range, but the most abundant in the soft, unconsolidated sediments of inner Kongsfjorden. A similar habitat preference of *Eudorella* spp. was observed in Norwegian (Holte, 1989) and Antarctic fjords (Błażewicz and Jażdżewski, 1995). *Eudorella* has been classified as a phytodetritus feeder (Błażewicz-Paszkowycz and Ligowski, 2002; Legeżyńska et al., 2012). Other important members of the glacial bay communities were the oedicerotids *Arrhis phyllonyx* and *Monoculodes packardi*. Oedicerotidae species are known to dominate soft bottoms and are especially dominant in the fjords (Buhl-Mortensen, 1996). They are highly mobile forms, capable of exploiting both sediment and epibenthic food sources such as detritus and meiofauna (Enequist, 1949; Legeżyńska et al., 2012). In accordance with the general trends observed in macrofauna (e.g. Włodarska-Kowalczuk et al., 2005, 2012), the Malacostraca of the outer fjord basins were functionally more diversified. A more compact bottom and higher primary production (Piwosz et al., 2009) promotes the occurrence of tube-dwelling amphipods such as *Ampelisca eschrichtii*, *Haploops tubicola* and *Unciola leucopis*, which are 'interface feeders', using their antennae to collect particles from both the sediment surface and the water column (Legeżyńska et al., 2012).

5.4. Kongsfjorden vs. Hornsund

The results of the PERMANOVA analysis suggest different taxonomic, functional and size compositions of the malacostracan assemblages in the two fjords, but these differences can be regarded as different expressions of the same species pool since they were largely due to the varying dominance patterns of the same set of species. This concurs with the results of the study by Berge et al. (2009) on Decapoda in Isfjorden (Spitsbergen). Although some 30 species were unique to each fjord, none of these taxa was numerous or frequent. It, thus, appears that the 'core set' of species is common to both fjords.

The different performance of the same species pool in the two fjords could be due to several factors. Firstly, Kongsfjorden and Hornsund differ in terms of geomorphology and dominant water masses. The geomorphological features at the mouth of Kongsfjorden permit a twofold faster rate of water exchange with this fjord (Promińska et al., 2017), which receives warm Atlantic water from the West Spitsbergen Current via the deep Kongsfjordrenna. In contrast, the advection of shelf waters is weaker in Hornsund, the mouth area of which is rather shallow (maximum depth about 150 m; Promińska et al., 2017). Furthermore, the strong hydrological front on the adjacent shelf partially blocks the inflow of Atlantic waters which, along with the stronger penetration of Arctic waters carried by the Sørkapp Current from the Barents Sea, results in the more Arctic character of this fjord (Walczowski, 2013). Shelf water advection has a major impact on the pelagic system (Buchholz et al., 2010; Dalpadado et al., 2016; Gluchowska et al., 2016). The absolute predominance of *T. abyssorum* observed in Kongsfjorden is in accordance with the recent study by Dalpadado et al. (2016). The dominance of this species, together with the

presence of Atlantic euphausiid species such as *Meganyctiphanes norvegica* and *Nematoscelis megalops* (Buchholz et al., 2010), has been recognized as a clear sign of the "Atlantification" of Kongsfjorden, which is happening as a result of the rising temperatures of the Atlantic waters penetrating into it (Dalpadado et al., 2016). On the other hand, the predominance of a more Arctic species, *T. inermis*, in Hornsund has been attributed to the cold conditions persisting due to the influence of the coastal Sørkapp Current (Buchholz et al., 2010). The input of coastal currents may also explain the high dominance level of Decapoda larvae in Hornsund (this study). The shallow rocky bottom on the shelf south of Hornsund is an important spawning ground for the hermit crab *P. pubescens* (Balazy et al., 2015). The direct influence of different water masses on benthic fauna distribution seems less probable, but benthic communities may be impacted indirectly, e.g. by changes in the planktonic community possibly modifying feeding conditions. We observed higher proportions of suspension-feeding species in Hornsund, which is in accordance with the higher primary production rates reported for this fjord by Piwosz et al. (2009). These species may also be benefitting temporarily from sedimenting ice-algae diatoms, which are associated with pack ice remnants carried by the Sørkapp Current from the Barents Sea.

According to our results the benthic malacostracan community of inner Hornsund is more impoverished than that of the corresponding area of Kongsfjorden. A significant drop in species richness was observed in both fjords, but only in Hornsund was it accompanied by a significant decrease in density and diversity. This seems quite surprising since the organic carbon content is higher in the Hornsund glacial bay than in the inner Kongsfjorden (Drewnik et al., 2016; Kędra et al., 2010; Włodarska-Kowalczuk and Pearson, 2004). However, higher percentages of terrestrial organic carbon are characteristic of the surface sediments in Hornsund (Zaborska et al., 2016). Koziorowska et al. (2016) reported that terrestrial organic carbon makes up to 82% of total carbon pool in the inner Hornsund. Compared to fresh marine organic matter, terrestrial carbon is regarded as a less suitable food source because most marine organisms appear to be unable to digest and assimilate refractory compounds such as cellulose and lignin without their prior microbial breakdown (Antonio et al., 2010).

The poor performance of malacostracans in the inner Hornsund may also be due to its greater isolation. Hornsund contains several distinct basins, and only a very narrow (1.7 km) passage connects the innermost glacial bay (Brepollen) with the main fjord basin (Drewnik et al., 2016; Moskalik et al., 2013). As a result, Brepollen is a truly isolated habitat, with very limited water exchange and a persistent near-bottom layer of cold winter waters. In contrast, Kongsfjorden's central basin takes the form of an elongated deep trough that almost reaches the inner sill. The narrowest cross section (~4 km) is located in the central part of the fjord; closer to the glacier there is a broad connection allowing unhampered penetration of upper water layers into the glacial bay.

Based on observations from Brepollen, where the near-bottom temperature has remained between −1.8°C and −0.6°C during the last 30 years, Węsławski et al. (2011) suggested that the inner fjord basins may be acting as refugia for stenothermic Arctic species. Although the dominance of widely distributed Arcto-boreal taxa in the inner fjords demonstrated in this study does not support this concept, we did observe a clear preference for the inner bay habitats in two typical Arctic species — *Onisimus caricus* and *Lepidepecreum umbo*.

6. Conclusions

There is general agreement that the Arctic Ocean is currently in a transition towards a new, warmer state (Narayanaswamy et al., 2010). Oceanographic variability has been proven to have a direct and detectable influence on pelagic (Dalpadado et al., 2016) and benthic fauna (Berge et al., 2005; Beuchel et al., 2006; Kortsch et al., 2012) in Spitsbergen fjords. Owing to the influence of different water masses, 'warm' Kongsfjorden and 'cold' Hornsund could serve respectively as examples of areas in a transition state and true Arctic areas. Our results suggest that the contrasting hydrological regimes have a strong impact on the pelagic malacostracan communities, but govern neither the distribution nor the diversity of benthic taxa, which are influenced more by the interaction of several factors, such as depth, sediment type, microhabitat variety and food availability and quality. The majority of species collected were widely distributed Arctic-boreal forms, capable of surviving over the whole range of temperatures and salinities noted in both fjords. Our results suggest that habitat homogenization resulting from the predicted increase of sediment discharge associated with accelerated glacier melt will severely affect benthic malacostracan communities. A clear decline of species richness was observed on the uniform muddy bottoms of the glacial bays of both fjords, although the patterns of species density and diversity differed in Kongsfjorden and Hornsund. The greater impoverishment of the benthic malacostracan community found in the Hornsund glacial bay was probably due to its greater isolation and poorer quality of sediment organic matter in comparison with the corresponding area of Kongsfjorden. Trends common to the glacial bays of both fjords were the numerical dominance of individuals belonging to the smallest species and the reduced trophic diversity. The variability in the taxonomic, size and functional composition of pelagic and benthic malacostracan communities may be ecologically important, and therefore requires further detailed study. As the heterogeneous habitats of the shallow sublittoral are likely to be diversity and density hot spots for benthic malacostracans, an extensive survey across the entire range of shallow water habitats is needed in order to obtain a realistic inventory of the fjords' species.

Acknowledgements

This study was conducted as part of the 'Growing of the Arctic Marine Ecosystem' project and financed by the Polish National Science Centre by grants 2012/04/A/NZ8/00661, 2012/05/B/ST10/01908 and 2012/05/B/NZ8/02652 and IO PAN statutory activities (Theme III). We thank the captain and crew of r/v *Oceania* and the whole scientific team for their support and assistance at sea during the sampling.

References

Anderson, M.J., Gorley, R.N., Clarke, K.R., 2008. PERMANOVA+ for PRIMER: Guide to Software and Statistical Methods. PRIMER-E Ltd., Plymouth, 214 pp.

Antonio, E.S., Kasai, A., Ueno, M., Kurikawa, Y., Tsuchiya, K., Toyohara, H., Yamashita, Y., 2010. Consumption of terrestrial organic matter by estuarine molluscs determined by analysis of their stable isotopes and cellulase activity. Estuar. Coast. Shelf Sci. 86 (3), 401—407, http://dx.doi.org/10.1016/j.ecss.2009.05.010.

Balazy, P., Kukliński, P., Włodarska-Kowalczuk, M., Barnes, D., Kędra, M., Legeżyńska, J., Węsławski, J.M., 2015. Hermit crabs (*Pagurus* spp.) at their northernmost range: distribution, abundance and shell use in the European Arctic. Polar Res. 34, 1—17, http://dx.doi.org/10.3402/polar.v34.21412.

Berge, J., Johnsen, G., Nilsen, F., Gulliksen, B., Slagstad, D., 2005. Ocean temperature oscillations causes the reappearance of blue mussels in Svalbard after 1000 years of absence. Mar. Ecol.-Prog. Ser. 303, 167—175, http://dx.doi.org/10.3354/meps/303167.

Berge, J., Renaud, P.E., Eiane, K., Gulliksen, B., Cottier, F.R., Varpe, Ø., Brattegard, T., 2009. Changes in the decapod fauna of an Arctic fjord during the last 100 years (1908—2007). Polar Biol. 32 (7), 953—961, http://dx.doi.org/10.1007/s00300-009-0594-5.

Beuchel, F., Gulliksen, B., Carroll, M.L., 2006. Long-term patterns of rocky bottom macrobenthic community structure in an Arctic fjord (Kongsfjorden, Svalbard) in relation to climate variability (1980—2003). J. Marine Syst. 63, 35—48.

Błażewicz, M., Jażdżewski, K., 1995. Cumacea (Crustacea, Malacostraca) of Admiralty Bay, King George Island: a preliminary note. Pol. Polar Res. 16 (1—2), 71—86.

Błażewicz-Paszkowycz, M., 2007. A revision of the family Typhlotanaidae Sieg 1984 (Crustacea: Tanaidacea) with the remarks on the Nototanaidae Sieg, 1976. Zootaxa 1958, 1—141.

Błażewicz-Paszkowycz, M., Bamber, R., Anderson, G., 2012. Diversity of tanaidacea (crustacea: Peracarida) in the world's oceans — how far have we come? PLoS ONE 7 (4), 1—11, http://dx.doi.org/10.1371/journal.pone.0033068.

Błażewicz-Paszkowycz, M., Ligowski, R., 2002. Diatoms as food source indicator for some Antarctic Cumacea and Tanaidacea (Crustacea). Antarct. Sci. 14 (1), 11—15, http://dx.doi.org/10.1017/S0954102002000524.

Błażewicz-Paszkowycz, M., Sekulska-Nalewajko, J., 2004. Tanaidacea (Crustacea, Malacostraca) of two polar fjords: Kongsfjorden (Arctic) and Admiralty Bay (Antarctic). Polar Biol. 27 (4), 222—230, http://dx.doi.org/10.1007/s00300-003-0585-x.

Brandt, A., 1993. Composition, abundance, and diversity of peracarid crustaceans on a transect of the Kolbeinsey Ridge, north of Iceland. Polar Biol. 13, 565—576, http://dx.doi.org/10.1007/BF00236399.

Brandt, A., 1995. The perecarid fauna (Crustacea, Malacostraca) of the Northeast Water Polynya, off Greenland, documenting close benthic-pelagic coupling. Mar. Ecol.-Prog. Ser. 121, 39—51, http://dx.doi.org/10.3354/meps121039.

Brandt, A., 1997. Biodiversity of peracarid crustaceans (Malacostraca) from the shelf down to the deep Arctic Ocean. Biodivers. Conserv. 6 (11), 1533—1556, http://dx.doi.org/10.1023/a:1018318604032.

Brandt, A., Barthel, D., 1995. An improved supra- and epibenthic sledge for catching Peracarida (Crustacea, Malacostraca). Ophelia 43 (1), 15—23.

Brandt, A., Błażewicz-Paszkowycz, M., Bamber, R.N., Mühlenhardt-Siegel, U., Malyutina, M.V., Kaiser, S., de Broyer, C., Havermans, C., 2012. Are there widespread peracarid species in the deep sea (Crustacea: Malacostraca)? Pol. Polar Res. 33 (2), 139—162, http://dx.doi.org/10.2478/v10183-012-0012-5.

Brandt, A., Schnack, K., 1999. Macrofaunal abundance at 79°N off East Greenland: opposing data from epibenthic-sledge and box-corer samples. Polar Biol. 22 (2), 75—81, http://dx.doi.org/10.1007/s003000050392.

Brattegard, T., Holthe, T. (Eds.), 2001. Distribution of marine, benthic macroorganisms in Norway. A tabulated catalogue.Oppdatering av utredning for DN 1997-1. Res. Rep. 2001—3. Dir. Nature Manag., Trondheim, 159—220.

Bryazgin, V., 1997. Diversity, distribution and ecology of benthic amphipods (Amphipoda, Gammaridea) in the Barents Sea sublittoral. Pol. Polar Res. 18, 89—106.

Buchholz, F., Buchholz, C., Weslawski, J.M., 2010. Ten years after: krill as indicator of changes in the macro-zooplankton communities of two Arctic fjords. Polar Biol. 33 (1), 101—113, http://dx.doi.org/10.1007/s00300-009-0688-0.

Buhl-Mortensen, L., 1996. Amphipod fauna along an offshore-fjord gradient. J. Nat. Hist. 30 (1), 23—49, http://dx.doi.org/10.1080/00222939600770031.

Carey, A.G., Boudrias, M.A., 1987. Feeding ecology of *Pseudalibrotus* (=*Onisimus*) *litoralis* Krøyer (Crustacea: Amphipoda) on the Beaufort Sea inner continental shelf. Polar Biol. 8 (1), 29—33, http://dx.doi.org/10.1007/BF00297161.

Chao, A., 2004. Species richness estimation. In: Kotz, S., Read, C.B., Balakrishnan, N., Vidakovic, B. (Eds.), Encyclopedia of Statistical Sciences. Wiley, New York, 1—23.

Clarke, K.R., Gorley, R.N., 2006. PRIMER v6. User Manual/Tutorial. PRIMER-E Ltd., Plymouth, 190 pp.

Cochrane, S.K.J., Pearson, T.H., Greenacre, M., Costelloe, J., Ellingsen, I.H., Dahle, S., Gulliksen, B., 2012. Benthic fauna and functional traits along a Polar Front transect in the Barents Sea — advancing tools for ecosystem-scale assessments. J. Marine Syst. 94, 204—217, http://dx.doi.org/10.1016/j.jmarsys.2011.12.001.

Colwell, R.K., 2013. EstimateS: Statistical estimation of species richness and shared species from samples. Version 9. Persistent URL.

Conlan, K., Hendrycks, E., Aitken, A., Williams, B., Blasco, S., Crawford, E., 2013. Macrofaunal biomass distribution on the Canadian Beaufort Shelf. J. Marine Syst. 127, 76—87, http://dx.doi.org/10.1016/j.jmarsys.2013.07.013.

Cottier, F., Tverberg, V., Inall, M., Svendsen, H., Nilsen, F., Griffiths, C., 2005. Water mass modification in an Arctic fjord through cross-shelf exchange: the seasonal hydrography of Kongsfjorden, Svalbard. J. Geophys. Res. 110, C12005, http://dx.doi.org/10.1029/2004JC002757.

Dalpadado, P., Hop, H., Rønning, J., Pavlov, V., Sperfeld, E., Buchholz, F., Rey, A., Wold, A., 2016. Distribution and abundance of euphausiids and pelagic amphipods in Kongsfjorden, Isfjorden and Rijpfjorden (Svalbard) and changes in their relative importance as key prey in a warming marine ecosystem. Polar Biol. 39 (10), 1765—1784, http://dx.doi.org/10.1007/s00300-015-1874-x.

Dauby, P., Scailteur, Y., De Broyer, C., 2001. Trophic diversity within the eastern Weddell Sea amphipod community. Hydrobiologia 443 (1), 69—86, http://dx.doi.org/10.1023/A:1017596120422.

Drewnik, A., Węsławski, J.M., Włodarska-Kowalczuk, M., Łącka, M., Promińska, A., Zaborska, A., Gluchowska, M., 2016. From the worm's point of view. I: Environmental settings of benthic ecosystems in Arctic fjord (Hornsund, Spitsbergen). Polar Biol. 39 (8), 1411—1424, http://dx.doi.org/10.1007/s00300-015-1867-9.

Dunton, K.H., Schell, D.M., 1987. Dependence of consumers on macroalgal (*Laminaria solidungula*) carbon in an arctic kelp community: $\delta^{13}C$ evidence. Mar. Biol. 93 (4), 615—625, http://dx.doi.org/10.1007/BF00392799.

Elverhøi, A., Lønne, O., Seland, R., 1983. Glaciomarine sedimentation in a modern fjord environment, Spitsbergen. Polar Res. 1 (2), 127—149, http://dx.doi.org/10.1111/j.1751-8369.1983.tb00697.

Enequist, P., 1949. Studies on the soft bottom amphipods of the Skagerrak. Zool. Bidrag Uppsala 28, 297—492.

Flannery, E., Przeslawski, R., 2015. Comparison of sampling methods to assess benthic marine biodiversity: are spatial and ecological relationships consistent among sampling gear? Geoscience Australia, record 2015/07. Canberra. 1—65.

Gluchowska, M., Kwaśniewski, S., Promińska, A., Olszewska, A., Goszczko, I., Falk-Petersen, S., Węsławski, J.M., 2016. Zooplankton in Svalbard fjords on the Atlantic—Arctic boundary. Polar Biol. 39 (10), 1785—1802, http://dx.doi.org/10.1007/s00300-016-1991-1.

Görlich, K., Węsławski, J.M., Zajączkowski, M., 1987. Suspension settling effect on macrobenthos biomass distribution in the Hornsund fjord, Spitsbergen. Polar Res. 5 (2), 175—192, http://dx.doi.org/10.1111/j.1751-8369.1987.tb00621.x.

Grebmeier, J.M., McRoy, P., Feder, H.M., 1989. Pelagic—benthic coupling on the shelf of the northern Bering and Chukchi Seas. II. Benthic community structure. Mar. Ecol.-Prog. Ser. 51, 253—268, http://dx.doi.org/10.3354/meps048057.

Gulliksen, B., Palerud, R., Brattegard, T., Sneli, J.A., 1999. Distribution of marine benthic organisms at Svalbard (including Bjornøya) and Jan Mayen. Res. Rep. Direct. Nature Manag. (DN) no. 4, Trondheim, 148 pp.

Hessler, R.R., Stromberg, J.-O., 1989. Behavior of janiroidean isopods (Asellota), with special reference to deep-sea genera. Sarsia 74 (3), 145—159, http://dx.doi.org/10.1080/00364827.1989.10413424.

Highsmith, R.C., Coyle, K.O., 1990. High productivity of northern Bering Sea benthic amphipods. Nature 344, 862—864, http://dx.doi.org/10.1038/344862a0.

Hirche, H.-J., Laudien, J., Buchholz, F., 2015. Near-bottom zooplankton aggregations in Kongsfjorden: implications for pelago—benthic coupling. Polar Biol. 39 (10), 1897—1912, http://dx.doi.org/10.1007/s00300-015-1799-4.

Holte, B., 1989. The macrofauna and main functional interactions in the sill basin sediments of the pristine Holandsfjord, northern Norway, with autecological reviews for some key-species. Sarsia 83 (1), 55—68, http://dx.doi.org/10.1080/00364827.1998.10413669.

Hop, H., Pearson, T., Hegseth, E.N., Kovacs, K., Wiencke, C., Kwaśniewski, S., Eiane, K., Mehlum, F., Gulliksen, B., Włodarska-Kowalczuk, M., Lydersen, C., Węsławski, J.M., Cochrane, S., Gabrielsen, G.W., Leakey, R., Lønne, O.J., Zajączkowski, M., Falk-Petersen, S., Kendall, M., Wängber, S.A., Bischof, K., Voronkov, A., Kovaltchouk, N.A., Wiktor, J., Poltermann, M., di Prisco, G., Papucci, C., Gerland, S., 2002. The marine ecosystem of Kongsfjorden, Svalbard. Polar Res. 21 (1), 167—208, http://dx.doi.org/10.1111/j.1751-8369.2002.tb00073.x.

Hopkins, C.C.E., Sargent, J.R., Nilssen, E.M., 1993. Total lipid content and lipid and fatty acid composition of the deep-water prawn *Pandalus borealis* from Balsfjord, northern Norway: growth and feeding relationships. Mar. Ecol.-Prog. Ser. 96, 217—228, http://dx.doi.org/10.3354/meps096217.

Huenerlage, K., Graeve, M., Buchholz, C., Buchholz, F., 2015. The other krill: overwintering physiology of adult *Thysanoessa inermis* (Euphausiacea) from the high-Arctic Kongsfjord. Aquat. Biol. 23, 225—235, http://dx.doi.org/10.3354/ab00622.

Jakobsson, M., Andreassen, K., Bjarnadóttir, L.R., Dove, D., Dowdeswell, J.A., England, J.H., Funder, S., Hogan, K., Ingólfsson, O., Jennings, A., Larsen, N.K., Kirchner, N., Landvik, J.Y., Mayer, L., Mikkelsen, N., Möller, P., Niessen, F., Nilsson, J., O'Regan, M., Polyak, L., Nørgaard-Pedersen, N., Stein, R., 2014. Arctic Ocean glacial history. Q. Sci. Rev. 92, 40—67, http://dx.doi.org/10.1016/j.quascirev.2013.07.033.

Jażdżewski, K., Węsławski, J.M., De Broyer, C., 1995. A comparison of the amphipod diversity in two polar fjords: Admiralty Bay, King George Island (Antarctica) and Horsund, Spitsbergen (Arctic). Pol. Arch. Hydrobiol. 42 (4), 367—384.

Jørgensen, L.L., Renaud, P., Cochrane, S., 2011. Improving benthic monitoring by combining trawl and grab surveys. Mar. Poll. Bull. 62 (6), 1183—1190, http://dx.doi.org/10.1016/j.marpolbul.2011.03.035.

Kaczmarek, H., Włodarska-Kowalczuk, M., Legeżyńska, J., Zajaczkowski, M., 2005. Shallow sublittoral macrozoobenthos in Kongsfjord, West Spitsbergen, Svalbard. Pol. Polar Res. 26 (2), 137—155.

Kędra, M., Pabis, K., Gromisz, S., Węsławski, J.M., 2013. Distribution patterns of polychaete fauna in an Arctic fjord (Hornsund, Spitsbergen). Polar Biol. 36 (10), 1463—1472, http://dx.doi.org/10.1007/s00300-013-1366-9.

Kędra, M., Włodarska-Kowalczuk, M., Węsławski, J.M., 2010. Decadal change in macrobenthic soft-bottom community structure in a high Arctic fjord (Kongsfjorden, Svalbard). Polar Biol. 33 (1), 1—11, http://dx.doi.org/10.1007/s00300-009-0679-1.

Kortsch, S., Primicerio, R., Beuchel, F., Renaud, P.E., Rodrigues, J., Lønne, O.J., Gulliksen, B., 2012. Climate-driven regime shifts in Arctic marine benthos. PNAS 109 (35), 14052—14057, http://dx.doi.org/10.1073/pnas.1207509109.

Koziorowska, K., Kuliński, K., Pempkowiak, J., 2016. Sedimentary organic matter in two Spitsbergen fjords: terrestrial and marine contributions based on carbon and nitrogen contents and stable isotopes composition. Cont. Shelf Res. 113, 38—46, http://dx.doi.org/10.1016/j.csr.2015.11.010.

Kuliński, K., Kędra, M., Legeżyńska, J., Gluchowska, M., Zaborska, A., 2014. Particulate organic matter sinks and sources in high Arctic fjord. J. Marine Syst. 139, 27—37, http://dx.doi.org/10.1016/j.jmarsys.2014.04.018.

Laudien, J., Herrmann, M., Arntz, W.E., 2007. Soft bottom species richness and diversity as a function of depth and iceberg scour in Arctic glacial Kongsfjorden (Svalbard). Polar Biol. 30 (8), 1035—1046, http://dx.doi.org/10.1007/s00300-007-0263-5.

Legeżyńska, J., 2001. Distribution patterns and feeding strategies of lysianassoid amphipods in shallow waters of an Arctic fjord. Pol. Polar Res. 22 (3—4), 173—186.

Legeżyńska, J., 2008. Food resource partitioning among Arctic sublittoral lysianassoid amphipods in summer. Polar Biol. 31 (6), 663—670, http://dx.doi.org/10.1007/s00300-008-0404-5.

Legeżyńska, J., Kędra, M., Walkusz, W., 2012. When season does not matter: summer and winter trophic ecology of Arctic amphipods. Hydrobiologia 684 (1), 189—214, http://dx.doi.org/10.1007/s10750-011-0982-z.

Legeżyńska, J., Węsławski, J.M., Presler, P., 2000. Benthic scavengers collected by baited traps in the high Arctic. Polar Biol. 23 (8), 539—544, http://dx.doi.org/10.1007/s003000000118.

Lippert, H., Iken, K., Rachor, E., Wiencke, C., 2001. Macrofauna associated with macroalgae in the Kongsfjord (Spitsbergen). Polar Biol. 24 (7), 512—522, http://dx.doi.org/10.1007/s003000100250.

Macdonald, T.A., Burd, B.J., Macdonald, V.I., van Roodselaar, A., 2010. Taxonomic and feeding guild classification for the marine benthic macroinvertebrates of the Strait of Georgia, British Columbia. Can. Tech. Rep. Fisheries Aquatic Sci. 2874, 1—63.

Macnaughton, M.O., Thormar, J., Berge, J., 2007. Sympagic amphipods in the Arctic pack ice: redescriptions of *Eusirus holmii* Hansen, 1887 and *Pleusymtes karstensi* (Barnard, 1959). Polar Biol. 30 (8), 1013—1025, http://dx.doi.org/10.1007/s00300-007-0260-8.

McMeans, B.C., Rooney, N., Arts, M.T., Fisk, A.T., 2013. Food web structure of a coastal Arctic marine ecosystem and implications for stability. Mar. Ecol.-Prog. Ser. 482, 17—28, http://dx.doi.org/10.3354/meps10278.

Moskalik, M., Grabowiecki, P., Tęgowski, J., Żulichowska, M., 2013. Bathymetry and geographical regionalization of Brepollen (Hornsund, Spitsbergen) based on bathymetric profiles interpolations. Pol. Polar Res. 34 (1), 1—22, http://dx.doi.org/10.2478/popore-2013-0001.

Narayanaswamy, B.E., Renaud, P.E., Duineveld, G.C.A., Berge, J., Lavaleye, M.S.S., Reiss, H., Brattegard, T., 2010. Biodiversity trends along the western European margin. PLoS ONE 5 (12), e14295, http://dx.doi.org/10.1371/journal.pone.0014295.

Nygård, H., 2011. Studies of benthic and sympagic amphipods in the genera *Onisimus* and *Anonyx*. (Ph.D. thesis). Univ. Centre in Svalbard, Univ. Tromsø.

Nygård, H., Wallenschus, J., Camus, L., Varpe, Ø., Berge, J., 2010. Annual routines and life history of the amphipod *Onisimus litoralis*: seasonal growth, body composition and energy budget. Mar. Ecol.-Prog. Ser. 417, 115—126, http://dx.doi.org/10.3354/meps08798.

Pabis, K., Błażewicz-Paszkowycz, M., 2011. Distribution and diversity of cumacean assemblages in Admiralty Bay, King George Island. Pol. Polar Res. 32 (4), 341—354, http://dx.doi.org/10.2478/v10183-011-0024-6.

Palerud, P., Gulliksen, B., Brattegard, T., Sneli, J.-A., Vader, W., 2004. The marine macro-organisms in Svalbard waters. In: Prestrud, P., Strom, H., Goldman, H.V. (Eds.), A Catalogue of the Terrestrial and Marine Animals of Svalbard. Norwegian Polar Inst., Tromsø, 5—56.

Piwosz, K., Walkusz, W., Hapter, R., Wieczorek, P., Hop, H., Wiktor, J., 2009. Comparison of productivity and phytoplankton in a warm (Kongsfjorden) and a cold (Hornsund) Spitsbergen fjord in midsummer 2002. Polar Biol. 32 (4), 549—559, http://dx.doi.org/10.1007/s00300-008-0549-2.

Postel, L., Fock, H., Hagen, W., 2000. Biomass and abundance. In: Harris, R., Wiebe, P., Lens, J., Skjoldal, H.R., Huntley, M. (Eds.), ICES Zooplankton Methodology Manual. Acad. Press, San Diego, 83—192.

Renaud, P.E., Løkken, T.S., Jørgensen, L.L., Berge, J., Johnson, B.J., 2015. Macroalgal detritus and food-web subsidies along an Arctic fjord depth-gradient. Front. Mar. Sci. 2, 1—15, http://dx.doi.org/10.3389/fmars.2015.00031.

Ronowicz, M., Legeżyńska, J., Kukliński, P., Włodarska-Kowalczuk, M., 2013. Kelp forest as a habitat for mobile epifauna: case study of *Caprella septentrionalis* Kröyer, 1838 (Amphipoda, Caprellidae) in an Arctic glacial fjord. Polar Res. 32, 21037, http://dx.doi.org/10.3402/polar.v32i0.21037.

Sainte-Marie, B., 1986. Feeding and swimming of lysianassoid amphipods in a shallow cold-water bay. Mar. Biol. 91 (2), 219—229, http://dx.doi.org/10.1007/BF00569437.

Sainte-Marie, B., Brunel, P., 1985. Suprabenthic gradients of swimming activity by cold-water gammaridean amphipod Crustacea over a muddy shelf in the Gulf of Saint Lawrence. Mar. Ecol.-Prog. Ser. 23, 57—69, http://dx.doi.org/10.3354/meps023057.

Sirenko, B.I., 2001. List of species of free-living invertebrates of Eurasian Arctic seas and adjacent deep waters. Russ. Acad. Sci. St. Petersburg 131 pp..

Smith, R., Bianchi, S.T., Allison, M., Savage, C., Galy, V., 2015. High rates of organic carbon burial in fjord sediments globally. Nat. Geosci. 8, 450—454, http://dx.doi.org/10.1038/ngeo2421.

Stransky, B., Brandt, A., 2010. Occurrence, diversity and community structures of peracarid crustaceans (Crustacea, Malacostraca) along the southern shelf of Greenland. Polar Biol. 33 (6), 851—867, http://dx.doi.org/10.1007/s00300-010-0785-0.

Svavarsson, J., 1997. Diversity of isopods (Crustacea): new data from the Arctic and Atlantic Oceans. Biodivers. Conserv. 6 (11), 1571—1579, http://dx.doi.org/10.1023/A:1018322704940.

Svendsen, H., Beszczynska-Möller, A., Hagen, J.O., Lefauconnier, B., Tverberg, V., Gerland, S., Ørbæk, J.B., Bischof, K., Papucci, C., Zajączkowski, M., Azzolini, R., Bruland, O., Wiencke, C., Winther, J.-G., Dallmann, W., 2002. The physical environment of Kongsfjorden—Krossfjorden, an arctic fjord system in Svalbard. Polar Res. 21, 133—166, http://dx.doi.org/10.1111/j.1751-8369.2002.tb00072.x.

Szczuciński, W., Schettler, G., Zajączkowski, M., 2006. Sediment accumulation rates, geochemistry and provenance in complex High Arctic fjord, Hornsund, Svalbard. In: Fourth ESF SEDIFLUX Sci. Meeting & First Workshop of I.A.G./A.I.G. SEDIBUD: Source_-to_Sink_Fluxes and Sediment Budgets in Cold Environments. NGF Abstr. Proc. Geolog. Soc. Norway 4. p. 65.

Tatarek, A., Wiktor, J., Kendall, M.A., 2012. The sublittoral macroflora of Hornsund. Polar Res. 31, 18900, http://dx.doi.org/10.3402/polar.v31i0.18900.

Trusel, L.D., Powell, R.D., Cumpston, R.M., Brigham-Grette, J., 2011. Modern glacimarine processes and potential future behaviour of Kronebreen and Kongsvegen polythermal tidewater glaciers, Kongsfjorden, Svalbard. In: Howe, J.A., Austin, W.E.N., Forwick, M., Paetzel, M. (Eds.), Fjord Systems and Archives. Spec. Publ., vol. 344. Geological Soc., London, 89—102, http://dx.doi.org/10.1144/SP344.9.

Voronkov, A., Hop, H., Gulliksen, B., 2013. Diversity of hard-bottom fauna relative to environmental gradients in Kongsfjorden, Svalbard. Polar Res. 32 (1), 11208, http://dx.doi.org/10.3402/polar.v32i0.11208.

Walczowski, W., 2013. Frontal structures in the West Spitsbergen Current margins. Ocean Sci. 9, 957—975, http://dx.doi.org/10.5194/os-9-957-2013.

Weisshappel, J.B.F., Svavarsson, J., 1998. Benthic amphipods (Crustacea: Malacostraca) in Icelandic waters: diversity in relation to faunal patterns from shallow to intermediate deep Arctic and North Atlantic Oceans. Mar. Biol. 131 (1), 133—143, http://dx.doi.org/10.1007/s002270050304.

Węsławski, J.M., 1990. Distribution and ecology of coastal waters Amphipoda from south Spitsbergen. Pol. Arch. Hydrobiol. 37, 503—519.

Węsławski, J.M., Kendall, M., Włodarska-Kowalczuk, M., Iken, K., Kedra, M., Legeżyńska, J., Sejr, M.K., 2011. Climate change effects on Arctic fjord and coastal macrobenthic diversity — observations and predictions. Mar. Biodivers. 41 (1), 71—85, http://dx.doi.org/10.1007/s12526-010-0073-9.

Węsławski, J.M., Opanowski, A., Legeżyńska, J., Maciejewska, B., Włodarska-Kowalczuk, M., Kędra, M., 2010. Hidden diversity in Arctic crustaceans. How many roles can a species play? Pol. Polar Res. 31 (3), 205—216, http://dx.doi.org/10.2478/v10183-010-0001-5.

Węsławski, J.M., Pedersen, G., Petersen, S.F., Poraziński, K., 2000. Entrapment of macroplankton in an Arctic fjord basin, Kongsfjorden, Svalbard. Oceanologia 42 (1), 57—69.

Węsławski, J.M., Wiktor, J., Zajączkowski, M., Swerpel, S., 1993. Intertidal zone of Svalbard, Macroorganism distribution and biomass. Polar Biol. 13 (2), 73—79, http://dx.doi.org/10.1007/BF00238538.

Winkelmann, D., Knies, J., 2005. Recent distribution and accumulation of organic carbon on the continental margin west off Spitsbergen. Geochem. Geophys. Geosyst. 6 (9), Q09012, http://dx.doi.org/10.1029/2005gc000916.

Włodarska-Kowalczuk, M., 2007. Molluscs in Kongsfjorden (Spitsbergen, Svalbard): a species list and patterns of distribution and diversity. Polar Res. 26 (1), 48—63, http://dx.doi.org/10.1111/j.1751-8369.2007.00003.x.

Włodarska-Kowalczuk, M., Kędra, M., 2007. Surrogacy in natural patterns of benthic distribution and diversity: selected taxa versus lower taxonomic resolution. Mar. Ecol.-Prog. Ser. 351 (1), 53—63, http://dx.doi.org/10.3354/meps07127.

Włodarska-Kowalczuk, M., Kukliński, P., Ronowicz, M., Legeżyńska, J., Gromisz, S., 2009. Assessing species richness of macrofauna associated with macroalgae in Arctic kelp forests (Hornsund, Svalbard). Polar Biol. 32, 897—905, http://dx.doi.org/10.1007/s00300-009-0590-9.

Włodarska-Kowalczuk, M., Pearson, T.H., 2004. Soft-bottom macrobenthic faunal associations and factors affecting species distributions in an Arctic glacial fjord (Kongsfjord, Spitsbergen). Polar Biol. 27 (3), 155—167, http://dx.doi.org/10.1007/s00300-003-0568-y.

Włodarska-Kowalczuk, M., Pearson, T.H., Kendall, M.A., 2005. Benthic response to chronic natural physical disturbance by glacial sedimentation in an Arctic fjord. Mar. Ecol.-Prog. Ser. 303, 31—41, http://dx.doi.org/10.3354/meps303031.

Włodarska-Kowalczuk, M., Renaud, P.E., Węsławski, J.M., Cochrane, S.K.J., Denisenko, S.G., 2012. Species diversity, functional complexity and rarity in Arctic fjordic versus open shelf benthic systems. Mar. Ecol.-Prog. Ser. 463, 73—87, http://dx.doi.org/10.3354/meps09858.

Włodarska-Kowalczuk, M., Węsławski, J., 2008. Mesoscale spatial structures of soft-bottom macrozoobenthos communities: effects of physical control and impoverishment. Mar. Ecol.-Prog. Ser. 356, 215—224, http://dx.doi.org/10.3354/meps07285.

Zaborska, A., Pempkowiak, J., Papucci, C., 2006. Some sediment characteristics and sedimentation rates in an Arctic fjord (Kongsfjorden, Svalbard). Ann. Environ. Prot. 8 (2), 79—96.

Zaborska, A., Włodarska-Kowalczuk, M., Legeżyńska, J., Jankowska, E., Winogradow, A., Deja, K., 2016. Sedimentary organic matter sources, benthic consumption and burial in west Spitsbergen fjords — signs of maturing of Arctic fjordic systems? J. Marine Syst., (in press), http://dx.doi.org/10.1016/j.jmarsys.2016.11.005.

Zajaczkowski, M., 2008. Sediment supply and fluxes in glacial and outwash fjords, Kongsfjorden and Adventfjorden, Svalbard. Pol. Polar Res. 29 (1), 59—72.

Oceanologia (2017) 59, 565—575

Available online at www.sciencedirect.com

ScienceDirect

journal homepage: www.journals.elsevier.com/oceanologia/

ORIGINAL RESEARCH ARTICLE

Benthic *Crustacea* and *Mollusca* distribution in Arctic fjord — case study of patterns in Hornsund, Svalbard

Anna Drewnik [a,b,*], **Jan Marcin Węsławski** [a], **Maria Włodarska-Kowalczuk** [a]

[a] *Institute of Oceanology, Polish Academy of Sciences, Sopot, Poland*
[b] *GIS Centre, University of Gdańsk, Poland*

Received 26 September 2016; accepted 6 January 2017
Available online 4 July 2017

KEYWORDS
Arctic;
Fjord;
Benthos;
Species distribution modeling;
Near-bottom waters

Summary We present the results of species distribution modeling conducted on macrobenthic occurrence data collected between 2002 and 2014 in Arctic fjord — Hornsund. We focus on species from *Mollusca* and *Crustacea* taxa. This study investigates the importance of individual environmental factors for benthic species distribution, with a special emphasis on bottom water temperature. It aims to verify the hypothesis that the distribution of species is controlled by low water temperatures in the fjord and that the inner basins of the fjord serve as potential refugia for Arctic species threatened by the climate change-related intensification of warmer water inflows. Our results confirm the importance of bottom water temperature in regulating the presence of benthic fauna in the Hornsund fjord. The distribution of studied species is clearly related to specific water mass — colder (<1°C) or warmer (>1°C); and the preferred temperature regimes seem to be species specific and unrelated to analyzed groups. This study supports the notion that inner basins of the Hornsund fjord are potential refugia for cold water Arctic fauna, while the outer and central basins provide suitable habitats for fauna that prefer warmer waters.

1. Introduction

Svalbard archipelago is one of the most rapidly warming regions in the Northern hemisphere (Acia, 2005). One of the main drivers of this warming is the West Spitsbergen Current (WSC). Recently, studies have shown that the WSC is responsible for the majority of Atlantic Water (AW) fluxes, which carries heat into the central Arctic (Pavlov et al., 2013; Schauer et al., 2008; Smedsrud et al., 2010; Walczowski and Piechura, 2007). Moreover, warming and northernmost extension of these waters has been observed (Schauer

* Corresponding author at: Institute of Oceanology, Polish Academy of Sciences, Powstańców Warszawy 55, 81-712 Sopot, Poland.
E-mail address: drewnik.anna@gmail.com (A. Drewnik).
Peer review under the responsibility of Institute of Oceanology of the Polish Academy of Sciences.

Production and hosting by Elsevier

http://dx.doi.org/10.1016/j.oceano.2017.01.005

et al., 2008; Spielhagen et al., 2011; Walczowski and Piechura, 2006, 2007). Inflows from the WSC have been noted in the fjord systems around Svalbard (Berge et al., 2005; Cottier et al., 2005; Nilsen et al., 2006, 2008; Pavlov et al., 2013; Skogseth et al., 2005; Teigen et al., 2011) and account for the instability and increasing temperatures in the fjords' waters (Pavlov et al., 2013).

Atlantic water carried from a region of higher biodiversity (Norwegian Sea) may also affect the Arctic ecosystem by mediating the northern expansion of certain boreal taxa (Węsławski et al., 2009). The WSC that flows along the Norwegian coast is one of the primary pathways of boreal species advection to the Arctic (Berge et al., 2005; Węsławski et al., 2011). Poleward shifts of pelagic as well as benthic species and communities have been broadly documented (Beaugrand et al., 2002; Berge et al., 2005; Drinkwater, 2006; Grebmeier et al., 2006; Piepenburg, 2005). Initial observations have also demonstrated that boreal fauna starts to dominate near the mouths of Spitsbergen fjords (Svalbard archipelago) (Węsławski et al., 2011). Overall, climate change may significantly affect the physical conditions and local Arctic ecosystems. Examples of such impacts on these ecosystems' structure and functioning (Basedow et al., 2004; Berge et al., 2005, 2009; Hop et al., 2002), as well as of fauna migrations and changes in species composition (Falk-Petersen et al., 2007; Jónsson and Valdimarsson, 2005; Wassmann et al., 2011), have already been noted. These changes may affect Arctic biodiversity and even lead to the supplanting of indigenous Arctic species (Dawson et al., 2011; Węsławski et al., 2009).

On the other hand, species that are relicts of past climate regimes are known to persist in many places. In the Baltic, approximately 5% of the macrofauna species present evolved under former, cold Yoldia sea conditions. Cold, brackish water species have also survived in several large lakes in Scandinavia and Russia (Leppäkoski and Olenin, 2001). Relict populations of cold-water species have also been reported in boreal fjords (Drainville, 1970; Freeland et al., 1980). Norwegian fjords are known to host cold water species in their innermost basins, while the outer basins are dominated by warm water Atlantic species (Freeland et al., 1980). The same distribution of species may occur in the future in the fjords of the European Arctic. Some diversification is already being observed in Spitsbergen fjords, and it may be enhanced further by climate change and continual Atlantic water inflows. Semi-closed fjords or topographically isolated inner basins have more homogeneous and uniform fauna, and they support a greater proportion of Arctic-origin species than outer areas under the influence of shelf waters (Kendall et al., 2003; Kędra et al., 2009; Renaud et al., 2007; Weslawski, 1990; Wlodarska-Kowalczuk et al., 1998; Włodarska-Kowalczuk and Węsławski, 2008). Their isolation enables these fjords to retain cold, dense, oxygen-rich bottom water that is produced in the fjords during annual ice formation (Svendsen et al., 2002; Syvitski et al., 1987; Weslawski et al., 2010; Węsławski et al., 2011; Wlodarska-Kowalczuk and Pearson, 2004). As a result, these sheltered bays create stable conditions and may serve as suitable refuges for cold water Arctic species facing ongoing warming in the region (Lydersen et al., 2014).

One way to investigate the mechanism and potential consequences of climate warming on biocoenosis and its components is through the application of species distribution modeling, a method that is gaining increasing attention in marine environmental studies (Degraer et al., 2008; Glockzin et al., 2009; Gogina et al., 2010; Reiss et al., 2011; Robinson et al., 2011). It has been used frequently to model habitat suitability and the spatial patterns of benthic fauna distribution, inter alia, under different climate change scenarios (Degraer et al., 2008; Ellis et al., 2006; Gogina and Zettler, 2010; Gogina et al., 2010; Inglis et al., 2006; Meißner et al., 2008; Thrush et al., 2003; Willems et al., 2008; Ysebaert et al., 2002). In such cases, a crucial step is to include climatic factors or their proxies in a model. In the case of benthic assemblages, in particular those inhabiting Arctic regions, the bottom water temperature has been identified as the most significant one. The purpose of our study is to investigate whether benthic fauna distribution in one of the Spitsbergen fjords – Hornsund – is controlled by the occurrence of cold water masses. We aim to determine whether and how climate change-related Atlantic warm water inflows affect benthos, and we seek to identify potential refugia for these Arctic communities in the fjord. In doing so, we aim to verify whether inner fjord basins could serve as such shelters. We present data on deeper soft bottom sublittoral (<50 m), with no data from shallows or hard substrata. Summer temperatures were analyzed only, as during winter season an entire water column in the fjord is isothermal and isohaline (Swerpel, 1985; Weslawski et al., 1991). Moreover, benthic fauna is the long-living part of the ecosystem with longer life cycles than planktonic communities, ability to incubate eggs or slowing the growth in the winter (Hop et al., 2002; Warwick, 1993; Weslawski et al., 1991). Hence, benthos can integrate hydrographic processes over the years and is believed to serve as a great indicator of long-term environmental changes (Kröncke, 1995; Renaud et al., 2008). The results of our study are discussed on the background of observed changes in Arctic biodiversity to highlight the need for, and usefulness of, collecting data on the distribution of individual species and communities as indicators of Arctic ecosystem change.

2. Material and methods

2.1. Study area

The study area was Hornsund – the southernmost fjord of west Spitsbergen, located at 76 to 77°N. Hornsund is a medium-sized fjord (24 km long, 11 km wide at its mouth) with a strongly developed coastline that includes five secondary bays (see www.iopan.gda.pl/projects/Visual). The Hornsund fjord is under the influence of the coastal Sørkapp Current, which carries cold, less saline Arctic water from the northeastern Barents Sea, and the West Spitsbergen Current, which carries saline Atlantic water from the Norwegian Sea (Cottier et al., 2005; Piechura et al., 2001). Both water masses can penetrate the fjord area because Hornusnd does not have a sill at its entrance. Circulation pattern in Hornsund is similar to other West Spitsbergen fjords. Water entering the fjord tend to inflow along the southern coast and outflow along northern coast (Cottier et al., 2010). Atlantic water (modified by mixing with Arctic Water) is usually observed as a bottom inflow. Its distribution and range differ from

summer to summer; however, a few shallow sills occur throughout the fjord and separate the outer and central parts of Hornsund from its inner basins (Drewnik et al., 2016), thereby limiting the distribution of Atlantic water fluxes (Promińska et al. unpublished data). The deepest layers of isolated basins are reservoirs of cold, saline winter water produced through salt rejection during sea-ice formation (fall-winter period). Tides in Hornsund fjord are regular, semidiurnal with range from 0.8 to 1.8 m (Węsławski et al., 1993; Zagórski et al., 2015). Due to the local climate, topographic conditions and Atlantic water fluxes, the Hornsund region is thought to be more vulnerable to climate-oceanic system changes than the rest of the Svalbard archipelago (Błaszczyk et al., 2013). Hence, it is a hotspot for observations related to the consequences of climate change on Artic ecosystems.

2.2. Benthic data

Sampling was performed during summer R V OCEANIA cruises performed by the Institute of Oceanology Polish Academy of Sciences between 2002 and 2014. Samples were collected using a Van Veen grab (0.1 m^2) at 130 stations dispersed across the Hornsund fjord (Fig. 1). The material was sieved onboard through a 0.5 mm mesh and preserved in a buffered 4% formaldehyde solution. In the laboratory macrofauna individuals were identified to the lowest possible taxonomic level (most often to the species level) using the taxonomic nomenclature after World Register of Marine Species: WoRMS (www.marinespecies.org). For the purposes of this study, only occurrence data for species in the *Mollusca* and *Crustacea* groups were used. Distribution data were compiled for species with at least 5 records of occurrence available for modeling. The "only-presence" occurrence data were imported into ArcGIS 10.1 and Maxent software for further processing and modeling.

2.3. Environmental data

The basic approach to species distribution modeling is to select physical factors (predictors) that are crucial for species persistence and that may control its distribution. For this study, we selected some of the factors known to be important to benthic fauna (Gogina and Zettler, 2010; McArthur et al., 2010; Olenin, 1997; Reiss et al., 2011) — topography and geomorphology (depth, slope, and rugosity), substratum (mean grain size of sediment) and near-bottom water characteristics (temperature, salinity and their derivatives — mean and range). Additionally, we used the distance from the glacier fronts as a proxy for glacier outflow, because no precise data on this predictor were available for the analyzed time period. Organic matter content in sediments was omitted since most of it consists of terrestrial, old carbon (www.iopan.gda.pl/projects/Game/prezentacje/Zaborska_et_al.pdf) that is of very limited use for benthic fauna. Furthermore, our previous studies concerning a detailed analysis of conditions prevailing at the bottom of the Hornsund revealed that organic matter content in sediments is stable across the fjord area (Drewnik et al., 2016). Hence, we consider this factor as insignificant in controlling benthic species distribution in Hornsund.

Sampling was performed during routine summer cruises between 2002 and 2014 (Fig. 1). Sediment grain size analysis was performed on surface (upper 5 cm) sediment samples collected using box corers, analyzed with a Malvern Mastersizer 2000 laser particle analyzer and calculated in GRADISTAT

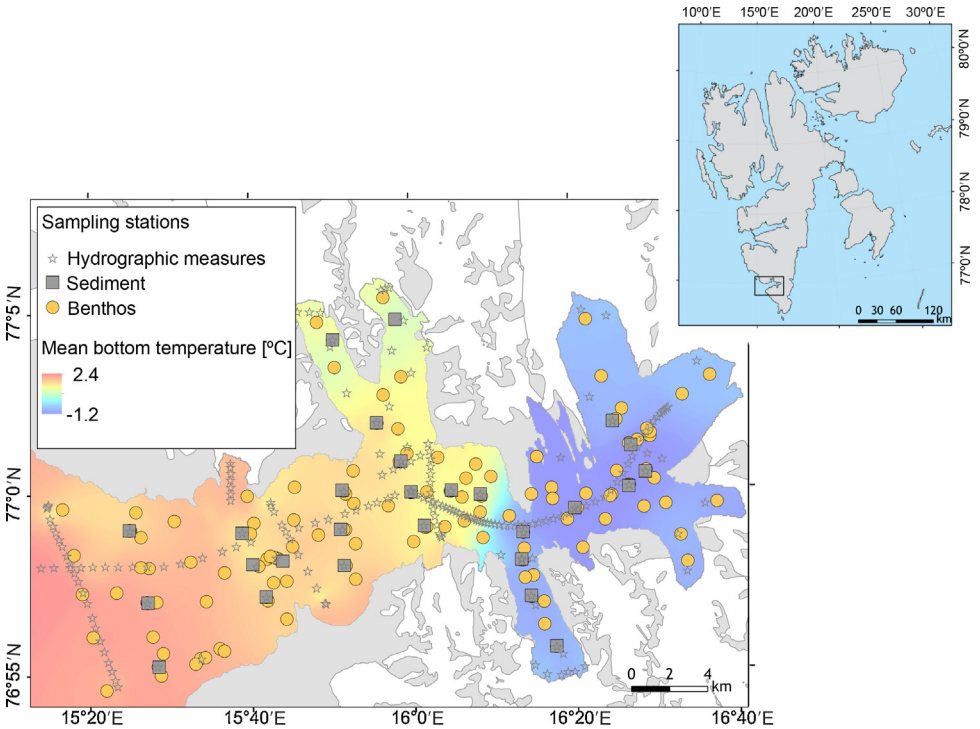

Figure 1 Study area and locations of sampling stations. Circles indicate benthos sampling locations; squares represent sediment collection sites and stars indicate hydrographic measurements; graduated color scale shows mean bottom water temperature.

8.0 using the geometric method of moments. Hydrographic measurements were collected using an SBE 49 probe. Near-bottom measurements were analyzed separately to model the conditions prevailing near the seabed. Water depth was measured simultaneously with other environmental factors at each sampling station (Echotrac MK III 12 kHz, Odom Hydrographic Systems). For more details on sampling and laboratory analysis see Drewnik et al. (2016). All continuous surfaces (raster layers) necessary for modeling were created and processed using ArcGIS 10.1 software.

2.4. Maximum entropy modeling

Maxent (maximum entropy model) is a general-purpose machine learning method used for species distribution modeling (SDM). Species distribution models are used to predict the actual (at present) or potential (at some other time period) distribution of habitats suitable for species survival over the studied area and to explore species–environment correlations. The models require data on species' occurrences in geographical space, as well as digital maps of environmental factors representing conditions encountered by the studied species (Beuchel et al., 2006; Franklin, 2009). The Maxent algorithm estimates a target probability distribution for each species by finding the distribution of maximum entropy (that is closest to uniform) and constraining the expected value of each environmental factor to match its empirical average (Phillips et al., 2006; Reiss et al., 2011). This method is equivalent to finding the maximum-likelihood distribution of a species (Bučas et al., 2013). The Maxent model's reliability has been confirmed in numerous studies (Elith et al., 2006; Hernandez et al., 2006; Hijmans and Graham, 2006; Ortega-Huerta and Peterson, 2008; Pearson et al., 2007; Wisz et al., 2008). The Maxent algorithm was chosen for the analysis because it is a generative, rather than the discriminative tool that allows the use of a limited amount of training data (as few as 4 sampling points; Pearson et al., 2007; Phillips et al., 2006). Benthos was sampled in a fixed net of 130 stations dispersed across the entire Hornsund fjord area (deterministic distribution), however, single species were present at far fewer localities – even 6 (Fig. 4). Moreover, Maxent builds the model using “only presence” biological data. Information about the absence of a species in the study area is not required so possible false absences are avoided. These are incredibly important advantages, especially in benthic marine studies where the capacity to sample at numerous locations is often limited and the species absence is never certain (only a subsample is studied; even several replicates of grab samples can miss the species and falsely provide absence information for the model).

2.5. Model processing and interpretation

In this study, we used Maxent software version 3.3.3k (http://www.cs.princeton.edu/~schapire/maxent). The description of the maximum-entropy approach for species habitat modeling as well as equations implemented in the software can be found in Elith et al. (2011), Phillips et al. (2004, 2006). The models were created using 10,000 pseudo-absence points; the convergence threshold was set at 10^{-5}, and the maximum iteration value was set at 500. Features (environmental factors or their functions) were selected automatically by the program depending on the number of presence records. A regularization value was also matched automatically to reduce over-fitting. The cumulative probability output format was chosen for the models' predictions. Cumulative probability ranges from 0 to 100% and indicates relative suitability. The value of a given map cell is calculated as the sum of that cell plus all other cells with equal or lower probability multiplied by 100 (for more details see Phillips et al., 2006). The cumulative output map also uses colors to indicate predicted probability – warmer colors show areas with better conditions predicted (http://www.cs.princeton.edu/~schapire/maxent). In other words, more suitable for that species (Phillips et al., 2006). Maxent automatically creates maps of this suitability that can be later transformed into simpler and clearer binary maps (1 – suitable vs. 0 – not suitable habitat) using a chosen threshold – a value above which model output is considered to be a prediction of presence. We transformed cumulative probability maps (Appendix A) using the ArcGIS 10.1 and the lowest presence threshold (LPT) – the lowest predicted value associated with any one of the observed presence records. It identifies sites that were at least as suitable as those where a species' presence has been recorded (Pearson et al., 2007). There are number of thresholds that are used in Species Distribution Modeling and applying a different one can slightly enlarge or decrease the areas predicted suitable for a species. We chose to use LPT threshold because it reduces false positive predictions, i.e., minimizes the proportion of the study area predicted as present. It is very conservative, hence sometimes the patches of suitability can be as small as a location where the species was recorded, but on the other hand, it enables to illustrate the most suitable sites for species in the studied area.

Supplementary Appendix A related to this article can be found, in the online version, at doi:10.1016/j.oceano.2017.01.005.

LPT values were also used to evaluate the performance of our models. We used the jackknife (or 'leave-one-out') validation approach, which is suitable for testing models with few observed location records available (fewer than 25 locations) (Hernandez et al., 2008; Pearson et al., 2007). We generated multiple models for each species; the number of models generated was equal to the number of occurrence locations of that species (n observed locations, n separate models). During each separate model run, one of the observed locations was removed from the data set and a model was built using the remaining $n - 1$ locations. Then, we assessed the ability of each model to predict the excluded location and calculated the significance of the prediction, and therefore the model, success rate (statistical significance was accepted at $p < 0.05$) (Pearson et al., 2007). For additional details about the jackknife calculation method and the software used see Pearson et al. (2007).

The importance of environmental factors for species distributions was assessed automatically in the Maxent software using a permutation importance measure that determined the contribution of each factor to each model. Values were normalized to give percentages and presented on a stacked bar graph illustrating the percentage contribution of each environmental factor in the creation of every model. Large values indicate that the model depends heavily on that

factor. The more model depends on some factor, the more that factor controls species distribution. To assess a prediction's dependence on individual factors and interpret the influence of those factors on the distribution of a species, we generated response curves. The curves plots present predicted probability of suitable conditions for a species corresponding with each factor value (Merow et al., 2013).

3. Results

In total, we developed 30 Maxent models for benthic fauna species in the *Mollusca* and *Crustacea* taxa found in Hornsund fjord. In each case, the model's success rate and statistical significance were tested to eliminate models with no or poor predictive and explanatory power. Consequently, data on 8 species of Mollusks and 7 species of Arthropods were further analyzed (Table 1).

The relative contributions of all environmental factors to the model predictions vary within and between analyzed groups. However, among all species, the most important predictors were mean grain size, distance from the glaciers, water depth, and mean temperature of bottom water (Fig. 2). The factor importance graphs (Fig. 2) and binary prediction maps (Fig. 4) illustrate the relationship between the importance of water temperature to species distribution and the amount of suitable area predicted. For species that were not significantly affected by temperature (*Dacrydium vitreum*, *Yoldiella solidula*, *Musculus niger*, *Neohela monstrosa*, *Anonyx nugax*, *Pagurus pubescens*), the models identified suitable habitat across most of the fjord. Those species that were more affected by temperature had smaller suitable habitat areas and were generally restricted to either the inner or outer basins of the fjord. The response curves analysis revealed that species representing the first case (distribution not governed by temperature, vast suitable area) are able to tolerate a slightly wider range in water temperature. The model calculated a high probability of suitable conditions for this group both below and above 0°C (Fig. 3). Species whose distributions were influenced by temperature and whose suitable habitat ranges were restricted could be categorized into two groups: (1) species whose response to temperature peaked at low values, mainly between −1 and +1°C (Fig. 3) and whose suitable conditions were located in the inner basins of the fjord, as defined by the algorithm (Fig. 4); and (2) species for whom suitable conditions were predicted at temperature values above 1°C (Fig. 3) and distributed at the fjord mouth and in the outer and central basins of the Hornsund fjord (Fig. 4). Among the

Table 1 Jackknife tests of distribution models for 30 species of *Mollusca* and *Crustacea* collected in Hornsund fjord; LPT – lowest presence threshold – applied. Significant impacts ($p < 0.05$) printed in bold.

Taxon	Class	Order	Species	Success rate	*p* value
Mollusca	*Bivalvia*	–	*Kurtiella tumida* (Carpenter, 1864)	0.9	**0.000**
	Bivalvia	*Nuculanida*	*Yoldia hyperborea* (Gould, 1841)	0.8	**0.001**
	Bivalvia	*Mytilida*	*Dacrydium vitreum* (Møller, 1842)	0.8	**0.001**
	Bivalvia	*Nuculanida*	*Yoldiella solidula* (Warén, 1989)	0.8	**0.002**
	Bivalvia	*Mytilida*	*Musculus glacialis* (Leche, 1883)	0.8	**0.011**
	Bivalvia	*Mytilida*	*Musculus niger* (J.E. Gray, 1824)	0.7	**0.028**
	Bivalvia	–	*Cuspidaria subtorta* (Sars G. O., 1878)	0.7	0.258
	Gastropoda	*Littorinimorpha*	*Onoba mighelsii* (Stimpson, 1851)	0.7	0.750
	Bivalvia	*Nuculanida*	*Portlandia arctica* (Gray, 1824)	0.6	**0.011**
	Bivalvia	*Cardiida*	*Ciliatocardium ciliatum* (Fabricius, 1780)	0.6	**0.019**
	Gastropoda	*Littorinimorpha*	*Frigidoalvania cruenta* (Odhner, 1915)	0.6	0.064
	Bivalvia	*Lucinida*	*Thyasira dunbari* (Lubinsky, 1976)	0.6	0.141
	Bivalvia	*Nuculanida*	*Yoldiella frigida* (Torell, 1859)	0.6	0.226
	Bivalvia	*Cardiida*	*Macoma moesta* (Deshayes, 1855)	0.5	0.136
	Bivalvia	*Lucinida*	*Thyasira gouldi* (Philippi, 1845)	0.5	0.146
	Gastropoda	–	*Margarites costalis* (Gould, 1841)	0.5	0.155
	Gastropoda	*Littorinimorpha*	*Euspira pallida* (Broderip & Sowerby, 1829)	0.4	0.323
Crustacea	*Malacostraca*	*Amphipoda*	*Neohela monstrosa* (Boeck, 1861)	0.9	**0.000**
	Malacostraca	*Amphipoda*	*Anonyx nugax* (Phipps, 1774)	0.9	**0.000**
	Malacostraca	*Amphipoda*	*Lepidepecreum umbo* (Goës, 1866)	0.8	**0.002**
	Malacostraca	*Amphipoda*	*Unciola leucopis* (Krøyer, 1845)	0.7	**0.000**
	Malacostraca	*Amphipoda*	*Orchomenella minuta* (Krøyer, 1846)	0.7	0.485
	Malacostraca	*Cumacea*	*Diastylis goodsiri* (Bell, 1855)	0.6	**0.006**
	Malacostraca	*Amphipoda*	*Melita formosa* (Murdoch, 1866)	0.6	**0.025**
	Malacostraca	*Amphipoda*	*Themisto abyssorum* (Boeck, 1870)	0.6	0.061
	Malacostraca	*Amphipoda*	*Pontoporeia femorata* (Krøyer, 1842)	0.6	0.221
	Malacostraca	*Euphausiacea*	*Thysanoessa inermis* (Krøyer, 1846)	0.6	0.267
	Malacostraca	*Decapoda*	*Pagurus pubescens* (Krøyer, 1838)	0.5	**0.001**
	Malacostraca	*Amphipoda*	*Monoculodes packardi* (Boeck, 1871)	0.5	0.129
	Malacostraca	*Decapoda*	*Sabinea septemcarinata* (Sabine, 1824)	0.4	0.650

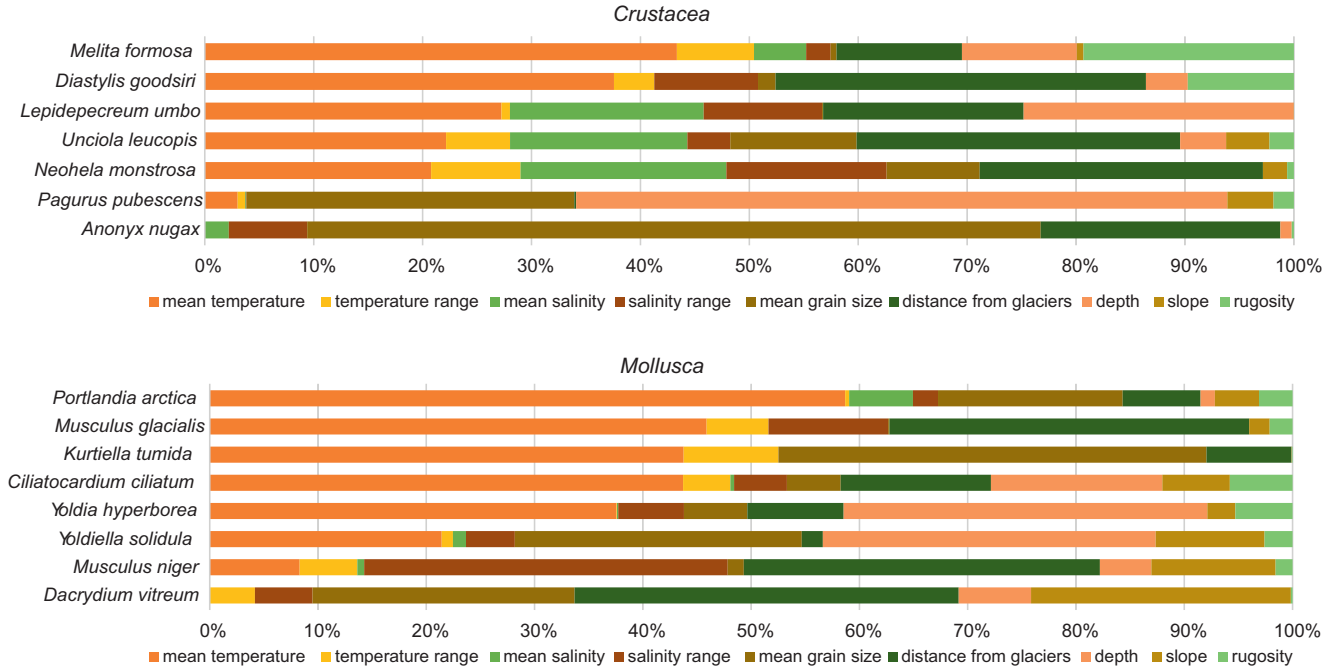

Figure 2 Environmental factors potentially affecting benthic species collected in the Hornsund fjord and those factors' percent contribution to species distribution, as determined in the Maxent models.

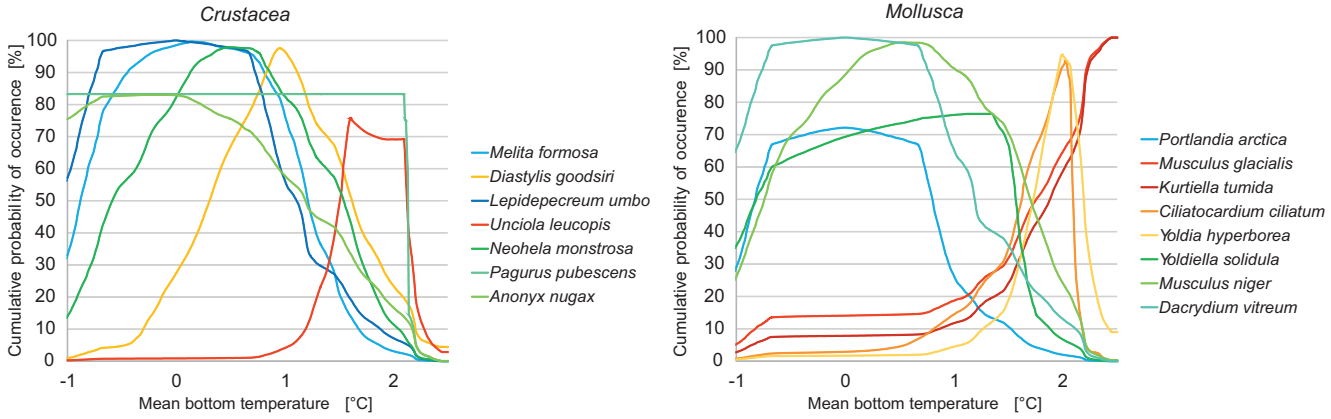

Figure 3 Response curves of benthic species collected in the Hornsund fjord to mean bottom water temperature (derived in Maxent).

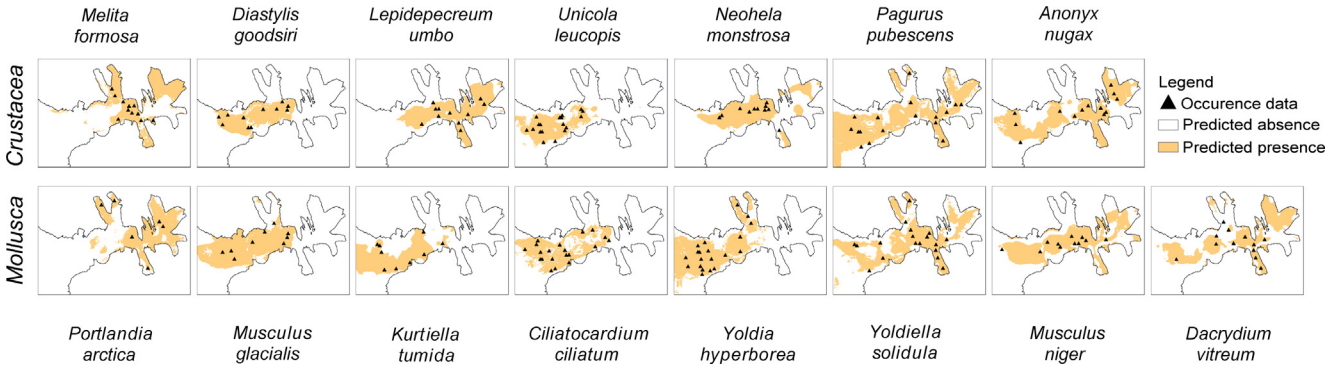

Figure 4 Modeled distributions for selected benthic species collected in Hornsund fjord; modeled using Maxent and applying LPT – the lowest presence threshold. Predicted areas are shaded; locations of observed occurrences are shown as black triangles.

latter group, differences in the influence of temperature on the probability of species occurrence were also observed. For certain species (*Yoldia hyperborea*, *Ciliatocardium ciliatum*, *Unciola leucopis*), the range of water temperature tolerance was incredibly narrow. In other cases (*Kurtiella tumida*, *Musculus glacialis*), the probability of finding a suitable habitat for a species continuously increased with temperature (Fig. 3).

In general, the importance of water temperature on benthic fauna distribution was demonstrated. However, the exact influence of this factor on benthos distribution and potential habitat preferences varied by species.

4. Discussion

Our study confirms the importance of bottom water temperature in the distribution of benthic fauna inhabiting an Arctic fjord — Hornsund. This was one of the most important factors controlling the distribution of the majority of analyzed species, along with the mean grain size, depth, and distance from the glaciers. Sediment characteristic is one of the most important factors for benthic fauna persistence and distribution. The fact that mean grain size is a vital factor in our analysis confirms this statement. However, Hornsund seafloor is quite homogenous in terms of granulometry. The fine fraction of sediment dominates throughout the fjord, with only single patches of coarse sediment. Our previous studies revealed no significant differences between individual fjord basins in terms of this factor (Drewnik et al., 2016). Hence, mean grain size of sediment is of minor importance in controlling benthic species distribution in Hornsund fjord (Drewnik et al., 2016). Same as depth which, although variable across fjord area, is rather stable parameter over time. Yet, the glacier movement (Błaszczyk et al., 2009, 2013) results in the appearance of new shallows (Moskalik et al., 2013) that may potentially serve as new habitats for benthic fauna. Distance from the glacier was used as a proxy for glacier outflow in order to confirm its importance and the need for extensive sampling of this parameter. Our results state this need, as a distance from the glacier fronts was an important predictor for some analyzed species. This will be the subject of our future research. Mean bottom temperature, on the other hand, was a very significant factor for most of analyzed species. Moreover, according to our previous findings, water temperature is the most spatially and temporally variable factor in the bottom habitat of the Hornsund fjord (Drewnik et al., 2016). Given that, bottom water temperature is potentially the most crucial determinant of benthic fauna distribution and habitat suitability in Hornsund. The importance of water temperature for benthic fauna persistence and distribution has also been emphasized in many previous studies (Callaway et al., 2002; Gray, 2002; McArthur et al., 2010; Neumann et al., 2009; Reiss et al., 2011; Snelgrove, 2001). Its influence may be even more visible and striking in semi-closed fjords (Freeland et al., 1980) with specific fauna compositions (Freeland et al., 1980; Görlich et al., 1987; Renaud et al., 2007; Sejr et al., 2000; Włodarska-Kowalczuk and Węsławski, 2008; Wlodarska-Kowalczuk et al., 2005; Włodarska-Kowalczuk et al., 2013) and unique environmental conditions (shelf water inflows). Our results support the significance of observed Atlantic warm water fluxes in benthic fauna persistence and composition in the Hornsund fjord.

Although the temperature is widely recognized as a factor limiting the occurrence and performance of Arctic marine invertebrates (Brown and Thatje, 2015; Petersen et al., 2003), many species inhabiting Hornsund are species of very wide thermal tolerance from the subarctic domain. Nevertheless, our studies show that the level of importance of bottom water temperature varies between species and individual species' responses to that factor should not be underestimated. We did not observe clear trends, similarities or differences between crustaceans and mollusc. Further analysis of the species' responses to specific temperature values (response curves graphs) and predicted occurrences in the fjord (binary prediction maps) indicated that interspecific differences were due to the temperature preferences of individual species. We identified species with a broad tolerance range to temperature, and suitable conditions for these species were modeled across a vast area of the fjord (low-temperature importance). We also identified species that preferred only warm (above 1°C) or only cold (below 1°C) waters with suitable habitats predicted in the outer and central, or in the central and inner basins of the fjord, respectively. This latter group's distribution was categorized as being temperature-dependent.

In terms of species physiology, potential consequences related to the continuous inflow of Atlantic warm water into the fjord may be the most severe for cold water species in the temperature-dependent group. However, Atlantic fluxes are believed to be limited to the outer and central basins of the fjords (Swerpel, 1985; Urbański et al., 1980). Long-term measurements of bottom water temperature in Hornsund fjord confirm that those basins, and not the inner basins, are influenced by shelf waters (Drewnik et al., 2016). On the other hand, the innermost basins contain cold water and are more stable (Weslawski et al., 2010). Consequently, cold-water benthic fauna that occupies the innermost basins of the fjord is isolated from the influence of shelf water inflows. Species that also inhabit the central and outer basins may be more vulnerable to the effects of Atlantic fluxes. As a result, their distributions may be limited to the inner basins when exposed to temperatures exceeding their maximum tolerance level. Either way, our results confirm that the inner most basins of Hornsund fjord likely serve as refugia for cold water Arctic fauna, as previously determined in Węsławski et al. (2011). Furthermore, our results show that the outer and central basins of the fjord create suitable habitats for fauna preferring warm Atlantic waters, assuming that they do not have a very narrow range of temperature tolerance. Nevertheless, these species may not tolerate exposure to higher temperatures for extended time periods, and they may become extinct if such conditions persist.

Overall, the constant inflow of warm shelf waters may potentially result in the division of Hornsund fjord into two biologically distinct zones. In this case, cold water fauna would dominate in the inner basins and warm water fauna in outer and central basins of the fjord. Biodiversity would remain stable unless certain species do not survive the changes in prevailing conditions. In that case, a decrease in the species pool would be expected. However, few documented marine extinctions have occurred (Dulvy et al., 2003; McCauley et al., 2015), and regional extinctions are considered unlikely (Carstensen and Weydmann, 2012; Flessa and Jablonski, 1995). Stuart-Smith et al. (2015) indicate the

importance of individual species' responses — particularly their thermal bias — and the need to investigate this topic to predict the future existence of species in warmed up areas. This will be the subject of the next paper to be published based on the present material.

The biodiversity of Hornsund fjord may also be affected by the northward advection of the North Atlantic Current. This current is able to carry boreal taxa from the Norwegian Sea shelf, an area distinctly richer in species than the European Arctic shelf of Svalbard, to the Hornsund fjord (Palerud et al., 2004). One possible scenario involves the increase of Hornsund diversity. Examples of such increases have already been observed in the Pacific Arctic (Grebmeier et al., 2006; Sirenko and Gagaev, 2007), in Svalbard fjord Kongsfjord (Beuchel et al., 2006; Kędra et al., 2009), as well as in Hornsund (Węsławski et al. unpublished data; Grzelak and Kotwicki unpublished data). This species enrichment applies to outer and central basins of Hornsund fjord. Inner, isolated basins of multiple fjords continue to contain less diverse fauna. Decreasing trend in biodiversity has already been observed in glacial impacted regions of Hornsund (Włodarska-Kowalczuk et al., 2013) and other glacial fjords off Spitsbergen (Renaud et al., 2007; Wlodarska-Kowalczuk et al., 2005; Włodarska-Kowalczuk and Węsławski, 2008), Greenland (Sejr et al., 2000), and the Canadian Arctic (Farrow et al., 1983). According to current knowledge, species pools may be enriched because closely related species coexist instead of replacing each other (Kwasniewski et al., 2010; Leppäkoski and Olenin, 2001; Weslawski et al., 2010).

In conclusion, the importance of water temperature in benthic fauna distribution in Hornsund fjord is clear. We have confirmed the significance of observed Atlantic warm water inflows in benthic fauna persistence and composition. Nevertheless, predicted responses to water temperature seem to be species specific. We did not find clear trends or similarities among modeled organisms. To understand and predict the possible consequences of environmental alterations in Arctic regions such as Spitsbergen, knowledge about individual species needs to be considered. For some species, changes in water characteristics may have physical consequences. For others, they may cause new interspecific interactions. Hence, an assessment of Arctic biodiversity should depend on detailed studies of individual species-environment relationships. Overall, the composition of Arctic communities and ecosystems may change in the future and may become more boreal in nature. Studying the distribution of individual species and communities as indicators of Arctic environmental and ecosystem change is of great value and importance.

Acknowledgements

This research was funded by the National Center for Science in Krakow, Poland ("Cold water benthic fauna relicts in warmed up fjords — GIS approach" 2012/05/N/ST10/03856, "GAME" 2012/04/A/NZ8/00661) and the Polish-Norwegian Research Programme operated by the National Centre for Research and Development under the Norwegian Financial Mechanism 2009—2014, Project Contract No POL-NOR/199377/91/2014 ("GLAERE"). IO PAN in Sopot contributed to this study by providing ship time and manpower. We thank Kajetan Deja from IO PAN for assisting with the laboratory analysis, and special thanks go to Agnieszka Promińska and Emilia Trudnowska from IO PAN for providing data on bottom water temperature and salinity.

References

ACIA, 2005. Arctic Climate Impact Assessment. ACIA Overview Report. Cambridge Univ. Press, 1042 pp.

Basedow, S., Eianeb, K., Tverbergc, V., Spindler, M., 2004. Advection of zooplankton in an Arctic fjord (Kongsfjorden, Svalbard). Estuar. Coast. Shelf Sci. 60 (1), 113—124, http://dx.doi.org/10.1016/j.ecss.2003.12.004.

Beaugrand, G., Reid, P.C., Ibañez, F., Lindley, J.A., Edwards, M., 2002. Reorganization of North Atlantic marine copepod biodiversity and climate. Science 296 (5573), 1692—1694, http://dx.doi.org/10.1126/science.1071329.

Berge, J., Johnsen, G., Nilsen, F., Gulliksen, B., Slagstad, D., 2005. Ocean temperature oscillations enable reappearance of blue mussels *Mytilus edulis* in Svalbard after a 1000 year absence. Mar. Ecol.-Prog. Ser. 303, 167—175, http://dx.doi.org/10.3354/meps303167.

Berge, J., Renaud, P.E., Eiane, K., Gulliksen, B., Cottier, F.R., Varpe, Ø., Brattegard, T., 2009. Changes in the decapod fauna of an Arctic fjord during the last 100 years (1908—2007). Polar Biol. 32 (7), 953—961, http://dx.doi.org/10.1007/s00300-009-0594-5.

Beuchel, F., Gulliksen, B., Carroll, M.L., 2006. Long-term patterns of rocky bottom macrobenthic community structure in an Arctic fjord (Kongsfjorden, Svalbard) in relation to climate variability (1980—2003). J. Marine Syst. 63 (1—2), 35—48, http://dx.doi.org/10.1016/j.jmarsys.2006.05.002.

Błaszczyk, M., Jania, J.A., Hagen, J.O., 2009. Tidewater glaciers of Svalbard: recent changes and estimates of calving fluxes. Pol. Polar Res. 30, 85—142.

Błaszczyk, M., Jania, J.A., Kolondra, L., 2013. Fluctuations of tidewater glaciers in Hornsund Fjord (Southern Svalbard) since the beginning of the 20th century. Pol. Polar Res. 34 (4), 327—352, http://dx.doi.org/10.2478/popore-2013-0024.

Brown, A., Thatje, S., 2015. The effects of changing climate on faunal depth distributions determine winners and losers. Glob. Change Biol. 21 (1), 173—180, http://dx.doi.org/10.1111/gcb.12680.

Bučas, M., Bergström, U., Downie, A.-L., Sundblad, G., Gullström, M., von Numers, M., Šiaulys, A., Lindegarth, M., 2013. Empirical modelling of benthic species distribution, abundance, and diversity in the Baltic Sea: evaluating the scope for predictive mapping using different modelling approaches. ICES J. Mar. Sci. 70 (6), 1233—1243, http://dx.doi.org/10.1093/icesjms/fst036.

Callaway, R., Alsvag, J., Boois, I., de Cotter, J., Ford, A., Hinz, H., Jennings, S., Kroncke, I., Lancaster, J., Piet, G., Prince, P., Ehrich, S., 2002. Diversity and community structure of epibenthic invertebrates and fish in the North Sea. ICES J. Mar. Sci. 59 (6), 1199—1214, http://dx.doi.org/10.1006/jmsc.2002.1288.

Carstensen, J., Weydmann, A., 2012. Tipping points in the Arctic: eyeballing or statistical significance? Ambio 41 (1), 34—43, http://dx.doi.org/10.1007/s13280-011-0223-8.

Cottier, F.R., Nilsen, F., Skogseth, R., et al., 2010. Arctic fjords: a review of the oceanographic environment and dominant physical processes. Geol. Soc. Lond. Spec. Publ. 344 (1), 35—50, http://dx.doi.org/10.1144/SP344.4.

Cottier, F., Tverberg, V., Inall, M., Svendsen, H., Nilsen, F., Griffiths, C., 2005. Water mass modification in an Arctic fjord through cross-shelf exchange: the seasonal hydrography of Kongsfjorden, Svalbard. J. Geophys. Res. Ocean. 110 (12), 1—18, http://dx.doi.org/10.1029/2004JC002757.

Dawson, T.P., Jackson, S.T., House, J.I., Prentice, I.C., Mace, G.M., 2011. Beyond predictions: biodiversity conservation in a changing

climate. Science 332 (6025), 53—58, http://dx.doi.org/10.1126/science.1200303.
Degraer, S., Verfaillie, E., Willems, W., Adriaens, E., Vincx, M., Van Lancker, V., 2008. Habitat suitability modelling as a mapping tool for macrobenthic communities: an example from the Belgian part of the North Sea. Cont. Shelf Res. 28 (3), 369—379, http://dx.doi.org/10.1016/j.csr.2007.09.001.
Drainville, G., 1970. The Saguenay fjord: the ichtyological fauna and ecological conditions. Nat. Can. 97 (6), 623—666.
Drewnik, A., Węsławski, J.M., Włodarska-Kowalczuk, M., Łącka, M., Promińska, A., Zaborska, A., Gluchowska, M., 2016. From the worm's point of view. I: Environmental settings of benthic ecosystems in Arctic fjord (Hornsund, Spitsbergen). Polar Biol., http://dx.doi.org/10.1007/s00300-015-1867-9.
Drinkwater, K.F., 2006. The regime shift of the 1920s and 1930s in the North Atlantic. Prog. Oceanogr. 68 (2—4), 134—151, http://dx.doi.org/10.1016/j.pocean.2006.02.011.
Dulvy, N., Sadovy, Y., Reynolds, J.D., 2003. Extinction vulnerability in marine populations. Fish Fish. 4 (1), 5—64, http://dx.doi.org/10.1046/j.1467-2979.2003.00105.x.
Elith, J., Graham, C.H., Anderson, R.P., Dudík, M., Ferrier, S., Guisan, A., Hijmans, R.J., Huettmann, F., Leathwick, J.R., Lehmann, A., Li, J., Lohmann, L.G., Loiselle, B.A., Manion, G., Moritz, C., Nakamura, M., Nakazawa, Y., Overton, J.M., Townsend Peterson, A., Phillips, S.J., Richardson, K., Scachetti-Pereira, R., Schapire, R.E., Soberón, J., Williams, S., Wisz, M. S., Zimmermann, N.E., 2006. Novel methods improve prediction of species' distributions from occurrence data. Ecography (Cop.). 29 (2), 129—151, http://dx.doi.org/10.1111/j.2006.0906-7590.04596.x.
Elith, J., Phillips, S.J., Hastie, T., Dudík, M., Chee, Y.E., Yates, C.J., 2011. A statistical explanation of MaxEnt for ecologists. Divers. Distrib. 17 (1), 43—57, http://dx.doi.org/10.1111/j.1472-4642.2010.00725.x.
Ellis, J., Ysebaert, T., Hume, T., Norkko, A., Bult, T., Herman, P., Thrush, S., Oldman, J., 2006. Predicting macrofaunal species distributions in estuarine gradients using logistic regression and classification systems. Mar. Ecol -Prog. Ser. 316, 69—83, http://dx.doi.org/10.3354/meps316069.
Falk-Petersen, S., Pavlov, V., Timofeev, S., Sargent, J., 2007. Climate variability and possible effects on arctic food chains: the role of Calanus. In: Ørbæk, J., Kallenborn, R., Tombre, I., Hegseth, E., Falk-Petersen, S., Hoel, A. (Eds.), Arctic Alpine Ecosystems and People in a Changing Environment. Springer, Berlin Heidelberg, 147—166, http://dx.doi.org/10.1007/978-3-540-48514-8_9.
Farrow, G.E., Syvitski, J.P.M., Tunnicliffe, V., 1983. Suspended particulate loading on the macrobenthos in a highly turbid fjord: Knight Inlet, British Columbia. Can. J. Fish. Aquat. Sci. 40 (S1), s273—s288, http://dx.doi.org/10.1139/f83-289.
Flessa, K.W., Jablonski, D., 1995. Biogeography of recent marine bivalve molluscs and its implications for paleobiogeography and the geography of extinction: a progress report. Hist. Biol. 10 (1), 25—47, http://dx.doi.org/10.1080/10292389509380512.
Franklin, J., 2009. Mapping Species Distributions: Spatial Inference and Prediction. Cambridge Univ. Press, New York, 340 pp.
Freeland, H.J., Farmer, D.M., Levings, C.D., 1980. Fjord Oceanography. Plenum Press, New York, 715 pp.
Glockzin, M., Gogina, M., Zettler, M.L., 2009. Beyond salty reins — modeling benthic species' spatial response to their physical environment in the Pomeranian Bay (Southern Baltic Sea). Balt. Coast. Zo. 13 (II), 79—95.
Gogina, M., Glockzin, M., Zettler, M.L., 2010. Distribution of benthic macrofaunal communities in the western Baltic Sea with regard to near-bottom environmental parameters. 2. Modelling and prediction. J. Marine Syst. 80 (1—2), 57—70, http://dx.doi.org/10.1016/j.jmarsys.2009.10.001.
Gogina, M., Zettler, M.L., 2010. Diversity and distribution of benthic macrofauna in the Baltic Sea. Data inventory and its use for species distribution modelling and prediction. J. Sea Res. 64 (3), 313—321, http://dx.doi.org/10.1016/j.seares.2010.04.005.
Görlich, K., Węslawski, J.M., Zajączkowski, M., 1987. Suspension settling effect on macrobenthos biomass distribution in the Hornsund fjord, Spitsbergen. Polar Res. 5 (2), 175—192.
Gray, J.S., 2002. Species richness of marine soft sediments. Mar. Ecol. -Prog. Ser. 244, 285—297, http://dx.doi.org/10.3354/meps244285.
Grebmeier, J.M., Overland, J.E., Moore, S.E., Farley, E.V., Carmack, E.C., Cooper, L.W., Frey, K.E., Helle, J.H., McLaughlin, F.A., McNutt, S.L., 2006. A major ecosystem shift in the northern Bering Sea. Science 311 (5766), 1461—1464, http://dx.doi.org/10.1126/science.1121365.
Hernandez, P.A., Franke, I., Herzog, S.K., Pacheco, V., Paniagua, L., Quintana, H.L., Soto, A., Swenson, J.J., Tovar, C., Valqui, T.H., Vargas, J., Young, B.E., 2008. Predicting species distributions in poorly-studied landscapes. Biodivers. Conserv. 17 (6), 1353—1366, http://dx.doi.org/10.1007/s10531-007-9314-z.
Hernandez, P.A., Graham, C.H., Master, L.L., Albert, D.L., Hernández Graham, C.H., Master, L.L., Albert, D.L., 2006. The effect of sample size and species characteristics on performance of different species distribution modeling methods. Ecography (Cop.). 29 (5), 773—785, http://dx.doi.org/10.1111/j.0906-7590.2006.04700.x.
Hijmans, R., Graham, C., 2006. The ability of climate envelope models to predict the effect of climate change on species distributions. Glob. Change Biol. 12 (12), 2272—2281, http://dx.doi.org/10.1111/j.1365-2486.2006.01256.x.
Hop, H., Pearson, T., Hegseth, E.N., Kovacs, K.M., Wiencke, C., Kwasniewski, S., Eiane, K., Mehlum, F., Gulliksen, B., Włodarska-Kowalczuk, M., Lydersen, C., Weslawski, J.M., Cochrane, S., Gabrielsen, G.W., Leakey, R.J.G., Lønne, O.J., Zajaczkowski, M., Falk-Petersen, S., Kendall, M., Wängberg, S.Å., Bischof, K., Voronkov, A.Y., Kovaltchouk, N.A., Wiktor, J., Poltermann, M., Di Prisco, G., Papucci, C., Gerland, S., 2002. The marine ecosystem of Kongsfjorden, Svalbard. Polar Res. 21 (1), 167—208, http://dx.doi.org/10.1111/j.1751-8369.2002.tb00073.x.
Inglis, G.J., Hurren, H., Oldman, J., Haskew, R., 2006. Using habitat suitability index and particle dispersion models for early detection of marine invaders. Ecol. Appl. 16 (4), 1377—1390, http://dx.doi.org/10.1890/1051-0761(2006)016[1377:UHSIAP]2.0.CO;2.
Jónsson, S., Valdimarsson, H., 2005. The flow of Atlantic water to the North Icelandic Shelf and its relation to the drift of cod larvae. ICES J. Mar. Sci. 62 (7), 1350—1359, http://dx.doi.org/10.1016/j.icesjms.2005.05.003.
Kendall, M., Widdicombe, S., Weslawski, J., 2003. A multi-scale study of the biodiversity of the benthic infauna of the high-latitude Kongsfjord, Svalbard. Polar Biol. 26 (6), 383—388.
Kędra, M., Włodarska-Kowalczuk, M., Węsławski, J.M., 2009. Decadal change in macrobenthic soft-bottom community structure in a high Arctic fjord (Kongsfjorden, Svalbard). Polar Biol. 33 (1), 1—11, http://dx.doi.org/10.1007/s00300-009-0679-1.
Kröncke, I., 1995. Long-term changes in North Sea benthos. Senck Marit. 26, 73—80.
Kwasniewski, S., Gluchowska, M., Jakubas, D., Wojczulanis-Jakubas, K., Walkusz, W., Karnovsky, N., Blachowiak-Samolyk, K., Cisek, M., Stempniewicz, L., 2010. The impact of different hydrographic conditions and zooplankton communities on provisioning Little Auks along the West coast of Spitsbergen. Prog. Oceanogr. 87 (1—4), 72—82, http://dx.doi.org/10.1016/j.pocean.2010.06.004.
Leppäkoski, E., Olenin, S., 2001. The meltdown of biogeographical peculiarities of the Baltic Sea: the interaction of natural and man-made processes. Ambio 30 (4—5), 202—209, http://dx.doi.org/10.1579/0044-7447-30.4.202.
Lydersen, C., Assmy, P., Falk-Petersen, S., Kohler, J., Kovacs, K.M., Reigstad, M., Steen, H., Strøm, H., Sundfjord, A., Varpe, Ø., Walczowski, W., Weslawski, J.M., Zajaczkowski, M., 2014. The

importance of tidewater glaciers for marine mammals and seabirds in Svalbard, Norway. J. Marine Syst. 129, 452—471, http://dx.doi.org/10.1016/j.jmarsys.2013.09.006.

McArthur, M.A., Brooke, B.P., Przeslawski, R., Ryan, D.A., Lucieer, V.L., Nichol, S., McCallum, A.W., Mellin, C., Cresswell, I.D., Radke, L.C., 2010. On the use of abiotic surrogates to describe marine benthic biodiversity. Estuar. Coast. Shelf Sci. 88 (1), 21—32, http://dx.doi.org/10.1016/j.ecss.2010.03.003.

McCauley, D.J., Pinsky, M.L., Palumbi, S.R., Estes, J.A., Joyce, F.H., Warner, R.R., 2015. Marine defaunation: animal loss in the global ocean. Science 347 (6219), 247—254, http://dx.doi.org/10.1126/science.1255641.

Meißner, K., Darr, A., Rachor, E., 2008. Development of habitat models for Nephtys species (Polychaeta: Nephtyidae) in the German Bight (North Sea). J. Sea Res. 60 (4), 271—286, http://dx.doi.org/10.1016/j.seares.2008.08.001.

Merow, C., Smith, M.J., Silander, J.A., 2013. A practical guide to MaxEnt for modeling species' distributions: what it does, and why inputs and settings matter. Ecography (Cop.). 36 (10), 1058—1069, http://dx.doi.org/10.1111/j.1600-0587.2013.07872.x.

Moskalik, M., Grabowiecki, P., Tęgowski, J., Żulichowska, M., 2013. Bathymetry and geographical regionalization of Brepollen (Hornsund, Spitsbergen) based on bathymetric profiles interpolations. Polish Polar Res. 34 (1), 1—22, http://dx.doi.org/10.2478/popore-2013-0001.

Neumann, H., Reiss, H., Rakers, S., Ehrich, S., Kroncke, I., 2009. Temporal variability in southern North Sea epifauna communities after the cold winter of 1995/1996. ICES J. Mar. Sci. 66 (10), 2233—2243, http://dx.doi.org/10.1093/icesjms/fsp203.

Nilsen, F., Cottier, F., Skogseth, R., Mattsson, S., 2008. Fjord-shelf exchanges controlled by ice and brine production: the interannual variation of Atlantic Water in Isfjorden, Svalbard. Cont. Shelf Res. 28 (14), 1838—1853, http://dx.doi.org/10.1016/j.csr.2008.04.015.

Nilsen, F., Gjevik, B., Schauer, U., 2006. Cooling of the West Spitsbergen Current: isopycnal diffusion by topographic vorticity waves. J. Geophys. Res. Ocean. 111 (8), 1—16, http://dx.doi.org/10.1029/2005JC002991.

Olenin, S., 1997. Benthic zonation of the Eastern Gotland Basin, Baltic Sea. Neth. J. Aquat. Ecol. 30 (4), 265—282, http://dx.doi.org/10.1007/BF02085871.

Ortega-Huerta, M.A., Peterson, A.T., 2008. Modeling ecological niches and predicting geographic distributions: a test of six presence-only methods. Rev. Mex. Biodivers. 79 (1), 205—216, http://dx.doi.org/10.1016/j.biocon.2004.07.008.

Palerud, R., Gulliksen, B., Brattegard, T., Sneli, J.-A., Vader, W., 2004. The marine macro-organisms in Svalbard waters. In: Prestrud, P., Strøm, H., Goldman, H.V. (Eds.), A Catalogue of Terrestrial and Marine Animals of Svalbard. Norwegian Polar Inst., Polar Environ. Centre, Tromsø, 5—56.

Pavlov, A.K., Tverberg, V., Ivanov, B.V., Nilsen, F., Falk-Petersen, S., Granskog, M.A., 2013. Warming of Atlantic Water in two west Spitsbergen fjords over the last century (1912—2009). Polar Res. 32, http://dx.doi.org/10.3402/polar.v32i0.11206.

Pearson, R.G., Raxworthy, C.J., Nakamura, M., Townsend Peterson, A., 2007. Predicting species distributions from small numbers of occurrence records: a test case using cryptic geckos in Madagascar. J. Biogeogr. 34 (1), 102—117, http://dx.doi.org/10.1111/j.1365-2699.2006.01594.x.

Petersen, J.K., Sejr, M.K., Larsen, J.E.N., 2003. Clearance rates in the Arctic bivalves *Hiatella arctica* and Mya sp. Polar Biol. 26 (5), 334—341, http://dx.doi.org/10.1007/s00300-003-0483-2.

Phillips, S.J., Anderson, R.P., Schapire, R.E., 2006. Maximum entropy modeling of species geographic distributions. Ecol. Modell. 190 (3—4), 231—259, http://dx.doi.org/10.1016/j.ecolmodel.2005.03.026.

Phillips, S.J., Dudík, M., Schapire, R.E., 2004. A maximum entropy approach to species distribution modeling. In: Proceedings of the Twenty-First International Conference on Machine Learning. ACM, New York, NY, 655—662, http://dx.doi.org/10.1145/1015330.1015412.

Piechura, J., Beszczyńska-Möller, A., Osiński, R., 2001. Volume, heat and salt transport by the West Spitsbergen Current. Polar Res. 20 (2), 233—240, http://dx.doi.org/10.1111/j.1751-8369.2001.tb00061.x.

Piepenburg, D., 2005. Recent research on Arctic benthos: common notions need to be revised. Polar Biol. 28 (10), 733—755, http://dx.doi.org/10.1007/s00300-005-0013-5.

Reiss, H., Cunze, S., König, K., Neumann, H., Kröncke, I., 2011. Species distribution modelling of marine benthos: a North Sea case study. Mar. Ecol.-Prog. Ser. 442, 71—86, http://dx.doi.org/10.3354/meps09391.

Renaud, P.E., Carroll, M.L., Ambrose Jr., W.G., 2008. Effects of global warming on Arctic sea-floor communities and its consequences for higher trophic levels. In: Duarte, C.M. (Ed.), Impacts of Global Warming on Polar Ecosystems. Fundacion BBVA, Madrid, 139—175.

Renaud, P.E., Włodarska-Kowalczuk, M., Trannum, H., Holte, B., Węsławski, J.M., Cochrane, S., Dahle, S., Gulliksen, B., 2007. Multidecadal stability of benthic community structure in a high-Arctic glacial fjord (van Mijenfjord, Spitsbergen). Polar Biol. 30 (3), 295—305, http://dx.doi.org/10.1007/s00300-006-0183-9.

Robinson, L.M., Elith, J., Hobday, A.J., Pearson, R.G., Kendall, B.E., Possingham, H.P., Richardson, A.J., 2011. Pushing the limits in marine species distribution modelling: lessons from the land present challenges and opportunities. Glob. Ecol. Biogeogr. 20 (6), 789—802, http://dx.doi.org/10.1111/j.1466-8238.2010.00636.x.

Schauer, U., Beszczynska-Möller, A., Walczowski, W., Fahrbach, E., Piechura, J., Hansen, E., 2008. Variation of measured heat flow through the fram strait between 1997 and 2006. In: Dickson, R.R., Meincke, J., Rhines, P. (Eds.), Arctic-Subarctic Ocean Fluxes. Springer, Netherlands, 65—85.

Sejr, M.K., Jensen, K.T., Rysgaard, S., 2000. Macrozoobenthic community structure in a high-arctic East Greenland fjord. Polar Biol. 23 (11), 792—801, http://dx.doi.org/10.1007/s003000000154.

Sirenko, B.I., Gagaev, S.Y., 2007. Unusual abundance of macrobenthos and biological invasions in the Chukchi Sea. Russ. J. Mar. Biol. 33 (6), 355—364, http://dx.doi.org/10.1134/S1063074007060016.

Skogseth, R., Haugan, P.M., Jakobsson, M., 2005. Watermass transformations in Storfjorden. Cont. Shelf Res. 25 (5—6), 667—695, http://dx.doi.org/10.1016/j.csr.2004.10.005.

Smedsrud, L.H., Ingvaldsen, R., Nilsen, J.E.Ø., Skagseth, Ø., 2010. Heat in the Barents Sea: transport, storage, and surface fluxes. Ocean Sci. 6 (1), 219—234, http://dx.doi.org/10.5194/os-6-219-2010.

Snelgrove, P.V.R., 2001. Diversity of marine species. In: Steele, J.H., Thorpe, S.A., Turekian, K.K. (Eds.), Encyclopedia of Ocean Sciences. Acad. Press, San Diego, 748—757.

Spielhagen, R.F., Werner, K., Sørensen, S.A., Zamelczyk, K., Kandiano, E., Budeus, G., Husum, K., Marchitto, T.M., Hald, M., 2011. Enhanced modern heat transfer to the Arctic by warm Atlantic Water. Science 331 (6016), 450—453, http://dx.doi.org/10.1126/science.1197397.

Stuart-Smith, R.D., Edgar, G.J., Barret, N.S., Kininmonth, S.J., Bates, A.E., 2015. Thermal biases and vulnerability to warming in the world's marine fauna. Nature 528 (7580), 88—92, http://dx.doi.org/10.1038/nature16144.

Svendsen, H., Beszczynska-Møller, A., Hagen, J.O., Lefauconnier, B., Tverberg, V., Gerland, S., Ørbæk, J.B., Bischof, K., Papucci, C., Zajaczkowski, M., Azzolini, R., Bruland, O., Wiencke, C., Winther, J.G., Dallmann, W., 2002. The physical environment of Kongsfjorden — Krossfjorden, an Arctic fjord system in Svalbard. Polar Res. 21 (1), 133—166, http://dx.doi.org/10.1111/j.1751-8369.2002.tb00072.x.

Syvitski, J.P.M., Burrell, D.C., Skei, J.M., 1987. Fjords. Processes and Products. Springer-Verlag, New York, 379 pp.

Swerpel, S., 1985. The Hornsund Fiord: water masses. Polish Polar Res. 6 (4), 475—496.

Teigen, S.H., Nilsen, F., Skogseth, R., Gjevik, B., Beszczynska-Möller, A., 2011. Baroclinic instability in the West Spitsbergen current. J. Geophys. Res. Ocean. 116 (7), 1—18, http://dx.doi.org/10.1029/2011JC006974.

Thrush, S.F., Hewitt, J.E., Norkko, A., Nicholls, P.E., Funnell, G.A., Ellis, J.I., 2003. Habitat change in estuaries: predicting broad-scale responses of intertidal macrofauna to sediment mud content. Mar. Ecol.-Prog. Ser. 263, 101—112, http://dx.doi.org/10.3354/meps263101.

Urbański, J., Neugenbauer, E., Spacjer, R., Falkowska, L., 1980. Physico-chemical characteristic of the waters of Hornsund Fjord on south-west Spitsbergen (Svalbard Archipelago) in the summer season 1979. Pol. Polar Res. 1 (4), 43—52.

Walczowski, W., Piechura, J., 2006. New evidence of warming propagating toward the Arctic Ocean. Geophys. Res. Lett. 33 (12), 1—5, http://dx.doi.org/10.1029/2006GL025872.

Walczowski, W., Piechura, J., 2007. Pathways of the Greenland Sea warming. Geophys. Res. Lett. 34 (10), 1—5, http://dx.doi.org/10.1029/2007GL029974.

Wassmann, P., Duarte, C.M., Agustí, S., Sejr, M.K., 2011. Footprints of climate change in the Arctic marine ecosystem. Glob. Change Biol. 17 (2), 1235—1249, http://dx.doi.org/10.1111/j.1365-2486.2010.02311.x.

Warwick, R.M., 1993. Environmental-impact studies on marine communities — pragmatical considerations. Aust. J. Ecol. 18, 63—80, http://dx.doi.org/10.1111/j.1442-9993.1993.tb00435.x.

Weslawski, J.M., 1990. Distribution and ecology of south Spitsbergen coastal marine amphipods (*Crustacea*). Pol. Arch. Hydrobiol. 37, 503—519.

Weslawski, J.M., Kwasniewski, S., Wiktor, J., 1991. Winter in a Svalbard fjord ecosystem. Arctic 44 (2), 115—123.

Weslawski, J.M., Wiktor, J., Kotwicki, L., 2010. Increase in biodiversity in the arctic rocky littoral, Sorkappland, Svalbard, after 20 years of climate warming. Mar. Biodivers. 40 (2), 123—130, http://dx.doi.org/10.1007/s12526-010-0038-z.

Węsławski, J.M., Kendall, M.A., Włodarska-Kowalczuk, M., Iken, K., Kędra, M., Legezynska, J., Sejr, M.K., 2011. Climate change effects on Arctic fjord and coastal macrobenthic diversity-observations and predictions. Mar. Biodivers. 41 (1), 71—85, http://dx.doi.org/10.1007/s12526-010-0073-9.

Węsławski, J.M., Kwaśniewski, S., Stempniewicz, L., 2009. Warming in the Arctic may result in the negative effects of increased biodiversity. Polarforschung 78 (3), 105—108.

Węsławski, J.M., Wiktor, J., Zajączkowski, M., Swerpel, S., 1993. Intertidal zone of Svalbard, macroorganism distribution and biomass. Polar Biol. 13 (2), 73—79, http://dx.doi.org/10.1007/BF00238538.

Willems, W., Goethals, P., Van den Eynde, D., Van Hoey, G., Van Lancker, V., Verfaillie, E., Vincx, M., Degraer, S., 2008. Where is the worm? Predictive modelling of the habitat preferences of the tube-building polychaete *Lanice conchilega*. Ecol. Modell. 212 (1—2), 74—79, http://dx.doi.org/10.1016/j.ecolmodel.2007.10.017.

Wisz, M.S., Hijmans, R.J., Li, J., Peterson, A.T., Graham, C.H., Guisan, A., Elith, J., Dudík, M., Ferrier, S., Huettmann, F., Leathwick, J.R., Lehmann, A., Lohmann, L., Loiselle, B.A., Manion, G., Moritz, C., Nakamura, M., Nakazawa, Y., Overton, J.M., Phillips, S.J., Richardson, K.S., Scachetti-Pereira, R., Schapire, R.E., Soberón, J., Williams, S.E., Zimmermann, N.E., 2008. Effects of sample size on the performance of species distribution models. Divers. Distrib. 14 (5), 763—773, http://dx.doi.org/10.1111/j.1472-4642.2008.00482.x.

Wlodarska-Kowalczuk, M., Pearson, T.H., 2004. Soft-bottom macrobenthic faunal associations and factors affecting species distributions in an Arctic glacial fjord (Kongsfjord, Spitsbergen). Polar Biol. 27 (3), 155—167, http://dx.doi.org/10.1007/s00300-003-0568-y.

Wlodarska-Kowalczuk, M., Pearson, T.H., Kendall, M., 2005. Benthic response to chronic natural physical disturbance by glacial sedimentation in an Arctic fjord. Mar. Ecol.-Prog. Ser. 303, 31—41, http://dx.doi.org/10.3354/meps303031.

Wlodarska-Kowalczuk, M., Weslawski, J.M., Kotwicki, L., 1998. Spitsbergen glacial bays macrobenthos — a comparative study. Polar Biol. 20 (1), 66—73, http://dx.doi.org/10.1007/s003000050277.

Włodarska-Kowalczuk, M., Pawłowska, J., Zajączkowski, M., 2013. Do foraminifera mirror diversity and distribution patterns of macrobenthic fauna in an Arctic glacial fjord? Mar. Micropaleontol. 103, 30—39, http://dx.doi.org/10.1016/j.marmicro.2013.07.002.

Włodarska-Kowalczuk, M., Węsławski, J.M., 2008. Mesoscale spatial structures of soft-bottom macrozoobenthos communities: effects of physical control and impoverishment. Mar. Ecol.-Prog. Ser. 356, 215—224, http://dx.doi.org/10.3354/meps07285.

Ysebaert, T., Meire, P., Herman, P.M.J., Verbeek, H., 2002. Macrobenthic species response surfaces along estuarine gradients: prediction by logistic regression. Mar. Ecol.-Prog. Ser. 225, 79—95, http://dx.doi.org/10.3354/meps225079.

Zagórski, P., Rodzik, J., Moskalik, M., Strzelecki, M.C., Lim, M., Błaszczyk, M., Promińska, A., Kruszewski, G., Styszyńska, A., Malczewski, A., 2015. Multidecadal (1960—2011) shoreline changes in Isbjørnhamna (Hornsund, Svalbard). Pol. Polar Res. 36 (4), 369—390.

Oceanologia (2017) 59, 576—584

Available online at www.sciencedirect.com

ScienceDirect

journal homepage: www.journals.elsevier.com/oceanologia/

ORIGINAL RESEARCH ARTICLE

Age, growth rate, and otolith growth of polar cod (*Boreogadus saida*) in two fjords of Svalbard, Kongsfjorden and Rijpfjorden

Dariusz P. Fey [a,*], **Jan M. Węsławski** [b]

[a] *National Marine Fisheries Research Institute, Gdynia, Poland*
[b] *Institute of Oceanology, Polish Academy of Sciences, Sopot, Poland*

Received 12 July 2016; accepted 22 March 2017
Available online 25 May 2017

KEYWORDS
Arctic;
Fish growth;
Annual rings;
Sagitta

Summary This work presents biological information for polar cod (*Boreogadus saida*) collected with a Campelen 1800 shrimp bottom trawl in Kongsfjorden (two stations located in the inner part of the fjord adjacent to the glacier) and Rijpfjorden (one station at the entrance to the fjord) in September and October 2013. The otolith-based ages of polar cod collected in Kongsfjorden (6.1—24 cm total length TL; $n = 813$) ranged from 0 to 4 years. The growth rate was relatively constant at approximately 4.7 cm year^{-1} between years 1 and 4, which indicates that growth was fast in the glacier area. The ages of polar cod collected in Rijpfjorden (8.6—15.9 cm TL; $n = 64$) ranged from 2 to 3 years. The fish from Rijpfjorden were smaller at age than those from Kongsfjorden, and their growth rate between years 2 and 3 (no other age classes were available) was approximately 3.3 cm year^{-1}. In both fjords, males and females were of the same size-at-age and the same weight-at-TL. The small sampling area means that the results on growth rate are not representative of the entire fjords. Instead, the results can be discussed as presenting the possible growth rates of some populations. A strong relationship was identified between otolith size (length and weight) and fish size (TL and TW), with no differences between males and females or the fjords. A significant, strong relationship was also noted between fish and otolith growth rates.

* Corresponding author at: National Marine Fisheries Research Institute, Kołłątaja 1, 81-332 Gdynia, Poland. Tel.: +48 587 356 232; fax: +48 587 356 110.
E-mail addresses: dfey@mir.gdynia.pl (D.P. Fey), weslaw@iopan.gda.pl (J.M. Węsławski).
Peer review under the responsibility of Institute of Oceanology of the Polish Academy of Sciences.

Production and hosting by Elsevier

http://dx.doi.org/10.1016/j.oceano.2017.03.011

1. Introduction

Polar cod (*Boreogadus saida*) is both a pelagic and demersal gadoid species that plays a key role in the Arctic shelf seas (Hop and Gjøsæter, 2013). It is distributed in open and ice-covered waters, and it provides a link between the lower (mainly zooplankton) and higher (seabirds and mammals) trophic levels (Christiansen et al., 2012; Hop and Gjøsæter, 2013). Closer association with ice, however, occurs particularly during the larval and juvenile stages (Bouchard and Fortier, 2011), whereas adult fish are primarily distributed in open or deeper waters below the ice (Geoffroy et al., 2011, 2016). From the point of view of population ecology, polar cod as an abundant planktivorous species could be a significant food competitor for other species (Renaud et al., 2012) such as capelin (*Mallotus villosus*) (Hedeholm et al., 2012). The level of competition depends, of course, on polar cod life stages. Additionally, the poleward expansion of Atlantic cod (*Gadus morhua*) and haddock (*Melanogrammus aeglefinus*) observed in recent years (Fossheim et al., 2015; Haug et al., 2017; Misund et al., 2016; Szczucka et al., 2017) increases the risk of predation by these species on polar cod. Another potential risk involves increased food competition between the young stages of Atlantic cod and haddock and polar cod, even if competition currently seems still to be at a low level (Renaud et al., 2012).

As the temperature is predicted to rise in the Arctic, further changes in species composition, their requirements, and processes such as predation and food competition are expected in the future (Berge et al., 2015; Fossheim et al., 2015; Haug et al., 2017; Misund et al., 2016). In regions such as Svalbard, these changes are likely to have serious consequences for the polar cod population. Therefore, obtaining a good understanding of polar cod life history strategies, biology, and ecology, including, for example, information on size range, growth rate, and length-weight relationship, is crucial. The amount of information of this kind for polar cod remains insufficient.

Otoliths are a useful tool in research on fish ecology. Information on the relationship between somatic growth and otolith growth as well as between otolith size and fish size is important for many applications, such as back-calculating growth rates (Francis, 1990), size estimates of fish from the guts of predators (Dietrich et al., 2006; Fritts and Pearsons, 2006; Takasuka et al., 2004), and age prediction (Boehlert, 1985; Fey and Linkowski, 2006). Although literature data on otolith size-fish size are available for polar cod (Christiansen et al., 2005; Frost and Lowry, 1981; Lidster et al., 1994), no data on the somatic growth-otolith growth relationship are available for this species except in a publication by Bouchard and Fortier (2008), who show that otolith growth is a reliable estimator of somatic growth for age-0 polar cod. Validating this assumption is necessary if growth back-calculation from otoliths or relative growth estimates from annual ring widths are to be conducted. The above-mentioned applications make otoliths a useful tool in research on the ecology of polar cod especially in light of the processes occurring in the Arctic ecosystems – increasing temperature and changes in community structure of different groups of sea animals (Fossheim et al., 2015; Haug et al., 2017; Misund et al., 2016) including mammals (Haug et al., 2017) that prey on polar cod.

This study determines the sex-specific size frequency, growth rate, and weight at length relationship for polar cod collected in two fjords – Kongsfjorden and Rijpfjorden. Because of the small sampling areas, we cannot treat the growth rate results as representative of the entire fjords. Instead, the results can be considered as indicative of the possible growth of some populations in the fjords analyzed. Additionally, the otolith size-fish size relationship as well as the fish growth rate-otolith growth rate relationships were analyzed to verify the usefulness of polar cod otoliths for their size and growth back-calculation. Possible sex and fjord effects were considered in these relationships.

2. Material and methods

2.1. Study area

Kongsfjorden is approximately 25 km long and 5–10 km wide and is located on the northwest coast of Svalbard (79°N, 12°E) (Fig. 1). Because it is an open fjord with no sill at the entrance, the influence of warm, saline Atlantic waters carried with the North Atlantic Current makes it sub-Arctic rather than Arctic. However, at the head of the fjord is an active tidal glacier that causes marked environmental gradients in salinity, temperature, and sedimentation rates (Walkusz et al., 2009). Rijpfjorden is approximately 40 km long and 12 km wide and is located in the high-Arctic on the northern side of Nordaustlandet, Svalbard (80°N, 22°30′E) (Fig. 1). The fjord is open toward the Arctic Ocean, and, because of the limited influence of warm Atlantic waters, its environment is truly arctic (Walkusz et al., 2009). The fjord is ice-covered for six to eight months annually (Wallace et al., 2010).

2.2. Fish collection

Polar cod (*B. saida*) were collected in Kongsfjorden and Rijpfjorden (Svalbard, Norway) between September 29 and October 4, 2013 during a cruise of the R V^{-1} *Helmer Hanssen* using a Campelen 1800 shrimp bottom trawl. The horizontal and vertical openings were 17 m and 4–5 m, respectively, and the door spread was about 45–50 m. Mesh size was 80 mm in the front and 22 mm in the cod end. The gear was towed on the bottom for approximately 10–15 min at 3 knots/h. The fish were collected at two stations in Kongsfjorden (depth: 134 m and 52 m) and at one in Rijpfjorden (depth: 280 m) (Fig. 1). Random sub-samples of polar cod were collected, and a total of 813 fish from Kongsfjorden and 64 from Rijpfjorden were used for the biological analysis, which included determining total length (TL, ±0.1 cm), total wet weight (TW, ±0.1 g), and sex. The fish were stored frozen before the measurements were taken. All the fish from Rijpfjorden (n = 64) and a sub-sample (n = 358) of fish from Kongsfjorden were used for otolith extraction (Fig. 2).

2.3. Otolith analysis

The sagittal otoliths were extracted from each fish non-randomly to cover the size range and to represent the fish size frequency in a given sample. The otoliths were cleaned

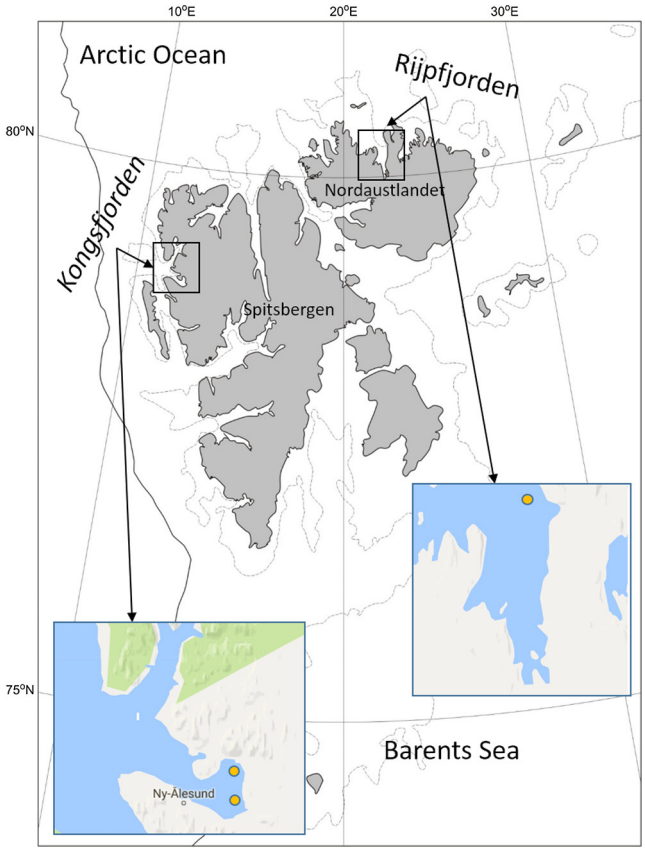

Figure 1 Map of sampling sites — Kongsfjorden and Rijpfjorden (Svalbard, Norway). The fish were collected at two stations in Kongsfjorden (depth: 134 m and 52 m, $n = 813$) and one station in Rijpfjorden (depth: 280 m, $n = 64$).

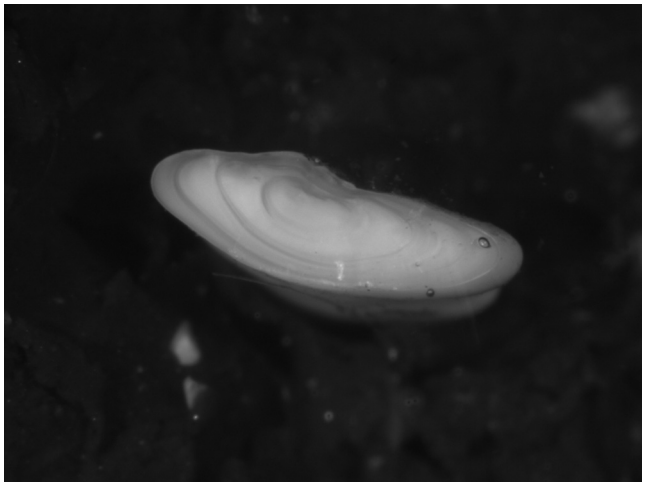

Figure 2 Annual rings in the sagittae of 13.4 cm TL polar cod.

in 96% ethanol, dried, and stored in paper envelopes for further analysis. Age was then estimated by counting the annual rings from broken otoliths. This was performed twice by the same person on different occasions using a compound microscope. The left or right sagitta was used for age estimation depending on the clarity of the increment pattern. No comparison of age estimates between the two otoliths were made. If the ages obtained from the two readings were different, the otolith was re-examined and another reader was consulted. If the two readers could not come to a decision about age, the otolith was excluded (13 of the 422 otoliths examined were excluded). Otolith length was measured for each fish from one of the sagittae with the Image Pro image analysis system (Media Cybernetics, USA). The same otolith was also weighed ($\pm$0.01 mg) on a Cahn C-31 microbalance (Thermo Orion, Beverly, MA).

2.4. Data analysis

The polar cod weight-at-length was described separately for males and females and fjord of origin with first order polynomial functions. The potential differences were evaluated with ANCOVAs after the data were log transformed to obtain linearity. The growth rate of cod was estimated from the length and weight at age data separately for the two fjords and for males and females. The age and sex effect as well as age and fjord effect on fish length and weight were evaluated for both locations with the application of two-way factorial ANOVAs.

The fish size (length and weight) and otolith size (length and weight) relationships were estimated with linear and polynomial functions, and potential differences between the sexes and fjords were evaluated with ANCOVAs. Data transformation (log) to obtain linear relationships was conducted if necessary.

Mean otolith growth rate was calculated for each specimen as otolith size divided by age, whereas the mean fish growth rate was calculated as fish size (TL and TW) divided by age. The size at hatch was omitted as insignificantly small for the analysis of adult fish growth. Fish age-0 were not included in this analysis. The significance of the otolith growth rate and fish growth rate relationship was then evaluated based on the coefficient of determination (r^2) of the first order polynomial functions fitted to the analyzed data within each age class separately. Eliminating the age effect permitted separating the somatic growth effect on otolith growth. Confirmation of the fish growth rate-otolith growth rate relationship is highly important, in addition to the otolith size-fish size relationship, if the fish growth rate is to be back-calculated or if the width of the otolith annual rings is to be interpreted as a proxy of fish growth in a corresponding year.

3. Results

3.1. Fish size and growth

The fish collected in Kongsfjorden ($n = 813$) ranged from 6.1 to 24 cm TL, and the dominant size-classes were 12–14 cm (Fig. 3). The fish collected in Rijpfjorden ($n = 64$) ranged from 8.6 to 15.9 cm TL and the dominant size-classes were 11–12 cm (Fig. 3). Males were generally more abundant among smaller fish and females among larger ones.

A significant relationship occurred between fish TL and TW ($TW = 0.0053TL^{3.042}$, $r^2 = 0.955$) (Fig. 4). The slope and intercept of the relationship were not affected by sex (ANCOVA, $n = 877$, $P > 0.05$) or fjord of origin (ANCOVA, $n = 877$, $P > 0.05$).

The otolith-based ages of the polar cod collected ranged from 0 to 4 years in Kongsfjorden and from 2 to 3 years in Rijpfjorden. TL-at-age and TW-at-age were not significantly affected by sex in either Kongsfjorden or Rijpfjorden (in all cases: two-way factorial ANOVA, $n = 409$, for age effect $P < 0.001$, for sex effect $P > 0.05$); therefore, the data were pooled for males and females (Fig. 5). Fish collected in Kongsfjorden were larger at age in comparison to those from Rijpfjorden for both size parameters – TL (two-way factorial ANOVA, $n = 409$, for fjord effect $P < 0.001$) and TW (two-way factorial ANOVA, $n = 409$, for fjord effect $P < 0.001$). The growth of polar cod in TL in Kongsfjorden was relatively

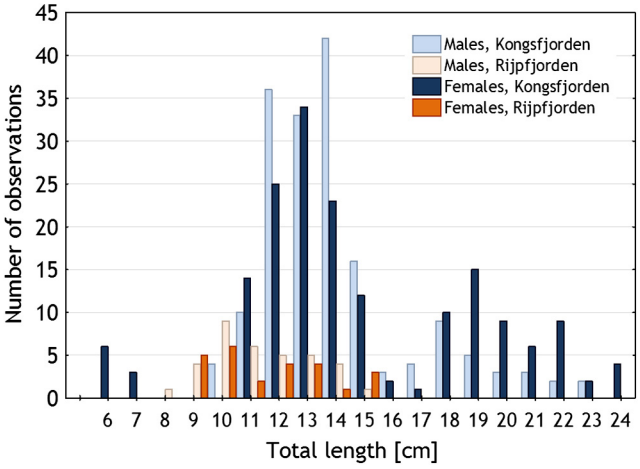

Figure 3 Total length frequency distribution of males and females collected at the Kongsfjorden and Rijpfjorden sites ($n = 877$).

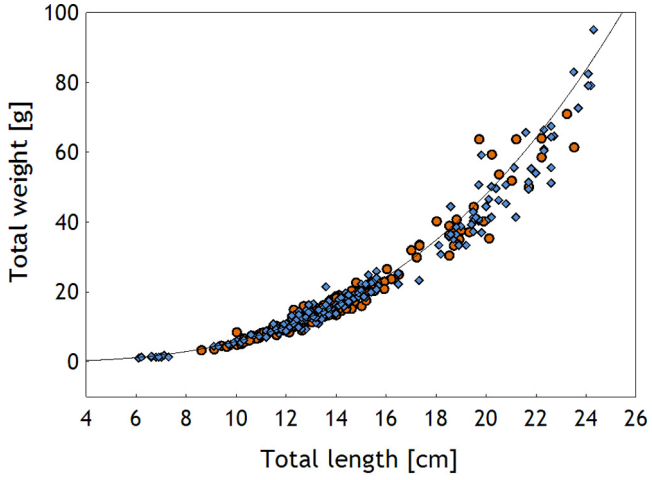

Figure 4 Relationship between total length and weight. Single function was fitted for males (circles) and females (diamonds) from Kongsfjorden and Rijpfjorden ($TW = 0.0053TL^{3.042}$, $n = 877$, $r^2 = 0.955$).

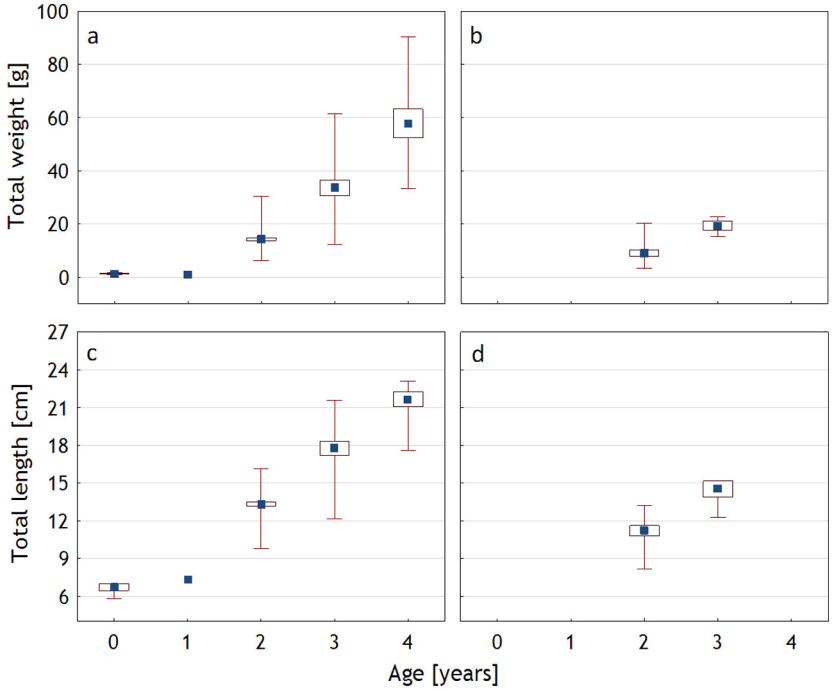

Figure 5 Total weight at age for Kongsfjorden (a) and Rijpfjorden (b), and total length at age for Kongsfjorden (c) and Rijpfjorden (d). Data for males and females are pooled. Square denotes mean, boxes 95% confidence intervals, and whiskers minimum and maximum. Number of data points for each age-group is given.

constant between years 1 and 4 at 4.7 cm year^{-1}. In Rijpfjorden, the growth between years 2 and 3 (no other year classes were available) was 3.3 cm year^{-1}.

3.2. Otolith size and growth

Both otolith size parameters (length and weight) expressed significant fish size-otolith size relationships. Because no differences in slope or intercept were recorded either between males and females or sampling locations (for all comparisons: ANCOVA, $n = 409$, $P > 0.05$), all the fish size-otolith size data were pooled for males and females and for Kongsfjorden and Rijpfjorden (Table 1, Fig. 6). Considering the high values of the coefficients of determination r^2 for these relationships that ranged from 0.861 to 0.947 (each r^2 was statistically significant, $P < 0.05$), both otolith length and weight can be used in the equation predicting fish TL and TW.

Fish growth rate-otolith growth rate relationships were significant for fish size expressed in both TL and TW ($P < 0.0001$) (Fig. 7). The r^2 of the polynomial equations fitted to these data ranged from 0.436 (age 4) to 0.884 (age 3) for TL, and from 0.401 (age 4) to 0.778 (age 3) for TW. The equations were developed just to show the strength of the relationships described. The exact formulas have no biological importance, and, as such, are not presented.

3.3. Discussion

The fish collected ranged from 6.1 to 24 cm TL. The dominant size classes were 11–14 cm with males more abundant among smaller fish and females among larger ones. This size structure and female/male ratio corresponds with other publications reporting polar cod size range ratios in the Beaufort Sea (Benoit et al., 2010; Craig et al., 1982), the east coast of Newfoundland (Lidster et al., 1994), Allen Bay, Canada (Matley et al., 2013), and Svalbard (Nahrgang et al., 2014). It was suggested previously that the relatively high frequency of females in upper age classes in samples collected in fall is related to higher male mortality during summer (Bain and Sekerak, 1978) and faster growth rates in females (Hop et al., 1997). In the present work, however, no differences in growth rates were found between males and females. Considering the age range, the oldest fish in the present work were 4 years old. Even if older polar cod were described in other studies – for example, age 5 (Matley et al., 2013), age 6 (Craig et al., 1982) or age 7 (Hop et al., 1997; Nahrgang et al., 2014) – they were not numerous.

TL-at-age and TW-at-age were not significantly affected by sex either in Kongsfjorden or in Rijpfjorden. Similar results showing no difference between males and females in fish size-at-age are reported by other researchers (Craig et al., 1982; Matley et al., 2013; Nahrgang et al., 2014). The growth of polar cod in TL in Kongsfjorden was relatively constant at

Table 1 Functions describing the relationship between fish size (total length, TL; and weight, TW) and otolith size (length, OL; and weight, OW). Data pooled for males and females, and for Kongsfjord and Rijpfjorden ($n = 409$).

Function	r^2
TL = 1.215 + 2.3297*OL	0.947
TL = 6.0655 + 0.7883·OW – 0.0159·OW^2 + 0.0001·OW^3	0.916
TW = 2.8226–3.558·OL + 1.1062·OL^2	0.861
TW = –2.4734 + 1.4402·OW	0.935

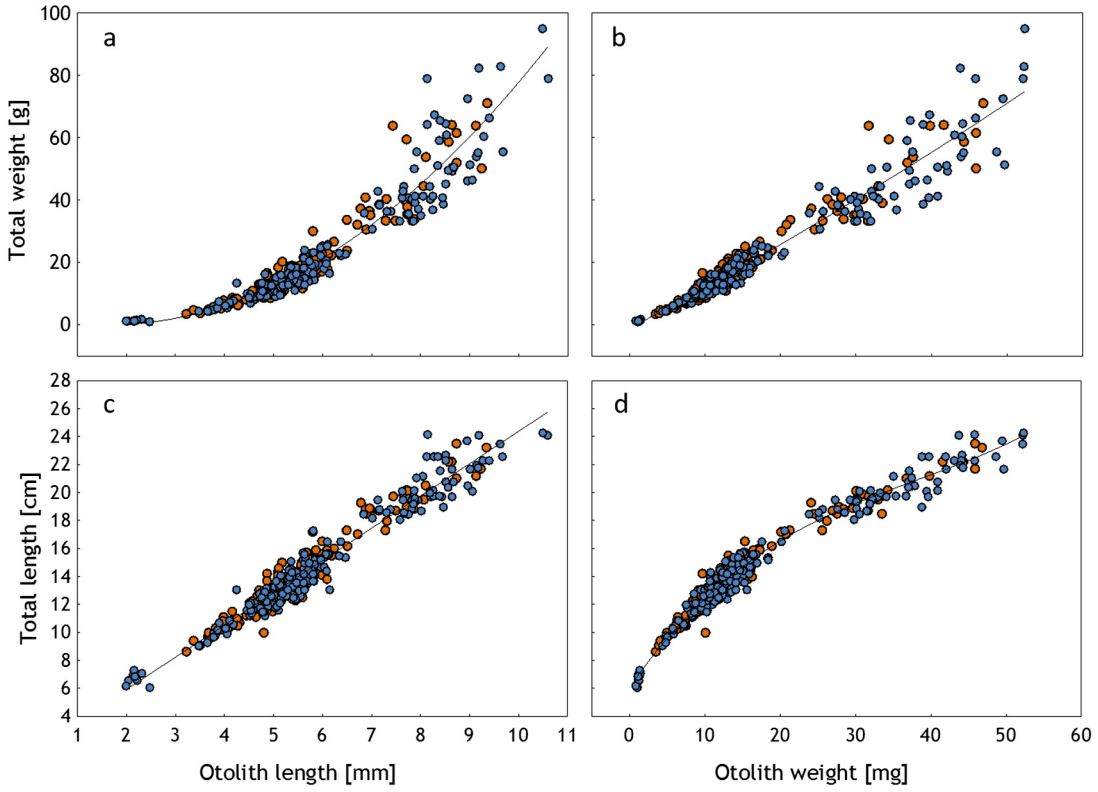

Figure 6 Relationship between: (a) total weight and otolith length, (b) total weight and otolith weight, (c) total length and otolith length, and (d) total length and otolith weight. Pooled data for males (orange points) and females (blue points) from Kongsfjorden and Rijpfjorden sites (n = 409). The formulas for these relationships are presented in Table 1. (For interpretation of the references to color in this figure legend, the reader is referred to the web version of this article.)

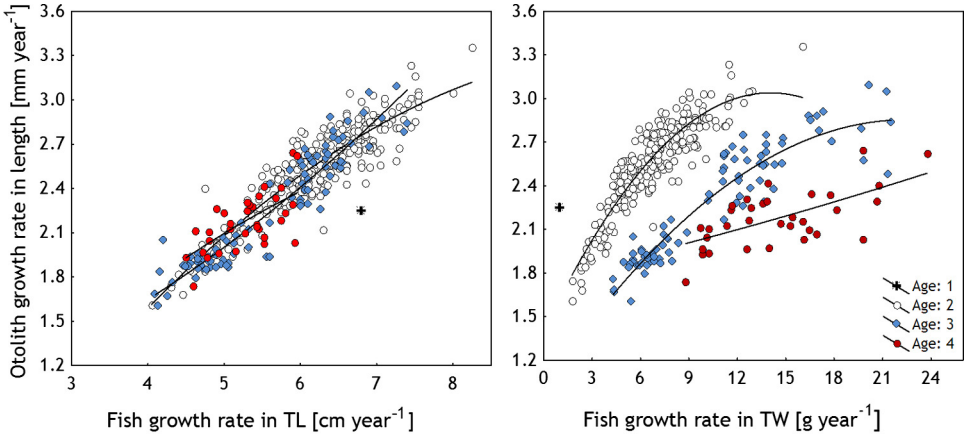

Figure 7 Relationships describing the dependence of otolith growth rates in length on fish growth rate in length (left panel) and weight (right panel) (n = 409 for both figures). The curves have no biological significance and were fitted just to exclude the potential age effect and to evaluate the significance of the relationships.

approximately 4.7 cm year^{-1} between years 1 and 4. The literature provides examples for polar cod of both relatively constant growth through the first four years of life (Nahrgang et al., 2014) and of slower growth after years 2 or 3 (Craig et al., 1982; Matley et al., 2013). To some extent this discrepancy could result from high variation in the reported size at age 4 since the number of fish of this age collected is usually low compared to the dominant age class 2 or even 3. This is why estimates for age 4 and higher are less accurate compared to those for younger age classes.

Generally, growth rate (size at age) variances related to geographical and latitudinal differences in the distribution of the fish analyzed are to be expected (Bain and Sekerak, 1978; Bradstreet et al., 1986). The growth rate of 4.7 cm year in

the current study was higher than that reported for the same age classes by Craig et al. (1982) for polar cod from Alaska and Matley et al. (2013) for polar cod from Canada, who found that 4-year-old fish were 18 cm and 18.2 cm FL, respectively, compared to 21.5 cm TL in the present study. Lønne and Gulliksen (1989) reported slower polar cod growth in the western Barents Sea of 11 cm TL at age 2 (no older fish were caught) compared to 13.5 cm noted in the current work. Falk-Petersen et al. (1986) reported results that are similar (13 cm) to ours for age 2 polar cod from Spitzbergen coastal waters.

In addition to large-scale geographical and latitudinal differences in sample origin, differences in environmental conditions within the same fjord can result in growth differences. The size at age data presented in the current work indicate significantly faster growth in polar cod from the glacial area compared to results presented for the same species from the same fjord, but which was collected in the entrance to the fjord (Nahrgang et al., 2014): for example, age 2: 13.5/13; age 3: 18/14 cm; age 4: 21.5/15 cm (present work/Nahrgang et al., 2014). On the one hand, distinct differences were noted in fish collected at the same time (September 2013) and based on a relatively numerous sample of fish (345 – our study and 199 – Nahrgang et al., 2014), so the results are reliable and provide evidence for growth differences within the fjord with faster growth in the subpopulation located in the direct glacial area. On the other hand, the strength of this finding is reduced by the fact that the fish were only collected in one season (September) and at one (Nahrgang et al., 2014) and two stations (present work).

In the present study, the comparison of the growth of fish from the two fjords sampled indicated that the fish collected in Kongsfjorden were larger at age in comparison to those from Rijpfjorden for both of the size parameters – TL and TW. However, the fish from Rijpfjorden represented only year classes 2 and 3, and their number was low (64) compared to the number of analyzed fish from Kongsfjorden (345). The results for Rijpfjorden should, therefore, be treated with more caution. Nahrgang et al. (2014) reported opposite results – faster growth in Rijpfjorden compared to Kongsfjorden, and their results for Rijpfjorden also are based on a relatively small sample size (97) that was collected at one station only. This disagreement clearly shows not only the need for more research presenting polar cod size-at-age data from different geographical areas, but also the importance of sampling strategy based on appropriate spatial and temporal scales. Any comparison based on small samples from one point in time and space is questionable, as it is in the comparison of Rijpfjorden to Kongsfjorden described above.

Otoliths found in the stomachs of predators, such as fish, birds, and seals, can be used to identify fish species and to determine their size (Dietrich et al., 2006; Jobling and Breiby, 1986; Wigley et al., 2003). The otolith size-fish size relationship, however, must be clearly described and take into consideration variables that can affect this relationship, such as, sex or population origin. In this work, neither the sex nor the sampling location had an effect on the relationships analyzed. Because both otolith length and weight provided good relationships, the two otolith size dimensions can be used in equations predicting fish TL and TW. The regression describing the relationship between polar cod length and their otolith length presented here is in agreement (linear character and almost identical otolith size at fish size) with regressions presented for this species by other authors (Christiansen et al., 2005; Frost and Lowry, 1981; Lidster et al., 1994). Otolith morphometrics were used successfully, for example, by Short et al. (2006) to separate small walleye pollock from Arctic cod in mixed samples. However, if otolith size measurements are to be used to determine the size of individual specimens found in the stomachs of consumers, it must be remembered that the rate of otolith dissolution is very fast and, for example, it can be as high as several percents in seal stomachs just within the first hour (Christiansen et al., 2005).

One of the most useful methods in fish biology for employing otolith size analysis is in the back-calculation of growth rates (Francis, 1990). In the present work on polar cod, a very significant relationship was determined between the growth rates of fish and otolith growth within each of the analyzed age classes. Similar verification was performed for other fish species, for example, the round goby (*Neogobius melanostomus*) (Sokołowska and Fey, 2011) and Atlantic menhaden (*Brevoortia tyrannus*) (Fey and Hare, 2012), but not for polar cod. The width of annual rings formed at a given age can be used as an indication of fish growth in corresponding years. Unfortunately, growth back-calculation is frequently performed for different species without verifying the relationship between somatic and otolith growth. The estimation of the fish size-otolith size model itself permits performing back-calculations, because otolith size generally increases with age (Thorrold and Hare, 2002). It does not, however, automatically indicate that the otolith growth rate is significantly correlated with the fish growth rate. Thorrold and Hare (2002) demonstrated that otolith and somatic size can be positively correlated even if the relationship between otolith and somatic growth is negative. Moreover, as previously evidenced, otolith growth might be related more to temperature than to somatic growth (Fey, 2005). The latter issue, however, is not of great importance for cod inhabiting Arctic waters. Therefore, data presented here supporting the fish growth-otolith growth relationship are very important, because they provide the basis for future studies that can benefit from otolith analysis.

In conclusion, the present work provided, in addition to some basic biological information (e.g., size frequency distribution, male/female ratio, and the fish size-weight relationship), growth rate data that indicate the presence of a fast-growing subpopulation (approximately 4.7 cm $year^{-1}$ between ages 1 and 4) located in the glacial area in one of the Spitzbergen fjords – Kongsfjorden. The results presented here on fish size at age, after comparing them with data available in the literature, indicate there is substantial variability in the growth rates reported for polar cod depending on both large-scale differences in geographical origin of the samples as well as small-scale differences at sampling locations within the fjord. The fact that most of the age-length data available in the literature are based on small sample sizes that were frequently obtained from one or two stations in a given geographical area underscores the need to improve sampling strategy in order to increase the value and strength of results. In addition to biological information, the existence of a significant somatic growth-otolith growth relationship was confirmed in polar cod, and no data of this kind have been available to date.

Acknowledgements

The study was supported by GAME (National Center for Science) and GLAERE (Norwegian funding mechanism) projects.

References

Bain, H., Sekerak, A.D., 1978. Aspects of the Biology of Arctic Cod (*Boreogadus saida*) in the Central Canadian Arctic. LGL Ltd., Ontario (for Polar Gas Project, Toronto), 104 pp. (unpubl. rept.).

Benoit, D., Simard, Y., Gagne, J., Geoffroy, M., Fortier, L., 2010. From polar night to midnight sun: photoperiod, seal predation, and the diel vertical migrations of polar cod (*Boreogadus saida*) under landfast ice in the Arctic Ocean. Polar Biol. 33 (11), 1505–1520, http://dx.doi.org/10.1007/s00300-010-0840-x.

Berge, J., Heggland, K., Lønne, O.J., Cottier, F., Hop, H., Gabrielsen, G.W., Nottestad, L., Misund, O.A., 2015. First records of Atlantic Mackerel (*Scomber scombrus*) from the Svalbard Archipelago, Norway, with possible explanations for the extension of its distribution. Arctic 68 (1), 4–61, http://dx.doi.org/10.14430/arctic4455.

Boehlert, G.W., 1985. Using objective criteria and multiple regression models for age determination in fishes. Fish. Bull. NOAA 83 (2), 103–117.

Bouchard, C., Fortier, L., 2008. Effects of polynyas on the hatching season, early growth and survival of polar cod *Boreogadus saida* in the Laptev Sea. Mar. Ecol. Prog. Ser. 355, 247–256.

Bouchard, C., Fortier, L., 2011. Circum-arctic comparison of the hatching season of polar cod *Boreogadus saida*: a test of the freshwater winter refuge hypothesis. Progr. Oceanogr. 90 (1–4), 105–116, http://dx.doi.org/10.1016/j.pocean.2011.02.008.

Bradstreet, M.S.W., Finley, K.J., Sekerak, A.D., Griffiths, W.B., Evans, C.R., Fabijan, M.F., Stallard, H.E., 1986. Aspects of the biology of Arctic cod (*Boreogadus saida*) and its importance in Arctic marine food chains. Can. Tech. Rep. Fish. Aquat. Sci. No. 1491 193 pp.

Christiansen, J.S., Gamst Moen, A.-G., Hansen, T.H., Nilssen, K.T., 2005. Digestion of capelin, *Mallotus villosus* (Müller), herring, *Clupea harengus* L., and polar cod *Boreogadus saida* (Lepechin), otoliths in a simulated seal stomach. ICES J. Mar. Sci. 62, 86–92, http://dx.doi.org/10.1016/j.icesjms.2004.06.022.

Christiansen, J.S., Hop, H., Nilssen, E.M., Joensen, J., 2012. Trophic ecology of sympatric Arctic gadoids, *Arctogadus glacialis* (Peters, 1872) and *Boreogadus saida* (Lepechin, 1774), in NE Greenland. Polar Biol. 35 (8), 1247–1257, http://dx.doi.org/10.1007/s00300-012-1170-y.

Craig, P.C., Griffiths, W.B., Haldorson, L., McElderry, H., 1982. Ecological studies of Arctic Cod (*Boreogadus saida*) in Beaufort Sea Coastal Waters, Alaska. Can. J. Fish. Aquat. Sci. 39 (3), 395–406, http://dx.doi.org/10.1139/f82-057.

Dietrich, J.P., Morrison, B.J., Hoyle, J.A., 2006. Alternative ecological pathways in the eastern Lake Ontario food web – round goby in the diet of Lake Trout. J. Great Lakes Res. 32 (2), 395–400, http://dx.doi.org/10.3394/0380-1330(2006)32[395:AEPITE]2.0.CO;2.

Falk-Petersen, I.B., Frivoll, V., Gulliksen, B., Haug, T., 1986. Occurrence and age/size relations of polar cod, *Boreogadus saida* (LEPECHIN), in Spitsbergen coastal waters. Sarsia 71 (3–4), 235–245, http://dx.doi.org/10.1080/00364827.1986.10419693.

Fey, D.P., 2005. Is the marginal otolith increment width a reliable recent growth index for larval and juvenile herring? J. Fish Biol. 66 (6), 1692–1703, http://dx.doi.org/10.1111/j.0022-1112.2005.00716.x.

Fey, D.P., Hare, J.A., 2012. Temperature and somatic growth effects on otolith growth of larval Atlantic menhaden, *Brevoortia tyrannus* (Actinopterygii: Clupeiformes: Clupeidae). Acta Ichthyol. Piscat. 42 (3), 215–222, http://dx.doi.org/10.3750/AIP2011.42.3.05.

Fey, D.P., Linkowski, T.B., 2006. Predicting juvenile Baltic cod (*Gadus morhua*) age from body and otolith size measurements. ICES J. Mar. Sci. 63 (6), 1045–1052, http://dx.doi.org/10.1016/j.icesjms.2006.03.019.

Fossheim, M., Primicerio, R., Johannesen, E., Ingvaldsen, R.B., Aschan, M.M., Dolgov, A.V., 2015. Recent warming leads to a rapid borealization of fish communities in the Arctic. Nat. Clim. Change 5, 673–677, http://dx.doi.org/10.1038/NCLIMATE2647.

Francis, R.I.C., 1990. Back-calculation of fish length: a critical review. J. Fish Biol. 36 (6), 883–902, http://dx.doi.org/10.1111/j.1095-8649.1990.tb05636.x.

Fritts, A.L., Pearsons, T.N., 2006. Effects of predation by non-native smallmouth bass on native salmonid prey: the role of predator and prey size. Trans. Am. Fish. Soc. 135 (4), 853–860, http://dx.doi.org/10.1577/T05-014.1.

Frost, K.J., Lowry, L.F., 1981. Trophic importance of some marine gadoids in Northern Alaska and their body-otolith size relationships. Fish. Bull. U.S. 79 (1), 187–192.

Geoffroy, M., Majewski, A., LeBlanc, M., Gauthier, S., Walkusz, W., Reist, J.D., Fortier, L., 2016. Vertical segregation of age-0 and age-1þ polar cod (*Boreogadus saida*) over the annual cycle in the Canadian Beaufort Sea. Polar Biol. 39 (6), 1023–1037, http://dx.doi.org/10.1007/s00300-015-1811-z.

Geoffroy, M., Robert, D., Darnis, G., Fortier, L., 2011. The aggregation of polar cod (*Boreogadus saida*) in the deep Atlantic layer of ice-covered Amundsen Gulf (Beaufort Sea) in winter. Polar Biol. 34 (12), 1959–1971, http://dx.doi.org/10.1007/s00300-011-1019-9.

Hedeholm, R., Gronkjaer, P., Rysgaard, S., 2012. Feeding ecology of capelin (*Mallotus villosus* Muller) in West Greenland waters. Polar Biol. 35 (10), 1533–1543, http://dx.doi.org/10.1007/s00300-012-1193-4.

Hop, H., Gjøsæter, H., 2013. Polar cod (*Boreogadus saida*) and capelin (*Mallotus villosus*) as key species in marine food webs of the Arctic and the Barents Sea. Mar. Biol. Res. 9 (9), 878–894, http://dx.doi.org/10.1080/17451000.2013.775458.

Hop, H., Welch, H., Crawford, R., 1997. Population structure and feeding ecology of Arctic cod schools in the Canadian High Arctic. In: Reynolds, J. (Ed.), Fish Ecology in Arctic North America. Am. Fisheries Soc., Bethesda, MD, 68–79.

Haug, T., Bogstad, B., Chierici, M., Gjøsæter, H., Hallfredsson, E.H., Høines, Å.S., Hoel, A.H., Ingvaldsen, R.B., Jørgensen, L.L., Knutsen, T., Loeng, H., Naustvoll, L.J., Røttingen, I., Sunnanå, K., 2017. Future harvest of living resources in the Arctic Ocean north of the Nordic and Barents Seas: a review of possibilities and constraints. Fish Res. 188, 38–57, http://dx.doi.org/10.1016/j.fishres.2016.12.002.

Jobling, M., Breiby, A., 1986. The use and abuse of fish otoliths in studies of feeding habits of marine piscivores. Sarsia 71 (3–4), 265–274, http://dx.doi.org/10.1080/00364827.1986.10419696.

Lønne, O.J., Gulliksen, B., 1989. Size, age and diet of polar cod, *Boreogadus saida* (Lepechin 1773), in ice covered waters. Polar Biol. 9 (3), 187–191, http://dx.doi.org/10.1007/BF00297174.

Lidster, W.W., Lilly, G.R., Dawe, E.G., 1994. Otoliths of arctic cod (*Boreogadus saida*), small atlantic cod (*Gadus morhua*), and three other fish species from Newfoundland waters: description and relationship of body length to otolith length. J. Northw. Atl. Fish. Sci. 16, 33–40.

Matley, J.K., Fisk, A.T., Dick, T.A., 2013. The foraging ecology of Arctic cod (*Boreogadus saida*) during open water (July–August) in Allen Bay, Arctic Canada. Mar. Biol. 160 (11), 2993–3004, http://dx.doi.org/10.1007/s00227-013-2289-2.

Misund, O.A., Heggland, K., Skogseth, R., Falck, E., Gjøsæter, H., Sundet, J., Watne, J., Lønne, O.J., 2016. Norwegian fisheries in the Svalbard zone since 1980. Regulations, profitability and warming waters affect landings. Polar Sci. 10 (3), 312–322, http://dx.doi.org/10.1016/j.polar.2016.02.001.

Nahrgang, J., Varpe, Ø., Korshunova, E., Murzina, S., Hallanger, I.G., Vieweg, I., Berge, J., 2014. Gender specific reproductive strategies of an arctic key species (*Boreogadus saida*) and implications of climate change. PLOS ONE 9 (5), e98452, http://dx.doi.org/10.1371/journal.pone.0098452.

Renaud, P.E., Berge, J., Varpe, Ø., Lønne, O.J., Nahrgang, J., Ottesen, C., Hallanger, I., 2012. Is the poleward expansion by Atlantic cod and haddock threatening native polar cod, *Boreogadus saida*? Polar Biol. 35 (3), 401–412, http://dx.doi.org/10.1007/s00300-011-1085-z.

Short, J.A., Gburski, C.M., Kimura, D.K., 2006. Using otolith morphometrics to separate small Wallaye Pollock *Theragra chalcogramma* from Arctic Cod *Boreogadus saida* in mixed samples. Alaska Fish. Res. Bull. 12 (1), 147–152.

Sokołowska, E., Fey, D.P., 2011. Age and growth of round goby *Neogobius melanostomus* in the Gulf of Gdańsk 16 years after invasion: can the Baltic Sea be a new promised land? J. Fish Biol. 78 (7), 1993–2009, http://dx.doi.org/10.1111/j.1095-8649.2011.02986.x.

Szczucka, J., Hoppe, Ł., Schmidt, B., Fey, D.P., 2017. Acoustical estimation of fish distribution and abundance in two Spitsbergen fjords. Oceanologia 59 (4), 585–591, http://dx.doi.org/10.1016/j.oceano.2017.04.007.

Takasuka, A., Oozeki, Y., Kimura, R., Kubota, H., Aoki, I., 2004. Growth-selective predation hypothesis 1 revisited for anchovy larvae in offshore waters: cannibalism by juveniles 2 versus predation by skipjack tunas. Mar. Ecol.-Prog. Ser. 278, 297–302, http://dx.doi.org/10.3354/meps278297.

Thorrold, S.R., Hare, J.A., 2002. Application of otoliths to the study of coral reef fishes. In: Sale, P.F. (Ed.), Ecology of Coral Reef Fishes. Academic Press, San Diego, CA, 243–264.

Walkusz, W., Kwasniewski, S., Falk-Petersen, S., Hop, H., Tverberg, V., Wieczorek, P., Weslawski, J.M., 2009. Seasonal and spatial changes in the zooplankton community of Kongsfjorden, Svalbard. Polar Res. 28 (2), 254–281, http://dx.doi.org/10.1111/j.1751-8369.2009.00107.x.

Wallace, M.I., Cottier, F.R., Berge, J., Tarling, G.A., Griffiths, C., Brierley, A.S., 2010. Comparison of zooplankton vertical migration in an ice-free and a seasonally ice-covered Arctic fjord: an insight into the influence of sea ice cover on zooplankton behavior. Limnol. Oceanogr. 55 (2), 831–845, http://dx.doi.org/10.4319/lo.2010.55.2.0831.

Wigley, S.E., McBride, H.M., McHugh, N.J., 2003. Length-Weight Relationships for 74 Fish Species Collected during NEFSC Research Vessel Bottom Trawl Surveys, 1992–99. NOAA Tech.l Memo. NMFS NE 171, 26 pp.

Oceanologia (2017) 59, 585—591

Available online at www.sciencedirect.com

ScienceDirect

journal homepage: www.journals.elsevier.com/oceanologia/

ORIGINAL RESEARCH ARTICLE

Acoustical estimation of fish distribution and abundance in two Spitsbergen fjords

Joanna Szczucka [a,*], Łukasz Hoppe [a], Beata Schmidt [b], Dariusz P. Fey [b]

[a] *Institute of Oceanology, Polish Academy of Sciences, Sopot, Poland*
[b] *National Marine Fisheries Research Institute, Gdynia, Poland*

Received 13 July 2016; accepted 11 April 2017
Available online 28 May 2017

KEYWORDS
Arctic fish;
Multifrequency acoustics;
West Spitsbergen

Summary Over recent decades, the Arctic region has been subjected to rapid climate change stemming from global warming. The advance of Atlantic waters to high latitudes is notable. The increased abundance of fish, such as cod (*Gadus morhua*) and haddock (*Melanogrammus aeglefinus*), has been reported near the western coast of Spitsbergen and entering fjords together with Atlantic waters. This study used multifrequency acoustics to measure fish distribution and abundance in 2013—2014 in two Arctic fjords, the colder Hornsund, which is typically of Arctic character, and the warmer Kongsfjorden, which is more of Atlantic character. The study revealed a bimodal fish size distribution with larger fish in the deep parts of fjords, and smaller fish distributed in more shallow waters. An evident increase in the abundance of large fish, most probably Atlantic cod, was observed in Hornsund and especially in Kongsfjorden in 2014 in comparison to 2013. The intense inflow of Atlantic water on the shelf in 2014 is suggested as the explanation for this phenomenon.

1. Introduction

Over recent decades, the Arctic region has been subjected to rapid climate change stemming from global warming. Temperature increases have caused decreases in sea ice cover extent and duration (Barber et al., 2015; Falk-Petersen et al., 2015). The warmer Atlantic waters of the West Spitsbergen Current have shifted northward (Walczowski et al., 2012; Walczowski, 2014). Consequently, there has been a shift in ecological zones. The occurrence of increased

* Corresponding author at: Institute of Oceanology, Polish Academy of Sciences, Powstańców Warszawy 55, 81-712 Sopot, Poland. Tel.: +48 587311824; fax: +48 585512130.
E-mail address: szczucka@iopan.gda.pl (J. Szczucka).
Peer review under the responsibility of Institute of Oceanology of the Polish Academy of Sciences.

Production and hosting by Elsevier

http://dx.doi.org/10.1016/j.oceano.2017.04.007

abundance of fish such as cod (*Gadus morhua*) and haddock (*Melanogrammus aeglefinus*) (Eriksen et al., 2015; Renaud et al., 2012), and most recently Atlantic mackerel (*Scomber scombrus*) (Berge et al., 2015), have been reported near the western coast of Spitsbergen and in fjords. Furthermore, sub-Arctic species such as capelin (*Mollotus villosus*) have extend their distribution further north in warm years (Hop and Gjøsæter, 2013). The increasing temperature in Svalbard fjords supports the survival of fish species that are not typically Arctic during the winter and provides better feeding conditions during summer and autumn. Fossheim et al. (2015) and Haug et al. (2017) recently documented the rapid northward shift in the distribution of boreal fish communities in the Barents Sea because of warming, and concluded that climate warming is inducing structural change over large spatial scales at high latitudes leading to a borealization of fish communities in the Arctic. Similar conclusions can be drawn from a publication by Misund et al. (2016) who analyzed detailed data on fisheries activity in the Svalbard zone since 1980 to show how fisheries for different species have developed as the Arctic ice sheet retreats and new waters open up for boreal fish species. The results clearly indicate a northward trend in landings of many fish species. All of these changes in hydrological conditions and fish community structure are expected to have significant consequences, mostly stemming from increased risk of predation and food competition, for typically Arctic species like the polar cod (*Boreogadus saida*) (Benoit et al., 2014; Berge et al., 2015; Christiansen et al., 2012; Geoffroy et al., 2011; Hop and Gjøsæter, 2013; Renaud et al., 2012).

This study focused on fish as a key component of the marine ecosystem. Fish distribution and abundance were measured in two hydrologically different Arctic fjords, the colder Hornsund and the warmer Kongsfjorden. The main measurement tool was acoustics (3-frequency echo sounder) supported by net catches.

2. Study area

This study was conducted in two West Spitsbergen fjords, Hornsund and Kongsfjorden, during cruises of r/v *Oceania* in the summer seasons of 2013 and 2014, as a part of the GAME (Growing of the Arctic Marine Ecosystem) project. Spitsbergen is the largest island of the Svalbard archipelago located north of Norway. The area is influenced by two water masses. Hornsund is regarded as a cold fjord, under the influence of the South Cape Current, while Kongsfjorden is influenced by warmer Atlantic waters carried by the West Spitsbergen Current. The area of Hornsund is 275 km^2, its volume is 25.7 km^3, and its maximum depth is 260 m. The area of Kongsfjorden is 209 km^2, its volume is 40.5 km^3, and its maximum depth is 394 m. In addition to differences in temperature, significant differences in fish prey species composition and size structure (Węsławski et al., 2006) are also observed between Hornsund and Kongsfjorden.

3. Material and methods

3.1. Survey design

Since Arctic expeditions are multidisciplinary, their scientific programs are very extensive and time-consuming, which means that the time planned for specific tasks is severely limited. The typical acoustic survey design for fish distribution and abundance estimation (e.g., systematic zig-zag) could not, therefore, be implemented, and it was necessary to reduce the cruise track to a few sections. Acoustic surveys were carried out together with continuous CTD measurements. The main transect was planned along the fjord axis extending from the mouth of the fjord to the easternmost glacier, with two or three additional transverse transects (Fig. 1a and b). A total of 66.7 nautical miles of acoustic transects were sampled in Hornsund (40.6 nmi in 2013 and 26.1 nmi in 2014), while in Kongsfjorden the measurements covered 53.7 nmi (27 nmi in 2013 and 26.7 nmi in 2014).

The technical specifications of concurrent CTD and acoustic surveys limited the ship speed to 3–4 knots. The speed was further reduced to 1–2 knots when ice floes appeared in the fjords.

3.2. Data acquisition

Acoustic data were collected with a Simrad EK60 split-beam echo sounder operating at frequencies of 70, 120, and 200 kHz, and all three transducers with 7 degrees beam angle at −3 dB. Acoustic transducers were mounted on a rigid frame attached to the broadside of the vessel, approximately 1 m below the sea surface. All three echo sounders used a 256 μs pulse length, with 525, 200, and 120 W of power, respectively. The ping rate was set to 2 s^{-1} and pulse transmission was synchronized for each transmitter. Calibration was performed before the first season (2013) using the standard target method (Foote et al., 1987). Acoustic signals were collected with dedicated Simrad ER60 software and stored digitally in raw format for later analysis in Echoview and Matlab.

Fish were collected at two stations in Kongsfjorden (at depths of 134 m and 52 m) between September 29 and October 4, 2013 during a cruise of the r/v *Helmer Hanssen* using a bottom Campelen 1800 shrimp trawl (Fey and Węsławski, in this issue). The horizontal and vertical openings were 17 m and 4–5 m, respectively, and the door spread was about 45–50 m. The mesh size was 80 mm in the front and 22 mm in the cod end. The gear was towed at the bottom for approximately 10–15 min, at 3 knots. More than 600 specimens of polar cod in the size range 6.1–24.3 cm and several individuals of other small pelagic species were measured (±1 cm) and weighed (±1 g). The only fish collected in Hornsund were small demersal species and larvae caught in a Tucker Trawl and several epibenthic sledge hauls in August 2015.

3.3. Data pre-processing

Acoustic data were pre-processed in Echoview software (Sonardata Pty Ltd.), which automatically delivered the values of S_V (volume backscattering strength) integrated into selected cells (distance by depth). Fish biomass calculations were based on 70 and 120 kHz records, while 200 kHz echoes were contaminated by the interfering ADCP signals and had to be neglected. Multi-frequency analysis required all frequency data to be unbiased from any noise (Korneliussen, 2000). A special algorithm for noise removal was developed

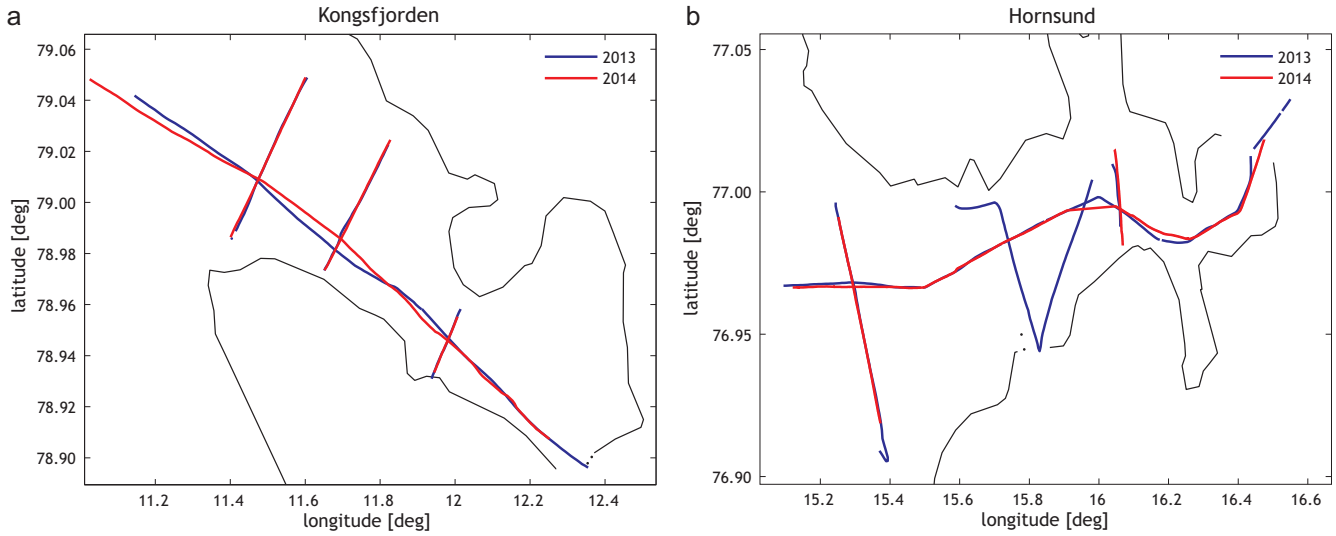

Figure 1 Acoustic transects in West Spitsbergen fjords: (a) Kongsfjorden (north) and (b) Hornsund (south).

and applied. To remove spike noise, the samples in each ping were compared to the same-range samples in the previous and following pings. If the ping-to-ping difference was greater than 10 dB, the value of the sample was replaced with the value of the previous sample. The threshold of 10 dB was determined after visual inspection of echograms before and after spike removal. "Second bottom reflections" were removed. Finally, the difference between volume backscattering strength recorded at 120 and 70 kHz, $S_{V,120} - S_{V,70}$, was used to discern fish from other scatterers, mainly zooplankton. Based on the fact that in the range of 70–120 kHz fish with swim bladder scatter more sound at a lower frequency than at a higher one (Pedersen and Korneliussen, 2009) and that scattering on zooplankton shows a reverse tendency, all the samples with the difference $S_{V,120} - S_{V,70} > 0$ were classified as "no fish" and were removed from the 70 kHz echogram.

The effectiveness of the algorithm for removing noise and zooplankton contributions was tested by calculating the differences in ΔS_V between backscattering strength before and after correction. This was performed at 0.1 nmi intervals for all longitudinal and transverse transects in both fjords and seasons. An example is presented in Fig. 2 showing the histogram of ΔS_V for Kongsfjorden in the 2014 season. The median of this distribution is 1.69 dB. Considerably higher median values of ΔS_V were obtained for the three other

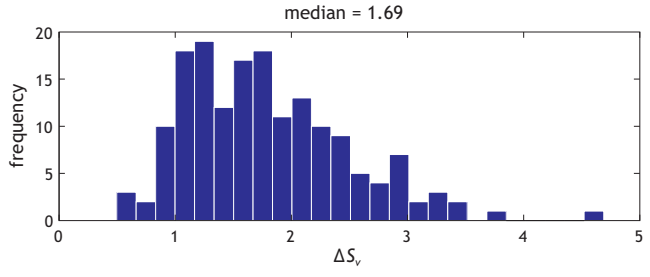

Figure 2 Histogram of differences between raw and corrected values of backscattering strength $S_{V,0} - S_{V,1}$ obtained in Kongsfjorden in 2014.

cases: 6.37 for Kongsfjorden'2013, 3.79 for Hornsund'2013, and 2.76 for Hornsund'2014. This was probably the result of the more serious contamination (mainly electrical) of the echo signals obtained.

3.4. Computational algorithms for fish abundance, biomass concentration, total fish biomass

The volume backscattering strength is the logarithmic measure of the volume backscattering coefficient. They are related as follows (Medwin and Clay, 1998):

$$\langle S_V \rangle = 10 \log \langle s_V \rangle. \tag{1}$$

In the case of bimodal fish size distribution, the backscattering coefficient can be expressed as (Simmonds and MacLennan, 2005):

$$s_V = s_{V,1} + s_{V,2} = (f_1 + f_2) s_V, \tag{2}$$

where f_1 and f_2 – weighting coefficients; $f_1 + f_2 = 1$ and numerical concentration of the ith fish size class (Nakken and Dommasnes, 1977):

$$N_{fish,i} = \frac{\langle s_{V,1} \rangle}{\langle \sigma_{bs,i} \rangle} = f_i \frac{\langle s_V \rangle}{\langle \sigma_{bs,i} \rangle}, \tag{3}$$

where σ_{bs} is the backscattering cross section of individual fish.

Biomass concentration estimates were derived by multiplying numerical concentration by the mean weight of acoustically detected fish of the ith size class:

$$M_i = N_{fish,i} W_i. \tag{4}$$

The weight-length dependence for fish was adopted as:

$$W(L) = AL^B, \tag{5}$$

where W is fish weight in g, L is fish length in cm. $A = 0.008$, $B = 3.05$ for Atlantic cod was taken from the literature (Wigley et al., 2003). These values for polar cod were based on our own trawl catch and were calculated with linear

regression at $A = 0.005$, $B = 3.04$, $R = 0.98$. The length of the analyzed fish was in the range of 6.1–24.3 cm.

Calculating fish target strength *TS* was done with Echoview single echo detection and the fish tracking tool. The fish tracking criteria were as follows: minimum number of single targets in a track – 3; minimum number of pings in track – 3; maximum gap between single targets – 2. This delivered the *TS* distribution, and its depth dependence. When there was bimodal *TS* distribution, weighting coefficients f_1 and f_2 (expression (2)) were determined.

The fish target strength dependence on fish length was adopted as:

$$TS(L) = m\log(L) + b, \tag{6}$$

where L is fish length in cm, $m = 21.8$, $b = -72.7$ dB for polar cod (Benoit et al., 2008) and $m = 20$, $b = -68.9$ dB for Atlantic cod (Simmonds and MacLennan, 2005), which were the two most abundant species occurring in the study area.

Because target strength is equivalent to fish length, the size of individuals or the dominant size of the fish could be determined.

The fish biomass for each integration interval was determined using the relationship between the weight of fish and its length (5) and between *TS* and fish length (6).

Volume backscattering strength values S_V extracted from the cleaned 70 kHz data, integrated horizontally over 0.5 nmi and vertically by 5 m depth layers, were used to visualize the depth distribution of fish biomass along each transect.

S_V values obtained for the entire water column were integrated horizontally over 0.1 nmi to determine fish concentration, abundance, and total biomass. Sampled volume was also calculated in each interval, so the product of biomass concentration and sampled volume resulted in the total mass of fish. Finally, the sum of biomass calculated for all transects of the fjord and the knowledge of the total fjord volume permitted approximating the total tonnage of fish in the fjord.

4. Results and discussion

Target strength distribution determined for each fjord and each year using the fish tracking tool combined with target strength dependence on fish length permitted finding the dominant fish size in any specific situation. In the first research season (2013), in Hornsund, unimodal *TS* distribution was obtained (Fig. 3a), while in Kongsfjorden analogous distribution was bimodal, with a relatively high number of small fish in comparison to large ones (Fig. 4a).

Hornsund was dominated by fish with a *TS* mean = –54.12 dB (fish length ≅ 7.1 cm) occurring to a depth of 200 m (Fig. 3b). In Kongsfjorden, the *TS* mean of small fish = –54.87 dB, which corresponded to a $L \cong 6.6$ cm, while the *TS* mean for large fish = –32.89 dB, which corresponded to $L = 80$ cm. Small fish, most likely polar cod, with $TS < -45$ dB, occurred in shallow layers to a depth of 200 m, while large Atlantic cod with $TS > -40$ dB occupied the lower part of the water column below 200 m.

This situation changed radically in summer 2014, when very large Atlantic cod with $TS > -40$ dB (up to 1 m in length) appeared in Hornsund (Fig. 5a), and the proportions of the *TS*

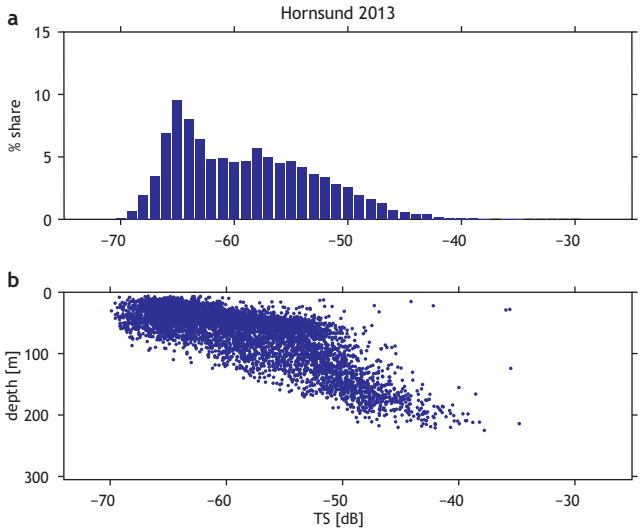

Figure 3 (a) *TS* distribution obtained for Hornsund in 2013. (b) Depth distribution of *TS* values measured in Hornsund in 2013.

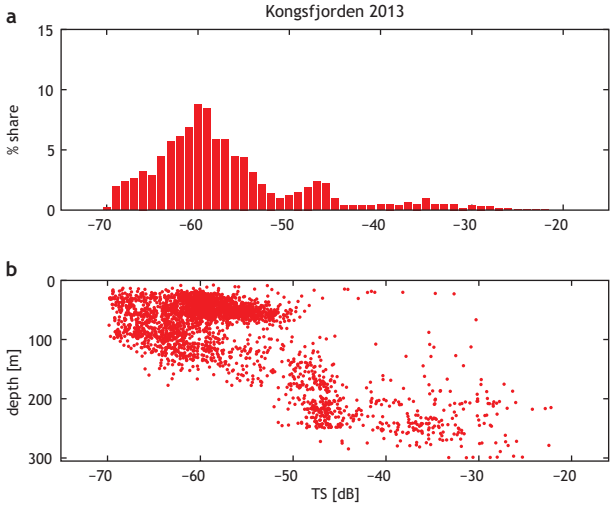

Figure 4 (a) *TS* distribution obtained for Kongsfjorden in 2013. (b) Depth distribution of *TS* values measured in Kongsfjorden in 2013.

bimodal distribution in Kongsfjorden changed with large fish predominating in number over small ones (Fig. 6a). Large fish also appeared in more shallow water than they had a year earlier (Fig. 6b).

Generally, except for the first season (2013) with hardly any large fish in Hornsund, bimodal *TS* distributions were the most common, with distinct local maximums of small and large fish.

The mean values of *TS* for one or both modes are presented in Table 1. They were used in fish abundance computations (formulae 2 and 3).

Because of fish mobility, we decided to apply the general *TS* distribution, which was universal for the entire fjord in each season, in the final computations instead of separate *TS* distributions for individual transects.

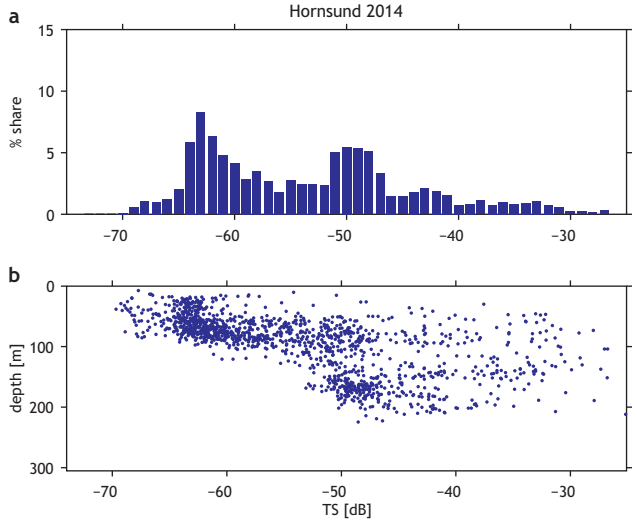

Figure 5 (a) *TS* distribution obtained for Hornsund in 2014. (b) Depth distribution of *TS* values measured in Hornsund in 2014.

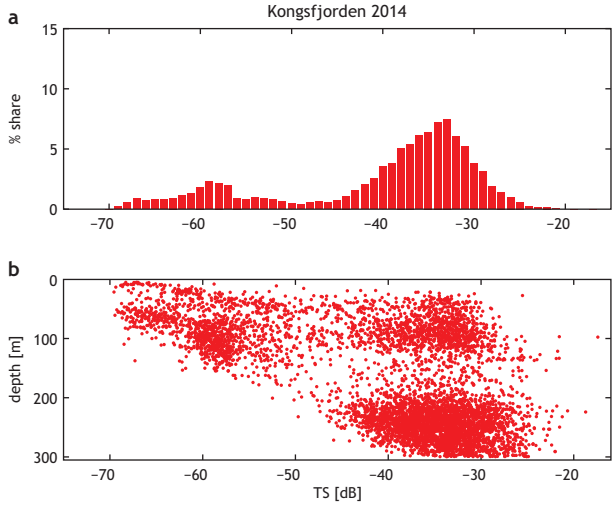

Figure 6 (a) *TS* distribution obtained for Kongsfjorden in 2014. (b) Depth distribution of *TS* values measured in Kongsfjorden in 2014.

Fig. 7a presents an example of fish biomass distribution in the external transverse transect of Kongsfjorden in 2014. The maximum biomass is concentrated in the deep water of the fjord, and a distinct fish layer exists at a depth of 100 m. The dependence of fish target strength on depth for the same transect is presented in Fig. 7b. Deep-water fish are probably large Atlantic cod grazing close to the bottom. Comparisons with trawl catch data indicate that the small fish are mainly polar cod with an admixture of capelin, while the large fish are Atlantic cod with an admixture of haddock.

TS means calculated for the individual modes can be attributed to the dominant size of fish in clusters. According to formula (6), small fish *TS* values correspond to a fish length of 7–8 cm. Minimum *TS* values (−70 dB) correspond to a fish length of 1 cm. The polar cod in the current study measured to determine the relationship *TS*(*L*) were caught in September 2013, and they were all longer than 6.1 cm. Nevertheless, during the polar expedition of 2015, polar cods as short as 13–23 mm were caught in the upper 20 m water layer.

The combination of acoustic methods and net-captured fish analysis suggests that the dominant species observed during this study was polar cod. Although significant differences in polar cod vertical distribution can occur depending on time of year, area, and environmental conditions such as food availability, the presence of predators, or light intensity (Benoit et al., 2010), the general pattern of smaller specimens occurring in shallow waters and large ones distributed in deeper layers is the most common for this species (Benoit et al., 2010, 2014; Falk-Petersen et al., 1986). This pattern of size-dependent vertical distribution was found in the present work in both 2013 and 2014. However, fish size differences among different depths are related not only to the behaviour (e.g., migrations) of polar cod, the most common species in Svalbard fjords, but also to the presence of other species in the same water masses. The large fish measuring up to 1 m observed in the present research must have been Atlantic cod. Although its presence in Svalbard fjords is not surprising (Renaud et al., 2012), especially in Kongsfjorden which is under strong Atlantic water influence, this is still not an ordinary situation.

The total fish biomass estimated for 2014 was 35 tonnes in Hornsund and 241 tonnes in Kongsfjorden, and the fish density was 1.4×10^{-3} g m^{-3} and 6×10^{-3} g m^{-3}, respectively. The abundance of Atlantic cod in Spitsbergen fjords in 2014 compared to that in 2013 was related to the intense influx of Atlantic water on the shelf in that year. The water temperature in both fjords was higher than the long-term average (2001–2015) by almost 1.5 degrees, and Atlantic water had the greatest reach in this period. It filled almost the entire water column in Kongsfjorden, from 20 m down to 250 m (Promińska et al., 2017). The northward expansion of the distribution of large predatory species such as Atlantic cod is a consequence of the warming observed in the Arctic

Table 1 Weighting coefficients *f* and mean *TS* for small and large fish in both fjords in both years.

Area/year	Small fish		Large fish	
	f_1	TS_1	f_2	TS_2
Hornsund'2013	1	−54.12	0	
Hornsund'2014	0.823	−52.66	0.177	−35.69
Kongsfjorden'2013	0.914	−54.87	0.086	−32.89
Kongsfjorden'2014	0.237	−53.79	0.763	−32.51

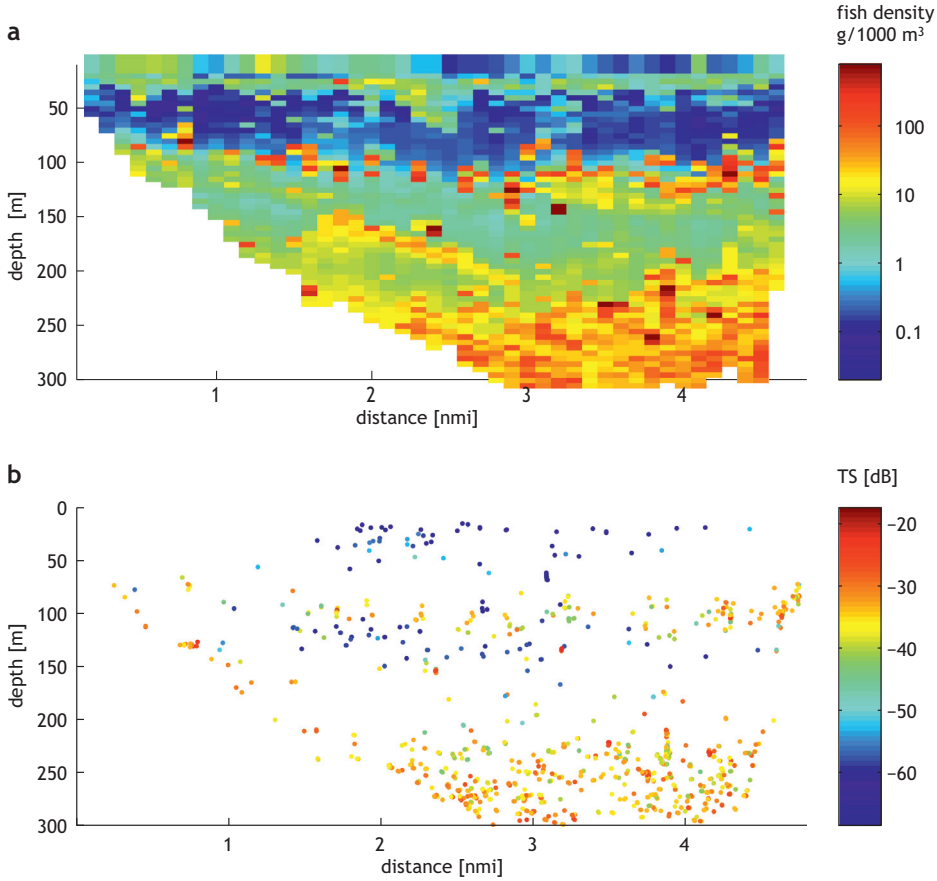

Figure 7 (a) Fish biomass along the external transverse transect of Kongsfjorden in 2014. S_V integrated horizontally over 0.5 nmi and vertically by 5 m depths. (b) Fish target strength vs depth for the same transect.

that is leading to structural changes in and the borealization of fish communities (Fossheim et al., 2015). The consequences of these changes are difficult to predict because of the complexity of the processes such as increasing food competition and predation (Hop and Gjøsæter, 2013; Renaud et al., 2012) among typical Arctic species like polar cod and incoming species like Atlantic cod, haddock, mackerel, and capelin. The intensity and mechanisms of competition and predation will vary significantly not only among fjords, but also at different times of the year. It should be remembered that these mechanisms also involve higher level predators such as birds and mammals, and polar cod is an important, valuable food source in this food chain component (Crawford and Jorgenson, 1996; Harter et al., 2013; Weslawski et al., 1994).

To sum up, the results presented here provide another example of size-related differences in the vertical distribution of polar cod, and the northern migration of typical Atlantic species such as Atlantic cod into Svalbard fjords as a consequence of environmental warming and the inflow of warm Atlantic waters into fjords.

Acknowledgements

This work was supported by the GAME project of the National Science Centre no. DEC-2012/04/A/NZ8/00661 and the GLAERE project of the Norwegian Funding Mechanism no. DZP/POL-Nor/1876/2013.

References

Barber, D.G., Hop, H., Mundy, C.J., Else, B., Dmitrenko, I.A., Tremblay, J.E., Ehn, J.K., Assmy, P., Daase, M., Candlish, L.M., Rysgaard, S., 2015. Selected physical, biological and biogeochemical implications of a rapidly changing Arctic Marginal Ice Zone. Prog. Oceanogr. 139, 122—150, http://dx.doi.org/10.1016/j.pocean.2015.09.003.

Benoit, D., Simard, Y., Fortier, L., 2008. Hydroacoustic detection of large winter aggregations of Arctic cod (*Boreogadus saida*) at depth in ice-covered Franklin Bay (Beaufort Sea). J. Geophys. Res. 113 (6), 1—9, http://dx.doi.org/10.1029/2007JC004276.

Benoit, D., Simard, Y., Fortier, L., 2014. Pre-winter distribution and habitat characteristics of polar cod (*Boreogadus saida*) in southeastern Beaufort Sea. Polar Biol. 37 (2), 149—163, http://dx.doi.org/10.1007/s00300-013-1419-0.

Benoit, D., Simard, Y., Gagne, J., Geoffroy, M., Fortier, L., 2010. From polar night to midnight sun: photoperiod, seal predation, and the diel vertical migrations of polar cod (*Boreogadus saida*) under landfast ice in the Arctic Ocean. Polar Biol. 33 (11), 1505—1520, http://dx.doi.org/10.1007/s00300-010-0840-x.

Berge, J., Heggland, K., Lønne, O.J., Cottier, F., Hop, H., Gabrielsen, G.W., Nottestad, L., Misund, O.A., 2015. First records of Atlantic Mackerel (*Scomber scombrus*) from the Svalbard Archipelago, Norway, with possible explanations for the extension of its distribution. Arctic 68 (1), 4—61, http://dx.doi.org/10.14430/arctic4455.

Christiansen, J.S., Hop, H., Nilssen, E.M., Joensen, J., 2012. Trophic ecology of sympatric Arctic gadoids, *Arctogadus glacialis* (Peters, 1872) and *Boreogadus saida* (Lepechin, 1774), in NE Greenland.

Polar Biol. 35 (8), 1247—1257, http://dx.doi.org/10.1007/s00300-012-1170-y.

Crawford, R.E., Jorgenson, J.K., 1996. Quantitative studies of Arctic Cod (*Boreogadus saida*) schools: important energy stores in the arctic food web. Arctic 49 (2), 181—193, http://dx.doi.org/10.14430/arctic1196.

Eriksen, E., Ingvaldsen, R.B., Nedreaas, K., Prozorkevich, D., 2015. The effect of recent warming on polar cod and beaked redfish juveniles in the Barents Sea. Reg. Stud. Mar. Sci. 2, 105—112.

Falk-Petersen, I.B., Frivoll, V., Gulliksen, B., Haug, T., 1986. Occurrence and size/age relations of polar cod, *Boreogadus saida* (Lepechin), in Spitsbergen coastal waters. Sarsia 71 (3—4), 235—245, http://dx.doi.org/10.1080/00364827.1986.10419693.

Falk-Petersen, S., Pavlov, V., Berge, J., Cottier, F., Kovacs, K.M., Lydersen, Ch., 2015. At the rainbow's end: high productivity fueled by winter upwelling along an Arctic shelf. Polar Biol. 38 (1), 5—11, http://dx.doi.org/10.1007/s00300-014-1482-1.

Fey, D.P., Węsławski, J.M., 2017. Age, growth rate, and otolith growth of polar cod (*Boreogadus saida*) in two fjords of Svalbard, Kongsfjorden and Rijpfjorden. Oceanologia 59 (4), 576—584, http://dx.doi.org/10.1016/j.oceano.2017.03.011.

Foote, K.G., Knudsen, H.P., Vestnes, G., MacLennan, D.N., Simmonds, E.J., 1987. Calibration of Acoustic Instruments for Fish Density Estimation: A Practical Guide. ICES Coop. Res. Rep., 144, 69 pp.

Fossheim, M., Primicerio, R., Johannesen, E., Ingvaldsen, R.B., Aschan, M.M., Dolgov, A.V., 2015. Recent warming leads to a rapid borealization of fish communities in the Arctic. Nat. Clim. Change 5, 673—677, http://dx.doi.org/10.1038/nclimate2647.

Geoffroy, M., Robert, D., Darnis, G., Fortier, L., 2011. The aggregation of polar cod (*Boreogadus saida*) in the deep Atlantic layer of ice-covered Amundsen Gulf (Beaufort Sea) in winter. Polar Biol. 34, 1959—1971, http://dx.doi.org/10.1007/s00300-011-1019-9.

Harter, B.B., Elliott, K.H., Divoky, G.J., Davoren, G.K., 2013. Arctic cod (*Boreogadus saida*) as prey: fish length-energetics relationships in the Beaufort Sea and Hudson Bay. Arctic 66 (2), 191—196, http://dx.doi.org/10.14430/arctic4290.

Haug, T., Bogstad, B., Chierici, M., Gjøsæter, H., Hallfredsson, E.H., Høines, Å.S., Hoel, A.H., Ingvaldsen, R.B., Jørgensen, L.L., Knutsen, T., Loeng, H., Naustvoll, L.J., Røttingen, I., Sunnanå, K., 2017. Future harvest of living resources in the Arctic Ocean north of the Nordic and Barents Seas: a review of possibilities and constraints. Fish. Res 188, 38—57, http://dx.doi.org/10.1016/j.fishres.2016.12.002.

Hop, H., Gjøsæter, H., 2013. Polar cod (*Boreogadus saida*) and capelin (*Mallotus villosus*) as key species in marine food webs of the Arctic and the Barents Sea. Mar. Biol. 9 (9), 878—894, http://dx.doi.org/10.1080/17451000.2013.775458.

Korneliussen, R.J., 2000. Measurement and removal of echo integration noise. ICES J. Mar. Sci. 57 (4), 1204—1217, http://dx.doi.org/10.1006/jmsc.2000.0806.

Medwin, H., Clay, C.S., 1998. Fundamentals of Acoustical Oceanography. Acad. Press, Boston, 712 pp.

Misund, O.A., Heggland, K., Skogseth, R., Falck, E., Gjøsæter, H., Sundet, J., Watne, J., Lønne, O.J., 2016. Norwegian fisheries in the Svalbard zone since 1980. Regulations, profitability and warming waters affect landings. Polar Sci. 10 (3), 312—322, http://dx.doi.org/10.1016/j.polar.2016.02.001.

Nakken, O., Dommasnes, A., 1977. Acoustic estimates of the Barents Sea capelin stock 1971—1976. Meet. Int. Explor. Sea (H:35) 1—6.

Pedersen, G., Korneliussen, R.J., 2009. The relative frequency response derived from individually separated targets of northeast Arctic cod (*Gadus morhua*), saithe (*Pollachius virens*), and Norway pout (*Trisopterus esmarkii*). ICES J. Mar. Sci. 66 (6), 1149—1154, http://dx.doi.org/10.1093/icesjms/fsp070.

Promińska, A., Cisek, M., Walczowski, W., 2017. Kongsfjorden and Hornsund hydrography - comparative study based on a multiyear survey in fjords of west Spitsbergen. Oceanologia 59 (4), 397—412, http://dx.doi.org/10.1016/j.oceano.2017.07.003.

Renaud, P.E., Berge, J., Varpe, Ø., Lønne, O.J., Nahrgang, J., Ottesen, C., Hallanger, I., 2012. Is the poleward expansion by Atlantic cod and haddock threatening native polar cod, *Boreogadus saida*? Polar Biol. 35 (3), 401—412, http://dx.doi.org/10.1007/s00300-011-1085-z.

Simmonds, J., MacLennan, D., 2005. Fisheries Acoustics. Theory and Practice, 2nd edn. Blackwell Publ., Oxford, http://dx.doi.org/10.1002/9780470995303, 437 pp.

Walczowski, W., 2014. Atlantic Water in the Nordic Seas. Properties, Variability, Climatic Importance, GeoPlanet: Earth and Planetary Sciences. Springer Int. Publ., London, 174 pp., http://dx.doi.org/10.1007/978-3-319-01279-7.

Walczowski, W., Piechura, J., Goszczko, I., Wieczorek, P., 2012. Changes of the Atlantic Water properties as an important factor of the European Arctic marine climate. ICES J. Mar. Sci. 69 (5), 864—869, http://dx.doi.org/10.1093/icesjms/fss068.

Weslawski, J.M., Ryg, M.S., Smith, T.G., Oritsland, N.A., 1994. Diet of ringed seals (Phoca Hispida) in a fjord of West Svalbard. Arctic 47 (2), 109—114, http://dx.doi.org/10.14430/arctic1279.

Węsławski, J.M., Kwaśniewski, S., Stempniewicz, L., Błachowiak-Samołyk, K., 2006. Biodiversity and energy transfer to top trophic levels in two contrasting Arctic fjords. Pol. Polar Res. 27 (3), 259—278.

Wigley, S.E., McBride, H.M., McHugh, N.J., 2003. Length-Weight Relationships for 74 Fish Species Collected during NEFSC Research Vessel Bottom Trawl Surveys, 1992—99. NOAA Tech. Memo. NMFS-NE-171, 26 pp.

Oceanologia (2017) 59, 592—602

Available online at www.sciencedirect.com

ScienceDirect

journal homepage: www.journals.elsevier.com/oceanologia/

ORIGINAL RESEARCH ARTICLE

Ecosystem maturation follows the warming of the Arctic fjords

Jan Marcin Węsławski [a,*], Friedrich Buchholz [b], Marta Głuchowska [a], Agata Weydmann [a,c]

[a] *Institute of Oceanology, Polish Academy of Sciences, Sopot, Poland*
[b] *Alfred Wegener Institute for Polar and Marine Research, Bremerhaven, Germany*
[c] *Institute of Oceanography, University of Gdansk, Gdynia, Poland*

Received 8 July 2016; accepted 3 February 2017
Available online 24 May 2017

KEYWORDS
Climate change;
Regime shift;
Biodiversity;
Arctic;
Svalbard;
Fjords

Summary Two fjords in West Spitsbergen (Hornsund 77°N and Kongsfjorden 79°N) differ with regard to their exposure towards increasingly warm Atlantic water inflow. Hornsund remains in many respects cooler than Kongsfjorden (on average 2°C SST in summer) and is less influenced by warmer and more saline Atlantic waters. Reported changes in the physical environment (temperature rise, freshwater inflow, salinity drop, turbidity, fast-ice reduction, coastal change) are discussed in the context of biological observations in the pelagic and benthic realms with special reference to krill (Euphausiacea). We conclude that well-documented changes in the physical environment have had little effect on the fjord biota and that both organisms and their ecological functions in the fjords are well adapted to the scale of ongoing change. The observed changes fit the definition of ecosystem maturation, with greater diversity, a more complex food web and dispersed energy flow at the warmer site.

1. Introduction

Currently observed environmental changes — specifically those in the marine ecosystem reported in the last IPCC document (2014) — are well documented, yet their predicted consequences are a matter for debate. We selected two Svalbard fjords as a case study, since they are among the best studied Arctic regions (Hop et al., 2002; Svendsen et al., 2002), and because the archipelago lies in the centre of reported environmental change (ACIA, 2004; Pavlov et al.,

* Corresponding author at: Institute of Oceanology, Polish Academy of Sciences, Powstańców Warszawy 55, 81-712 Sopot, Poland. Tel.: +6042516.
E-mail address: weslaw@iopan.gda.pl (J.M. Węsławski).
Peer review under the responsibility of Institute of Oceanology of the Polish Academy of Sciences.

ELSEVIER Production and hosting by Elsevier

http://dx.doi.org/10.1016/j.oceano.2017.02.002

2013; Walczowski and Piechura, 2006). Public concern about Arctic change is understandable, as the visible element – ice, disappears before our eyes (Duarte et al., 2012). When traditional marine biogeography came into being (Ekman, 1953), the Arctic was given the status of a fully "independent province", owing to the obvious ice cover and its cold character, not because of its faunistic or functional uniqueness. This stands in stark contrast to the other polar area, the Antarctic, which is a hydrologically separate entity with a rich endemic fauna and long evolutionary history (McIntyre, 2010).

The Svalbard archipelago has most often been placed at the boundary between the High Arctic and Arctic or the Arctic and Sub-Arctic, with the borderline along the west coast of the island of Spitsbergen (Backus, 1986; Ekman, 1953; Sherman et al., 1990). Some authors have used the more general expression "temperate and cold waters of the Northern Hemisphere" (Golikov et al., 1990). The present paper summarizes and reviews data recently acquired within the GAME (Growing of Arctic Marine Ecosystem) project. We are going to demonstrate that most of the changes to the fjord ecosystem, reported from Spitsbergen, are in fact shifts within one large system. The changes resemble the process of ecosystem maturation as described by Odum (1969), namely, the development of more complex and balanced food webs and a higher level of carbon metabolism.

2. Material and methods

The data discussed below were collected from r/v *Oceania* during late July–early August surveys in 2013–2015, in the central basins of Hornsund (77°N) and Kongsfjorden (79°N), on a flat, even seabed of 100 m depth as part of the GAME project. There, an array of multidisciplinary observations were gathered from the water column and seabed, relating to hydrography, water column optics, water chemistry, plankton (from piko- to macroplankton), fish, as well as sediment biogeochemistry, bacteria, and meio- and macrofaunal assessments. The oxygen consumptions of the sediment and dominant taxa were also measured. In order to ensure the best possible comparability of the data, the same group of people made the observations, within a short time window, using the same equipment and measuring techniques. The specific methodologies are described in separate papers. Archival hydrographic data, collected in the two fjords between 2000 and 2015, were also used as background to give the fresh data a long-term environmental perspective (specific data are cited in the paper). All the data are accessible on the project's website and an illustrated summary can be found at http://www.iopan.gda.pl/projects/Game/deliverables.html.

To place the above-mentioned observations in a wider perspective, we took the case study of the expansion of Euphausiacea to the Spitsbergen fjords, studied by the second author (literature cited in the text).

3. Results and discussion

3.1. Environmental drivers

Table 1 shows that the two fjords (Hornsund at 77°N and Kongsfjorden at 79°N) are similar in size (300 and 210 km^2 respectively), volume (25 km^3) and shape with semi-separated inner fjord branches (Fig. 1) http://www.iopan.gda.pl/projects/Visual/index.html. The general circulation pattern is also similar, with shelf waters entering the fjord along the southern shore and flowing back out along the northern (Jakacki et al., 2017; Svendsen et al., 2002). Both fjords lack a sill at their entrances, yet depth is the important difference: Hornsund is shallower (max. depth 220 m) with a flat bottom profile, whereas Kongsfjorden is deep (max. depth 350 m) with a V-shaped bottom profile. Kongsfjorden's bathymetry links it directly to the outer shelf and slope via the Kongsfjordrenna (Włodarska-Kowalczuk, 2007). Hornsund is

Table 1 Observed physical differences between "cold" Hornsund and "warm" Kongsfjorden; data from cruises of r/v *Oceania* in 2010–2013 and Urbański et al. (1980), Swerpel (1985), Beszczynska-Möller et al. (1997), Blaszczyk et al. (2013), Drewnik et al. (2016), GAME project web page http://www.iopan.gda.pl/projects/Visual/index.html.

Factor	Hornsund	Kongsfjorden
Average near-bottom temperature in summer at 100 m depth (°C)	2	4
Average summer surface temperature	4	6
Fast ice: % of fjord area	20–25%	5–10%
Fast ice duration	3–5 months	1–3 months
Freshwater (glacial melt) volume in summer	0.7 km^3	0.3 km^3
Coastal change (new areas uncovered by glaciers between 1936 and 2000)	8% increase in sea bed shallower than 50 m	13% increase in sea bed shallower than 50 m
Winter cooled water retention in summer, volume	Always, usually 0.2–0.45 km^3	Seldom, 0–0.02 km^3 at best
Wind pattern	High percentage of local easterly winds driving freshwater out of the fjord	High percentage of westerly winds driving shelf water into the fjord
Atlantic core water inflow from shelf	Rare, outer part of fjord only	Regular in summer, deep into the fjord
Fjord topography	Shallow (max. depth 220 m)	Deep (max. depth 350 m)
Fjord area	300 km^2	210 km^2

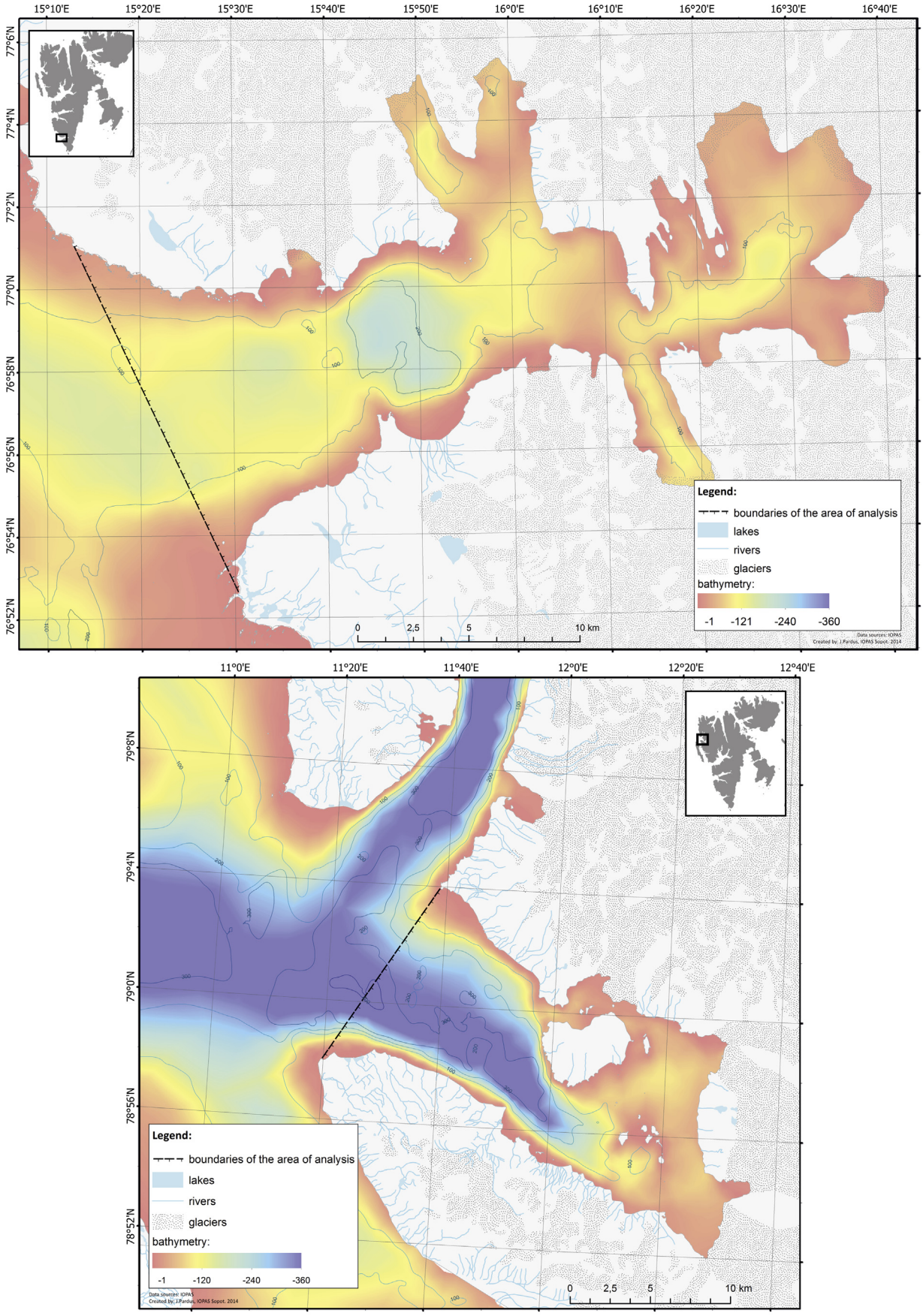

Figure 1 The bathymetry and topography of two fjords upper Hornsund, lower Kongsfjord, compared in the paper, modified after http://www.iopan.gda.pl/projects/Visual/index.html.

colder, fresher and less influenced by Atlantic shelf waters than Kongsfjorden (Table 1). The wind pattern is slightly different, with a more local, easterly circulation in Hornsund and more often westerly, open sea winds in Kongsfjorden (Table 1).

Kongsfjorden is treated here as an example of an already warmed system, whereas Hornsund remains relatively cold. The long-term hydrographic monitoring show that along the west coast of Spitsbergen, the sea surface temperature and volume of Atlantic waters, though variable, are steadily increasing (Walczowski, 2014). It is difficult to separate a local sea temperature rise from the general temperature increase of Atlantic waters, as the two most often go together. There have been specific situations, as in 2004, when during a strong inflow of Atlantic water, easterly winds moved cold, freshened water with sea ice from east Svalbard over the top of the warm saline waters flowing along the west coast, then in "warm year" we have got cold water and sea ice (Promińska et al., 2017). Another important environmental driver is the vertical partitioning of the fjord waters. The dynamics of the thin, freshened layer at the surface with its turbid glacial outflow is controlled mainly by the wind pattern and is highly changeable. In contrast, the near-bottom waters, especially in the inner fjord basins, are more stable, slow-moving, and respond to changes at the surface after a time lag (Drewnik et al., 2016). The intermediate water column also shows a different pattern in the two fjords: the deep canyon of the Kongsfjordrenna easily directs Atlantic waters from the outer shelf deep into the fjord, whereas this happens only rarely in the shallower Hornsund (Table 1, Węsławski et al., 2016).

In contrast to the increasing numbers of krill in the Arctic (Eriksen et al., 2016), the truly polar Antarctic krill, *Euphausia superba*, is diminishing dramatically (Atkinson et al., 2004). Only a few krill species have managed to adapt to the polar environment over the last 20 my, meaning that they are irreplaceable, not even by the "ice-krill", *E. crystallorophias*, because this is eco-physiologically completely bound to the ice edge. Instead, *E. superba* is being replaced by herbivorous tunicate *Salpa thompsoni*, which prefer warmer waters (Pakhomov et al., 2002). Antarctic krill stocks are thought to have been reduced to one third during the last two decades. The reason for this is an ice-effect: with the sea ice around the Antarctic strongly receding, krill is losing an essential habitat, particularly for overwintering. Here we have a clear response to global warming, evidently associated with ice retreat. This is very unlike what we are seeing in the Arctic and in Northern Hemisphere krill.

An interesting chapter in (Arctic-) ocean warming and the associated faunal changes is the history of krill in Kongsfjorden. There are now five euphausiid species regularly present in the pelagic fauna instead of the original two; this change took place at some time before the turn of the last century. In contrast, the colder Hornsund is still at the two-species level (Buchholz et al., 2010). First of all, we would like to take a rather more global perspective by comparing and trying to predict what may happen to the zooplankton community and its associated flora and fauna in Kongsfjorden. Then, we propose to consider physiological traits in the species, because, quite obviously, their specific adaptive capacity determines their ability to persist in new regions. Thirdly, euphausiids make good water body indicators, partly because they are good swimmers and can maintain their position within a specific water mass following favourable trophic and abiotic gradients; in other words, they are micronekton rather than zooplankton.

The first question to clear up is that there is no such thing as the "Arctic" krill. The two krill species *Thysanoessa inermis* and *Thysanoessa raschii* are non-reproducing expatriates from the Barents Sea, which are regularly carried by the remnants of the North Atlantic Current along western Spitsbergen into Kongsfjorden and beyond. However, *T. raschii* was found spawning there recently and a complete reproductive cycle can be expected soon, as the temperature increases further and the trophic environment improves, which will better match the environmental conditions of their boreal-subarctic origin. In fact, though non-Arctic, both species are definitely cold-stenothermal: they do have an upper thermal limit in terms of respiration efficiency and a heat-shock protection repertoire (Huenerlage, 2014). Indeed, their southern survival limit has already shifted northwards: in Canadian waters their numbers have fallen off dramatically (Obradovich et al., 2014) and they seem to have disappeared altogether from the warming Kattegat and the nearby Gullmarn Fjord in south-western Sweden (Buchholz and Saborowski, unpublished). It appears that they have to move to the north, evading warming waters and following the cold. We can expect them to play an increasing role in the Arctic environment as more and more of them arrive with advecting Atlantic water masses. Strangely enough, although both species thrive during the spring plankton bloom in Kongsfjorden, they then regress during summer in terms of reproduction and growth. This implies that there must be some factor either present in the water or missing from it that does not suit them, underlining that environmental improvement is a multifactorial process: not only thermal but also trophic conditions count.

Our studies of another *Euphausia* species may be helpful in understanding adaptive capacity in krill: *E. hanseni* is like its Antarctic congener — equally bound to a specific ecological situation, namely, to the upwelling regions off the West African coast on both sides of the equator and nowhere else (Huenerlage and Buchholz, 2013). The associated physiological trait is the smallest capacity for storing lipids as reserves so far found in euphausiids: only 5% of is dry weight. This means that the "upwelling-krill" depends completely on a constant food supply that is provided within one of the most productive zones of the world all the year round. This trait is found when the animals are experimentally starved: they reduce their metabolism immediately by 70%, thereby saving energy. The opposite extreme in starvation capacity as well as associated lipid storage is our "fjord-krill": *T. inermis* can go with no food for three weeks without any reduction in respiratory metabolism: it makes use of the huge lipid store that fills most of the carapace (the lipid body constitutes a lipid reserve of at least 40% of a specimen's dry weight). So, here we have a perfect example of cold water adaptation that allows survival over most of the productionless boreal-subarctic winter.

The three Atlantic invaders *Thysanoessa longicaudata*, *Meganyctiphanes norvegica* and *Nematoscelis megalops* are all showing an increasing trend in Kongsfjorden. First of all, they underline the "Atlantification" taking place (Huenerlage et al., 2014). Secondly, they will have a different impact in Kongsfjorden, both as consumers and competitors within the regional food web. The rather small *T. longicaudata*,

though truly oceanic and therefore a suitable indicator of immediate Atlantic influx, is probably ecologically the least important. This may not be the case with the strongly carnivorous *N. megalops*, a bi-hemispheric species of subtropical to cold temperate origin, but which seems to thrive, i.e. feeds, moults and exhibits reproductive traits, in the Arctic environment during summer. We have not tested this yet, but judging from physiological experience it may be its extraordinary hypoxia-tolerance in warm waters (Werner et al., 2012) that is responsible for its unexpected cold-tolerance. In the end, a critical cold temperature leads to cellular hypoxia, which can be counteracted by a switch of the cell metabolism to anaerobiosis, as happens in any case under external oxygen depletion. Be that as it may, this species has to be taken seriously in view of the changing food web. The greatest impact, however, will be exerted by *M. norvegica*, often called the Northern krill which, like the previous species, has a very widespread distribution and seems to be expanding everywhere, in the Mediterranean as well as in the St. Lawrence River or Georges Bank and lately in the Norwegian and Barents seas (Eriksen and Dalpadado, 2011; Link et al., 2009). In Canada this species is even being considered for commercial harvesting, with the aim of using it in natural products, e.g. medical additives (Winkler, Gesche, ref. Natural Sci. Res. Council, Canada). We have physiologically compared Northern krill from the cool north-eastern Atlantic and the warm Mediterranean (Buchholz and Saborowski, 2000): its pronounced expansive capacity is due to a combination of its very high thermal tolerance in terms of phenotypic adaptability and its being the greatest opportunist as regards food selection. Consequently, this offers the greatest opportunity to expand, always provided this happens along with the occurrence of their food. So far, we have observed *M. norvegica* feeding very well in Kongsfjorden, better than *T. inermis* (fullness of stomachs compared); the swarms of juveniles also present merely serve to underline the trend (Huenerlage et al., 2014).

Accordingly, it is quite likely that *T. inermis* and *T. raschii* will have to compete with the Atlantic newcomers. And it looks as if the latter are already doing better in terms of food choice or selective feeding. The former species are apparently more narrowly oriented, meaning that in fact they will only thrive when their matching trophic environment moves northwards and becomes established in Arctic waters. Because of their thermal upper limit they may even have to abandon the southern parts of their range. What then? In contrast to the Antarctic, the "Arctic" krill species are numerous and in terms of quantity may compensate losses and possibly improve food web quality as a whole. However, the trump card held by the *Thysanoessa* species in the Arctic environment is their huge lipid store: this trait will always be advantageous to their survival. The other species have much smaller amounts of lipids and also of poorer quality because they store other lipid types, e.g. energy rich wax esters vs. rather poor TAGs (Tri Acyl Glycerols). In the context of food web functioning, the loss of high quality lipids vs. gain in quantity through increasing krill numbers should be considered seriously – a nice task for ecosystem modellers! At any rate, the study of the interplay of different species of one (small) crustacean family may be considered as an interesting natural experiment in climatic adaptation.

3.2. Ecosystem response — species change

In general the biomass and biodiversity of Kongsfjorden are distinctly higher in both the water column and the sediment (Ormanczyk et al., 2017; Zaborska et al., 2016). The number of species is not very different, however, with Crustacea, for instance, represented by 120 species in Hornsund and 130 in Kongsfjorden (Legeżyńska et al., 2017). There are similar small differences among other taxonomic groups like Bryozoa (Gontar et al., 2001; Kuklinski et al., 2005), Mollusca (Włodarska-Kowalczuk, 2007), Polychaeta (Kędra et al., 2015) and various groups of marine algae (Smoła et al., 2017b).

The marine species distribution shifts observed in the two fjords (Table 2) can be attributed to different phenomena (and to the data deficit as well). Species often occur naturally over a large area, yet only a part of their distribution range is actually known, so new findings are interpreted as a distribution change – a typical situation in difficult taxonomic groups (e.g. meiobenthic Nematoda – Grzelak, pers. comm.).

Another process is the delayed reaction: a species occurs under certain physical conditions, but then disappears from part of its range as a result of, for instance, disease, overharvesting, predation pressure or breeding failure. It may attempt to return to its former range of occurrence, but is prevented from doing so by new competitors or the distance from the source population. To give an example: physical conditions favourable to blue mussel *Mytilus edulis* have existed off Svalbard since the beginning of the 20th century, yet the species did not reappear until over 100 years later (Berge et al., 2005).

Again, a species is theoretically capable of living in a certain area (habitat-related, physical–chemical limits), yet some factor prevents it from colonizing that area. Once this factor changes, however, invasion is likely to ensue. The above mentioned reappearance of blue mussel in Svalbard was made possible by the unusually high northward mass transport of warm Atlantic water resulting in elevated sea-surface temperatures (Berge et al., 2005). Another example, it is the mechanical ice scouring that prevents a number of intertidal species from occurring along the shores of east Spitsbergen, but in areas where the ice cover has receded, colonization has been rapid (Weslawski et al., 2010).

A common phenomenon is dispersal: expatriates of large, long-lived species are transported passively or may swim actively far away from their natural range of distribution. This has been demonstrated for ice amphipods (*Gammarus wilkitzkii*, *Apherusa glacialis*) expatriated south with the East Greenland Current (Duris and Weslawski, 1995; Lonne and Gulliksen, 1989). See also the krill case study below.

In general, we believe that the explanation for the phenomena listed in Table 2 is the common species pool over a large area. Conditions for several of these species may be suboptimal around its edges, hence they are rare on the peripheries, even though they are supplied from an extensive area and can move their distribution back and forth. For instance, only seven Polychaeta species are dominant sublittoral benthic dwellers from central Europe to the European Arctic (Weslawski et al., 2012). The dominance of particular species may vary from year to year, yet the species pool remains the same (Beuchel et al., 2006; Renaud et al., 2007).

Table 2 Observed changes in species occurrence in Hornsund and Kongsfjorden and adjacent shelf waters.

Species	Remarks	References
New arrivals		
Meganyctiphanes norvegica	Range extension, limit to temperature tolerance for breeding	Buchholz et al., 2010
Nematoscelis megalops	Range extension, high tolerance to temperature and hypoxia	Buchholz et al., 2010
Mackerel, Herring, Atlantic cod	Advection of Atlantic waters	Own observations
Themisto compressa	Advection of Atlantic waters	Kraft et al., 2013
Mytilus edulis	Local environmental change	Berge et al., 2005
Limacina retroversa	Advection of Atlantic waters	Weslawski et al., 2009
Local species loss		
Gammarus wilkitzki	Able to live intertidally, with at least two closely related species	Weslawski, 1994
Apherusa glacialis	Able to live in shallow littoral with a number of closely related species	
Local species range extension		
Gammarus oceanicus	Expansion towards inner fjords and along the coast	Weslawski et al., 2010
Fucus sp. and macroalgae	Expansion towards upper littoral and newly de-iced areas	
Calanus finmarchicus	Expansion towards inner fjords	Kwaśniewski et al., 2010

3.3. The ecosystem response — functional change

Serious functional alteration is usually connected to climate change or attributed to fishery collapse (Mollmann et al., 2015) or other forms of human ecosystem usage, what can lead to regime shifts (Carstensen and Weydmann, 2012). The large-scale occurrence of Atlantic cod off Svalbard, not to mention capelin, mackerel and herring, was reported recently and is likely to induce changes in the food web (Renaud et al., 2012). Boreal pelagic fish are turning up along with their food (advection of Atlantic water with plankton), but so far no perceptible changes have been reported in the benthos (Kędra et al., 2015) and the Atlantic cod in Kongsfjorden feeds mainly on krill (Węsławski et al., 2016).

The specific functions associated with sea ice are likely to be lost in warmed-up fjords, as the ice cover has retreated markedly in recent years (Table 1). However, the sea ice habitat in fjords (fast ice) adds relatively little to the benthic realm (Weslawski et al., 1993), although it is still important for the zooplankton community, which feeds on ice algal bloom as the first source of food after polar winter (Søreide et al., 2010; Weydmann et al., 2013) and acts as a breeding habitat for ringed seals (Lydersen and Ryg, 1991). As ice scouring has decreased, there are certainly more macroalgae on the coast (Weslawski et al., 2010), and consequently macro-algal detritus is recorded in the food of the deep sublittoral benthos (Legeżyńska et al., 2014; Renaud et al., 2011).

Energy flow redirection as a functional change was envisaged by Hopner-Petersen and Curtis (1980), as strong pelago-benthic coupling is believed to be typical of Arctic waters, whereas a stronger pelagic energy flow is a sign of a boreal system. Comparison of organic carbon sedimentation rates (Table 3) reveals a higher level of carbon sedimentation in Kongsfjorden, associated with a higher level of carbon metabolism in the sediments. As a large part of the organic carbon in Hornsund is of terrestrial origin (Koziorowska et al., 2016; Zaborska et al., 2016), the marine organic matter in Kongsfjorden is being recycled whereas the terrestrial matter is being buried (Zaborska et al., 2016). The pelagic energy flow is certainly stronger in Kongsfjorden than in Hornsund as a consequence of the larger biomass and greater diversity of grazers and micropredators (Ormanczyk et al., 2017).

Another fjord function is the production of winter cooled water (in Svalbard its temperature is below -1.5°C and the salinity over 34) and its retention through the summer. This process is almost defunct in Kongsfjorden but still occurs in Hornsund (Table 1). Basins with cold, dense waters are apparently refugia for cold-water species (Drewnik et al., 2016b), but such a function may persist even in warmer sites, as exemplified by the presence of glacial relicts in the innermost fjord basins in the much warmer present-day temperatures in continental Norway and in the Baltic (Segerstråle, 1982).

An important function that is likely to differ between the two fjords is microbial loop activity, namely, a higher level of bacterial production and biomass in a warmer Kongsfjorden than in Hornsund (Ameryk et al., 2017; Kalinowska et al., 2015). The temperature-related bacterial processes and sediment carbon burial in fjords will most likely result in biogeochemical changes (sulphur cycle and alkalinity) to the sediments, as was demonstrated in two Greenland fjords by Rysgaard and Glud (2007). The microbial-dominated sediment oxygen uptake expressed per gC m^{-2} is not statistically different between the two fjords; the higher oxygen consumption and deeper oxygen penetration in Kongsfjorden is associated with the higher biomass and the more complex benthic community there (Kotwicki et al., 2016).

Table 3 Examples of functional changes in the fjords.

Change	Hornsund	Kongsfjord	Function change
Primary production [gC m^{-2} $year^{-1}$]	71	42	Higher proportion of macrophytes in KGF (Smoła et al., 2017a)
Carbon mineralization in sediments (% of acc.)	26%	46%	Higher proportion of marine carbon in KGF (Zaborska et al., 2016)
Energy transfer to top predators (4th TL [gC m^{-2} $year^{-1}$])	0.7	0.6	More energy to top predators in Hornsund
Carbon accumulation in sediment [g m^{-2} $year^{-1}$]	90	47	Larger carbon sink in Hornsund (Zaborska et al., 2016)
Carbon demand in sediment [g m^{-2} $year^{-1}$]	51.6	85.5	Biomass and metabolic levels higher in KGF (Kotwicki et al., 2016)
Carbon demand in water column			
Microbial production in sediments [μg C kg^{-1} h^{-1}]	0.3	0.5	More microbial production and biomass in KGF sediment, less in KGF water column (Ameryk et al., 2017)
Meiofauna size structure (length to width ratio, <12)	4%	12%	Nematoda short and stout in Hornsund, long and slender in KGF (Grzelak et al., 2016)

3.4. The alteration of a whole system

This is a rare event in the natural environment, e.g. a change in the Bering Sea food web (Grebmeier et al., 2006) or the large-scale disappearance of sea ice and its consequences for the Central Arctic sympagic biota (Berge et al., 2012).

Some papers discussing large-scale environmental change predict mass extinctions of species in sea waters (Worm et al., 2006), yet there are very few documented cases of such extinctions (Dulvy et al., 2003). Flessa and Jablonski (1995) published an extensive biogeographical analysis discussing the extinction probabilities of different bivalve fauna. They demonstrated that because there is no endemism, Arctic bivalves are so widespread that the threat of regional extinction is unlikely. The cosmopolitan nature of distribution and the natural variability of the Spitsbergen fjord environment (from fresh to marine, and from frozen to warm) prevent the colonization of stenotopic species and the consequent threats to their existence.

4. Conclusions

At a large scale, because of recent glaciation, the uniqueness of the Arctic marine fauna has just begun to be formed but has not yet had enough time to generate a new, independent ecosystem (Wares and Cunningham, 2001). Now, with increasing Atlantic water inflow and atmospheric warming of the coasts, the peripheries of the Atlantic Ocean are going to become more similar to its source, with little change in function. For the coastal marine Arctic, the sea ice is an inversed sea bottom, the habitat of a very few species that can leave the littoral for the sea ice in winter and move back to their original benthic habitat in summer (Weslawski, 1994). In general, and in contrast to the old paradigm (Beaugrand et al., 2002; Blacker, 1957), closely related species are not really replacing each other. What is currently taking place is that newcomers are arriving from warmer waters, thereby creating a richer species pool with the original, local cold water species still present. For example, Atlantic zooplankter *Calanus finmarchicus* is not expelling the Arctic *Calanus glacialis*, although changes in species proportions are observed (Kwaśniewski et al., 2010, Weydmann et al., 2014), *Gammarus setosus* shares space with *Gammarus oceanicus* (Weslawski et al., 2010), and echinoderms are widely distributed across previously well-delimited zoogeographical boundaries (Deja et al., 2016).

Similar observations have been made in the Baltic Sea, where recently settled species add to the species pool and cause the meltdown of former zoogeographical borders (Leppakoski and Olenin, 2001).

As a consequence, observed and predicted changes in the west Spitsbergen fjords are happening within the boundaries of one, large North Atlantic biogeographical province (Sherman et al., 1990). In fact, there is not a single species from the known species lists published for the two fjords that would not be recorded in continental Norway or the Murman Coast/Kola Peninsula (see Kędra et al., 2010; Prestrud et al., 2004). The little-known biogeographical concept of Golikov et al. (1990) is based on the temperature span between extreme warm seasons in the south and extreme cold seasons in the northern range of a species' distribution (Fig. 2). This shows how large the potential space is for changes in species distribution. The differences between the colder, Arctic fjord (Hornsund) and the warmer, more open Kongsfjord are unlikely to be close to "tipping points" – irreversible change of structure and function of the system (Duarte et al., 2012), or "regime shifts" – replacement of the local ecosystem structure and function with such from the neighbouring boreal area (ACIA, 2004); it is rather a case that is fulfilling the definition of ecosystem maturation as described by Odum (1969) and Saint-Beat et al. (2015). The key phenomena observed are increases in biomass, species richness and functional group diversity, a more evenly-balanced and effective food web, and a higher proportion of organic matter metabolized within the system compared to deposited carbon, with little change in species distribution or their functions.

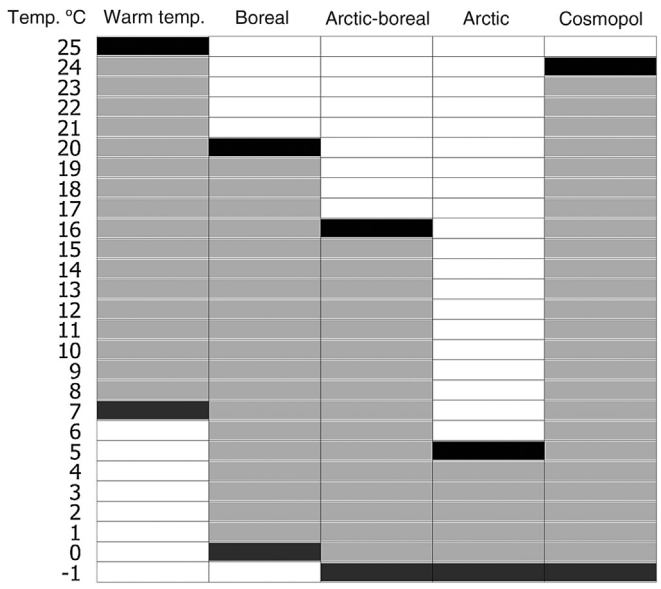

Figure 2 General scheme of temperature tolerance span among different marine zoogeographical regions: range from extreme cold (winter in northern distribution limit) to extreme warm (summer at southern distribution limit); modified after Golikov et al. (1990), temperature data after Levitus (2006).

Acknowledgements

We are grateful for the fruitful discussions with participants of the Kongsfjorden Workshop held at Senja, Norway, in spring 2014. This paper was supported financially by the GAME project — Polish National Science Centre No. DEC-2012/04/A/NZ8/00661.

References

ACIA, 2004. Impacts of a Warming Arctic: Arctic Climate Impact Assessment. ACIA Overview Report. Cambridge Univ. Press, 140 pp.

Ameryk, A., Jankowska, K.M., Kalinowska, A., Węsławski, J.M., 2017. Comparison of bacterial production in the water column between two Arctic fjords, Hornsund and Kongsfjorden (West Spitsbergen). Oceanologia 59 (4), 496—507, http://dx.doi.org/10.1016/j.oceano.2017.06.001.

Atkinson, A., Siegel, V., Pakhomov, E., Rothery, P., 2004. Long-term decline in krill stock and increase in salps within the Southern Ocean. Nature 432 (7013), 100—103, http://dx.doi.org/10.1038/nature02996.

Backus, R.H., 1986. Biogeographic boundaries in the open ocean. In: Pierrot-Bults, A., Van Der Spoel, S., Zahuranec, B.J., Johnson, R. K. (Eds.), Pelagic Biogeography. The Netherlands, Unesco Tech. Papers Mar. Sci., 9—13.

Beaugrand, G., Reid, P.C., Ibanez, F., Lindlay, J.A., Edwards, M., 2002. Reorganisation of North Atlantic marine copepod biodiversity and climate. Science 296 (5573), 168—170, http://dx.doi.org/10.1126/science.1071329.

Berge, J., Johnsen, G., Nilsen, F., Gulliksen, B., Slagstad, D., 2005. Ocean temperature oscillations causing the reappearance of blue mussels in Svalbard after 1000 years of absence. Mar. Ecol.-Prog. Ser. 303, 167—175, http://dx.doi.org/10.3354/meps303167.

Berge, J., Varpe, Ø., Moline, M.A., Wold, A., Renaud, P.E., Daase, M., Falk-Petersen, S., 2012. Retention of ice-associated amphipods: possible consequences for an ice-free Arctic Ocean. Biol. Lett. UK 8 (6), http://dx.doi.org/10.1098/rsbl.2012.0517, 4 pp.

Beszczynska-Möller, A., Weslawski, J.M., Walczowski, W., Zajaczkowski, M., 1997. Estimation of glacial meltwater discharge into Svalbard coastal water. Oceanologia 39 (3), 289—297, http://www.iopan.gda.pl/oceanologia/39_3.htm#A8.

Beuchel, F., Gulliksen, B., Caroll, M.L., 2006. Long-term patterns of rocky bottom macrobenthic community structure in an Arctic fjord (Kongsfjorden, Svalbard) in relation to climate variability (1980—2003). J. Marine Syst. 63 (1—2), 35—48, http://dx.doi.org/10.1016/j.jmarsys.2006.05.002.

Blacker, R.W., 1957. Benthic animals as indicators of hydrographic conditions and climatic change in Svalbard waters. Fish. Invest. 2, 1—59.

Blaszczyk, M., Jania, J., Kolondra, L., 2013. Fluctuations of tidewater glaciers in Hornsund Fjord (Southern Svalbard) since the beginning of the 20th century. Pol. Polar Res. 34 (4), 327—352, http://dx.doi.org/10.2478/popore-2013-0024.

Buchholz, F., Buchholz, C., Weslawski, J.M., 2010. Ten years after: krill as indicator of changes in the macro-zooplankton communities of two Arctic fjords. Polar Biol. 33 (1), 101—113, http://dx.doi.org/10.1007/s00300-009-0688-0.

Buchholz, F., Saborowski, R., 2000. Metabolic and enzymatic adaptations in northern krill, *Meganyctiphanes norvegica*, and Antarctic krill, *Euphausia superba*. Can. J. Fish. Aquat. Sci. 57 (S3), 115—129, http://dx.doi.org/10.1139/f00-168.

Carstensen, J., Weydmann, A., 2012. Tipping points in the Arctic: eyeballing or statistical significance? AMBIO 41 (1), 34—43, http://dx.doi.org/10.1007/s13280-011-0223-8.

Deja, K., Węsławski, J.M., Borszcz, T., Włodarska- Kowalczuk, M., Kuklinski, P., Bałazy, P., Kwiatkowska, P., 2016. Recent distribution of *Echinodermata* species in Spitsbergen coastal waters. Pol. Polar Res. 37 (4), 511—526.

Drewnik, A., Weslawski, J.M., Włodarska-Kowalczuk, M., Łącka, M., Romińska, A., Zaborska, A., Głuchowska, M., 2016. From the worm's point of view. Physical environment of an Arctic fjord benthos. Polar Biol. 39 (8), 1411—1424, http://dx.doi.org/10.1007/s00300-015-1867-9.

Duarte, C.M., Lenton, T.M., Wadhams, P., Wassmann, P., 2012. COMMENTARY: abrupt climate change in the Arctic. Nat. Clim. Change 2 (2), 60—62, http://dx.doi.org/10.1038/nclimate1386.

Dulvy, N.K., Sadovy, Y., Reynolds, J.D., 2003. Extinction vulnerability in marine populations. Fish Fish. 4, 25–64.

Duris, Z., Weslawski, J.M., 1995. Range extensions of some decapod crustaceans of North East Greenland. Acta Facultat. Rerum Natur. Univ. Ostraviensis 148, 81–92.

Ekman, S., 1953. Zoogeography of the Seas. Sidgewick and Jackson, London, 417 pp.

Eriksen, E., Dalpadado, P., 2011. Long-term changes in Krill biomass and distribution in the Barents Sea: are the changes mainly related to capelin stock size and temperature conditions? Polar Biol. 34 (9), 1399–1409.

Eriksen, E., Skjoldal, H.R., Dolgov, A.V., Dalpadado, P., Orlova, E.L., Prozorkevich, D.V., 2016. The Barents Sea euphausiids: methodological aspects of monitoring and estimation of abundance and biomass. ICES J. Mar. Sci. 73 (6), 1533–1544, http://dx.doi.org/10.1093/icesjms/fsw022.

Flessa, K.W., Jablonski, D., 1995. Biogeography of recent marine bivalve molluscs and its implications for paleobiogeography and the geography of extinction: a progress report. Histor. Biol. 10 (1), 25–47, http://dx.doi.org/10.1080/10292389509380512.

Golikov, A.N., Dolgolenko, M.A., Maximovich, N.V., Scarlato, O.A., 1990. Theoretical approaches to marine biogeography. Mar. Ecol.-Prog. Ser. 63, 289–301, http://dx.doi.org/10.3354/meps063289.

Gontar, V.I., Hop, H., Voronkov, A.Y., 2001. Diversity and distribution of Bryozoa in Kongsfjorden, Svalbard. Pol. Polar Res. 22 (3–4), 187–204.

Grebmeier, J.M., Overland, J.E., Moore, S.E., Farley, E.V., Carmack, E.C., Cooper, L.W., Frey, K.E., Helle, J.H., McLaughlin, F.A., McNutt, S.L., 2006. A major ecosystem shift in the Northern Bering Sea. Science 311 (5766), 1461–1464, http://dx.doi.org/10.1126/science.1121365.

Grzelak, K., Głuchowska, M., Gregorczyk, K., Winogradowa, A., Weslawski, J.M., 2016. Nematode biomass and morphometric attributes as biological indicators of local environmental conditions in Arctic fjords. Ecol. Indic. 69, 368–380, http://dx.doi.org/10.1016/j.ecolind.2016.04.036.

Hop, H., Pearson, T., Hegseth, E.N., Kovacs, K.M., Wiencke, Ch., Kwasniewski, S., Eiane, K., Mehlum, F., Gulliksen, B., Wlodarska-Kowalczuk, M., Lydersen, Ch., Weslawski, J.M., Cochrane, S., Gabrielsen, G.W., Leakey, R.J.G., Lønne, O.J., Zajaczkowski, M., Falk-Petersen, S., Kendall, M., Wängberg, S.A., Bischof, K., Voronkov, A.Y., Kovaltchouk, N.A., Wiktor, J., Poltermann, M., di Prisco, G., Papucci, C., Gerland, S., 2002. The marine ecosystem of Kongsfjord, Svalbard. Polar Res. 21 (1), 67–208.

Hopner-Petersen, G., Curtis, M.A., 1980. Differences in energy flow through major components of subarctic, temperate and tropical marine shelf ecosystems. Dana 1, 53–64.

Huenerlage, K., 2014. Krill in the Arctic and the Atlantic – Climatic Variability and Adaptive Capacity. (Diss). Univ. Hamburg, 174 pp.

Huenerlage, K., Buchholz, F., 2013. Krill of the northern Benguela Current and the Angola-Benguela frontal zone compared: physiological performance and short-term starvation in *Euphausia hanseni*. J. Plankton Res. 35 (2), 337–435, http://dx.doi.org/10.1093/plankt/fbs086.

Huenerlage, K., Graeve, M., Buchholz, F., 2014. Lipid composition and trophic relationships of krill species in a high Arctic fjord. Polar Biol. 39 (10), 1803–1817, http://dx.doi.org/10.1007/s00300-014-1607-6.

IPCC, 2014. Climate Change, Synthesis Rep., www.ipcc.ch.

Jakacki, J., Przyborska, A., Kosecki, S., Sunfjord, A., Albretsen, J., 2017. Modelling of the Svalbard fjord, Hornsund. Oceanologia 59 (4), 473–495, http://dx.doi.org/10.1016/j.oceano.2017.04.004.

Kalinowska, A., Ameryk, A., Jankowska, K., 2015. Microbiological survey in two Arctic fjords: total bacterial number and biomass comparison of Hornsund and Kongsfjorden. In: Zielinski, T., Weslawski, M., Kuliński, K. (Eds.), Impact of Climate Changes on Marine Environments. Geo Planet: Earth and Planetary Sci. Ser. Springer, Heidelberg/New York/Dordrecht/London, 115–126, http://dx.doi.org/10.1007/978-3-319-14283-8_9.

Kędra, M., Gromisz, S., Jaskula, R., Legezynska, J., Maciejewska, B., Malec, E., Opanowski, A., Ostrowska, K., Wlodarska-Kowalczuk, M., Weslawski, J.M., 2010. Soft bottom fauna of an All Taxa Biodiversity Site – Hornsund (77°N, Svalbard). Pol. Polar Res. 31, 309–326, http://dx.doi.org/10.2478/v10183-010-0008-y.

Kędra, M., Moritz, Ch., Choy, E.S., David, C., Degen, R., Duerksen, S., Ellingsen, I., Górska, B., Grebmeier, J.M., Kirievskaya, D., van Oevelen, D., Piwosz, K., Samuelsen, A., Węsławski, J.M., 2015. Status and trends in the structure of Arctic benthic food webs. Polar Res. 34 (1), http://dx.doi.org/10.3402/polar.v34.23775.

Kotwicki, L., Grzelak, K., Opalinski, K., Jankowska, K.M., Weslawski, J.M., 2016. Total benthic oxygen uptake in two Spitsbergen Arctic fjords under different hydrological regimes. Oceanologia (submitted for publication).

Koziorowska, K., Kulinski, K., Pempkowiak, J., 2016. Sedimentary organic matter in two Spitsbergen fjords: terrestrial and marine contributions based on carbon and nitrogen contents and stable isotopes composition. Cont. Shelf Res. 113, 38–46, http://dx.doi.org/10.1016/j.csr.2015.11.010.

Kraft, A., Nöthig, E.M., Bauerfeind, E., Wildish, D.J., Pohle, G.W., Bathmann, U.V., Beszczynska-Möller, A., Klages, M., 2013. First evidence of reproductive success in a southern invader indicates possible community shifts among Arctic zooplankton. Mar. Ecol.-Prog. Ser. 493, 291–296, http://dx.doi.org/10.3354/meps10507.

Kuklinski, P., Gulliksen, B., Lonne, O.J., Weslawski, J.M., 2005. Composition of bryozoan assemblages related to depth in Svalbard fjords and sounds. Polar Biol. 28 (8), 619–630, http://dx.doi.org/10.1007/s00300-005-0726-5.

Kwaśniewski, S., Gluchowska, M., Jakubas, D., Wojczulanis-Jakubas, K., Walkusz, W., Karnovsky, N., Blachowiak-Samolyk, K., Cisek, M., Stempniewicz, L., 2010. The impact of different hydrographic conditions and zooplankton communities on provisioning Little Auks along the West coast of Spitsbergen. Prog. Oceanogr. 87 (1–4), 72–82, http://dx.doi.org/10.1016/j.pocean.2010.06.004.

Legeżyńska, J., Włodarska-Kowalczuk, M., Gluchowska, M., Ormańczyk, M., Kędra, M., Węsławski, J.M., 2017. The malacostracan fauna of two Arctic fjords (west Spitsbergen): the diversity and distribution patterns of its pelagic and benthic components. Oceanologia 59 (4), 541–564, http://dx.doi.org/10.1016/j.oceano.2017.01.004.

Legeżyńska, J., Kędra, M., Walkusz, W., 2014. Identifying trophic relationships within the high Arctic benthic community: how much can fatty acids tell? Mar. Biol. 161, 821–836, http://dx.doi.org/10.1007/s00227-013-2380-8.

Leppakoski, E., Olenin, S., 2001. The meltdown of biogeographical peculiarities of the Baltic Sea: the interaction of natural and man-made processes. AMBIO 30 (4), 202–209, http://dx.doi.org/10.1579/0044-7447-30.4.202.

Levitus, S. (Ed.), 2006. World Ocean Atlas 2005, Vol. 1: Temperature. NOAA Atlas ESDIS 61, U.S. Gov. Printing Office, Washington, DC, 182 pp.

Link, J.S., Stockhausen, W.T., Skaret, G., Overholtz, W., Megrey, B.A., Gjøs, H., Gaichas, S., Dommasnes, A., Falk-Petersen, J., Kane, J., Mueter, F.J., Friedland, K.D., Hare, J.A., 2009. A comparison of biological trends from four marine ecosystems: synchronies, differences, and commonalities. Prog. Oceanogr. 81 (1–4), 29–46, http://dx.doi.org/10.1016/j.pocean.2009.04.004.

Lonne, O.J., Gulliksen, B., 1989. Occurrence and ecological importance of sympagic fauna in Fram Strait, Svalbard area and Eastern Barents Sea. Rapp. Et Proc. Verb du CIEM 188, 170–188.

Lydersen, Ch., Ryg, M., 1991. Evaluating breeding habitat and population of ringed seal *Phoca hispida* in Svalbard fjords. Polar Rec. 27 (162), 223–228, http://dx.doi.org/10.1017/S0032247400012614.

McIntyre, A.D. (Ed.), 2010. Life in the World's Oceans. Blackwell Publ. Ltd., Chichester, 362 pp.

Mollmann, C., Folke, C., Edwards, M., Conversi, A., 2015. Marine regime shifts around the globe: theory drivers and impacts. Philos. Trans. R. Soc. B 370 (1659), http://dx.doi.org/10.1098/rstb.2013.0260, 5 pp.

Obradovich, S.G., Carruthers, E.H., Rose, G.A., 2014. Bottom-up limits to Newfoundland capelin (*Mallotus villosus*) rebuilding: the euphausiid hypothesis. ICES J. Mar. Sci. 71 (4), 775—783, http://dx.doi.org/10.1093/icesjms/fst184.

Odum, E.P., 1969. The strategy of ecosystem development. Science 164 (3877), 262—270, http://dx.doi.org/10.1126/science.164.3877.262.

Ormanczyk, M.R., Gluchowska, M., Olszewska, A., Kwasniewski, S., 2017. Zooplankton structure in high latitude fjords with contrasting oceanography (Hornsund and Kongsfjorden, Spitsbergen). Oceanologia 59 (4), 508—524, http://dx.doi.org/10.1016/j.oceano.2017.06.003.

Pakhomov, E.A., Froneman, P.W., Perissinotto, R., 2002. Salp/krill interactions in the Southern Ocean: spatial segregation and implications for the carbon flux. Deep-Sea Res. II 49 (9—10), 1881—1907, http://dx.doi.org/10.1016/S0967-0645(02)00017-6.

Pavlov, A.K., Tverberg, V., Nilsen, F., 2013. Warming of Atlantic Water in two west Spitsbergen fjords over the last century (1912—2009). Polar Res. 32 (1), 11206, http://dx.doi.org/10.3402/polar.v32i0.11206.

Prestrud, P., Strøm, H., Goldman, H.V., 2004. A catalogue of the terrestrial and marine animals of Svalbard. Norsk Polar. Inst. Skrift. 201, 142 pp.

Promińska, A., Cisek, M., Walczowski, W., 2017. Kongsfjorden and Hornsund hydrography — comparative study based on a multiyear survey in fjords of west Spitsbergen. Oceanologia 59 (4), 397—412, http://dx.doi.org/10.1016/j.oceano.2017.07.003.

Renaud, P., Berge, J., Varpe, O., Lonne, O.J., Nahrgang, J., Ottesen, C., Hallanger, I., 2012. Is the poleward expansion by Atlantic cod and haddock threatening native polar cod, *Boreogadus saida*? Polar Biol. 35 (3), 401—412, http://dx.doi.org/10.1007/s00300-011-1085-z.

Renaud, P.E., Tessmann, M., Evenset, A., Christensen, G.N., 2011. Benthic food-web structure of an Arctic fjord (Kongsfjorden, Svalbard). Mar. Biol. Res. 7 (1), 13—26, http://dx.doi.org/10.1080/17451001003671597.

Renaud, P.E., Wlodarska-Kowalczuk, M., Trannum, H., Holte, B., Weslawski, J.M., Cochrane, S., Dahle, S., Gulliksen, B., 2007. Multidecadal stability of benthic community structure in a high-arctic glacial fjord (Van Mijenfjord, Spitsbergen). Polar Biol. 30 (3), 295—305, http://dx.doi.org/10.1007/s00300-006-0183-9.

Rysgaard, S., Glud, R., 2007. Carbon cycling and climate change. Predictions for a High Arctic marine ecosystem (Young sound, NE Greenland). Medd. om Grønland Biosci. 58, 206—214.

Saint-Beat, B., Baird, D., Asmus, H., Asmus, R., Bacher, C., Pacella, S.R., Johnson, G.A., David, V., Vezina, A.F., Niquill, N., 2015. Trophic networks: how do theories link ecosystem structure and functioning to stability properties? A review. Ecol. Indic. 52, 458—471, http://dx.doi.org/10.1016/j.ecolind.2014.12.017.

Segerstråle, S.G., 1982. The immigration of glacial relicts into Northern Europe in the light of recent geological research. Fennia — Int. J. Geogr. 160 (2), 303—312.

Sherman, K., Alexander, L.M., Gold, B.D. (Eds.), 1990. Large Marine Ecosystems: Patterns, Processes, and Yields. AAAS Publ., Washington, DC, USA, 242 pp.

Smoła, Z., Tatarek, A., Wiktor, J., Wiktor Jr., J., Hapter, R., Kubiszyn, A., Weslawski, J.M., 2017a. Primary producers and production in two West Spitsbergen fjords (Hornsund and Kongsfjorden) — a review. Pol. Polar Res. 38 (2).

Smoła, Z., Tatarek, A., Wiktor, J., Wiktor Jr., J., Kubiszyn, A., Węsławski, J.M., 2017b. Primary producers and production in two West Spitsbergen ljords — comparison of two frord systems (Hornsund and Kongsftorden). Pol. Polar Res. (in press).

Søreide, J.E., Leu, E., Berge, J., Graeve, M., Falk-Petersen, S., 2010. Timing of blooms, algal food quality and *Calanus glacialis* reproduction and growth in a changing Arctic. Glob. Change Biol. 16 (11), 3154—3163, http://dx.doi.org/10.1111/j.1365-2486.2010.02175.x.

Svendsen, H., Beszczynska-Möller, A., Hagen, J.O., Lefauconnier, B., Tverberg, V., Gerland, S., Bischof, K., Papucci, C., Zajaczkowski, M., Azzolini, R., Bruland, O., Wiencke, C., Winther, J.G., Dallmann, W., 2002. The physical environment of Kongsfjorden—Krossfjorden, an arctic fjord system in Svalbard. Polar Res. 21 (1), 133—166, http://dx.doi.org/10.1111/j.1751-8369.2002.tb00072.x.

Swerpel, S., 1985. The Hornsund fjord — water masses. Pol. Polar Res. 6, 475—496.

Urbański, J., Neugenbauer, E., Spacjer, R., Falkowska, L., 1980. Physico-chemical characteristic of the waters of Hornsund Fjord on south-west Spitsbergen (Svalbard Archipelago) in the summer season 1979. Pol. Polar Res. 1, 43—52.

Walczowski, W., 2014. Dynamics of the west Spitsbergen current. In: Atlantic Water in the Nordic Seas. GeoPlanet: Earth and Planetary Sci. Springer, Cham/Heidelberg/New York/Dordrecht/London, 111—127.

Walczowski, W., Piechura, J., 2006. New evidence of warming propagation toward the Arctic Ocean. Geophys. Res. Lett. 33 (12), L1212601, http://dx.doi.org/10.1029/2006GL025872.

Wares, J.P., Cunningham, C.W., 2001. Phylogeography and historical ecology of the North Atlantic intertidal. Evolution 55 (12), 2455—2469, http://dx.doi.org/10.1554/0014-3820(2001)055[2455:PAHEOT]2.0.CO;2.

Werner, T., Hünerlage, K., Verheye, H., Buchholz, F., 2012. Thermal constraints on the respiration and excretion rates of krill, *Euphausia hanseni* and *Nematoscelis megalops*, in the northern Benguela upwelling system off Namibia. Afr. J. Mar. Sci. 34 (3), 391—399, http://dx.doi.org/10.2989/1814232X.2012.689620.

Weslawski, J.M., 1994. Genus *Gammarus* (Crustacea, Amphipoda) from Svalbard and Franz Josef Land. Distribution and density. Sarsia 79 (2), 145—150, http://dx.doi.org/10.1080/00364827.1994.10413553.

Weslawski, J.M., Kwasniewski, S., Wiktor, J., Zajaczkowski, M., 1993. Observations on the fast ice biota in the fjords of Spitsbergen. Pol. Polar Res. 14 (4), 331—343.

Weslawski, J.M., Kwasniewski, S., Stempniewicz, L., 2009. Warming in the Arctic may result in the negative effects of increased biodiversity. Polarforschung 78 (3), 105—108.

Weslawski, J.M., Wiktor jr., J., Kotwicki, L., 2010. Increase in biodiversity in the Arctic rocky littoral, Sorkappland, Svalbard after 20 years of climate warming. Mar. Biodivers. 40 (2), 123—130, http://dx.doi.org/10.1007/s12526-010-0038-z.

Weslawski, J.M., Włodarska-Kowalczuk, M., Kędra, M., Legeżyńska, J., Kotwicki, L., 2012. Eight species that rule today's European Arctic fjord benthos. Pol. Polar Res. 33 (3), 225—238, http://dx.doi.org/10.2478/v10183-012-0016-1.

Węsławski, J.M., Szczucka, J., Głuchowska, M., Ormańczyk, M., Hoppe, Ł., Schmidt, B., Promińska, A., Kwaśniewski, S., Berge, J., Deja, K., Fey, D.P., 2016. A comparative study of the fish community in two fjords on Svalbard. J. Mar. Syst. (submitted for publication).

Weydmann, A., Søreide, J.E., Kwasniewski, S., Leu, E., Falk-Petersen, S., Berge, J., 2013. Ice-related seasonality in zooplankton community composition in a high Arctic fjord. J. Plankton Res. 35 (4), 831—842, http://dx.doi.org/10.1093/plankt/fbt031.

Weydmann, A., Carstensen, J., Goszczko, I., Dmoch, K., Olszewska, A., Kwasniewski, S., 2014. Shift towards the dominance of boreal species in the Arctic: inter-annual and spatial zooplankton variability in the West Spitsbergen Current. Mar. Ecol.-Prog. Ser. 501, 41—52, http://dx.doi.org/10.3354/meps10694.

Włodarska-Kowalczuk, M., 2007. Molluscs in Kongsfjorden (Spitsbergen, Svalbard): a species list and patterns of distribution and diversity. Polar Res. 26 (1), 48—63, http://dx.doi.org/10.1111/j.1751-8369.2007.00003.x.

Worm, B., Barbier, E.B., Beraumont, J.E., Duffy, C., Folke, B.S., Halpern, J.B.C., Jackson, J.B.C., Lotze, H.K., Micheli, F., Palumbi, S.R., Sala, E., Selkoe, K.A., Stachowicz, J.J., Watson, R., 2006. Impacts of biodiversity loss on ecosystem services. Science 314 (5800), 787—790, http://dx.doi.org/10.1126/science.1132294.

Zaborska, A., Włodarska-Kowalczuk, M., Legeżyńska, J., Jankowska, E., Winogradow, A., Deja, K., 2016. Sedimentary organic matter sources, benthic consumption and burial in west Spitsbergen fjords — signs of maturing of Arctic fjordic systems? J. Mar. Syst., (in press), http://dx.doi.org/10.1016/j.jmarsys.2016.11.005.

Oceanologia (2017) 59, 603—611

Available online at www.sciencedirect.com

ScienceDirect

journal homepage: www.journals.elsevier.com/oceanologia/

RESEARCH NOTE

Can seabirds modify carbon burial in fjords?

Jan Marcin Węsławski [a,*], Jacek Urbański [c], Marta Głuchowska [a], Katarzyna Grzelak [a], Lech Kotwicki [a], Sławomir Kwaśniewski [a], Joanna Legeżyńska [a], Józef Wiktor [a], Maria Włodarska-Kowalczuk [a], Agata Zaborska [a], Marek Zajączkowski [a], Lech Stempniewicz [b]

[a] *Institute of Oceanology, Polish Academy of Sciences, Sopot, Poland*
[b] *Department of Vertebrate Ecology and Zoology, University of Gdańsk, Poland*
[c] *GIS Centre, University of Gdańsk, Poland*

Received 8 July 2016; accepted 30 January 2017
Available online 7 June 2017

KEYWORDS
Arctic;
Svalbard;
Fjords;
Carbon;
Seabirds

Summary Two high latitude fjords of Spitsbergen (Hornsund 77°N and Kongsfjorden 79°N) are regarded as being highly productive (70 g and 50 gC m^{-2} $year^{-1}$) and having organic-rich sediments. Hornsund has more organic matter in its sediments (8%), nearly half of it of terrestrial origin, while most of that in Kongsfjorden (5%) comes from fresh, marine sources (microplankton). Analysis of the carbon sources in both fjords shows that a major difference is the much larger seabird population in Hornsund-dominated with over 100 thousands pairs of plankton feeding little auks in Hornsund versus 2 thousand pairs in Kongsfjorden, and marine food consumption estimated as 5573 tonnes of carbon in Hornsund, versus 3047 tonnes in Kongsfjorden during one month of chick feeding period. Seabird colonies supply rich ornithogenic tundra (595 tonnes of C, as against only 266 tonnes of C in the Kongsfjorden tundra). No much of the terrestrial carbon, flushed out or wind-blown to the fjord, is consumed on the seabed — a state of affairs that is reflected by the low metabolic activity of bacteria and benthos and the lower benthic biomass in Hornsund than in Kongsfjorden.

* Corresponding author at: Institute of Oceanology, Polish Academy of Sciences, Powstańców Warszawy 55, 81-712 Sopot, Poland. Tel.: +48 58731171884.
E-mail address: weslaw@iopan.gda.pl (J.M. Węsławski).
Peer review under the responsibility of Institute of Oceanology of the Polish Academy of Sciences.

Production and hosting by Elsevier

http://dx.doi.org/10.1016/j.oceano.2017.01.006

1. Introduction

Carbon burial in Arctic fjords has recently become the focus of international research efforts, as these coastal areas have been recognized as being disproportionally (to their area) important as regards the carbon sink in the Arctic (Smith et al., 2015). General information on carbon in the Svalbard archipelago sediments was given by Winkelmann and Knies (2005). Coastal areas and fjords of the Svalbard archipelago are characterized by turbid waters derived from intense glacial discharge (Görlich et al., 1987). The Spitsbergen fjords Kongsfjorden and Hornsund are among the best studied Arctic areas (e.g. Hop et al., 2002; Svendsen et al., 2002), from where the most complete data sets are available for modelling and synthesis. Other well-studied Arctic fjords are Godhabsfjord and Young Sound on Greenland (Glud and Rysgaard, 2007), from which detailed information about carbon cycling is available. The data already published indicates that the organic carbon contents in Hornsund and Kongsfjorden differ markedly, since Hornsund is dominated by terrestrial carbon, whereas Kongsfjorden exhibits a higher proportion of fresh marine carbon (Koziorowska et al., 2016; Zaborska et al., 2016). Both fjords receive extensive glacial meltwater discharges estimated at between 0.4 and 1.5 km^{-3} per year (Węsławski et al., 1995). Terrestrial carbon in marine sediments is regarded as a low-quality energy source and should first be transformed by heterotrophic bacteria before it can enter the food web (Glud et al., 1998). There have already been reports on the importance of refractory carbon in Svalbard sediments (Kim et al., 2011). There are several scenarios that may explain the extensive proportion of terrestrial organic matter (OM) in Arctic fjords: washout from melting permafrost (Anderson and Macdonald, 2015), local rocks with carbon ground by glaciers (Syvitski et al., 1987), terrestrial vegetation supplied by rivers (Anderson and Macdonald, 2015; Rysgaard and Sejr, 2007) and retreating glaciers that may release old organic deposits (vegetation). In this paper, we provide data on the terrestrial vegetation around two Spitsbergen fjords against the background of published and archival data on marine carbon sources in them. Our aim is to test the hypothesis that seabirds play an important role in modifying the carbon budget in Arctic fjords.

2. Material and methods

2.1. Marine biogeochemical sampling

Summer data from 2015 were used for calculating the organic carbon distribution in biota and sediments (stations as in Fig. 1). The three sampling stations in both fjords were carefully selected in order to: (1) represent the central fjord basin, (2) be comparable between and within the fjord, thus the flat, even, soft sediment seabed at 100 m depth was chosen and (3) create a replicate representative for the central fjord basin — the three selected stations were separated by less than 1 N m between each other. As routinely three replicates were collected for each type of sample on each of the three stations, finally at least nine samples of every type were taken from the fjord. All samples were collected during the same cruise in the period of one week in July 2015.

The top 2 cm of sediment was collected from 30 cm long Niemistö cores, and sediment slices were analyzed according to the procedure described in Zaborska et al. (2016). Meiofauna was collected from 10 cm × 10 cm Box Core samples, 2 cm diameter subsamples were collected and analyzed as described in Grzelak et al. (2016), and macrofauna was sampled using Van Veen grabs. All water column samples were collected from the same sites during the same sampling campaign, and details on the methodology are presented in specific works that are cited in Tables 2 and 3. The most important for this paper were carbon analyses, performed in a specialized analytical lab at IO PAN with the use of CHN analyser. The bacterial count in the water column and sediment is given in Ameryk et al. (2017). The pelagic organisms were assessed in Ormanczyk et al. (2017). For recalculating biomass to carbon where no specific data were available, we used, following Kleiber (1961) the relationship: 1 g organism wet weight = 0.25 g dry weight = 0.1 g C = 1 cal = 4.184 J. The carbon consumption by seabirds was recalculated from joules after Węsławski et al. (2006).

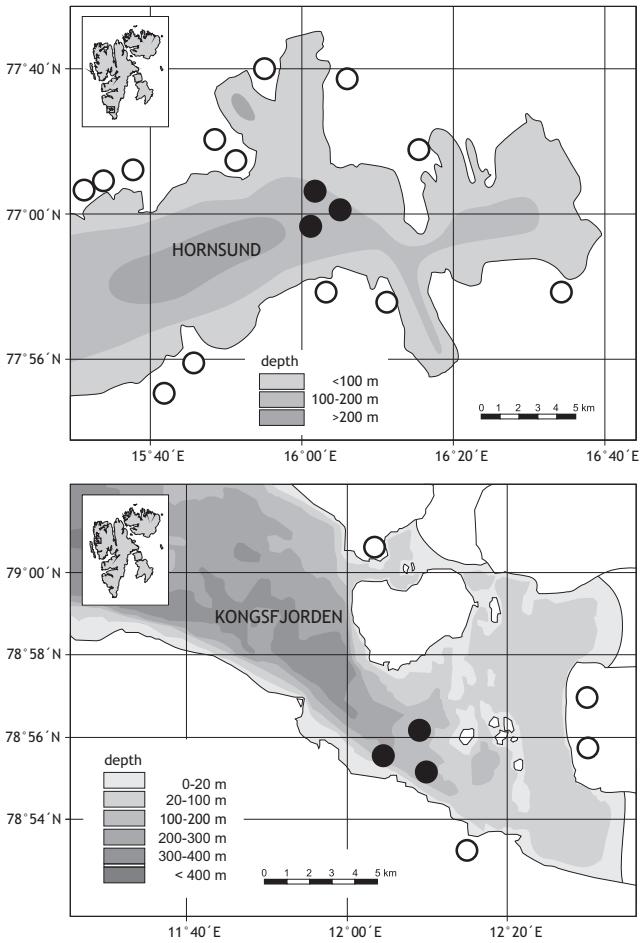

Figure 1 Study area: black dots — sampling stations of marine biota and sediments in 2013–2014; open circles denote major seabird colonies.

2.2. Study area

Two west Spitsbergen fjords of similar size – Hornsund (77°N) 300 km^2 and Kongsfjorden (79°N) 210 km^2 – have been extensively studied in recent years (see reviews in Drewnik et al., 2016; Görlich et al., 1987; Hop et al., 2002; Svendsen et al., 2002; Węsławski et al., 2017). In many respects the two sites are similar: the occurrence of rapidly melting tidal glaciers, a thick layer of glaciomarine sediments, the absence of a sill in the outer fjord, the ice cover limited to the innermost basins. In general, the shallower Hornsund is more exposed to coastal and cold local waters of Atlantic/Arctic origin, whereas the deeper Kongsfjorden has a good connection with the outer shelf through a deep renna (furrow), which directs warm Atlantic waters into the fjord. Hornsund is dominated by large colonies of little auks, accompanied by kittiwakes and Brünnich's guillemots, whereas much smaller and less dense colonies are present in Kongsfjorden (Węsławski et al., 2006). The seabird colonies in the two fjords have been studied with regard to bird density, foraging, guano production and its influence on ornithogenic tundra plant and animal communities by many authors (Hop et al., 2002; Isaksen and Bakken, 1995; Jakubas et al., 2008; Skrzypek et al., 2015; Stempniewicz et al., 2007; Stempniewicz, 1990; Wojczulanis-Jakubas et al., 2008; Zmudczyńska et al., 2012; Zmudczyńska-Skarbek et al., 2015; Zwolicki et al., 2013).

2.3. GIS methodology

The Digital Elevation Model of the Svalbard archipelago with a spatial resolution of 20 m was used to delineate the Hornsund and Kongsfjorden watershed areas. The model is the result of an ongoing project of the Norwegian Polar Institute: it is generated mainly from stereo models and partly from elevation contours, lakes and coastlines. For our project, we used the model updated on 14.01.2015 (Norwegian Polar Institute, 2014). Landsat 8 is the latest satellite in the Landsat Project and has been operational since June 2014; its image quality and geometric accuracy is superior to its predecessors. Cloudless images of the area of interest were acquired from GloVis Viewer (available from the U.S. Geological Survey) to cover the entire watershed areas in summer. For Hornsund the images were taken on 31 July 2015 and for an additional small part of this fjord on 6 July 2015. For Kongsfjorden the image was taken on 7 August 2015. In addition, the vegetation cover on four homogeneous areas by Hornsund was recorded photographically on 1 August 2015. The borders of the polygons with a mean area of 0.3 ha were determined using GPS.

ArcGIS software (ESRI, 2015) was the main data processing tool. The DEM model was preprocessed to match the glacier margins on the satellite images by clipping the land part of DEM by land polygons. The watershed areas were delineated using a standard spatial analysis procedure that uses a flow direction raster. Each band of Landsat scenes was first converted to TOA reflectance with correction for the Sun's angle according to the USGS Landsat 8 product instructions (USGS, 2015). Following this, an atmospheric correction using dark object subtraction (DOS) was carried out, assuming as 1% surface reflectance from dark objects (Chavez, 1988).

The intensity and density of green vegetation can be estimated using the remote-sensing Normalized Differential Vegetation Index (NDVI). This index is often used because it compensates for variable factors like illumination, slopes and aspects (Lillesand et al., 2004). Two bands are used to calculate this index: the red band (R), with a high absorption of chlorophyll, and the near-infrared band (NIR), which accounts for the relatively high reflectance of vegetation. The difference in reflectance of the two bands is divided by the sum of reflectances in the same two bands to normalize for differing illumination conditions (NDVI = (NIR – R)/(NIR + R)). Using the corrected reflectance for bands 4 and 5 of Landsat 8, the NDVI indexes were calculated for both watershed areas as raster layers with a spatial resolution of 30 m.

NDVI has been used by several researchers for modelling numerous biophysical properties of arctic tundra, including the above-ground phytomass. The quantitative phytomass sampling method was described by Walker et al. (2003) and then used by other researchers (Johansen and Tømmervik, 2013; Raynolds et al., 2006). They all used the regression model to find the relation between NDVI and phytomass. Several researchers discovered linear relationships between NDVI and phytomass, but for a larger range of NDVI the relationship takes a curved form (Raynolds et al., 2006). In our project we used the formula originally proposed by Walker et al. (2003) and modified by Raynolds et al. (2006) in the form Phytomass = 26.58 * EXP(6.9357 * NDVI). This formula gives similar results to the one used by Johansen and Tømmervik (2013) for Svalbard. However, the main limitation of their formula is the narrower range of NDVI values than those we obtained. As low phytomass values ($<$200 g m^{-2}) in Svalbard conditions indicate a partial cover of mainly lichen and moss with no peat layer, the contribution of such a vegetation subzone to the carbon flux as a result of surface run-off will be negligible. Consequently, only phytomass values $>$200 g m^{-2} were summed for both watershed areas (Table 1). According to Walker et al. (2003) this method in similar conditions of Alaska gave a relative standard errors of about 15% of estimated values.

3. Results

The areas analyzed for terrestrial vegetation ranged from 1150 km^2 in Hornsund to 1449 km^2 in Kongsfjorden (Fig. 2). Four types of terrestrial vegetation were identified for the biomass calculations (Fig. 3a) (a) sparse, dry vegetation on stony and gravel substrata, (b) poor moss tundra on semi-dry land, (c) wet rich moss tundra and (d) rich ornithogenic vegetation with variable plants and a high biomass. Four categories of biomass were associated with the areas of particular vegetation types (Table 1). The overall calculation yields 595 tonnes of carbon in the terrestrial vegetation around Hornsund, compared to 266 tonnes in the Kongsfjorden area.

4. Discussion

How representative are presented data for the seasons, interannual variability and regional scale? The circulation models published for the Spitsbergen fjords (Ingvaldsen

Table 1 Areas and land vegetation biomass (July–August 2015).

Biomass class [wet weight g m^{-2}]	Hornsund [km^{-2}]	Hornsund estimated biomass (595 tonnes C)	Kongsfjord [km^{-2}]	Kongsfjord estimated biomass (266 tonnes C)
0–100	115	42	168	47.12
100–250	14	156	22	147
250–500	5	345	2.8	323
500–1000	2.6	695	0.81	698
1000–2500	1.1	1421	0.33	1453
2500–more	0.08	3135	0.027	2905

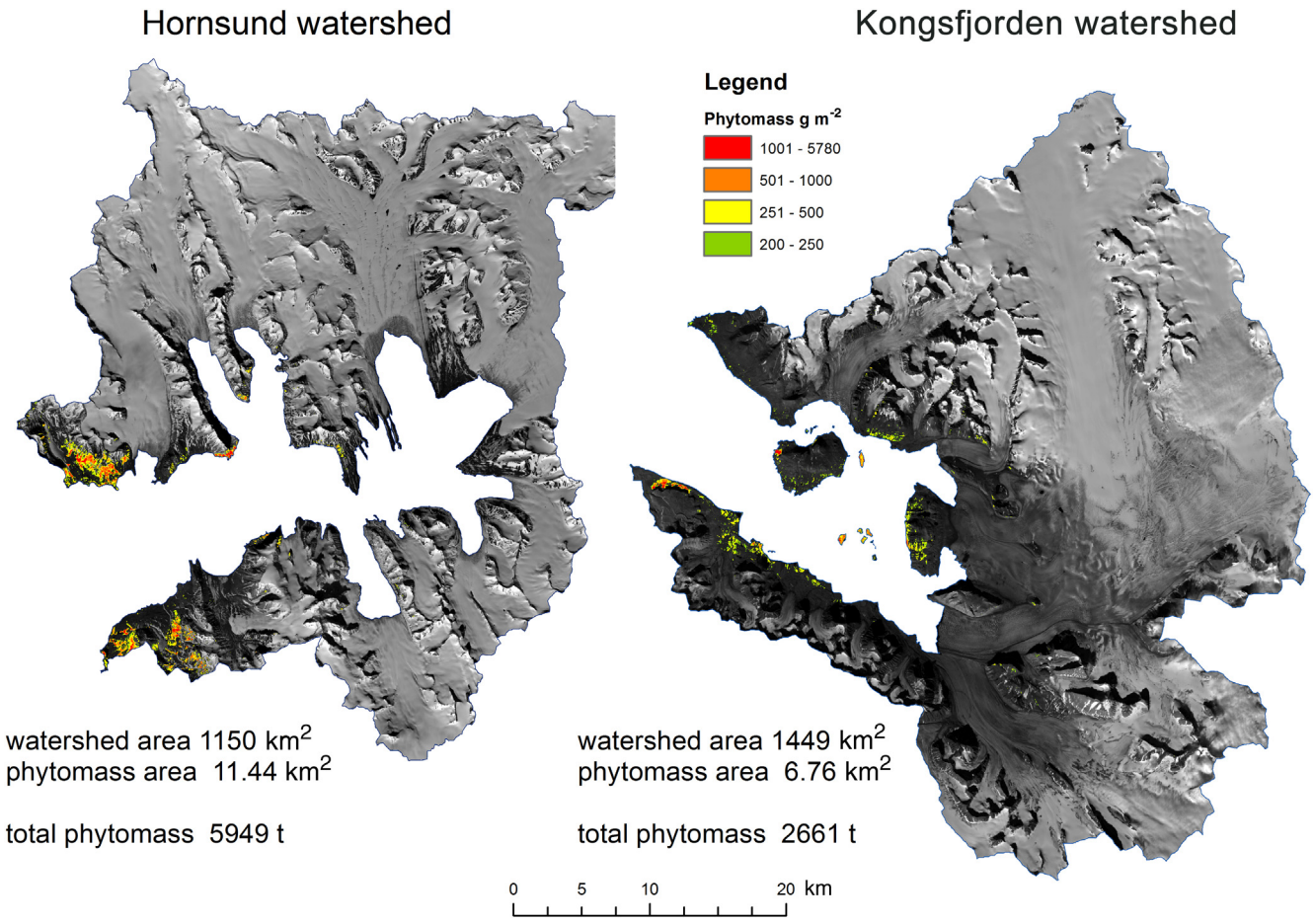

Figure 2 Hornsund and Kongsfjorden water shed areas and terrestrial vegetation cover.

et al., 2001; Jakacki et al., 2017) show that our sampling sites were placed in the gyre that is formed in the central fjord part, and is separated hydrologically from both innermost fjord basins (where the water used to be more stagnant) and outer fjord part (with frequent water exchange with shelf). The seasonal aspect (samples were collected in the mid of summer) represents situation after the peak of vegetation period and settling the bloom in Spitsbergen fjords (Węsławski et al., 1988). As most of the benthos of Svalbard are long living (perennial) species, the seasonal difference in biomass and density is low (Berge et al., 2015), and summer sampling shows the peak of the annual growth, the general – annual situation. Carbon accumulation in the sediment is an integrated value of year-long processes and is not very changeable (Pawłowska et al., 2011), hence our data are comparable in two analyzed fjords and likely representative for the given spatial scale and time.

Seston (dead organic matter suspended in the water column) contributes 45% of the carbon in Hornsund and 33% in Kongsfjorden (Table 2). The carbon stored in living organisms (biomass) in the water column differs between fjords in some important aspects: there are more bacteria and microplankton in Hornsund, whereas macroplankton is more important in Kongsfjorden (Fig. 4).

The percentage of detritus in sedimentary organic carbon is even higher than in the water column, with values of 97%

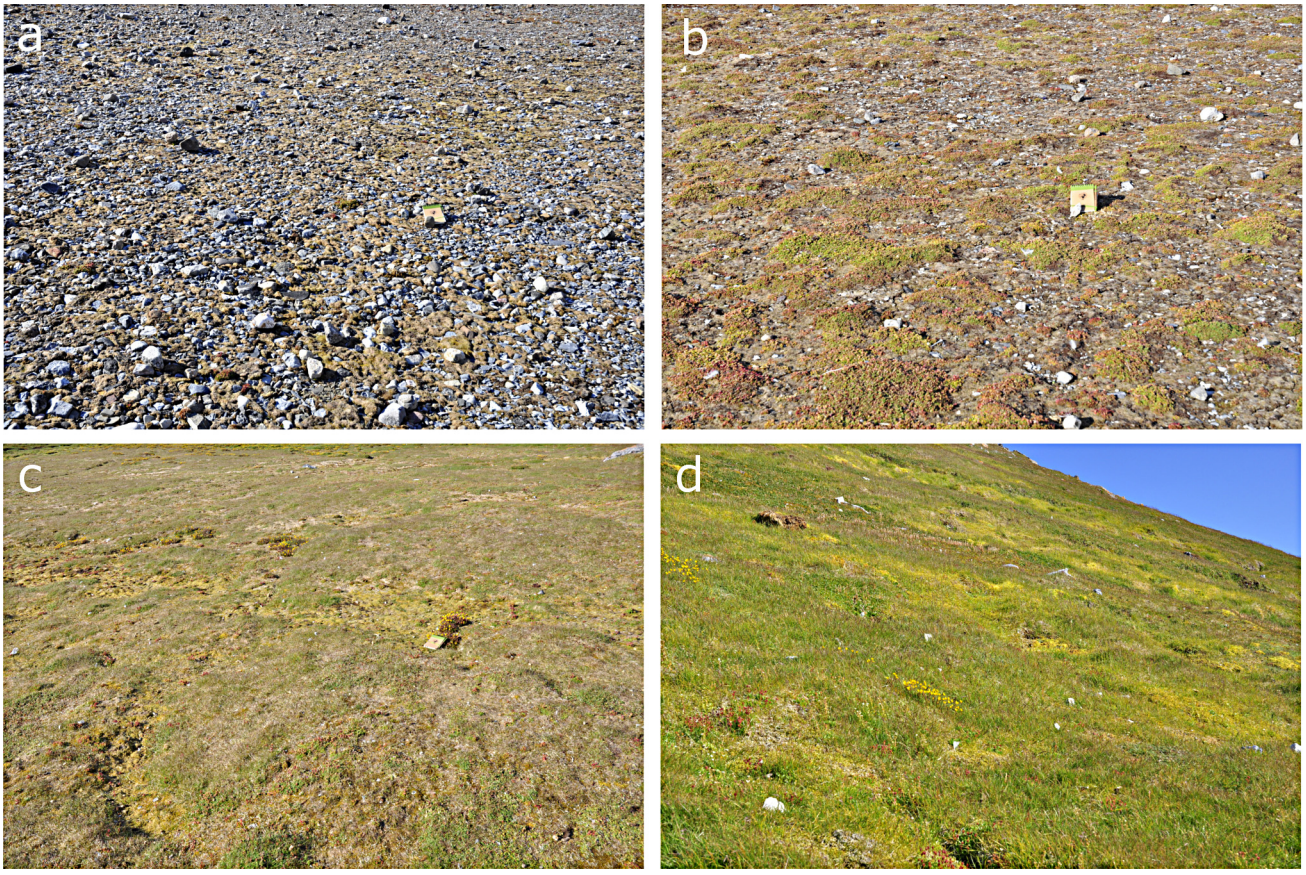

Figure 3 Types of terrestrial vegetation used for calculating biomass in Hornsund and Kongsfjorden.

Table 2 Carbon sources in both fjords (summer biomass values); the total carbon content calculated for each fjord is given in brackets.

Biomass source	Hornsund	Kongsfjorden	Reference
Microplankton [gC m^{-2}] (100 m water column)	0.8 (94 tC)	2.5 (70 tC)	Smoła et al. (2016)
Mesozooplankton [gC m^{-3}]	0.050 (549 tC)	0.075 (893 tC)	Ormanczyk et al. (2017)
Macroplankton [gC m^{-3}]	0.040 (140 tC)	0.135 (415 tC)	Ormanczyk et al. (2017)
Fish [tC $fjord^{-1}$]	2.2	18.8	Szczucka et al. (2017)
Pelagic bacteria [gC m^{-2}] (100 m water column)	1.2	0.7	Ameryck et al. (2017)
Meiofauna [gC m^{-2}] (top 1 cm)	0.45 (58 tC)	0.2 (63 tC)	Grzelak et al. (2016)
Macrofauna [gC m^{-2}]	4 (791 tC)	10 (1413 tC)	Zaborska et al. (2016)
Benthic bacteria [gC m^{-2}] (top 1 cm)	0.11	0.52	Ameryck et al. (2017)
Macroalgae [tC $fjord^{-1}$]	1282	1936	Smoła et al. (2016)
Terrestrial vegetation [tC $fjord^{-1}$] watershed area	600	290	Present work
Food consumed by sea birds in July (30 days) [tC $fjord^{-1}$]	5573	3047	Węsławski et al. (2006)
Organic carbon in suspended matter [mgC dm^{-3}]	0.19	0.33	Present work

and 81% in Hornsund and Kongsfjorden, respectively (Table 2). The biomass proportion in the sediment shows the greater importance of meiofauna in Hornsund and the greater significance of macrofauna in Kongsfjorden (Fig. 5).

Carbon accumulation and burial is greater in Hornsund (Table 3), whereas carbon mineralization is disproportionally higher (3 vs. 50%) in Kongsfjorden, owing to the fresh, marine origin of organic matter (up to 50% in Hornsund and up to 80% in Kongsfjorden) (Table 3). The rates of carbon accumulation in the surface sediments of both fjords are almost equal (42.6 and 32.5 gC m^{-2} $year^{-1}$), although the carbon content per gram of sediment in Hornsund is more than twice as high as in Kongsfjorden (Table 2). These differences result from the fact that the sediment accumulation rate in Kongsfjorden is twice as fast as in Hornsund. Carbon accumulation in the surface sediments of both fjords was higher than the highest values reported for Storfjorden in Svalbard — from 5.5 to 17.2 gC m^{-2} $year^{-1}$ (Winkelmann and Knies, 2005) — as well

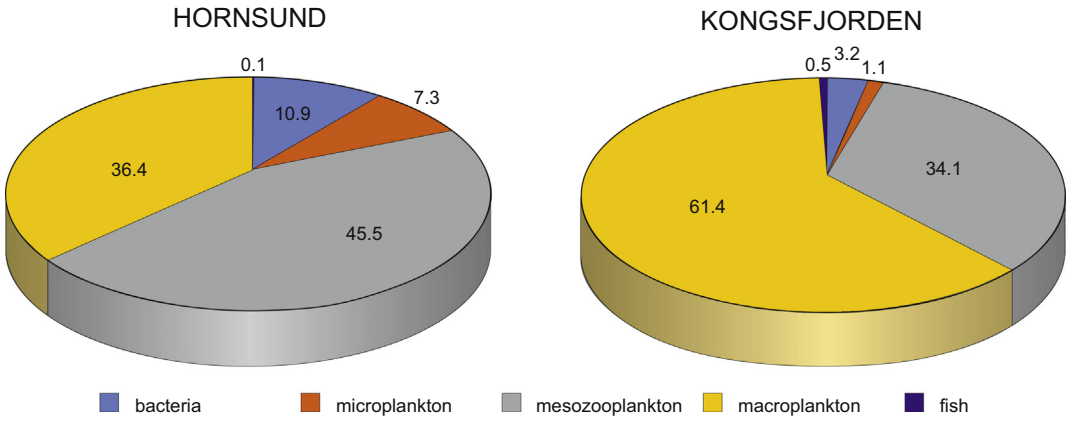

Figure 4 Percentage of biomass in the water column of the two fjords — expressed in gC m^{-3} (for data, see Table 2).

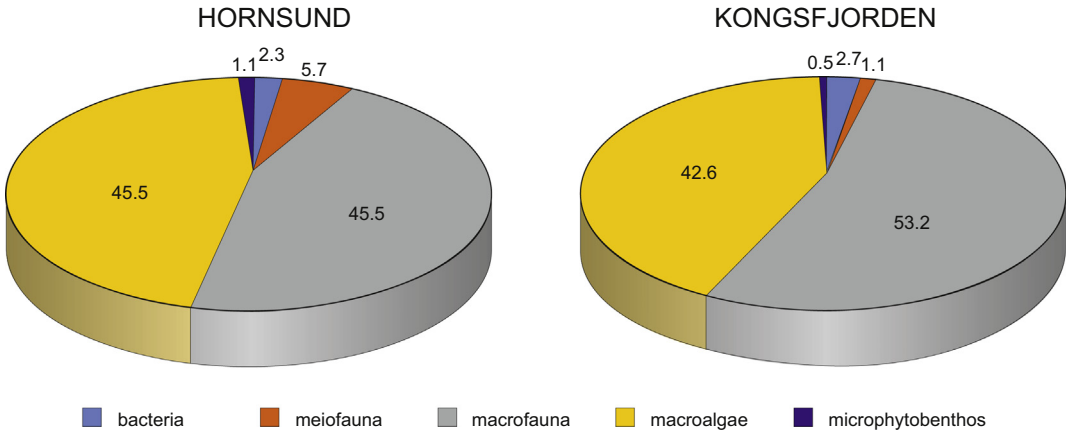

Figure 5 Percentage of organic carbon in sediment — expressed in gC m^{-2} (for data, see Table 2).

Table 3 Carbon fate in the two fjords.

Process	Hornsund	Kongsfjorden
Carbon content in sediment [gC m^{-3}] (top 1 cm)	252.4	98.3
Carbon content in sediment [mg g^{-1}]	14.2	5.46
Carbon accumulation [gC m^{-2} $year^{-1}$] (top 1 cm)	43.2	32.5
Mass accumulation rate of sediment [g m^{-2} $year^{-1}$]	3041	5947
Carbon burial [gC m^{-2} $year^{-1}$]	41.4	16.3
Carbon mineralization (in top 20 cm) [gC m^{-2} $year^{-1}$]	1.3 (3%)	16.2 (50%)

Modified from Zaborska et al. (2016).

as those from a Greenland fjord (Glud et al., 1998). In Young Sound (NE Greenland), the benthic carbon mineralization was 70% per annum (Thamdrup et al., 2007).

In general, the seabirds in Spitsbergen colonies feed their nestlings between mid-July and mid-August. During that brief period most of the marine food is carried to the colonies, where excreta and food remnants discarded by juveniles and adults become buried; during the rest of the year, the birds feed and excrete mostly away from the nesting area (Stempniewicz et al., 2007; Stempniewicz, 1990). Carbon burial is effectively enhanced in a bird-dominated fjord, compared to a bird-poor fjord (Figs. 6 and 7).

The type of the seabirds' food plays a substantial role in biogeochemistry: Zwolicki et al. (2013) presented the difference in N and P deposition in two types of seabird colonies in Hornsund: more P in fish eaters (kittiwakes and Brünnich's guillemots) and more N in the colonies of crustacean eaters (little auks).

Assumptions of the birds excreta nutrition effect on the coastal marine ecosystem and relations between bird colony

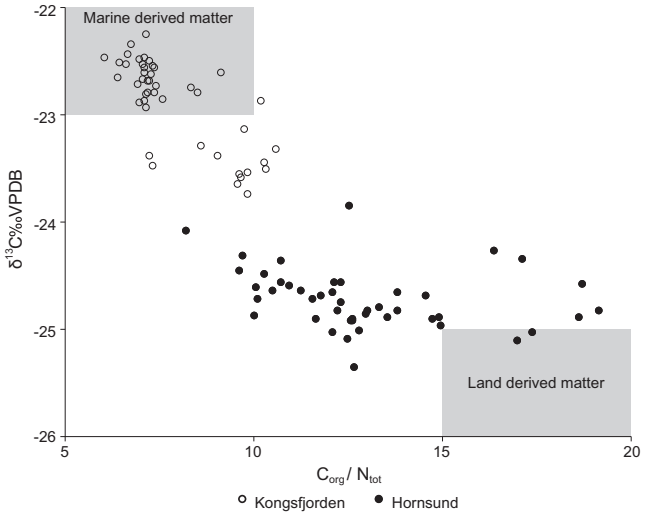

Figure 6 Origin and degree of degradation of organic matter in surface sediments in Kongsfjorden and Hornsund. Modified from Zaborska et al. (2016).

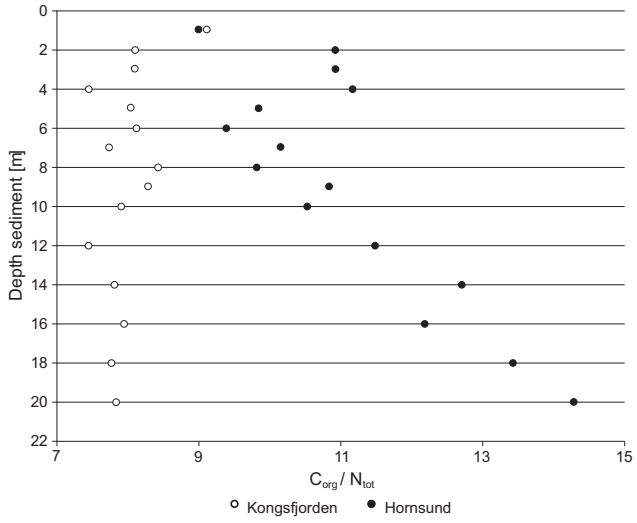

Figure 7 Degree of decomposition of organic matter in surface sediments (Kongsfjorden and Hornsund). Modified from Zaborska et al. (2016).

and adjacent waters were discussed in the literature (Stempniewicz, 1990; Wainright et al., 1998; Zelickman and Golovkin, 1972).

Assuming here that 10% of the terrestrial plant biomass is lost annually through weathering and being washed into the sea, we obtained 0.2 gC m^{-2} of seabed, whichmakes an important contribution to the carbon balance of the fjords. If to this we add direct input from seabirds — assuming that 10% of the seafood delivered to the colonies ends up there as excreta and leftovers — we have at least 500 and 300 tonnes of C delivered to the two fjords annually (during one month of chick feeding), an amount similar to that estimated from tundra carbon.

The high percentage of terrestrial organic matter can be explained by the higher amount of organic carbon stored in the ornithogenic tundra (Table 3), which yields 595 and 266 tonnes of carbon in Hornsund and Kongsfjorden, respectively.

Another possible explanation for the disproportionally high terrestrial proportion of organic carbon in Hornsund might be a riverine outflow. However, there are only small rivers in both areas, discharging between 0.03 and 0.095 km^3 $year^{-1}$ according to Lefauconnier (personal communication) and Węsławski et al. (1995). This is in contrast to Young Sound (NE Greenland), where a riverine discharge ranges from 0.1 to 0.3 km^3 per annum (Mernild et al., 2007), thereby providing 1–6 thousand tonnes of terrestrial carbon, which is equal to 40% of the local sediment carbon pool (Mernild et al., 2007; Rysgaard and Sejr, 2007).

The different rocks that are ground by the glaciers may also carry different carbon loads, but there is no statistical difference in the proportion of organic carbon in glacial suspensions in the two fjords (Zaborska et al., 2016). Suspended POC in both fjords contains almost pure marine fresh carbon in summer (Zaborska et al., 2016), which suggests that terrestrial carbon is delivered as a bedload transport or that it sinks faster than the marine component. A further possibility, but which is very difficult to verify, is the release of organic deposits from below the glacier foot (tundra) from previous warm periods (the climate optimum 7–9 thousand years ago) — J. Jania, personal communication. Yet another possibility of terrestrial carbon transport is advection, often regarded as a key factor in fjord biogeochemistry (Aksnes et al., 1989), but the West Spitsbergen Current that supplies water to both fjords does not carry measurable amounts of terrestrial carbon (Kuliński et al., 2014; Winkelmann and Knies, 2005).

There is a growing amount of information that glaciers may supply fjords with much more than freshwater alone — there are nutrients, organic carbon from aerial deposition, mineral and refractory carbon as well as the microbes (Hagvar et al., 2016; Wynn et al., 2007).

We need to learn more about the melting glacier contribution to carbon budget in fjords, yet from the information available the seabirds and their nutrition input into ornithogenic tundra are the most likely explanation of high values of terrestrial carbon in Hornsund fjord sediments.

Acknowledgements

This paper was funded by the NCN GAME project — Polish National Science Centre No. DEC-2012/04/A/NZ8/00661 and the GLAERE project of Norwegian Funding Mechanism.

References

Aksnes, D.L., Aure, J., Kaartvedt, S., Magnesen, T., Richard, J., 1989. Significance of advection for the carrying capacities of fjord populations. Mar. Ecol.-Prog. Ser. 50 (3), 263—274, http://dx.doi.org/10.3354/meps050263.

Ameryk, A., Jankowska, K.M., Kalinowska, A., Węsławski, J.M., 2017. Comparison of bacterial production in the water column between two Arctic fjords, Hornsund and Kongsfjorden (West Spitsbergen). Oceanologia 59 (4), 496—507, http://dx.doi.org/10.1016/j.oceano.2017.06.001.

Anderson, L.G., Macdonald, R.W., 2015. Observing the Arctic Ocean carbon cycle in a changing environment. Polar Res. 34 (1), 26891, http://dx.doi.org/10.3402/polar.v34.26891.

Berge, J., Renaud, P.E., Darnis, G., Cottier, F., Last, K., Gabrielsen, T. M., Johnsen, G., Seuthe, L., Weslawski, J.M., Leu, E., Moline, M., Nahrgang, J., Søreide, J.E., Varpe, O., Lønne, O.J., Daase, M., Falk-Petersen, S., 2015. In the dark: a review of ecosystem processes during the Arctic polar night. Prog. Oceanogr. 139, 258—271, http://dx.doi.org/10.1016/j.pocean.2015.08.005.

Chavez, P.S., 1988. An improved dark — object subtraction technique for atmospheric scattering correction of multispectral data. Remote Sens. Environ. 24 (3), 459—479, http://dx.doi.org/10.1016/0034-4257(88)90019-3.

Drewnik, A., Węsławski, J.M., Włodarska-Kowalczuk, M., Łącka, M., Romińska, A., Zaborska, A., Głuchowska, M., 2016. From the worm's point of view. Physical environment of an Arctic fjord benthos. Polar Biol. 39 (8), 1411—1424, http://dx.doi.org/10.1007/s00300-015-1867-9.

ESRI, 2015. ArcGIS Desktop: Release 10.3. Environ. Syst. Res. Inst., Redlands, CA.

Glud, R.N., Holby, O., Hoffmann, F., Canfield, D.E., 1998. Benthic mineralization and exchange in Arctic sediments (Svalbard, Norway). Mar. Ecol.-Prog. Ser. 173, 237—251, http://dx.doi.org/10.3354/meps173237.

Glud, R.N., Rysgaard, S., 2007. The annual organic carbon budget of Young Sound, NE Greenland. In: Rysgaard, S., Glud, R.N. (Eds.), Carbon Cycling in Arctic Marine Ecosystems: Case Study Young Sound. Meddr. Grønland, Bioscience, vol. 58, 194—203.

Görlich, K., Węsławski, J.M., Zajączkowski, M., 1987. Suspensions settling effect on macrobenthos biomass distribution in the Hornsund fjord, Spitsbergen. Polar Res. 5 (2), 175—192.

Grzelak, K., Głuchowska, M., Gregorczyk, K., Winogradowa, A., Weslawski, J.M., 2016. Nematode biomass and morphometric attributes as biological indicators of local environmental conditions in Arctic fjords. Ecol. Indic. 69, 368—380, http://dx.doi.org/10.1016/j.ecolind.2016.04.036.

Hagvar, S., Ohlson, M., Brittain, J.E., 2016. A melting glacier feeds aquatic and terrestrial invertebrates with ancient carbon and supports early succession. Arctic Antarctic Alpine Res. 48 (3), 551—562, http://dx.doi.org/10.1657/AAAR0016-027.

Hop, H., Pearson, T., Hegseth, E.N., Kovacs, K.M., Wiencke, C., Kwasniewski, S., Eiane, K., Mehlum, F., Gulliksen, B., Włodarska-Kowalczuk, M., Lydersen, C., Weslawski, J.M., Cochrane, S., Gabrielsen, G.W., Leakey, R.J.G., Lønne, O.J., Zajaczkowski, M., Falk-Petersen, S., Kendall, M., Wängberg, S.-Å., Bischof, K., Voronkov, A.Y., Kovaltchouk, N.A., Wiktor, J., Poltermann, M., di Prisco, G., Papucci, C., Gerland, S., 2002. The marine ecosystem of Kongsfjorden, Svalbard. Polar Res. 21 (1), 167—208.

Ingvaldsen, M., Reitan, M.B., Svendsen, H., Asplin, L., 2001. The upper layer circulation in Kongsfjorden and Krossfjorden — a complex fjord system on the west coast of Spitsbergen. Mem. Nat. Inst. Polar Res. 54 (SI), 393—407.

Isaksen, K., Bakken, V. (Eds.), 1995. Seabird Populations in the Northern Barents Sea: Source Data for the Impact Assessment of the Effects of Oil Drilling Activity, Meddelelser, vol. 135, 136 pp.

Jakacki, J., Przyborska, A., Kosecki, S., 2017. Modelling of the Svalbard fjord, Hornsund. Oceanologia 59 (4), 473—495, http://dx.doi.org/10.1016/j.oceano.2017.04.004.

Jakubas, D., Zmudczyńska, K., Wojczulanis-Jakubas, K., Stempniewicz, L., 2008. Faeces deposition and numbers of vertebrate herbivores in the vicinity of planktivorous and piscivorous seabird colonies in Hornsund, Spitsbergen. Pol. Polar Res. 29 (1), 45—58.

Johansen, B., Tømmervik, H., 2013. The relationship between phytomass, NDVI and vegetation communities on Svalbard. Int. J. Appl. Earth Obs. 27 (Pt. A), 20—30, http://dx.doi.org/10.1016/j.jag.2013.07.001.

Kim, J.-H., Peterse, F., Willmott, V., Klitgaard Kristensen, D., Baas, M., Schouten, S., Sinninghe Damste, J.S., 2011. Large ancient organic matter contributions to Arctic marine sediments (Svalbard). Limnol. Oceanogr. 56 (4), 1463—1474, http://dx.doi.org/10.4319/lo.2011.56.4.1463.

Koziorowska, K., Kulinski, K., Pempkowiak, J., 2016. Sedimentary organic matter in two Spitsbergen fjords: terrestrial and marine contributions based on carbon and nitrogen contents and stable isotopes composition. Cont. Shelf Res. 113, 38—46, http://dx.doi.org/10.1016/j.csr.2015.11.010.

Kuliński, K., Kędra, M., Legeżynska, J., Gluchowska, M., Zaborska, A., 2014. Particulate organic matter sinks and sources in high Arctic fjord. J. Mar. Syst. 139, 27—37, http://dx.doi.org/10.1016/j.jmarsys.2014.04.018.

Lillesand, T.M., Keifer, R.W., Chipman, J.W., 2004. Remote Sensing and Image Interpretation, 5th edn., Wiley, New York, 804 pp.

Mernild, S.H., Sigsgaard, C., Rasch, M., Hasholt, B., Hansen, B.U., Stjernholm, M., Petersen, D., 2007. Climate, river discharge and suspended sediment transport in the Zackenberg River drainage basin and Young Sound/Tyrolerfjord, Northeast Greenland, 1995—2003. In: Rysgaard, S., Glud, R.N. (Eds.), Carbon Cycling in Arctic Marine Ecosystems: Case Study Young Sound. Meddr. Grønland, Bioscience, vol. 58., 23—43.

Norwegian Polar Institute, 2014. Terrengmodell Svalbard (S0 Terrengmodell). Norwegian Polar Inst., Tromsø, Norway, https://data.npolar.no/dataset/dce53a47-c726-4845-85c3-a65b46fe2fea.

Ormanczyk, M., Gluchowska, M., Olszewska, A., Kwasniewski, S., 2017. Zooplankton structure in high latitude fjords with contrasting oceanography (Hornsund and Kongsfjorden, Spitsbergen). Oceanologia 59 (4), 508—524, http://dx.doi.org/10.1016/j.oceano.2017.06.003.

Pawłowska, J., Włodarska-Kowalczuk, M., Zajączkowski, M., Nygard, H., Berge, J., 2011. Seasonal variability of meio- and macrobenthic standing stocks and diversity in an Arctic fjord (Adventfjorden, Spitsbergen). Polar Biol. 34 (6), 833—845, http://dx.doi.org/10.1007/s00300-010-0940-7.

Raynolds, M.K., Walker, D.A., Maier, H.A., 2006. NDVI patterns and phytomass distribution in the circumpolar Arctic. Remote Sens. Environ. 102 (3—4), 271—281.

Rysgaard, S., Sejr, M.K., 2007. Vertical flux of particulate organic matter in high Arctic fjord. In: Rysgaard, S., Glud, R.N. (Eds.), Carbon Cycling in Arctic Marine Ecosystems: Case Study Young Sound. Meddr. Grønland, Bioscience, vol. 58., 110—119.

Skrzypek, G., Wojtuń, B., Richter, D., Jakubas, D., Wojczulanis-Jakubas, K., Samecka-Cymerman, A., 2015. Diversification of

nitrogen sources in various tundra vegetation types in the High Arctic. PLOS ONE 10 (9), e0136536, http://dx.doi.org/10.1371/journal.pone.0136536.

Smith, R.W., Bianchi, T.S., Allison, M., Savage, C., Galy, V., 2015. High rates of organic carbon burial in fjord sediments globally. Nat. Geosci. 8 (6), 450–453, http://dx.doi.org/10.1038/ngeo2421.

Smoła, Z., Tatarek, A., Wiktor, J., Wiktor, J.jr., Hapter, R., Kubiszyn, A., Weslawski, J.M., 2016. Primary producers and production in two West Spitsbergen fjords (Hornsund and Kongsfjorden) a review. Pol. Polar Res. 38 (3), http://dx.doi.org/10.1515/popore-2017-0013.

Stempniewicz, L., 1990. Biomass of dovekie excreta in the vicinity of a breeding colony. Colon. Waterbird. 13 (1), 62–66, http://dx.doi.org/10.2307/1521421.

Stempniewicz, L., Blachowiak-Samołyk, K., Weslawski, J.M., 2007. Impact of climate change on zooplankton communities, seabird populations and arctic terrestrial ecosystem – a scenario. Deep-Sea Res. Pt. II 54 (23–26), 2934–2945, http://dx.doi.org/10.1016/j.dsr2.2007.08.012.

Svendsen, H., Beszczyńska-Moller, A., Hagen, J.O., Lefauconnier, B., Tverberg, V., Gerland, S., Orbaek, J.B., Bischof, K., Papucci, C., Zajączkowski, M., Azzolini, R., Bruland, O., Wiencke, C., Winther, J.G., Dallmann, W., 2002. The physical environment of Kongsfjorden–Krossfjorden, an Arctic fjord system in Svalbard. Polar Res. 21 (1), 133–166.

Syvitski, J.P.M., Burrel, D.C., Skei, J.M., 1987. Fjords: Processes and Products. Springer-Verlag, New York, 375 pp.

Szczucka, J., Hoppe, Ł., Schmidt, B., 2017. Acoustical estimation of fish distribution and abundance in two Spitsbergen fjords. Oceanologia 59 (4), 585–591.

Thamdrup, B., Glud, R., Hansen, J.W., 2007. Benthic carbon cycling in Young Sound, Northeast Greenland. In: Rysgaard, S., Glud, R.N. (Eds.), Carbon Cycling in Arctic Marine Ecosystems: Case study Young Sound. Meddr. Grønland, Bioscience, vol. 58, 137–157.

USGS, 2015. Landsat 8 (L8) Data Users Handbook. Department of the Interior U.S. Geological Survey.

Wainright, S., Haney, J., Kerr, C., Golovkin, A.N., Flint, M.V., 1998. Utilization of nitrogen derived from seabird guano by terrestrial and marine plants at St. Paul, Pribilof Islands, Bering Sea, Alaska. Mar. Biol. 131 (1), 63–71, http://dx.doi.org/10.1007/s002270050297.

Walker, D.A., Epstein, H.E., Jia, G.J., Balser, A., Copass, C., Edwards, E.J., Gould, W.A., Hollingsworth, J., Knudson, J., Maier, H.A., Moody, A., Raynolds, M.K., 2003. Phytomass, LAI, and NDVI in northern Alaska: relationships to summer warmth, soil pH, plant functional types, and extrapolation to the circumpolar Arctic. J. Geophys. Res. 108 (D2), 8169, http://dx.doi.org/10.1029/2001JD000986 18 PDF pp.

Węsławski, J.M., Koszteyn, J., Zajączkowski, M., Wiktor, J., Kwaśniewski, S., 1995. Fresh water in the Svalbard fjord ecosystem. In: Skjoldal, H.R., Hopkins, C., Erikstad, K.E., Leinaas, H.P. (Eds.), Proceedings of the Mare Nor Symposium on the Ecology of Fjords and Coastal Waters, Tromso, Norway, 5–9 December 1994. Elsevier, Amsterdam, 229–241.

Węsławski, J.M., Kwaśniewski, S., Stempniewicz, L., Błachowiak-Samołyk, K., 2006. Biodiversity and energy transfer to top trophic levels in two contrasting Arctic fjords. Pol. Polar Res. 27 (3), 259–278.

Węsławski, J.M., Szczucka, J., Głuchowska, M., Ormańczyk, M., Hoppe, Ł., Schmidt, B., Promińska, A., Kwaśniewski, S., Berge, J., Deja, K., Fey, D.P., 2017. A comparative study of the fish community in two fjords on Svalbard. J. Marine Syst. (submitted for publication).

Węsławski, J.M., Zajaczkowski, M., Kwaśniewski, S., Jezierski, J., Moskal, W., 1988. Seasonality in an Arctic fjord ecosystem, Hornsund, Spitsbergen. Polar Res. 6 (2), 185–189, http://dx.doi.org/10.3402/polar.v6i2.6861.

Winkelmann, D., Knies, J., 2005. Recent distribution and accumulation of organic carbon on the continental margin west off Spitsbergen. Geochem. Geophy. Geosyst. 6 (9), 1–22, http://dx.doi.org/10.1029/2005GC000916.

Wojczulanis-Jakubas, K., Jakubas, D., Stempniewicz, L., 2008. Avifauna of Hornsund area, SW Spitsbergen: present state and recent changes. Pol. Polar Res. 29 (2), 187–197.

Wynn, P.M., Hodson, A.J., Heaton, T.H.E., Chenery, S.R., 2007. Nitrate production beneath a High Arctic glacier, Svalbard. Chem. Geol. 244 (1–2), 88–102.

Zaborska, A., Włodarska-Kowalczuk, M., Legeżyńska, J., Jankowska, E., Winogradow, A., Deja, K., 2016. Sedimentary organic matter sources, benthic consumption and burial in west Spitsbergen fjords – Signs of maturing of Arctic fjordic systems? J. Mar. Syst., (in press), http://dx.doi.org/10.1016/j.jmarsys.2016.11.005.

Zelickman, E.A., Golovkin, A.N., 1972. Composition, structure and productivity of neritic plankton communities near the bird colonies of the northern shores of Novaya Zemlya. Mar. Biol. 17 (3), 265–274, http://dx.doi.org/10.1007/BF00366302.

Zmudczyńska, K., Olejniczak, I., Zwolicki, A., Iliszko, L., Convey, P., Stempniewicz, L., 2012. Influence of allochthonous nutrients delivered by colonial seabirds on soil collembolan communities on Spitsbergen. Polar Biol. 35 (8), 1233–1245, http://dx.doi.org/10.1007/s00300-012-1169-4.

Zmudczyńska-Skarbek, K., Balazy, P., Kuklinski, P., 2015. An assessment of seabird influence on Arctic coastal benthic communities. J. Marine Syst. 144, 48–56, http://dx.doi.org/10.1016/j.jmarsys.2014.11.013.

Zwolicki, A., Zmudczyńska-Skarbek, K., Iliszko, L., Stempniewicz, L., 2013. Guano deposition and nutrient enrichment in the vicinity of planktivorous and piscivorous seabird colonies in Spitsbergen. Polar Biol. 36 (3), 363–372, http://dx.doi.org/10.1007/s00300-012-1265-5.

Oceanologia (2017) 59, 612—619

Available online at www.sciencedirect.com

ScienceDirect

journal homepage: www.journals.elsevier.com/oceanologia/

RESEARCH NOTE

Svalbard as a study model of future High Arctic coastal environments in a warming world

Jacek Piskozub *

Institute of Oceanology, Polish Academy of Sciences, Sopot, Poland

Received 22 June 2017; accepted 29 June 2017
Available online 18 July 2017

KEYWORDS
Arctic;
Svalbard;
Climate;
Temperature;
Sea-ice;
Clouds

Summary Svalbard archipelago, a high latitude area in a region undergoing rapid climate change, is relatively easily accessible for field research. This makes the fjords of Spitsbergen, its largest island, some of the best studied Arctic coastal areas. This paper aims at answering the question of how climatically diverse the fjords are, and how representative they are for the expected future Arctic diminishing range of seasonal sea-ice. This study uses a meteorological reanalysis, sea surface temperature climatology, and the results of a recent one-year meteorological campaign in Spitsbergen to determine the seasonal differences between different Spitsbergen fjords, as well as the sea water temperature and ice ranges around Svalbard in recent years. The results show that Spitsbergen fjords have diverse seasonal patterns of air temperature due to differences in the SST of the adjacent ocean, and different cloudiness. The sea water temperatures and ice concentrations around Svalbard in recent years are similar to what is expected most of the Arctic coastal areas in the second half of this century. This makes Spitsbergen a unique field study model of the conditions expected in future warmer High Arctic.

* Corresponding author at: Institute of Oceanology, Polish Academy of Sciences, Powstańców Warszawy 55, 81-712 Sopot, Poland. Tel.: +48 587311802; fax: +48 585512130.
E-mail address: piskozub@iopan.gda.pl.
Peer review under the responsibility of Institute of Oceanology of the Polish Academy of Sciences.

http://dx.doi.org/10.1016/j.oceano.2017.06.005

1. Introduction

Arctic Ocean and the adjacent land masses are undergoing intensive climate change (IPCC, 2013). It is a region where temperature changes are 3–4 times greater than the average for the Northern Hemisphere, as evidenced both by observational (Serreze et al., 2009) and paleo-data (Miller et al., 2010). This phenomenon, called Arctic amplification (Manabe and Stouffer, 1980), which makes the Arctic climate change caused by any global radiative forcing greater than in other climate zones, is caused by albedo changes due to the decline in sea-ice extent and land snow cover, atmospheric and oceanic heat advection, as well as changes in cloud cover and water vapour (Serreze and Barry, 2011). This amplified warming continues unabated as evidenced by some parts of the Arctic Ocean up to +4°C warmer in August 2015 than the 1982–2010 August mean in these regions (Timmermans and Proshutinsky, 2015) and lands north of 60°N being +2.9°C warmer in the period of October 2014–September 2015 than in the beginning of 20th Century, being the warmest 12 month period in the observational record beginning in 1900 (Overland et al., 2015).

The increasing Arctic temperatures go hand-in-hand with the decline of the sea-ice extent, with trends negative in all months (Simmonds, 2015), the smallest magnitude in May (-30.45×10^3 km^2 year^{-1}), and the largest in September (-88.96×10^3 km^2 year^{-1}). These trends are expected to result in seasonal sea-ice or even all-year absence of ice over almost the whole Arctic Ocean before year 2100 (Stroeve et al., 2012) or even before 2040 (Wang and Overland, 2009, 2012) although different prediction approaches still leave a large uncertainty as to the date of the free of sea-ice summer in the Arctic (Overland and Wang, 2013). Even in a seasonal sea-ice mode, the Arctic Ocean is expected to be covered by ice for a decreasing amount of days per annum. According to recent estimates, the Arctic coastal waters will be covered with ice for only half of the year in most High Arctic coasts by 2015 and almost everywhere by 2070 (Barnhart et al., 2016).

Less sea-ice coverage will mean a more dynamic Arctic Ocean with larger waves (Thomson and Rogers, 2014), more intense storms (Long and Perrie, 2012) and more intensive vertical mixing within the water column (Zhang et al., 2013), which will increase the sea-ice retreat rate even further. All these changes will influence the ecology of the Arctic Ocean and the adjacent land masses (Post et al., 2009). The warming Arctic Ocean may also release large volumes of methane stored in the form of hydrates and permafrost within shallow marine sediments (Biastoch et al., 2011), creating a strong positive feedback of the global warming (DeConto et al., 2012), although the time scale of the involved processes is still poorly constrained (James et al., 2016).

Rapid warming of the Arctic has not omitted Spitsbergen, the main island of the Svalbard archipelago. The summer temperatures in 2015 were the highest in recorded history (Overland et al., 2015), including the composite Longyearbyen-Svalbard Airport record, which goes back to 1898 (Nordli et al., 2014). The Atlantic waters of the West Spitsbergen Current are getting warmer (Piechura et al., 2002; Walczowski et al., 2012), which in turn increases the calving rates of the Svalbard tidewater glaciers (Luckman et al., 2015). The glaciers are retreating (Błaszczyk et al., 2009), which expands the area of Svalbard fjords such as Horsund (Błaszczyk et al., 2013) in such a spectacular way that the misnamed fjord may become a real sound before 2035 (Ziaja and Ostafin, 2015).

This paper aims at answering the question, whether this easily accessible archipelago, a popular place for Arctic research (Research in Svalbard database, https://www.researchinsvalbard.no/, lists 413 ongoing projects) may already be a study model of the environment of High Arctic coastal areas as it is expected to become in the next decades of the 21st century.

2. Methods

For the values of climate-related fields in the region of Svalbard, I used NCEP/NCAR reanalysis (Kalnay et al., 1996). It is a lower resolution reanalysis ($2.5^\circ \times 2.5^\circ$) than ERA-40 (Uppala et al., 2005), but it avoids the spurious Arctic temperature trends of ERA-40 (Screen and Simmonds, 2011). The low resolution also has the advantage of not introducing too many degrees of freedom to the temperature fields in a region sparsely and non-uniformly covered by data. For the sea surface temperatures (SST), I used a recent SST climatology, in situ merging and satellite data, created for the WMO recommended base for the period 1981–2010 (Xue et al., 2011), a $1^\circ \times 1^\circ$ update of an earlier SST climatology (Xue et al., 2003), available at http://origin.cpc.ncep.noaa.gov/products/people/yxue/sstclim/. Because there is little long term temperature data from inland Spitsbergen for seasonal temperature averages available, I used results from a recent 12 month measurement campaign (Przybylak et al., 2014), involving 30 meteorological stations placed all over Svalbard. All figures were prepared using the R language (R Core Team, 2017).

3. Results and discussion

The NCEP/NCAR reanalysis provides fields of meteorological parameters which, although of low spatial resolution, are temporally homogeneous since mid-20th century in the Arctic (Screen and Simmonds, 2011). Svalbard is covered very sparsely with meteorological stations and most of them are placed on the warmer western side. I used the reanalysis node with a centre in South-West Spitsbergen (77.5°N, 15°E) to analyse the warming trend in Svalbard. This approach has an additional advantage, which is the possibility to check the trends against the neighbouring stations, the data from which has recently been analysed by Gjelten et al. (2016). The annual averages for the NCEP/NCAR near-surface atmospheric temperature time series (1950–2015) are shown in Fig. 1 together with the trend line and trend 95% confidence range. The linear trend for the annual average temperatures since 1950 is +0.60 K decade^{-1} (with uncertainty of ±0.17 K decade^{-1} at 95% confidence). This corresponds to a 3.9 K warming since 1950. The trend is over 4 times the global one, showing that Svalbard is a good study case of the Arctic amplification. Because the Gjelten et al. (2016) temperature trends are calculated for the period 1979–2015, I have also calculated the linear temperature trend for the same period. Its value is +0.89 K decade^{-1}

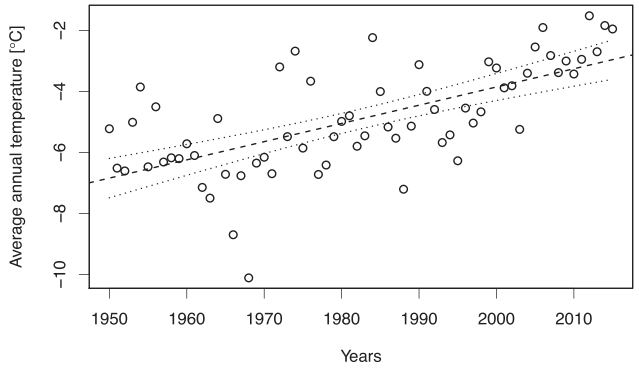

Figure 1 The annual near-surface air temperature averages, 1950–2015 from NCEP/NCAR reanalysis for South-West Spitsbergen. Linear trend and its uncertainty (95% confidence level) are marked with the dashed and the dotted line respectively.

(±0.32 K decade^{-1} at 95% confidence). This trend from the NCEP/NCAR reanalysis is lower than the station trends which are as follows: 0.96 K decade^{-1} for Ny-Ålesund, 1.03 K decade^{-1} for Hornsund, 1.06 K decade^{-1} for Barentsburg and 1.29 K decade^{-1} for the Svalbard Airport. The difference in the trends lies within statistical uncertainty, but it may also be caused by the larger spatial range of the reanalysis node covering also parts of the adjacent sea.

Fig. 2 shows the average near-surface atmospheric temperature data for all months since the year 1950. It presents 12 temperature graphs next to one another in a way that makes it possible to visually estimate the variability and trends for each month. The monthly averages in the recent years are similar to the locally measured ones (Cisek et al., 2017). It is clear from the figure that most of the warming since 1950 is confined to the coldest months, while the summers (especially June and July) have no warming trend. In fact the two months are the only ones with no statistically significant warming trend since 1950. The trends for the remaining ten months vary between +0.17 K decade^{-1} (±0.16 K decade^{-1} at 95% confidence) for May and +1.42 K decade^{-1} (±0.50 K decade^{-1} at 95% confidence) for January.

Recent temperature data measured at 30 Svalbard stations during a one-year campaign (Przybylak et al., 2014).

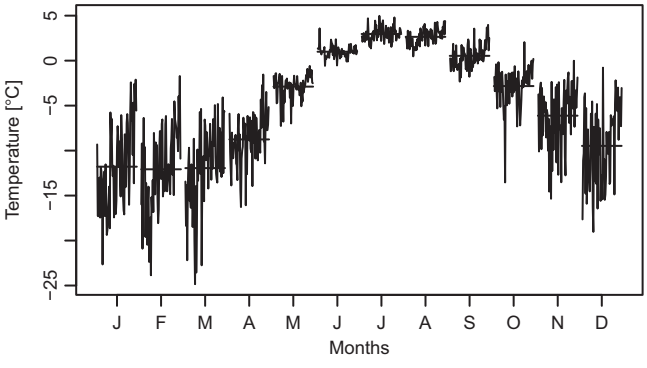

Figure 2 Near-surface air temperature averages for each month. Each month graph presents averages of each year in the range of 1950–2015 from NCEP/NCAR reanalysis for South-West Spitsbergen near Hornsund. Monthly means for the whole period are marked with horizontal lines.

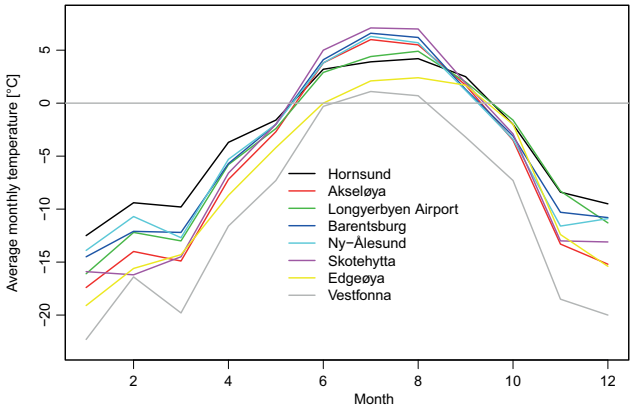

Figure 3 Monthly average near-surface temperatures recorded by meteorological stations in different Svalbard fjords from a one-year campaign of Przybylak et al. (2014).

Fig. 3 shows the monthly average temperatures from eight stations. Six of them are located in different Spitsbergen fjords, all close to sea-level to avoid the effect of altitude: Hornsund, Akseløya (in Bellsund), Longyearbyen Airport and Barentsburg (both in Isfjorden), Ny-Ålesund (in Kongsfjorden) and Skotehytta (near Pyramiden). The remaining two are placed on different islands, Edgeøya and Nordaustlandet (near Vestfonna glacier). Although the data is only from one year, the seasonal differences between Hornsund and Ny-Ålesund are similar to the ones derived from longer series (Cisek et al., 2017), which increases the confidence that the temperature range is representative for Svalbard fjords. The largest temperature differences are in winter (with the range of average January temperatures between −16.1 and −12.5°C (respectively for Akseloya and Hornsund) and in summer (from +3.9 to +7.1°C, respectively for Hornsund and Skotehytta). It is worthy of note that not the same fjords are warmest in summer and in winter (with Hornsund warmest in winter and coldest in summer). Coastal areas of Nordaustlandet island (represented by the Vestfonna station) are colder than all the coastal Spitsbergen stations during all seasons. Its annual monthly mean temperature variability if from −22.3°C in January to +1.1°C in July. This is caused by its north-eastern position and sea-ice coverage of adjacent ocean during most of the year. On the other hand, the Edgeøya station on an island east of Spitsbergen shows seasonal variability different than other stations with temperatures similar to the Spitsbergen coastal regions in autumn and winter while colder during the spring and summer. This shows the Svalbard fjords to be a diverse ensemble with different seasonal temperature patterns controlled by different processes.

One of the sources of differences in climate of different parts of Spitsbergen is the amount of clouds, influencing radiative fluxes. Fig. 4 shows the cloud coverage for the four seasons (averaged from the period 2010 to 2014) from NCEP/NCAR reanalysis. The cloudiness values from this product are underestimations of observed values, but they are useful for radiative forcing calculations (Weare, 1997) and no other analysis correlates better with satellite derived Arctic cloudiness on the time-scale of months (Liu and Key, 2016). In winter and spring, the largest cloudiness is over the warm waters of the West Spitsbergen Current and the

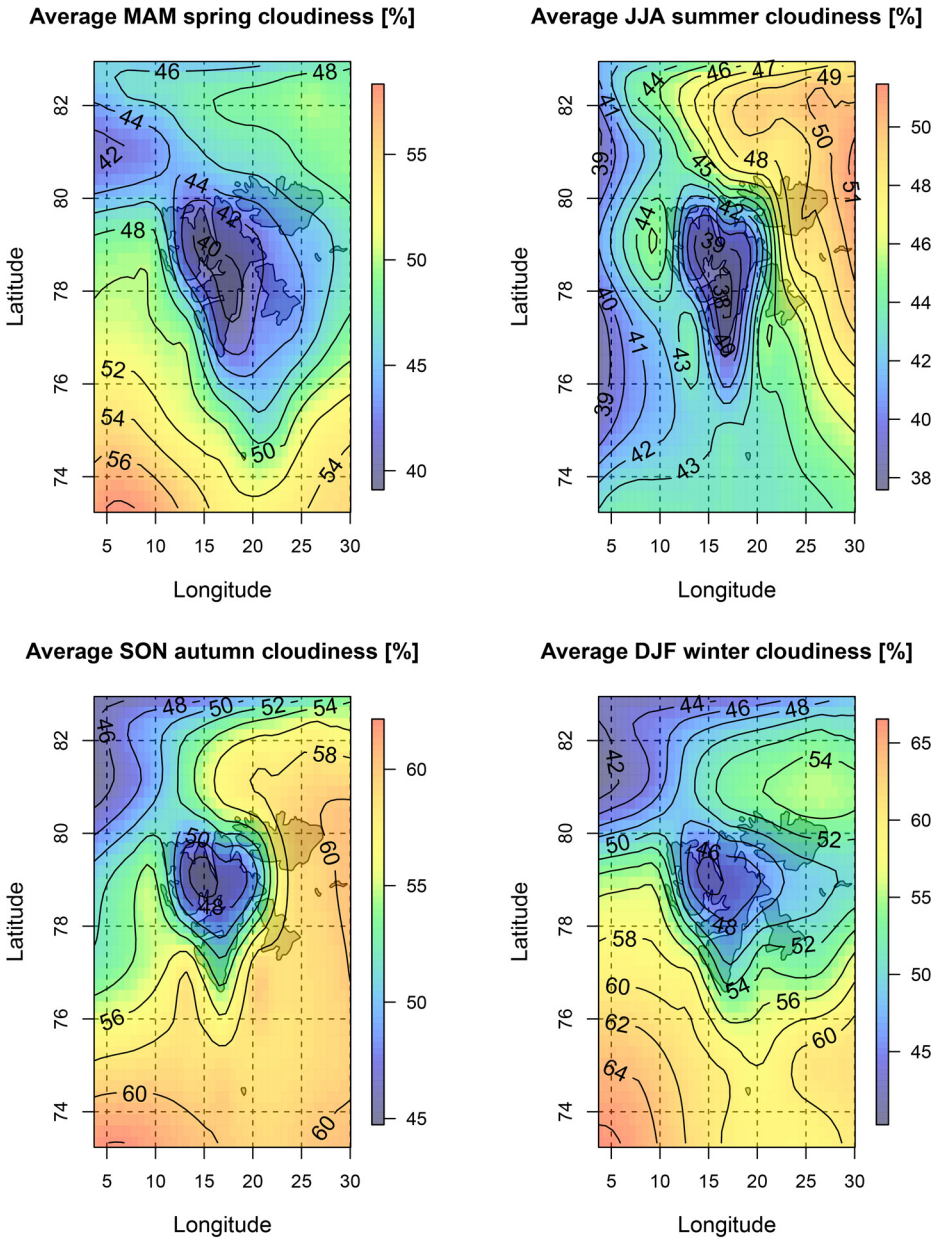

Figure 4 The average cloud coverage (2011–2015) for each season calculated from NCEP/NCAR reanalysis data.

south-eastern part of Svalbard, including Hornsund (a result confirmed by the local station data analysis from Hornsund and Ny-Ålesund in Cisek et al., 2017). In summer and autumn, the coastal areas both in the east and west of the island, have more clouds than the inland Spitsbergen. These patterns explain why Hornsund is warmest in winter when clouds have a warming forcing in the Arctic (Lubin and Vogelmann, 2006), while Skotehytta (the most inland station in Fig. 3) is warmest in summer. Arctic clouds work as a positive radiative forcing because the effect of blocking outgoing longwave radiation (the Arctic emits to space on average net 100 W m^{-2}) is more important than blocking incoming (solar) shortwave radiation during autumn and winter months of the "polar night" (Porter et al., 2010) and also, more surprisingly, during the spring (Francis and Hunter, 2007).

The cloud coverage is related to the SST, as the sea surface is the source of atmospheric water vapour (although other factors, such as wind direction, are also important). Fig. 5 shows the seasonal averages from a SST 1981 to 2010 climatology (Xue et al., 2011). The average sea surface temperatures to the west of Spitsbergen, in the Greenland Sea, are above zero in all months while to the east, in the Barents Sea, they are below zero for five months in the year (January–May). This East–West difference is larger then the South–North one along the Svalbard shores. The difference between the western part of the archipelago warmed by the West Spitsbergen Current (Walczowski and Piechura, 2011) and the cold eastern one, creates the large variability of environment in Svalbard, influencing the length of the snow-free and ice-free seasons, on the islands and in the adjacent seas respectively.

Fig. 6 presents the seasonal average sea-ice concentration for the period 2011–2015 calculated from the NCEP/NCAR reanalysis. It shows that Svalbard is recently practically free

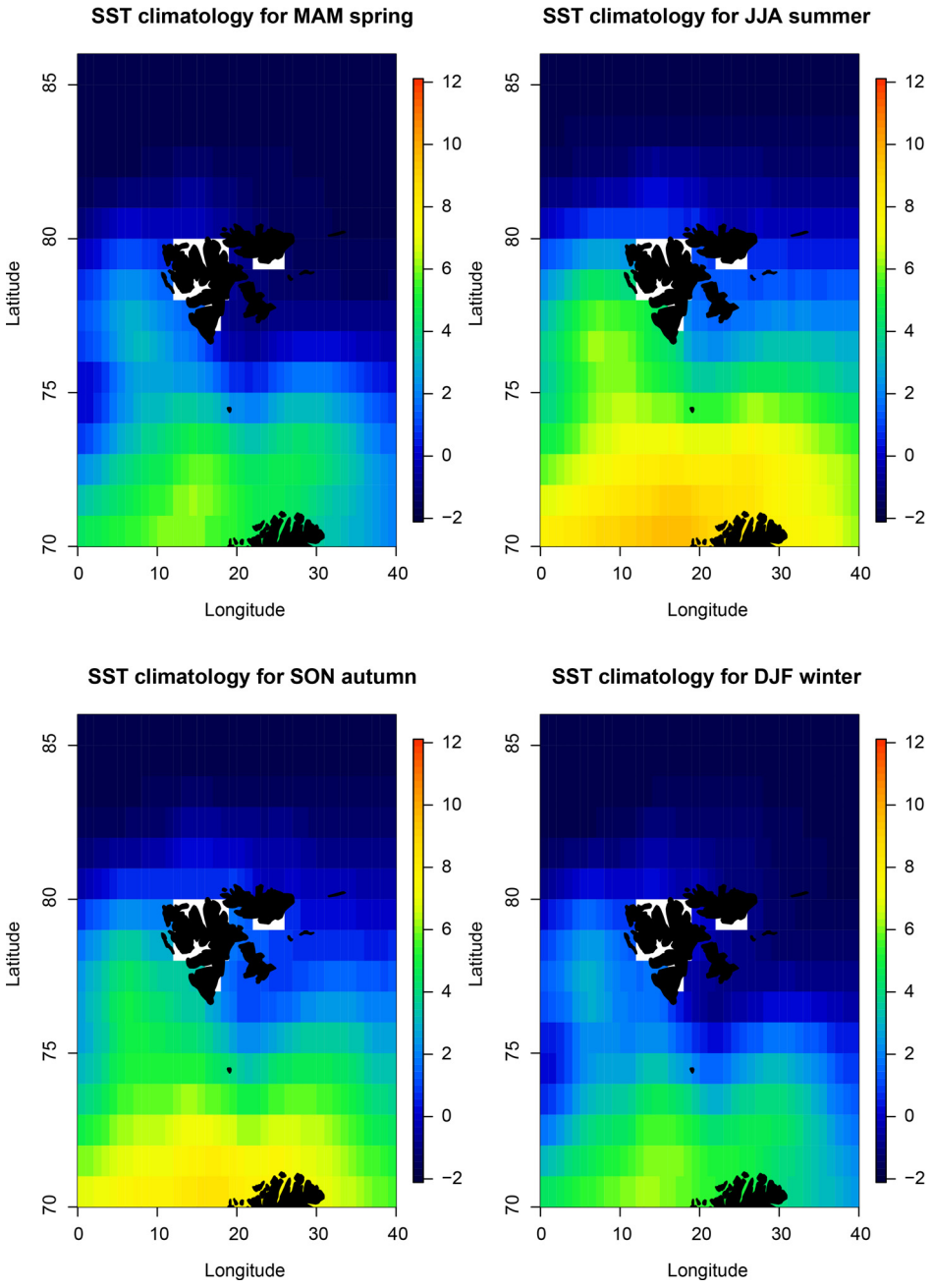

Figure 5 The sea surface temperature seasonal averages calculated from SST 1981–2010 climatology (Xue et al., 2011). The climatology $1^\circ \times 1^\circ$ grid data have not been interpolated. The white areas are grid nodes treated as land in the climatology.

of sea-ice in autumn. During the summer (JJA) sea-ice is sporadic in the north and east. On the other hand, winter and spring are the seasons in which the east coast of Svalbard is ice bound. The sea-ice reaches its maximum extent in May, when in the east of Svalbard, in the Barents Sea, it sometimes reaches Bjørnøya (Bear Island). This seasonal pattern means that the east and north coasts of Svalbard are ice-bound for about half a year, a state expected to be typical of the Arctic coastal areas only in about 50 years (Barnhart et al., 2016) while its West coast, with most of the easily accessible fjords, is already similar in to the ice-free conditions expected in the Arctic close to the end of the 21st century. The seasonal patterns of the sea-ice explain the SST patterns from Fig. 5, as sea water temperature cannot be positive with sea-ice present, therefore implying similar ones for the future High Arctic (IPCC, 2013). This makes Svalbard in general, and Spitsbergen fjords in particular, a natural laboratory of environmental changes expected in the future in the coasts of regions such as Greenland or the Canadian Arctic Archipelago.

4. Conclusions

Svalbard is an Arctic archipelago with warming trends exceeding the global average by at least four times with

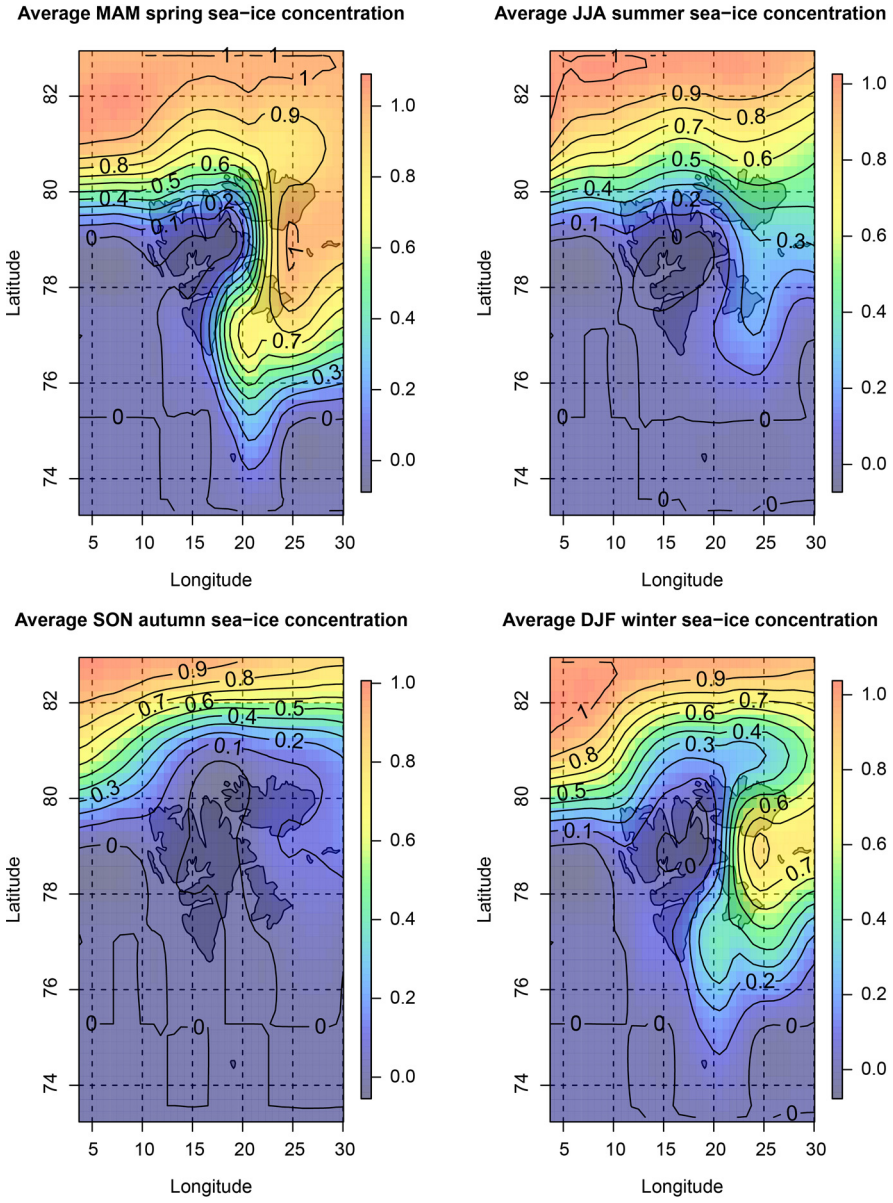

Figure 6 The average sea-ice concentration (2011–2015) for each season calculated from NCEP/NCAR reanalysis data.

most of the warming in the coldest months of the year. Its fjords represent diverse seasonal patterns of temperature due to some differences in the SST of the adjacent ocean, and the resulting different cloudiness. The sea water temperatures and ice concentrations in recent years are similar to what is expected in most of the Arctic coastal areas later this century. All this argues for using Svalbard as a model of future changes in the Arctic coastal ecosystems.

Acknowledgements

The study has been supported from the GAME "Growing of Marine Arctic Ecosystem" project, funded by the Polish National Science Centre [grant number DEC-2012/04/A/NZ8/00661]. The author is not aware of any conflicts of interest associated with this publication.

References

Barnhart, K.R., Miller, C.R., Overeem, I., Kay, J.E., 2016. Mapping the future expansion of Arctic open water. Nat. Clim. Change 6 (3), 280–285, http://dx.doi.org/10.1038/nclimate2848.

Biastoch, A., Treude, T., Rüpke, L.H., Riebesell, U., Roth, C., Burwicz, E.B., Park, W., Latif, M., Böning, C.W., Madec, G., Wallmann, K., 2011. Rising Arctic Ocean temperatures cause gas hydrate destabilization and ocean acidification. Geophys. Res. Lett. 38 (8), L08602, http://dx.doi.org/10.1029/2011GL047222.

Błaszczyk, M., Jania, J.A., Hagen, J.O., 2009. Tidewater glaciers of Svalbard: recent changes and estimates of calving fluxes. Polish Polar Res. 30 (2), 85–142.

Błaszczyk, M., Jania, J.A., Kolondra, L., 2013. Fluctuations of tidewater glaciers in Hornsund Fjord (Southern Svalbard) since the beginning of the 20th century. Pol. Polar Res. 34 (4), 327–352.

Cisek, M., Makuch, P., Petelski, T., 2017. Comparison of meteorological conditions in Svalbard fjords: Hornsund and Kongsfjorden. Oceanologia 59 (4), 413—421, http://dx.doi.org/10.1016/j.oceano.2017.06.004.

DeConto, R.M., Galeotti, S., Pagani, M., Tracy, D., Schaefer, K., Zhang, T., Pollard, D., Beerling, D.J., 2012. Past extreme warming events linked to massive carbon release from thawing permafrost. Nature 484 (7392), 87—92, http://dx.doi.org/10.1038/nature10929.

Francis, J.A., Hunter, E., 2007. Changes in the fabric of the Arctic's greenhouse blanket. Environ. Res. Lett. 2 (4), 045011, 6 pp., http://dx.doi.org/10.1088/1748-9326/2/4/045011.

Gjelten, H.M., Nordli, O., Isaken, K., Forland, E.J., Sviashchennikov, P.N., Wyszynski, P., Prokhorova, U.V., Przybylak, R., Ivanov, B.V., Urazgildeeva, A.V., 2016. Air temperature variations and gradients along the coast and fjords of western Spitsbergen. Polar Res. 35 (1), 29878, http://dx.doi.org/10.3402/polar.v35.29878.

IPCC, 2013. In: Stocker, T.F., et al. (Eds.), Climate Change 2013: The Physical Science Basis. Contribution of Working Group I to the Fifth Assessment Report of the Intergovernmental Panel on Climate Change. Cambridge Univ. Press, Melbourne, Madrid, Cape Town, Singapore, São Paolo, Delhi, Mexico City, 1535 pp.

James, R.H., Bousquet, P., Bussmann, I., Haeckel, M., Kipfer, R., Leifer, I., Niemann, H., Ostrovsky, I., Piskozub, J., Rehder, G., Treude, T., Vielstädte, L., Greinert, J., 2016. Effects of climate change on methane emissions from seafloor sediments in the Arctic Ocean: a review. Limnol. Oceanogr. 61 (S1), 283—299, http://dx.doi.org/10.1002/lno.10307.

Kalnay, E., Kanamitsu, M., Kistler, R., Collins, W., Deaven, D., Gandin, L., Iredell, M., Saha, S., White, G., Woollen, J., Zhu, Y., Chelliah, M., Ebisuzaki, W., Higgins, W., Janowiak, J., Mo, K.K. C., Ropelewski, C., Wang, J., Leetmaa, A., Reynolds, R., Jenne, R., Joseph, D., 1996. The NCEP/NCAR 40-year reanalysis project. Bull. Am. Meteor. Soc. 77 (3), 437—471, http://dx.doi.org/10.1175/1520-0477(1996)077<0437:TNYRP>2.0.CO;2.

Liu, Y., Key, J.R., 2016. Assessment of Arctic cloud cover anomalies in atmospheric reanalysis products using satellite data. J. Climate 29 (17), 6065—6083, http://dx.doi.org/10.1175/JCLI-D-15-0861.1.

Long, Z., Perrie, W., 2012. Air-sea interactions during an Arctic storm. J. Geophys. Res. 117 (D15), 20 pp., http://dx.doi.org/10.1029/2011JD016985.

Lubin, D., Vogelmann, A.M., 2006. A climatologically significant aerosol longwave indirect effect in the Arctic. Nature 439 (7075), 453—456, http://dx.doi.org/10.1038/nature04449.

Luckman, A., Benn, D.I., Cottier, F., Bevan, S., Nilsen, F., Inall, M., 2015. Calving rates at tidewater glaciers vary strongly with ocean temperature. Nat. Commun. 6, 8566, 1—7, http://dx.doi.org/10.1038/ncomms9566.

Manabe, S., Stouffer, R.J., 1980. Sensitivity of a global climate model to an increase of CO_2 concentration in the atmosphere. J. Geophys. Res. 85 (C10), 5529—5554, http://dx.doi.org/10.1029/JC085iC10p05529.

Miller, G.H., Alley, R.B., Brigham-Grette, J., Fitzpatrick, J.J., Polyak, L., Serreze, M.C., White, J.W.C., 2010. Arctic amplification: can the past constrain the future? Quat. Sci. Rev. 29 (15—16), 1779—1790, http://dx.doi.org/10.1016/j.quascirev.2010.02.008.

Nordli, Ö., Przybylak, R., Ogilvie, A.E.J., Isaksen, K., 2014. Long-term temperature trends and variability on Spitsbergen: the extended Svalbard Airport temperature series, 1898—2012. Polar Res. 33 (1), 21349, http://dx.doi.org/10.3402/polar.v33.21349#sthash.bFu0CZ1B.dpuf.

Overland, J.E., Hanna, E., Hanssen-Bauer, I., Kim, B.-M., Kim, S.-J., Walsh, J., Wang, M., Bhatt, U., Thoman, R.L., 2015. Air Temperature, Arctic Report Card 2015; http://www.arctic.noaa.gov/Report-Card.

Overland, J.E., Wang, M., 2013. When will the summer Arctic be nearly sea ice free? Geophys. Res. Lett. 40 (10), 2097—2101, http://dx.doi.org/10.1002/grl.50316.

Piechura, J., Osinski, R., Petelski, T., Woźniak, S.B., 2002. Heat and salt fluxes in the West Spitsbergen current area in summer. Oceanologia 44 (3), 307—321.

Porter, D.F., Cassano, J.J., Serreze, M.C., Kindig, D.N., 2010. New estimates of the large-scale Arctic atmospheric energy budget. J. Geophys. Res. 115 (D08), 20 pp. http://dx.doi.org/10.1029/2009JD012653.

Post, E., Forchhammer, M.C., Bret-Harte, M.S., Callaghan, T.V., Christensen, T.R., Elberling, B., Fox, A.D., Gilg, O., Hik, D.S., Hoye, T.T., Ims, R.A., Jeppesen, E., Klein, D.R., Madsen, J., McGuire, A.D., Rysgaard, S., Schindler, D.E., Stirling, I., Tamstorf, M.P., Tyler, N.J.C., van der Wal, R., Welker, J., Wookey, P.A., Schmidt, N.M., Aastrup, P., 2009. Ecological dynamics across the arctic associated with recent climate change. Science 325 (5946), 1355—1358, http://dx.doi.org/10.1126/science.1173113.

Przybylak, R., Arazny, A., Nordli, O., Finkelnburg, R., Kejna, M., Budzik, T., Migała, K., Sikora, S., Puczko, D., Rymer, K., Rachlewicz, G., 2014. Spatial distribution of air temperature on Svalbard during 1 year with campaign measurements. Int. J. Climatol. 34 (14), 3702—3719, http://dx.doi.org/10.1002/joc.3937.

R Core Team, 2017. R: A Language and Environment for Statistical Computing. R Foundation for Statistical Computing, Vienna, Austria, https://www.R-project.org/.

Screen, J.A., Simmonds, I., 2011. Erroneous Arctic temperature trends in the ERA-40 reanalysis: a closer look. J. Climate 24 (10), 2620—2627, http://dx.doi.org/10.1175/2010JCLI4054.1.

Serreze, M.C., Barrett, A.P., Stroeve, J.C., Kindig, D.N., Holland, M. M., 2009. The emergence of surface-based Arctic amplification. Cryosphere 3 (1), 11—19, http://dx.doi.org/10.5194/tc-3-11-2009.

Serreze, M.C., Barry, R.G., 2011. Processes and impacts of Arctic amplification: a research synthesis. Glob. Planet. Change 77 (1—2), 85—96, http://dx.doi.org/10.1016/j.gloplacha.2011.03.004.

Simmonds, I., 2015. Comparing and contrasting the behaviour of Arctic and Antarctic sea ice over the 35 year period 1979—2013. Ann. Glaciol. 56 (69), 18—28.

Stroeve, J.C., Kattsov, V., Barrett, A., Serreze, M., Pavlova, T., Holland, M., Meier, W.N., 2012. Trends in Arctic sea ice extent from CMIP5, CMIP3 and observations. Geophys. Res. Lett. 39 (16), L16502, 7 pp. http://dx.doi.org/10.1029/2012GL052676.

Thomson, J., Rogers, W.E., 2014. Swell and sea in the emerging Arctic Ocean. Geophys. Res. Lett. 41 (9), 3136—3140, http://dx.doi.org/10.1002/2014GL059983.

Timmermans, M.-L., Proshutinsky, A., 2015. Sea Water Temperature, Arctic Report Card 2015; http://www.arctic.noaa.gov/Report-Card.

Uppala, S.M., Kållberg, P.W., Simmons, A.J., Andrae, U., Bechtold, V. D.C., Fiorino, M., Gibson, J.K., Haseler, J., Hernandez, A., Kelly, G.A., Li, X., Onogi, K., Saarinen, S., Sokka, N., Allan, R.P., Andersson, E., Arpe, K., Balmaseda, M.A., Beljaars, A.C.M., Berg, L.V.D., Bidlot, J., Bormann, N., Caires, S., Chevallier, F., Dethof, A., Dragosavac, M., Fisher, M., Fuentes, M., Hagemann, S., Hólm, E., Hoskins, B.J., Isaksen, L., Janssen, P.A.E.M., Jenne, R., Mcnally, A.P., Mahfouf, J.-F., Morcrette, J.-J., Rayner, N.A., Saunders, R.W., Simon, P., Sterl, A., Trenberth, K.E., Untch, A., Vasiljevic, D., Viterbo, P., Woollen, J., 2005. The ERA-40 re-analysis. Q.J.R. Meteorol. Soc. 131 (612), 2961—3012, http://dx.doi.org/10.1256/qj.04.176.

Walczowski, W., Piechura, J., 2011. Influence of the West Spitsbergen current on the local climate. Int. J. Climatol. 31 (7), 1088—1093, http://dx.doi.org/10.1002/joc.2338.

Walczowski, W., Piechura, J., Goszczko, I., Wieczorek, P., 2012. Changes in Atlantic water properties: an important factor in

the European Arctic marine climate. ICES J. Mar. Sci. 69 (5), 864–869, http://dx.doi.org/10.1093/icesjms/fss068.

Wang, M., Overland, J.E., 2009. A sea ice free summer Arctic within 30 years? Geophys. Res. Lett. 36 (7), L07502, 5 pp., http://dx.doi.org/10.1029/2009GL037820.

Wang, M., Overland, J.E., 2012. A sea ice free summer Arctic within 30 years: an update from CMIP5 models. Geophys. Res. Lett. 39 (18), L18501, 6 pp., http://dx.doi.org/10.1029/2012GL052868.

Weare, B.C., 1997. Comparison of NCEP–NCAR cloud radiative forcing reanalyses with observations. J. Climate 10 (9), 2200–2209, https://doi.org/10.1175/1520-0442(1997)010<2200:CONNCR>2.0.CO;2.

Xue, Y., Reynolds, R.W., Banzon, V.F., Smith, T.M., Rayner, N.A., 2011. Global oceans: sea surface temperature. In: Arndt, D.S., Baringer, M.O., Johnson, M.R. (Eds.), State of the Climate in 2010. Bull. Amer. Meteorol. Soc., 92 (6), S78–S81.

Xue, Y., Smith, T.M., Reynolds, R.W., 2003. Interdecadal changes of 30-yr SST normals during 1871–2000. J. Clim. 16 (10), 1601–1612.

Zhang, J., Lindsay, R., Schweiger, A., Steele, M., 2013. The impact of an intense summer cyclone on 2012 Arctic sea ice retreat. Geophys. Res. Lett. 40 (4), 720–726, http://dx.doi.org/10.1002/grl.50190.

Ziaja, W., Ostafin, Z., 2015. Landscape–seascape dynamics in the isthmus between Sørkapp Land and the rest of Spitsbergen: will a new big Arctic island form? Ambio 44 (4), 332–342, http://dx.doi.org/10.1007/s13280-014-0572-1.